

UNIVERSITÀ DELLA CALABRIA



## **UNIVERSITA' DELLA CALABRIA**

Dipartimento di Farmacia e Scienze della Salute e della Nutrizione

**Dottorato di Ricerca in**

**MEDICINA TRASLAZIONALE (XXX CICLO)**

# **Targeting systems vulnerabilities in uveal melanoma by CRISPR Cas/9 focal adhesion kinase (FAK) genome editing and therapeutic inhibition**

**Settore Scientifico Disciplinare MED/04**

**Coordinatore del Dottorato:** Ch.mo Prof. Sebastiano Ando'

**Tutor:** Ch.mo Prof. Marcello Maggiolini

**Dottorando:** Dott. Damiano Cosimo Rigracciolo

# **Index**

Italian Abstract.....	1
English Abstract.....	2

## **Chapter 1**

### **Introduction**

1.1 Uveal Melanoma:clinical burden.....	3
1.2 Epidemiology.....	3
1.3 Etiology and risk factors.....	4
1.4 Clinical presentation and diagnosis.....	4
1.5 Primary treatment of Uveal Melanoma.....	5
1.6 Metastatic Uveal Melanoma treatments.....	7
1.7 Systemic therapies in Uveal Melanoma.....	9
1.8 Genetic mutations in Uveal Melanoma.....	10
1.9 Clinical implications.....	13
1.10 Focal adhesion kinase (FAK).....	14
1.11 FAK structure organization.....	15
1.12 Regulation of FAK expression.....	16
1.13 Regulation of FAK activity.....	17
1.14 Role of FAK in cancer cells.....	18
1.15 Novel strategies targeting FAK with pharmacological inhibitors.....	20

<b>Aim of the study.....</b>	<b>23</b>
------------------------------	-----------

## **Chapter 2**

### **Materials and methods**

2.1	Cell lines, culture procedures, and chemicals.....	24
2.2	Mutational analysis.....	24
2.3	Immunoblot analysis.....	24
2.4	Immunoprecipitation assay.....	25
2.5	siRNA transfection.....	25
2.6	Cell proliferation analysis.....	25
2.7	Focal adhesion assay.....	25
2.8	Methylcellulose growth assay.....	25
2.9	Genetic editing with CRISPR/Cas9.....	26
2.10	In vivo mice experiments and VS4718 treatment.....	26
2.11	Data and statistical analysis.....	26

## **Chapter 3**

### **Results**

3.1	PTK2 gene is overexpressed in Uveal Melanoma.....	27
3.2	GNAQ activates FAK in UM cancer cells .....	29
3.3	FAK mediates the proliferation of uveal melanoma cells through the PI3K/AKT/mTOR signaling pathway .....	32
3.4	Targeting FAK in vivo .....	34

## **Chapter 4**

**Discussion**.....36

**References**.....39

**Publications**.....54

# Abstract

Il Melanoma Uveale rappresenta la neoplasia intraoculare più frequente nell'età adulta. Colpisce circa 2,500 individui ogni anno negli USA ed il 50% dei pazienti affetti da tale neoplasia sviluppa metastasi entro 5 anni dalla diagnosi. Non essendo state ancora identificate terapie efficaci, la sopravvivenza in presenza di metastasi è di circa 6 mesi. Il Melanoma Uveale è geneticamente caratterizzato dalla presenza di mutazioni somatiche attivanti a carico degli oncogeni *GNAQ* e *GNA11*, che codificano per due diverse subunità  $\alpha$  delle proteine G. Tali mutazioni sono state identificate rispettivamente in circa il 94% dei casi di Melanoma Cutaneo ed il 4% dei casi di Melanoma Uveale.

Sulla base di tali osservazioni, nel presente lavoro di tesi è stato valutato il ruolo esercitato da una proteina citoplasmatica ad attività tirosin-chinasica associata ai recettori per le integrine denominata FAK (focal adhesion kinase), nella progressione del Melanoma Uveale, sia *in vitro* che *in vivo*. In particolare, mediante analisi bioinformatica ([www.cbioportal.com](http://www.cbioportal.com)) delle alterazioni genomiche di campioni estratti da pazienti affetti da melanoma uveale ( $n=80$ ), è stato inizialmente determinato che il gene codificante per FAK (PTK2) risulta over-espresso nel 56% dei casi. Inoltre, il presente studio condotto in cellule di Melanoma Uveale OMM1.3 (*GNAQ/11* mutate) e in cellule ingegnerizzate per l'espressione di un recettore di membrana accoppiato a proteine-G ( $G\alpha_q$ ) attivato esclusivamente da ligandi sintetici denominate HEK293 DREADD/ $G_q$ , ha dimostrato il coinvolgimento di segnali mediati da GNAQ nell'attivazione di FAK attraverso il reclutamento del fattore coinvolto nello scambio di nucleotidi guaninici denominato TRIO e la proteina appartenente alla super-famiglia di Ras denominata Rho-A. A riprova, saggi biologici hanno dimostrato l'efficacia di specifici inibitori di FAK nei processi di proliferazione cellulare sia in cellule di Melanoma Uveale derivanti da lesioni primarie che da metastasi epatiche. Attraverso l'innovativo approccio genetico denominato CRISPR/Cas 9 genome editing (Clustered Regularly Interspaced Short Palindromic Repeats), il silenziamento dell'espressione di FAK ha ridotto significativamente la crescita del melanoma uveale in modelli sperimentali utilizzati *in vivo*. Collettivamente, i risultati ottenuti indicano che FAK può essere considerato un potenziale target terapeutico per il trattamento del Melanoma Uveale e di altre neoplasie caratterizzate da mutazioni oncogeniche a carico delle subunità  $\alpha_q/\alpha_{11}$  dei recettori di membrana accoppiati a proteine G.

# Abstract

Uveal melanoma (UM) is the most common primary cancer of the eye in adults. It is diagnosed in about 2,500 adults in USA every year and approximately 50% of UM patients develop liver metastasis mostly within 5 years after diagnosis, independently of the successful treatment of the primary lesions. The survival of metastatic UM patients is often only few (2-6) months. To date, there are not effective options to treat or prevent UM metastasis. UM is genetically characterized by mutually exclusive activating mutations in the *GNAQ* and *GNA11* oncogenes, which encode heterotrimeric Gαq family members. These mutations have been identified in about 92% and 4% of uveal and skin melanomas, respectively. Here, we focused on a cytoplasmic protein tyrosine kinase associated with integrins namely focal adhesion kinase (FAK), which modulates important cell processes such as growth, survival, migration and angiogenesis. By the analysis of UM genomic alterations (TCGA), we found that the gene encoding FAK (PTK2) is amplified or overexpressed in >56% of all UM lesions. UM represents the human cancer harboring the highest levels of FAK, which we confirmed by immune histochemical analysis of a large collection of UM lesions. We found that Gq-GPCRs triggers a rapid phosphorylation of FAK at position Y397, which reflects its activation, through a guanine nucleotide exchange factor (TRIO)/Rho-A signaling circuitry. This promotes the assembly of focal adhesions, independently of the PLCβ/Ca<sup>2+</sup> second messenger system and the canonical PKC pathway. Next, we have assessed whether Gαq promotes the FAK-dependent proliferation of uveal melanoma cells. Both, CRISPR/Cas9 genome editing of FAK as well as the use of FAK inhibitors under clinical evaluation for other diseases resulted in reduction of UM tumor growth *in vivo*. The impact of these FAK inhibiting strategies in UM metastasis is under current evaluation. Collectively, our findings support the potential clinical benefit of targeting FAK as a precision therapy approach for UM and other *GNAQ*-driven malignancies and pathological conditions.

# Chapter 1

## Introduction

### 1.1 Uveal Melanoma: clinical burden

Uveal melanoma (UM) is the most common primary intraocular malignancy in adults displaying a high propensity for metastasis to the liver within 5-10 years after diagnosis, independently of the successful treatment of the primary lesions [1]. UM is a rare subtype of melanoma, representing ~5% of all melanoma tumors. Approximately 90% of all uveal melanomas involve the choroid, with the remainder arising in the ciliary body or the iris of the eye (**Fig. 1.1**) [1]. The terms choroidal melanoma and ocular melanoma are alternative terms for this cancer, because most of the uveal tract is choroidal. However, the term ocular melanoma should be avoided, because it implies the inclusion of conjunctival and adnexal melanomas, which behave like cutaneous rather than uveal primaries. UM can also rarely arise in melanocytes in the conjunctiva—melanoma of the conjunctiva accounts for ~2% – 3% of all eye neoplasms.

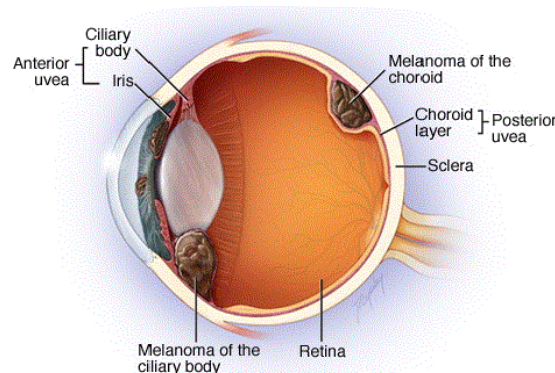


**Figure 1.1:** schematic representation of uveal melanoma origin sites

### 1.2 Epidemiology

The incidence rate of UM ranges from 0.2 to 0.3 per million individuals in African/Asian populations to up to 6 per million individuals in white population [2]. The average age of diagnosis is ~60 years and it affects both sexes equally or slightly more frequently males as per some reports [2] (**Fig. 1.2**). More recently, an increase in the mean age at diagnosis for the interval between 1973 and 2009 was described based on the analysis of 7043 UM patients from the Surveillance, Epidemiology, and End Results Program (SEER) database [3]. Furthermore, there is a strong difference in the incidence of UM for different ethnic groups: the annual age-adjusted incidence is 0.31 for Afro-Americans, 0.38 for Asians, 1.67 for Hispanics, and 6.02 for non-Hispanic whites [4], yet prognosis does not differ for ethnic groups [4]. The European Cancer Registry-based study on survival and care of cancer patients (EUROCORE) for the years 1983–1994 reported similar incidence rates with a characteristic increase from south to north Europe, from <2 per million in Spain and Southern Italy to >8 per million in Norway and Denmark [5].

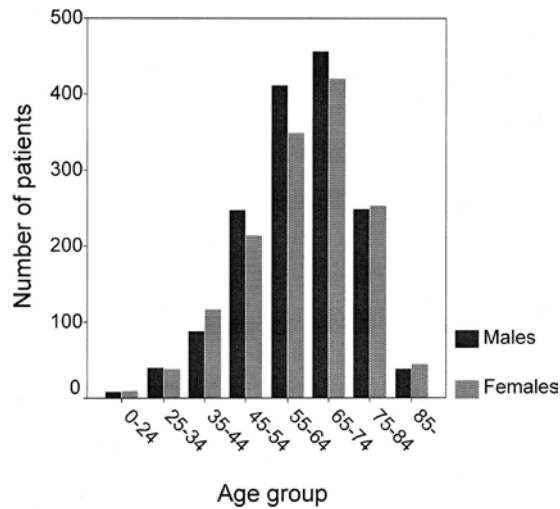


**Figure 1.2:** epidemiology of uveal melanoma in both sexes

### ***1.3 Etiology and risk factors***

The etiology of UM is still unclear. A variety of risk factors have been identified, including the presence of light eyes, fair skin color, red/blond hair, and *BAP1* mutations [6]. In contrast to Cutaneous Melanoma, the impact of ultraviolet (UV) light exposure is less clear for UM: although there are effective therapeutic strategies to eradicate primary UM. Cornea, lens, and vitreous body absorb almost all wavelengths below 300 nm and much of the spectrum between 300 and 400 nm. However, age-dependent alterations of the vitreous body [might alter the absorptive capacity of the latter. The associations between UM risk and blue iris or a generally weakly pigmented phenotype and sun exposure suggest a role for UV radiation in the etiology of UM [6]. If there is a role for UV light in UM etiology, it is certainly by far weaker than that for CM. The etiologic effect of UV radiation for UM is likely too weak to overcome confounding factors such as co-distribution of weakly pigmented skin and iris and latitude, co-occurrence of UV radiation with light of longer wavelengths, and protective, vitamin D-mediated effects of sun exposure. Interestingly, a recent study has demonstrated that posterior choroidal melanomas occurring in illuminated areas were associated with frequent adenine-to-cytosine mutations, whereas ciliochoroidal melanoma arising from unilluminated areas are associated with frequent adenine-to-thymine mutations and light eye color, suggesting that both light eye color and sunlight may be independent risk factors associated with different anatomic and mutation profiles [7].

### ***1.4 Clinical presentation and diagnosis***

The most common presenting symptom in patients with primary UM is blurred vision (37.8%); however, many patients are asymptomatic at the time of diagnosis (30.2%). Other common symptoms at presentation include: painless loss or distortion of vision (metamorphopsia) (2.2%), a serous (fluid) retinal detachment, (photopsia) (8.6%), floaters (7%), visual field loss (6.1%), visible tumor (3.1%) and pain (2.4%). Other diagnoses to be considered when assessing lesions concerning for UM are dependent upon location based on

the evaluation of iris or posterior lesions of the eye (**Fig.1.4**). For example, when UM affects the anterior segment of the eye, patients may notice discoloration of the iris or persistent injection of the episclera; also, chronic conjunctivitis may represent a referring diagnosis. Rarely, a blind eye or an eye with a dense cataract may harbor an occult melanoma. Patients with suspicious pigmented lesions should be assessed by an ophthalmologist who has clinical expertise in ocular tumors. The presence of subretinal fluid and orange pigment and the documented growth on fundus photography are findings that support the diagnosis of UM. Drusen and pigment epithelial changes are more suggestive of a benign lesion. Fluorescein angiography can demonstrate an intrinsic secondary vasculature of the choroid; however, ocular echography is the single most effective diagnostic tool available to the clinician. Melanomas tend to exhibit low internal reflectivity as well as an intrinsic acoustic quiet zone on ultrasound. Most are dome-shaped, but a collarstud or mushroom configuration is highly suggestive of melanoma. The shape occurs after a break in Bruch's membrane, a structure of the retina. Some reports suggest a correlation between increased tumor thickness and the risk of distant metastasis. Most experts agree that a lesion measuring >3 mm in apical height is likely a melanoma. Rarely is a clinical biopsy necessary to confirm the diagnosis of UM. The Collaborative Ocular Melanoma Study reported >99% diagnostic accuracy for eyes with typical features that were enucleated [8]. In some instances, a diagnostic biopsy may be indicated, particularly when the lesion is amelanotic or difficult to assess because of vitreous hemorrhage or debris. Fine-needle aspiration can be performed but requires the assistance of a skilled cytologist who is familiar with ocular pathology.

<b>Iris lesion</b>	<b>Posterior lesion</b>
• Primary iris cyst	• Choroidal nevus
• Iris nevus	• Disciform degeneration
• Essential iris atrophy	• Peripheral disciform degeneration
• Foreign body	• Retinal pigment epithelium hypertrophy
• Peripheral anterior synechia	• Hemangioma
• Secondary metastasis	

**Figure 1.4:** different diagnosis of uveal melanoma by location

### ***1.5 Primary treatment of Uveal Melanoma***

Before ocular therapy, a systemic workup should be performed to demonstrate lack of distant metastasis; once it is confirmed that disease is limited to the eye, local ophthalmic therapy can be focused on the primary neoplasm. Distant metastasis is rare at the time of initial UM presentation, occurring in <5% of patients. If distant disease is present, a local therapy for the eye may be deferred in favor of systemic treatment, although this depends on the symptomatology of the patient with regard to the eye. It cannot be emphasized enough that the management of UM is highly individualized; what follows are general guidelines and principles used by leading ocular oncologists in North America and Western Europe.

- ❖ *Close serial observation:* in most instances, it is best to consider this approach for patients who have ocular lesions with indeterminate findings that are not typical of melanoma. The ophthalmologist will

often monitor patients for definitive features, such as rapid growth or the development of subretinal fluid. In very rare instances, observation may be the preferred approach if the patient is too frail for surgical intervention to either enucleate or place a radionuclide plaque.

- ❖ *Laser therapy*: diode laser therapy, also known as transpupillary thermo therapy (TTT) and photodynamic laser photocoagulation are modalities that direct focused energy to destroy tumor vascular supplies and reduce local recurrences by injecting and activating light-sensitive compounds and free radicals. Well tolerated but has limited value, because local relapse rates are as high as 20%. TTT has been effective as primary therapy in up to 80% of cases of small or indeterminate lesions with few risk factors. However, the rate of tumor control with laser therapy varies inversely with tumor size. Therefore, it is best considered for small tumors (<3mm thickness) arising at a distance from the macula and the optic nerve. More commonly, this modality is used in an adjuvant setting after radiation.
- ❖ *Radiation therapy*: focal radiation therapy is the most common globe-salvaging approach used by ocular oncologists. The Collaborative Ocular Melanoma Study medium-size trial randomized patients who had tumors that measured from 2.5 to 10.0 mm in apical height to primary brachytherapy (with iodine-125 plaques) or enucleation. In that trial, no statistically significant difference was observed in melanoma-related mortality between the 2 cohorts [9]. Since then, ocular brachytherapy has emerged as the most common globe-sparing modality for tumors within these parameters. Patients who have melanomas with an apical height >10.0 mm can be treated using this approach but are more likely to experience severe radiation retinopathy and visual loss. In USA, iodine-125 is the most commonly used isotope. Other radioisotopes are also used; ruthenium-106 is the preferred isotope in many European centers. If available, charged-particle and proton-beam radiation are alternative to brachytherapy. Most clinicians agree that both modalities have high rates of local tumor control, as high as 98% in some series.
- ❖ *Surgery*: enucleation (removal of the globe) is the most common surgery performed for UM, and is appropriate for patients with vision loss, extensive extraocular growth, circumferential tumor invasion and large tumor diameter. Alternative surgical modalities include transretinal endoresection and transscleral resection: both procedures are site- and surgeon-dependent, with the majority of data coming from single-institution case series. Uvectomy (selective excision of the tumor with retention of the globe) is best limited to small anterior tumors of the eye, such as iris melanomas. Patients who undergo selective choroidal resection of their melanomas may benefit from adjuvant plaque radiotherapy to reduce the risk of ocular recurrence. Surgery affords the most detailed histopathologic assessment and can confirm microscopic extraocular extension. Epithelioid cell type and the presence of microvascular loops are associated with a worse prognosis. Exenteration (surgical removal of the globe and adjacent orbital contents) is rarely indicated and is limited to extreme cases of massive orbital involvement and patients who are receiving palliative care.

In addition, in patients with UM, it's believed that survival and the risk of distant relapse are independent of the method selected for primary tumor management. Some authorities have suggested that micrometastatic disease precedes local therapy. However, because metastatic risk correlates with the size of the primary tumor, some ocular oncologists now take a more aggressive local approach to the management of smaller primary and indeterminate tumors. A few adjuvant studies have been conducted in UM in an attempt to prevent metastatic disease. However, none of these studies demonstrated meaningful metastasis free survival benefit or overall survival (OS) benefit, including a small phase 3 using methanolextracted residue of bacillus Calmette-Guerin [10] and 2 single-arm studies of interferon- $\alpha$  using matched historic controls. Adjuvant intra-arterial hepatic infusion of the alkylating agent, *fotemustine*, was studied in an effort to reduce the occurrence of liver metastasis, because the liver is the most common site of metastasis and cause of death from UM [11]. In that study, 22 UM patients with choroidal involvement, and longest basal dimension >20 mm, extrascleral extension or apical height >15 mm were treated with *fotemustine* for 6 months. In this contest, adjuvant intra-arterial hepatic *fotemustine* was not shown to improve survival compared with matched historical controls. There are several ongoing adjuvant clinical trials in the USA such as ipilimumab, sunitinib, valproic acid, and crizotinib for high-risk patients. These agents or classes of agents have been chosen for study based on the molecular characteristics of UM cells or expected immunomodulatory or microenvironment effects.

### ***1.6 Metastatic Uveal Melanoma treatments***

Since the liver represents the first and only site of metastasis in most patients with UM, and the prognosis of patients with metastatic UM is highly dependent on the presence of liver metastasis and disease progression in the liver [12], liver-directed local treatments such as surgical resection, hepatic artery embolization, hepatic arterial infusion of chemotherapy, and radiofrequency ablation have been used in patients with metastatic uveal melanoma. A survival benefit has been demonstrated in patients who undergo surgical resection of liver metastasis compared with non-surgical control groups in multiple retrospective studies, but this benefit is limited to those who have minimal tumor volume that is limited to the liver and who also are fit enough for surgery (in a population with an average age at diagnosis of 70 years); and, according to these criteria, <10% of patients who have metastatic UM are candidates for liver resection [13].

Direct targeting of the hepatic arterial circulation is an enticing anatomic option for patients with liver-predominant disease, because the normal liver will receive blood supply from the portal system, whereas metastatic tumors generally are supplied predominantly by the hepatic artery. Hepatic arterial infusion of *fotemustine* (**Fig. 1.6.1**) has been studied in patients with UM metastatic to the liver in a randomized phase 3 study that assigned 171 patients to receive *fotemustine* either intravenously or by hepatic arterial infusion [14]. Although hepatic arterial infusion of *fotemustine* significantly improve progression-free survival (PFS) compared with intravenous administration (median PFS, 4.5 vs 3.5 months; hazard ratio [HR], 0.62; 95%

confidence interval [CI], 0.45-0.84;  $P = .002$ ), there was no improvement in OS (median OS, 14.6 vs 13.8 months;  $P = .59$ ).

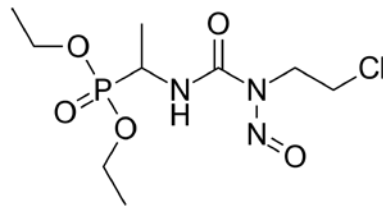


**Figure 1.6.1:** chemical structure of fotemustine

Isolated hepatic perfusion (IHP) is another option. In contrast to hepatic arterial infusion, IHP is a closed-circuit perfusion that delivers high doses of chemotherapy to the liver with minimized systemic drug exposure (**Figure 1.6.2**). IHP is an invasive and precise operative procedure that requires great skill and a period of extracorporeal circulation. A simple derivative percutaneous procedure known as percutaneous hepatic perfusion (PHP) has been developed. In a phase 3 trial, 93 patients were randomized to either PHP with melphalan or best supportive care, and crossover to PHP was allowed for those in the best supportive care arm after hepatic progression [15]. In that trial, there was a significant improvement in the median hepatic PFS (245 vs 49 days;  $P < .001$ ) and the overall response rate (34.1% vs 2%;  $P < .001$ ) compared with best supportive care.

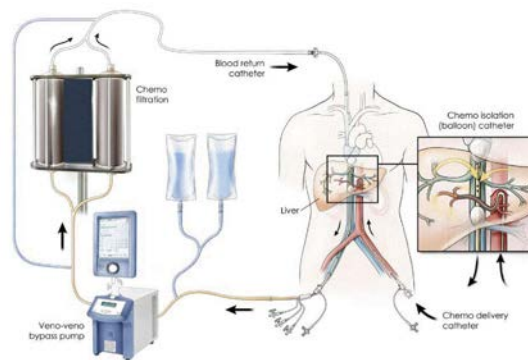


**Figure 1.6.2:** isolated hepatic perfusion circuit

Chemoembolization which combines hepatic artery embolization with infusion of concentrated doses of chemotherapeutic agents like cisplatin and 1,3-bis (2-chloroethyl)-1-nitrosourea, is another commonly used liver-directed therapy for metastatic UM. Gelatin sponge and non spherical polyvinyl alcohol particles have been used as embolic agents for chemoembolization. Because these embolic agents have an unpredictable level of arterial occlusion on account of their irregular shape and heterogeneous calibration, spherical embolic agents and drug-eluting microspheres have been developed and increasingly are being used. In a retrospective study of 201 patients with UM involving the liver, systemic chemotherapy, intra-arterial hepatic chemotherapy, and chemoembolization were compared [12]. In that study, although the rate of objective response to systemic treatment was  $<1\%$ , chemoembolization induced a 36% objective response rate with a median response duration of 6 months.

Also, another important liver-directed approach is the radioembolization by using yttrium-90 (90Y) radiospheres. 90Y is small enough to pass deep into tumor vessels (2-4 mm tissue penetration of radiation) but not through the capillary, thus sparing normal liver surrounding the tumor (**Figure 1.6.3**). Two retrospective studies of 90Y produced high response rates of up to 62% (8 of 13 patients) with a median OS of 7 to 10 months [16-17]. Currently, a prospective phase 2 study of 90Y plus ipilimumab is ongoing to evaluate the clinical activity in patients with UM metastatic to the liver.

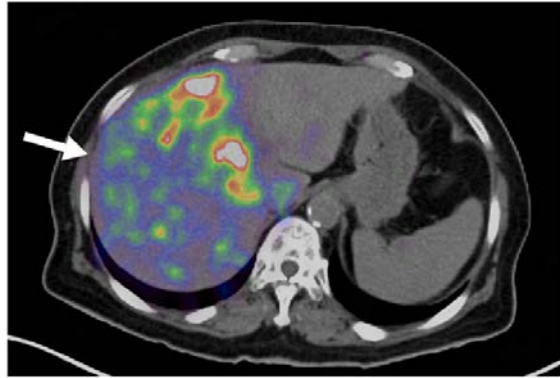


**Figure 1.6.3:** Yttrium-90 PET following radioembolization

### ***1.7 Systemic therapies in uveal melanoma***

**Chemotherapy:** UM is highly resistant to systemic cytotoxic chemotherapy. Several clinical trials of single-agent or combination chemotherapy have produced disappointing results, with objective response rates of <1%. [18-20]. On the basis of promising activity in patients with advanced cutaneous melanoma, biochemotherapy with either bleomycin, vincristine, lomustine, dacarbazine, and interferon- $\alpha$  or with fotemustine, interferon- $\alpha$ , and interleukin-2 has been studied in 4 phase 2 trials for patients with metastatic UM [21-22]. Objective response rates in those studies were <20%, and the median OS was only 12 months with significant pulmonary toxicities, neurotoxicities, and myelosuppression. To date, no clear role has been established for chemotherapy or biochemotherapy in patients with metastatic UM.

**Immunotherapy:** in March 2011, ipilimumab, a human antibody that blocks the immune checkpoint interaction between cytotoxic T-lymphocyte-associated protein 4 (CTLA4) and B7 protein 1 (B7.1) on antigen-presenting cells and/or target tumor cells, was approved for the treatment of advanced melanoma based on improved OS in a large, randomized, phase 3 study [23]. Although ipilimumab has been extensively studied in cutaneous melanoma, only limited data for ipilimumab are available in UM. For example, in a retrospective review of 39 patients with metastatic UM who received ipilimumab at doses of either 3 mg/kg (N 5 34 patients) or 10 mg/kg (N 5 5 patients) [24], the objective response and disease control rates (with the addition of patients who had stable disease at 12 weeks to objective responders) were 2.6% and 46%, respectively, at week 12 and 2.6% and 28.2%, respectively at week 23. The median OS was only 9.6 months. The efficacy of ipilimumab in UM also was investigated in other studies.

The programmed death 1 protein (PD-1) is another important immune checkpoint receptor expressed on the surface of T cells. PD-1 has 2 known ligands, PD-L1 (B7-H1) and PD-L2 (B7-DC). The ligation of PD-1 with PDL1 inhibits T-cell proliferation and activation and induces apoptosis of antigen-specific T cells to suppress antitumor immunity. Recently, pembrolizumab (humanized) and nivolumab (human) immunoglobulin G4 (IgG4) anti-PD1 monoclonal antibodies were approved by the Food and Drug Administration for the treatment of metastatic melanoma after ipilimumab (and v-Raf murine sarcoma viral oncogene homolog [BRAF] inhibitor therapy for patients who have melanoma with BRAF mutations). The efficacy of PD-1 blockade has not yet been reported in metastatic UM. In a single-center EAP, 7 patients with metastatic UM received 2 mg/kg of pembrolizumab every 3 weeks [25]. Two patients had objective responses (1 complete response and 1 partial response), and the median PFS was 12.2 weeks in that report. Currently, several clinical trials of immunotherapy including adoptive cell therapy and combined ipilimumab and nivolumab, are under way to identify effective immunotherapeutic approaches in metastatic UM.

*Targeted therapy:* 80% of UMs have oncogenic mutations in *GNAQ* or *GNA11*, and these mutations are potential drivers of mitogen-activated protein kinase (MAPK) activation, similar to oncogenic *BRAF* mutations in cutaneous melanoma [26]. Therefore, inhibition of the MAPK pathway has been studied in metastatic UM. A randomized phase 2 trial of selumetinib, a selective MAPK kinase (MEK) inhibitor, produced promising preliminary outcomes for UM [27]. In that study, 101 patients with metastatic UM were randomized to receive either selumetinib or temozolomide (or dacarbazine). The median PFS in the selumetinib group was 15.9 weeks with a median OS of 11.8 months, whereas the chemotherapy group had a median PFS of 7 weeks and a median OS of 9.1 months (P 5 .09 for OS). This was the first randomized study to demonstrate improved PFS in patients with metastatic UM, although an OS benefit was not observed. Currently, several MEK-inhibitors based clinical trials are underway or have been completed, including a randomized, double-blind, phase 3 study called SUMIT comparing selumetinib plus dacarbazine versus placebo plus dacarbazine (completed; no difference in PFS) and studies of MEK inhibitors with protein kinase C or AKT inhibitors. These studies will provide insight into the role of MEK inhibitors, their molecular targets, and other interacting pathways in the treatment of metastatic UM.

### ***1.8 Genetic mutations in uveal melanoma***

Oncogene and tumor-suppressor mutations that are common in other cancers are mostly absent in UM, a disease that is characterized by a low mutation burden. UM also differs in its genetic mutation profile from conventional cutaneous melanoma, in which BRAF and NRAS mutations dominate. These driver mutations, which control the biology of up to 70% of cutaneous melanomas, are absent/rare in UM [28]. UM has, in many cases, a poor prognosis since about half of all patients develop metastatic disease, predominantly to the liver. By using gene expression profile (GEP) classification, UM can be stratified into two distinct molecular classes with a significant difference in prognosis [29]. Class 1 tumors can be further divided into two

subgroups (class *IA* and *IB*) and has in general a good prognosis and low metastatic risk, whereas class 2 tumors have high metastatic risk and thereby a worse prognosis. The risk of metastasis has been determined to be 2% for class *IA* tumors, 21% for *IB* tumors, and finally 72% for class 2. The different molecular classes are also associated with mutations in different UM driver genes [30]. The most frequently mutated genes that are considered to be drivers in UM development and progression are: BAP1, EIF1AX, GNA11, GNAQ, and SF3B1 [26, 30-32]. Also, activating mutations occur in PLC $\beta$ 4 (phospholipase C  $\beta$ 4), the downstream effector of G $\alpha$ q signaling [26, 31] and in cysteinyl leukotriene receptor 2 (CYSLTR2), a seven-transmembrane G-protein-coupled receptor (GPCR), which functions in leukotriene-mediated signaling [33]. Microarrays and gene copy numbers from single nucleotide polymorphism arrays revealed that 42.2% of uveal melanoma samples harbored mutated *GNAQ*, 32.6% harbored mutated *GNA11*, 31.5% harbored mutated BAP1, 9.7% harbored mutated SF3B1, 18.9% harbored mutated EIF1AX and 1% harbored mutated TERT [34]. Of these, *GNAQ* and *GNA11* mutations are usually mutually exclusive, but both can coexist with BAP1 or SF3B1 mutations [52]. Likewise, BAP1 and SF3B1 mutations are mutually exclusive, as are EIF1AX and SF3B1 mutations, whereas TERT mutations appear to coexist specifically with *GNA11* or EIF1AX mutations [32, 34].

- ***BRCA1-associated protein 1 (BAP1)***: BAP1 encodes a deubiquitinating hydrolase with multiple cellular functions, such as regulation of chromatin dynamics, DNA damage response, cell cycle regulation, and cell growth. It is involved in the polycomb multiprotein repressor complex that is critical for transcriptional silencing of target genes by removing ubiquitin molecules from histone H2A. As a consequence of this functional loss, an accumulation of monoubiquitinated histone H2A has been revealed, which in turn was found to cause a more de-differentiated phenotype [35]. Furthermore it has been shown that BAP1 may interact with promoters regulated by the E2F transcription factor 1 gene (E2F1) and, thus, may affect the cell cycle progression genes controlled by E2F [36]. BAP1 is able to display tumor suppressor capacity by binding to the BRCA1 protein and thereby enhancing BRCA1-mediated tumor suppression [37]. BAP1 mutations strongly correlate with metastatic disease in UM: over 80% of metastasizing UM has been found to carry a mutation in this gene [30]. Most of the BAP1 mutations are truncating variants or missense variants affecting the ubiquitin carboxyl-terminal hydrolase domain. In some cases, BAP1 is not altered by a sequence mutation but by hemizygous deletion of one or more exons. Such alterations may be missed by traditional Sanger sequencing because of the presence of normal DNA in the sample. Also, BAP1 is frequently mutated in other tumor types, including cholangiocarcinoma, renal cell carcinoma, mesothelioma, and bladder cancer ([www.cbioportal.org](http://www.cbioportal.org)). Several of these cancer types are part of the hereditary cancer syndrome known as tumor predisposition syndrome that is characterized by germline mutations of BAP1 in patients belonging to cancer-prone families. Currently, there is no consensus among genetic counseling groups regarding who should be screened and surveillance strategies for patients who have germline BAP1 aberrancy.

- ***Splicing factor 3b subunit 1 (SF3B1)***: SF3B1 located at chromosome 2 is another driver gene identified by whole-exome sequencing of UM tumors. SF3B1 is essential in pre-mRNA splicing by encoding the unit of the splicing factor 3b protein complex that is a critical part of both major (U2-like) and minor (U12-like) spliceosomes. SF3B1 has recently also been designated as a factor involved in DNA damage repair [38]. Missense mutations in specific regions of the *SF3B1* gene have been found to alter the splicing of many target genes [39]. Uveal melanoma is among a small group of cancers associated with SF3B1 mutations: these mutations define a genetic subset of uveal melanoma that have been reported to be associated with favorable prognostic features and to be nearly always mutually exclusive of BAP1 mutations [30]. SF3B1 mutations are observed in codon 65 and mostly in tumors without loss of all or part of chromosome 3. Furney et al. have reported an association of these mutations with alternative splicing of transcripts [40].
- ***Eucaryotic Translation Initiation Factor 1A X-Linked (EIF1AX)***: EIF1AX, located on the Xp22 chromosome, encodes the eukaryotic translation initiation factor 1A (eIF1A). This factor is essential in the initiation phase of translation of eukaryotic cells by the transfer of methionyl initiator tRNA to the small (40S) ribosomal unit and stabilizes the formation of the ribosome around the AUG start codon, which enables translation. EIF1AX was identified as a UM driver gene by whole-exome sequencing [32]. Approximately 14%–20% of all UM carries a mutation in this gene, with most mutations found in exons 1 and 2 [32, 34]. EIF1AX mutations usually occur in non metastatic cases, are associated with class 1 GEP tumors and good prognosis, and are inversely associated with metastasis [41]. EIF1AX mutations are usually mutually exclusive with BAP1 mutations and to a large extent also to SF3B1 mutations. As expected most EIF1AX mutations are identified in tumors with disomy 3 (48%) and rarely occur in monosomy 3 tumors (3%) [32]. In contrast to, for example, BAP1 mutations, which mainly are truncating and loss-of-function variants, the majority of the EIF1AX mutations are heterozygous non synonymous variants, or in some cases splicing variants, leading to deletions of one or two amino acids. Thus, in most cases, the core protein remains unchanged.
- ***GNAQ and GNA11***: GNAQ encodes the alpha subunit (Gaq) and GNA11 the alpha subunit 11 (Gα11), both being guanine nucleotide-binding proteins belonging to the heterotrimeric protein family, which are of importance in transmembrane signaling systems. The alpha subunits serve as a switch between the G-proteins active state – when bound to guanosine triphosphate (GTP) – and the inactive state – when GTP is hydrolyzed to guanosine diphosphate. Activating mutations in GNAQ/GNA11 were the first described driver mutations in UMs. GNAQ and GNA11 mutations occur in a mutual exclusive pattern and are exclusively found in codon 209 and in some cases in codon 183 [26, 31]). Mutations at these positions lead to a constitutive activation of the Gaq and Gα11 subunits by abolishing their intrinsic GTPase activity, thereby preventing the return to an inactive state. In total, ~85% of all UMs carry a mutation in either of these genes. Both GNAQ and GNA11 have been found to upregulate the MAP kinase pathway when constitutively activated in a similar fashion as BRAF and NRAS mutations (**Figure 1.8.1**).

The activation of the MAPK pathway in the absence of BRAF/NRAS mutations in UMs was at first unforeseen until the identification of GNAQ and later GNA11 mutations that had the same effect as the *V600EBRAF* mutation. Cell lines with a GNAQ Q209L mutation have also been found to be highly sensitive to mitogen-activated protein kinase (MEK) inhibition [31]. Mutations in these genes have not been associated with the two different molecular classes of UM tumors. In addition, GNAQ/GNA11 mutations have not been reported to be of prognostic value and they occur at similar frequencies in metastatic and non-metastatic lesions. Furthermore, they have not been linked to patient outcomes. Taken all this data into consideration is supportive of GNAQ/GNA11 being early events. The hotspot mutations in GNAQ or GNA11 are also commonly found in benign nevi such as blue nevi [26, 42]. Actually, GNAQ Q209 was most frequently found in blue nevi, observed in 55% of the lesions, whereas 45% of the primary UMs and 22% of the metastatic UM, respectively, carry this mutation [26]. Inverse relationship was seen for the GNA11 Q209 mutation where metastatic lesions showed the highest number (56%) followed by primary UM tumors (32%) and lastly blue nevi (6%) [26]. Mutations affecting codon R183 are less frequent, present in 2% of the blue nevi and 5% of primary UM tumors, GNAQ and GNA11 mutations combined [26].

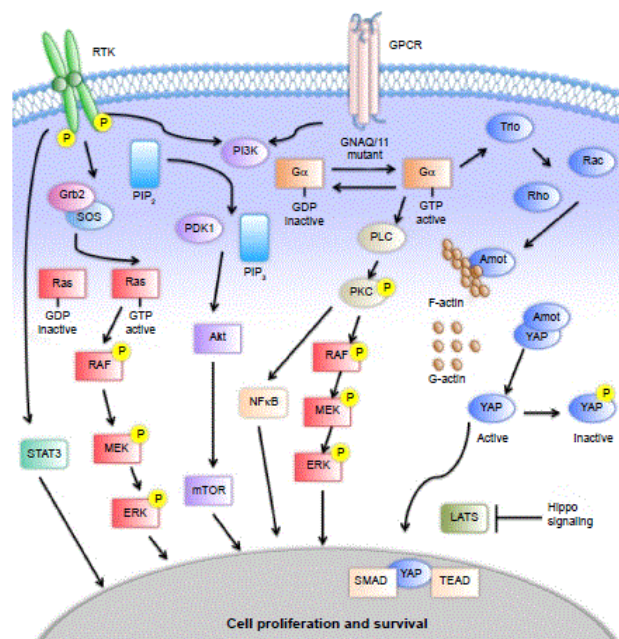


**Figure 1.8.1:** signaling pathways in uveal melanoma

## 1.9 Clinical implications

The identification of driver genes has led to the identification of novel treatment targets and several clinical trials are ongoing investigating these targets in UM therapy. Targeting mutated GNQ/GNA11 directly is difficult because of the molecular nature of the mutations causing an inactivation of intrinsic GTPase within the cell. However, for several downstream molecules of GNAQ/GNA11, targeted therapies have become

available. These include mitogenic activated protein kinase/extracellular signal-regulated kinase (MEK) that is shown to be upregulated in *GNAQ/GNA11* mutated tumors [43]. Inhibition of MEK has actually been found to decrease the proliferation of UM tumors both in vivo and in vitro [44]. Furthermore, a clinical Phase II trial has shown a prolonged progression-free survival of nearly 9 weeks when treating patients with the MEK inhibitor selumetinib compared to chemotherapy (temozolamide) [45]. However, in another Phase II trial, there was no significant effect on overall survival when treating with semurafenib compared to chemotherapy, although there was a modest increase in response rate and progression-free survival [27]. Other putative downstream targets of *GNAQ/GNA11* mutated tumors are protein kinase C and molecules of the protein kinase B (AKT)/mammalian target of rapamycin pathway [46-47]. Also BAP1 mutations are difficult to target directly because of their recessive nature. However, the effects of the mutations are possible to target by the use of histone deacetylase (HDAC) inhibitors in tumors with loss of BAP1 function. The absence of functional BAP1 protein leads to hyperubiquitination of H2A in the cells [35]. The use of HDAC inhibitors can reverse this phenotype, thereby causing a shift from aggressive, de-differentiated class-2 UM cells to more differentiated and less aggressive cells [35]. HDAC inhibitors have also been suggested as adjuvant treatment in high-risk patients [48].

In familial cancer combining clinical and genetic information can be used to improve prognostic estimates and to improve strategies for early diagnosis. By genetic testing of cancer-prone families, the clinical outcome can in many situations be improved, by detecting precursor lesions and tumors at an early stage in members of mutation-positive families. Often, however, this is not straight forward, as in familial melanoma, where a low frequency of mutations in high penetrance genes is seen and risk estimates for mutation carriers have not been well established at this point. Genetic testing is often only recommended when the result is of importance in the management of the patient and where there is a possibility of improving the clinical outcome. However, in families exhibiting the phenotype specific for *BAP1* tumor predisposition syndrome, genetic testing should be offered. Additional research will be of importance to elucidate the penetrance and risk of developing different types of cancer in mutation carriers. Identifying the susceptibility factor in cancer-prone families will be of importance for choice of surveillance programs and follow-up of the patient and their relatives. For families with a high cancer burden but without mutation in any known high predisposing gene, next-generation sequencing will be the natural choice to search for novel susceptibility genes. This will subsequently increase the knowledge about genetic susceptibility and may in the future be the basis for improved early detection and prevention of UM as well as lead to the development of new targeted treatments.

### ***1.10 Focal adhesion kinase (FAK)***

Focal Adhesion Kinase (FAK) is a 125 kDa non-receptor tyrosine kinase also known as PTK2, that resides at the sites of integrin clustering, known as focal adhesions. FAK plays a significant role in adhesion, survival,

motility, metastasis, angiogenesis, lymphangiogenesis, cancer stem cell functions [49-50], tumor microenvironment and epithelial to mesenchymal transition (EMT) [51]. FAK was first discovered in 1992 by several different groups [52], the next year human FAK was isolated [53] and later it was found in *Drosophila* and other species [54]. Once FAK was isolated in humans it was directly linked to cancer due to its high expression in primary tumors and overexpression in nearly all metastatic tumors, with no detectable FAK mRNA or protein in normal tissues [53].

### 1.11 FAK structure organization

The human gene encoding FAK namely PTK2 is localized on chromosome 8q24, a region characterized by frequent aberrations in human cancers [55]. Structurally, FAK consists of an amino-terminal regulatory FERM domain, a central catalytic kinase domain, two proline-rich motifs, and a carboxy-terminal focal adhesion targeting domain FAT (a four helix bundle) (**Fig. 1.11.1**).

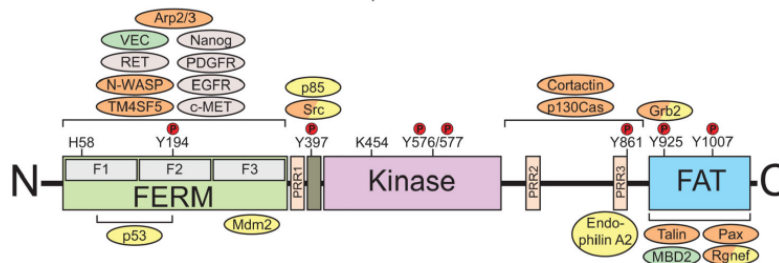


**Figure 1.11.1:** FAK domain structure model

The N-terminal FERM domain of FAK contains one nuclear export sequence (NES) and one nuclear localization sequence (NLS), whereas the FAK kinase domain contains another NES sequence close to the major FAK phosphorylation sites Y576/Y577 suggesting the regulation of FAK through nucleo-cytoplasmic shuttling and supporting nuclear functions of FAK (binding with p53 [56], and Mdm-2 [57] and other partners) [58].

The C-terminal domain of FAK contains two proline-rich regions that function as binding sites for SRC-homology (SH)3-domain-containing proteins. SH3-domain-mediated binding of the adaptor protein p130Cas to FAK is important in promoting cell migration through the coordinated activation of Rac at membrane extensions [59]. The SH3-mediated binding of other proteins, such as GRAF (GTPase regulator associated with FAK) and ASAP1 (Arf GTPase-activating protein (GAP) containing SH3, ankyrin repeat and pleckstrin homology (PH) domains-1), connects FAK to the regulation of cytoskeletal dynamics and focal contact assembly. However, the downstream connections of GRAF and ASAP1 remain undefined. Furthermore, the C-terminal domain encompasses the FAT region which promotes the co-localization of FAK with integrins at focal contacts. The FAK FAT domain also binds directly to an activator of Rho-family GTPases that is known as p190 RhoGEF, and FAK-mediated tyrosine phosphorylation of p190 RhoGEF might be a direct

link to RhoA activation [60]. Interestingly, FAK is phosphorylated (P) on several tyrosine residues, including Tyr397, 407, 576, 577, 861 and 925. Tyrosine phosphorylation of FAK on its major site Tyr397 creates a Src-homology-2 (SH2) binding site for Src [61-62]. The interaction between Y397-activated FAK and Src leads to a cascade of tyrosine phosphorylation of multiple sites in FAK, as well as other signaling molecules such as p130CAS and paxillin, resulting in cytoskeletal changes and activation of other downstream signaling pathways [59]. Also, FAK phosphorylation leads to activation of phospholipase C $\gamma$  (PLC $\gamma$ ), suppressor of cytokine signalling (SOCS), growth-factor-receptor bound protein 7 (GRB7), the Shc adaptor protein, p120 RasGAP and the p85 subunit of phosphatidylinositol 3-kinase (PI3K) [55]. Phosphorylation of Tyr576 and Tyr577 within the kinase domain is required for maximal FAK catalytic activity, whereas the binding of FAK-family interacting protein of 200 kDa (FIP200) to the kinase region inhibits FAK catalytic activity [63]. Also, FAK phosphorylation at Tyr925 creates a binding site for GRB2 [63]. These structural studies provided a basis for developing of small molecule inhibitors targeting FAK.

### ***1.12 Regulation of FAK expression***

Nuclear factor  $\kappa$ B (NF $\kappa$ B) and p53 are well-characterized transcription factors which activate and repress the *PTK2* promoter, respectively [64-65]. Also, other transcription factors like Nanog [66], Argonaute2 (Ago2) [67], and PEA3 [68] increase *PTK2* promoter activity. Nanog promotes FAK expression in colon carcinoma cells and as part of a signaling loop, Nanog activity is increased by FAK phosphorylation [66]. Ago2, a part of the cellular RNA interference machinery, is amplified in hepatocellular carcinoma and induces FAK transcription [67]. Ago2-silencing reduces FAK levels and concomitantly blocks tumorigenesis and metastasis in mice. Elevated PEA3 and FAK levels correlate with metastatic stages in human oral squamous cell carcinoma [68]. PEA3 induces FAK expression *in vitro* and silencing of either PEA3 or FAK reduces metastasis of human melanoma xenografts. Given the complexity and size of the *PTK2* promoter region, it is likely that transcription factor combinatorial effects regulate *PTK2* transcription.

FAK is also subject to alternative splicing as *PTK2* with deletion of exon 33 (FAK amino acids 956–982), identified in a subset of breast and thyroid patient samples, results in enhanced cell motility and invasion [69]. However, this deletion disrupts FAK linkage to integrins and it is unclear how truncated FAK may function. At the protein levels, FAK is subject to proteasomal or calpain-mediated degradation [70]. Poly-ubiquitination by the E3 ligase mitsugumin 53 (also known as TRIM72) promotes FAK proteasomal degradation during myogenesis, but this has not been tested in tumor cells [71]. However, in general, FAK protein levels are elevated in advanced stage of solid tumors. Together, these results support the notion that elevated FAK expression is connected to several tumor-associated phenotypes.

### ***1.13 Regulation of FAK activity***

Several types of signaling events initiate FAK activation. The best-characterized mechanism promoting FAK activation involves engagement of integrins with the ECM and the subsequent co-clustering of proteins like talin and paxillin with the cytoplasmic tail of integrin [72]. This leads to the recruitment of FAK to sites of integrin clustering via interactions with integrin-associated proteins, leading to FAK activation. Other examples of signaling stimuli promoting FAK activation include stimulation by specific growth factors like epithelial growth factor (EGF), hepatocyte growth factor (HGF), vascular endothelial growth factor (VEGF) and platelet derived growth factor (PDGF), activation of particular G-protein-coupled receptors, and the binding of interacting partners of the FAK FERM domain such as ezrin in an integrin-independent manner [63, 70, 72].

The first step in FAK activation involves displacement of the FERM domain from the kinase domain, presumably reflecting binding of a phospholipid or peptide ligand to the FERM domain, allowing rapid autophosphorylation of Y397 [72]. This then creates a high affinity binding site for the SH2 domain of Src, or other SFKs, leads to exposure of the activation loop, and prevents further interactions between the FERM and kinase domains. Src then transphosphorylates additional sites on FAK (Y576 and Y577) on the kinase domain activation loop, leading to full activation [72]. The phosphorylated activation loop also precludes the inhibitory docking of the FERM domain.

Recent studies provide additional mechanistic insights into FAK activation, one of which establishes a phospholipid, phosphatidylinositol-4,5-bisphosphate (PI(4,5)P<sub>2</sub>), as an important signaling messenger linking integrin signaling to FAK regulation [74]. Integrin-mediated local production of PI(4,5)P<sub>2</sub> promotes binding of PI(4,5)P<sub>2</sub> to a basic region (K216AKTLRK222) of the regulatory FAK FERM domain, inducing FAK clustering in focal adhesions [74]. FAK subsequently transits into a partially open conformation where the autophosphorylation site Y397 is exposed without re-leasing the autoinhibitory interaction of FERM-kinase domains, but this is sufficient to facilitate autophosphorylation and subsequent Src recruitment to Y397 [74]. Src-phosphorylation of the activation loop then releases the FERM/kinase domain leading to a fully active conformation. Using a variety of complementary approaches including structural and biophysical analyses, Brami-Cherrier et al, identified that autophosphorylation of Y397 requires FAK dimerization, mediated via FERM:FERM and FERM:FAT interactions, and occurs in trans FERM:FAT interaction involves binding of FAT to a basic patch on the FERM domain. Interestingly, paxillin contributes to positive regulation of FAK activity by clustering FAK at focal adhesions and reinforcing FERM:FAT association [75]. In addition, different types of cellular stimuli impact upon FAK activation. For example, elevated intracellular pH positively regulates FAK, in which deprotonation of the His58 FAK residue at high intracellular pH initiates conformational changes that may enhance Y397 autophosphorylation [76].

### 1.14 Role of FAK in cancer cells

FAK is at the intersection of various signaling pathways promoting cancer growth and metastasis (**Fig. 1.14.1**). These include kinase-dependent control of cell motility, invasion, cell survival, and transcriptional events promoting epithelial-mesenchymal transition (EMT) [70, 72]. Additionally, kinase-independent scaffolding functions of FAK can influence cell survival or cancer stem cell proliferation [59, 70, 72]. Understanding the balance between kinase-dependent and -independent functions is the key to the interpretation of FAK-related phenotypes.

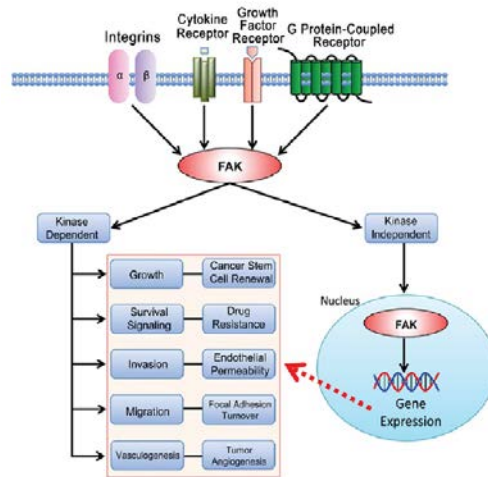


**Figure 1.14.1:** Kinase dependent and independent-FAK signalling pathways

Conditional tissue-specific FAK floxed mouse models and chemical FAK inhibitors have allowed the delineation of several FAK-associated pathways. For example, several groups have used polyoma virus middle T antigen (PyMT)-driven breast tumor models combined with tissue-specific FAK knockout through the mouse mammary tumor virus (MMTV) promoter (MMTV-PyMT model) [49, 77] to assess FAK function in tumor progression.

- ❖ **Survival and apoptosis:** the first demonstration of a survival function for FAK was performed by Frisch et al, where expression of active FAK was shown to suppress anoikis in Madin Darbin canine kidney (MDCK) and immortalized keratinocyte HaCat epithelial cells [78]. Then, FAK was linked to apoptosis in cancer cells, in which the inhibition of FAK with anti-sense oligonucleotides or with dominant negative FAK (FAK-CD (FAK C-terminal domain)) caused loss of adhesion and apoptosis in tumor cells [79]. Also, down-regulation of FAK with FAK siRNA decreased MCF-7 breast cancer viability and inhibited tumor growth [80]. In addition, FAK was shown to interact with p53 and inhibit its apoptotic activity [56]. Furthermore, nuclear FAK regulated survival through its direct binding to Mdm-2, which promoted p53 ubiquitination and degradation [57]. The anti-apoptotic function of FAK was demonstrated in HL-60 leukemia cells, where

FAK activated the PI-3-Kinase/AKT pathway and induced functions of NF-kappa B and inhibitor of apoptosis proteins (IAPs) [81].

- ❖ **Motility:** FAK was shown to play a pivotal role for motility in cancer cells [82]. FAK-null embryos exhibited decreased cell motility [83], whereas overexpression of FAK induced cell motility [84]. The Src and PI-3 Kinase downstream signaling pathways have been shown to be an important role for FAK-mediated cell motility [70].
- ❖ **Invasion and metastasis:** tumor cell invasion into the surrounding microenvironment is an important step in cancer progression, allowing cancer cells to form metastasis at secondary locations. This requires transition to a motile phenotype through changes in focal adhesions (FAs) and cytoskeletal dynamics, and alterations in matrix metalloproteinase (MMP) expression or activation to facilitate ECM invasion. EMT, which is driven by a transcriptional program, supports the progression to these invasive properties. FAK was shown to mediate cell invasion and metastasis through promotion of EMT (**Fig. 1.14.2**). For example, FAK promotes cellular membrane expression of MT1-MMP, a matrix metalloproteinase, which serves to degrade the ECM [85]. Also, FAK activity increases MMP-9 expression and spontaneous breast carcinoma metastasis in a syngeneic and orthotopic mouse model [86]. Other studies show that MMPs regulation and surface presentation in cancer cells involves multiple downstream pathways such as p130Cas58 and the PI3K/Akt/mTOR cascade [87]. Thus, FAK plays an important role in EMT, invasion and metastasis and the details of the down-stream molecular mechanisms of FAK-regulated EMT and E-cadherin mediated cell-cell adhesions or integrin-ECM mediated adhesions and their cross-talk and role in metastasis remain to be discovered.

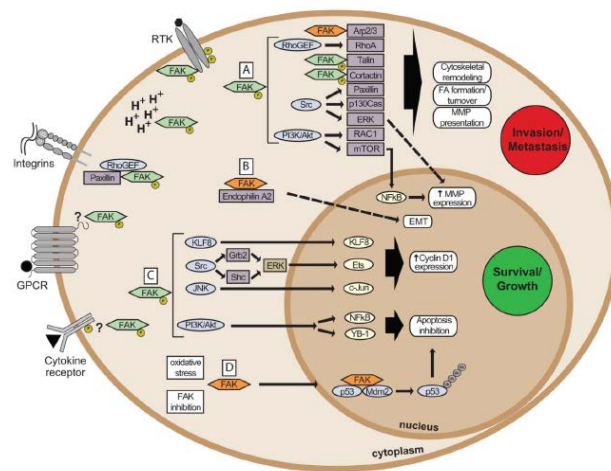


**Figure 1.14.2:** FAK promotes survival and invasion in cancer

- ❖ **Angiogenesis:** angiogenesis is critical to malignant progression and involves the local formation of nascent blood vessels from pre-existing vasculature through stimulation of ECs and subsequent mobilization, proliferation and sprout formation [63]. FAK integrates angiogenic signals from vascular endothelial growth factor receptors (VEGFRs) and integrin receptors, and directs the migration and growth of endothelial cells

to promote angiogenesis [88]. The requirement of FAK in angiogenesis was initially suggested by early observations of restricted patterns of enriched FAK expression in the embryonic vasculature and the embryonic lethality conferred upon FAK gene ablation in mice, which is due to cardiovascular defects [89]. VEGF-induced FAK activation promotes rapid localization of FAK to endothelial adherens junctions and binding of FAK to vascular endothelial (VE)-cadherin via its FERM domain and FAK-mediated phosphorylation of  $\beta$ -catenin. This subsequently induces  $\beta$ -catenin/VE-cadherin dissociation and increased junctional breakdown. In the context of cancer, the angiogenic function of FAK was demonstrated using EC-specific FAK-null melanoma- or lung-carcinoma bearing mice, which exhibit suppressed VEGF-mediated tumor angiogenesis and growth [90]. Additionally, elevated FAK expression was observed in the vascular and tumor cell compartments of invasive breast cancer specimens [91]. A key mechanism underpinning the pro-angiogenic role of tumoral FAK is induction of VEGF expression. Inhibition of FAK catalytic activity in breast carcinoma cells by stable expression of FRNK reduces FAK Y925 phosphorylation, the ability of the Grb2 adaptor protein to bind to FAK, as well as Erk2 activation [92]. The concomitant impairment of FAK–Grb2–Erk2 signaling results in decreased VEGF expression *in vitro* and *in vivo* together with small avascular tumors in mice without affecting cell survival or proliferation *in vitro* [92]. Reconstitution experiments with a FAK Y925F or impaired kinase activity mutants in Src-transformed FAK-null fibroblasts confirmed the role of this FAK phosphorylation site and catalytic activity in regulating VEGF-associated angiogenesis. Suppression of FAK expression in neuroblastoma, breast and prostate carcinoma cells also results in reduced VEGF expression [72]. Overall, these findings indicate that FAK can play contrasting roles within cancer cells and the surrounding tumor microenvironment, and highlight novel rationales for therapeutic targeting of FAK.

### ***1.15 Novel strategies targeting FAK with pharmacological inhibitors***

FAK has long been considered as a potential target for cancer therapeutics, reflecting its pivotal role in governing malignant characteristics and the evidence of its high expression and activity in both preclinical tumor models and human cancers. A number of inhibitory approaches were initially employed to functionally interrogate the oncogenic role of FAK. These include antisense oligonucleotide, siRNA- and shRNA-based abrogation of FAK expression), and overexpression of FRNK [93-95]. Attenuation of FAK signaling through these approaches led to decreased cell viability by induction of apoptosis, as well as impaired migratory and angiogenic capacity of cancer cells *in vitro* and *in vivo*, and provided proof-of-principle for the development of more clinically relevant pharmacologic approaches such as small molecule inhibitors. Over the past decade, a number of preclinical and clinical studies have employed a variety of pharmacologic agents with different mechanisms for the blockade of FAK signaling in cancer (**Fig. 1.15.1**). Of these, several orally bioavailable ATP-competitive FAK inhibitors have entered early clinical testing. FAK small molecule inhibitors can be divided into two main groups: the first group includes inhibitors

targeting enzymatic or kinase-dependent functions of FAK, such as inhibitors targeting the ATP-binding site domain and allosteric inhibitors that target other sites of FAK yet still block kinase activity, and the second group includes inhibitors that target the scaffolding function of FAK [96].

Name	Alt. Name	Type	Specificity	Phase	Trial#	Reference
GSK2266998		N.A.	N.A.	I	NCT01938443, NCT01138033, NCT00996671	N.A.
NVP-TAC544		KI	FAK	PC	none	(24)
PF 573,228	PF-228	KI	FAK	PC	none	(120)
TAE226	NVP-226	KI	FAK/Pyk2	PC	none	(119)
VS-4718	PND-1186	KI	N.A.	I	NCT01849744	(122)
VS-6062	PF 562,271 PF-271	KI	FAK/Pyk2	I	NCT00666926	(121)(132)
VS-6063	PF-04554878 defactinib	KI	N.A.	I/II, II	NCT01951690, NCT00787033, NCT01943292, NCT02004028, NCT01778803	(65)(132)
1H-Pyrrolo[2,3-b]pyridine		aKI	N.A.	PC	none	(128)
Compound 1 and 2		aKI	N.A.	PC	none	(127)
Y15	Compound 14	aKI	FAK	PC	none	(130)
C4	chloropyramine hydrochloride	SI	N.A.	PC	none	(130)
R2	Rosins	SI	N.A.	PC	none	(131)
Y11		SI	FAK	PC	none	(129)

**Figure 1.15.1:** Anti-cancer compound targeting FAK

- **Small molecule ATP-competitive kinase inhibitors:** small molecules inhibitors that bind within the active site of kinases compete with relatively high levels of ATP present in cells. These inhibitors are designed to make binding interactions with residues surrounding the ATP binding pocket of kinases and the advantage of this approach is that it blocks the FAK enzymatic activity with high efficiency. The best characterized cellular-active and selective nanomolar affinity FAK inhibitors are comprised of pyrimidine (*TAE-226*, *PF 573,228*, *PF 562,271*) or pyridine (*VS-4718*) ATP site hinge binders [97-99].
  - *TAE-226* effectively inhibited *in vitro* kinase activity of recombinant FAK with an IC<sub>50</sub> of 5.5 nM, caused apoptosis and decreased tumor growth in glioma and ovarian cancer xenograft models *in vivo* [100]. TAE226 not only caused tumor regression, but also affected tumor microenvironment, blocked production of VEGF and reduced micro vessel density [100]. TAE-226 also was shown to inhibit IGFR-1 at 120 nM [101]. Since FAK and IGFR-1 were shown to interact and increase cancer cell survival [102], their dual targeting with TAE-226 inhibitor can be very effective. In fact, TAE226 inhibited pancreatic cell growth and decreased phosphorylation of ERK and AKT as well [102];
  - *PF-573,228* is the mother compound for the derivative FAK-directed drugs (*VS-6062* and *VS6063*) that are currently being evaluated by Verastem. PF-573,228 exhibits an IC<sub>50</sub> value of 4 nM, and inhibits cell migration by blocking focal adhesion turnover, but has no effect on cell growth or survival in fibroblast or prostate cancer cell lines [103]. Despite its potent efficacy in FAK inhibition, PF-573,228 showed limited anticancer effects possibly due to the compensatory role of the FAK homologue namely Pyk2 [104]. There is no report that further evaluates this compound in the pre-clinical or clinical settings.
  - *PF-562,271* effectively inhibited *in vitro* FAK activity with an IC<sub>50</sub> of 1.5 nM, and also inhibited Pyk2 kinase activity (IC<sub>50</sub>=13 nM) [98]. Since Pyk2 was shown to compensate for FAK functions in angiogenesis, metastasis and tumorigenicity in FAK-deficient cells [105], dual-targeting of FAK and Pyk-2 is beneficial for effective therapy. PF-562,271 effectively decreased tumor growth in many xenograft

models [98], and also it inhibited pancreatic tumor growth, invasion and metastasis in an orthotopic murine model [106]. This inhibitor blocked not only tumor growth and proliferation, and also inhibited pancreatic tumor microenvironment components such as tumor associated fibroblasts and macrophages [106].

- *VS-4718* is the newest FAK inhibitor acquired by Verastem. *VS-4718* is a potent reversible inhibitor of FAK, exhibiting an IC<sub>50</sub> of 1.5 nM, and is able to induce a robust FAK inhibition in cultured breast carcinoma cells at a concentration of 0.1 μM [99]. An initial preclinical study indicated that *VS-4718* showed limited effects on cell proliferation in adherent cancer cells, whereas it induced marked inhibition of FAK and p130Cas phosphorylation in cells grown in suspension or as spheroids, resulting in caspase-3 activation and apoptosis [99]. Additionally, *VS-4718* exerted anti-tumor and anti-metastatic effects in orthotopic breast and ovarian carcinoma mouse tumor models (4T1 and MDA-MB-231) without conferring animal morbidity, death or weight loss [99]. The efficacy of *VS-4718* was demonstrated by a marked reduction in both sub-cutaneous tumor growth of breast carcinoma cells and their metastasis to lungs that was accompanied by inhibition of FAK Y397 and p130Cas phosphorylation and elevated caspase-mediated apoptosis [99]. *VS-4718* inhibitor is currently in clinical trials in subjects with metastatic non-hematologic malignancies (phase I clinical trial # NCT01849744, <http://www.clinicaltrials.gov>).

Another important approach is to target the FAK autophosphorylation site, which was reported recently with allosteric FAK inhibitor 14 or compound Y15 to block tumor growth [107-108]. The inhibitor effectively inhibited FAK autophosphorylation activity at 25 nM-1 μM, did not inhibit Pyk-2, EGFR, Src, IGFR-1 and other enzymes *in vitro* and decreased tumor growth *in vivo* at 30 mg/kg by intraperitoneal delivery or at 120 mg/kg by oral delivery using breast, pancreatic, neuroblastoma, glioblastoma and colon cancer xenograft mice models. The inhibitor caused apoptosis and decreased proliferation in xenograft tumors *in vivo*. The advantage of this approach is the high specificity of targeting Y397, the main autophosphorylation site of FAK. This inhibitor also decreased Y418-phosphorylation of down-stream Src in colon cancer cells [108], which can be also beneficial for development of future therapies. FAK has additional functions independent of its autophosphorylation activity or kinase activity [109], which is evident from the different phenotypes of FAK<sup>-/-</sup> cells and cells with deleted Y397 site [110], or with knock-in point mutation (lysine 454 to arginine) [109], which is important for future therapeutic design of the enzymatic inhibitors. Takeda also developed non-ATP-competitive FAK allosteric inhibitors that efficiently decreased FAK functions [111]. The Takeda identified tricyclic sulfonamides (compound 1 and compound 2) that targeted a novel allosteric site in the C-lobe of the FAK-kinase domain, caused conformational changes of the kinase domain and induced disruption of ATP pocket formation and inhibition of FAK kinase activity with an IC<sub>50</sub> of 4.2 and 8.7 μM, respectively [111]. The compounds required pre-incubation of kinase with inhibitor to cause allosteric ATP-non competitive inhibition. Both allosteric inhibitors were highly selective among 288 kinases, with only 10 kinases other than FAK inhibited by >50% and Pyk-2 inhibited by 25%. The compound 2 was more selective

than compound 1, as it did not inhibit 10 kinases >50% and did not inhibit Pyk-2 at 10  $\mu$ M. This approach reveals novel allosteric and selective way of FAK inhibition. The *in vivo* studies in xenograft mice models need to demonstrate efficacy on these allosteric inhibitors.

- ***Inhibitors targeting FAK scaffold:*** FAK also signals via non-kinase scaffold functions that cannot be affected using conventional small molecule FAK inhibitors. Since FAK has so many binding partners such as Src, EGFR, Her-2, c-Met, PI-3K, disruption of these complexes is an additional therapeutic approach to disrupt signals that FAK integrates and effectively block FAK regulated functions. A small number of compounds developed by CureFAKtor Pharmaceutical are currently undergoing pre-clinical testing. In particular, a compound known as C4 disrupts FAK and VEGFR4 interactions [112], whereas the M13 compound blocks FAK and Mdm-2 interaction [113]. Other inhibitors of FAK-scaffold functions include INT2-31 that blocks FAK and c-Met/IGFR1 interactions [114] and R2 which targets the FAK-p53 interaction [115]. All of these inhibitors effectively reduce cell viability and tumor growth through inhibiting angiogenesis and Akt signaling, or by activating p53 signaling with a resulting enhanced expression of downstream targets of p53 such as p21 and Bax. Also, the inhibitors targeting FAK scaffolding function displayed efficacy at submicromolar and low micromolar doses *in vitro* and at 15–60 mg/kg *in vivo* in mice xenograft models. Since there are other many important scaffolding partners of FAK, disrupting FAK-protein interactions based on structural studies is a very perspective approach and will show the efficacy of this approach in future.

## **Aim of the study**

On the basis of the aforementioned findings highlighting the potential involvement of FAK in the development of certain tumors, the present study aimed to address the role of FAK toward the progression of UM in a *GNAQ*-dependent manner. In particular, our investigation focused on the mechanisms by which *Gaq* may activate FAK and the identification of the effectors determining the biological function of the *Gaq*-FAK transduction signaling. Next, the benefit of FAK inhibition in UM was ascertained both *in vitro* and *in vivo* using CRISPR/Cas9 genome editing as well as specific inhibitors that are currently under advanced clinical evaluation.

## Chapter 2

### *Materials and methods*

**2.1 Cell lines, culture procedures, and chemicals:** HEK293 DREADD/Gq cells were cultured in DMEM (Invitrogen, CA) containing 10% FBS (Sigma-Aldrich Inc., MO) and 1× antibiotic/antimycotic solution (Sigma-Aldrich Inc., MO). OMM1.3 and Mel270 Uveal Melanoma cells have been described elsewhere [116]. All cell lines were grown in a 37°C incubator with 5% CO<sub>2</sub> and underwent to mycoplasma contamination by using Mycoplasma Detection Kit (Roche) prior to the described experiments. Y-27632 (Tocris Cookson Inc., MO) (10µM), PKC inhibitor (Tocris Cookson Inc., MO) (10µM), Blebbistatin (Tocris Cookson Inc., MO) (100nM), VS-4718/PND-1186 (Selleckchem, CA) (1µM) and PF-562271 (Selleckchem, CA) (1µM) were dissolved in DMSO and were used to treat HEK293 DREADD/Gq cells and uveal melanoma cells for different time points before to perform the experiments.

**2.2 Mutational analysis:** bioinformatic whole-genome sequencing of UM samples ( $n=80$ ) derived from The Cancer Genome Atlas (TCGA) ([www.cbioportal.org](http://www.cbioportal.org)). mRNA expression z-Scores (RNA seq V2 RSEM) selected was  $\pm 1.5$ .

**2.3 Immunoblot analysis:** cells were lysed in RIPA buffer containing Halt protease and phosphatase inhibitor cocktail (Thermo Scientific, Rockford, IL). Protein concentration was measured by Bio-Rad Protein Assay (Bio-Rad, Hercules, CA). Equal amounts of total proteins were subjected to SDS-polyacrylamide gel electrophoresis and transferred to PVDF membranes. Membranes were blocked with 5% non-fat dry milk in T-TBS buffer (50 Mm Tris/HCL, pH 7.5, 0.15 M NaCl, 0.1% [v/v] Tween-20) for 1 hour at room temperature, and then incubated with primary antibodies in blocking buffer at 4°C overnight. Primary antibodies were diluted 1:1000 unless otherwise stated. (anti-Gαq (E-17; Santa Cruz Biotech., CA), anti-RhoA (C-18; Santa Cruz Biotech., CA), anti-Rac1 (BD Biosciences, CA), anti-Trio (H120; Santa Cruz Biotech., CA), anti-GAPDH (14C10; Cell Signaling Technology, MA), anti-FAK (Cell Signaling Technology, MA), anti-pFAK (Y397) (Cell Signaling Technology, MA), anti-pY (Santa Cruz Biotech., CA), anti-AKT (Cell Signaling Technology, MA), anti-pAKT (S473) (Cell Signaling Technology, MA), anti-ERK1/2 (Cell Signaling Technology, MA), anti-pERK<sup>42/44</sup> (Cell Signaling Technology, MA), anti-S6 (Cell Signaling Technology, MA), anti-pS6 (Cell Signaling Technology, MA), anti-α-Tubulin (Cell Signaling Technology, MA). Detection was conducted by incubating the membranes with horseradish peroxidase-conjugated goat anti-rabbit and anti-mouse IgG secondary antibodies (Southern Biotech, Birmingham, AL) that were used at a dilution of 1:50,000 in 5% milk-T-TBS buffer at room temperature for 1 hour, and visualized with Immobilon Western Chemiluminescent HRP Substrate (Millipore, Billerica, MA).

**2.4 Immunoprecipitation assay:** cells were lysed with lysis buffer [10mM Tris-Cl (pH 8.0), 150mM NaCl, 1mM EDTA, 0.3% CHAPS, 50mM NaF, 1.5mM Na<sub>3</sub>VO<sub>4</sub>, protease inhibitor (Thermo Scientific, CO), 1mM DTT and 1mM PMSF], and centrifuged at 16,000 rpm for 10 min at 4°C. Supernatants were incubated with primary antibody for 2h at 4°C, and protein G or protein A conjugated resin for another 1 hour. Resins were then washed 3 times with lysis buffer and boiled in SDS-loading buffer.

**2.5 siRNA transfection:** all human siRNA sequences and providers are described in the following table. All the cells were transfected when 40% confluent using Lipofectamine RNAiMAX Reagent (Invitrogen, CA) according to manufacturer's instructions, using 50nM of each siRNA, and experiments were performed, when the cells were confluent. Detail of RNAi and oligonucleotide sequences used in this study:

siRNA	Source	Homology	Details
siRNA Control	Thermo Scientific	-	SIC001
Hs_GNAQ	Thermo Scientific (Smart Pool)	Homo Sapiens	Human (GNAQ 2776)
Hs Trio	Thermo Scientific (Smart Pool)	Homo Sapiens	Human (TRIO 7204)
Hs_RhoA	Thermo Scientific (Smart Pool)	Homo Sapiens	Human (RhoA 387)
Hs_Rac1	Thermo Scientific (Smart Pool)	Homo Sapiens	Human (RAC1 5879)
Hs_PTK2	Thermo Scientific (Smart Pool)	Homo Sapiens	Human (PTK2 5747)

**2.6 Cell proliferation analysis:** Alamar Blue Cell Viability Reagent was purchased from Life Technologies (Grand Island, NY). In brief, OMM1.3 and MEL270 UM cell lines were cultured in 96-well plates and then treated with VS4718 and PF-562271 for 72 hours. The manufacturer's instructions were followed to complete the assay.

**2.7 Focal adhesion assay:** cells cultured on fibronectin-coated coverslips were washed three times with PBS, were fixed with 3.7% formaldehyde in phosphate-buffered saline (PBS) for 30 minutes, and permeabilized using 0.05% Triton X-100 for 10 minutes. Cells were blocked with 3% FBS-containing PBS for 30 min, and incubated with anti-pFAK (Y397) (Cell Signaling Technology, MA) and anti-paxillin (Cell Signaling Technology, MA) (in 3% FBS-PBS otherwise stated) for 1 hour at room temperature. The reaction was visualized with Alexa-labeled secondary antibodies (Invitrogen, CA) and using also Alexa Fluor 488 Phalloidin (Invitrogen, CA). Cells were incubated in PBS buffer containing Hoechst 33342 (Molecular Probes, OR) for nuclear staining. Images were acquired with an Axio Imager Z1 microscope equipped with ApoTome system controlled by ZEN 2012 software (Carl Zeiss, NY).

**2.8 Methylcellulose growth assay:**  $5 \times 10^3$  uveal melanoma cells were embedded in 1% methylcellulose (R&D HSC001) diluted in growth media and plated onto 6-well-poly-hydroxyethyl methacrylic acid (poly-HEMA) – coated plates (Costar). At the indicated time, colonies were imaged in phase contrast, and

enumerated by counting five different fields of each well. All experimental points were performed in triplicate and repeated at least two times.

**2.9 Genetic editing with CRISPR/Cas9:** OMM1.3 and MEL20 UM cells were infected with a specific FAK-sgRNA (# AATACTCGCTCCATTGCACC) cloned into a CRISPR/Cas9 All-in-One Lentivector. After ~1 week of puromycin-selection, we selected several single clones and assessed FAK editing by direct sequencing and by lack of FAK protein through western blot analysis. MEL270 FAK KO generated by CRISPR/Cas9 genome editing were also injected in female NOD.Cg-Prkdc<sup>scid</sup> Il2rgt<sup>m1wjl</sup>/SzJ mice (commonly known as NOD *scid* gamma, Jackson Laboratory, Maine).

**2.10 In vivo mice experiments and VS4718 treatment:** female NOD.Cg-Prkdc<sup>scid</sup> Il2rgt<sup>m1wjl</sup>/SzJ mice (commonly known as NOD *scid* gamma, Jackson Laboratory, Maine), 5 to 6 weeks of age and weighing 18 to 20g, were used to evaluate the potential clinical benefit of targeting FAK by using VS4718 and by CRISPR/Cas9 genetic approach, housed in appropriate sterile filter-capped cages, and provided food and water ad libitum. Briefly, exponentially growing cultures were harvested, washed, resuspended in RPMI 1640, and  $1.5 \times 10^6$  viable cells were transplanted subcutaneously into the flanks of the mice. To administer VS4718, an appropriate amount of VS4718 was added to the vehicle prepared with 0.5% carboxymethyl cellulose (CMC) (C5678, Sigma-Aldrich; St. Louis, MO) and 0.1% Tween 80 (P1754, Sigma Aldrich; St. Louis, MO) in sterile water, to make 100 mg/ml stock. The formulation was mixed with constant gentle stirring and sonicated for 5-10 minutes to make a uniform suspension. The VS4718 suspension was administered via oral gavage twice daily at a dose of 100 mg/kg. For tumor growth analysis, tumor volume was assessed as  $[(LW^2)/2]$ ; where L and W represent the length and the width of the tumor]. The animals were monitored twice weekly for tumor development. Results of animal experiments were expressed as mean  $\pm$  SEM of a total of 6 tumors analyzed. All the mice studies were carried out according to National Institutes of Health (NIH) approved protocols (ASP #13-695) in compliance with the NIH Guide for the Care and Use of Laboratory Mice.

**2.11 Data and statistical analysis:** data were analyzed using GraphPad Prism version 6 (GraphPad Software, San Diego, CA). Comparisons between experimental groups were made using unpaired t test.  $P < 0.05$  was considered to be statistically significant.

## Chapter 3

### Results

#### 3.1 PTK2 gene is overexpressed in Uveal Melanoma

It has been well established that FAK is overexpressed in various types of solid and non-solid tumors to mediate survival and other important functions [117-119]. A potential link between FAK and cancer was first reported over twenty years ago in a study that identified elevated levels of FAK transcripts in various tumor contexts [53]. Similarly, a number of subsequent evidences reported up-regulation of FAK in a wide range of malignancies including ovarian, cervical, kidney, lung, pancreatic, brain, colon, breast, and skin cancer [80]. In addition, several studies have confirmed a correlation between FAK overexpression levels and poorer clinical prognosis in different types of human tumors [120]. Here, we focused on uveal melanoma (UM), a type of cancer harboring only a handful of mutations as compared to hundreds in other cancers. We started our study from the analysis of the possible drug targets that lead to selective death or growth suppression specifically in Gαq-activated tumors. In a preliminary analysis performed to this end in collaboration with the Ruppin's Laboratory (UCLA), we started with a set of genes that can be targeted by approved and experimental drugs (N=756) [121]. By comparing the TCGA UM dataset (N=80) with skin melanoma samples that do not harbor GNAQ genomic alterations (N=209) as control, we first identified the genes that are highly overexpressed in UM. We validated this approach by confirming that the genes over- and under-expressed in UM and *GNAQ*-altered skin melanomas are highly overlapping (hyper-geometric  $p < 1E-198$  and  $p < 1E-232$ , respectively). Next, we filtered the genes for those whose inactivation leads to better patient survival in UM based on TCGA survival data, and finally we used large datasets of gene essentiality [122-124], and drug response screenings [122-126] in cancer cells to identify genes that are predicted to reduce cell viability when targeted in *GNAQ*-expressing tumors. In accordance with the aforementioned observations, we summarized the 5 top predicted drug targets emerging from our computational screening pipeline (**Fig.3.1A**). Among them, based on all the three steps described above, the top predicted gene target resulted PTK2, suggesting the potential benefit of targeting the PTK2 gene product (a non-receptor tyrosine kinase known as FAK) in *GNAQ*-induced tumors. Also, in order to identify novel genetic alterations correlated with oncogenic drivers in UM, we curated whole-genome sequencing data for 80 UM samples derived from The Cancer Genome Atlas (TCGA). The analysis of UM genomic alterations revealed that the gene encoding for FAK (PTK2) is amplified or overexpressed in 56% of UM lesions (**Fig.3.1B**) even without the amplification of MYC proto-oncogene located close the PTK2 locus, suggesting that UM represents the human cancer harboring the highest level of FAK overexpression (**Fig.3.1C**). Furthermore, we found that the patients with high PTK2 expression (red) show poorer survival than the patients with low PTK2 expression (blue) (Fig. 1), align with its potential biological role in UM (**Fig.3.1D**). These findings implicate FAK as a novel uveal melanoma up-regulated gene and highlight its critical role in UM pathogenesis.

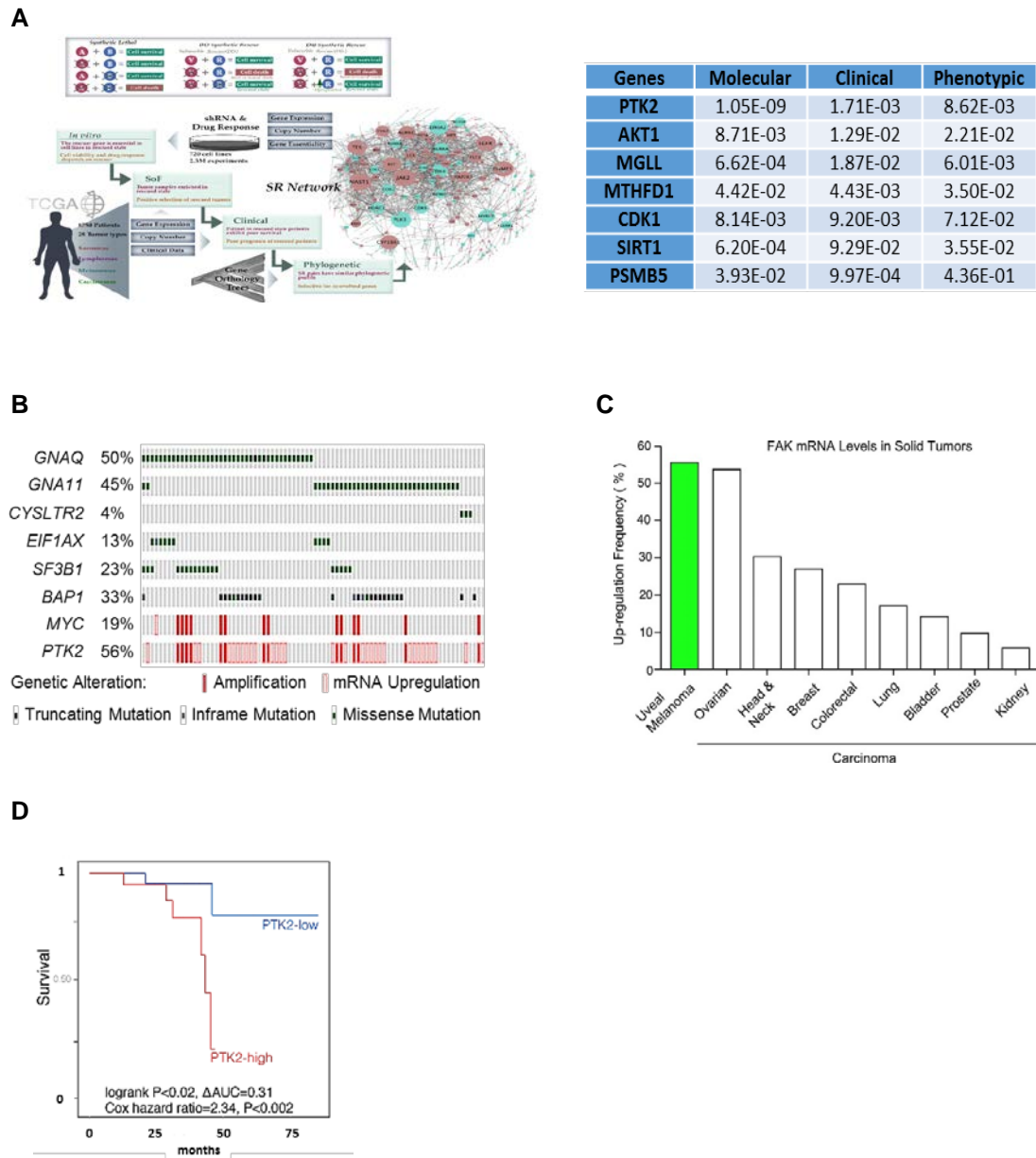


**Fig. 3.1 PTK2 gene is overexpressed in UM.** (A) Potential target genes and their molecular, clinical phenotypic significance values. The genes are listed based on their combined significance identified by combined ranking of their significance (molecular: genes are up-regulated in UM based on TCGA gene expression data; clinical: down-regulation of the gene leads to better prognosis in TCGA UM survival data; phenotypic: inactivation of the gene in GNAQ-altered contexts leads to a reduced cell growth, based on shRNA knockdown or drug inhibition screens); (B) Genetic alteration of UM from cBioPortal analysis of UM patients (N=80); (C) Percent of tumor samples with elevated FAK Mrna; (D) UM patients with high PTK2 expression (top 40-percentile, N=32; red) shows poorer survival than the patients with low PTK2 expression (bottom 40-percentile, N=32; blue), (data from UM TCGA).

### 3.2 GNAQ activates FAK in UM cancer cells

FAK is a cytoplasmatic tyrosine kinase that modulates cell growth, survival and movement, with phosphorylation at position Y397 representing a common marker of FAK activation [63]. As the phosphorylation of many proteins has been largely involved in cancer [127-128], we first investigated whether *GNAQ* and its coupled GPCRs trigger multiple tyrosine phosphorylation sites. As model system, we used HEK293 cells expressing a synthetic GPCRs linked to Gq, also known as DREADD (designer receptors exclusively activated by a designer drug) which is activated by the pharmacologically inert compound namely clozapine-N-oxide (CNO) [129]. Whortly, we observed that CNO induced a rapid tyrosine phosphorylation of diverse cellular proteins, as evaluated by using different anti-pY antibodies. Tyrosine phosphorylation started upon only 2 minutes agonist addition and increase up to 1h of treatment (**Fig. 3.2A**). In accordance with other previous studies showing the induction of tyrosine phosphorylation by agonist-activated-GPCRs [130-131], our previous investigation has demonstrated that fully transforming GPCRs may mediate tyrosine phosphorylation of a set of cellular proteins, including p125<sup>FAK</sup> and the p130 v-*src* substrate [132]. Performing western blotting analysis and phospho-tyrosine immunoprecipitations of lysates obtained by HEK293 DREADD/Gq cells treated with CNO, we observed a remarkable activation of FAK (**Fig. 3.2B-C**). On the basis of these findings, it can be argued that *GNAQ* activating circuitry may lead to tyrosine phosphorylation of diverse cellular proteins such as p125<sup>FAK</sup>. Next, we asked whether FAK is activated in UM cells expressing the *GNAQ* oncogene. Of note, *GNAQ* silencing prevented FAK phosphorylation in OMM1.3 UM cells (**Fig. 3.2D**), providing a multifaceted regulation of FAK activity in UM cells harboring *GNAQ* mutation.

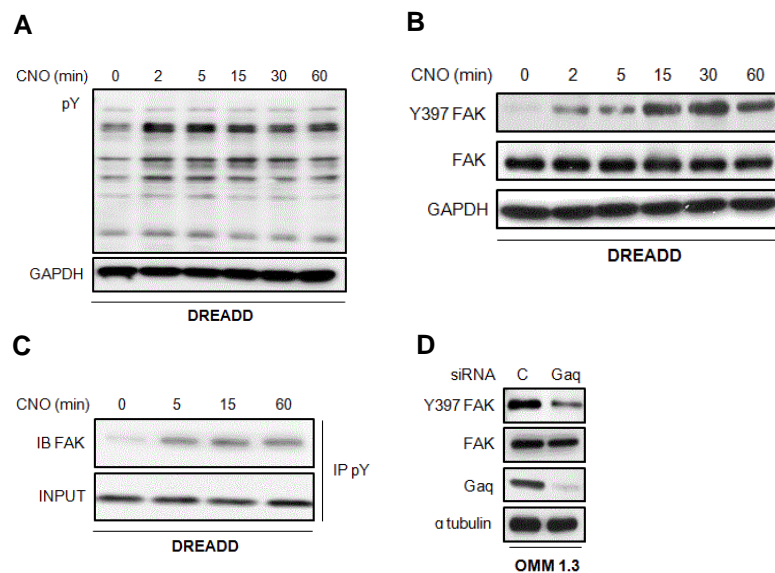


**Fig. 3.2 GNAQ activates FAK in UM cancer cells.** (A) Western blot analysis of time-dependent pY phosphorylation in HEK293 DREADD/Gq cells treated with Clozapine N-oxide (CNO). (B) Western blot analysis of time-dependent FAK Y397 phosphorylation in HEK293 DREADD/Gq cells treated with CNO. (C) Anti-pY immunoprecipitates from HEK293 DREADD/Gq cells treated with CNO for the indicated times and then analyzed for FAK protein expression (D) Western blot analysis of FAK Y397 phosphorylation in OMM1.3 UM cells transfected with siRNA Control and siRNA Gaq.  $\alpha$ -tubulin serves as a loading control.

So far, it is not clearly understood which of the multiple Gαq-initiated pathways regulates and activates FAK and how the interplay between FAK and GNAQ-mediated signaling contributes to the transduction of proliferative prompts. For instance, the activation of PKC is one of the best-known downstream target activated by Gαq [133]. Using a PKC inhibitor (PKCi), we observed that the phosphorylation of FAK by Gαq was still evident in both HEK293 DREADD/Gq cells and in OMM1.3 UM cells (**Fig. 3.2E-F**), suggesting that the activation of FAK may occur in a PKC- independent manner. Recently, a genome wide dsRNA screen in drosophila cells has revealed that Trio, which is a guanine nucleotide exchange factor, may be involved in the transduction of many signals mediated by Gαq through the activation of Rho-GTPases and their associated signaling circuitries [134]. These findings prompted us to investigate whether Trio and its regulated GTPase, like RhoA and Rac1, may participate to FAK phosphorylation mediated by Gαq signaling pathway. As evaluated by western blot assays, we observed that the knock down of RhoA and Trio prevented FAK activation in HEK293 DREADD/Gq cells upon stimulation with CNO, while the knock down of RAC1 did not affect the activation of FAK (**Fig. 3.2G-I**). Also, the silencing of RhoA prevented the phosphorylation of FAK in OMM1.3 UM cells (**Fig. 3.2J**). Taken together, these results suggest that Gαq signals through Trio and RhoA leading to the phosphorylation of FAK without the PKC involvement.

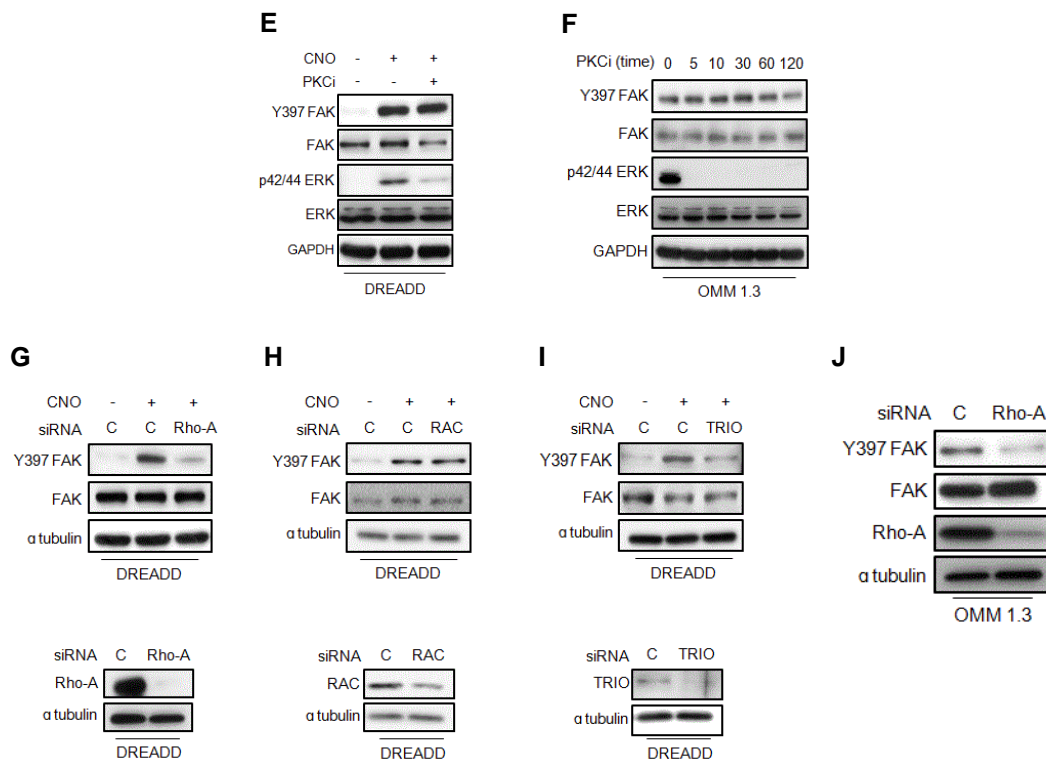


**Fig. 3.2 GNAQ activates FAK in uveal melanoma cancer cells.** (E) FAK Y397 phosphorylation and p42/44 ERK in HEK293 DREADD/Gαq cells treated with a specific PKC inhibitor (PKCi) and then stimulated with CNO. (F) FAK Y397 phosphorylation and p42/44 ERK in OMM1.3 cells treated with a PKCi for the indicated times. (G) FAK Y397 phosphorylation in HEK293 DREADD/Gαq cells transfected with siRNA Rho-A and stimulated with CNO. α-tubulin serves as a loading control. (H) FAK Y397 phosphorylation in HEK293 DREADD/Gαq cells transfected with siRNA RAC and stimulated with CNO. α-tubulin serves as a loading control. (I) FAK Y397 phosphorylation in HEK293 DREADD/Gαq cells transfected with siRNA TRIO and treated with CNO. α-tubulin serves as a loading control. (J) FAK Y397 phosphorylation in OMM1.3 cells transfected with siRNA Rho-A. α-tubulin serves as a loading control.

Several studies have demonstrated that FAK is linked to focal adhesion formation and turnover through the binding to guanine nucleotide exchange factor (GEF) and then the dynamic rearrangement of the actin cytoskeleton [59-60, 70, 82]. In order to provide novel evidence on the role of activated FAK in stress fiber polymerization and contraction, we used the ROCK inhibitor Y-27632 and the selective myosin II inhibitor namely blebbistatin. Both compounds, decreased FAK phosphorylation in HEK293 DREADD/Gq and in OMM1.3 uveal melanoma cells (**Fig. 3.2K-N**). Next, the focal adhesion formation observed upon CNO stimulation in HEK293 DREADD/Gq cells was repressed inhibiting ROCK and in the presence of blebbistatin (**Fig. 3.2O**). Collectively, these findings demonstrated the importance of RhoA-ROCK-dependent assembly of focal adhesion complexes through the activation of GNAQ signaling pathway.

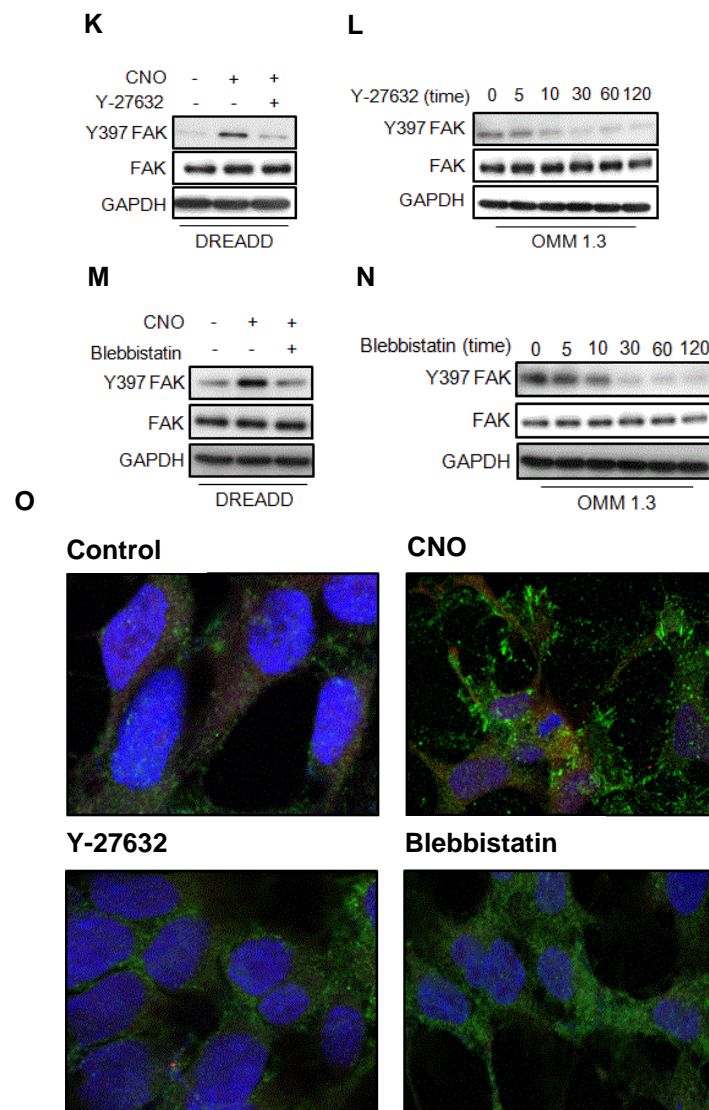


**Fig. 3.2 GNAQ activates FAK in uveal melanoma cancer cells.** (K) Y397 phosphorylation in HEK293 DREADD/Gaq cells treated with ROCK inhibitor Y-27632 and then stimulated with CNO. (L) FAK Y397 phosphorylation in OMM1.3 UM cells treated with Y-27632 for the indicated times. (M) FAK Y397 phosphorylation in HEK293 DREADD/Gaq cells treated with blebbistatin and then stimulated CNO. (N) FAK Y397 phosphorylation in OMM1.3 UM cells treated with blebbistatin for the indicated times. (O) Immunofluorescence assay for FAK Y397 in HEK293 DREADD/Gaq cells treated with Y-27632 or Blebbistatin and CNO. FAK Y397 (green), Hoechst stains nuclear DNA (blue) and paxillin stains F-actin (red).

### 3.3 FAK mediates the proliferation of uveal melanoma cells through the PI3K/AKT/mTOR signaling pathway

Recent evidences have demonstrated the involvement of FAK in tumorigenesis by promoting sustained proliferative and survival signals [107]. Given its apparent role in cancer progression, small molecule FAK inhibitors are emerging as promising chemotherapeutic agents [98-100, 103-104], suggesting that FAK inhibition could be an appropriate approach to targeted cancer treatment. In order to investigate the significance of FAK activation in the biology of UM, we transfected OMM1.3 and MEL270 UM cells with siRNA targeting FAK (siRNA PTK2). FAK silencing led to reduced AKT and S6 phosphorylation in both UM cell lines, without altering ERK activation (**Fig. 3.3A-B**). Furthermore, FAK knock down lowered the proliferation of UM cells (**Fig. 3C**). These results may suggest that FAK activation by *Gaq* triggers the PI3K/AKT/mTOR signaling pathway toward the growth of UM cells.

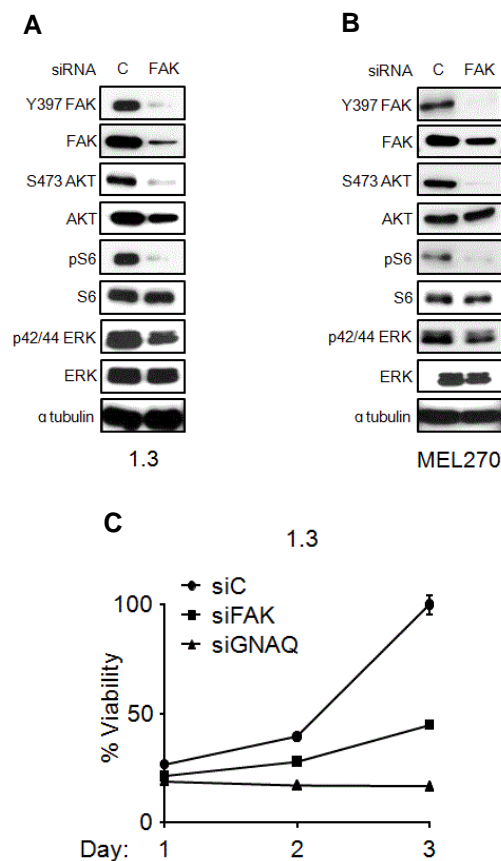


**Fig. 3.3 FAK mediates the proliferation of uveal melanoma cells through the PI3K/AKT/mTOR signaling pathway.** (A) FAK Y397, AKT S473, pS6, p42/44 ERK phosphorylation in OMM1.3 cells transfected with siRNA FAK.  $\alpha$ -tubulin serves as a loading control. (B) FAK Y397, AKT S473, pS6, p42/44 ERK phosphorylation in MEL270 cells transfected with siRNA FAK.  $\alpha$ -tubulin serves as a loading control. (C) Alamar Blue assay performed in OMM1.3 cells transfected with siRNAs FAK or Gaq.

Two ATP-competitive FAK kinase inhibitors, namely VS-4718 (PND-1186) and PF-562271 (**Fig. 3.3D**) are under clinical evaluation for their antitumor activity [98-99]. Therefore, we asked whether these inhibitors may exert inhibitory effects on the proliferation of UM cells. Interestingly, both compounds reduced AKT and S6 phosphorylation without altering ERK activation in both OMM1.3 and MEL270 cells (**Fig. 3.3E-F**). Moreover, both compounds decreased the proliferation of UM cells with an IC<sub>50</sub> around 1 μM (**Fig. 3.3G**). VS-4718 treatment led also to a reduced number of colonies in OMM1.3 cells cultured in 3D matrix (**Fig. 3.3H**). Overall, these results may provide novel insights into FAK inhibition by VS-4718 and PF-562271 toward further therapeutic approach in patients with UM.

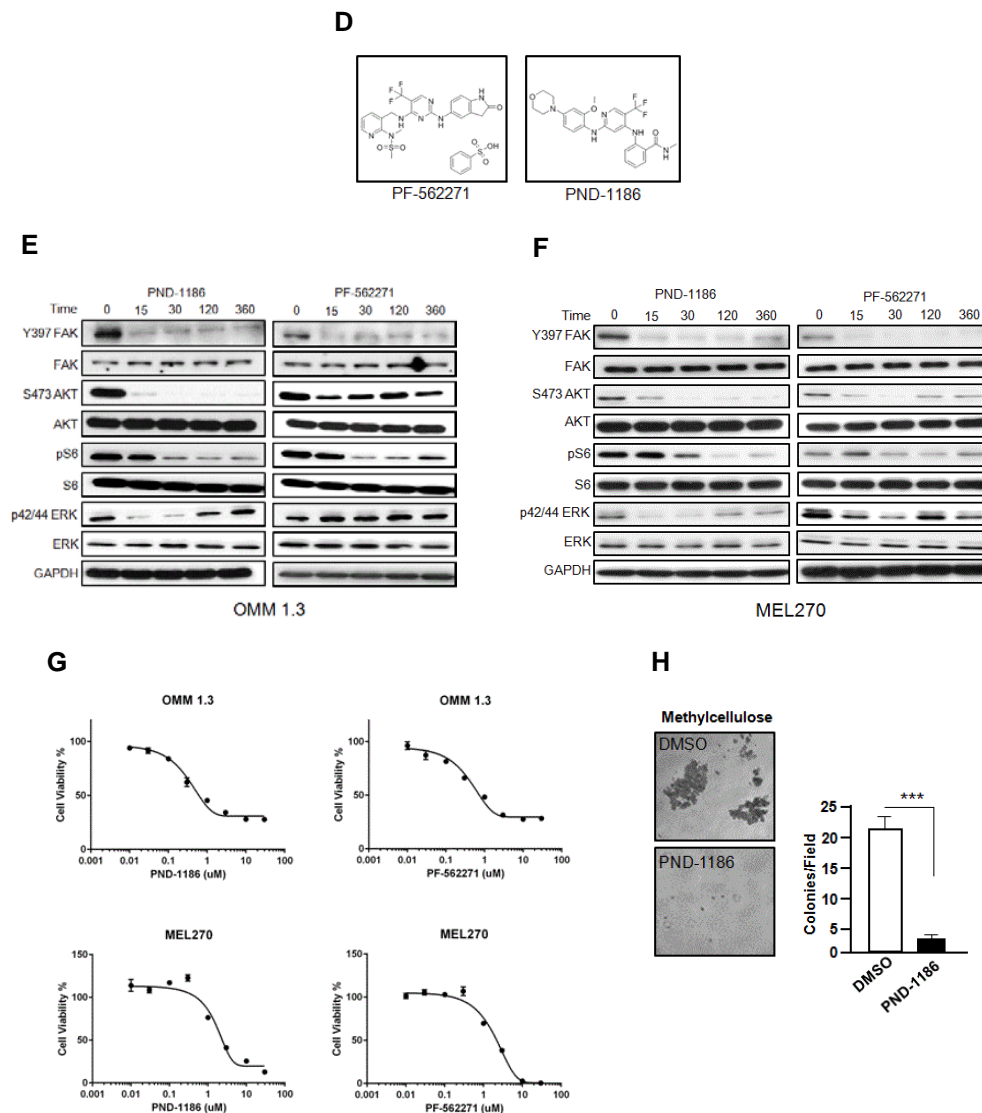


**Fig. 3.3 FAK mediates the proliferation of uveal melanoma cells through the PI3K/AKT/mTOR signaling pathway.** (D) Chemical structure of the FAK inhibitors VS-4718 and PF-562271. (E) FAK Y397, AKT S473, pS6 and p42/44 ERK phosphorylation in OMM1.3 cells treated with 1 μM VS-4718 and μM PF-562271 for the indicated times. (F) FAK Y397, AKT S473, pS6 and p42/44 ERK phosphorylation in MEL270 cells treated with VS-4718 and PF-562271 for the indicated times. (G) Alamar Blue assay performed in OMM1.3 and MEL270 cells after 3 days of treatment with increasing concentrations of VS-4718 and PF-562271. (H) OMM1.3 cells were embedded in 0.1% methylcellulose, vehicle (DMSO) or 1 μM VS-4718 were added and after 10 days the colonies were imaged by phase contrast microscopy.

### 3.4 Targeting FAK in vivo

Previous studies in human xenograft or syngeneic mouse tumor models have associated some FAK small-molecules inhibitors oral administration with the inhibition of breast, liver, prostate, pancreatic, and squamous cell carcinoma tumor growth with a dose-range from 5 to 50 mg/kg and twice-daily administration (BID) has shown greatest efficacy [99-101]. As part of a translational effort, we first investigated the potential therapeutic benefit of targeting FAK in UM *in vivo* by using the specific inhibitor VS-4718 (PND-1186) that is under advanced clinical evaluation. We used as xenograft models female non-obese diabetic/severe combined immunodeficiency (NOD-SCID) gamma (NSG) mice. We inoculated in their flank UM cells and allowed to grow until they reach a volume of 200 mm<sup>3</sup>, at which time they were randomized into the corresponding treatment and control arms. We treated the mice twice daily with VS-4718 (100 mg/kg via oral gavage) and finally we assessed the tumor volume thrice weekly by Vernier caliper, as we described previously [134-135]. At different experimental days, mice were euthanized and we found that VS-4718 treated mice showed significantly smaller primary tumors (or reduced tumor volume) than vehicle-treated control mice (**Fig. 3.4A-D**). Taken together, our results show that VS-4718 inhibits the growth of UM cells *in vivo*.

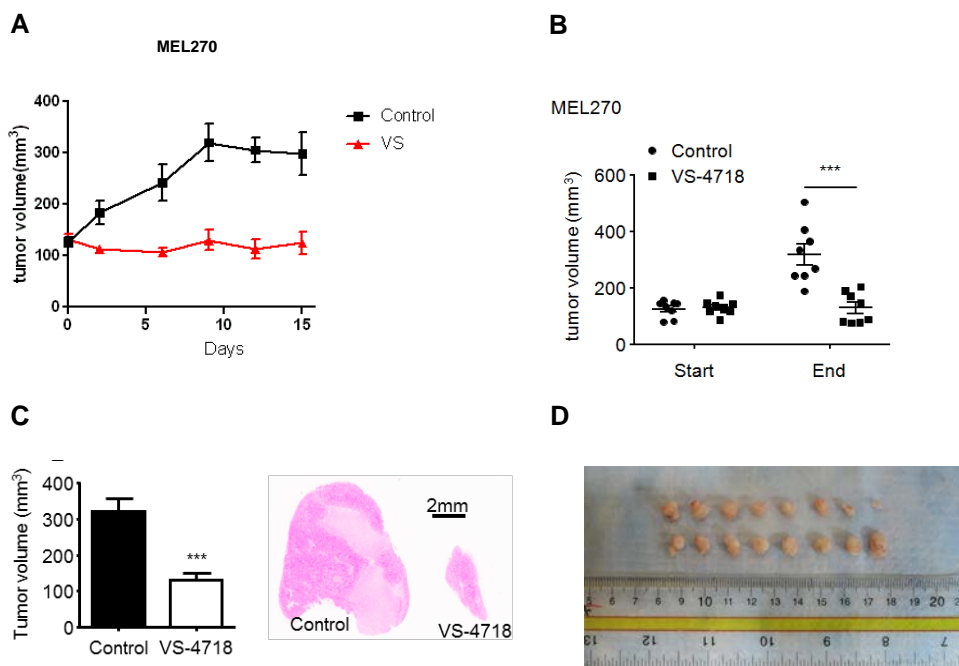


**Fig. 3.4 Targeting FAK in vivo:** (A-B) MEL270 UM cell were injected into both flanks of NOD-SCID mice. Animals were treated with either vehicle or VS-4718 as indicated by oral gavage twice daily for 3 weeks. Tumor size were measured at the indicated time points. Tumor volumes were calculated and blotted. \*\*\* denotes a statistically significant difference ( $p < 0.01$ ) comparing with vehicle-treated group. (C-D) Tumor weights from different groups at the end of experiments (mean  $\pm$  SEM,  $n=8$ ;  $n$ = number of tumors analyzed), and hematoxylin and eosin (H&E)-stained sections of representative tumors from each group are shown.

Next, we used the new CRISPR/Cas9 genome editing technique [136] (**Fig. 3.4E**), to induce the loss of FAK expression both in OMM1.3 and MEL270 UM cells. Firstly, we investigated the system by infecting *in vitro* UM cells with a lentivector (gRNA CRISPR/Cas9 All-in-One Lentivector) containing inside a sequence targeting directly a specific exon nucleotide region located on PTK2 gene locus. After 1 week of cell puromycin-selection, we collected the samples and we found that the genome editing induced the KO of FAK with an high efficiency both in MEL270 and OMM1.3 UM cells (**Fig. 3.4F**). Also, we explored the system to target directly FAK *in vivo*. We inoculated in the flanks of female non-obese diabetic/severe combined immunodeficiency (NOD-SCID) gamma (NSG) mice both MEL270/FAK WT UM cells as control group and MEL270/FAK KO UM cells that we previous generated. We obtained evidence that MEL270 FAK-KO using CRISPR/Cas9 reduced tumor formation compared to MEL270 FAK-WT mice models displaying a remarkable anti-tumor activity (**Fig. 3.4G-H**). Collectively, our findings confirm and extend our previous observations, providing further support to the notion that FAK could be a promising therapeutic target in UM and other GNAQ-driven malignancies and pathological conditions.

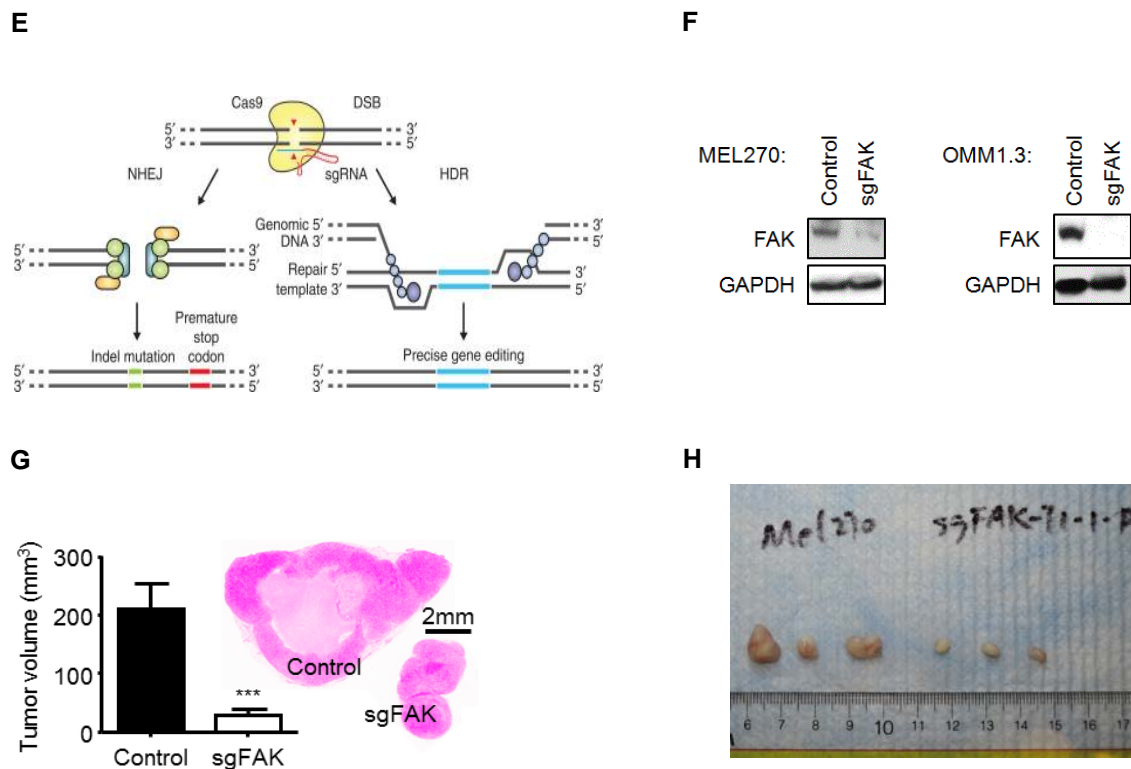


**Fig. 3.4 Targeting FAK *in vivo*:** (E) DSB repair promotes gene editing. DSBs induced by Cas9 (yellow) can be repaired in one of two ways. In the error-prone NHEJ pathway, the ends of a DSB are processed by endogenous DNA repair machinery and rejoined, which can result in random indel mutations at the site of junction. Indel mutations occurring within the coding region of a gene can result in frameshifts and the creation of a premature stop codon, resulting in gene knockout. Alternatively, a repair template in the form of a plasmid or ssODN can be supplied to leverage the HDR pathway, which allows high fidelity and precise editing. (F) Western blot analysis of FAK CRISPR/Cas9-edited in MEL270 and OMM1.3 UM; GAPDH serves as loading control. (G-H) UM tumors (MEL270) formation *in vivo* in cells expressing control sgRNA and FAK KO (sgRNA-FAK). Tumor size at the end of the study was measured (mean  $\pm$  SEM, n=4), hematoxylin and eosin (H&E)-stained sections of representative tumors from each group are shown (middle panel).

## *Chapter 4*

### *Discussion*

Numerous melanomas show oncogenic mutations in signaling components of the MAP kinase pathway, in particular *BRAF* and *NRAS* [137], nevertheless a subset of melanocytic neoplasms does not show these mutations [138]. UM, which arises from melanocytes within the choroidal plexus of the eye, exhibits biologically distinct characteristics from CM including peculiar liver metastasis [30]. In this respect, in the majority of UMs and in a subset of melanomas arising in the skin [31] have been assessed mutations in the  $G\alpha$  subunits named *GNAQ* and *GNA11* as genetic initiating events. On the basis of these findings, we have ascertained that FAK represents a key driver of *GNAQ*-induced tumorigenesis both in UM cells harboring activating *GNAQ/GNA11* mutations and in xenograft models. Furthermore, we have provided evidence that FAK activation may play a role in the functional network between the  $G\alpha_q$  transduction pathway and the tyrosine phosphorylation signaling involved in the UM development. Overall, our novel data may suggest that the inhibition of FAK does represent a suitable pharmacological treatment in UM and other tumors harboring *GNAQ/GNA11* mutations.

FAK is a non-receptor protein tyrosine kinase identified as a critical signaling molecule leading to cell adhesion, invasion, angiogenesis and metastasis through a cooperation with src, integrin and growth factor receptor-mediated transduction pathways [70]. In addition, increased FAK expression and activity have been associated with the progression of various malignancies and a poor prognosis [53]. Few studies have addressed the role of G-proteins in the regulation of FAK activity. GPCRs may induce FAK activation through both Rho-dependent and Rho-independent mechanisms, hence triggering subsequent signaling cascades involved in relevant biological responses [139-140]. In addition, previous investigations have determined that the growth promoting pathways activated by GPCRs might involve the tyrosine phosphorylation of substrates for oncogene-encoded tyrosine kinases [132].

In the present study, we first performed a computational screening pipeline comparing the TCGA UM dataset (n=80) with skin melanomas samples that do not harbor *GNAQ* genomic alterations (n=209), in order to identify genes that are predicted to reduce cell viability when targeted in *GNAQ*-expressing tumors. Interestingly, we found that *PTK2* is the top predicted gene among the major 5 drug targets genes. Accordingly, a further bio-informatic analysis of UM genetic alterations ([www.cbioportal.com](http://www.cbioportal.com)), evidenced that *PTK2* is over-expressed in more than 50% of all UM lesions. Remarkably, patients with high *PTK2* expression showed poor survival rates. Next, to dissect the mechanisms involved in FAK activation by  $G\alpha_q$ , we used as experimental model a cell line named Designer Receptor Exclusively Activated by Designer Drugs (DREADD), which expresses an ectopic GPCR activated solely by the synthetic ligand clozapine-N-oxide (CNO) [129]. We found that CNO induces FAK phosphorylation in a time-dependent manner through a guanine-nucleotide exchange factor namely Trio as well as through the Trio-dependent-Rho GTPase, Rho-

A. These events lead, in turn, to increased stress fiber polymerization and contraction as evaluated by knock down experiments and using specific pharmacological inhibitors.

As FAK exerts a significant role in the survival and proliferation of cancer cells [139], initial efforts were made to inhibit its activity transfecting cells with a dominant negative C-terminal plasmid named FAK-CD and silencing FAK expression by FAK siRNA [80]. In this regard, mammary gland-specific deletion of FAK in mice expressing the polyoma middle T (PyMT) oncogene under control of the MMTV promoter resulted in delayed mammary tumor formation and reduced tumor incidence [77]. Likewise, the deletion of FAK from MMTV-PyMT-transformed mammary epithelial cells *in vitro* led to a decreased proliferation and invasion and an enhanced sensitivity to anoikis [77]. In the current study, we have demonstrated that FAK knock down by FAK siRNA reduces the proliferation of UM cells as observed silencing *GNAQ* expression. Of note, FAK inhibition potentially lowered the PI3K/AKT/mTOR survival pathway, as determined evaluating the phosphorylation of the downstream targets pAKT and pS6, either in OMM1.3 UM primary cells or MEL270 UM cells derived from metastatic lesions. Overall, these results indicate the partial knowledge of Gαq-FAK signaling, including the targets and the compensatory changes of the intracellular transduction network.

Considering that FAK activation plays an important role in tumor progression, several FAK inhibitors (FAKi) have been generated [104]. Accordingly, certain FAK inhibitors have shown the ability to prevent the growth of xenograft tumors [98] as well as the metastasis of diverse tumors [106]. In our study, two different FAKi have been used in order to target UM cells: the FAKi namely PF-562271 and a new generation orally-bioavailable FAKi known as VS-4718. Both agents were able to elicit anti-tumor activity in ovarian cancer models, which is characterized by a high frequency of FAK amplification and overexpression [99]. Both compounds reduced UM cell growth *in vitro* and VS-4718 was able to inhibit UM tumor formation *in vivo*. To further validate the clinical benefit targeting FAK in UM *in vivo*, the silencing of FAK through the novel genetic approach namely CRISPR/Cas9 nearly abolished tumor formation in our xenograft models. Collectively, our findings suggest that FAK may represent a suitable therapeutic target for the treatment of uveal melanoma and other malignancies that originate from function mutations in the *GNAQ* and *GNA11* oncogenes.

### ***Future direction targeting FAK***

Although FAK was first identified over twenty years ago, studies on this multifunctional kinase and scaffold still continue apace providing significant surprises. Major progresses have been achieved during the past few years targeting FAK and the first Phase I trial has been promising. Nevertheless, many questions remain open as the mechanisms involved in FAK up-regulation in the early cancer stages. In this respect, it could be exciting to evaluate the cross-signaling between FAK, WNT, Sonic Hedgehog, Gli and Notch toward further transcription factors and markers involved in the regulation of FAK expression. In addition, as FAK inhibits cancer stem cells through kinase-dependent and independent functions, the dissection of the mechanisms

involved is very important toward the design of future therapies. Likewise, the regimen of FAK inhibitors used alone or in combination treatments, pharmacodynamics and toxicology studies would be important to set in order to propose suitable clinical trials. Targeting FAK scaffold together with FAK enzymatic inhibitors and dissecting their functions may also represent a future translational perspective.

In conclusion, the past twenty years of FAK research answered many questions regarding FAK binding partners, the structure of its major domains and the mechanisms of survival signaling, although remains unsolved further questions about FAK biology that should be answered in the next future.

## *Chapter 5*

### *References*

1. Singh AD, Bergman L, Seregard S. Uveal Melanoma: epidemiologic aspects. *Ophthalmol Clin North Am*, 2005. 18:75-84.
2. Nathan P, Cohen V, Coupland S, Curtis K, Damato B, Evans J, Fenwick S, Kirkpatrick L, Li O, Marshall E, McGuirk K, Ottensmeier C, Pearce N, Salvi S, Stedman B, Szlosarek P, Turnbull N; United Kingdom Uveal Melanoma Guideline Development Working Group. Uveal Melanoma UK National Guidelines. *Eur J Cancer*, 2015. 51:2404-2412.
3. Andreoli MT, Mieler WF, Leiderman YI. Epidemiological trends in uveal melanoma. *The British Journal of Ophthalmology*, 2015. 99:1550–1553.
4. Hu DN, Yu GP, McCormick SA, Schneider S, Finger PT. Population-based incidence of uveal melanoma in various races and ethnic groups. *Am J of Ophthalmol*, 2005. 140:612-617.
5. Virgili G, Gatta G, Ciccolallo L, Capocaccia R, Biggeri A, Crocetti E, Lutz JM, Paci E; EUROCORE Working Group. Incidence of uveal melanoma in Europe. *Ophthalmology*, 2007. 114:2309-2315.
6. Weis E, Shah CP, Lajous M, Shields JA, Shields CL. The association between host susceptibility factors and uveal melanoma: a metaanalysis. *Arch Ophthalmol*, 2006. 124:54–60.
7. de Lange MJ, Razzaq L, Versluis M, Verlinde S, Dogrusöz M, Böhringer S, Marinkovic M, Luyten GP, de Keizer RJ, de Gruijl FR, Jager MJ, van der Velden PA. Distribution of GNAQ and GNA11 mutation signatures in uveal melanoma points to a light dependent mutation mechanism. *PloS One*, 2015. 10:e0138002.
8. Accuracy of diagnosis of choroidal melanomas in the Collaborative Ocular Melanoma Study. COMS Report No. 1. *Arch Ophthalmol*, 1990. 108:1268-1273.
9. Diener-West M, Earle JD, Fine SL, Hawkins BS, Moy CS, Reynolds SM, Schachat AP, Straatsma BR; Collaborative Ocular Melanoma Study Group. The COMS randomized trial of iodine 125 brachytherapy for choroidal melanoma, III: initial mortality findings. COMS Report No. 18. *Arch Ophthalmol*, 2001. 119:969-982.
10. McLean IW, Berd D, Mastrangelo MJ, Shields JA, Davidorf FH, Grever M, Makley TA, Gamel JW. A randomized study of methanol-extraction residue of bacille Calmette-Guerin as postsurgical adjuvant therapy of uveal melanoma. *Am J Ophthalmol*, 1990. 110:522-526.
11. Voelter V, Schalenbourg A, Pampallona S, Peters S, Halkic N, Denys A, Goitein G, Zografos L, Leyvraz S. Adjuvant intraarterial hepatic fotemustine for high-risk uveal melanoma patients. *Melanoma Res*, 2008. 18:220-224.
12. Gragoudas ES, Egan KM, Seddon JM, Glynn RJ, Walsh SM, Finn SM, Munzenrider JE, Spar MD. Survival of patients with metastases from uveal melanoma. *Ophthalmology*, 1991. 98:383-389.

13. Rivoire M, Kodjikian L, Baldo S, Kaemmerlen P, Négrier S, Grange JD. Treatment of liver metastases from uveal melanoma. *Ann Surg Oncol*, 2005. 12:422-428.
14. Leyvraz S, Piperno-Neumann S, Suciú S, Baurain JF, Zdzienicki M, Testori A, Marshall E, Scheulen M, Jouary T, Negrier S, Vermorken JB, Kaempgen E, Durando X, Schadendorf D, Gurnath RK, Keilholz U. Hepatic intra-arterial versus intravenous fotemustine in patients with liver metastases from uveal melanoma (EORTC 18021): a multicentric randomized trial. *Ann Oncol*, 2014. 25:742-746.
15. Pingpank JF et al. A phase III random assignment trial comparing percutaneous hepatic perfusion with melphalan (PHP-mel) to standard of care for patients with hepatic metastases from metastatic ocular or cutaneous melanoma [abstract]. *J Clin Oncol*. 2010.
16. Gonsalves CF, Eschelman DJ, Sullivan KL, Anne PR, Doyle L, Sato T. Radioembolization as salvage therapy for hepatic metastasis of uveal melanoma: a single-institution experience. *AJR Am J Roentgenol*, 2011. 196:468-473.
17. Klingenstein A, Haug AR, Zech CJ, Schaller UC. Radioembolization as locoregional therapy of hepatic metastases in uveal melanoma patients. *Cardiovasc Intervent Radiol*, 2013. 36:158-165.
18. Schmittl A, Schmidt-Hieber M, Martus P, Bechrakis NE, Schuster R, Siehl JM, Foerster MH, Thiel E, Keilholz U. A randomized phase II trial of gemcitabine plus treosulfan versus treosulfan alone in patients with metastatic uveal melanoma. *Ann Oncol*, 2006. 17:1826-1829.
19. Atzpodien J, Terfloth K, Fluck M, Reitz M. Cisplatin, gemcitabine and treosulfan is effective in chemotherapy-pretreated relapsed stage IV uveal melanoma patients. *Cancer Chemother Pharmacol*, 2008. 62:685-688.
20. O'Neill PA, Butt M, Eswar CV, Gillis P, Marshall E. A prospective single arm phase II study of dacarbazine and treosulfan as first-line therapy in metastatic uveal melanoma. *Melanoma Res*, 2006. 16:245-248.
21. Becker JC, Terheyden P, Kämpgen E, Wagner S, Neumann C, Schadendorf D, Steinmann A, Wittenberg G, Lieb W, Bröcker EB. Treatment of disseminated ocular melanoma with sequential fotemustine, interferon alpha, and interleukin 2. *Br J Cancer*, 2002. 87:840-845.
22. Kivelä T, Suciú S, Hansson J, Kruit WH, Vuoristo MS, Kloke O, Gore M, Hahka-Kemppinen M, Parvinen LM, Kumpulainen E, Humblet Y, Pyrhönen S. Bleomycin, vincristine, lomustine and dacarbazine (BOLD) in combination with recombinant interferon alpha-2b for metastatic uveal melanoma. *Eur J Cancer*, 2003. 39:1115-1120.
23. Hodi FS, O'Day SJ, McDermott DF, Weber RW, Sosman JA, Haanen JB, Gonzalez R, Robert C, Schadendorf D, Hassel JC, Akerley W, van den Eertwegh AJ, Lutzky J, Lorigan P, Vaubel JM, Linette GP, Hogg D, Ottensmeier CH, Lebbé C, Peschel C, Quirt I, Clark JI, Wolchok JD, Weber JS, Tian J, Yellin MJ, Nichol GM, Hoos A, Urba WJ. Improved survival with ipilimumab in patients with metastatic melanoma. *N Engl J Med*, 2010. 363:711-723.

24. Luke JJ, Callahan MK, Postow MA, Romano E, Ramaiya N, Bluth M, Giobbie-Hurder A, Lawrence DP, Ibrahim N, Ott PA, Flaherty KT, Sullivan RJ, Harding JJ, D'Angelo S, Dickson M, Schwartz GK, Chapman PB, Wolchok JD, Hodi FS, Carvajal RD. Clinical activity of ipilimumab for metastatic uveal melanoma: a retrospective review of the Dana-Farber Cancer Institute, Massachusetts General Hospital, Memorial Sloan-Kettering Cancer Center, and University Hospital of Lausanne experience. *Cancer*, 2013. 119:3687-3695.
25. Kottschade LA, McWilliams RR, Markovic SN, Block MS, Villasboas Bisneto J, Pham AQ, Esplin BL, Dronca RS. The use of pembrolizumab for the treatment of metastatic uveal melanoma. *Melanoma Res*, 2016. 26:300-303.
26. Van Raamsdonk CD, Griewank KG, Crosby MB, Garrido MC, Vemula S, Wiesner T, Obenaus AC, Wackernagel W, Green G, Bouvier N, Sozen MM, Baimukanova G, Roy R, Heguy A, Dolgalev I, Khanin R, Busam K, Speicher MR, O'Brien J, Bastian BC. Mutations in GNA11 in uveal melanoma. *N Engl J Med*, 2010. 363:2191-2199.
27. Carvajal RD, Sosman JA, Quevedo JF, Milhem MM, Joshua AM, Kudchadkar RR, Linette GP, Gajewski TF8, Lutzky J, Lawson DH, Lao CD, Flynn PJ, Albertini MR, Sato T, Lewis K, Doyle A, Ancell K, Panageas KS, Bluth M, Hedvat C, Erinjeri J, Ambrosini G, Marr B, Abramson DH, Dickson MA, Wolchok JD, Chapman PB, Schwartz GK. Effect of selumetinib vs chemotherapy on progression-free survival in uveal melanoma: a randomized clinical trial. *JAMA*, 2014. 311:2397-2405.
28. Krauthammer M, Kong Y, Ha BH, Evans P, Bacchiocchi A, McCusker JP, Cheng E, Davis MJ, Goh G, Choi M, Ariyan S, Narayan D, Dutton-Regester K, Capatana A, Holman EC, Bosenberg M, Sznol M, Kluger HM, Brash DE, Stern DF, Materin MA, Lo RS, Mane S, Ma S, Kidd KK, Hayward NK, Lifton RP, Schlessinger J, Boggon TJ, Halaban R. Exome sequencing identifies recurrent somatic RAC1 mutations in melanoma. *Nat Genet*, 2012. 44:1006–1014.
29. Onken MD, Worley LA, Ehlers JP, Harbour JW. Gene expression profiling in uveal melanoma reveals two molecular classes and predicts metastatic death. *Cancer Res*, 2004. 64:7205–7209.
30. Harbour JW, Onken MD, Roberson ED, Duan S, Cao L, Worley LA, Council ML, Matatall KA, Helms C, Bowcock AM. Frequent mutation of BAP1 in metastasizing uveal melanomas. *Science*, 2010. 330:1410–1413.
31. Van Raamsdonk CD, Bezrookove V, Green G, Bauer J, Gaugler L, O'Brien JM, Simpson EM, Barsh GS, Bastian BC. Frequent somatic mutations of GNAQ in uveal melanoma and blue naevi. *Nature*, 2009. 457:599–602.
32. Martin M, Maßhöfer L, Temming P, Rahmann S, Metz C, Bornfeld N, van de Nes J, Klein-Hitpass L, Hinnebusch AG, Horsthemke B, Lohmann DR, Zeschnigk M. Exome sequencing identifies recurrent somatic mutations in EIF1AX and SF3B1 in uveal melanoma with disomy 3. *Nat Genet*, 2013. 45:933–936.

33. Moore AR, Ceraudo E, Sher JJ, Guan Y, Shoushtari AN, Chang MT, Zhang JQ, Walczak EG, Kazmi MA, Taylor BS, Huber T, Chi P, Sakmar TP, Chen Y. Recurrent activating mutations of G-protein coupled receptor *CYSLTR2* in uveal melanoma. *Nat Genet*, 2016. 48:675-680.
34. Dono M, Angelini G, Cecconi M, Amaro A, Esposito AI, Mirisola V, Maric I, Lanza F, Nasciuti F, Viaggi S, Gualco M, Bandelloni R, Truini M, Coviello DA, Zupo S, Mosci C, Pfeffer U. Mutation frequencies of *GNAQ*, *GNA11*, *BAP1*, *SF3B1*, *EIF1AX* and *TERT* in uveal melanoma: detection of an activating mutation in the *TERT* gene promoter in a single case of uveal melanoma. *Br J Cancer*, 2014. 110:1058-1065.
35. Landreville S, Agapova OA, Matatall KA, Kneass ZT, Onken MD, Lee RS, Bowcock AM, Harbour JW. Histone deacetylase inhibitors induce growth arrest and differentiation in uveal melanoma. *Clin Cancer Res*, 2012. 18:408–416.
36. Pan H, Jia R, Zhang L, Xu S, Wu Q, Song X, Zhang H, Ge S, Xu XL, Fan X. *BAP1* regulates cell cycle progression through *E2F1* target genes and mediates transcriptional silencing via *H2A* monoubiquitination in uveal melanoma cells. *Int J Biochem Cell Biol*, 2015. 60:176-184.
37. Jensen DE, Proctor M, Marquis ST, Gardner HP, Ha SI, Chodosh LA, Ishov AM, Tommerup N, Vissing H, Sekido Y, Minna J, Borodovsky A, Schultz DC, Wilkinson KD, Maul GG, Barlev N, Berger SL, Prendergast GC, Rauscher FJ 3rd. *BAP1*: a novel ubiquitin hydrolase which binds to the *BRCA1* RING finger and enhances *BRCA1*- mediated cell growth suppression. *Oncogene*, 1998. 16:1097–1112.
38. Te Raa GD, Derks IA, Navrkalova V, Skowronska A, Moerland PD, van Laar J, Oldreive C, Monsuur H, Trbusek M, Malcikova J, Lodén M, Geisler CH, Hülleln J, Jethwa A, Zenz T, Pospisilova S, Stankovic T, van Oers MH, Kater AP, Eldering E. The impact of *SF3B1* mutations in CLL on the DNA-damage response. *Leukemia*, 2015. 29:1133–1142.
39. Quesada V, Conde L, Villamor N, Ordóñez GR, Jares P, Bassaganyas L, Ramsay AJ, Beà S, Pinyol M, Martínez-Trillos A, López-Guerra M, Colomer D, Navarro A, Baumann T, Aymerich M, Rozman M, Delgado J, Giné E, Hernández JM, González-Díaz M, Puente DA, Velasco G, Freije JM, Tubío JM, Royo R, Gelpí JL, Orozco M, Pisano DG, Zamora J, Vázquez M, Valencia A, Himmelbauer H, Bayés M, Heath S, Gut M, Gut I, Estivill X, López-Guillermo A, Puente XS, Campo E, López-Otín C. Exome sequencing identifies recurrent mutations of the splicing factor *SF3B1* gene in chronic lymphocytic leukemia. *Nat Genet*, 2011. 44:47–52.
40. Furney SJ, Pedersen M, Gentien D, Dumont AG, Rapinat A, Desjardins L, Turajlic S, Piperno-Neumann S, de la Grange P, Roman-Roman S, Stern MH, Marais R. *SF3B1* mutations are associated with alternative splicing in uveal melanoma. *Cancer Discov*, 2013. 3:1122–1129.
41. Decatur CL, Ong E, Garg N, Anbunathan H, Bowcock AM, Field MG, Harbour JW. Driver mutations in uveal melanoma: associations with gene expression profile and patient outcomes. *JAMA Ophthalmol*, 2016. 134:728–733.

42. Emley A, Nguyen LP, Yang S, Mahalingam M. Somatic mutations in GNAQ in amelanotic/hypomelanotic blue nevi. *Hum Pathol*, 2011. 42:136–140.
43. Weber A, Hengge UR, Urbanik D, Markwart A, Mirmohammadsaegh A, Reichel MB, Wittekind C, Wiedemann P, Tannapfel A. Absence of mutations of the BRAF gene and constitutive activation of extracellularregulated kinase in malignant melanomas of the uvea. *Lab Invest*, 2003. 83:1771–1776.
44. von Euw E, Atefi M, Attar N, Chu C, Zachariah S, Burgess BL, Mok S, Ng C, Wong DJ, Chmielowski B, Lichter DI, Koya RC, McCannel TA, Izmailova E, Ribas A. Antitumor effects of the investigational selective MEK inhibitor TAK733 against cutaneous and uveal melanoma cell lines. *Mol Cancer*, 2012. 11:22.
45. Selumetinib shows promise in metastatic uveal melanoma. *CancerDiscov*, 2013. 3(7):OF8.
46. Patel M, Smyth E, Chapman PB, Wolchok JD, Schwartz GK, Abramson DH, Carvajal RD. Therapeutic implications of the emerging molecular biology of uveal melanoma. *Clin Cancer Res*, 2011. 17:2087–2100.
47. Khalili JS, Yu X, Wang J, Hayes BC, Davies MA, Lizee G, Esmaeli B, Woodman SE. Combination small molecule MEK and PI3K inhibition enhances uveal melanoma cell death in a mutant GNAQ- and GNA11-dependent manner. *Clin Cancer Res*, 2012. 18:4345–4355.
48. Harbour JW, Chao DL. A molecular revolution in uveal melanoma: implications for patient care and targeted therapy. *Ophthalmology*, 2014. 121:1281–1288.
49. Luo M, Fan H, Nagy T, Wei H, Wang C, Liu S, Wicha MS, Guan JL. Mammary epithelial-specific ablation of the focal adhesion kinase suppresses mammary tumorigenesis by affecting mammary cancer stem/progenitor cells. *Cancer Res*, 2009. 69:466–474.
50. Schober M, Fuchs E. Tumor-initiating stem cells of squamous cell carcinomas and their control by TGF-beta and integrin/focal adhesion kinase (FAK) signaling. *Proc Natl Acad Sci U S A*, 2009. 108:10544–10549.
51. Scheel C, Weinberg RA. Phenotypic plasticity and epithelial-mesenchymal transitions in cancer and normal stem cells? *Int J Cancer*, 2011. 129:2310–2314.
52. Schaller MD, Borgman CA, Cobb BS, Vines RR, Reynolds AB, Parsons JT. pp125fak a structurally distinctive protein-tyrosine kinase associated with focal adhesions. *Proc Natl Acad Sci USA*, 1992. 89:5192–5196.
53. Weiner TM, Liu ET, Craven RJ, Cance WG. Expression of focal adhesion kinase gene and invasive cancer. *Lancet*, 1993. 342:1024–1025.
54. Palmer RH, Fessler LI, Edeen PT, Madigan SJ, McKeown M, Hunter T. DFak56 is a novel *Drosophila melanogaster* focal adhesion kinase. *J Biol Chem*, 1999. 274:35621–35629.
55. Schaller MD. Cellular functions of FAK kinases: insight into molecular mechanisms and novel functions. *J Cell Sci*, 2010. 123:1007–1013.

56. Golubovskaya VM, Finch R, Cance WG. Direct Interaction of the N-terminal Domain of Focal Adhesion Kinase with the N-terminal Transactivation Domain of p53. *J Biol Chem*, 2005. 280:25008–25021.
57. Lim ST, Chen XL, Lim Y, Hanson DA, Vo TT, Howerton K, Larocque N, Fisher SJ, Schlaepfer DD, Ilic D. Nuclear FAK promotes cell proliferation and survival through FERM-enhanced p53 degradation. *Mol Cell*, 2008. 29:9–22.
58. Lim ST. Nuclear FAK: a new mode of gene regulation from cellular adhesions. *Mol Cells*, 2013. 36:1–6.
59. Hanks SK, Ryzhova L, Shin NY, Brábek J. Focal adhesion kinase signaling activities and their implications in the control of cell survival and motility. *Front Biosci*, 2003. 8:982–996.
60. Zhai J, Lin H, Nie Z, Wu J, Cañete-Soler R, Schlaepfer WW, Schlaepfer DD. Direct interaction of focal adhesion kinase with p190RhoGEF. *J Biol Chem*, 2003. 278:24865–24873.
61. Cobb BS, Schaller MD, Leu TH, Parsons JT. Stable association of pp60src and pp59fyn with the focal adhesion-associated protein tyrosine kinase, pp125FAK. *Mol Cell Bio*, 1994. 14:147–55.
62. Schaller MD, Hildebrand JD, Shannon JD, Fox JW, Vines RR, Parsons JT. Autophosphorylation of the focal adhesion kinase, pp125FAK, directs SH2-dependent binding of pp60src. *Mol Cell Bio*, 1994. 14:1680–1688.
63. Sulzmaier FJ, Jean C, Schlaepfer DD. FAK in cancer: mechanistic findings and clinical applications. *Nat Rev Cancer*, 2014. 14:598-610.
64. Corsi JM, Rouer E, Girault JA, Enslin H. Organization and post-transcriptional processing of focal adhesion kinase gene. *BMC Genomics*, 2006. 7:198
65. Cance WG, Golubovskaya VM. Focal adhesion kinase versus p53: apoptosis or survival? *Sci Signal*, 2008. 1:pe22.
66. Ho B, Olson G, Figel S, Gelman I, Cance WG, Golubovskaya VM. Nanog increases focal adhesion kinase (FAK) promoter activity and expression and directly binds to FAK protein to be phosphorylated. *J Biol Chem*, 2012. 287:18656–73.
67. Cheng N, Li Y, Han ZG. Argonaute2 promotes tumor metastasis by way of up-regulating focal adhesion kinase expression in hepatocellular carcinoma. *Hepatology*, 2013. 57:1906–1918.
68. Li S, Huang X, Zhang D, Huang Q, Pei G, Wang L, Jiang W, Hu Q, Tan R, Hua ZC. Requirement of PEA3 for transcriptional activation of FAK gene in tumor metastasis. *PLoS One*, 2013. 8:e79336.
69. Fang XQ, Liu XF, Yao L, Chen CQ, Gu ZD, Ni PH, Zheng XM, Fan QS. Somatic mutational analysis of FAK in breast cancer: A novel gain-of-function mutation due to deletion of exon 33. *Biochem Biophys Res Commun*. 2014; 443:363–369.
70. Mitra SK, Hanson DA, Schlaepfer DD. Focal adhesion kinase: in command and control of cell motility. *Nat Rev Mol Cell Biol*, 2005. 6:56–68.
71. Nguyen N, Yi JS, Park H, Lee JS, Ko YG. MG53 ubiquitinates focal adhesion kinase during skeletal myogenesis. *J Biol Chem*, 2013. 289:3209-3216.

72. Mitra SK, Schlaepfer DD. Integrin-regulated FAK-Src signaling in normal and cancer cells. *Curr Opin Cell Biol*, 2006. 18:516–523.
73. Frame MC, Patel H, Serrels B, Lietha D, Eck MJ. The FERM domain: organizing the structure and function of FAK. *Nat Rev Mol Cell Biol*, 2010. 11:802–814.
74. Goñi GM, Epifano C, Boskovic J, Camacho-Artacho M, Zhou J, Bronowska A, Martín MT, Eck MJ, Kremer L, Gräter F, Gervasio FL, Perez-Moreno M, Lietha D. Phosphatidylinositol 4,5-bisphosphate triggers activation of focal adhesion kinase by inducing clustering and conformational changes. *Proc Natl Acad Sci U S A*, 2014. 111:3177–3186.
75. Brami-Cherrier K1, Gervasi N, Arsenieva D, Walkiewicz K, Bouterin MC, Ortega A, Leonard PG, Seantier B, Gasmi L, Bouceba T, Kadaré G, Girault JA, Arold ST. FAK dimerization controls its kinase-dependent functions at focal adhesions. *EMBO J*, 2014. 33:356–370.
76. Choi CH, Webb BA, Chimenti MS, Jacobson MP, Barber DL. pH sensing by FAK-His58 regulates focal adhesion remodeling. *J Cell Biol*, 2013. 202:849–859.
77. Pylayeva Y, Gillen KM, Gerald W, Beggs HE, Reichardt LF, Giancotti FG. Ras- and PI3K-dependent breast tumorigenesis in mice and humans requires focal adhesion kinase signaling. *J Clin Invest*, 2009. 119:252–266.
78. Frisch SM, Vuori K, Ruoslahti E, Chan-Hui PY. Control of adhesion-dependent cell survival by focal adhesion kinase. *Journal of Cell Biology*, 1996. 134:793–799.
79. Xu LH, Yang X, Bradham CA, Brenner DA, Baldwin AS Jr, Craven RJ, Cance WG. The focal adhesion kinase suppresses transformation-associated, anchorage-Independent apoptosis in human breast cancer cells. Involvement of death receptor-related signaling pathways. *J Biol Chem*, 2000. 275:30597–30604.
80. Golubovskaya VM, Zheng M, Zhang L, Li JL, Cance WG. The direct effect of focal adhesion kinase (FAK), dominant-negative FAK, FAK-CD and FAK siRNA on gene expression and human MCF-7 breast cancer cell tumorigenesis. *BMC Cancer*, 2009. 9:280–285.
81. Sonoda Y, Matsumoto Y, Funakoshi M, Yamamoto D, Hanks SK, Kasahara T. Anti-apoptotic role of focal adhesion kinase (FAK). Induction of inhibitor-of-apoptosis proteins and apoptosis suppression by the overexpression of FAK in a human leukemic cell line, HL-60. *J Biol Chem*, 2000. 275:16309–16315.
82. Schlaepfer DD, Mitra SK, Ilic D. Control of motile and invasive cell phenotypes by focal adhesion kinase. *Biochim Biophys Acta*, 2004. 1692:77–102.
83. Ilić D, Furuta Y, Kanazawa S, Takeda N, Sobue K, Nakatsuji N, Nomura S, Fujimoto J, Okada M, Yamamoto T. Reduced cell motility and enhanced focal adhesion contact formation in cells from FAK-deficient mice. *Nature*, 1995. 377:539–544.
84. Sieg DJ, Hauck CR, Schlaepfer DD. Required role of focal adhesion kinase (FAK) for integrin-stimulated cell migration. *J Cell Sci*, 1999. 112:2677–2691.
85. Wu X, Gan B, Yoo Y, Guan JL. FAK-mediated src phosphorylation of endophilin A2 inhibits endocytosis of MT1-MMP and promotes ECM degradation. *Dev Cell*, 2005. 9:185–196.

86. Mitra SK, Lim ST, Chi A, Schlaepfer DD. Intrinsic focal adhesion kinase activity controls orthotopic breast carcinoma metastasis via the regulation of urokinase plasminogen activator expression in a syngeneic tumor model. *Oncogene*, 2006. 25:4429–4440.
87. Chen JS, Huang XH, Wang Q, Huang JQ, Zhang LJ, Chen XL, Lei J, Cheng ZX. Sonic hedgehog signaling pathway induces cell migration and invasion through focal adhesion kinase/AKT signaling-mediated activation of matrix metalloproteinase (MMP)-2 and MMP-9 in liver cancer. *Carcinogenesis*, 2013. 34:10–19.
88. Veikkola T, Karkkainen M, Claesson-Welsh L, Alitalo K. Regulation of angiogenesis via vascular endothelial growth factor receptors. *Cancer Res*, 2000. 60:203–212.
89. Ilic D, Kovacic B, McDonagh S, Jin F, Baumbusch C, Gardner DG, Damsky CH. Focal adhesion kinase is required for blood vessel morphogenesis. *Circ Res*, 2003. 92:300–307.
90. Tavora B, Batista S, Reynolds LE, Jadeja S, Robinson S, Kostourou V, Hart I, Fruttiger M, Parsons M, Hodivala-Dilke KM. Endothelial FAK is required for tumour angiogenesis. *EMBO Mol Med*, 2106. 2: 516–528.
91. Alexopoulou AN, Ho-Yen CM, Papalazarou V, Elia G, Jones JL, Hodivala-Dilke K. Tumour-associated endothelial-FAK correlated with molecular sub-type and prognostic factors in invasive breast cancer. *BMC Cancer*, 2014. 14:237.
92. Mitra SK, Mikolon D, Molina JE, Hsia DA, Hanson DA, Chi A, Lim ST, Bernard-Trifilo JA, Ilic D, Stupack DG, Cheresch DA, Schlaepfer DD. Intrinsic FAK activity and Y925 phosphorylation facilitate an angiogenic switch in tumors. *Oncogene*, 2006. 25:5969–5984.
93. Lim ST, Mikolon D, Stupack DG, Schlaepfer DD. FERM control of FAK function: implications for cancer therapy. *Cell Cycle*, 2008. 7:2306–2314.
94. Huang YT, Lee LT, Lee PP, Lin YS, Lee MT. Targeting of focal adhesion kinase by flavonoids and small-interfering RNAs reduces tumor cell migration ability. *Anticancer Res*, 2005. 25:2017–2025.
95. Taylor JM, Mack CP, Nolan K, Regan CP, Owens GK, Parsons JT. Selective expression of an endogenous inhibitor of FAK regulates proliferation and migration of vascular smooth muscle cells. *Mol Cell Biol*, 2001. 21:1565–1572.
96. Golubovskaya VM, Virnig C, Cance WG. TAE226-induced apoptosis in breast cancer cells with overexpressed Src or EGFR. *Mol Carcinog*, 2008. 47:222–234.
97. Shi Q, Hjelmeland AB, Keir ST, Song L, Wickman S, Jackson D, Ohmori O, Bigner DD, Friedman HS, Rich JN. A novel low-molecular weight inhibitor of focal adhesion kinase, TAE226, inhibits glioma growth. *Mol Carcinog*, 2007. 6:488–496.
98. Roberts WG, Ung E, Whalen P, Cooper B, Hulford C, Autry C, Richter D, Emerson E, Lin J, Kath J, Coleman K, Yao L, Martinez-Alsina L, Lorenzen M, Berliner M, Luzzio M, Patel N, Schmitt E, LaGreca S, Jani J, Wessel M, Marr E, Griffor M, Vajdos F. Antitumor activity and pharmacology of a selective focal adhesion kinase inhibitor, PF-562,271. *Cancer Res*, 2008. 68:1935–1944.

99. Tanjoni I, Walsh C, Uryu S, Tomar A, Nam JO, Mielgo A, Lim ST, Liang C, Koenig M, Sun C, Patel N, Kwok C, McMahon G, Stupack DG, Schlaepfer DD. PND-1186 FAK inhibitor selectively promotes tumor cell apoptosis in three-dimensional environments. *Cancer Biol Ther*, 2010. 9:764–777.
100. Halder J, Lin YG, Merritt WM, Spannuth WA, Nick AM, Honda T, Kamat AA, Han LY, Kim TJ, Lu C, Tari AM, Bornmann W, Fernandez A, Lopez-Berestein G, Sood AK. Therapeutic efficacy of a novel focal adhesion kinase inhibitor TAE226 in ovarian carcinoma. *Cancer Res*, 2007. 67:10976–10983.
101. Liu TJ, La Fortune T, Honda T, Ohmori O, Hatakeyama S, Meyer T, Jackson D, de Groot J, Yung WK. Inhibition of both focal adhesion kinase and insulin-like growth factor-I receptor kinase suppresses glioma proliferation in vitro and in vivo. *Mol Cancer Ther*, 2007. 6:1357–1367.
102. Liu W, Bloom DA, Cance WG, Kurenova EV, Golubovskaya VM, Hochwald SN. FAK and IGFIR interact to provide survival signals in human pancreatic adenocarcinoma cells. *Carcinogenesis*, 2008. 29:1096–1107.
103. Slack-Davis JK, Martin KH, Tilghman RW, Iwanicki M, Ung EJ, Autry C, Luzzio MJ, Cooper B, Kath JC, Roberts WG, Parsons JT. Cellular characterization of a novel focal adhesion kinase inhibitor. *J Biol Chem*, 2007. 282:14845–14852.
104. Schultze A, Fiedler W. Therapeutic potential and limitations of new FAK inhibitors in the treatment of cancer. *Expert Opin Investig Drugs*, 2010. 19:777–788.
105. Fan H, Guan JL. Compensatory function of Pyk2 protein in the promotion of focal adhesion kinase (FAK)-null mammary cancer stem cell tumorigenicity and metastatic activity. *J Biol Chem*, 2011. 286:18573–15582.
106. Stokes JB, Adair SJ, Slack-Davis JK, Walters DM, Tilghman RW, Hershey ED, Lowrey B, Thomas KS, Bouton AH, Hwang RF, Stelow EB, Parsons JT, Bauer TW. Inhibition of focal adhesion kinase by PF-562,271 inhibits the growth and metastasis of pancreatic cancer concomitant with altering the tumor microenvironment. *Mol Cancer Ther*, 2011. 10:2135–2145.
107. Golubovskaya VM, Nyberg C, Zheng M, Kweh F, Magis A, Ostrov D, Cance WG. A Small Molecule Inhibitor, 1,2,4,5-Benzenetetraamine Tetrahydrochloride, Targeting the Y397 Site of Focal Adhesion Kinase Decreases Tumor Growth. *J Med Chem*, 2008. 51:7405–7416.
108. Heffler M, Golubovskaya VM, Dunn KM, Cance W. Focal adhesion kinase autophosphorylation inhibition decreases colon cancer cell growth and enhances the efficacy of chemotherapy. *Cancer Biol Ther*, 2013. 14:761–772.
109. Lim ST, Chen XL, Tomar A, Miller NL, Yoo J, Schlaepfer DD. Knockin mutation reveals an essential role for focal adhesion kinase (FAK) activity in blood vessel morphogenesis, cell motility-polarity, but not cell proliferation. *J Biol Chem*, 2010. 285:21526–21536.
110. Corsi JM, Houbron C, Billuart P, Brunet I, Bouvrée K, Eichmann A, Girault JA, Enslen H. Autophosphorylation-independent and dependent functions of Focal Adhesion Kinase during development. *J Biol Chem*, 2009. 284:34769–34776.

111. Iwatani M, Iwata H, Okabe A, Skene RJ, Tomita N, Hayashi Y, Aramaki Y, Hosfield DJ, Hori A, Baba A, Miki H. Discovery and characterization of novel allosteric FAK inhibitors. *Eur J Med Chem*, 2012. 61:49–60.
112. Kurenova EV, Hunt DL, He D, Magis AT, Ostrov DA, Cance WG. Small molecule chloropyramine hydrochloride (C4) targets the binding site of focal adhesion kinase and vascular endothelial growth factor receptor 3 and suppresses breast cancer growth in vivo. *J Med Chem*, 2009. 52:4716–4724.
113. Golubovskaya VM, Palma NL, Zheng M, Ho B, Magis A, Ostrov D, Cance WG. A small-molecule inhibitor, 5'-O-tritylthymidine, targets FAK and Mdm-2 interaction, and blocks breast and colon tumorigenesis in vivo. *Anticancer Agents Med Chem*, 2013. 13:532–545.
114. Ucar DA, Magis AT, He DH, Lawrence NJ, Sebti SM, Kurenova E, Zajac-Kaye M, Zhang J, Hochwald SN. Inhibiting the interaction of cMET and IGF-1R with FAK effectively reduces growth of pancreatic cancer cells in vitro and in vivo. *Anticancer Agents Med Chem*, 2013. 13:595–602.
115. Golubovskaya VM, Ho B, Zheng M, Magis A, Ostrov D, Morrison C, Cance WG. Disruption of focal adhesion kinase and p53 interaction with small molecule compound R2 reactivated p53 and blocked tumor growth. *BMC Cancer*, 2103. 13:342.
116. Zuidervaart W, van Nieuwpoort F, Stark M, Dijkman R, Packer L, Borgstein AM, Pavey S, van der Velden P, Out C, Jager MJ, Hayward NK, Gruis NA. Activation of the MAP pathway is a common event in uveal melanomas although it rarely occurs through mutation of BRAF or RAS. *Br J Cancer*, 2005. 92:2032-2038.
117. Ocak S, Chen H, Callison C, Gonzalez AL, Massion PP. Expression of focal adhesion kinase in small-cell lung carcinoma. *Cancer*, 2012. 118:1293–1301.
118. Owens LV, Xu L, Craven RJ, Dent GA, Weiner TM, Kornberg L, Liu ET, Cance WG. Overexpression of the focal adhesion kinase (p125FAK) in invasive human tumors. *Cancer Research*, 1995. 55:2752–2755.
119. Lark AL, Livasy CA, Calvo B, Caskey L, Moore DT, Yang X, Cance WG. Overexpression of focal adhesion kinase in primary colorectal carcinomas and colorectal liver metastases: immunohistochemistry and real-time PCR analyses. *Clin Cancer Res*, 2003. 9:215–222.
120. Yom CK, Noh DY, Kim WH, Kim HS. Clinical significance of high focal adhesion kinase gene copy number and overexpression in invasive breast cancer. *Breast Cancer Res Treat*, 2011. 128:647-655.
121. Law V, Knox C, Djoumbou Y, Jewison T, Guo AC, Liu Y, Maciejewski A, Arndt D, Wilson M, Neveu V, Tang A, Gabriel G, Ly C, Adamjee S, Dame ZT, Han B, Zhou Y, Wishart DS. DrugBank 4.0: shedding new light on drug metabolism. *Nucleic acids research*, 2014. 42:D1091-1097.
122. Marcotte R, Brown KR, Suarez F, Sayad A, Karamboulas K, Krzyzanowski PM, Sircoulomb F, Medrano M, Fedyshyn Y, Koh JLY, van Dyk D, Fedyshyn B, Luhova M, Brito GC, Vizeacoumar FJ, Vizeacoumar FS, Datti A, Kasimer D, Buzina A, Mero P, Misquitta C, Normand J, Haider M, Ketela T, Wrana JL, Rottapel R, Neel BG, Moffat J. Essential gene profiles in breast, pancreatic, and ovarian cancer cells. *Cancer Discov*, 2012. 2:172-189.

123. Marcotte R, Sayad A, Brown KR, Sanchez-Garcia F, Reimand J, Haider M, Virtanen C, Bradner JE, Bader GD, Mills GB, Pe'er D, Moffat J, Neel BG. Functional Genomic Landscape of Human Breast Cancer Drivers, Vulnerabilities, and Resistance. *Cell*, 2016. 164:293-309.
124. Cheung HW, Cowley GS, Weir BA, Boehm JS, Rusin S, Scott JA, East A, Ali LD, Lizotte PH, Wong TC, Jiang G, Hsiao J, Mermel CH, Getz G, Barretina J, Gopal S, Tamayo P, Gould J, Tsherniak A, Stransky N, Luo B, Ren Y, Drapkin R, Bhatia SN, Mesirov JP, Garraway LA, Meyerson M, Lander ES, Root DE, Hahn WC. Systematic investigation of genetic vulnerabilities across cancer cell lines reveals lineage-specific dependencies in ovarian cancer. *Proc Natl Acad Sci U S A*, 2011. 108:12372-12377.
125. Iorio F, Knijnenburg TA, Vis DJ, Bignell GR, Menden MP, Schubert M, Aben N, Gonçalves E, Barthorpe S, Lightfoot H, Cokelaer T, Greninger P, van Dyk E, Chang H, de Silva H, Heyn H, Deng X, Egan RK, Liu Q, Mironenko T, Mitropoulos X, Richardson L, Wang J, Zhang T, Moran S, Sayols S, Soleimani M, Tamborero D, Lopez-Bigas N, Ross-Macdonald P, Esteller M, Gray NS, Haber DA, Stratton MR, Benes CH, Wessels LFA, Saez-Rodriguez J, McDermott U, Garnett MJ. A Landscape of Pharmacogenomic interactions in cancer. *Cell*, 2016. 166:740-754.
126. Basu A, Bodycombe NE, Cheah JH, Price EV, Liu K, Schaefer GI, Ebright RY, Stewart ML, Ito D, Wang S, Bracha AL, Liefeld T, Wawer M, Gilbert JC, Wilson AJ, Stransky N, Kryukov GV, Dancik V, Barretina J, Garraway LA, Hon CS, Munoz B, Bittker JA, Stockwell BR, Khabele D, Stern AM, Clemons PA, Shamji AF, Schreiber SL. An Interactive resource to identify cancer genetic and lineage dependencies targeted by small molecules. *Cell*, 2013. 154:1151-1161.
127. Hunter T. Tyrosine phosphorylation: thirty years and counting. *Curr Opin Cell Biol*, 2009. 21:140-146.
128. Lemmon MA, Schlessinger J. Cell signaling by receptor tyrosine kinases. *Cell*, 2010. 141:1117-1134.
129. Armbruster BN, Li X, Pausch MH, Herlitz S, Roth BL. Evolving the lock to fit the key to create a family of G protein-coupled receptors potently activated by an inert ligand. *Proc Natl Acad Sci USA*, 2007. 104:5163-5168.
130. Zachary I, Sinnott-Smith J, Rozengurt E. Stimulation of tyrosine kinase activity in anti-phosphotyrosine immune complexes of Swiss 3T3 cell lysates occurs rapidly after addition of bombesin, vasopressin, and endothelin to intact cells. *J Biol Chem*, 1991. 266:24126-24133.
131. Huckle WR, Prokop CA, Dy RC, Herman B, Earp S. Angiotensin II stimulates protein-tyrosine phosphorylation in a calcium-dependent manner. *Mol Cell Biol*, 1990. 10:6290-6298.
132. Gutkind JS, Robbins KC. Activation of transforming G protein-coupled receptors induces rapid tyrosine phosphorylation of cellular proteins, including p125FAK and the p130 v-src substrate. *Biochem Biophys Res Commun*, 1992. 188:155-161.
133. Hubbard KB, Hepler JR. Cell signalling diversity of the Gqalpha family of heterotrimeric G proteins. *Cell Signal*, 2006. 18:135-150.

134. Vaqué JP, Dorsam RT, Feng X, Iglesias-Bartolome R, Forsthoefel DJ, Chen Q, Debant A, Seeger MA, Ksander BR, Teramoto H, Gutkind JS. A genome-wide RNAi screen reveals a Trio-regulated Rho GTPase circuitry transducing mitogenic signals initiated by G protein-coupled receptors. *Mol Cell*, 2013. 49:94-108.
135. Feng X, Degese MS, Iglesias-Bartolome R, Vaque JP, Molinolo AA, Rodrigues M, Zaidi MR, Ksander BR, Merlino G, Sodhi A, Chen Q, Gutkind JS. Hippo-independent activation of YAP by the GNAQ uveal melanoma oncogene through a trio-regulated rho GTPase signaling circuitry. *Cancer Cell*, 2104. 25:831-845.
136. Joung J, Konermann S, Gootenberg JS, Abudayyeh OO, Platt RJ, Brigham MD, Sanjana NE, Zhang F. Genome-scale CRISPR/Cas9 knockout and transcriptional activation screening. *Nat Prot*, 2017. 12:828-863.



## *Università degli Studi della Calabria*

Dipartimento di Farmacia e Scienze della Salute e della Nutrizione

### **Dottorato di Ricerca in Medicina Traslationale (XXX Ciclo)**

**Relazione sull'attività scientifica svolta dal Dr. Damiano Cosimo Rigracciolo  
nel corso del Dottorato (Docente Tutor: Prof. M. Maggiolini)**

Nel corso del Dottorato, l'attività di ricerca ha riguardato inizialmente i meccanismi molecolari coinvolti dal rame nella stimolazione dell'angiogenesi in cellule tumorali. Gli esperimenti condotti e i risultati ottenuti hanno dimostrato che il rame ( $\text{CuSO}_4$ ), attraverso la generazione di radicali liberi ed il coinvolgimento del pathway trasduzionale EGFR/ERK/MAPK, è in grado di indurre l'up-regolazione dei livelli di mRNA e proteici del fattore trascrizionale indotto dall'ipossia HIF-1 $\alpha$ , del fattore di crescita dell'endotelio vascolare VEGF e del recettore di membrana responsivo agli estrogeni GPER, sia in cellule tumorali mammarie SkBr3 che epatiche HepG2. In tale contesto, utilizzando specifici silenziatori è stato inoltre osservato il coinvolgimento di HIF-1 $\alpha$  e GPER nell'up-regolazione di VEGF indotta dal rame. E' stato infine valutato il ruolo del cross-talk funzionale tra HIF-1 $\alpha$ , VEGF e GPER nelle risposte biologiche mediate dal rame, utilizzando come modello sperimentale cellule HUVECs (Human Umbilical Vein Endothelial Cells), nelle quali il metallo ha indotto la formazione di un intricato network di strutture tubulari simil-vascolari e la migrazione cellulare.

L'attività di ricerca ha inoltre riguardato la caratterizzazione dei pathway trasduzionali coinvolti negli effetti mediati dall'aldosterone in cellule tumorali mammarie. Attraverso saggi di co-immunoprecipitazione ed immunofluorescenza è stato dimostrata l'esistenza di un'interazione diretta tra il recettore dell'aldosterone MR e GPER, il quale è stato coinvolto nella regolazione dello scambiatore  $\text{Na}^+/\text{H}^+$  denominato NHE-1 la cui attività è regolata dal complesso aldosterone/MR. Gli studi condotti hanno infine specificato il ruolo di MR e GPER in alcuni effetti biologici mediati dall'aldosterone, utilizzando come modello sperimentale cellule endoteliali derivate da tumore mammario denominate B-TEC. In tale contesto cellulare, il silenziamento dell'espressione di GPER e di MR ha infatti inibito la capacità dell'aldosterone di indurre la proliferazione e la migrazione cellulare.

Nel corso del dottorato, è stato inoltre svolto uno stage di un anno (Gennaio 2016-Dicembre 2016) a San Diego presso il Laboratorio diretto dal Prof. J. Silvio Gutkind – John & Rebecca Moores Cancer Center, dell'Università della California (USA).

Durante tale stage, l'attività di ricerca ha riguardato il ruolo esercitato da una proteina citoplasmatica ad attività tirosin-chinasica associata ai recettori per le integrine, denominata FAK (focal adhesion kinase), nella progressione del Melanoma Uveale. A riguardo, si precisa che tale tumore è caratterizzato dalla presenza di mutazioni somatiche attivanti a carico degli oncogeni GNAQ e GNA11, che codificano per due diverse subunità  $\alpha$  delle proteine G. Attraverso analisi bioinformatica lo studio ha inizialmente determinato che il gene codificante per FAK (PTK2) è over-espresso nel 56% dei casi di Melanoma Uveale. Sulla base di tale osservazione, sono stati successivamente valutati i meccanismi mediati da GNAQ nell'attivazione di FAK, utilizzando come modelli sperimentali cellule di Melanoma Uveale OMM1.3 (GNAQ/11 mutate) e cellule denominate HEK293 DREADD/Gq che sono state ingegnerizzate per l'espressione di un recettore di membrana accoppiato a proteine-G ( $\text{G}\alpha\text{q}$ ) attivato da ligandi sintetici. I saggi biologici effettuati hanno dimostrato l'attività antitumorale di specifici inibitori di FAK, come osservato negli esperimenti

realizzati in cellule di Melanoma Uveale derivanti sia da lesioni primarie che da metastasi epatiche. Infine, attraverso l'innovativo approccio genetico CRISPR/Cas9, il silenziamento dell'espressione di FAK ha ridotto significativamente la crescita del melanoma uveale anche in saggi condotti *in vivo*.

## **Pubblicazioni del Dottor Damiano Cosimo Rigracciolo durante il corso di Dottorato:**

1. **Rigracciolo DC**, Xiadong F, Maggiolini M, Gutkind JS. Targeting systems vulnerabilities in uveal melanoma by CRISPR/Cas9 focal adhesion kinase (FAK) genome editing and therapeutic inhibition. *Cancer Research*, Submitted.
2. Lappano R, Sebastiani A, Cirillo F, **Rigracciolo DC**, Galli GR, Curcio R, Malaguarnera R, Belfiore A, Cappello AR, Maggiolini M. The lauric acid-activated signaling prompts apoptosis in cancer cells. *Cell Death Discov*, 2017. 3:17063.
3. Cirillo F, Pellegrino M, Malivindi R, Rago V, Avino S, Muto L, Dolce V, Vivacqua A, **Rigracciolo DC**, De Marco P, Sebastiani A, Abonante S, Nakajima M, Lappano R, Maggiolini M. GPER is involved in the regulation of the estrogen-metabolizing CYP1B1 enzyme in breast cancer. *Oncotarget*, in press, 2017.
4. De Francesco EM, Rocca C, Scavello F, Amelio D, Pasqua T, **Rigracciolo DC**, Scarpelli A, Avino S, Cirillo F, Amodio N, Cerra MC, Maggiolini M, Angelone T. Protective Role of GPER Agonist G-1 on Cardiotoxicity Induced by Doxorubicin. *J Cell Physiol*, 2017. 232:1640-1649.
5. **Rigracciolo DC**, Scarpelli A, Lappano R, Pisano A, Santolla MF, Avino S, De Marco P, Bussolati B, Maggiolini M, De Francesco EM. GPER is involved in the stimulatory effects of aldosterone in breast cancer cells and breast tumor-derived endothelial cells. *Oncotarget*, 2016. 7:94-111.
6. Serra R, Gallelli L, Perri P, De Francesco EM, **Rigracciolo DC**, Mastroberto P, Maggiolini M, de Franciscis S. Estrogens Receptors and Chronic Venous Disease. *Eur J Endovasc Surg*, 2016. 52:114-118.
7. Pisano A, Santolla MF, De Francesco EM, De Marco P, **Rigracciolo DC**, Perri MG, Vivacqua A, Abonante S, Cappello AR, Dolce V, Belfiore A, Maggiolini M, Lappano R. GPER, IGF-1R, and EGFR transduction signaling are involved in stimulatory effects of zinc in breast cancer cells and cancer-associated fibroblasts. *Mol Carcinog*, 2017. 56:580-593.

8. Avino S, De Marco P, Cirillo F, Santolla MF, De Francesco EM, Perri MG, **Rigiracciolo DC**, Dolce V, Belfiore A, Maggiolini M, Lappano R, Vivacqua A. Stimulatory actions of IGF-1 are mediated by IGF-1R cross-talk with GPER and DDR1 in mesothelioma and lung cancer cells. *Oncotarget*, 2016. 7:52710-52728.
9. Lappano R, **Rigiracciolo DC**, De Marco P, Avino S, Cappello AR, Rosano C, Maggiolini M, De Francesco EM. Recent Advances on the Role of G Protein-Coupled Receptors in Hypoxia-Mediated Signaling. *AAPS J*, 2016. 18:305-310.
10. Tropea T, De Francesco EM, **Rigiracciolo DC**, Maggiolini M, Wareing M, Osol G, Mandalà M. Pregnancy Augments G Protein Estrogen Receptor (GPER) Induced Vasodilation in Rat Uterine Arteries via the Nitric Oxide-cGMP Signaling Pathway. *PloS One*, 2015. 10:e0141997.
11. **Rigiracciolo DC**, Scarpelli A, Lappano R, Pisano A, Santolla MF, De Marco P, Cirillo F, Cappello AR, Dolce V, Belfiore A, Maggiolini M, De Francesco EM. Copper activates HIF-1 $\alpha$ /GPER/VEGF signalling in cancer cells. *Oncotarget*, 2015. 6:34158-34177.
12. Santolla MF, Avino S, Pellegrino M, De Francesco EM, De Marco P, Lappano R, Vivacqua A, Cirillo F, **Rigiracciolo DC**, Scarpelli A, Abonante S, Maggiolini M. SIRT1 is involved in oncogenic signaling mediated by GPER in breast cancer. *Cell Death Dis*, 2015. 6:e1834.

**Dr. Damiano Cosimo Rigiracciolo**

- **Partecipazioni a Congressi**

8-9 Giugno 2017. **The future of cancer therapy: the genome editing era.**  
University Magna Graecia, Catanzaro (Italy).

6-8 Maggio 2015. **Novel mechanisms of signal transduction involved in cancer chemoresistance: focus on IGF signaling integration and cross-talk.**  
University Campus ‘‘S. Venuta’’- Catanzaro, Italy. Lecture Hall G3.

- **Stage**

Stage di un anno (Gennaio 2016-Dicembre 2016) presso il Laboratorio di Ricerca diretto dal Prof. Jorge Silvio Gutkind – John & Rebecca Moores Cancer Center – University of San Diego, California, USA.

- **Corsi**

- 24 Novembre - 3 Dicembre 2015. NMR for organic and biological chemistry: Old experiments for new applications. Theoretical and practical overview. Docente del corso: Ignacio Delso Hernández. Sala Terenzi.

- 22 Febbraio – 15 Marzo 2017. Advanced English. Docente del corso: Dott.ssa Anna Franca Plastina.

- 19 Aprile – 30 Maggio 2017. Appr. Class. Analisi Dati. Docente del corso: Ing. A. Tagarelli.

- **Partecipazioni a Seminari**

- 11 Dicembre 2014. Titolo del seminario: “*Recent Advances in Computational Proteomics*”. Relatore: Prof. Pedro A. Fernandes - Università di Porto. Sala Terenzi del Dipartimento di Chimica (cubo 12c, 6 piano).

- 28 Gennaio 2015. Titolo del seminario: “*Rational design of glycomimetic compounds targeting fungal transglycosylases*”. Relatore: Prof. Merino, Universidad de Zaragoza, Departamento de Química Orgánica Facultad de Ciencias, Campus San Francisco 50009 Zaragoza, Aragon. SPAIN. Aula “M. Terenzi” del Dipartimento di Chimica e Tecnologie Chimiche.
  
- 15 Giugno 2015. Titolo del seminario: “*Interaction of graphene with biological and biomimetic membranes*”. Relatore: Dr. Aravind Vijayaraghavan Lecturer in Graphene Science and Nanotechnology School of Materials, University of Manchester. Aula Circolare del Dipartimento di Farmacia e Scienze della Salute e della Nutrizione.
  
- 17 Giugno 2015. Titolo del seminario: “*Accreditamento dei laboratori e sicurezza degli alimenti*”. Relatori: Dott.ssa Silvia Tramontin e Dott. Federico Pecoraro - Dipartimento Laboratori di prova ACCREDIA. Aula Circolare del Dipartimento di Farmacia e Scienze della Salute e della Nutrizione.
  
- 22-23 Giugno 2015. Titolo del seminario: “*La chimica scienza della sicurezza e dello sviluppo sostenibile*”. Aula Magna dell’Università della Calabria.
  
- 12 Giugno 2017. Titolo del seminario: “*Conditional Targeted Somatic Mutagenesis In the Mouse*”. Prof. Daniel Metzger, direttore di ricerca dell’Istituto di Genetica e Biologia Molecolare e Cellulare (IGBMC9, di Strasburgo. Aula Seminari del Centro Sanitario, cubo 34/b (piano 3).

**GPER is involved in the regulation of the  
estrogen-metabolizing CYP1B1 enzyme in breast cancer**

Francesca Cirillo<sup>1\*</sup>, Michele Pellegrino<sup>1\*</sup>, Rocco Malivindi<sup>1</sup>, Vittoria Rago<sup>1</sup>, Silvia Avino<sup>1</sup>, Luigina Muto<sup>1</sup>, Vincenza Dolce<sup>1</sup>, Adele Vivacqua<sup>1</sup>, Damiano Cosimo Rigidacciolo<sup>1</sup>, Paola De Marco<sup>1</sup>, Anna Sebastiani<sup>1</sup>, Sergio Abonante<sup>2</sup>, Miki Nakajima<sup>3</sup>, Rosamaria Lappano<sup>1#</sup>, Marcello Maggiolini<sup>1#</sup>

<sup>1</sup>Department of Pharmacy, Health and Nutritional Sciences, University of Calabria, Rende, Italy;

<sup>2</sup>Regional Hospital Cosenza, Italy; <sup>3</sup>Faculty of Pharmaceutical Sciences, Kanazawa University, Kanazawa 920-1192, Japan.

\*The first two Authors contributed equally to the work

# Correspondence to:

Prof. Marcello Maggiolini, email: marcellomaggiolini@yahoo.it; marcello.maggiolini@unical.it

Dr. Rosamaria Lappano, email: lappanorosamaria@yahoo.it; [rosamaria.lappano@unical.it](mailto:rosamaria.lappano@unical.it)

## **Abstract**

The cytochrome P450 1B1 (CYP1B1) is a heme-thiolate monooxygenase involved in both estrogen biosynthesis and metabolism. For instance, CYP1B1 catalyzes the hydroxylation of E2 leading to the production of 4-hydroxyestradiol that may act as a potent carcinogenic agent. In addition, CYP1B1 is overexpressed in different tumors including breast cancer. In this scenario, it is worth mentioning that CYP1B1 expression is triggered by estrogens through the estrogen receptor (ER) $\alpha$  in breast cancer cells. In the present study, we evaluated whether the G protein estrogen receptor namely GPER may provide an alternate route toward the expression and function of CYP1B1 in ER-negative breast cancer cells, in main players of the tumor microenvironment as cancer associated fibroblasts (CAFs) that were obtained from breast cancer patients, in CAFs derived from a cutaneous metastasis of an invasive mammary ductal carcinoma and in breast tumor xenografts. Our results show that GPER along with the EGFR/ERK/c-Fos transduction pathway can lead to CYP1B1 regulation through the involvement of a half-ERE sequence located within the CYP1B1 promoter region. As a biological counterpart, we found that both GPER and CYP1B1 mediate growth effects *in vitro* and *in vivo*. Altogether, our data suggest that estrogens in ER-negative cell contexts may engage the alternate GPER signaling toward CYP1B1 regulation. Estrogen-CYP1B1 landscape via GPER should be taken into account in setting novel pharmacological approaches targeting breast cancer development.

**Keywords:** Breast cancer; Cancer-associated fibroblasts; CYP1B1; Estrogen; GPER.

## **Introduction**

Breast cancer is the most frequently diagnosed malignancy and the leading cause of cancer death in women worldwide [1]. A prolonged exposure to estrogens has been considered an important factor driving the initiation and progression of diverse hormone-dependent malignancies, including breast tumor [2]. The multifaceted biological effects triggered by estrogens are mainly mediated by the estrogen receptor (ER) $\alpha$  and ER $\beta$ , which acting as ligand-activated transcription factors stimulate cell survival, proliferation and migration [3]. The G protein estrogen receptor, GPER (also known as GPR30), has been recently shown to mediate estrogen action in both normal and malignant cells as well as in main components of the tumor stroma namely cancer-associated fibroblasts (CAFs) [4-5]. In this regard, it has been demonstrated that estrogenic GPER signaling triggers a network of transduction pathways including the transactivation of the epidermal growth factor receptor (EGFR), an increase of intracellular cyclic AMP (cAMP), calcium mobilization, the activation of mitogen-activated protein kinase (MAPK) and phosphatidylinositol 3-kinase/protein kinase B (PI3K/Akt) cascades [6]. These rapid GPER-mediated responses then lead to gene expression changes, cancer cell proliferation and migration [4]. Accordingly, GPER expression has been negatively correlated with relapse free survival and positively associated with tamoxifen resistance in patients with breast tumor [7-8].

Previous studies have indicated that certain metabolites of 17 $\beta$ -estradiol (E2) may influence the development of breast malignancy, therefore great attention has been addressed to a better understanding of the mechanisms involved in estrogen biosynthesis and metabolism as well as in the biological effects of estrogen metabolites [9-10]. For instance, it has been reported that diverse cytochrome P450 enzymes (CYP) contribute to key processes leading to the metabolism of E2 [11]. CYP1B1 (cytochrome P450, family 1, subfamily B, polypeptide 1), which is a heme-thiolate monooxygenase mainly expressed in endocrine-regulated tissues like breast, uterus and ovary, has been indicated as a primary enzyme involved in estrogen metabolism [12]. In addition, CYP1B1 has

been suggested to play an essential role in the development of various hormone-dependent tumors, including breast cancer, through the bio-transformation of endogenous estrogens and environmental carcinogens [9,13-16]. In this context, CYP1B1 is responsible for the metabolism of E2 into 4-hydroxyestradiol (4OHE2) that forms DNA adducts and generates free radicals leading to DNA damage and tumorigenesis in different tissues like breast [2,17-18]. Several compounds as dioxin, benzo(a) pyrene (BaP) and polycyclic aromatic hydrocarbons (PAHs) stimulate the transcription of CYP1B1 [19-20] as well as its metabolic activity [2]. It is worth noting that estrogens generate a feed-forward loop triggering the transcription of CYP1B1, which in turn is primarily involved in the metabolic conversion of these steroids [19,21-22]. For instance, the transcription of CYP1B1 was induced in breast and endometrial cancer cells by E2 through the activation of ER $\alpha$  and its binding to an estrogen responsive element (ERE) located within the CYP1B1 promoter sequence [21]. These findings may underline the physiological relevance of CYP1B1 regulation by estrogens in the landscape of the estrogen homeostasis and action, in particular in hormone-sensitive tissues [2, 21-22].

In order to provide a more comprehensive scenario through which estrogens may trigger the transcription of CYP1B1 and its metabolic activity in a feed-forward manner, we have ascertained that estrogenic GPER signaling regulates CYP1B1 expression in ER-negative and GPER-positive breast cancer cells, CAFs obtained from breast cancer patients and CAFs derived from a cutaneous metastasis of an invasive mammary ductal carcinoma (met-CAF). In addition, we have determined that ligand-activated GPER and CYP1B1 contribute to the proliferative responses observed in the aforementioned cells and also in breast tumor xenografts. Thus, GPER may be included among the transduction mediators through which estrogens generate a feed-forward loop driving CYP1B1 expression and its metabolic action toward breast cancer development.

## Results

**E2 and G-1 induce CYP1B1 expression through GPER-mediated signaling.** Previous studies ascertained that estrogens up-regulate CYP1B1 levels through ER $\alpha$  in diverse cancer cells [22], therefore we asked whether estrogens may trigger CYP1B1 expression through GPER in an ER-independent manner. Of note, E2 and the selective GPER agonist G-1 induced CYP1B1 mRNA (Fig. 1 A-B) and protein levels (Supplementary Figure S1) in cell contexts lacking ER but expressing GPER as SkBr3 breast cancer cells, CAFs and met-CAFs. Next, the silencing of GPER expression abrogated the CYP1B1 protein induction by E2 and G-1 in SkBr3 cells (Fig. 1 C-D), CAFs (Fig. 1 G-H) and met-CAFs (Fig. 1 K-L). In addition, we found that the EGFR inhibitor AG1478 (AG) and the MEK inhibitor PD98059 (PD) abrogate the increased expression of CYP1B1 upon E2 and G-1 treatments in SkBr3 cells (Fig. 1 E-F), CAFs (Fig. 1 I-J) and met-CAFs (Fig. 1 M-N). Taken together, these findings suggest that the GPER/EGFR/ERK transduction pathway is involved in CYP1B1 expression upon exposure to E2 and G-1 in our model systems.

**A half-ERE site is required for CYP1B1 transcription by E2 and G-1.** In order to provide novel insights into the transcriptional activation of CYP1B1 by E2 and G-1, we first ascertained that E2 and G-1 stimulate the luciferase activity of diverse CYP1B1 promoter deletion constructs in SkBr3 cells (Fig. 2 A), CAFs and met-CAFs (data not shown). Among other sequences, we focused on a half-ERE site [23-24] located from -120 to -110 respect to the transcription initiation site (TIS) of the CYP1B1 promoter (Fig. 2 B). By site-directed mutagenesis, we generated (see material and methods) two further deleted CYP1B1 promoter constructs containing (Fig. 2 C) or lacking (Fig. 2 D) the half-ERE site. Worthy, E2 and G-1 stimulated the luciferase activity only transfecting in SkBr3 cells (Fig. 2 E), CAFs (Fig. 2 F) and met-CAFs (Fig. 2 G) the plasmid containing the half-ERE site, hence suggesting that this site is involved in CYP1B1 transcription upon treatment with ligands used (see below). Thereafter, the luciferase activity of representative CYP1B1 promoter constructs induced by E2 and G-1 was no longer evident silencing GPER expression or in the

presence of the EGFR inhibitor AG1478 (AG) and the MEK inhibitor PD 98059 (PD) in SkBr3 cells (Supplementary Figure S2), both CAFs and met-CAFs (data not shown), in accordance with the results shown in figure 1. Collectively, these results indicate that E2 and G-1 regulate CYP1B1 transcription through the GPER/EGFR/ERK transduction pathway.

**c-Fos is involved in CYP1B1 expression by E2 and G-1.** In order to further assess the transduction mechanisms leading to the CYP1B1 expression, we ascertained that E2 and G-1 trigger c-Fos expression at both mRNA and protein levels in SkBr3 cells (Supplementary Figure S3 A-C), CAFs (Supplementary Figure S3 D-F) and met-CAFs (Supplementary Figure S3 G-I), according to our previous studies [25]. Considering that a half-ERE sequence may differ in only one nucleotide from a canonical AP1 binding site [23-24], we then established that E2 and G-1 trigger the recruitment of c-Fos to the half-ERE site located within the CYP1B1 promoter in SkBr3 cells (Fig. 3 A), CAFs and met-CAFs (data not shown), however this response was no longer evident transfecting the DN/c-Fos construct in SkBr3 cells (Fig. 3 B), CAFs and met-CAFs (data not shown). Further supporting these findings, the up-regulation of CYP1B1 protein levels and the transactivation of a representative CYP1B1 construct induced by E2 and G-1 was prevented transfecting SkBr3 cells, CAFs and met-CAFs with the DN/c-Fos (Fig. 3 C-H). Taken together, these data indicate that c-Fos is involved in the regulation of CYP1B1 by E2 and G-1.

**CYP1B1 activity is stimulated by E2 and G-1.** Previous investigations have suggested that an increased expression of CYP1B1 leads to its enhanced enzymatic activity in cancer cells [14, 26-27]. Therefore, we assessed that a treatment for 18 h with E2 and G-1 stimulate CYP1B1 activity in SkBr3 cells (Fig. 3 I), CAFs (Fig. 3 J) and met-CAFs (Fig. 3 K), as evaluated by EROD assay. Accordingly, we found that the selective CYP1B1 inhibitor named TMS abolishes the CYP1B1 enzymatic activity induced by E2 and G-1 (Fig. 3 I-K), thus suggesting its usefulness toward the evaluation of CYP1B1 involvement in certain biological responses (see below).

**GPER and CYP1B1 are involved in the up-regulation of growth regulatory genes by E2 and G-1.** Estrogenic GPER signaling has been shown to trigger relevant effects in cancer cells as well as in CAFs through the induction of growth regulators like cyclins [28-30]. Accordingly, we found that E2 and G-1 stimulate the expression of cyclin D1, cyclin E and cyclin A at both mRNA and protein levels in SkBr3 cells, CAFs and met-CAF, however these responses were abrogated using the GPER antagonist G15 as well as in the presence of the CYP1B1 inhibitor TMS (Fig. 4). Nicely fitting with these findings, the proliferative effects elicited by E2 and G-1 in SkBr3 cells, CAFs and met-CAF were prevented silencing GPER or CYP1B1 as well as in the presence of the GPER and CYP1B1 inhibitors, G15 and TMS, respectively (Fig. 5). Taken together, these results suggest that both GPER and CYP1B1 contribute to the growth responses prompted by E2 and G-1 in our model systems.

**GPER and CYP1B1 are involved in the growth effects triggered by E2 and G-1 in breast cancer xenografts.** In order to strengthen the aforementioned observations we turned to the high metastatic and invasive MDA-MB-231 breast cancer cells [31] that were used both *in vitro* and *in vivo* studies. First, we determined that E2 and G-1 induce CYP1B1 expression at both mRNA (Fig. 6 A) and protein levels through GPER (Fig. 6 B-E) also in these cells. Corroborating the results obtained in SkBr3 cells, CAFs and met-CAF, we thereafter ascertained that E2 and G-1 stimulate the luciferase activity of diverse CYP1B1 promoter constructs (Fig. 6 F) except for the half-ERE deleted plasmid (Fig. 6 G). Likewise, we found that E2 and G-1 up-regulate the expression of cyclin D1, cyclin E and cyclin A in MDA-MB-231 cells, however these responses were no longer evident silencing GPER (Fig. 6 H-I) or using the GPER antagonist G15 (Fig. 6 J) and the CYP1B1 inhibitor TMS (Fig. 6 K). Recapitulating the abovementioned findings, E2 and G-1 promoted the proliferation of MDA-MB-231 cells through GPER and CYP1B1, as ascertained silencing their expression (Fig. 6 L-N) and using G15 or TMS (Fig. 6 O). Then, in order to evaluate the role of CYP1B1 on tumor growth *in vivo*, 45-day-old female nude mice were injected with MDA-MB-231

cells into the mammary fat pad region and treated with vehicle, G-1 and TMS alone or in combination. These treatments were well tolerated as no change in body weight and in food or water consumption were observed together with no evidence of reduced motor function. Among the different groups of mice, no significant difference was assessed after the sacrifice in the mean weights or histologic features of the major organs (liver, lung, spleen and kidney), thus indicating a lack of toxic effects. Of note, TMS treatment prevented the tumor growth induced by G-1 (Fig. 7 A-B) and the up-regulation of cyclin protein levels in tumor homogenates (Fig. 7 C). In addition, an increased expression of the proliferative marker Ki67, together with that of cyclin D1, cyclin E and cyclin A was found in tumor tissue sections obtained from G-1 treated mice with respect to those treated with vehicle (Fig. 7 D). Worthy, these effects were prevented in the group of animals receiving G-1 in combination with TMS (Fig. 7 D). Overall, these data suggest that GPER and CYP1B1 are involved in the stimulatory effects exerted by E2 and G-1 in MDA-MB-231 breast cancer cells both *in vitro* and *in vivo*.

## Discussion

In the present study we have ascertained that estrogens through the alternate route, namely GPER, regulate CYP1B1 expression and function in diverse ER-negative breast cancer cells, CAFs obtained from breast cancer patients, CAFs derived from a cutaneous metastasis of an invasive mammary ductal carcinoma and in MDA-MB-231 that were used both *in vitro* and *in vivo*. In particular, we have demonstrated that estrogenic GPER signaling stimulate CYP1B1 expression through the activation of the GPER/EGFR/ERK transduction pathway and the recruitment of c-Fos to the half-ERE site located within the CYP1B1 promoter sequence. We have also disclosed that CYP1B1 is involved in the growth effects elicited by GPER ligands, as demonstrated silencing both GPER and CYP1B1 or using their inhibitors named G15 and TMS, respectively. In accordance with these findings, TMS abrogated the increase of the proliferative index Ki67 and the expression of diverse cyclins upon exposure to the selective GPER ligand G-1, as assessed in tumor homogenates and tissue sections. Overall, these findings provide novel evidence regarding the role of GPER on the estrogen-CYP1B1 landscape toward breast tumor progression, as recapitulated in figure 8.

Estrogens are involved in important physiological functions as the maintenance of the female reproductive system, however these steroids may also contribute to the development of breast malignancies [32]. Estrogen mainly act through the classical ER, nevertheless several studies have demonstrated that GPER can mediate the stimulatory effects of estrogens in both normal and malignant tissues, including breast cancer [4,28,33-34]. For instance, ligand-activated GPER triggers a network of transduction pathways such as EGFR, intracellular cyclic AMP, calcium mobilization, MAPK and PI3K, thus leading to the induction of genes involved in the proliferation, migration and invasion of cancer cells including breast tumor cells [33]. Likewise, a clinical correlation between GPER expression and increased tumor size, distant metastasis and recurrence has been found in human breast tumor specimens, suggesting that GPER levels may be predictive of aggressive breast malignancies [7,34]. Various studies have also revealed that certain GPER-

mediated responses to estrogens target important components of the tumor microenvironment driving cancer progression as CAFs [5]. In particular, GPER has been involved in the transcription of genes toward the proliferation, migration and adhesion/spreading of CAFs derived from breast tumor patients [5]. Worthy, in the present study we have ascertained that GPER mediates the stimulatory action of estrogens not only in CAFs obtained from primary breast malignancies but also in CAFs derived from a cutaneous metastasis of an invasive mammary ductal carcinoma. In this regard, it is worthy mentioning that metastasis-associated CAFs may elicit stimulatory effects in metastatic cancer cells similar to those triggered by CAFs at primary tumor sites [35]. Indeed, it is now unquestioned that both tumor growth and the essential steps of the metastatic process are not only dependent on cancer cells, but rather involve a promiscuous interaction between tumor cells and components of the tumor microenvironment as CAFs [36]. Likewise, recent observations have indicated that cancer cells might carry CAFs during their migration to metastatic sites, in such way these co-traveling cells may facilitate tumor development in further tissues [37].

Several studies have suggested that estrogens play a role in the development of hormone-sensitive tumors via oxidative estrogen metabolism [19]. CYP1B1 is a major E2 hydroxylase involved in estrogen biosynthesis and metabolism, generation of DNA damaging pro-carcinogens and resistance to anti-hormone therapies [14]. For instance, CYP1B1 catalyzes the hydroxylation of E2 leading to the formation of 4OHE2 [10], which may trigger the induction of estradiol-3,4-quinone, the strongest ultimate carcinogenic estrogen metabolite that, binding to the N-7 position of guanine, leads to the destabilization of the glycosidic bond and the subsequent DNA depurination and mutagenesis [2,20,22,38]. Considering that CYP1B1 expression has been reported increased in tumor tissues compared to the normal counterpart [16,39] and given that the levels of 4OHE2 have been found higher in hormone-sensitive tumors like breast cancer respect to normal tissues [20], this cytochrome has attracted increasing interest as potential target in further anticancer strategies, especially in the treatment of hormone-related tumors [40].

The transcription of CYP1B1 is mainly regulated by the aryl hydrocarbon receptor (AhR) that acts as a ligand-activated transcription factor [41]. Xenobiotics like dioxin, halogenated aromatic hydrocarbons, BaP and PAHs, are AhR activators of CYP1B1 transcription [20,41]. In accordance with our findings, it has been recently reported that G-1 is also able to up-regulate the expression of both AhR and CYP1B1 in ER-positive MCF-7 breast cancer cells, although the molecular mechanisms involved remain to be elucidated [42]. Furthermore, CYP1B1 can be regulated by other transcription factors as AhR nuclear translocator (ARNT) complex (AhR/ARNT), Sp1, cAMP-response element binding protein (CREB) and ER [22]. In this context, it is worth noting that CYP1B1 may be induced by its own substrates [2]. For instance, E2-activated ER $\alpha$  triggered the transcription of CYP1B1 through an estrogen responsive element (ERE) located within the CYP1B1 promoter sequence in MCF-7 cells [21]. These findings may indicate that the regulation of CYP1B1 expression and activity by its own substrates like estrogens would be pathophysiologically important for their metabolism and homeostasis in hormone-responsive tissues. In this scenario, our data provide novel insights into the current knowledge regarding the regulation of CYP1B1 by estrogens. Using as model systems ER-negative breast cancer cells, CAFs from a primary tumor, CAFs from a metastatic site and breast xenografts, we have determined that GPER may be an alternate route toward the regulation of CYP1B1 expression and function by estrogens in different biological targets. Worthy, the CYP1B1 inhibitor TMS prevented the stimulatory effects on tumor growth exerted by estrogenic GPER signaling both *in vitro* and *in vivo*, in accordance with previous studies that highlighted the ability of this agent to delay tumor progression in xenograft models [13]. TMS has been also proposed as a potential chemopreventive agent in hormone-sensitive tumors as it prevented the formation of the carcinogenic estrogen metabolite 4OHE2, it induced apoptotic cell death selectively in cancer cells and it reduced tumor volume of tamoxifen-resistant breast cancer xenografts [11,13,15,43-44]. Collectively, our findings suggest that GPER

may be included among the transduction mediators involved by estrogens in the regulation of CYP1B1 toward the development of breast cancer at both primary and metastatic sites.

## Materials and Methods

**Reagents.** 17 $\beta$ -Estradiol (E2), salicylamide (2-hydroxybenzamide), resorufin (7-hydroxy-3H-phenoxazin-3-one) and resorufin ethyl ether (7-ethoxy-3H-phenoxazin-3-one) were purchased from Sigma-Aldrich (Milan, Italy). G-1 (1-[4-(6-bromobenzol [1,3]diodo-5-yl)-3a,4,5,9b-tetrahydro3H5cyclopenta[c]quinolin-8yl]-ethanone), G-15 (3aS,4R,9bR)-4-(6-bromo-1,3-benzodioxol-5-yl)-3a,4,5,9b-3H-cyclopenta[c]quinolone and TMS 1-[2,(3,5-Dimethoxyphenyl)ethenyl]-2,4-dimethoxybenzene were obtained from Tocris Bioscience (Space, Milan, Italy). Tyrphostin AG1478 (AG) and PD98059 (PD) were obtained from Calbiochem (DBA, Milan, Italy). All the aforementioned compounds were dissolved in dimethyl sulfoxide (DMSO), except for salicylamide that was dissolved in methanol.

**Ethics statement.** All procedures conformed to the Helsinki Declaration for the research on humans. Signed informed consent was obtained from all patients and the experimental research has been performed with the ethical approval provided by the “Comitato Etico Regione Calabria, sezione area nord c/o azienda ospedaliera di Cosenza, Italy”.

**Cell cultures.** SkBr3 and MDA-MB-231 breast cancer cells were obtained by ATCC (Manassas, VA, USA), used less than 6 months after resuscitation and routinely tested and authenticated according to the ATCC suggestions. SkBr3 cells were maintained in RPMI-1640 (Life Technologies, Milan, Italy) without phenol red, supplemented with 10% fetal bovine serum (FBS) and 100 $\mu$ g/ml penicillin/streptomycin (Life Technologies, Milan, Italy). MDA-MB231 cells were maintained in DMEM (Dulbecco's modified Eagle's medium) (Life Technologies, Milan, Italy) with phenol red, with a supplement of 5% FBS and 100  $\mu$ g/ml of penicillin/streptomycin. CAFs obtained from breast malignancies and met-CAF obtained from biopsy of cutaneous metastasis in a patient with a primary invasive mammary ductal carcinoma, who previously had undergone surgery, were characterized and maintained as we have previously described [28,45]. Briefly, specimens were cut into smaller pieces (1–2mm diameter), placed in digestion solution (400 IU

collagenase, 100 IU hyaluronidase, and 10% serum, containing antibiotic and antimycotic solution) and incubated overnight at 37 °C. The cells were then separated by differential centrifugation at 90× g for 2min. Supernatant containing fibroblasts was centrifuged at 485× g for 8min; the pellet obtained was suspended in fibroblasts growth medium (Medium 199 and Ham's F12 mixed 1:1 and supplemented with 10% FBS) and cultured at 37°C in 5% CO<sub>2</sub>. Primary cells cultures of metastasis-derived fibroblasts were characterized by immunofluorescence. Briefly, cells were incubated with human anti-vimentin (V9) and human anti-cytokeratin 14 (LL001), both from Santa Cruz Biotechnology (DBA, Milan, Italy). To characterize fibroblasts activation, we used anti-fibroblast activated protein  $\alpha$  (FAP $\alpha$ ) antibody (H-56; Santa Cruz Biotechnology, DBA, Milan, Italy) (data not shown). CAFs and metastasis-derived CAFs were maintained in Medium 199 and Ham's F12 (mixed 1:1) supplemented with 10% FBS and 100 $\mu$ g/ml penicillin/streptomycin. All cell lines were grown in a 37°C incubator with 5% CO<sub>2</sub>. All cell lines to be processed for immunoblot and RT-PCR assays were switched to medium without serum and phenol red the day before treatments.

**Gene expression studies.** Total RNA was extracted and cDNA was synthesized by reverse transcription as previously described [46]. The expression of selected genes was quantified by real-time PCR using platform Quant Studio7 Flex Real-Time PCR System (Life Technologies). Gene-specific primers were designed using Primer Express version 2.0 software (Applied Biosystems). For CYP1B1, c-Fos, cyclin D1, cyclin E, cyclin A and the ribosomal protein 18S, which was used as a control gene to obtain normalized values, the primers were: 5'-TGTGCCTGTCACTATTCCTCATG-3' (CYP1B1 forward) and 5'-GGGAATGTGGTAGCCCAAGA-3' (CYP1B1 reverse); 5'-CGAGCCCTTTGATGACTTCCT-3' (c-Fos forward) and 5'-GGAGCGGGCTGTCTCAGA-3' (c-Fos reverse); 5'-GTCTGTGCATTTCTGGTTGCA-3' (cyclin D1 forward) and 5'-GCTGGAAACATGCCGGTTA-3' (cyclin D1 reverse); 5'-GCATGTCACCGTTCCTCCTTG-3' (cyclin A forward) and 5'-GGGCATCTTCACGCTCTATTTT-3' (cyclin A reverse); 5'-GATGACCGGGTTTACCCAAAC-3'

(cyclin E forward) and 5'-GAGCCTCTGGATGGTGCAA-3' (cyclin E reverse); 5'-GGCGTCCCCCAACTTCTTA-3' (18S forward) and 5'-GGGCATCACAGACCTGTTATT-3' (18S reverse). Assays were performed in triplicate and the results were normalized for 18S expression and then calculated as fold induction of RNA expression.

**Western Blot analysis.** Cells were grown in 10-cm dishes, exposed to treatments and then lysed in 500  $\mu$ L of 50 mmol/L NaCl, 1.5 mmol/L MgCl<sub>2</sub>, 1 mmol/L EGTA, 10% glycerol, 1% Triton X-100, 1% sodium dodecyl sulfate (SDS), and a mixture of protease inhibitors containing 1mmol/L aprotinin, 20 mmol/L phenylmethylsulfonyl fluoride and 200 mmol/L sodium orthovanadate. Protein lysates from tumor homogenates obtained from nude mice were processed as previously described [47]. Protein concentration was determined using Bradford reagent according to the manufacturer's recommendations (Sigma-Aldrich, Milan, Italy). Equal amounts of whole protein extract were resolved on a 10% SDS-polyacrylamide gel, transferred to a nitrocellulose membrane (Amersham Biosciences, Sigma-Adrich, Milan, Italy), probed overnight at 4 °C with antibodies against CYP1B1 (TA339934), cyclin D1 (TA801655), cyclin E (TA590076), cyclin A (TA890057) (OriGene Technologies, DBA, Milan, Italy), c-Fos (E8), GPER (N-15) and  $\beta$ -actin (C-2) (Santa Cruz Biotechnology, DBA). Proteins were detected by horseradish peroxidase-linked secondary antibodies (Santa Cruz Biotechnology, DBA) and then revealed using the chemiluminescent substrate for western blotting Westar Nova 2.0 (Cyanagen, Biogenerica, Catania, Italy).

**Gene Silencing Experiments.** Cells were plated into 10-cm dishes and transfected using X-treme GENE 9 DNA Transfection Reagent (Roche Diagnostics, Sigma-Adrich, Milan, Italy) for 24 h before treatments with a control shRNA, a shRNA for GPER (shGPER) or a shRNA for CYP1B1 (shCYP1B1, Santa Cruz Biotechnology, DBA, Milan, Italy). The silencing of GPER expression was obtained by using the constructs which we have previously described, and used [48].

**Bioinformatic tools.** The putative promoter sequences of CYP1B1 was retrieved from the National Center for Biotechnology Information (NCBI) (<http://www.ncbi.nlm.nih.gov>). Prediction of

transcription factors for CYP1B1 was performed using TRANSFAC (<http://www.generegulation.com>) site.

**Plasmids.** The plasmid DN/c-Fos, which encodes a c-Fos mutant that heterodimerizes with c-Fos dimerization partners but does not allow DNA binding, was a kind gift from Dr C Vinson (NIH, Bethesda, MD, USA). pGL3-promoter plasmid containing the 5'-flanking region from -2299 to +25 respect to the transcription initiation site (TIS) [49] of the CYP1B1 gene and CYP1B1 promoter deletion constructs containing fragments -1652 to +25, -1243 to +25, -1022 to +25, -988 to +25, -910 to +25 respect to TIS were generated as previously described [50].

**Site-directed mutagenesis.** The p-GL3-promoter plasmid containing the 5'-flanking region from -1652 to +25 respect to TIS of the CYP1B1 gene was used as template to generate as previously described [51] the DNA fragment from -513 to -95 respect to TIS containing a half-ERE site (see results section), which was amplified by PCR using the following primers: sense 5'-CGAGGTACCCTGATCTCGCCGCAAGAACT-3' and anti-sense 5'-GTCGCTAGCGCCGCACACCAGGCC-3'. The CYP1B1 deletion construct from -513 to -95 lacking the half-ERE site (see results section) was amplified by PCR using the following primers: sense 5'-CGAGGTACCCTGATCTCGCCGCAAGAACT-3' and anti-sense 5'-GTCGCTAGCGCCGCACACCAGGCCGACTCCCGTCCAGG-3'. The amplified DNA fragments were digested with KpnI and NheI and cloned into the pGL3-promoter plasmid (Promega, Milan, Italy). The sequence of each construct was verified by nucleotide sequence analysis.

**Transfections and luciferase assays.** Cells ( $1 \times 10^5$ ) were plated into 24-well dishes with 500  $\mu$ l/well of regular growth medium the day before transfection. Growth medium was replaced with medium lacking serum on the day of transfection, which was performed using X-tremeGene9 reagent, as recommended by the manufacturer (Roche Diagnostics), with a mixture containing 0.5  $\mu$ g of each reporter plasmid and 1 ng of pRL-TK. After 8 h, the medium was replaced with fresh medium lacking serum and the cells were incubated for 18 h with treatments. Luciferase activity

was then measured with the Dual Luciferase Kit (Promega, Milan, Italy) according to the manufacturer's recommendations. Firefly luciferase activity was normalized to the internal transfection control provided by the Renilla luciferase activity. The normalized relative light unit values obtained from cells treated with vehicle (-) were defined as one fold induction, relative to which the activity induced by treatments was calculated.

**Chromatin immunoprecipitation (CHIP) assay.** The cells grown on 10-cm plates were shifted for 24 h in a medium lacking serum and then exposed to treatments for 3 h. Thereafter, cells were cross-linked with 1% formaldehyde and sonicated. Supernatants were immuno-cleared with salmon DNA/protein A-agarose (Upstate Biotechnology, Inc., Lake Placid, NY, USA) and immunoprecipitated with anti c-Fos (H-125) or nonspecific IgG (Santa Cruz Biotechnology, DBA). Pellets were washed, eluted with a buffer consisting of 1% SDS and 0.1 mol/L NaHCO<sub>3</sub> and digested with proteinase K. DNA was obtained by phenol/chloroform extractions and precipitated with ethanol. A 4µl volume of each immunoprecipitated DNA sample and input were used as a template to amplify by PCR the region containing a half-ERE site located in the CYP1B1 promoter region. The primers used to amplify this fragment were as follows: 5'-CTGCTGGTAGAGCTCCGAGG-3' (forward) and 5'-CCCGCTGCTCTGCTTCTTAC-3' (reverse). Data were normalized to the input for the immunoprecipitation.

**Ethoxyresorufin-O-deethylase activity assay.** The cells ( $7 \times 10^4$  cells/ml) were grown in 24-well plates for 48 h, then were shifted for 24 h in a medium lacking serum and then treated for 18 h. The cells were washed with PBS, and fresh medium containing salicylamide to inhibit conjugating enzymes (1.5 mM) was added to the wells. The plate was incubated at 37°C for 5 min, then 7-ethoxyresorufin was added (final concentration of 5 µM) and the reaction was carried out for 1 hour at 37°C with gentle stirring of the plate every 5 min. Aliquots of cell suspensions (200 µL) were transferred to tubes and the reaction was terminated by the addition of an equal volume of ice-cold methanol, which resulted in immediate cell lysis. Then, samples were centrifuged at 3,000 rpm for

10 min and the supernatants transferred to an opaque 96-well plate and the fluorescence was read using Gene5 2.01 Software in Synergy H1 Hybrid Multi-Mode Microplate Reader (BioTek, AHSI, Milan Italy) with excitation and emission at 530 and 590 nm, respectively. Standard curves for resorufin formation were also performed. Data were normalized to total protein content, which was determined using the Bradford reagent according to the manufacturer's recommendations (Sigma-Aldrich, Milan, Italy).

**Proliferation assay.** Cells ( $1 \times 10^5$ ) were seeded in 24-well plates in regular growth medium, washed once they had attached and then incubated in medium containing 2.5% charcoal-stripped FBS, transfected for 24 h and then exposed to treatments. Transfection were renewed every 2 days and treatments every days. Cells were counted on day 5 using the Countess Automated Cell Counter, as recommended by the manufacturer's protocol (Life Technologies, Milan, Italy).

***In vivo* studies.** Female 45-day-old athymic nude mice (nu/nu Swiss; Envigo Laboratories) were maintained in a sterile environment. At day 0, exponentially growing MDA-MB-231 cells ( $2.5 \times 10^6$  per mouse) were inoculated in mammary fat pad in 0.1 mL of Matrigel (Cultrex; Trevigen Inc.). When the tumors reached average  $\sim 0.15 \text{ cm}^3$  (i.e., in about 1 week), mice were randomized and divided into four groups, according to treatments administered by intramuscular (G-1) and/or subcutaneous (TMS) injection for 21 days. The first group of mice ( $n = 7$ ) was treated daily with vehicle (0.9% NaCl with 0.1% albumin and 0.1% Tween-20; Sigma-Aldrich), the second group of mice ( $n = 7$ ) was treated daily with G-1 (0.5 mg/kg/die), the third group of mice ( $n = 7$ ) was treated daily with TMS (0.3 mg/kg/die), and the fourth group of mice ( $n = 7$ ) was treated daily with G-1 in combination with TMS (the concentrations were similar to those described above). G-1 and TMS were dissolved in DMSO at 1 mg/mL. MDA-MB-231 xenograft tumor growth was evaluated twice a week by caliper measurements, along two orthogonal axes: length (L) and width (W). Tumor volumes (in cubic centimeters) were estimated by the following formula:  $TV = L \times (W^2)/2$ . After 21 days of treatment, the animals were killed following the standard protocols and tumors were

dissected from the neighboring connective tissue. Specimens of tumors were frozen in nitrogen and stored at  $-80\text{ }^{\circ}\text{C}$ ; the remaining tumor tissues of each sample were fixed in 4% paraformaldehyde and embedded in paraffin for the histologic analyses. Animal experiments were conducted according to Italian law (D.L. 26/2014), the Guide for Care and Use of Laboratory Animals published by the US National Institutes of Health (2011), and the Directive 2010/63/EU of the European Parliament on the protection of animals used for Scientific research. The animal research project was approved by the Italian Ministry of Health, Rome (authorization n. 199/2015-PR).

**Immunohistochemistry.** Paraffin embedded sections,  $5\text{ }\mu\text{m}$  thick, were mounted on slides precoated with poly-lysine, and then they were deparaffinized and dehydrated (7-8 serial sections). Immunohistochemical experiments were performed after heat-mediated antigen retrieval. Hydrogen peroxide (3% in distilled water) was used, for 30 min, to inhibit endogenous peroxidase activity while normal goat serum (10%) was utilized, for 30 min, to block the non-specific binding sites. Immunodetection was carried out using anti-Ki67 and cyclin D1 (1:100) (DAKO, Denmark), cyclin E (1:200) (Bethyl Laboratories, Texas, USA) and cyclin A (1:50) (Abcam, DBA) primary antibodies at  $4^{\circ}\text{C}$  overnight. Then, a universal biotinylated IgG was applied (1:600) for 1 hour at RT, followed by ABC/HRP. Immunoreactivity was visualized by using DAB. The negative controls were made with DAKO mouse IGg1 (cod.X0931) for Ki67, DAKO immunoglobulin fraction (cod.X0936) for cyclin D1 at the same concentration of primary antibodies, rabbit serum at 5% for cyclin E and cyclin A. Sections were also counterstained with haematoxylin. Six-seven serial sections were processed for each sample from two independent operators.

**Imaging.** Tissue samples were visualized using an OLYMPUS BX41 microscope (Olympus Europa, Germany) and the images were taken with CSV1.14 software using a CAM XC-30 for images acquisition.

**Statistical analysis.** Statistical analysis was performed using ANOVA followed by Newman-Keuls' testing to determine differences in means. Statistical comparisons for in vivo studies were made using the Wilcoxon–Mann–Whitney test.  $P < 0.05$  was considered statistically significant.

## Abbreviations

**4OHE2:** 4-Hydroxyestradiol. **CAFs:** Cancer-associated fibroblasts. **CYP1B1:** Cytochrome P450, family 1, subfamily B, polypeptide 1. **E2:** 17 $\beta$ -estradiol. **EGFR:** Epidermal growth factor receptor. **ERE:** estrogen responsive element. **EROD:** Ethoxyresorufin-O-deethylase activity assay. **ER $\alpha$ :** Estrogen receptor  $\alpha$ . **GPGR:** G protein estrogen receptor. **MAPK:** Mitogen-activated protein kinase. **met-CAFs:** CAFs derived from a cutaneous metastasis of an invasive mammary ductal carcinoma. **TIS:** Transcription initiation site. **TMS:** 1-[2,(3,5-Dimethoxyphenyl)ethenyl]-2,4-dimethoxybenzene.

## Author contributions

Francesca Cirillo, Silvia Avino, Adele Vivacqua, Rosamaria Lappano and Marcello Maggiolini conceived and designed the experiments. Michele Pellegrino, Rocco Malivindi, Vittoria Rago, Sergio Abonante provided animals, acquired and managed patients and provided facilities. Luigina Muto, Vincenza Dolce, Miki Nakajima provided plasmids. Francesca Cirillo, Silvia Avino, Paola De Marco, Damiano Cosimo Rigracciolo, Anna Sebastiani performed experiments. Francesca Cirillo, Adele Vivacqua, Rosamaria Lappano analysed and interpreted data. Francesca Cirillo, Rosamaria Lappano and Marcello Maggiolini wrote the manuscript. All authors read and approved the final manuscript.

## Conflicts of interest

The authors have no financial or commercial conflicts of interest to declare

## Funding

This work was supported by Associazione Italiana per la Ricerca sul Cancro (IG 16719/2015).

## References

1. Siegel R, Naishadham D, Jemal A. Cancer Statistics, 2012. *CA Cancer J Clin.* 2012; 62: 10-29.
2. Tsuchiya Y, Nakajima M, Yokoi T. Cytochrome P450-mediated metabolism of estrogens and its regulation in human. *Cancer Lett.* 2005; 227: 115–124.
3. Yager JD, Davidson NE. Estrogen carcinogenesis in breast cancer. *N Engl J Med.* 2006; 354: 270-82.
4. Pandey DP, Lappano R, Albanito L, Madeo A, Maggiolini M, Picard D. Estrogenic GPR30 signalling induces proliferation and migration of breast cancer cells through CTGF. *EMBO J.* 2009; 28: 523–532.
5. Lappano R, Maggiolini M. GPER is involved in the functional liaison between breast tumor cells and cancer-associated fibroblasts (CAFs). *J Steroid Biochem Mol Biol.* 2017.
6. Prossnitz ER, Maggiolini M. Mechanisms of estrogen signaling and gene expression via GPR30. *Mol Cell Endocrinol.* 2009; 308: 32-8.
7. Filardo EJ, Graeber CT, Quinn JA, Resnick MB, Giri D, DeLellis RA, Steinhoff MM, Sabo E. Distribution of GPR30, a seven membrane-spanning estrogen receptor, in primary breast cancer and its association with clinicopathologic determinants of tumor progression. *Clin Cancer Res.* 2006; 12: 6359-66.
8. Ignatov A, Ignatov T, Weissenborn C, Eggemann H, Bischoff J, Semczuk A, Roessner A, Costa SD, Kalinski T. G-protein-coupled estrogen receptor GPR30 and tamoxifen resistance in breast cancer. *Breast Cancer Res Treat.* 2011; 128: 457-66.

9. Lu F, Zahid M, Wang C, Saeed M, Cavalieri EL, Rogan EG. Resveratrol Prevents Estrogen-DNA Adduct Formation and Neoplastic Transformation in MCF-10F Cells. *Cancer Prevention Research*. 2008; 1: 135-45.
10. Cavalieri EL, Rogan EG. Depurinating estrogen-DNA adducts generators of cancer initiation: their minimization leads to cancer prevention. *Clin Trans Med*. 2016; 5: 12.
11. Bruno RD, Njar VC. Targeting cytochrome P450 enzymes: A new approach in anti-cancer drug development. *Bioorg Med Chem*. 2007; 15: 5047–5060.
12. Parl FF, Dawling S, Roodi N, Crookeb PS. Estrogen Metabolism and Breast Cancer A Risk Model. *Steroid Enzymes and Cancer*. *Ann NY Acad Sci*. 2009; 1155: 68–75.
13. Liu J, Sridhar J, Foroozesh M. Cytochrome P450 Family 1 Inhibitors and Structure-Activity Relationships. *Molecules*. 2013; 18: 14470-14495.
14. Blackburn HL, Ellsworth DL, Shriver CD, Ellsworth RE. Role of cytochrome P450 genes in breast cancer etiology and treatment: effects on estrogen biosynthesis, metabolism, and response to endocrine therapy. *Cancer Causes Control*. 2015; 26: 319–332.
15. Kim T, Park H, Yue W, Wang J, Atkins KA, Zhang Z, Rogan EG, Cavalieri EL, Mohammad KS, Kim S, Santen RJ, and Sarah E. Tetra-methoxystilbene modulates ductal growth of the developing murine mammary gland. *Breast Cancer Res Treat*. 2011; 126: 779–789.
16. Kwon Y, Baek H, Ye D, Shin S, Kim D, Chun Y. CYP1B1 Enhances Cell Proliferation and Metastasis through Induction of EMT and Activation of Wnt/ $\beta$ -Catenin Signaling via Sp1 Upregulation. *PLoS ONE*. 2016; 11:e0151598.
17. Cavalieri E, Rogan E. Catechol quinones of estrogens in the initiation of breast, prostate, and other human cancers: keynote lecture. *Ann N Y Acad Sci*. 2006; 1089: 286-301.

18. Saini S, Hirata H, Majid S, Dahiya R. Functional Significance of Cytochrome P450 1B1 in Endometrial Carcinogenesis. *Cancer Res.* 2009; 69: 7038-45.
19. Gajjar K, Martin-Hirsch PL, Martin FL. CYP1B1 and hormone-induced cancer. *Cancer Letters.* 2012; 324: 13–30.
20. Go R, Hwang K, Choi K. Cytochrome P450 1 family and cancers. *Journal of Steroid Biochemistry & Molecular Biology.* 2015; 147: 24–30.
21. Tsuchiya Y, Nakajima M, Kyo S, Kanaya T, Inoue M, Yokoi T. Human CYP1B1 Is Regulated by Estradiol via Estrogen Receptor. *Cancer Research.* 2004; 64: 3119–3125.
22. Sissung TM, Price DK, Sparreboom A, Figg WD. Pharmacogenetics and Regulation of Human Cytochrome P450 1B1: Implications in Hormone-Mediated Tumor Metabolism and a Novel Target for Therapeutic Intervention. *Mol Cancer Res.* 2006; 4: 135–50.
23. Gaub MP, Bellard M, Scheuer I, Chambon P, Sassone-Corsi P. Activation of the Ovalbumin Gene by the Estrogen Receptor Involves the Fos- Jun Complex. *Cell Press.* 1990; 63: 1267-1276.
24. Kato S, Tora L, Yamauchi J, Masushige S, Beilard M, Chambon P. A Far Upstream Estrogen Response Element of the Ovalbumin Gene Contains Several Half-Palindromic 5'-TGACC-3' Motifs Acting Synergistically. *Cell Press.* 1992; 68: 731-742.
25. Santolla MF, Lappano R, De Marco P, Pupo M, Vivacqua A, Sisci D, Abonante S, Iacopetta D, Cappello AR, Dolce V, Maggiolini M. G protein-coupled estrogen receptor mediates the up-regulation of fatty acid synthase induced by 17 $\beta$ -estradiol in cancer cells and cancer-associated fibroblasts. *J Biol Chem.* 2012; 287: 43234-45.
26. Loaiza-Perez AI, Kenney S, Boswell J, Hollingshead M, Alley MC, Hose C, Ciolino HP, Yeh GC, Trepel JB, Vistica DT and Sausville EA. Aryl hydrocarbon receptor activation of an antitumor

- aminoflavone: Basis of selective toxicity for MCF-7 breast tumor cells. *Mol Cancer Ther.* 2004; 3: 715–25.
27. Martinez VG, O'Connor R, Liang Y, Clynes M. CYP1B1 expression is induced by docetaxel: effect on cell viability and drug resistance. *British Journal of Cancer.* 2008; 98: 564–570.
28. Madeo A, Maggiolini M. Nuclear alternate estrogen receptor GPR30 mediates 17 $\beta$ -estradiol - Induced gene expression and migration in breast cancer-associated fibroblasts. *Cancer Res.* 2010; 70: 6036–6046.
29. Vivacqua A, Romeo E, De Marco P, De Francesco EM, Abonante S, Maggiolini M. GPER mediates the Egr-1 expression induced by 17 $\beta$ -estradiol and 4-hydroxitamoxifen in breast and endometrial cancer cells. *Breast Cancer Res Treat.* 2012; 133: 1025.
30. Pisano A, Santolla MF, De Francesco EM, De Marco P, Rigracciolo DC, Perri MG, Vivacqua A, Abonante S, Cappello AR, Dolce V, Belfiore A, Maggiolini M, R Lappano. GPER, IGF-IR, and EGFR transduction signaling are involved in stimulatory effects of zinc in breast cancer cells and cancer-associated fibroblasts. *Mol Carcinog.* 2017; 56: 580-593.
31. de Ruijter TC, Veeck J, de Hoon JP, van Engeland M, Tjan-Heijnen VC. Characteristics of triple-negative breast cancer. *J Cancer Res Clin Oncol.* 2011; 137: 183-92.
32. Deroo BJ, Korach KS. Estrogen receptors and human disease. *J Clin Invest.* 2006; 116: 561–570.
33. Maggiolini M, Picard D. The unfolding stories of GPR30, a new membrane-bound estrogen receptor. *J Endocrinol.* 2010; 204: 105-14.
34. Prossnitz ER, Hathaway HJ. What have we learned about GPER function in physiology and disease from knockout mice? *J Steroid Biochem Mol Biol.* 2015; 153: 114-26.

35. Tommelein J, Verset L, Boterberg T, Demetter P, Bracke M, De Wever O. Cancer-associated fibroblasts connect metastasis-promoting communication in colorectal cancer. *Front Oncol.* 2015; 5: 63.
36. Guan X. Cancer metastases: challenges and opportunities. *Acta Pharm Sin B.* 2015; 5: 402-18.
37. Del Valle PR, Milani C, Brentani MM, Hirata Katayama ML, Carneiro de Lyra E, Carraro DM, Brentani H, Puga R, Lima LA, Bortman Rozenchan P, dos Santos Nunes B, Guedes Sampaio Góes JC, and MA Azevedo Koike Folgueira. Transcriptional profile of fibroblasts obtained from the primary site, lymph node and bone marrow of breast cancer patients. *Genetics and Molecular Biology.* 2014; 37: 480-489.
38. Chun Y, Kim S, Kim D, Lee S, Guengerich FP. A New Selective and Potent Inhibitor of Human Cytochrome P450 1B1 and Its Application to Antimutagenesis. *Cancer Research.* 2001; 61: 8164–8170.
39. Murray GI, Taylor MC, McFadyen MC, Melvin WT. Tumor-specific expression of cytochrome P450 CYP1B1. *Cancer Res.* 1997; 57: 3026–31.
40. Rochat B, Morsman JM, Murray GI, Figg WD, McLeod HL. Human CYP1B1 and anticancer agent metabolism: mechanism for tumor-specific drug inactivation? *J Pharmacol Exp Ther.* 2001; 296: 537–41.
41. Nebert DW, Dalton TP. The role of cytochrome P450 enzymes in endogenous signalling pathways and environmental carcinogenesis. *Nat Rev.* 2006; 6: 947–960.
42. Tarnow P, Tralau T, Luch A. G protein-coupled receptor 30 ligand G-1 increases aryl hydrocarbon receptor signalling by inhibition of tubulin assembly and cell cycle arrest in human MCF-7 cells. *Arch Toxicol.* 2016; 90(8):1939-48.

43. Chun Y, Lee S, Kim MY. Modulation of human Cytochrome P450 1B1 expression by 2,4,3',5'-tetramethoxystilbene. *Drug Metabolism and Disposition*. 2005; 33: 1771–1776.
44. Park H, Aiyar SE, Fan P, Wang J, Yue W, Okouneva T, Cox C, Jordan MA, Demers L, Cho H, Kim S, Song RX, Santen RJ. Effects of Tetramethoxystilbene on Hormone-Resistant Breast Cancer Cells: Biological and Biochemical Mechanisms of Action. *Cancer Res*. 2007; 67: 5717–26.
45. De Marco P, Lappano R, De Francesco EM, Cirillo F, Pupo M, Avino S, Vivacqua A, Abonante S, Picard D, and Maggiolini M. GPER signalling in both cancer-associated fibroblasts and breast cancer cells mediates a feedforward IL1 $\beta$ /IL1R1 response. *Sci Rep*. 2016; 6: 24354.
46. Rigracciolo DC, Scarpelli A, Lappano R, Pisano A, Santolla MF, De Marco P, Cirillo F, Cappello AR, Dolce V, Belfiore A, Maggiolini M, De Francesco EM. Copper activates HIF-1 $\alpha$ /GPER/VEGF signalling in cancer cells. *Oncotarget*. 2015; 6: 34158-77.
47. Santolla MF, Avino S, Pellegrino M, De Francesco EM, De Marco P, Lappano R, Vivacqua A, Cirillo F, Rigracciolo D C, Scarpelli A, Abonante S, and Maggiolini M. SIRT1 is involved in oncogenic signaling mediated by GPER in breast cancer. *Cell Death Dis*. 2015; 6: e1834.
48. Albanito L, Sisci D, Aquila S, Brunelli E, Vivacqua A, Madeo A, Lappano R, Pandey DP, Picard D, Mauro L, Andò S, Maggiolini M. Epidermal Growth Factor Induces G Protein-Coupled Receptor 30 Expression in Estrogen Receptor-Negative Breast Cancer. *Cells Endocrinology*. 2008; 149: 3799–3808.
49. Tang YM, Wo YP, Stewart J, Hawkins AL, Griffin CA, Sutter TR, Greenlee WF. Isolation and Characterization of the Human Cytochrome P450 CYP1B1 Gene. *J Biol Chem*. 1996; 271: 28324–28330.
50. Tsuchiya Y, Nakajima M, Yokoi T. Critical Enhancer Region to Which AhR/ARNT and Sp1 Bind in the Human CYP1B1 Gene. *J Biochem*. 2003; 133: 583–592.

51. Bonofiglio D, Santoro A, Martello E, Vizza D, Rovito D, Cappello AR, Barone I, Giordano C, Panza S, Catalano S, Iacobazzi V, Dolce V, Andò S. Mechanisms of divergent effects of activated peroxisome proliferator-activated receptor- $\gamma$  on mitochondrial citrate carrier expression in 3T3-L1 fibroblasts and mature adipocytes. *Biochim Biophys Acta*. 2013; 1831: 1027-36.

## Figure legends

### **Figure 1.** *GPER mediates CYP1B1 induction by E2 and G-1 in SkBr3 cells, CAFs and met-CAFs.*

E2 (10 nM) (A) and G-1 (100 nM) (B) induce the mRNA expression of CYP1B1, as indicated. Data obtained by real-time PCR in three independent experiments performed in triplicate were normalized to 18S expression and shown as fold changes of CYP1B1 expression upon treatments with E2 and G-1 respect to cells treated with vehicle (-). (■)  $P < 0.05$  for cells receiving treatments versus vehicle. The up-regulation of CYP1B1 protein levels induced by 10 nM E2 and 100 nM G-1 is abrogated in SkBr3 cells (C), CAFs (G) and met-CAFs (K) transfected for 24 h with shRNA or shGPER and then treated for 6 h with vehicle (-), 10 nM E2 and 100 nM G-1. (D, H, L) Efficacy of GPER silencing. Evaluation of CYP1B1 protein levels in SkBR3 cells (E-F), CAFs (I-J) and met-CAFs (M-N) upon treatment for 6 h with vehicle, 10 nM E2 and 100 nM G-1 alone or in combination with 1  $\mu$ M EGFR inhibitor AG1478 (AG) or 10  $\mu$ M MEK inhibitor PD98059 (PD).  $\beta$ -actin serves as a loading control. Results shown are representative of at least two independent experiments.

### **Figure 2.** *E2 and G-1-stimulate the transcriptional activation of CYP1B1 promoter constructs.* (A)

SkBr3 cells were transiently transfected for 8 h with the indicated CYP1B1 promoter constructs, then cells were treated for 18 h with vehicle (-), 10 nM E2 or 100 nM G-1. Schematic representation of the CYP1B1 5'-flanking region containing a half-ERE binding motif (B), a deletion construct containing a half-ERE binding motif (C) and a deletion construct lacking a half-ERE binding motif (D), as indicated. SkBr3 cells (E), CAFs (F) and met-CAFs (G) were transiently transfected for 8 h with the deleted CYP1B1 promoter constructs shown in panels C and D, then treated for 18 h with vehicle, 10 nM E2 and 100 nM G-1, as indicated. The luciferase activities were normalized to the internal transfection control and values of cells receiving vehicle were set as 1-fold induction upon which the activities induced by treatments were calculated. Each column

represents the mean  $\pm$  SD for three independent experiments, each performed in triplicate. (■) indicates  $P < 0.05$  for cells receiving treatments versus vehicle.

**Figure 3.** *c-Fos* is involved in the up-regulation of *CYP1B1* by *E2* and *G-1* in *SkBr3* cells, *CAFs* and *met-CAFs*. (A) Recruitment of *c-Fos* induced by 10 nM *E2* and 100 nM *G-1* to the half-ERE site located within the *CYP1B1* promoter sequence in *SkBr3* cells. In control samples non-specific IgG was used instead of the primary antibody. (B) *SkBr3* cells were transfected for 18 h with a vector or a construct encoding for a dominant negative form of *c-Fos* (DN/*c-Fos*), then treated for 3 h with vehicle (–), 10 nM *E2* and 100 nM *G-1* and thereafter submitted to the chromatin immunoprecipitation procedure using anti-*c-Fos* or nonspecific anti-IgG antibodies. The amplified sequences were evaluated by real-time PCR. *CYP1B1* protein levels in *SkBr3* cells (C), *CAFs* (E) and *met-CAFs* (G) transfected for 18 h with a vector or DN/*c-Fos* and then treated for 6 h with vehicle, 10 nM *E2* and 100 nM *G-1*, as indicated.  $\beta$ -actin serves as a loading control. Results shown are representative of at least two independent experiments. *SkBr3* cells (D), *CAFs* (F) and *met-CAFs* (H) were transfected for 18 h with a *CYP1B1* construct, a vector or DN/*c-Fos* and then treated for 18 h with vehicle, 10 nM *E2* and 100 nM *G-1*. The luciferase activities were normalized to the internal transfection control and values of cells receiving vehicle were set as 1-fold induction upon which the activities induced by treatments were calculated. *CYP1B1* activity evaluated by EROD assay in *SkBr3* cells (I), *CAFs* (J) and *met-CAFs* (K) treated for 18 h with vehicle (–), 10 nM *E2* and 100 nM *G-1* alone or in combination with 5 $\mu$ M *CYP1B1* inhibitor TMS. Fluorescence values of cells receiving vehicle were set as 1-fold induction upon which values induced by treatments were calculated. Each column represents the mean  $\pm$  SD for three independent experiments, each performed in triplicate. (■) indicates  $P < 0.05$  for cells receiving treatments versus vehicle (–).

**Figure 4.** *GPER* and *CYP1B1* mediate the up-regulation of cyclins *D1*, cyclin *E* and cyclin *A* by *E2* and *G-1* in *SkBr3* cells, *CAFs* and *met-CAFs*. Cyclin *D1*, cyclin *E* and cyclin *A* mRNA expression

in SkBr3 cells (A), CAFs (C) and met-CAFs (E) treated for 18 h with vehicle (–), E2 (10 nM) and G-1 (100 nM) alone or in combination with 100 nM GPER antagonist G15 and 5  $\mu$ M CYP1B1 inhibitor TMS, as evaluated by real-time PCR. Data obtained in three independent experiments performed in triplicate were normalized to 18S expression and shown as fold changes upon E2 and G-1 treatments respect to cells treated with vehicle. (■)  $P < 0.05$  for cells receiving treatments versus vehicle. Cyclin D1, cyclin E and cyclin A protein levels in SkBr3 cells (B), CAFs (D) and met-CAFs (F) upon treatments for 18 h with vehicle (–), E2 (10 nM) and G-1 (100 nM) alone or in combination with 100 nM GPER antagonist G15 and 5  $\mu$ M CYP1B1 inhibitor TMS.  $\beta$ -actin serves as a loading control. Results shown are representative of at least two independent experiments.

**Figure 5.** *GPER and CYP1B1 are involved in the proliferative effects induced by E2 and G1 in SkBr3 cells, CAFs and met-CAFs.* The proliferation of SkBr3 cells (A), CAFs (E) and met-CAFs (I) induced by 10 nM E2 or 100 nM G-1 is prevented silencing GPER or CYP1B1 expression. Cells were transfected every 2 days with shRNA, shGPER or shCYP1B1, treated every day with ligands and then counted on day 5. Efficacy of GPER (B, F, J) and CYP1B1 (C, G, K) silencing.  $\beta$ -actin serves as a loading control. The proliferation of SkBr3 cells (D), CAFs (H) and met-CAFs (L) induced by 10 nM E2 or 100 nM G-1 is prevented by 100 nM GPER antagonist G15 and 1  $\mu$ M CYP1B1 inhibitor TMS. Proliferation of cells treated with vehicle (–) was set as 100% upon which cell growth induced by treatments was calculated. Each data point is the mean  $\pm$  SD of three independent experiments performed in triplicate. (■)  $P < 0.05$  for cells receiving treatments versus vehicle.

**Figure 6.** *E2 and G-1 induce CYP1B1 expression through GPER in MDA-MB-231 breast cancer cells.* (A) E2 (10 nM) and G-1 (100 nM) induce CYP1B1 mRNA expression in MDA-MB-231 cells, as evaluated by real-time PCR. Data obtained in three independent experiments performed in triplicate were normalized to 18S expression and shown as fold changes upon E2 and G-1 treatments respect to cells exposed to vehicle (–). (B-C) CYP1B1 protein levels in MDA-MB-231

cells treated with 10 nM E2 and 100 nM G-1, as indicated. (D) CYP1B1 protein levels upon treatments with 10 nM E2 and 100 nM G-1 in cells transfected with shRNA or shGPER. (E) Efficacy of GPER silencing.  $\beta$ -actin serves as a loading control. Results shown are representative of at least two independent experiments. (F) Cells were transiently transfected for 8 h with the indicated CYP1B1 promoter constructs, then cells were treated for 18 h with vehicle (-), 10 nM E2 or 100 nM G-1. (G) Cells were transiently transfected for 8 h with the deleted CYP1B1 promoter constructs shown in figure 2C and 2D, then treated for 18 h with vehicle, 10 nM E2 and 100 nM G-1, as indicated. The luciferase activities were normalized to the internal transfection control and values of cells receiving vehicle were set as 1-fold induction upon which the activities induced by treatments were calculated. Each column represents the mean  $\pm$  SD for three independent experiments, each performed in triplicate. (H) Cyclin D1, cyclin E and cyclin A protein levels in cells transiently transfected with a shRNA or shGPER for 24 h, then treated for 18 h with vehicle, 10 nM E2 or 100 nM G-1. (I) Efficacy of GPER silencing. Cyclin D1, cyclin E and cyclin A protein levels in cells treated for 18 h with vehicle, 10 nM E2 and 100 nM G-1 alone or in combination with 100 nM GPER antagonist G15 (J) and 5  $\mu$ M CYP1B1 inhibitor TMS (K).  $\beta$ -actin serves as a loading control. Results shown are representative of at least two independent experiments. (L) Cell proliferation induced by 10 nM E2 or 100 nM G-1 is prevented silencing GPER or CYP1B1 expression. Cells were transfected every 2 days with shRNA, shGPER or shCYP1B1, treated every day with ligands and then counted on day 5. Efficacy of GPER (M) and CYP1B1 (N) silencing.  $\beta$ -actin serves as a loading control. (O) Cell proliferation induced by 10 nM E2 or 100 nM G-1 is prevented by 100 nM GPER antagonist G15 and 1  $\mu$ M CYP1B1 inhibitor TMS. Proliferation of cells treated with vehicle was set as 100% upon which cell growth induced by treatments was calculated. Each data point is the mean  $\pm$  SD of three independent experiments performed in triplicate. (■)  $P < 0.05$  for cells receiving treatments versus vehicle.

**Figure 7.** *CYP1B1* is involved in the growth of MDA-MB-231 xenografts. (A) Tumor volume from MDA-MB-231 xenografts implanted in female athymic nude mice treated for 21 days with vehicle, G-1, TMS or both compounds, as indicated. (\*) indicates  $P < 0.05$  for animals treated with G-1 versus animals treated with vehicle. (B) Representative images of explanted tumors at day 21, scale bar, 0.3 cm. (C) Cyclin D1, cyclin E, cyclin A protein levels in tumor homogenates from MDA-MB-231 xenografts treated as reported above.  $\beta$ -actin serves as loading control. Results shown are representative of two independent experiments. (D) Ki67, cyclin D1, cyclin E and cyclin A immunodetection in paraffin embedded sections of explanted tumors from breast cancer xenografts treated with vehicle, G-1 and TMS alone or in combination, as indicated. Scale bar: 25 $\mu$ m. Insert: negative control. Histograms represent the percentage ( $\pm$  SD) of immunostained positive cells treated with G-1 and TMS alone or in combination versus vehicle treated cells. (\*) indicates  $P < 0.05$ .

**Figure 8.** *Schematic representation of CYP1B1 regulation by GPER-mediated signaling, as evidenced in breast cancer cells, CAFs and met-CAFs.*

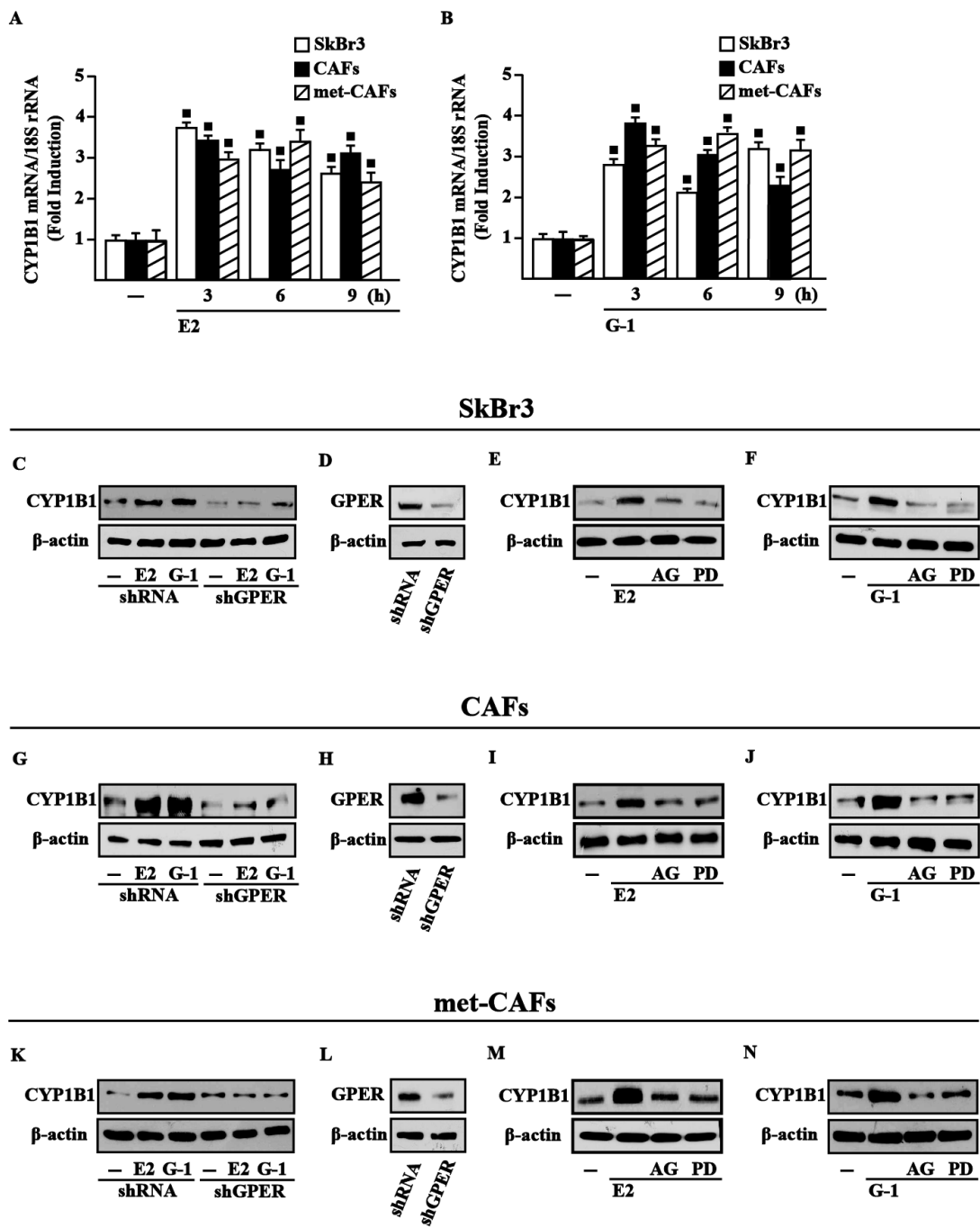


**Fig.1**

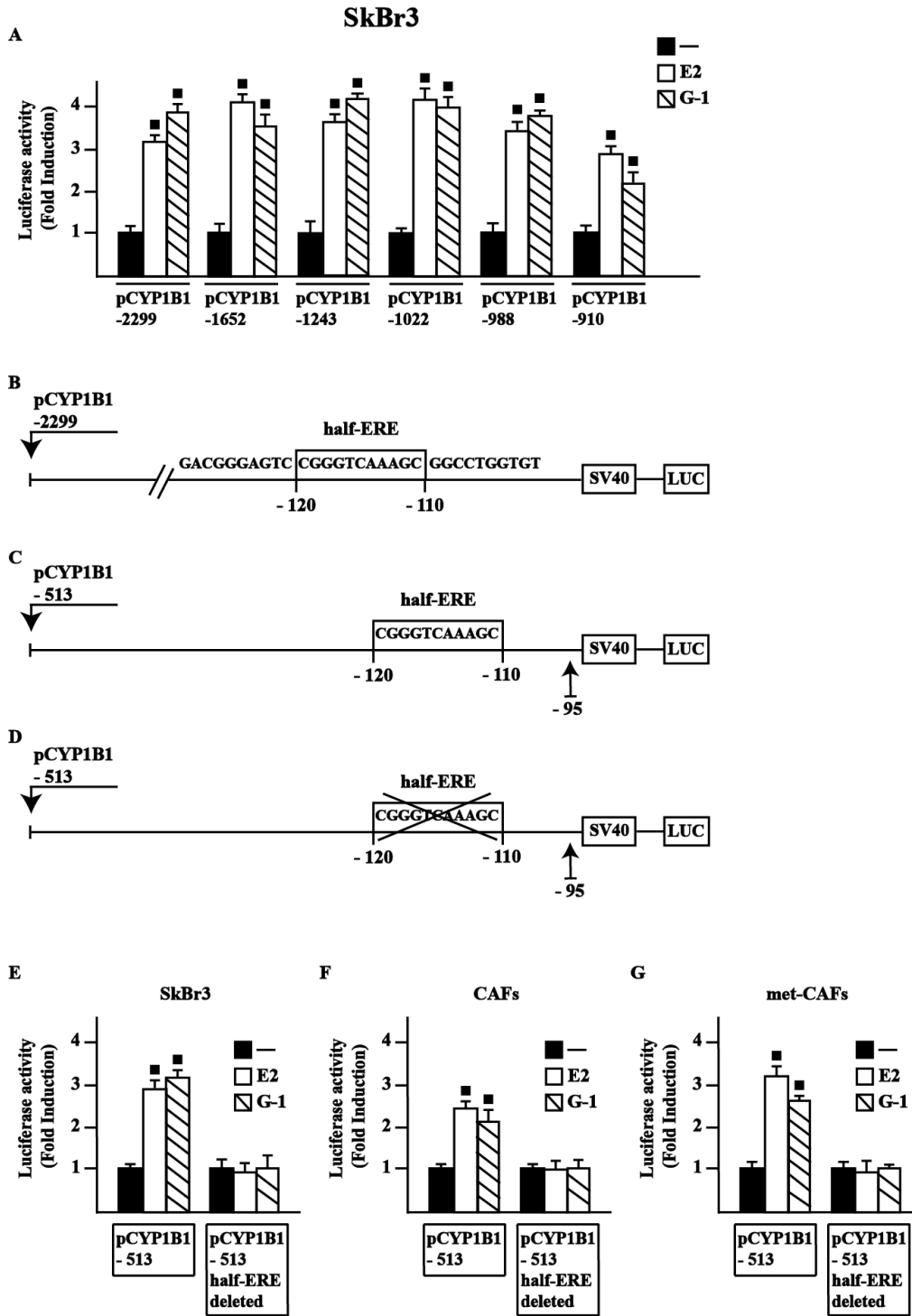
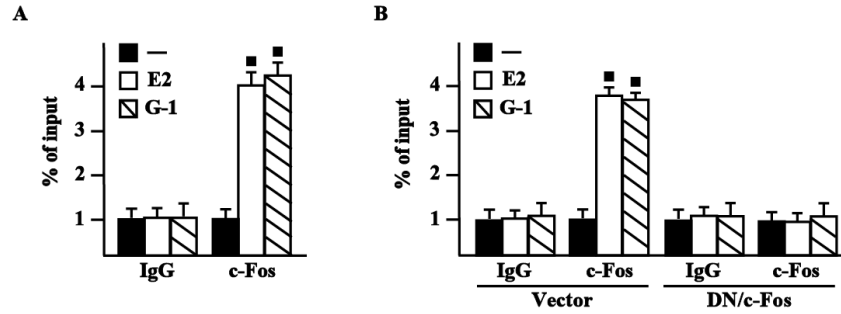
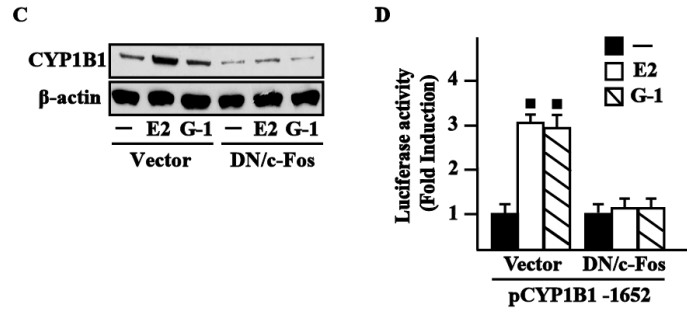


Fig.2

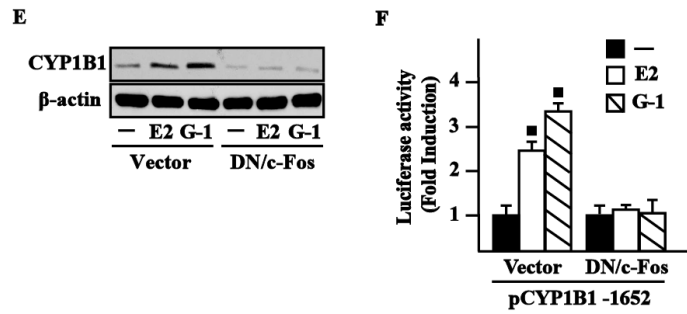
### SkBr3



### SkBr3



### CAFs



### met-CAFs

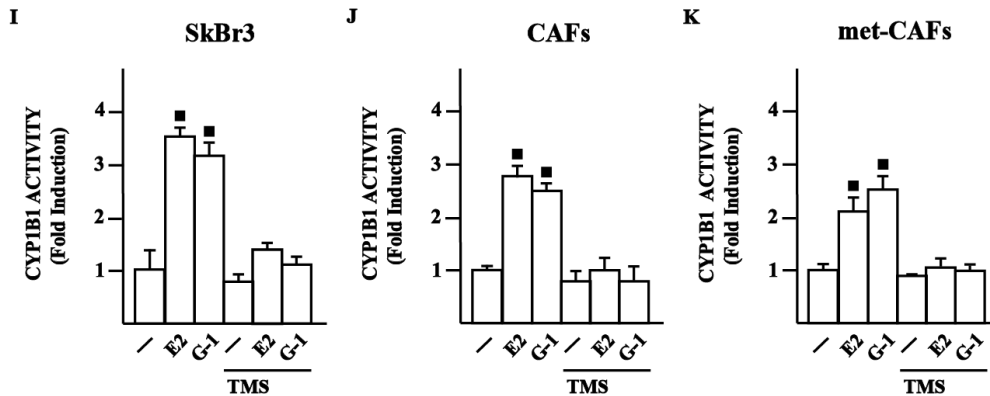
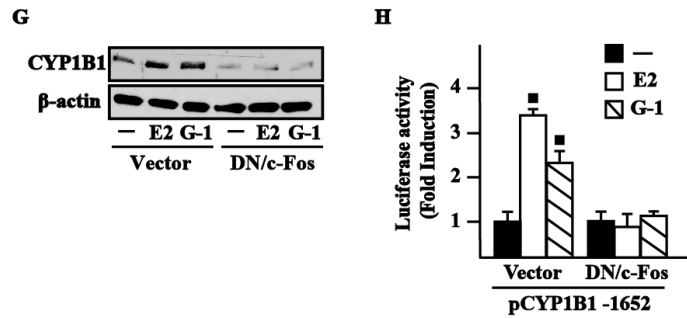
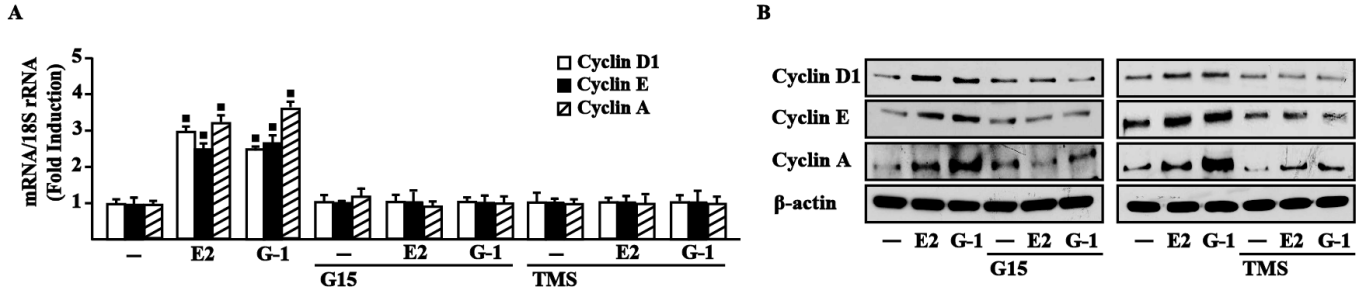
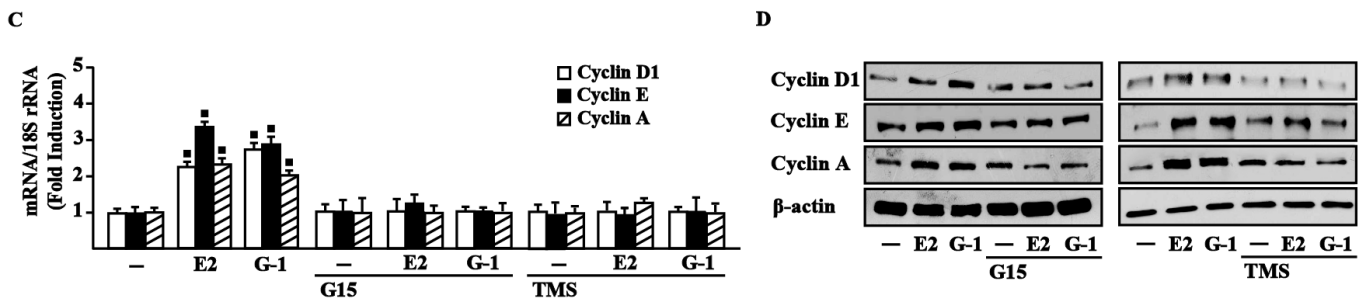


Fig.3

### SkBr3



### CAFs



### met-CAFs

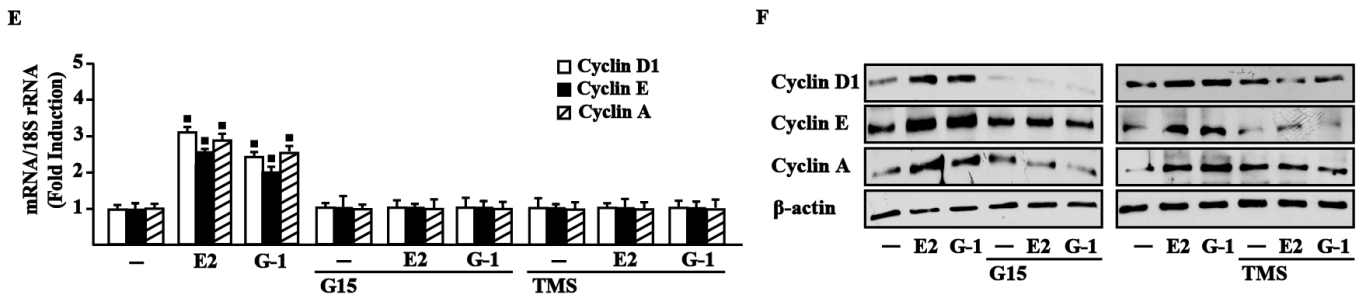
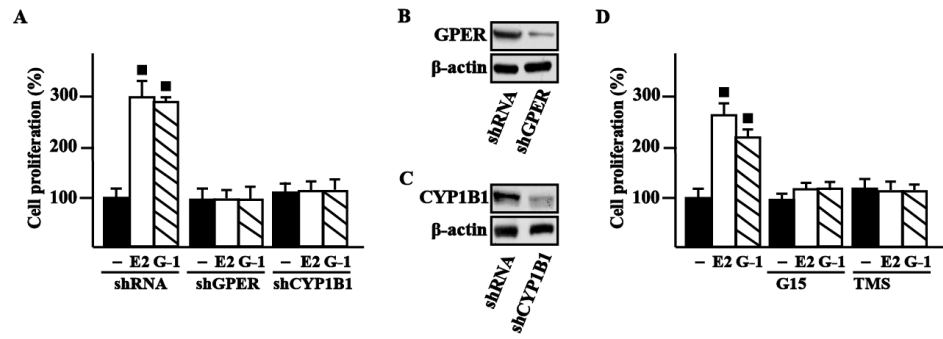
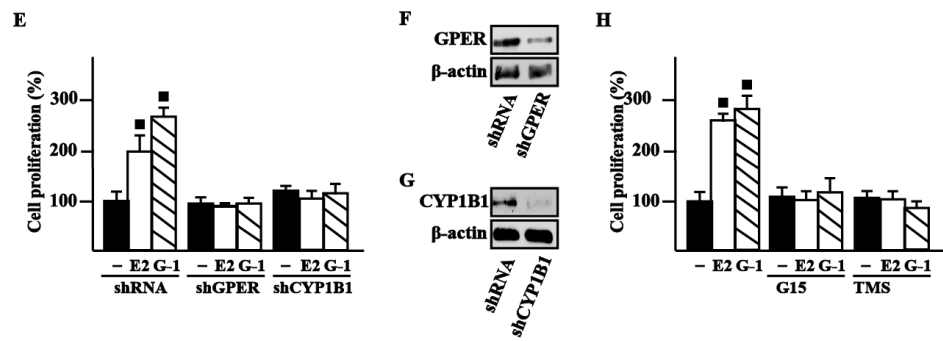


**Fig.4**

### SkBr3



### CAFs



### met-CAFs

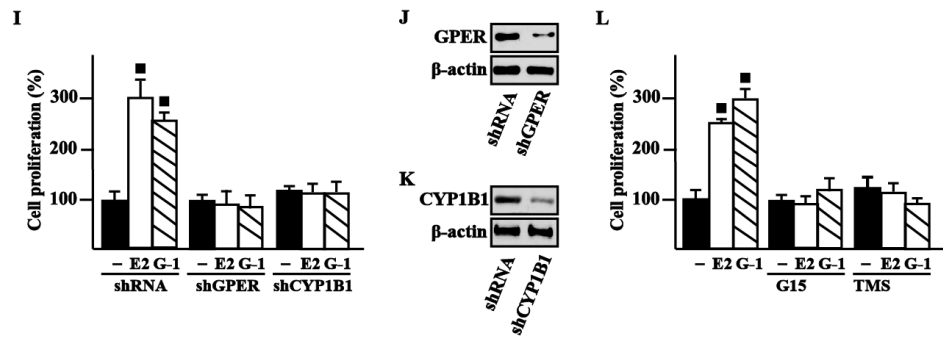


**Fig.5**

MDA-MB-231

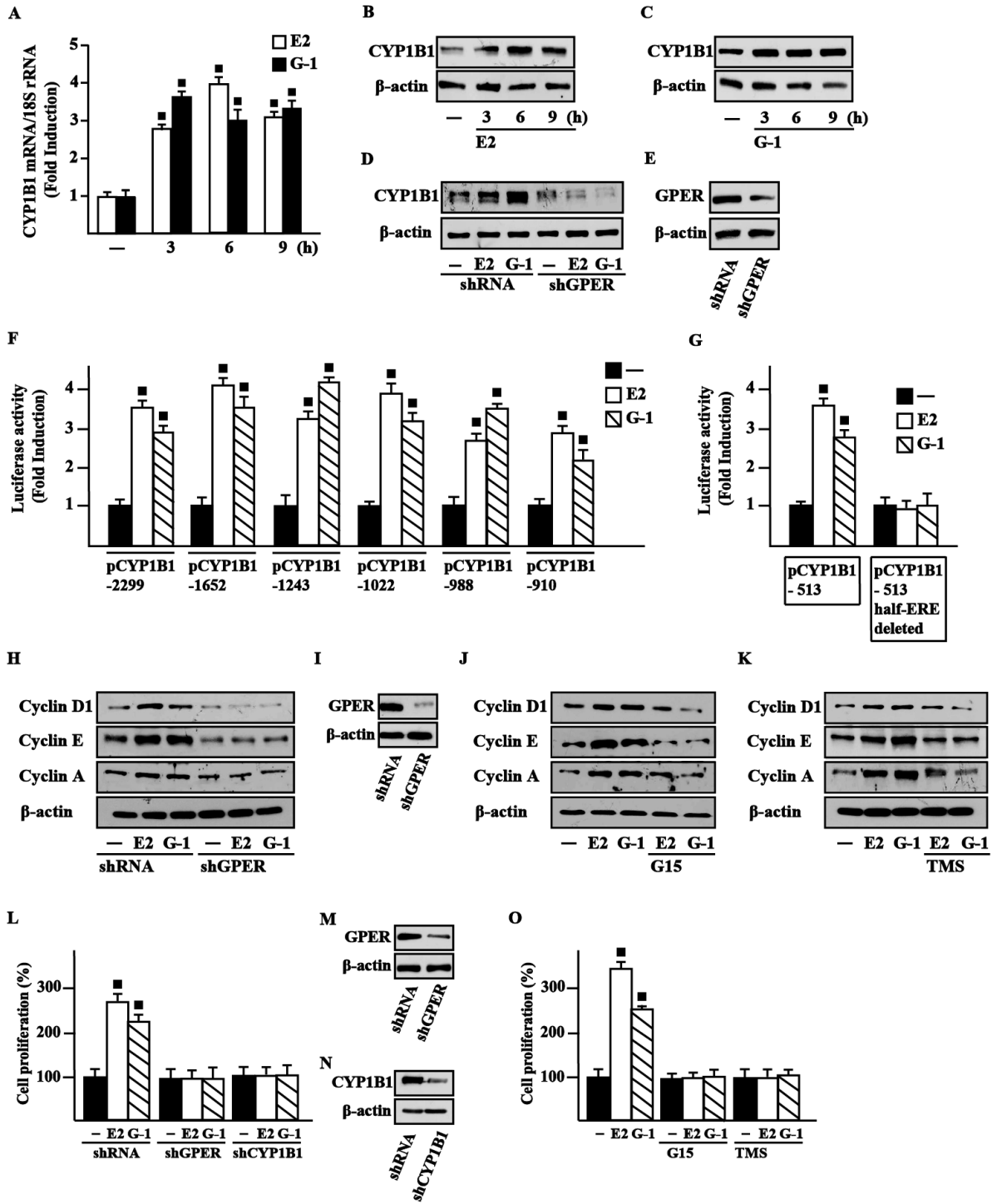
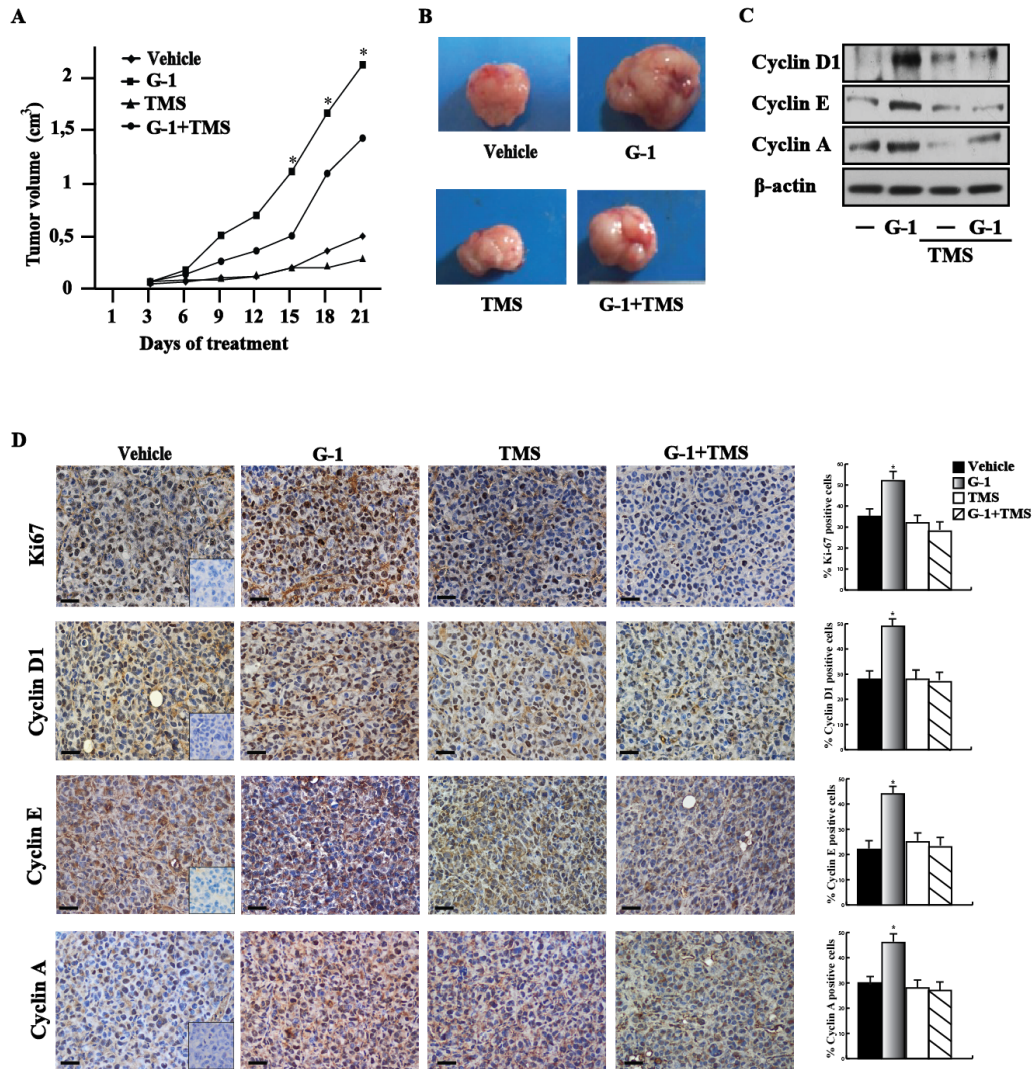


Fig.6



**Fig.7**

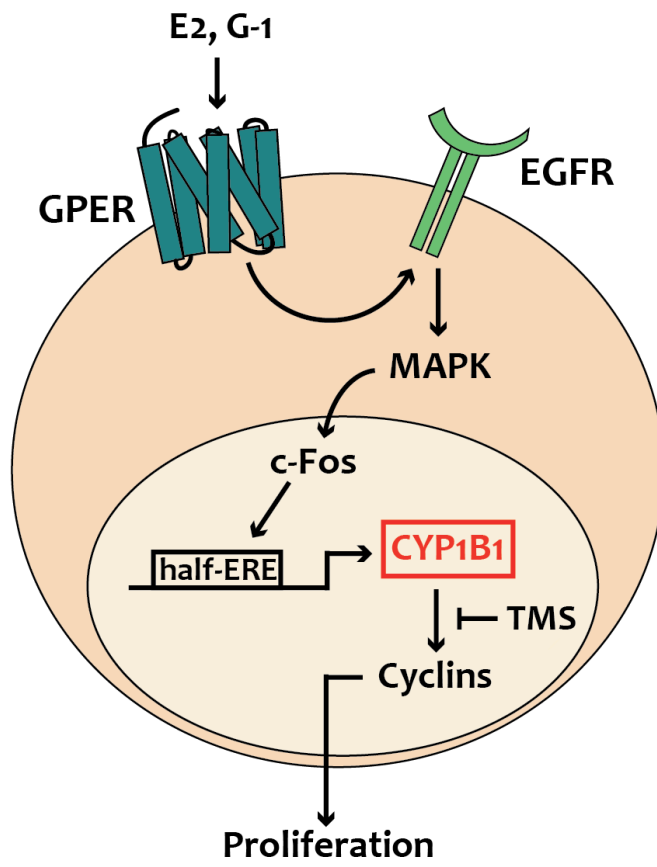


Fig. 8

## ARTICLE

# The lauric acid-activated signaling prompts apoptosis in cancer cells

Rosamaria Lappano<sup>1</sup>, Anna Sebastiani<sup>1</sup>, Francesca Cirillo<sup>1</sup>, Damiano Cosimo Rigracciolo<sup>1</sup>, Giulia Raffaella Galli<sup>1</sup>, Rosita Curcio<sup>1</sup>, Roberta Malaguarnera<sup>2</sup>, Antonino Belfiore<sup>2</sup>, Anna Rita Cappello<sup>1</sup> and Marcello Maggiolini<sup>1</sup>

The saturated medium-chain fatty-acid lauric acid (LA) has been associated to certain health-promoting benefits of coconut oil intake, including the improvement of the quality of life in breast cancer patients during chemotherapy. As it concerns the potential to hamper tumor growth, LA was shown to elicit inhibitory effects only in colon cancer cells. Here, we provide novel insights regarding the molecular mechanisms through which LA triggers antiproliferative and pro-apoptotic effects in both breast and endometrial cancer cells. In particular, our results demonstrate that LA increases reactive oxygen species levels, stimulates the phosphorylation of EGFR, ERK and c-Jun and induces the expression of c-fos. In addition, our data evidence that LA via the Rho-associated kinase-mediated pathway promotes stress fiber formation, which exerts a main role in the morphological changes associated with apoptotic cell death. Next, we found that the increase of p21<sup>Cip1/WAF1</sup> expression, which occurs upon LA exposure in a p53-independent manner, is involved in the apoptotic effects prompted by LA in both breast and endometrial cancer cells. Collectively, our findings may pave the way to better understand the anticancer action of LA, although additional studies are warranted to further corroborate its usefulness in more comprehensive therapeutic approaches.

*Cell Death Discovery* (2017) 3, 17063; doi:10.1038/cddiscovery.2017.63; published online 18 September 2017

## INTRODUCTION

Fatty acids are acyclic carboxylic acids with aliphatic tails of different lengths. Based on their carbon atom chain length, fatty acids are classified into the following three groups: short-chain fatty acids with < 6 carbon atoms, medium-chain fatty acids (MCFAs) and long-chain fatty acids that contain 6–12 carbons and > 12 carbons, respectively.<sup>1</sup> Fatty acids are major components of triacylglycerols, phospholipids and other complex lipids, therefore representing main contributors to dietary fat in humans.<sup>2</sup> Plant oils like palm, coconut and olive oils, nuts, seeds and seed oils, cocoa butter and animal-derived fats as lard, tallow and butter, are rich of fatty acids that are important components of cell membranes and essential sources of energy.<sup>2</sup> Previous studies have demonstrated that fatty acids are also involved in diverse transduction pathways, in gene transcription and relevant biological events as cell metabolism, inflammation, apoptosis and production of bioactive lipid mediators, thus contributing to multiple patho-physiological responses.<sup>2–7</sup>

Lauric acid (LA), which is a saturated MCFA with 12 carbon atoms and the primary fatty acid of coconut oil, has been associated with certain health benefits of coconut oil intake.<sup>8–10</sup> LA is also contained in plant oils, fruits, seeds and in breast milk.<sup>11,12</sup> LA has been shown to elicit diverse actions in various tissues, including a potent antimicrobial property.<sup>8</sup> For instance, LA and the derivative monolaurin were reported to destroy cell membranes of gram-positive bacteria and lipid-coated viruses, to interfere with main cellular responses as the activation of transduction cascades and gene transcription, to stabilize cell membranes toward the prevention of bacterial resistance.<sup>8</sup> In addition, LA promoted inflammatory processes activating the

nuclear factor- $\kappa$ B transcription factor as well as stimulating the expression of cyclooxygenase-2 and pro-inflammatory cytokines.<sup>13</sup> LA was also associated with beneficial effects on the cardiovascular system due to its ability to increase the high-density lipoproteins<sup>14</sup> and to reduce the blood pressure and heart rate in both normotensive and hypertensive rats.<sup>15</sup> Moreover, LA prevented the prostatic hyperplasia induced by testosterone in rats,<sup>16</sup> triggered apoptosis in colon cancer cells through oxidative stress<sup>17</sup> and improved the sensitization of the EGFR inhibitor cetuximab in KRAS/BRAF mutated colorectal cancer cells.<sup>18</sup> It is worth mentioning that the consumption of virgin coconut oil during chemotherapy improved the global quality of life in patients with breast cancer.<sup>19</sup>

Here, we show for the first time that LA elicits antiproliferative and pro-apoptotic effects in breast and endometrial cancer cells promoting the generation of reactive oxygen species (ROS), the activation of transduction pathways and gene expression changes. In particular, the upregulation of the cyclin-dependent kinase inhibitor p21<sup>Cip1/WAF1</sup> upon LA exposure was found to be required for its anticancer properties. Our findings shed new light on the molecular mechanisms through which LA induces antiproliferative and pro-apoptotic responses in both breast and endometrial cancer cells toward its usefulness in more comprehensive therapeutic approaches.

## RESULTS

LA inhibits cancer cell viability

On the basis of previous findings showing that MCFAs may elicit apoptosis in certain cancer cells<sup>17,20</sup> and considering that in our

<sup>1</sup>Department of Pharmacy, Health and Nutritional Sciences, University of Calabria, Rende, Italy and <sup>2</sup>Department of Health Sciences, University Magna Graecia of Catanzaro, Catanzaro, Italy.

Correspondence: R Lappano (rosamaria.lappano@unical.it) or AR Cappello (annarita.cappello@unical.it)

Received 24 July 2017; accepted 2 August 2017; Edited by A Rufini

recent investigation LA exerted antiproliferative activity in diverse types of tumor cells,<sup>21</sup> we began the present study evaluating whether LA (Figure 1a) and a further MCFA namely capric acid (CA) (Figure 1b) may affect the viability of SkBr3 breast and Ishikawa endometrial cancer cells, which were used as model system. Only LA inhibited the viability of both cancer cell types (Figures 1c and d) without altering the growth of MCF-10A normal breast epithelial cells (Figure 1e), thus suggesting its specific potential to trigger antiproliferative effects in malignant cells.

#### LA triggers ROS generation and EGFR, ERK and c-Jun phosphorylation

To evaluate the molecular mechanisms involved in the ability of LA to lower cancer cell viability, we ascertained that LA triggers the phosphorylation of EGFR, ERK and c-Jun in both SkBr3 and Ishikawa cells (Figures 2a and b). These responses were no longer observed in the presence of the EGFR inhibitor (AG) (Figures 2c and d), whereas ERK activation by LA was abolished using the MEK inhibitor (PD) and the Rho-associated kinase (ROCK) inhibitor (Y) but it still persisted using the JNK inhibitor (SP) (Figures 2c and d). The phosphorylation of c-Jun by LA was prevented in the presence of PD or SP, but not using the ROCK inhibitor Y (Figures 2c and d). Reminiscing previous data on the ability of LA to induce ROS levels in colon cancer cells,<sup>17</sup> we found that LA triggers ROS generation in our model system, yet this response was no longer evident using the ROS scavenger *N*-acetyl-L-cysteine (NAC, Figure 3a). Thereafter, we established that the phosphorylation of EGFR, ERK and c-Jun upon LA exposure is strictly dependent on ROS generation, as ascertained using NAC in both cell types (Figures 3b and c).

#### LA induces gene expression changes

Then, we assessed the expression levels of well-known cell cycle regulators as the member of the AP1 transcription factor complex namely c-fos, the tumor suppressor p53 and the cyclin-dependent kinase inhibitor p21<sup>Cip1/WAF1</sup>. In both SkBr3 and Ishikawa cells, LA upregulated the mRNA expression of c-fos and p21<sup>Cip1/WAF1</sup>, without altering the levels of p53 (Figures 4a and b). In addition, LA transactivated the AP1-luc responsive collagenase promoter construct that was transiently transfected in SkBr3 and Ishikawa cells and stimulated the transcriptional activity of reporter plasmids containing the c-fos and p21<sup>Cip1/WAF1</sup> promoter sequences (Figures 4c and d). According to the results obtained in real-time PCR, LA did not modify the p53 protein levels, whereas

it increased c-fos and p21<sup>Cip1/WAF1</sup> protein expression in both cell types (Figures 4e and f). We next ascertained that the ROS scavenger NAC, the EGFR inhibitor AG, the MEK inhibitor PD and the ROCK inhibitor Y prevent c-fos induction by LA (Figures 5a and b). Likewise, these compounds together with the JNK inhibitor SP repressed the increase of p21<sup>Cip1/WAF1</sup> protein levels elicited by LA (Figures 5a and b). As the upregulation of p21<sup>Cip1/WAF1</sup> protein levels was no longer evident transfecting a dominant-negative form of c-fos (DN/c-fos) in both SkBr3 and Ishikawa cells (Figures 5c and d), we ascertained by chromatin immunoprecipitation assay that LA induces the recruitment of c-fos to the AP1 site located within the p21<sup>Cip1/WAF1</sup> promoter sequence (Figure 5e). Overall, these data indicate that c-fos-AP1 transduction signaling is involved in the upregulation of p21<sup>Cip1/WAF1</sup> induced by LA.

LA promotes stress fiber formation and apoptosis in cancer cells Rho GTPases and their effectors as the Rho-associated protein kinase (ROCK) are key regulators of the cytoskeleton reorganization and the generation of the contractile force required for stress fiber formation.<sup>22</sup> In line with the aforementioned findings regarding the capability of the ROCK inhibitor to prevent LA-induced responses, in both SkBr3 and Ishikawa cells LA promoted the formation of stress fibers in a ROCK-dependent manner as this effect was abrogated in the presence of its inhibitor (Figures 6a-f) that alone did not show any effects (data not shown). Then, we assessed that LA increases the percentage of SkBr3 (Figures 7a-c) and Ishikawa (Figures 7d-f) TdT-mediated dUTP nick-end-labeling (TUNEL)-positive cells, however this effect was prevented in the presence of the ROS scavenger NAC (Figure 7). In addition, the apoptotic effects induced by LA were blocked in the presence of the p21<sup>Cip1/WAF1</sup> inhibitor UC2288 (Figure 7), suggesting that p21<sup>Cip1/WAF1</sup> is involved in the pro-apoptotic activity exerted by LA in breast and endometrial cancer cells.

#### DISCUSSION

The present study provides novel evidence regarding the molecular mechanisms through which LA elicits antiproliferative and pro-apoptotic effects in breast and endometrial cancer cells. In particular, we have ascertained that ROS generation induced by LA triggers the activation of the EGFR/ERK/AP1 transduction pathway, leading to the upregulation of p21<sup>Cip1/WAF1</sup> in a p53-independent manner.

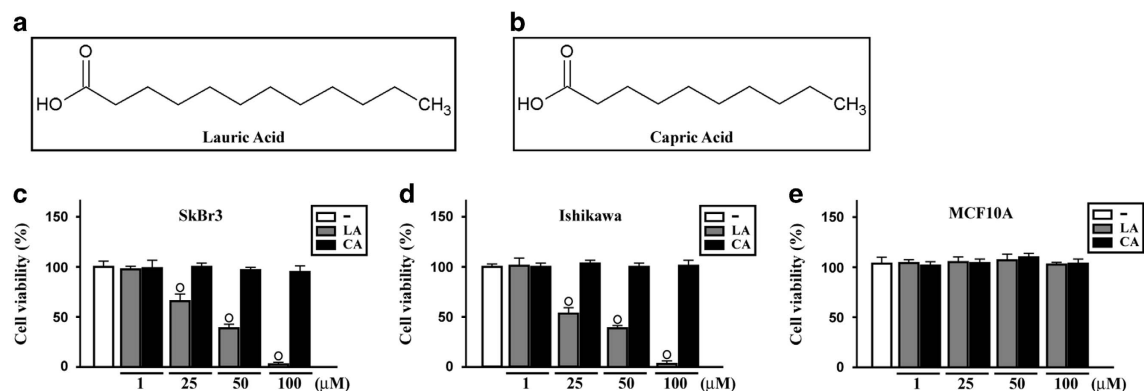


**Figure 1.** Lauric acid inhibits the proliferation of breast and endometrial cancer cells. (a, b) Chemical structures of lauric acid (LA) and capric acid (CA). (b-d) MTT growth assays in SkBr3 (c), Ishikawa (d) and MCF-10A (e) cells treated for 48 h with vehicle (-) or increasing concentrations of LA and CA, as indicated. Cell viability is expressed as the percentage of cells upon treatments respect to cells treated with vehicle. Values shown are mean  $\pm$  S.D. of three independent experiments performed in triplicate. (○) indicates  $P < 0.05$  for cells receiving vehicle versus treatments.

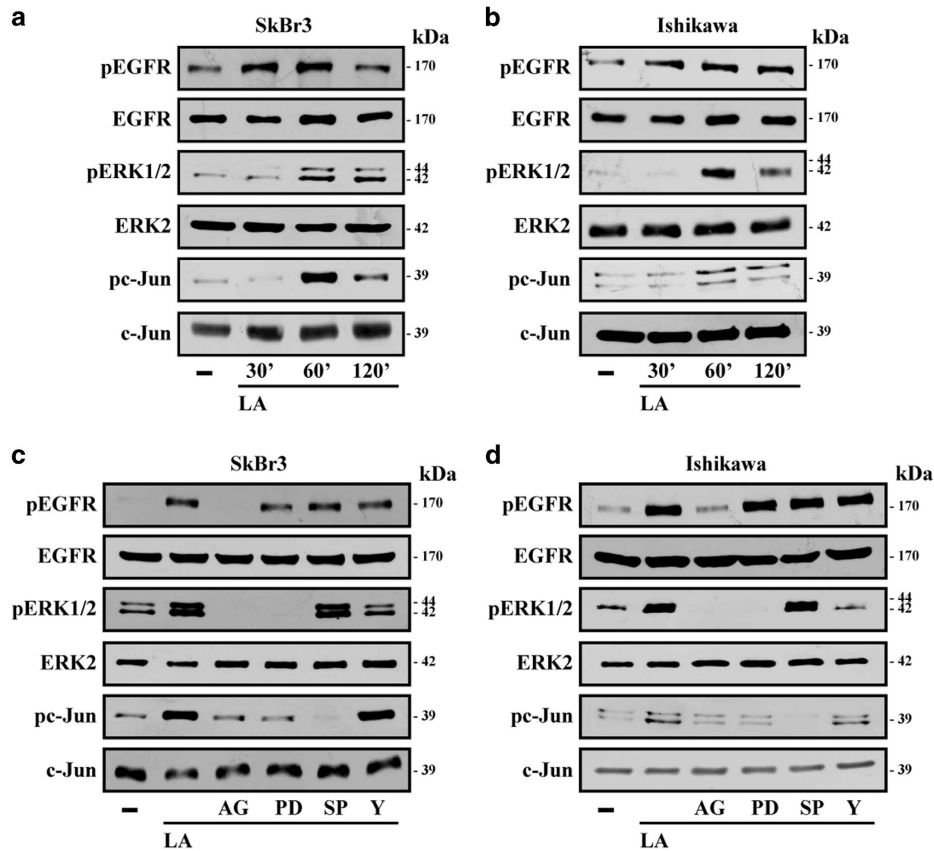


**Figure 2.** Lauric acid triggers rapid responses in breast and endometrial cancer cells. (a, b) Phosphorylation of EGFR, ERK1/2 and c-Jun in SkBr3 (a) and Ishikawa (b) cells treated with vehicle (–) and 100  $\mu$ M LA, as indicated. (c, d) EGFR, ERK1/2 and c-Jun activation in SkBr3 (c) and Ishikawa (d) cells treated for 60 min with vehicle or 100  $\mu$ M LA alone or in combination with 10  $\mu$ M EGFR inhibitor AG1478 (AG), 10  $\mu$ M MEK inhibitor PD98089 (PD), 1  $\mu$ M JNK inhibitor SP 600125 (SP) and 10  $\mu$ M ROCK inhibitor Y-27632 (Y). EGFR, ERK2 and c-Jun were used as loading controls for pEGFR, pERK1/2 and pc-Jun, respectively. Results shown are representative of at least two independent experiments.

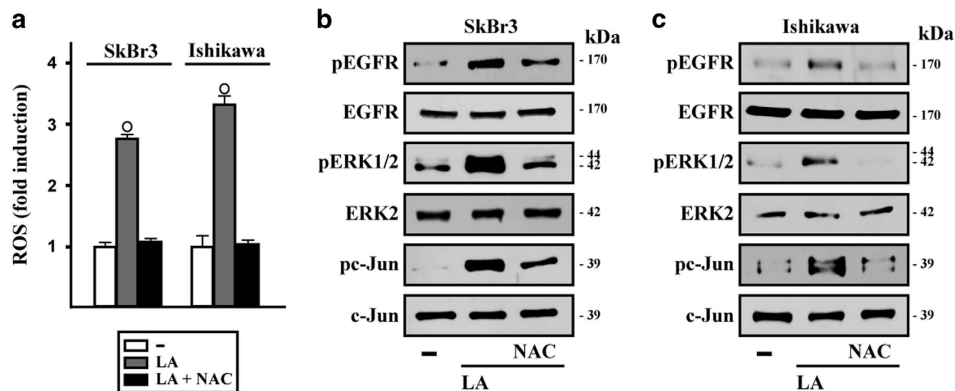


**Figure 3.** ROS generation by lauric acid is involved in the activation of transduction signaling observed in breast and endometrial cancer cells. (a) ROS production determined as DCF fluorescence in SkBr3 and Ishikawa cells treated for 60 min with vehicle (–) or 100  $\mu$ M LA alone or in combination with 300  $\mu$ M free radical scavenger NAC. DCF fluorescence obtained in cells treated with vehicle was set as onefold induction upon which ROS levels induced by treatments were calculated. Data shown are the mean  $\pm$  S.D. of three independent experiments performed in triplicate. (○) indicates  $P < 0.05$  for cells receiving vehicle versus treatments. EGFR, ERK1/2 and c-Jun activation in SkBr3 (b) and Ishikawa (c) cells treated for 60 min with vehicle or 100  $\mu$ M LA alone or in combination with 300  $\mu$ M NAC. EGFR, ERK2 and c-Jun were used as loading controls for pEGFR, pERK1/2 and pc-Jun, respectively. Results shown are representative of at least two independent experiments.

Fatty acids are structural components of cellular membranes either alone or together with other molecules as phospholipids and triacylglycerides.<sup>23</sup> In addition, fatty-acid oxidation occurring at the mitochondrial level plays a pivotal role in maintaining energy homeostasis during catabolic states.<sup>24</sup> Nevertheless, fatty acids are currently no longer considered as mere membrane structure regulators or energy sources as they also influence

diverse transduction signaling and cellular functions.<sup>2–7</sup> For instance, regulating transcription factors involved in lipid metabolism and inflammation, saturated fatty acids as LA may influence the biosynthesis of cholesterol and triacylglycerols, the assembly, secretion and clearance of lipoproteins, various metabolic and inflammatory processes.<sup>23</sup> Therefore, an increasing attention has been paid to the multifaceted role elicited by fatty

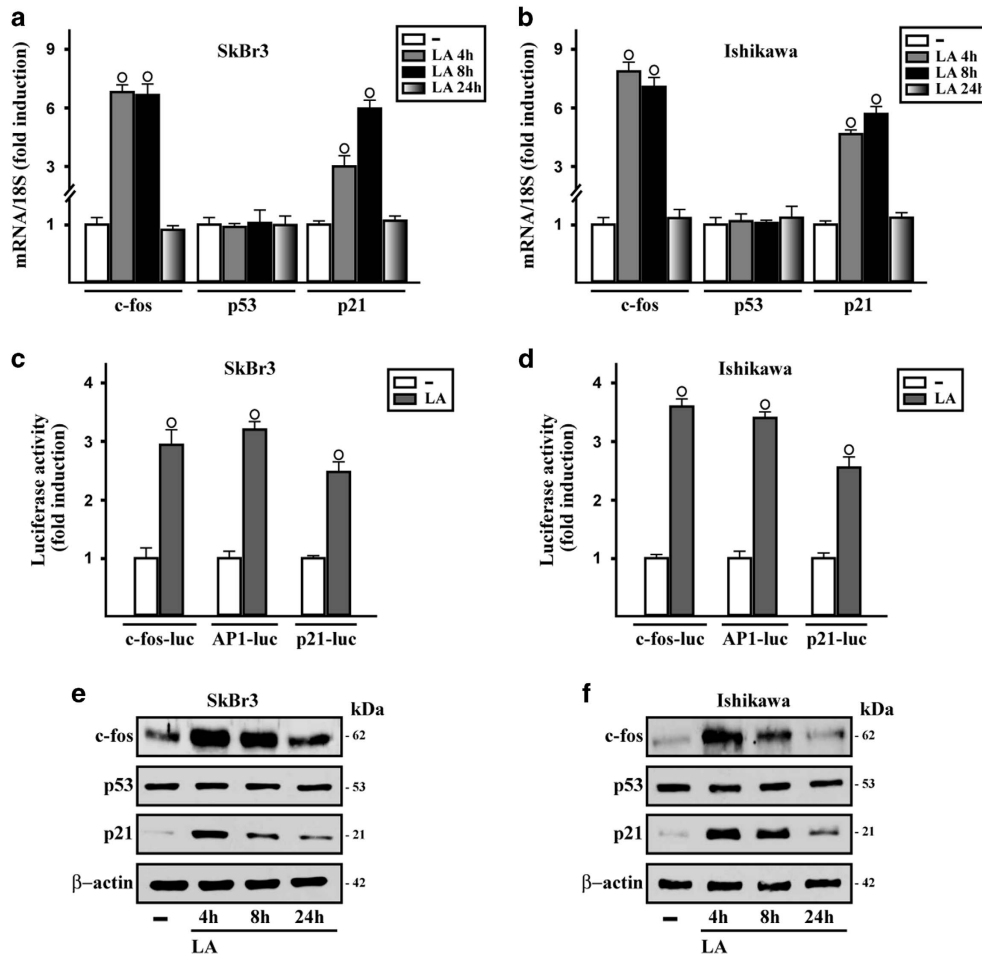


**Figure 4.** Lauric acid regulates the expression of cell cycle regulatory genes. The mRNA expression of c-fos, p53 and p21<sup>Cip1/WAF1</sup> (p21) was evaluated by real-time PCR in SkBr3 (a) and Ishikawa (b) cells treated with vehicle (–) or 100  $\mu$ M LA, as indicated. Data obtained from three independent experiments performed in triplicate were normalized to 18S expression and shown as fold changes of mRNA expression induced by LA respect to cells treated with vehicle. Evaluation of c-fos, AP1 and p21 luciferase reporter genes in SkBr3 (c) and Ishikawa (d) cells treated for 18 h with vehicle or 100  $\mu$ M LA. The luciferase activities were normalized to the internal transfection control, and values of cells receiving vehicle were set as onefold induction upon which the activity induced by treatments was calculated. Data shown are the mean  $\pm$  S.D. of three independent experiments performed in triplicate. (o) indicates  $P < 0.05$  for cells receiving vehicle versus treatments. c-fos, p53 and p21 protein levels in SkBr3 (e) and Ishikawa (f) cells treated with vehicle or 100  $\mu$ M LA, as indicated.  $\beta$ -actin was used as a loading control. Results shown are representative of at least two independent experiments.

acids on human health given that the amount and type of fatty acids contained in the diet are involved in the etiopathogenesis of diabetes, cancer and cardiovascular, immunity, inflammatory, renal, hepatic diseases.<sup>25</sup> In this context, coconut oil that is one of the richest sources of saturated fatty acids as LA, has attracted interest for its potential health benefits.<sup>26–29</sup> Furthermore, coconut oil has been shown to counteract the action of stimulatory agents in colon and mammary tumors in rats<sup>30,31</sup> and to improve the quality of life of breast cancer patients undergoing chemotherapy.<sup>19</sup> As it concerns LA, Fauser and co-workers<sup>17</sup> firstly demonstrated its ability to induce apoptosis in colon cancer cells through the reduction of glutathione levels and the generation of oxidative stress. In accordance with these and other observations showing that fatty acids may induce ROS generation in diverse types of cells,<sup>32–34</sup> we have extended these findings ascertaining that LA prompts ROS-mediated apoptosis also in breast and endometrial cancer cells through the subsequent activation of relevant transduction pathways. In this respect, it is worth mentioning that the EGFR and ERK signaling are mostly referred to as regulatory pathways of cell proliferation, migration and differentiation.<sup>35,36</sup> Nevertheless, these two main transduction mediators can also trigger apoptotic signals especially in the

context of tumor cells.<sup>35,36</sup> For instance, EGF through the cognate receptor induced the expression of the caspase 1 enzyme and p21<sup>WAF1/CIP1</sup> toward apoptosis and growth inhibition.<sup>35</sup> In addition, it has been demonstrated that free radicals generated by radiation exposure may elicit the activation of the EGFR/ERK signaling in cancer cells.<sup>36</sup> In line with these observations, we found that LA increases ROS levels that in turn trigger the EGFR/ERK transduction pathway and gene expression changes, therefore culminating in apoptotic responses in cancer cells.

Actin stress fibers have a pivotal role in many cellular functions, including cell adhesion, mobility, contraction and morphogenesis.<sup>37</sup> Stress fibers are also required for membrane blebbing, nuclear disintegration and apoptosis.<sup>38–41</sup> The small GTPase Rho and its main effector ROCK are involved in several cellular processes like the regulation of actin cytoskeleton, cell polarity, microtubule dynamics, gene transcription, cell cycle progression, differentiation, apoptosis and the formation of actin stress fibers.<sup>37,42–44</sup> In this vein, ROCK was shown to mediate the generation of stress fibers that in turn trigger the p21<sup>Cip1/WAF1</sup>-dependent apoptosis upon phorbol 12-myristate 13-acetate exposure in prostate cancer cells.<sup>40</sup> Further extending these data, our findings have determined for the first time that LA promotes

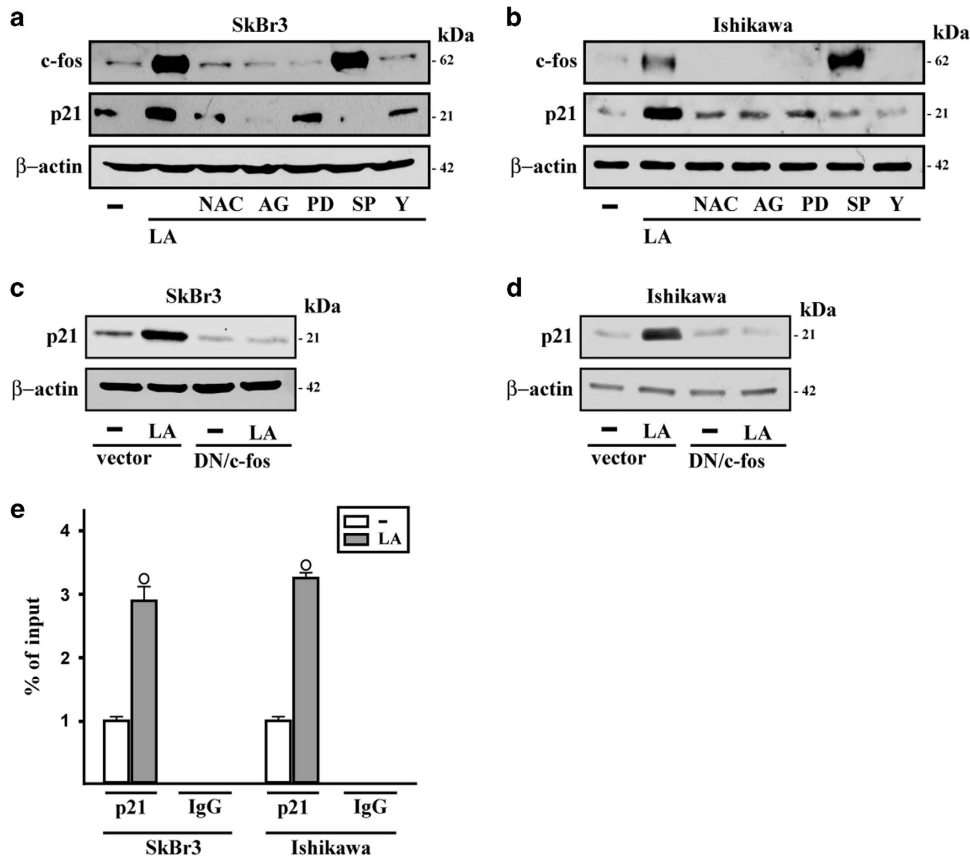


**Figure 5.** c-fos is involved in the upregulation of p21<sup>Cip1/WAF1</sup> induced by lauric acid. Immunoblots of c-fos and p21<sup>Cip1/WAF1</sup> (p21) in SkBr3 (a) and Ishikawa (b) cells treated for 4 h with vehicle (–) or 100  $\mu$ M LA alone or in combination with 300  $\mu$ M free radical scavenger NAC, 10  $\mu$ M EGFR inhibitor AG1478 (AG), 10  $\mu$ M MEK inhibitor PD98089 (PD), 1  $\mu$ M JNK inhibitor SP 600125 (SP) and 10  $\mu$ M ROCK inhibitor Y-27632 (Y). The expression vector encoding for a dominant-negative form of c-fos (DN/c-fos) blocked the upregulation of p21<sup>Cip1/WAF1</sup> protein levels induced by 100  $\mu$ M LA in SkBr3 (c) and Ishikawa (d) cells.  $\beta$ -actin was used as a loading control. Results shown are representative of at least two independent experiments. (e) Recruitment of c-fos induced by 100  $\mu$ M LA to the AP1 site located within the p21<sup>Cip1/WAF1</sup> promoter sequence in SkBr3 and Ishikawa cells, as indicated. In control samples non-specific IgG was used instead of the primary antibody. Each column represents the mean  $\pm$  S.D. of three independent experiments. (○) indicates  $P < 0.05$  for cells receiving vehicle versus treatments.

in breast and endometrial cancer cells the formation of stress fibers through the ROCK transduction pathway, thus suggesting that LA might be included among the activators of the Rho/ROCK signaling.

The cyclin-dependent kinase inhibitor p21<sup>Cip1/WAF1</sup> has an essential role in the cell cycle arrest, the transcriptional regulation, the inhibition of DNA replication, the DNA repair, the stress-induced premature senescence and the modulation of apoptosis.<sup>45–48</sup> Numerous studies have shown that p21<sup>Cip1/WAF1</sup> can mediate both pro- and anti-apoptotic functions depending on the type of stimulation and the cellular context.<sup>48</sup> For instance, p21<sup>Cip1/WAF1</sup> can prevent cells from undergoing apoptosis triggering cell cycle arrest, inactivating cyclin A/Cdk2 complexes, inhibiting the activity of procaspase 3, caspase 8 and 10, stress-activated protein kinases and apoptosis signal-regulating kinase 1.<sup>47,49</sup> Likewise, several reports have also suggested that p21<sup>Cip1/WAF1</sup> exerts a pro-apoptotic function under certain cellular stresses upregulating the pro-apoptotic protein Bax, activating the tumor necrosis factor family of death receptors and regulating components of the DNA repair machinery.<sup>47</sup> It is worth mentioning that even though p21<sup>Cip1/WAF1</sup> may represent a major p53 transcriptional target, it can promote apoptosis through both p53-dependent and independent mechanisms.<sup>47</sup> In addition, p21<sup>Cip1/WAF1</sup> can act as a tumor suppressor or an oncogene depending on the stimulations and the cellular context.<sup>45</sup> In particular, various compounds eliciting an anticancer activity such

as histone deacetylase inhibitors, cisplatin, phorbol 12-myristate 13-acetate and curcumin were shown to induce apoptotic cell death through the p21<sup>Cip1/WAF1</sup> induction.<sup>40,50–54</sup> Extending these findings, our data have ascertained that LA induces apoptosis in both breast and endometrial cancer cells upregulating the p21<sup>Cip1/WAF1</sup> expression levels via an AP1-mediated pathway.

Overall, the present results provide novel insights into the potential of LA to activate the EGFR/ERK/AP1/p21<sup>Cip1/WAF1</sup> transduction signaling toward antiproliferative and pro-apoptotic responses in tumor cells. Nevertheless, further experimental evidence are warranted to better define the action of LA alone or in the context of coconut oil consumption on tumor development as claimed by a current newsworthy debate.

## MATERIALS AND METHODS

### Reagents

LA, CA, NAC, Y-27632 (Y) and 2',7'-dichlorofluorescein diacetate (DCFDA) were purchased from Sigma-Aldrich (Milan, Italy). Tyrostatin AG1478 (AG), PD98059 (PD), SP 600125 (SP) and UC2288 were obtained from Calbiochem (DBA, Milan, Italy). All compounds were dissolved in dimethyl sulfoxide except LA, CA, NAC and Y-27632 (Y), which were solubilized in water.

### Cell cultures

SkBr3 breast cancer cells were obtained by ATCC, used < 6 months after resuscitation and maintained in RPMI 1640 without phenol red

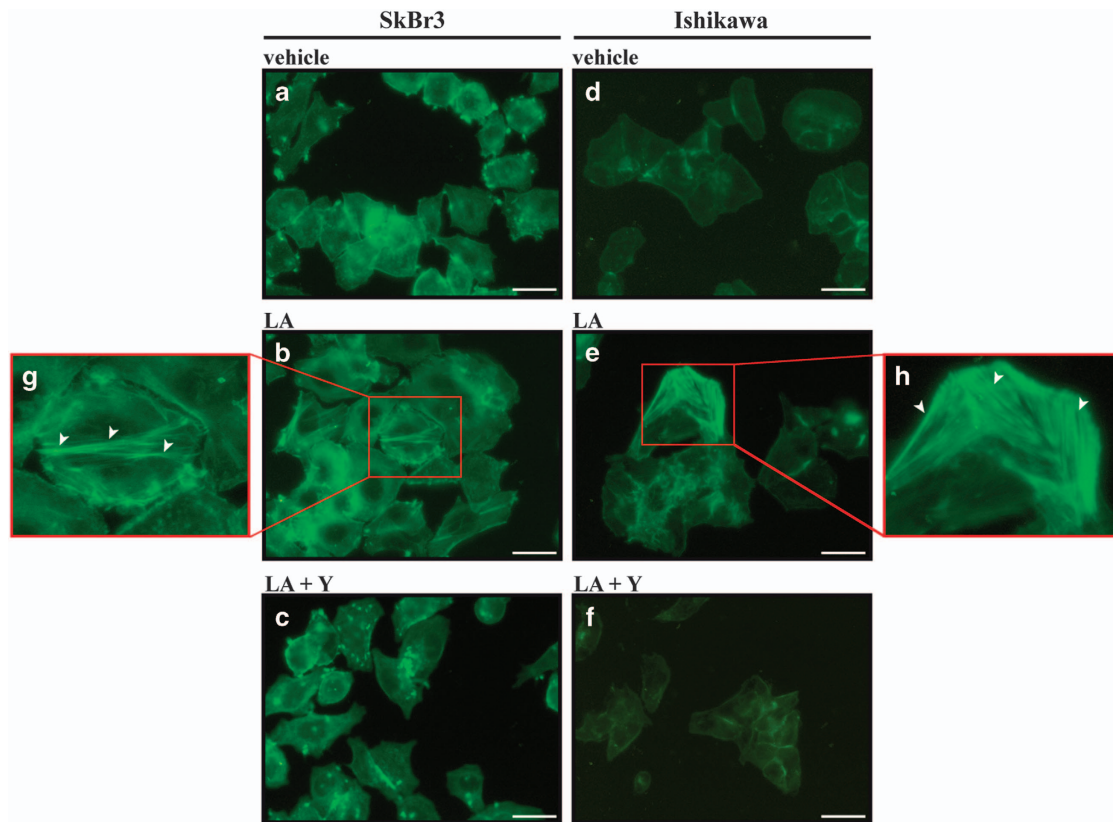


**Figure 6.** Lauric acid promotes the formation of stress fibers. SkBr3 and Ishikawa cells were treated for 4 h with vehicle (–) (**a, d**) or 100  $\mu\text{M}$  LA alone (**b, e**) or in combination with 10  $\mu\text{M}$  ROCK inhibitor Y-27632 (Y) (**c, f**) and subjected to phalloidin staining to visualize F-actin. (**g, h**) Enlarged details of stress fibers shown in **b** and **e**, respectively. White arrows indicate stress fibers. Images shown are representative of 30 random fields obtained in three independent experiments. Scale bar: 12.5  $\mu\text{m}$ .

supplemented with 10% FBS and 100 mg/ml penicillin/streptomycin (Life Technologies, Milan, Italy). Ishikawa endometrial cancer cells were obtained by D Picard (University of Geneva) and maintained in MEM supplemented with 10% FBS, 100  $\mu\text{g}/\text{ml}$  penicillin/streptomycin, 2 mM L-glutamine and 1% Non-Essential Amino Acids Solution Cells (Life Technologies). Cells were switched to medium without serum the day before immunoblots and reverse transcription-PCR experiments.

#### Cell viability assay

Cell viability was determined by the MTT [3-(4,5-dimethylthiazol-2-yl)-2,5-diphenyltetrazolium bromide] assay, which is based on the conversion of MTT to MTT formazan by mitochondrial enzyme. Cells were seeded in quadruplicate in 96-well plates in regular growth medium and grown until 70–80% confluence. Cells were washed once they had attached and then treated with increasing concentrations of each compound for 48 h in regular medium supplemented with 1% FBS. Relative cell viability was determined by MTT assay according to the manufacturer's protocol (Sigma-Aldrich). Mean absorbance of cells receiving vehicle (–) was set as onefold induction upon which the mean absorbance of treatments was calculated.

#### Plasmids, transfections and gene reporter assays

The luciferase reporter plasmid for c-fos encoding a 2.2-kb 5' upstream fragment of human c-fos was a gift from Dr. K Nose (Hatanodai, Shinagawa-ku, Tokyo). The luciferase reporter plasmid for AP1 responsive collagen promoter was a kind gift from H Van Dam (Department of Molecular Cell Biology, Leiden University, Leiden, Netherlands). The human p21<sup>Cip1/WAF1</sup> promoter-luciferase reporter was kindly provided by Dr T Sakai (Kyoto Prefectural University of Medicine, Kyoto, Japan). The *Renilla* luciferase expression vector pRL-TK (Promega, Milan, Italy) was used as internal transfection control in luciferase assays. Cells ( $1 \times 10^5$ ) were plated into 24-well plates with regular growth medium/well the day before transfection. Cell medium was replaced on the day of transfection with

serum-free medium and transfection was performed using X-tremeGENE 9 DNA Transfection Reagent (Sigma-Aldrich) and a mixture containing 0.5  $\mu\text{g}$  of each reporter plasmid and 5 ng of pRL-TK. After 6 h, treatments were added and cells were incubated for 18 h. Luciferase activity was measured using the Dual Luciferase Kit (Promega) according to the manufacturer's recommendations. Firefly luciferase activity was normalized to the internal transfection control provided by the *Renilla* luciferase activity. Normalized relative light unit values obtained from cells treated with vehicle were set as onefold induction upon which the activity induced by treatments was calculated.

The plasmid DN/c-fos, which encodes a c-fos mutant that heterodimerizes with c-fos dimerization partners but does not allow DNA binding,<sup>55</sup> was a kind gift from Dr C Vinson (NIH, Bethesda, MD, USA). Cells were plated onto 10-cm dishes and prior to treatments cells were transfected for 24 h using X-tremeGENE 9 DNA Transfection Reagent (Sigma-Aldrich) with a control vector and the plasmid DN/c-fos.

#### Gene expression studies

Total RNA was extracted and cDNA was synthesized by reverse transcription as previously described.<sup>56</sup> The expression of selected genes was quantified by real-time PCR using Step One (TM) sequence detection system (Applied Biosystems Inc, Milan, Italy). Gene-specific primers were designed using Primer Express version 2.0 software (Applied Biosystems). For c-fos, p53, p21<sup>Cip1/WAF1</sup> (p21) and the ribosomal protein 18S, which was used as a control gene to obtain normalized values, the primers were: 5'-CGAGCCCTTTGATGACTTCCT-3' (c-fos forward), 5'-GGAGCGGGCTGTCT CAGA-3' (c-fos reverse); 5'-GCTTCATGCCAGCTACTTC-3' (p53 forward), 5'-GGCATTCTGGGAGCTTCATCT-3' (p53 reverse); 5'-GCTTCATGCCAGCTA CTTCC-3' (p21 forward) and 5'-CTGTGCTCACTCAGGGTCA-3' (p21 reverse); 5'-GGCGTCCCCCAACTTCTTA-3' (18S forward) and 5'-GGGCATCACAGAC CTGTTAT-3' (18S reverse), respectively. Assays were performed in triplicate and the results were normalized for 18S expression and then calculated as fold induction of RNA expression.

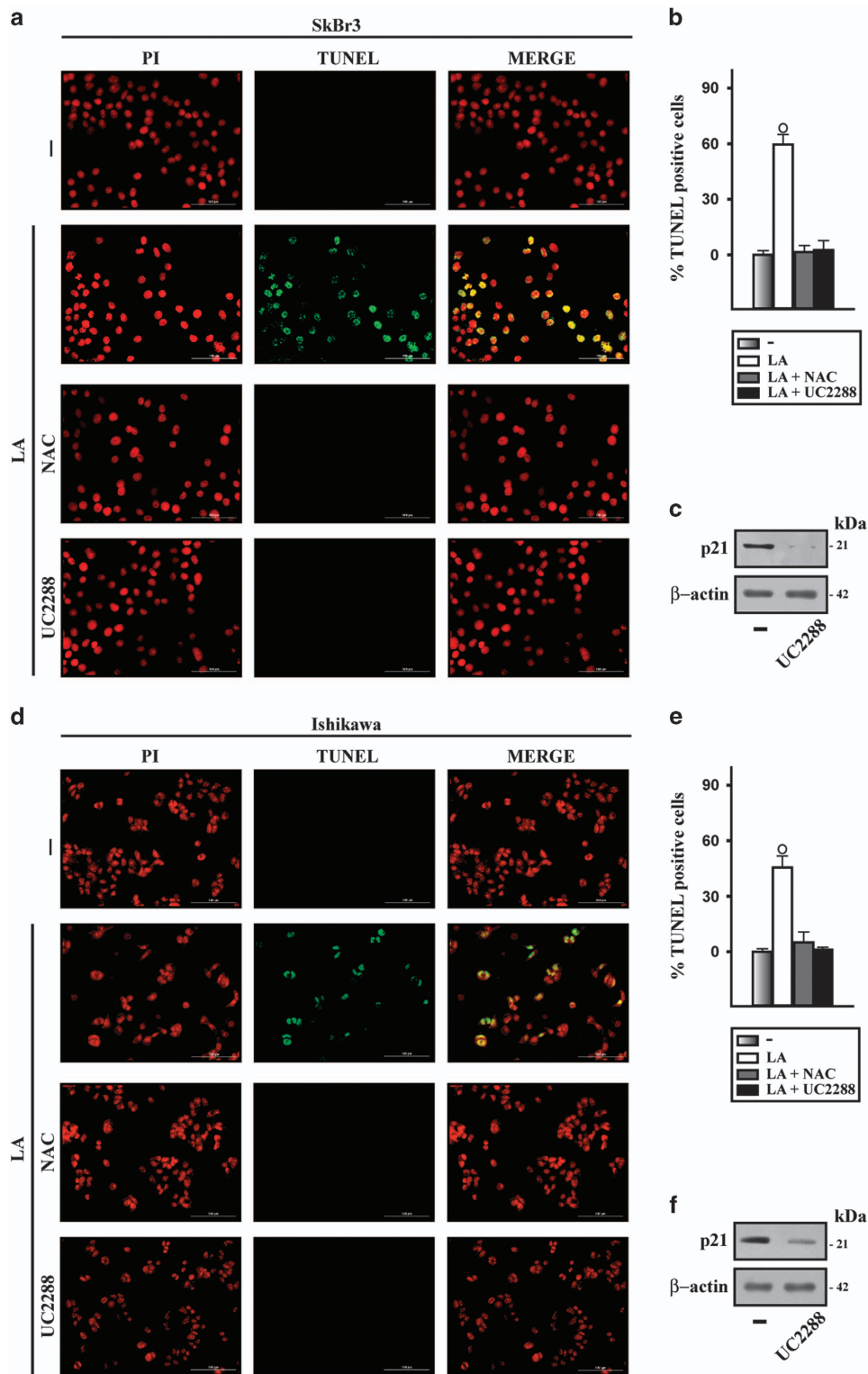


**Figure 7.** Lauric acid induces apoptotic cell death. **(a, d)** TdT-mediated dUTP nick-end-labeling (TUNEL) staining (green) in SkBr3 **(a)** and Ishikawa **(d)** cells treated for 18 h with vehicle (–) or 100  $\mu$ M LA alone or in combination with 300  $\mu$ M free radical scavenger NAC and 10  $\mu$ M p21<sup>Cip1/WAF1</sup> inhibitor UC2288, as indicated. Nuclei were stained by propidium iodide (PI, red). Magnification is indicated by bars (100  $\mu$ m). Each experiment shown is representative of 20 random fields observed. **(b, e)** Bar graphs represent the percentage of TUNEL-positive cells upon treatments versus vehicle. Values are the mean of three independent experiments. (○) indicates  $P < 0.05$  for cells receiving vehicle versus treatments. **(c, f)** Efficacy of p21<sup>Cip1/WAF1</sup> downregulation by UC2288.  $\beta$ -actin was used as a loading control. Results shown are representative of at least two independent experiments.

### Chromatin immunoprecipitation assay

Cells were grown in 10-cm dishes to 70–80% confluence, shifted to serum-free medium for 24 h and then treated with vehicle (–) or 100  $\mu$ M LA for 4 h. Thereafter, cells were cross-linked with 1% formaldehyde and sonicated. Supernatants were immunocleared with salmon DNA/protein A-agarose (Upstate Biotechnology, Inc., Lake Placid, NY, USA) and immunoprecipitated with anti c-fos (H-125) antibody or non-specific IgG (Santa Cruz Biotechnology, DBA, Milan, Italy). Pellets were washed, eluted with a buffer consisting of 1% SDS and 0.1 mol/l NaHCO<sub>3</sub>, and digested with proteinase K. DNA was obtained by phenol/chloroform extraction and precipitated with ethanol. A 4  $\mu$ l volume of each sample was used as template to amplify an AP1-containing region located in the p21<sup>Cip1/WAF1</sup> promoter by real-time PCR. The primers used were 5'-TCAGCTGCAT TGGGTAATCCT-3' (forward) and 5'-CTGGACATTTCCACGAA-3' (reverse). Data were normalized to the input for the immunoprecipitation.

### Western blot analysis

Cells were grown in 10-cm dishes, exposed to ligands, and then lysed as previously described.<sup>57</sup> Equal amounts of whole-protein extract were resolved on a 10% SDS-polyacrylamide gel and transferred to a nitrocellulose membrane (Amersham Biosciences, Sigma-Adrich, Milan, Italy), which were probed with primary antibodies against pEGFR Tyr 1173, EGFR (1005), phosphorylated ERK1/2 (E-4), ERK2 (C-14), p-c-Jun S73, c-Jun (N), c-fos (E8), p53 (DO-1), p21 (H164) and  $\beta$ -actin (C2) (Santa Cruz Biotechnology) and then revealed using the chemiluminescent substrate for western blotting Westar Nova 2.0 (Cyanagen, Biogenerica, Catania, Italy).

### ROS production

The non-fluorescent DCFDA probe, which becomes highly fluorescent on reaction with ROS, was used to evaluate intracellular ROS production. In brief, cells ( $2 \times 10^5$ ) were incubated with 10  $\mu$ M DCFDA (Sigma-Aldrich) at 37 °C for 30 min, washed with PBS and then exposed to treatments, as indicated. Cells were washed with PBS and the fluorescent intensity of DCF was measured (excitation at 485 nm and emission at 530 nm).

### Phalloidin staining

Cells were washed twice with PBS, fixed in 4% paraformaldehyde in PBS for 10 min, washed briefly with PBS, then incubated with Phalloidin-Fluorescent Conjugate (Santa Cruz Biotechnology) and visualized with the Olympus BX41 microscope and the images were taken with CSV1.14 software using a CAM XC-30 for images acquisition (Olympus Europa, Hamburg, Germany).

### TUNEL assay

Cell apoptosis was determined by TUNEL assay, conducted using DeadEnd Fluorometric TUNEL System (Promega) and performed according to the manufacturer's instructions. In brief, cells were treated for 18 h, as indicated, then were fixed in freshly prepared 4% paraformaldehyde solution in PBS (pH 7.4) for 25 min at 4 °C. After fixation, cells were permeabilized in 0.2% Triton X-100 solution in PBS for 5 min. After washing twice with washing buffer for 5 min, the cells were covered with equilibration buffer at room temperature for 5–10 min. The labeling reaction was performed using terminal deoxynucleotidyl transferase end-labeling TdT and fluorescein-dUTP cocktail for each sample and incubated for 1 h at 37 °C where TdT catalyses the binding of fluorescein-dUTP to free 3'OH ends in the nicked DNA. After rinsing, cells were washed with 2  $\times$  SSC solution buffer and subsequently incubated with propidium iodide (Sigma-Aldrich) to stain nuclei and analyzed using the Cytation 3 Cell Imaging Multimode Reader (BioTek, Winooski, VT, USA).

### Statistical analysis

Statistical analysis was done using ANOVA followed by Newman–Keuls' testing to determine differences in means.  $P < 0.05$  was considered as statistically significant.

### ACKNOWLEDGEMENTS

This work was supported by Associazione Italiana per la Ricerca sul Cancro (IG 16719 to MM; IG 19242 to AB).

### COMPETING INTERESTS

The authors declare no conflict of interest.

### PUBLISHER'S NOTE

Springer Nature remains neutral with regard to jurisdictional claims in published maps and institutional affiliations.

### REFERENCES

- Layden BT, Angueira AR, Brodsky M, Durai V, Lowe WL Jr. Short chain fatty acids and their receptors: new metabolic targets. *Transl Res* 2013; **161**: 131–140.
- Calder PC. Functional roles of fatty acids and their effects on human health. *JPEN J Parenter Enteral Nutr* 2015; **39**: 185–325.
- Bocca C, Bozzo F, Gabriel L, Miglietta A. Conjugated linoleic acid inhibits Caco-2 cell growth via ERK-MAPK signaling pathway. *J Nutr Biochem* 2007; **18**: 332–340.
- Engelbrecht AM, Toit-Kohn JL, Ellis B, Thomas M, Nell T, Smith R. Differential induction of apoptosis and inhibition of the PI3-kinase pathway by saturated, monounsaturated and polyunsaturated fatty acids in a colon cancer cell model. *Apoptosis* 2008; **13**: 1368–1377.
- Jump DB, Clarke SD. Regulation of gene expression by dietary fat. *Annu Rev Nutr* 1999; **19**: 63–90.
- Ris erus U. Fatty acids and insulin sensitivity. *Curr Opin Clin Nutr Metab Care* 2008; **11**: 100–105.
- Turcotte C, Chouinard F, Lefebvre JS, Flamand N. Regulation of inflammation by cannabinoids, the endocannabinoids 2-arachidonoyl-glycerol and arachidonoyl-ethanolamide, and their metabolites. *J Leukoc Biol* 2015; **97**: 1049–1070.
- Dayrit FM. The properties of lauric acid and their significance in coconut oil. *J Am Oil Chem Soc* 2015; **92**: 1–15.
- Kappally S, Shirwaikar A, Shirwaikar A. Coconut oil – a review of potential applications. *Hygeia J D Med* 2015; **7**: 34–41.
- Eyres L, Eyres MF, Chisholm A, Brown RC. Coconut oil consumption and cardiovascular risk factors in humans. *Nutr Rev* 2016; **74**: 267–280.
- Silva RB, Silva-J unior EV, Rodrigues LC, Andrade LH, da Silva SI, Harand W et al. A comparative study of nutritional composition and potential use of some underutilized tropical fruits of Arecaceae. *An Acad Bras Cienc* 2015; **87**: 1701–1709.
- Silberstein T, Burg A, Blumenfeld J, Sheizaf B, Tzur T, Saphier O. Saturated fatty acid composition of human milk in Israel: a comparison between Jewish and Bedouin women. *Isr Med Assoc J* 2013; **15**: 156–159.
- Huang WC, Tsai TH, Chuang LT, Li YY, Zouboulis CC, Tsai PJ. Anti-bacterial and anti-inflammatory properties of capric acid against Propionibacterium acnes: a comparative study with lauric acid. *J Dermatol Sci* 2014; **73**: 232–240.
- Temme EH, Mensink RP, Hornstra G. Comparison of the effects of diets enriched in lauric, palmitic, or oleic acids on serum lipids and lipoproteins in healthy women and men. *Am J Clin Nutr* 1996; **63**: 897–903.
- Alves NF, de Queiroz TM, de Almeida Travassos R, Magnani M, de Andrade Braga V. Acute treatment with lauric acid reduces blood pressure and oxidative stress in spontaneously hypertensive rats. *Basic Clin Pharmacol Toxicol* 2017; **120**: 348–353.
- Veeresh Babu SV, Veeresh B, Patil AA, Warke YB. Lauric acid and myristic acid prevent testosterone induced prostatic hyperplasia in rats. *Eur J Pharmacol* 2010; **626**: 262–265.
- Fauser JK, Matthews GM, Cummins AG, Howarth GS. Induction of apoptosis by the medium-chain length fatty acid lauric acid in colon cancer cells due to induction of oxidative stress. *Chemotherapy* 2013; **59**: 214–224.
- Weng WH, Leung WH, Pang YJ, Hsu HH. Lauric acid can improve the sensitization of Cetuximab in KRAS/BRAF mutated colorectal cancer cells by retrievable microRNA-378 expression. *Oncol Rep* 2016; **35**: 107–116.
- Law KS, Azman N, Omar EA, Musa MY, Yusoff NM, Sulaiman SA et al. The effects of virgin coconut oil (VCO) as supplementation on quality of life (QOL) among breast cancer patients. *Lipids Health Dis* 2014; **13**: 139.
- Narayanan A, Baskaran SA, Amalradjou MA, Venkitanarayanan K. Anticarcinogenic properties of medium chain fatty acids on human colorectal, skin and breast cancer cells in vitro. *Int J Mol Sci* 2015; **16**: 5014–5027.
- Abdullah FO, Hussain FH, Mannucci B, Lappano R, Tosi S, Maggiolini M et al. Composition, antifungal and antiproliferative activities of the hydrodistilled oils from leaves and flower heads of pteroccephalus nestorianus Nab. *Chem Biodivers* 2017; **14**: e1700009.
- Jaffe AB, Hall A. Rho GTPases: biochemistry and biology. *Annu Rev Cell Dev Biol* 2005; **21**: 247–269.
- Ibarguren M, L opez DJ, Escrib a PV. The effect of natural and synthetic fatty acids on membrane structure, microdomain organization, cellular functions and human health. *Biochim Biophys Acta* 2014; **1838**: 1518–1528.

- 24 Wanders RJ, Ruiter JP, IJLst L, Waterham HR, Houten SM. The enzymology of mitochondrial fatty acid beta-oxidation and its application to follow-up analysis of positive neonatal screening results. *J Inherit Metab Dis* 2010; **33**: 479–494.
- 25 Estadella D, da Penha Oller do Nascimento CM, Oyama LM, Ribeiro EB, Dâmaso AR, de Piano A. Lipotoxicity: effects of dietary saturated and trans fatty acids. *Mediators Inflamm* 2013; **2013**: 137579.
- 26 Babu AS, Veluswamy SK, Arena R, Guazzi M, Lavie CJ. Virgin coconut oil and its potential cardioprotective effects. *Postgrad Med* 2014; **126**: 76–83.
- 27 Mumme K, Stonehouse W. Effects of medium-chain triglycerides on weight loss and body composition: a meta-analysis of randomized controlled trials. *J Acad Nutr Diet* 2015; **115**: 249–263.
- 28 McCarty MF, DiNicolantonio JJ. Lauric acid-rich medium-chain triglycerides can substitute for other oils in cooking applications and may have limited pathogenicity. *Open Heart* 2016; **3**: e000467.
- 29 Stanhope JM, Sampson VM, Prior IA. The Tokelau Island Migrant Study: serum lipid concentration in two environments. *J Chronic Dis* 1981; **34**: 45–55.
- 30 Reddy BS, Maelura Y. Tumor promotion of dietary fat in azoxymethane-induced colon carcinogenesis in female F 344 rats. *J Natl Cancer Inst* 1984; **72**: 745–750.
- 31 Cohen LA, Thompson DO, Maelura Y, Choi K, Blank ME, Rose DP. Dietary fat and mammary cancer. Promoting effects of different dietary fats on N-nitrosomethylurea-induced rat mammary tumorigenesis. *J Natl Cancer Inst* 1986; **77**: 33–42.
- 32 Fukui M, Kang KS, Okada K, Zhu BT. EPA, an omega-3 fatty acid, induces apoptosis in human pancreatic cancer cells: role of ROS accumulation, caspase-8 activation, and autophagy induction. *J Cell Biochem* 2013; **114**: 192–203.
- 33 Shin S, Jing K, Jeong S, Kim N, Song KS, Heo JY *et al*. The omega-3 polyunsaturated fatty acid DHA induces simultaneous apoptosis and autophagy via mitochondrial ROS-mediated Akt-mTOR signaling in prostate cancer cells expressing mutant p53. *Biomed Res Int* 2013; **2013**: 568671.
- 34 Song Y, Li X, Li Y, Li N, Shi X, Ding H *et al*. Non-esterified fatty acids activate the ROS-p38-p53/Nrf2 signaling pathway to induce bovine hepatocyte apoptosis in vitro. *Apoptosis* 2014; **19**: 984–997.
- 35 Lehto VP. EGF receptor: which way to go? *FEBS Lett* 2001; **491**: 1–3.
- 36 Wada T, Penninger JM. Mitogen-activated protein kinases in apoptosis regulation. *Oncogene* 2004; **23**: 2838–2849.
- 37 Pellegrin S, Mellor H. Actin stress fibres. *J Cell Sci* 2007; **120**: 3491–3499.
- 38 Sebbagh M, Renvoizé C, Hamelin J, Riché N, Bertoglio J, Bréard J. Caspase-3-mediated cleavage of ROCK I induces MLC phosphorylation and apoptotic membrane blebbing. *Nat Cell Biol* 2001; **3**: 346–352.
- 39 Huang CY, Liang CM, Chu CL, Peng JM, Liang SM. A fibrillar form of fibronectin induces apoptosis by activating SHP-2 and stress fiber formation. *Apoptosis* 2010; **15**: 915–926.
- 40 Xiao L, Eto M, Kazanietz MG. ROCK mediates phorbol ester-induced apoptosis in prostate cancer cells via p21Cip1 up-regulation and JNK. *J Biol Chem* 2009; **284**: 29365–29375.
- 41 Coleman ML, Sahai EA, Yeo M, Bosch M, Dewar A, Olson MF. Membrane blebbing during apoptosis results from caspase-mediated activation of ROCK I. *Nat Cell Biol* 2001; **3**: 339–345.
- 42 Etienne-Manneville S, Hall A. Rho GTPases in cell biology. *Nature* 2002; **420**: 629–635.
- 43 Del Re DP, Miyamoto S, Brown JH. RhoA/Rho kinase up-regulate Bax to activate a mitochondrial death pathway and induce cardiomyocyte apoptosis. *J Biol Chem* 2007; **282**: 8069–8078.
- 44 Lai JM, Hsieh CL, Chang ZF. Caspase activation during phorbol ester-induced apoptosis requires ROCK-dependent myosin-mediated contraction. *J Cell Sci* 2003; **116**: 3491–3501.
- 45 Abbas T, Dutta A. p21 in cancer: intricate networks and multiple activities. *Nat Rev Cancer* 2009; **9**: 400–414.
- 46 Gartel AL. p21(WAF1/CIP1) and cancer: a shifting paradigm? *Biofactors* 2009; **35**: 161–164.
- 47 Gartel AL, Tyner AL. The role of the cyclin-dependent kinase inhibitor p21 in apoptosis. *Mol Cancer Ther* 2002; **1**: 639–649.
- 48 Karimian A, Ahmadi Y, Yousefi B. Multiple functions of p21 in cell cycle, apoptosis and transcriptional regulation after DNA damage. *DNA Repair (Amst)* 2016; **42**: 63–71.
- 49 Dotto GP. p21(WAF1/Cip1): more than a break to the cell cycle? *Biochim Biophys Acta* 2000; **1471**: M43–M56.
- 50 Ocker M, Schneider-Stock R. Histone deacetylase inhibitors: signalling towards p21<sup>Cip1/Waf1</sup>. *Int J Biochem Cell Biol* 2007; **39**: 1367–1374.
- 51 Gogada R, Amadori M, Zhang H, Jones A, Verone A, Pitarresi J *et al*. Curcumin induces Apaf-1-dependent, p21-mediated caspase activation and apoptosis. *Cell Cycle* 2011; **10**: 4128–4137.
- 52 Zhao B, He T. Chidamide, a histone deacetylase inhibitor, functions as a tumor inhibitor by modulating the ratio of Bax/Bcl-2 and P21 in pancreatic cancer. *Oncol Rep* 2015; **33**: 304–310.
- 53 Kondo S, Barna BP, Kondo Y, Tanaka Y, Casey G, Liu J *et al*. WAF1/CIP1 increases the susceptibility of p53 non-functional malignant glioma cells to cisplatin-induced apoptosis. *Oncogene* 1996; **13**: 1279–1285.
- 54 Lincet H, Poulain L, Remy JS, Deslandes E, Duigou F, Gauduchon P *et al*. The p21 (cip1/waf1) cyclin-dependent kinase inhibitor enhances the cytotoxic effect of cisplatin in human ovarian carcinoma cells. *Cancer Lett* 2000; **161**: 17–26.
- 55 Gerdes MJ, Myakishev M, Frost NA, Rishi V, Moitra J, Acharya A *et al*. Activator protein-1 activity regulates epithelial tumor cell identity. *Cancer Res* 2006; **66**: 7578–7588.
- 56 Lappano R, Santolla MF, Pupo M, Sinicropi MS, Caruso A, Rosano C *et al*. MIBE acts as antagonist ligand of both estrogen receptor  $\alpha$  and GPER in breast cancer cells. *Breast Cancer Res* 2012; **14**: R12.
- 57 Santolla MF, Avino S, Pellegrino M, De Francesco EM, De Marco P, Lappano R *et al*. SIRT1 is involved in oncogenic signaling mediated by GPER in breast cancer. *Cell Death Dis* 2015; **6**: e1834.



This work is licensed under a Creative Commons Attribution 4.0 International License. The images or other third party material in this article are included in the article's Creative Commons license, unless indicated otherwise in the credit line; if the material is not included under the Creative Commons license, users will need to obtain permission from the license holder to reproduce the material. To view a copy of this license, visit <http://creativecommons.org/licenses/by/4.0/>

© The Author(s) 2017

# Protective Role of GPER Agonist G-1 on Cardiotoxicity Induced by Doxorubicin

ERNESTINA M. DE FRANCESCO,<sup>1</sup> CARMINE ROCCA,<sup>2</sup> FRANCESCO SCAVELLO,<sup>2</sup> DANIELA AMELIO,<sup>2</sup> TERESA PASQUA,<sup>2</sup> DAMIANO C. RIGIRACCILO,<sup>1</sup> ANDREA SCARPELLI,<sup>1</sup> SILVIA AVINO,<sup>1</sup> FRANCESCA CIRILLO,<sup>1</sup> NICOLA AMODIO,<sup>3</sup> MARIA C. CERRA,<sup>2,4,\*</sup> MARCELLO MAGGIOLINI,<sup>1,\*\*</sup> AND TOMMASO ANGELONE<sup>2,4</sup>

<sup>1</sup>Department of Pharmacy, Health and Nutritional Sciences, University of Calabria, Rende (CS), Italy

<sup>2</sup>Department of Biology, Ecology, and E.S., University of Calabria, Rende (CS), Italy

<sup>3</sup>Department of Experimental and Clinical Medicine, University of Catanzaro Magna Græcia, Catanzaro, Italy

<sup>4</sup>National Institute of Cardiovascular Research, Bologna, Italy

The use of Doxorubicin (Dox), a frontline drug for many cancers, is often complicated by dose-limiting cardiotoxicity in approximately 20% of patients. The G-protein estrogen receptor GPER/GPR30 mediates estrogen action as the cardioprotection under certain stressful conditions. For instance, GPER activation by the selective agonist G-1 reduced myocardial inflammation, improved immunosuppression, triggered pro-survival signaling cascades, improved myocardial mechanical performance, and reduced infarct size after ischemia/reperfusion (I/R) injury. Hence, we evaluated whether ligand-activated GPER may exert cardioprotection in male rats chronically treated with Dox. 1 week of G-1 (50 µg/kg/day) intraperitoneal administration mitigated Dox (3 mg/kg/day) adverse effects, as revealed by reduced TNF-α, IL-1β, LDH, and ROS levels. Western blotting analysis of cardiac homogenates indicated that G-1 prevents the increase in p-c-jun, BAX, CTGF, iNOS, and COX2 expression induced by Dox. Moreover, the activation of GPER rescued the inhibitory action elicited by Dox on the expression of BCL2, pERK, and pAKT. TUNEL assay indicated that GPER activation may also attenuate the cardiomyocyte apoptosis upon Dox exposure. Using *ex vivo* Langendorff perfused heart technique, we also found an increased systolic recovery and a reduction of both infarct size and LDH levels in rats treated with G-1 in combination with Dox respect to animals treated with Dox alone. Accordingly, the beneficial effects induced by G-1 were abrogated in the presence of the GPER selective antagonist G15. These data suggest that GPER activation mitigates Dox-induced cardiotoxicity, thus proposing GPER as a novel pharmacological target to limit the detrimental cardiac effects of Dox treatment.

J. Cell. Physiol. 232: 1640–1649, 2017. © 2016 Wiley Periodicals, Inc.

Doxorubicin (Dox)-based treatments represent a highly effective therapeutic strategy in a large number of malignant diseases, including leukemias, lymphomas, sarcomas, and breast cancer (Young et al., 1981). However, Dox generates reactive oxygen species (ROS) that may trigger cardiotoxicity leading to cardiomyopathy and heart failure (Carvalho et al., 2014). This response to Dox has limited its clinical use, therefore, great attention has been addressed to the identification of novel pharmacological strategies able to mitigate the negative cardiovascular effects exerted by Dox.

The G-protein estrogen receptor GPER, also known as GPR30, has been largely implicated in the biological action of estrogens in diverse tissues, including the cardiovascular system (Maggiolini and Picard, 2010; Lindsey and Chappell, 2011; De Francesco et al., 2013a, 2014; Meyer et al., 2014; Zimmerman et al., 2016). In this regard, our and other previous studies have demonstrated that GPER is expressed in the rat and human heart and mediates a variety of beneficial cardiovascular effects (Filice et al., 2009; Patel et al., 2010). In addition, previous investigations have shown the cardioprotective actions mediated by GPER, particularly under stressful conditions characterized by increased ROS levels (Filice et al., 2009; Patel et al., 2010; Recchia et al., 2011; De Francesco et al., 2013a, 2014; Meyer et al., 2014). For instance, in a hypertensive rat heart model, the administration of the selective GPER ligand G-1 triggered beneficial negative inotropic and lusitropic effects, which were prevented in the presence of the selective GPER antagonist G15 (De Francesco et al., 2013a). These observations suggest that GPER may be

**Abbreviations:** GPER, G protein estrogen receptor; Dox, doxorubicin; ROS, reactive oxygen species; I/R, ischemia/reperfusion; IS, infarct size; LDH, lactate dehydrogenase; CTGF, connective tissue growth factor; TNF-α, tumor necrosis factor-α; COX2, cyclooxygenase 2; iNOS, inducible nitric oxide synthases; IL-1β, interleukin 1-β.

**Conflict of interest:** None declared.

**Contract grant sponsor:** Associazione Italiana per la Ricerca sul Cancro;

**Contract grant number:** 16719/2015.

**Contract grant sponsor:** Ministero della Salute;

**Contract grant number:** 67/GR-2010-2319511.

**Contract grant sponsor:** “Ministero dell’Università e Ricerca Scientifica e Tecnologica” (ex 60%).

**Contract grant sponsor:** “Dottorato di Ricerca in Scienze della Vita” (“Fondo Giovani”).

**Contract grant sponsor:** iCARE fellowship from the Associazione Italiana per la Ricerca sul Cancro (AIRC) cofunded by Marie Curie Actions.

\*Correspondence to: Prof. Maria Carmela Cerra, Department of Biology, Ecology, and E.S., University of Calabria, Rende (CS), Italy. E-mail: maria\_carmela.cerra@unical.it

\*\*Correspondence to: Prof. Marcello Maggiolini, Department of Pharmacy, Health and Nutritional Sciences, University of Calabria, Rende (CS), Italy. E-mail: marcellomaggiolini@yahoo.it; marcello.maggiolini@unical.it

Manuscript Received: 28 June 2016

Manuscript Accepted: 6 September 2016

Accepted manuscript online in Wiley Online Library (wileyonlinelibrary.com): 8 September 2016.

DOI: 10.1002/jcp.25585

considered as a valuable target in cardiovascular diseases characterized by increased oxidative stress. In this context, GPER activation by G-1 was shown to reduce infarct size and contractile dysfunctions after ischemia/reperfusion (I/R) injury through the involvement of PI3K kinase/AKT signaling pathway (Deschamps and Murphy, 2009). In addition, G-1 induced anti-inflammatory and pro-survival effects after I/R by reducing the production of TNF- $\alpha$ , interleukin (IL)-1 $\beta$ , and IL-6, as well as inhibiting mitochondria permeability transition pore opening (Bopassa et al., 2010; Weil et al., 2010). Consequently, GPER has emerged as a mediator of cardioprotection and a novel therapeutic target in cardiac diseases characterized by impaired oxidative balance.

In the present study, we demonstrate that GPER activation by G-1 inhibits the adverse effects of Dox, as revealed by reduced TNF- $\alpha$ , IL-1 $\beta$ , ROS, LDH plasma, and tissue levels. In rat heart homogenates, we found that G-1 also prevents the increase in p-c-jun, BAX, CTGF, iNOS, and COX2 expression upon Dox treatment. In addition, the activation of GPER prevented the inhibitory action elicited by Dox on BCL2, pERK, pAKT expression and attenuated the apoptotic actions exerted by Dox exposure. Likewise, GPER activation mitigated the adverse effects of Dox after I/R as evidenced by the increased systolic recovery and both reduced infarct size and LDH levels. Accordingly, the beneficial effects induced by G-1 were prevented in the presence of the GPER antagonist G15. These data suggest that GPER activation may mitigate Dox-induced cardiotoxicity, thus proposing GPER as a novel therapeutic target in cancer patients treated with Dox.

## Methods

### Animals

Male Wistar rats (~300 g body weight) (Harlan Laboratories, Udine, Italy), identically housed under controlled lighting and temperature conditions, fed a standard diet, and water ad libitum. All protocols were conducted in accordance with the Declaration of Helsinki, the Italian law (D.L. 26/2014), the Guide for the Care, and Use of Laboratory Animals published by the US National Institutes of Health (2011) and the Directive 2010/63/EU of the European Parliament on the protection of animals used for scientific. The project was approved by the Italian Ministry of Health, Rome and by the ethics review board.

### Drugs

Dox was from Sigma–Aldrich (Milan, Italy). 1-[4-(-6-Bromobenzol[1,3]diodo-5-yl)-3a,4,5,9-btetrahydro-3H-cyclopenta[c]-quinolin-8yl]ethanone (G-1) and (3aS,4R,9bR)-4-(6-bromo-1,3-benzodioxol-5-yl)-3a,4,5,9b-3H-cyclopenta[c]quinolone (G15) were from Tocris Bioscience, distributed by Space (Milan, Italy). G-1 and G15 were dissolved in DMSO. Preliminary experiments showed that the presence of equivalent amounts of DMSO in KHs solution do not modify basal cardiac performance.

### Experimental protocols

**In vivo treatment.** To evaluate whether G-1 counteracts Dox-induced cardiotoxicity, animals were divided in five groups:

Group I (control): normal saline was i.p. administered each day throughout 1 week at a dose of 3 ml/kg/day.

Group II (Doxorubicin: Dox): Dox was i.p. administered each day throughout 1 week at a dose of 3 mg/kg/day, resulting in a cumulative dose of 21 mg/kg (Saad et al., 2004).

Group III (G-1: G-1): G-1 was i.p. administered each day at a dose of 50  $\mu$ g/kg/day (Filice et al., 2009; De Francesco et al., 2013b).

Group IV (Doxorubicin + G-1: Dox + G-1): Dox (3 mg/kg/day) in combination with G-1 (50  $\mu$ g/kg/day) was i.p. administered throughout 1 week.

Group V (Doxorubicin + G-1 + G15: Dox + G-1 + G15): Dox (3 mg/kg/day) in combination with G-1 (50  $\mu$ g/kg/day) and G15 (160  $\mu$ g/kg/day) was i.p. administered throughout 1 week (Filice et al., 2009; De Francesco et al., 2013b).

Animals were sacrificed after 7 days in order to allow heart performance evaluation by Langendorff perfusion technique, plasma collection, as well as protein expression analysis on tissue homogenates. G-1 and G15 doses were chosen on the basis of preliminary dose-response curves (data not shown) and literature data (Filice et al., 2009; De Francesco et al., 2013a). Dox dose was chosen on the basis of literature data (Saad et al., 2004).

### Plasma collection

Blood samples were collected from the abdominal aorta with heparinized syringe. Plasma was then separated by centrifugation at 3000g (15 min, 4°C) and stored at –80°C until assays. Blood samples were used to measure plasma levels of ROS, TNF- $\alpha$ , IL-1 $\beta$ , and LDH, as described below.

### Enzyme-linked immunosorbent assay (ELISA)

TNF- $\alpha$  and IL-1 $\beta$  determinations were performed by using ELISA system according to manufacturer's instructions (Thermo Scientific, Rockford, IL). To determine tissue levels of TNF- $\alpha$  and IL-1 $\beta$ , left ventricle of hearts of each group was homogenized using Ultra-Turrax<sup>®</sup>. Plasma samples and cardiac tissue homogenates were incubated with antibodies against TNF- $\alpha$  or IL-1 $\beta$  that were pre-coated to wells of microplates. After discarding samples, biotinylated antibodies were added and the incubation was continued. Biotinylated antibody solution was discarded and further incubation with streptavidin-HRP was continued. Finally, TMB (3,3',5,5'-tetramethylbenzidine) solution was added and the absorbance was measured at 450 nm immediately after stopping the reaction by adding 2 M H<sub>2</sub>SO<sub>4</sub>.

### Lactate dehydrogenase (LDH) determinations

LDH was measured on both blood samples and samples of coronary effluent from isolated Langendorff heart perfusion. Samples of coronary effluent, during reperfusion, were withdrawn with a catheter inserted into the right ventricle via the pulmonary artery. Data (IU/L) were expressed as cumulative values for the entire reperfusion period. LDH released was determined by spectrophotometric analysis at 340 nM, using a classic procedure (Penna et al., 2006).

### ROS production

ROS production was evaluated using the ELISA system, according to the manufacturer (Sunred Biological Technology, Shanghai, China). Briefly, blood samples from rats belonging to all experimental groups were collected from the abdominal aorta with heparinized syringe and centrifuged at 3000g for 15 min (4°C) to obtain plasma. Fourty microliters of plasma samples were then incubated in the presence of ROS-antibody labeled with Biotin and Streptavidin-HRP for 60 min at 37°C. After chromogen addition, absorbance at 450 nM was immediately measured.

### Gene expression studies

After chronic treatments, rat hearts (n = 6) were dissected, homogenized, and processed for mRNA extraction, to

evaluate the expression of GPER by real-time PCR using the Step One™ sequence detection system (Applied Biosystems Inc., Milan, Italy), as previously described (De Francesco et al., 2013b). Gene-specific primers were designed using Primer Express version 2.0 software (Applied Biosystems Inc.) and are as follows: GPER Fwd: 5'-TCTACCTACCCTCCCCTGTGG-3' and Rev: 5'-AGGCAGGAGAGGAAGAGAGC-3'; I8S Fwd: 5'-TTTGTGGTTTTTCGGAAGTGA-3' and Rev: 5'-CGTTTATGGTCGGAAGTACGA-3'. I8S expression was used as a control.

### Immunoblotting analysis

After chronic treatments, rat hearts ( $n = 6$ ) were dissected, homogenized, and processed for protein extraction, to evaluate protein expression by immunoblotting, as previously described (De Francesco et al., 2013b). After loading and transfer, membranes were blocked and incubated with primary polyclonal IgG antibody for GPER (N-15) phosphorylated ERK1/2 (E-4), phosphorylated AKT1/2/3 Ser 473-R, phosphorylated-c-Jun Ser 73, ERK2 (C-14), AKT1/2/3 (H-136), c-Jun (N), iNOS (C11), COX2 (N-20), CTGF (L-20), BAX (6D150), BCL2 (C2),  $\beta$ -tubulin (H-235-2), and appropriate secondary HRP-conjugated antibodies, all purchased from Santa Cruz Biotechnology (DBA, Milan, Italy). Proteins and phosphoproteins levels were detected with horseradish peroxidase-linked secondary antibodies and revealed by using the Enhanced Chemiluminescence system (GE Healthcare, Milan, Italy).

### Histological analysis

After chronic treatments and sacrifice, ventricular sections (three hearts for each group), placed onto Superfrost Plus slides (Menzel-Glaser, Braunschweig-Germany), were deparaffined, rehydrated, and TUNEL staining (in situ Cell Death Detection Kit, POD from Roche Diagnostics-Germany) was performed, as previously described (Amelio et al., 2013). Briefly, sections incubated with proteinase K (20  $\mu$ g/ml; 37°C; 20-min) were washed, rinsed, and incubated with TUNEL (37°C, 60-min); reaction was blocked by 3% BSA in PBS at room temperature. Horseradish peroxidase-conjugated antibodies were added and incubated at 37°C. Terminal deoxynucleotidyl transferase (TdT) enzyme was omitted for negative control. Nuclei were counterstained with hematoxylin. Apoptotic Index (AI) was calculated as  $100 \times$  (number of myocytes TUNEL-positive cell nuclei per field/total number of cell nuclei per field). For each condition, four randomly selected fields were evaluated and averaged.

### Ex vivo studies

**Perfusion method.** In order to evaluate the cardiac parameters, at the end of the treatments rats were anesthetized with ethyl carbamate (2 g/kg body weight, i.p) and sacrificed. Then, hearts were rapidly excised, immediately placed in ice-cold perfusion buffer, cannulated via the aorta and perfused in the Langendorff apparatus at a constant flow-rate of 12 ml/min (37°C), as previously described (De Francesco et al., 2013a). To evaluate inotropism, the developed left ventricular pressure (dLVP; mmHg, index of contractile activity calculated from LVP-LVEDP) and the left ventricular end diastolic pressure (LVEDP; mmHg, index of contracture) were measured during the experiment by using PowerLab data acquisition system. Parameters were analyzed by using Chart software (ADInstruments, Oxford-UK), as previously reported (De Francesco et al., 2013a). Hearts were perfused with Krebs-Henseleit solution (KHs) (pH 7.4; gassed with 95% O<sub>2</sub> and 5% CO<sub>2</sub>) containing (in mmol/l): 113.0 mM NaCl; 4.7 mM KCl; 1.2 mM MgSO<sub>4</sub>; 25.0 mM NaHCO<sub>3</sub>; 1.2 mM

KH<sub>2</sub>PO<sub>4</sub>; 1.8 mM CaCl<sub>2</sub>; 11.0 mM glucose; 1.1 mM mannitol; 5 mM Na-pyruvate (Cerra et al., 2006).

**I/R protocols.** After chronic treatment, rats from each group were subjected to I/R protocol. Baseline parameters were recorded during the first 40 min of stabilization, then hearts were subjected to 30-min of global, no-flow ischemia followed by 120-min of reperfusion (I/R). The protocol of treatments for each group was as follows:

Group I (Saline): rats were treated each day throughout 1 week with saline solution;  $n = 6$  hearts were stabilized and subjected to I/R protocol.

Group II (Dox): rats were treated each day throughout 1 week with a single dose i.p. of Dox,  $n = 6$  hearts were stabilized and subjected to I/R protocol.

Group III (G-I): rats were treated once a day (a single i.p. dose) for 1 week with G-I,  $n = 6$  hearts were stabilized and subjected to I/R protocol.

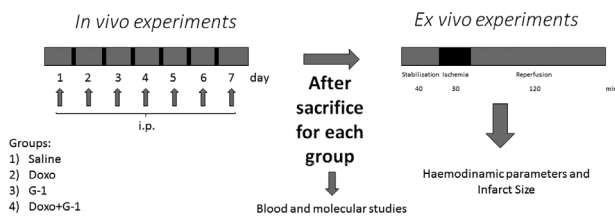
Group VI (Dox + G-I): rats were treated each day throughout 1 week with a single dose i.p. of G-I in combination with Dox,  $n = 6$  hearts were stabilized and subjected to I/R protocol.

Group V (Dox + G-I + G15): rats were treated each day throughout 1 week with a single dose i.p. of G-I in combination with Dox and G15,  $n = 6$  hearts were stabilized and subjected to I/R protocol.

At the end of treatments, cardiac parameters were analyzed by Langendorff technique. Administration of G15 alone, at the concentration used, did not influence I/R damages (data not shown). Cardiac performance before and after ischemia was evaluated by analyzing LVP recovery, as an index of contractile activity, and LVEDP as an index of contracture, defined as an increase in LVEDP of 4 mmHg above the baseline level (Cerra et al., 2006; Penna et al., 2006).

**Infarct size (IS).** Hearts were rapidly removed from the perfusion apparatus at the end of reperfusion. The left ventricle was dissected into 2–3-mm circumferential slices. After 20-min of incubation at 37°C in 0.1% solution of nitro blue tetrazolium in phosphate buffer, unstained necrotic tissue was carefully separated from stained viable tissue by an independent observer who was not aware of the nature of the intervention. The weights of the necrotic and non-necrotic tissues were then determined, and the necrotic mass was expressed as a percentage of total left ventricular mass, including septum (Penna et al., 2012).

A comprehensive diagram showing the experimental protocol for both in-vivo and ex-vivo studies is detailed below:



**Statistics.** All data were expressed as means  $\pm$  SEM. One-way ANOVA, non-parametric Mann-Whitney-U test and Newman-Keuls Multiple Comparison Test (for post-ANOVA comparisons) were used when appropriate (Graphpad Prism5). A  $P$ -value  $< 0.05$  was considered statistically significant.

### Results

#### GPER activation attenuates the increase of inflammatory and oxidative stress markers induced by Dox

We started our study by evaluating whether GPER mediates the reduction in inflammatory and oxidative stress markers in

TNF $\alpha$  and IL1 $\beta$  levels

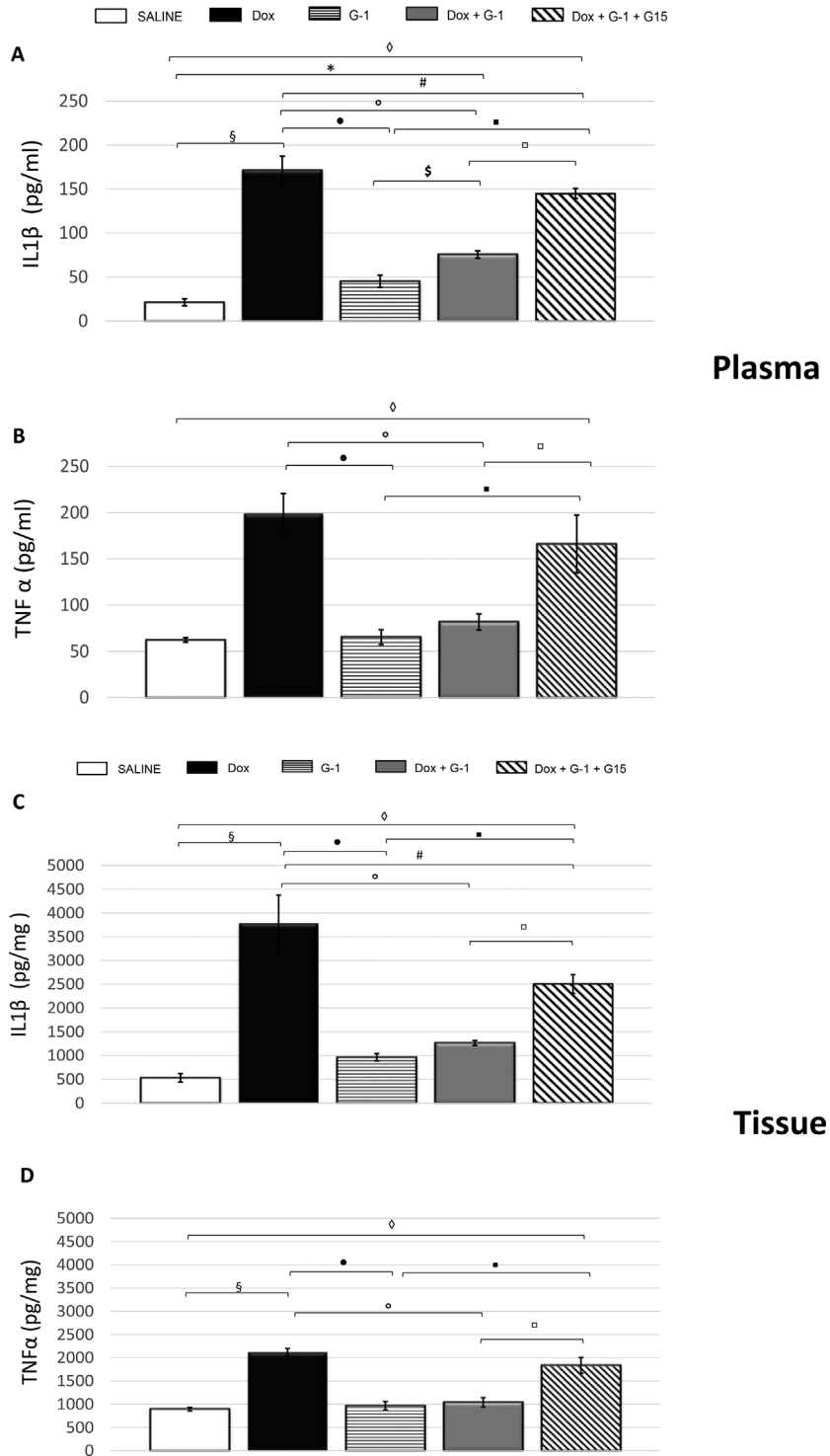


**Fig. 1.** Evaluation of IL-1 $\beta$  and TNF $\alpha$  plasma (A–B) and cardiac tissue (C–D) levels in saline, Dox, G-1, Dox + G-1, Dox + G-1 + G15 groups. Values are expressed as means  $\pm$  SEM with respect to saline group. Significance of differences from control value and comparison between groups by one-way ANOVA followed by Newman–Keuls Multiple Comparison Test. (§), (§), (°), (#), (◇), (◊), (●), (■), (□)  $P < 0.05$ .

rats treated with Dox alone and in combination with the GPER selective agonist G-1 as well as the GPER selective antagonist G15. Following the experimental protocol described in Material and Methods section, at the end of all treatments, heart ( $n = 6$  for each group) weights were: saline group:  $1.49 \pm 0.03$  g; Dox group:  $2.09 \pm 0.14$  g<sup>\*</sup>; G-1 group:  $1.43 \pm 0.07$  g; Dox in combination with G-1:  $1.52 \pm 0.05$  g; Dox in combination with G-1 and G15:  $1.96 \pm 0.1$  g<sup>\*</sup> ( $*P < 0.05$  vs. saline).

IL-1 $\beta$ , TNF- $\alpha$ , and LDH plasma levels were significantly increased in Dox-treated animals with respect to animals treated with saline (Figs. 1A and B and 2A). G-1 alone did not induce significant changes in IL-1 $\beta$ , TNF- $\alpha$ , and LDH plasma levels with respect to the saline group (Figs. 1A and B and 2A). However, G-1 lowered the IL-1 $\beta$ , TNF- $\alpha$ , and LDH plasma values observed upon Dox exposure, an effect no longer evident in the presence of the GPER antagonist G15 (Figs. 1A and B and 2A). In addition, G-1 counteracted the Dox-induced plasma levels of ROS, while G15 prevented the response triggered by G-1 (Fig. 2B). The levels of IL-1 $\beta$  were increased in the heart of rats treated with Dox alone and Dox in combination with G-1 and G15 with respect to animals treated with saline, G-1 and G-1 in combination with Dox (Fig. 1C). Similarly, TNF- $\alpha$  values were detected higher in animal groups treated with Dox alone and Dox in combination with G-1 and G15 respect to values detected in animals treated with saline, G-1 and G-1 in combination with Dox (Fig. 1D).

### LDH and ROS plasma levels

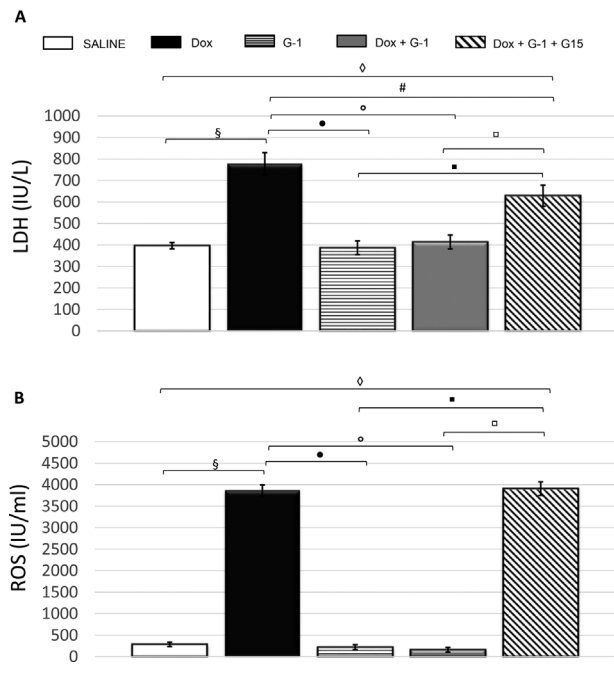


**Fig. 2.** Evaluation of LDH (A) and ROS (B) plasma levels in saline, Dox, G-1, Dox + G-1, Dox + G-1 + G15 groups. Values are expressed as means  $\pm$  SEM in respect to saline group. Significance of differences from control value and comparison between groups by one-way ANOVA followed by Newman-Keuls Multiple Comparison Test. (§), (◇), (#), (◊), (●), (■), (□)  $P < 0.05$ .

### Ligand-activated GPER reverses certain biological responses triggered by doxorubicin

On the basis of the above findings suggesting that GPER activation mitigates the detrimental cardiac effects of Dox, we analyzed whether GPER may reverse certain Dox-induced responses in cardiomyocytes. First, we assessed that in cardiac homogenates of all animal groups the chronic exposure to treatments do not determine any variation in GPER expression, as evaluated by real-time PCR and western blotting (Fig. 3A–C). Then, we evaluated main transduction signaling involved in cardiomyocytes survival as ERK1/2 and AKT (de Jonge et al., 2006). G-1 prevented the inhibition of ERK1/2 and AKT phosphorylation induced by Dox (Fig. 3D and E), while this effect was no longer evident in the presence of the GPER antagonist G15 (Fig. 3D and E). In addition, the phosphorylation of c-jun triggered by Dox was prevented by G-1 and rescued in the presence of G15 (Fig. 3D and E). Noteworthy, G-1 inhibited the up-regulation of BAX observed upon Dox treatment; however, this effect of G-1 was abolished in the presence of G15 (Fig. 3F and G). Conversely, the down-regulation of the antiapoptotic factor BCL2 observed upon Dox treatment was prevented using G-1, while this action of G-1 was rescued using G15 (Fig. 3F and G). In addition, the up-regulation of iNOS, COX2, and CTGF triggered by Dox was abrogated in the presence of G-1 and rescued in the presence of G15 (Fig. 3H and I). Next, we evaluated whether G-1 may inhibit cardiomyocyte apoptosis upon Dox exposure. As shown in Figure 4, vehicle-treated hearts exhibited limited TUNEL-positive nuclei, while Dox treatment substantially increased the positivity (Fig. 4B). Furthermore, G-1 used in combination with Dox significantly reduced the number of apoptotic myocytes (Fig. 4C and D); however, the action of G-1 was abolished using G15 (data not shown). Taken together, these data suggest that the activation of GPER may counteract certain biological responses involved in the cardiotoxicity induced by Dox (Octavia et al., 2012; Mantawy et al., 2014; Tocchetti et al., 2014; Vejpongsa and Yeh, 2014).

### GPER activation improves post-ischemic cardiac function

The possibility that G-1 treatment elicits cardioprotection was investigated in hearts from each group exposed to I/R manoeuvres by analyzing both systolic and diastolic function. For ex-vivo experiments, the following basal cardiac parameters were obtained after 40 min equilibration: LVP =  $74.13 \pm 2.13$ , LVEDP = 5–8 mmHg. The endurance and stability of the preparations, analyzed by measuring the performance variables every 10 min, showed that each heart was stable up to 180 min. Systolic function was represented by the level of developed left ventricular pressure (i.e., dLVP recovery). Results showed that the post ischemic performance of the heart from the saline group was characterized by a limited LVP recovery. In particular, at the end of reperfusion, dLVP was  $39.9 \pm 8.2$  mmHg (about 50% of the basal value). The post ischemic performance was lower (dLVP: about 38%) in hearts from the group treated with Dox alone, while it resulted similar to the basal value when Dox was administered in combination with G-1 that lost its protective action using the selective GPER antagonist G15 (Fig. 5). Diastolic function is expressed by contracture development (i.e., LVEDP 4 mmHg or more above baseline level) (Pagliaro et al., 2003). In the saline group, I/R markedly increased LVEDP which resulted  $38 \pm 10$  mmHg at the end of reperfusion with respect to  $6.8 \pm 0.8$  mmHg in the baseline. In the Dox group, LVEDP was higher ( $33 \pm 7$  mmHg) respect to the baseline value ( $8.3 \pm 1.4$  mmHg) (Fig. 5). In heart of rats exposed to Dox in combination with G-1 and in those exposed to G-1 alone, at the end of the reperfusion, LVEDP was not significantly modified,

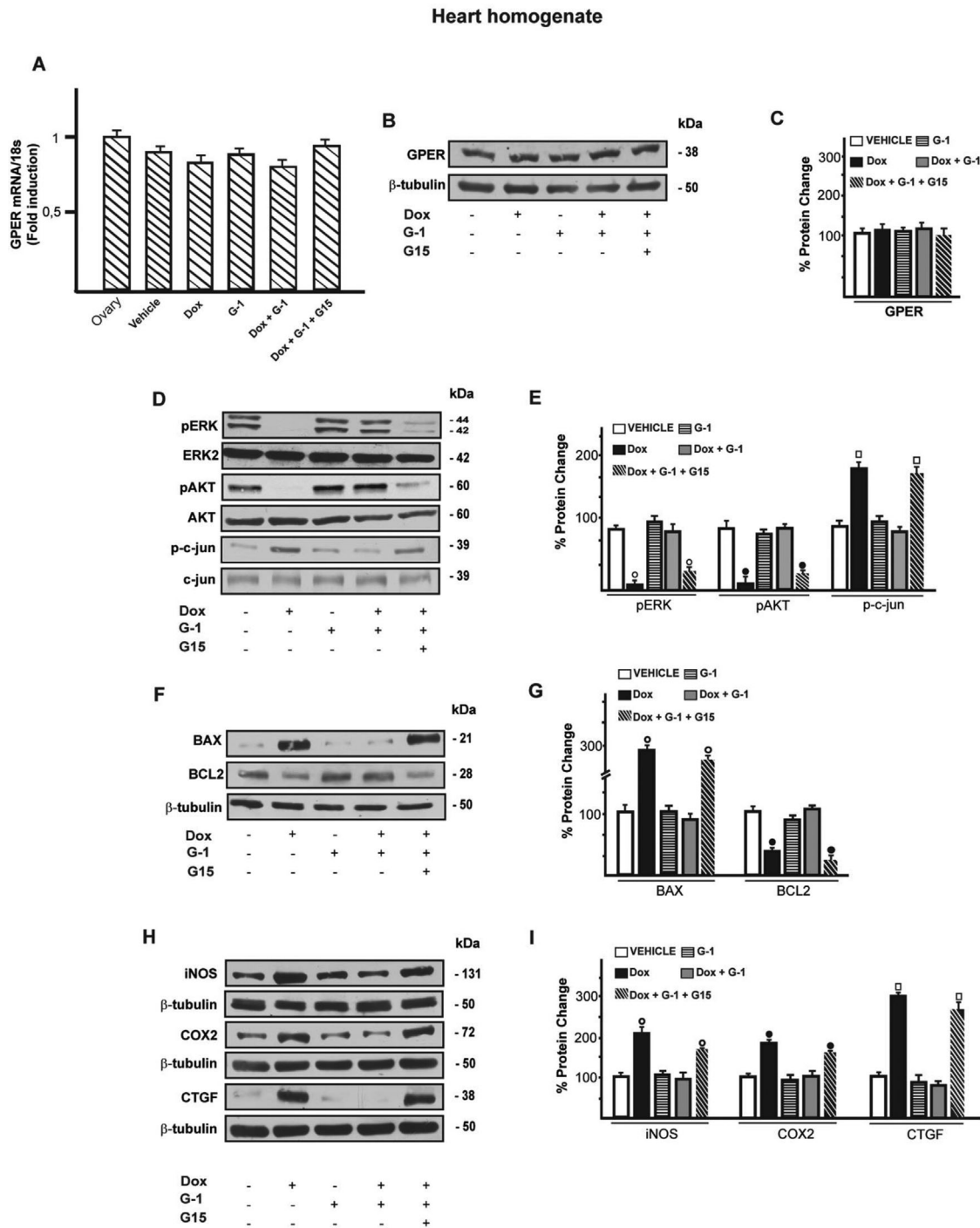


**Fig. 3. GPER mRNA (A) and protein (B and C) expression in heart homogenates from rats treated with vehicle (–), Dox, G-1 alone and in combination with Dox or G-1 in the presence of Dox and G15, as evaluated by real-time PCR and immunoblotting, respectively. In RNA experiments, PCR amplification in absence of cDNA was used as a control (–) and each data point represents the mean ± SD of three independent experiments performed in triplicate. In immunoblotting experiments, protein levels were quantified by densitometry and normalized to the expression of β-tubulin. Percentage changes were evaluated as the mean ± SD of six experiments for each group. (D,E) ERK, AKT, and c-jun phosphorylation in heart homogenates from rats treated with vehicle (–), Dox, G-1 alone and in combination with Dox or G-1 in the presence of both Dox and G15. The protein expression of pERK, pAKT, and p-c-jun was quantified by densitometry and normalized to total ERK, AKT, and c-jun, respectively. Changes were evaluated and expressed as the mean ± SD of six experiments for each group. (○), (●), (□) *P* < 0.05. (F and G) BAX and BCL2 expression in heart homogenates from rats treated with vehicle (–), Dox, G-1 alone and in combination with Dox or G-1 in the presence of both Dox and G15. The protein levels were quantified by densitometry and normalized to the expression of β-tubulin. Percentage changes were evaluated as the mean ± SD of six experiments for each group. (○), (●) *P* < 0.05. (H and I) iNOS, COX2, and CTGF expression in heart homogenates from rats treated with vehicle (–), Dox, G-1 alone and in combination with Dox or G-1 in the presence of Dox and G15. The protein levels were quantified by densitometry and normalized to the expression of β-tubulin. Percentage changes were evaluated as the mean ± SEM of six experiments for each group. (○), (●), (□) *P* < 0.05. Significance of difference from control value and comparison between groups (one-way ANOVA followed by Newman–Keuls Multiple Comparison Test).**

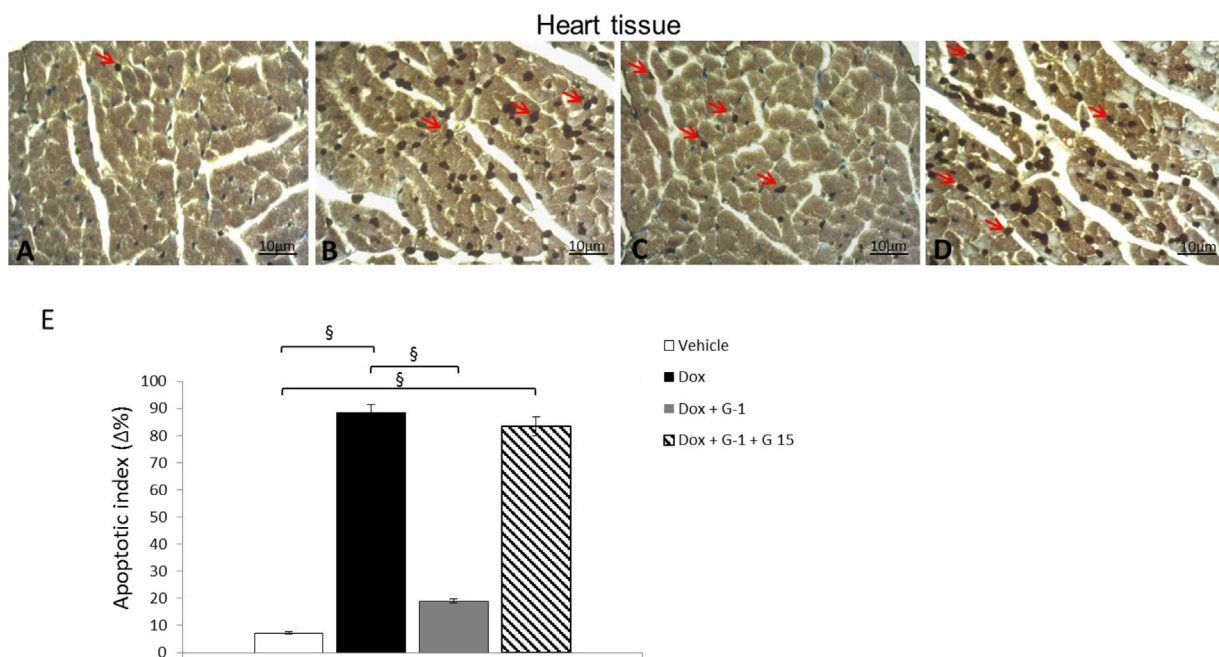


**Fig. 4.** (A–C) Representative images of Tunel-positive cardiomyocyte on rat hearts sections. Nuclei are indicated by red arrows. A (vehicle), B (Dox), C (Dox + G-1). (D) Apoptotic index of the cardiac muscle. Data shown are representative of three experiments for each group. Differences were evaluated by non-parametric Mann–Whitney–U test. (§)  $P < 0.05$ .

being  $5.6 \pm 0.3$  and  $6.7 \pm 1$  mmHg, respectively (Fig. 5). During reperfusion, G15 abolished the G-I associated protection on contracture, as LVEDP at the end of reperfusion was  $29.9 \pm 3.8$  mmHg (Fig. 5). Total infarct size (IS) was expressed as a percentage of left ventricular (LV) mass (Fig. 6). IS was  $68.6 \pm 3.4\%$  in saline group,  $78.2 \pm 4.8\%$  in Dox group,  $76.3 \pm 5\%$  in the animal group treated with G-I in combination with Dox and G15. The simultaneous administration of G-I and Dox determined an IS of  $44.5 \pm 2\%$ , which was similar to that observed in hearts exposed to G-I alone ( $52.6 \pm 2.6\%$ ) (Fig. 6), evidencing that G-I is able to reduce the IS area induced by Dox. Next, a slight decrease in IS and a small increase in dLVP functional recovery were observed in animals treated with Dox and G-I respect to the group treated with G-I alone (Figs. 5 and 6). Interestingly, in Dox group the cumulative LDH release during reperfusion was significantly increased with respect to the saline group, while in the group of animals treated with G-I in combination with Dox the release of LDH was significantly reduced. As expected, the levels of LDH increased in the group of animals treated with Dox in combination with G-I and G15 (data not shown).

## Discussion

Cardiotoxicity is one of the most important undesired complications of Dox treatment, which triggers the development of several dysfunctions and congestive heart failure (Octavia et al., 2012; Carvalho et al., 2014). Therefore, many approaches are currently investigated in order to minimize the severe side effects of Dox and improve its clinical effectiveness (Veijongsa and Yeh, 2014). In the present study, we demonstrated that ligand-activated GPER prevents the increase of TNF- $\alpha$ , IL-1 $\beta$ , ROS, and LDH plasma and tissue levels induced by Dox. Moreover, we showed that in rat heart homogenates GPER activation abolishes the increase in p-c-jun,

BAX, CTGF, iNOS, and COX2 expression triggered by Dox treatment. We also determined that the activation of GPER rescues the inhibitory action elicited by Dox on BCL2, pERK, pAKT expression, and attenuates apoptosis induced by Dox. Next, GPER activation mitigated the adverse effects of Dox after I/R insult, as evidenced by the ability of G-1 to increase systolic recovery, to reduce diastolic dysfunction and to decrease infarct size and plasma LDH levels. Further supporting the aforementioned data, the beneficial effects of G-1 on Dox-induced cardiotoxicity were prevented in the presence of the GPER antagonist G15, which has been largely acknowledged as specific inhibitor of GPER-mediated responses in diverse experimental models (Dennis et al., 2009). It should be noted that the experimental design was performed using male WKY rats that represent a unique model due to their minimal exposure to estrogens, which have been largely involved in GPER-mediated actions. Nonetheless, further studies are needed toward a better understanding of the potential of GPER to prevent the detrimental effects induced by Dox in the presence of different hormone exposures.

GPER mediates estrogenic signaling in diverse tissues like the cardiovascular system (Maggiolini and Picard, 2010; Meyer et al., 2011; Prossnitz and Barton, 2011; De Francesco et al., 2013a; Rigracchio et al., 2015a,b; Tropea et al., 2015; Lappano et al., 2016). In this regard, it has been demonstrated that GPER knockout mice exhibit both systolic and diastolic dysfunctions together with myocyte hypertrophy (Delbeck et al., 2011), suggesting that GPER may contribute to maintain cardiac mechanical performance. In addition, we have previously ascertained that GPER mediates a decreased contractility in Langendorff-perfused rat heart together with an increased phosphorylation of both ERK1/2 and eNOS (Filice et al., 2009), thus corroborating the cardiac beneficial effects mediated by GPER. Likewise, GPER has been involved in cell adaptation to stressful conditions like hypoxia and hypertension

### Isolated Langendorff Heart

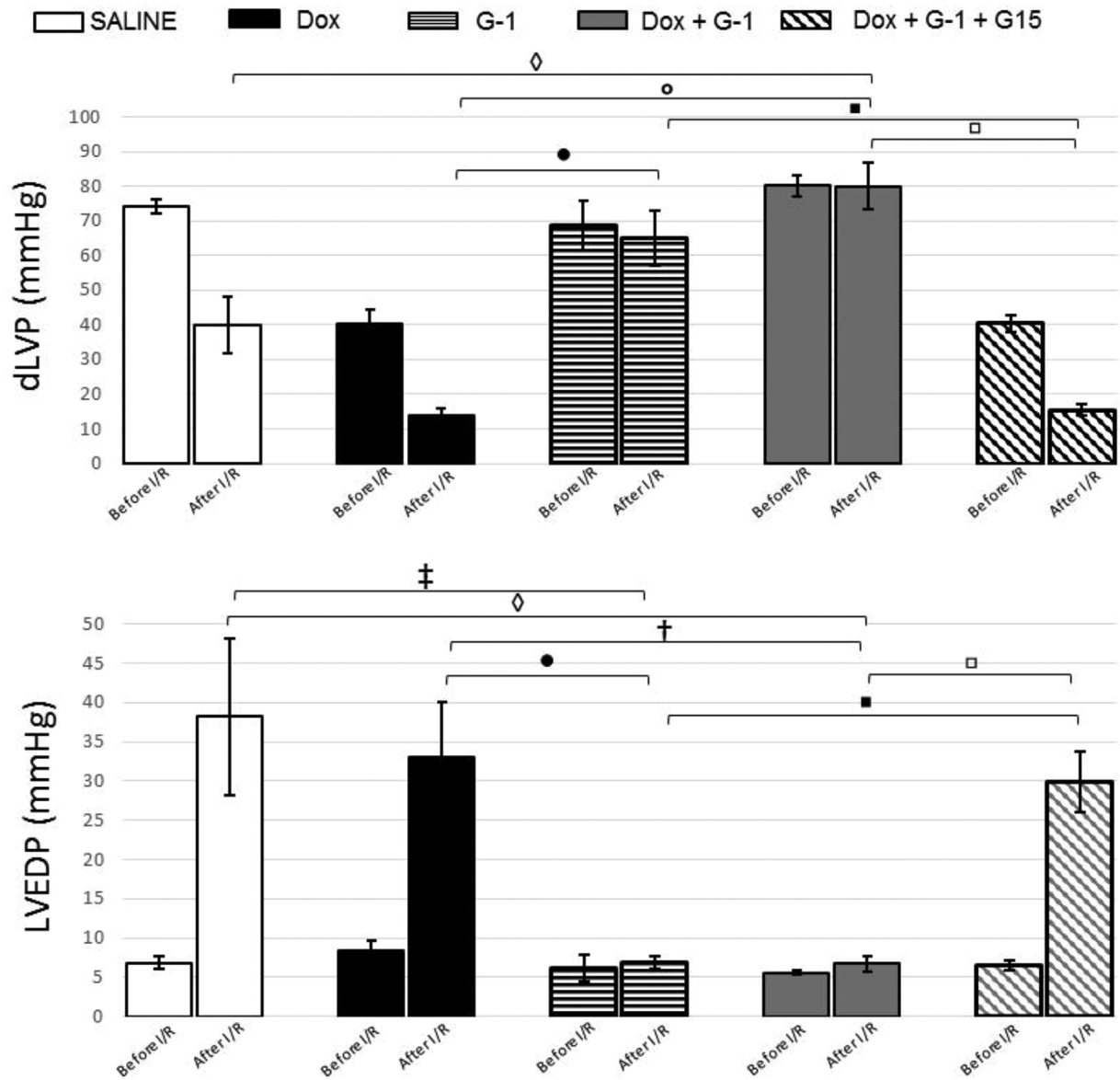


**Fig. 5.** Evaluation of LVP and LVEDP in saline, Dox, G-1, Dox + G-1, Dox + G-1 + G15 groups. Values are expressed as means  $\pm$  SD in respect to saline group from the stabilization to the end of the 150 min of reperfusion with respect to the baseline values for each group. Vertical lines indicate ischemic administration. Significance of differences from control value and comparison between groups by one-way ANOVA followed by Newman-Keuls Multiple Comparison Test: ( $\dagger$ ), ( $\ddagger$ ), ( $\diamond$ ), ( $\square$ ), ( $\blacksquare$ ), ( $\circ$ ), ( $\bullet$ )  $P < 0.05$ .

(Recchia et al., 2011; De Francesco et al., 2013a). Accordingly, GPER activation contributed to the negative inotropic and lusitropic effects in male spontaneously hypertensive rat hearts (De Francesco et al., 2013a). Further extending the ability of GPER in mediating beneficial cardiac effects in a stressful environment, it has been shown that in isolated mice and rat hearts exposed to I/R, G-1 pre-treatment reduces IS and preserves the cardiac function through AKT and ERK1/2 activation and the reduction of inflammation (Deschamps and Murphy, 2009; Weil et al., 2010). These data are in line with our findings showing that GPER activation may improve cardiac

function and decrease IS, hence attenuating the negative effects of Dox on cardiac performance, myocytes viability, and inflammation after I/R injury. Compelling evidence has involved in cardiomyocytes integrity after ischemic damage the AKT and ERK transduction signaling, also referred to as Reperfusion Injury Salvage Kinase (RISK) pathways, (de Jonge et al., 2006). In this regard, the downregulation of AKT and ERK transduction cascades has been shown to contribute to cardiomyocytes damage and apoptosis induced by Dox both in vitro and in vivo (Lou et al., 2005; Su et al., 2006). In accordance with these observations, our results suggest that GPER activation may

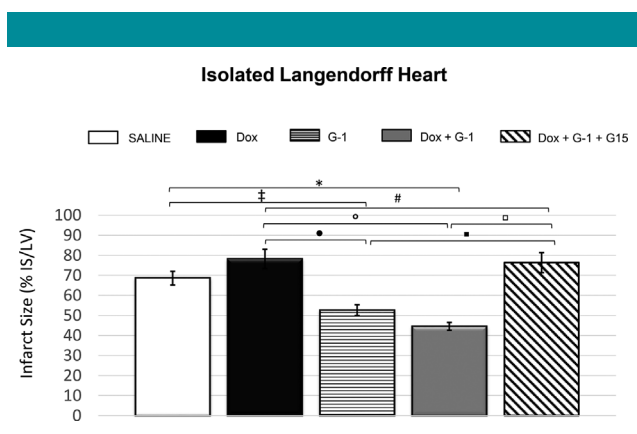


**Fig. 6. Infarct size (IS):** the amount of necrotic tissue is expressed as percentage of the left ventricle (% IS/LV), which is considered the risk area. Significance of differences from control value and comparison between groups by ANOVA followed by Newman-Keuls Multiple Comparison Test, ( $n = 6$  for each group) with respect to I/R (saline group). (\*), (#), (†), (‡), (○), (●), (■), (□)  $P < 0.05$ .

trigger AKT and ERK1/2 transduction signaling as downstream mediators toward cell survival during I/R.

It has been shown that the response of innate immunity and acute inflammation mediated by iNOS are activated after cardiac injury (Abe et al., 2001). Notably, in the present study, Dox-increased iNOS expression was prevented by G-1 treatment. In addition, G-1 reduced myocardial inflammation as evidenced by its ability to abolish the increase of COX2 and LDH cardiac levels upon Dox exposure. Moreover, G-1 administration counteracted the ability of Dox to increase the plasma and tissue levels of several inflammatory and damage markers like TNF- $\alpha$ , IL-1 $\beta$ , and LDH, hence suggesting that GPER activation may attenuate these detrimental effects elicited by Dox. According to these data, genetic ablation of GPER in mice was associated with a pro-inflammatory state while the treatment with G-1 was effective in reducing inflammation (Meyer et al., 2014; Barton and Prossnitz, 2015). Our data indicated also that GPER activation may prevent the fibrotic response to Dox treatment, thus corroborating the acknowledged role of GPER as anti-fibrotic mediator in rat heart (De Francesco et al., 2013a). As it concerns the pro-survival and anti-apoptotic actions induced by G-1 treatment in combination with Dox, we provided evidence that GPER activation prevents the harmful action of Dox on pro-survival signaling cascades like ERK1/2 and AKT. Indeed, the ability of G-1 to reduce the apoptotic response triggered by Dox nicely fits with previous investigations showing that GPER may mediate pro-survival effects in several model systems including keratinocytes, breast cancer cells, myocardial cells, and heart after I/R damage (Kanda and Watanabe, 2003; Weil et al., 2010; Delbeck et al., 2011; Barton and Prossnitz, 2015; Kabir et al., 2015).

Our findings pave the way for future investigations on the multifaceted mechanisms and mediators involved in GPER cardioprotection upon Dox exposure. In this regard, it has been demonstrated that Dox contributes to cardiac damage by inhibiting angiogenesis on human cardiac microvascular endothelial cells by reducing myocardial capillary density. This microvascular deficiency, described in cardiomyopathies such as diabetic and idiopathic dilated cardiomyopathies, promotes the progression of cardiac disease (Sun et al., 2016). On the contrary, GPER activation has been shown to contribute to the formation of new blood vessels particularly under stressful conditions (De Francesco et al., 2013b, Rigracciolo et al., 2015a). Additionally, Doxorubicin-dependent cardiomyopathy is associated with

impaired  $Ca^{2+}$  handling in the sarcoplasmic reticulum, which resulted markedly decreased in Dox-treated hearts, leading to a reduced cardiac function (Arai et al., 2000). At the same time, Kooptiwut et al. (2014) demonstrated in INS-1 cells that estrogen increases SERCA-2 expression. This suggests that the protective effect of G1 against Dox-dependent cardiotoxicity can be mediated by the increase of SERCA-2 expression.

Collectively, our results contribute to extend the current knowledge on the potential of GPER to exert beneficial cardiac effects in stressful conditions. As GPER activation may mitigate the cardiotoxicity exerted by Dox, our data suggest that combination therapies targeting GPER can represent a novel strategy in order to strengthen the usefulness of this anti-cancer drug.

## Acknowledgments

This work was supported by Associazione Italiana per la Ricerca sul Cancro (AIRC, grant n. 16719/2015), Ministero della Salute (grant n. 67/GR-2010-231951 I), “Ministero dell’Università e Ricerca Scientifica e Tecnologica” (ex 60%), and “Dottorato di Ricerca in Scienze della Vita” (“Fondo Giovani”). EMDF was supported by an iCARE fellowship from the Associazione Italiana per la Ricerca sul Cancro (AIRC) cofunded by Marie Curie Actions.

## Literature Cited

- Abe K, Tokumura M, Ito T, Murai T, Takashima A, Ibi N. 2001. Involvement of iNOS in postischemic heart dysfunction of stroke-prone spontaneously hypertensive rats. *Am J Physiol Heart Circ Physiol* 280:H668–H673.
- Amelio D, Garofalo F, Wong V, Chew SF, Ip YK, Cerra MC, Tota B. 2013. Nitric oxide synthase-dependent “on/off” switch and apoptosis in freshwater and aestivating lungfish, *Protopterus annectens*: Skeletal muscle versus cardiac muscle. *Nitric Oxide* 32:1–12.
- Arai M, Yaguchi A, Takizawa T, Yokoyama T, Kanda T, Kurabayashi M, Nagai R. 2000. Mechanism of doxorubicin-induced inhibition of sarcoplasmic reticulum  $Ca^{2+}$ -ATPase gene transcription. *Circ Res* 86:8–14.
- Barton M, Prossnitz ER. 2015. Emerging roles of GPER in diabetes and atherosclerosis. *Trends Endocrinol Metab* 26:185–192.
- Bopassa JC, Eghbali M, Toro L, Stefani E. 2010. A novel estrogen receptor GPER inhibits mitochondria permeability transition pore opening and protects the heart against ischemia-reperfusion injury. *Am J Physiol Heart Circ Physiol* 298:H16–H23.
- Carvalho FS, Burgeiro A, Garcia R, Moreno AJ, Carvalho RA, Oliveira PJ. 2014. Doxorubicin-induced cardiotoxicity: From bioenergetic failure and cell death to cardiomyopathy. *Med Res Rev* 34:106–135.
- Cerra MC, De Iuri L, Angelone T, Corti A, Tota B. 2006. Recombinant N-terminal fragments of chromogranin-A modulate cardiac function of the Langendorff-perfused rat heart. *Basic Res Cardiol* 101:43–52.
- De Francesco EM, Angelone T, Pasqua T, Pupo M, Cerra MC, Maggiolini M. 2013a. GPER mediates cardioprotective effects in spontaneously hypertensive rat hearts. *PLoS ONE* 8:e69322.
- De Francesco EM, Lappano R, Santolla MF, Marsico S, Caruso A, Maggiolini M. 2013b. HIF-1 $\alpha$ /GPER signaling mediates the expression of VEGF induced by hypoxia in breast cancer associated fibroblasts (CAFs). *Breast Cancer Res* 15:R64.
- De Francesco EM, Pellegrino M, Santolla MF, Lappano R, Ricchio E, Abonante S, Maggiolini M. 2014. GPER mediates activation of HIF1 $\alpha$ /VEGF signaling by estrogens. *Cancer Res* 74:4053–4064.
- de Jonge N, Goumans MJ, Lips D, Hassink R, Vlugs EJ, van der Meel R, Emmerson CD, Nijman J, de Windt L, Doevendans PA. 2006. Controlling cardiomyocyte survival. *Novartis Found Symp* 274:41–51. discussion 51–7, 152–5, 272–6.
- Delbeck M, Golz S, Vonk R, Janssen W, Hucho T, Isensee J, Schäfer S, Otto C. 2011. Impaired left-ventricular cardiac function in male GPR30-deficient mice. *Mol Med Rep* 4:37–40.
- Dennis MK, Burai R, Ramesh C, Petrie WK, Alcon SN, Nayak TK, Bologna CG, Leitao A, Brailoiu E, Deliu E, Dun NJ, Sklar LA, Hathaway HJ, Arterburn JB, Oprea TI, Prossnitz ER. 2009. In vivo effects of a GPR30 antagonist. *Nat Chem Biol* 5:421–427.
- Deschamps AM, Murphy E. 2009. Activation of a novel estrogen receptor, GPER, is cardioprotective in male and female rats. *Am J Physiol Heart Circ Physiol* 297: H1806–H1813.
- Filice E, Recchia AG, Pellegrino D, Angelone T, Maggiolini M, Cerra MC. 2009. A new membrane G protein-coupled receptor (GPR30) is involved in the cardiac effects of 17 $\beta$ -estradiol in the male rat. *J Physiol Pharmacol* 60:3–10.
- Kanda N, Watanabe S. 2003. 17 $\beta$ -estradiol inhibits oxidative stress-induced apoptosis in keratinocytes by promoting Bcl-2 expression. *J Invest Dermatol* 121:1500–1509.
- Kabir ME, Singh H, Lu R, Olde B, Leeb-Lundberg LM, Bopassa JC. 2015. G protein-coupled estrogen receptor 1 mediates acute estrogen-induced cardioprotection via MEK/ERK/GSK-3 $\beta$  pathway after Ischemia/Reperfusion. *PLoS ONE* 10:e0135988.
- Kooptiwut S, Mahawong P, Hanchang W, Sempasert N, Kaewin S, Limjindaporn T, Yenchitsomanus PT. 2014. Estrogen reduces endoplasmic reticulum stress to protect against glucotoxicity induced-pancreatic  $\beta$ -cell death. *J Steroid Biochem Mol Biol* 139:25–32.
- Lappano R, Rigracciolo D, De Marco P, Avino S, Cappello AR, Rosano C, Maggiolini M, De Francesco EM. 2016. Recent advances on the role of G protein-coupled receptors in hypoxia-mediated signaling. *AAPS J* 18:305–310.
- Lindsey SH, Chappell MC. 2011. Evidence that the G protein-coupled membrane receptor GPR30 contributes to the cardiovascular actions of estrogen. *Gen Med* 8:343–354.
- Lou H, Danielson I, Singal PK. 2005. Involvement of mitogen activated protein kinases in adriamycin-induced cardiomyopathy. *Am J Physiol Heart Circ Physiol* 288:H1925–H1930.

- Maggiolini M, Picard D. 2010. The unfolding stories of GPR30, a new membrane-bound estrogen receptor. *J Endocrinol* 204:105–114.
- Mantawy EM, El-Bakly WM, Esmat A, Badr AM, El-Demerdash E. 2014. Chrysin alleviates acute doxorubicin cardiotoxicity in rats via suppression of oxidative stress, inflammation and apoptosis. *Eur J Pharmacol* 728:107–118.
- Meyer MR, Fredette NC, Howard TA, Hu C, Ramesh C, Daniel C, Amann K, Arterburn JB, Barton M, Prossnitz ER. 2014. G protein-coupled estrogen receptor protects from atherosclerosis. *Sci Rep* 4:7564.
- Meyer MR, Prossnitz ER, Barton M. 2011. The G protein-coupled estrogen receptor GPER/GPR30 as a regulator of cardiovascular function. *Vascul Pharmacol* 55:17–25.
- Octavia Y, Tocchetti CG, Gabrielson KL, Janssens S, Crijns HJ, Moens AL. 2012. Doxorubicin-induced cardiomyopathy: From molecular mechanisms to therapeutic strategies. *J Mol Cell Cardiol* 52:1213–1225.
- Pagliari P, Mancardi D, Rastaldo R, Penna C, Gattullo D, Miranda KM, Feelisch M, Wink DA, Kass DA, Paolucci N. 2003. Nitroxyl affords thiol-sensitive myocardial protective effects akin to early preconditioning. *Free Radic Biol Med* 34:33–43.
- Patel VH, Chen J, Ramanjaneya M, Karteris E, Zachariades E, Thomas P, Been M, Randeve HS. 2010. G-protein coupled estrogen receptor 1 expression in rat and human heart: Protective role during ischaemic stress. *Int J Mol Med* 26:193–199.
- Penna C, Cappello S, Mancardi D, Raimondo S, Rastaldo R, Gattullo D, Losano G, Pagliaro P. 2006. Post-conditioning reduces infarct size in the isolated rat heart: Role of coronary flow and pressure and the nitric oxide/cGMP pathway. *Basic Res Cardiol* 101:168–179.
- Penna C, Pasqua T, Perrelli MG, Pagliaro P, Cerra MC, Angelone T. 2012. Postconditioning with glucagon like peptide-2 reduces ischemia/reperfusion injury in isolated rat hearts: Role of survival kinases and mitochondrial KATP channels. *Basic Res Cardiol* 107:272–283.
- Prossnitz ER, Barton M. 2011. The G-protein-coupled estrogen receptor GPER in health and disease. *Nat Rev Endocrinol* 7:715–726.
- Recchia AG, De Francesco EM, Vivacqua A, Sisci D, Panno ML, Andò S, Maggiolini M. 2011. The G protein-coupled receptor 30 is up-regulated by hypoxia-inducible factor-1alpha (HIF-1alpha) in breast cancer cells and cardiomyocytes. *J Biol Chem* 286:10773–10782.
- Rigiracciolo DC, Scarpelli A, Lappano R, Pisano A, Santolla MF, De Marco P, Cirillo F, Cappello AR, Dolce V, Belfiore A, Maggiolini M, De Francesco EM. 2015a. Copper activates HIF-1 $\alpha$ /GPER/VEGF signaling in cancer cells. *Oncotarget* 6:34158–34177.
- Rigiracciolo DC, Scarpelli A, Lappano R, Pisano A, Santolla MF, Avino S, De Marco P, Bussolati B, Maggiolini M, De Francesco EM. 2015b. GPER is involved in the stimulatory effects of aldosterone in breast cancer cells and breast tumor-derived endothelial cells. *Oncotarget* 7:94–111.
- Saad SY, Najjar TA, Alashari M. 2004. Cardiotoxicity of doxorubicin/paclitaxel combination in rats: Effect of sequence and timing of administration. *J Biochem Mol Toxicol* 18:78–86.
- Su HF, Samsamshariat A, Fu J, Shan YX, Chen YH, Piomelli D, Wang PH. 2006. Oleyethanolamide activates Ras-Erk pathway and improves myocardial function in doxorubicin-induced heart failure. *Endocrinology* 147:827–834.
- Sun Z, Schriewer J, Tang M, Marlin J, Taylor F, Shohet RV, Konorev EA. 2016. The TGF- $\beta$  pathway mediates doxorubicin effects on cardiac endothelial cells. *J Mol Cell Cardiol* 90:129–138.
- Tocchetti CG, Carpi A, Coppola C, Quintavalle C, Rea D, Campesan M, Arcari A, Piscopo G, Cipresso C, Monti MG, De Lorenzo C, Arra C, Condorelli G, Di Lisa F, Maurea N. 2014. Ranolazine protects from doxorubicin-induced oxidative stress and cardiac dysfunction. *Eur J Heart Fail* 16:358–366.
- Tropea T, De Francesco EM, Rigiracciolo D, Maggiolini M, Wareing M, Osol G, Mandalà M. 2015. Pregnancy augments G protein estrogen receptor (GPER) induced vasodilation in rat uterine arteries via the nitric oxide – cGMP signaling pathway. *PLoS ONE* 10:e0141997.
- Veijpongsa P, Yeh ET. 2014. Prevention of anthracycline-induced cardiotoxicity: Challenges and opportunities. *J Am Coll Cardiol* 64:938–945.
- Weil BR, Manukyan MC, Herrmann JL, Wang Y, Abarbanell AM, Poynter JA, Meldrum DR. 2010. Signaling via GPR30 protects the myocardium from ischemia/reperfusion injury. *Surgery* 148:436–443.
- Young RC, Ozols RF, Myers CE. 1981. The anthracycline antineoplastic drugs. *N Engl J Med* 305:139–153.
- Zimmerman MA, Budish RA, Kashyap S, Lindsey SH. 2016. GPER-novel membrane oestrogen receptor. *Clin Sci (Lond)* 130:1005–1016.

# GPER is involved in the stimulatory effects of aldosterone in breast cancer cells and breast tumor-derived endothelial cells

Damiano Cosimo Rigracciolo<sup>1</sup>, Andrea Scarpelli<sup>1</sup>, Rosamaria Lappano<sup>1</sup>, Assunta Pisano<sup>1</sup>, Maria Francesca Santolla<sup>1</sup>, Silvia Avino<sup>1</sup>, Paola De Marco<sup>1</sup>, Benedetta Bussolati<sup>2</sup>, Marcello Maggiolini<sup>1</sup> and Ernestina Marianna De Francesco<sup>1</sup>

<sup>1</sup> Department of Pharmacy, Health and Nutritional Sciences, University of Calabria, Rende, Italy

<sup>2</sup> Department of Molecular Biotechnology and Health Sciences, University of Torino, Turin, Italy

**Correspondence to:** Marcello Maggiolini, **email:** marcellomaggiolini@yahoo.it

Rosamaria Lappano, **email:** lappanorosamaria@yahoo.it

**Keywords:** GPER, aldosterone, mineralcorticoid receptor, breast cancer cells, breast tumor-derived endothelial cells, Pathology Section

**Received:** September 01, 2015

**Accepted:** November 22, 2015

**Published:** December 05, 2015

## ABSTRACT

**Aldosterone induces relevant effects binding to the mineralcorticoid receptor (MR), which acts as a ligand-gated transcription factor. Alternate mechanisms can mediate the action of aldosterone such as the activation of epidermal growth factor receptor (EGFR), MAPK/ERK, transcription factors and ion channels. The G-protein estrogen receptor (GPER) has been involved in the stimulatory effects of estrogenic signalling in breast cancer. GPER has been also shown to contribute to certain responses to aldosterone, however the role played by GPER and the molecular mechanisms implicated remain to be fully understood. Here, we evaluated the involvement of GPER in the stimulatory action exerted by aldosterone in breast cancer cells and breast tumor derived endothelial cells (B-TEC). Competition assays, gene expression and silencing studies, immunoblotting and immunofluorescence experiments, cell proliferation and migration were performed in order to provide novel insights into the role of GPER in the aldosterone-activated signalling. Our results demonstrate that aldosterone triggers the EGFR/ERK transduction pathway in a MR- and GPER-dependent manner. Aldosterone does not bind to GPER, it however induces the direct interaction between MR and GPER as well as between GPER and EGFR. Next, we ascertain that the up-regulation of the Na<sup>+</sup>/H<sup>+</sup> exchanger-1 (NHE-1) induced by aldosterone involves MR and GPER. Biologically, both MR and GPER contribute to the proliferation and migration of breast and endothelial cancer cells mediated by NHE-1 upon aldosterone exposure. Our data further extend the current knowledge on the molecular mechanisms through which GPER may contribute to the stimulatory action elicited by aldosterone in breast cancer.**

## INTRODUCTION

Aldosterone elicits multiple biological effects binding to the mineralcorticoid receptor (MR), which acts as a ligand-gated transcription factor [1]. In addition, rapid aldosterone signalling involves alternate mechanisms that include the activation of transduction pathways like tyrosine kinase c-Src, epidermal growth factor receptor (EGFR) and MAPK/ERK cascade [2-4]. Aldosterone is a key component of the renin-angiotensin-aldosterone system (RAAS), which is mainly implicated in maintaining

salt and water balance toward the regulation of systemic blood pressure [5]. In addition, aldosterone activates ionic membrane transporters as the Na<sup>+</sup>/H<sup>+</sup> exchanger (NHE-1) and Na<sup>+</sup>/HCO<sub>3</sub><sup>-</sup> cotransporter (NBC), which regulate the cellular pH and volume [6-7]. Aldosterone has been also involved in diverse cardio-metabolic diseases as it triggers inflammatory and fibrotic responses in both heart and vessels [8-11]. Recent studies have suggested that aldosterone/MR signalling may contribute to the progression of certain types of tumor [12-13]. For instance, it has been shown that aldosterone stimulates

the survival and proliferation of renal carcinoma cells by upregulating K-RAS and the activation of the Akt and Raf pathways [12]. Moreover, an aldosterone blocker inhibited the growth of hepatocellular carcinoma and angiogenesis both *in vitro* and *in vivo* [13].

The G-protein estrogen receptor namely GPER mediates several pathophysiological functions in the cardiovascular, immune and central nervous systems, glucose and fat metabolism [14]. In addition, our and other previous studies have largely demonstrated that estrogenic GPER signalling elicits stimulatory effects in cancer cells and tumor microenvironment toward cancer progression [14-19]. In this regard, it has been reported that GPER activation triggers diverse transduction pathways involved in the proliferation, invasion and migration of tumor cells, including the epidermal growth factor receptor (EGFR), the MAPK/ERK and PI3K/AKT transduction cascades, Ca<sup>2+</sup> mobilization and cAMP production [20-27]. Numerous endogenous, environmental and newly synthesized molecules have been shown to trigger relevant GPER-mediated responses in different cell contexts [28-36]. Aldosterone has been recently suggested to act through GPER in diverse models, including the cardiovascular and renal systems [6, 37-40]. For instance, it was demonstrated that GPER is involved in important effects exerted by aldosterone on vascular endothelial cells, cardiac vagal tone and connecting tubule glomerular feedback [37-40]. These observations have pointed out the potential of GPER to contribute to the aldosterone action, however the effective role played by GPER and the molecular mechanisms implicated are controversial as pharmacologic criteria for considering GPER as an aldosterone receptor have been not adequately fulfilled [41-43].

In the framework of the aforementioned observations, the current study provides novel insights into the role of GPER in mediating the action of aldosterone in breast tumor. In particular, our data show that a functional cross-talk between MR and GPER may occur upon aldosterone treatment leading to stimulatory effects in both breast cancer cells and endothelial cells obtained from breast malignancies.

## RESULTS

### Aldosterone activates the EGFR/ERK transduction pathway and induces the interaction between MR and GPER

We began our study evaluating whether aldosterone could be able to activate the EGFR/ERK transduction signalling in SkBr3 breast cancer cells and B-TEC breast tumor-derived endothelial cells, which were used as model systems. Both cell types express MR and GPER but not

ER $\alpha$  (Supplementary Figure 1). Of note, pM aldosterone concentrations induced the phosphorylation of EGFR and ERK1/2 in both SkBr3 cells and B-TEC (Figure 1A-1D), though these effects were no longer evident silencing the expression of MR (Figure 1E-1J). Recently, it has been reported that GPER contributes to aldosterone action although the mechanisms involved remain to be fully understood [6, 38-44]. In this vein, we therefore performed saturation curves and scatchard plot analyses using as radiotracers the GPER ligand [<sup>3</sup>H]E2 [28, 31-32, 34-36] and the MR ligand [<sup>3</sup>H]aldosterone. [<sup>3</sup>H]E2 showed an estimated Bmax corresponding to 6799  $\pm$  707.8 cpm/1  $\times$  10<sup>5</sup> SkBr3 cells and an estimated Kd corresponding to 8.16  $\pm$  1.70 nM (Figure 2A), whereas [<sup>3</sup>H]aldosterone showed an estimated Bmax corresponding to 2159  $\pm$  229.2 cpm/1  $\times$  10<sup>5</sup> SkBr3 cells and an estimated Kd corresponding to 0.42  $\pm$  0.08 nM (Figure 2B). In competition assays, E2 but not aldosterone displaced [<sup>3</sup>H]E2 (Figure 2C), while aldosterone but not E2 displaced [<sup>3</sup>H]Aldosterone (Figure 2D). Collectively, these findings argue that in SkBr3 cells aldosterone is not able to displace [<sup>3</sup>H]E2, which was used as a GPER radioligand.

In order to gain further insights into the role of GPER in certain biological responses to aldosterone, we then evaluated the possible interaction of GPER and MR and EGFR. Our immunoprecipitation data indicated that aldosterone triggers a direct interaction between GPER and MR as well as GPER and EGFR (Figure 2E-2L). Immunofluorescence experiments performed in SkBr3 cells further corroborated the aforementioned results as an increased merged (orange) signal of MR and GPER was observed upon a short (15 min) aldosterone treatment (Figure 2M-2O). Altogether, these data suggest that GPER may contribute to aldosterone/MR-activated EGFR signalling.

### GPER is involved in the aldosterone-mediated signalling

On the basis of the abovementioned observations, we performed gene silencing experiments in order to assess whether GPER is involved in the rapid signalling induced by aldosterone. Interestingly, the activation of both EGFR and ERK1/2 by aldosterone was no longer evident silencing GPER in both SkBr3 cells and B-TEC (Figure 3A-3F). In accordance with these findings, the GPER antagonist G15 prevented the EGFR/ERK phosphorylation upon aldosterone exposure (Figure 3G-3I). Next, the EGFR tyrosine kinase inhibitor AG1478 (AG) but not the MEK inhibitor PD98059 (PD) blocked EGFR phosphorylation by aldosterone (Figure 3G-3I), while ERK1/2 activation was prevented in the presence of both AG and PD. Hence, the MEK/ERK transduction pathway is activated afterward the engagement of EGFR upon aldosterone treatment in our model system.

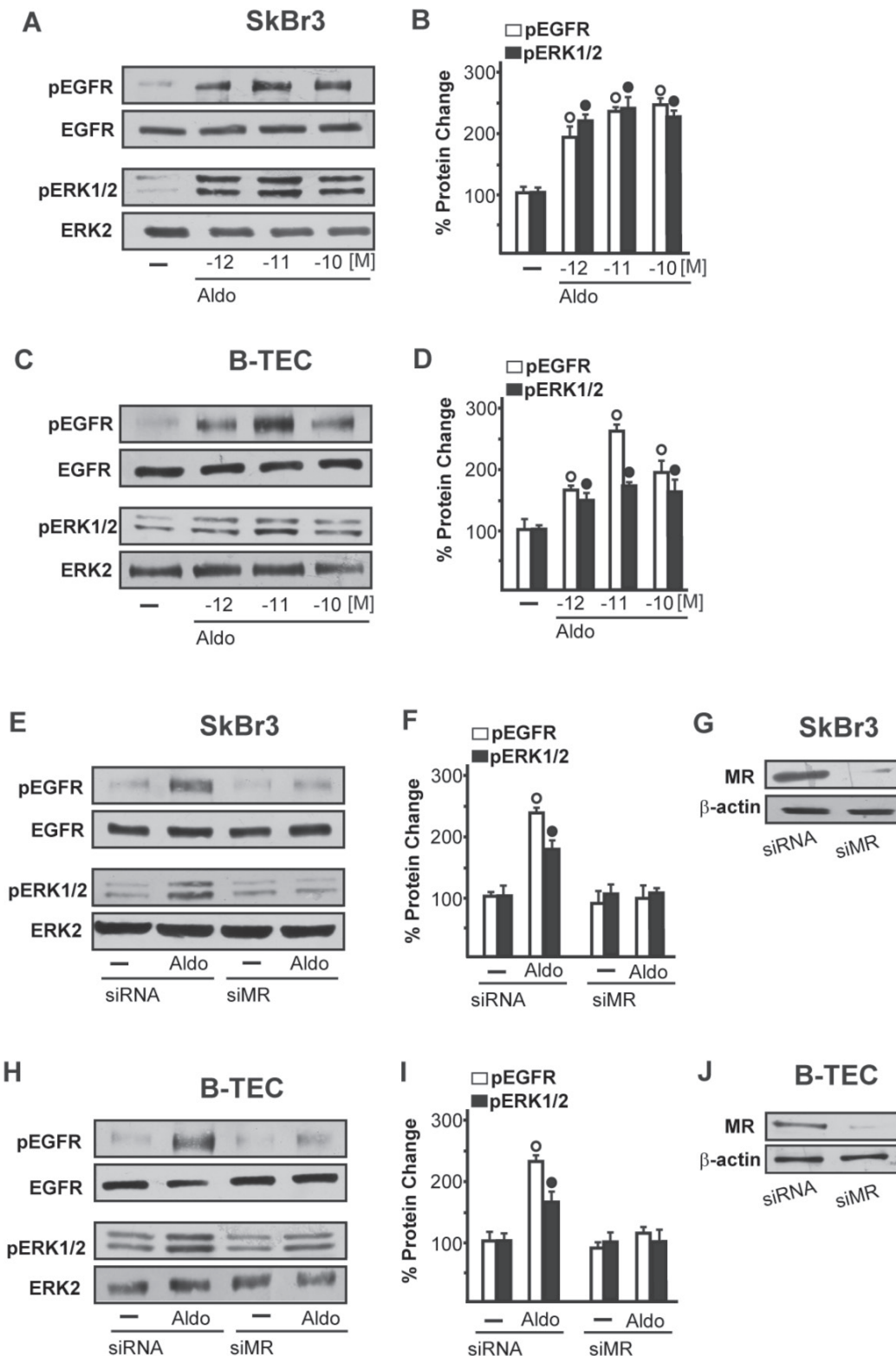


**Figure 1: EGFR and ERK1/2 phosphorylation in SkBr3 cells.** A., B. and B-TEC C., D. treated with Aldosterone (Aldo) for 15 min. EGFR and ERK1/2 phosphorylation in SkBr3 cells E., F. and B-TEC H., I. transfected for 24 h with siRNA or siMR and then treated with 10 pM Aldo for 15 min. G., J. Efficacy of MR silencing. The blots were normalized to EGFR or ERK2 and each data point represents the mean  $\pm$  SD of three independent experiments. (○) and (●) indicate  $p < 0.05$  for cells receiving vehicle (-) versus Aldo treatment.

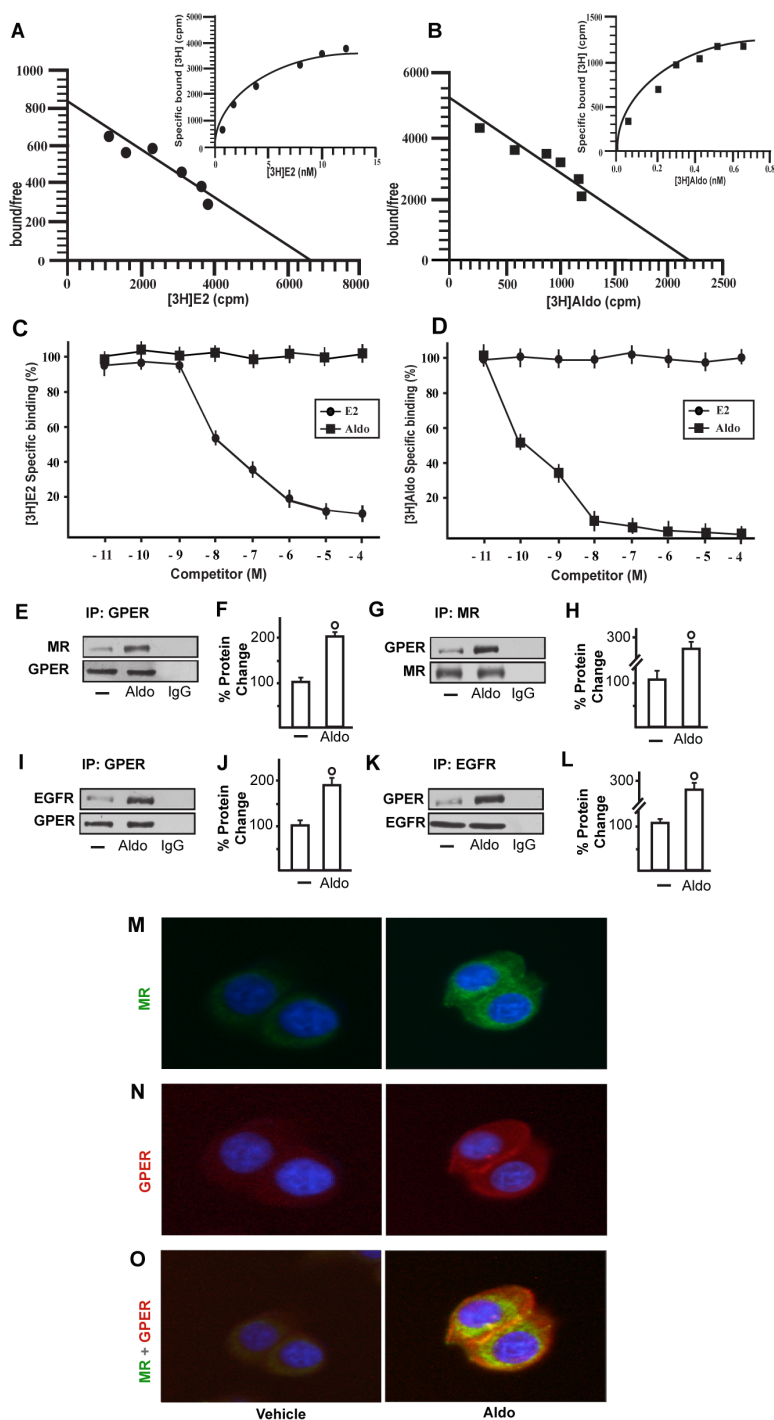


**Figure 2: Representative saturation curve and Scatchard plot of  $[^3\text{H}]$ 17 $\beta$ -estradiol (E2) binding** **A.** and  $[^3\text{H}]$ Aldosterone (Aldo) binding **B.** in SkBr3 cells. Each value represents the mean  $\pm$  SEM of three determinations. Ligand binding assay in SkBr3 cells incubated with  $[^3\text{H}]$ E2 and exposed to increasing concentrations of E2 and Aldo for 2 hours **C.** Ligand binding assay in SkBr3 cells incubated with  $[^3\text{H}]$ Aldo and exposed to increasing concentrations of E2 and Aldo for 2 hours **D.** Competition curves are expressed as a percentage of maximum specific  $[^3\text{H}]$ E2 or  $[^3\text{H}]$ Aldo binding. Each data point represents the mean  $\pm$  SEM of three independent experiments performed in triplicate. The co-immunoprecipitation of MR with GPER increases upon treatment with 10 pM Aldo for 15 min in SkBr3 cells **E.-H.** The blots were normalized to GPER or MR, respectively. The interaction between GPER and EGFR increases upon treatment with 10 pM Aldo for 15 min in SkBr3 cells **I.-L.** The blots were normalized to GPER or EGFR, respectively. In control samples, nonspecific IgG was used instead of the primary antibody, as indicated. Each data point represents the mean  $\pm$  SD of three independent experiments. (○) indicates  $p < 0.05$  for cells receiving vehicle (-) versus Aldo treatment. Localization of MR **M.** and GPER **N.** alone or in combination **O.**, as evaluated by immunofluorescence in SkBr3 cells treated with 10 pM Aldo for 15 min. Green signal: MR; Red signal: GPER; Blue signal: Nuclei. Images shown are representative of ten random fields from three independent experiments.

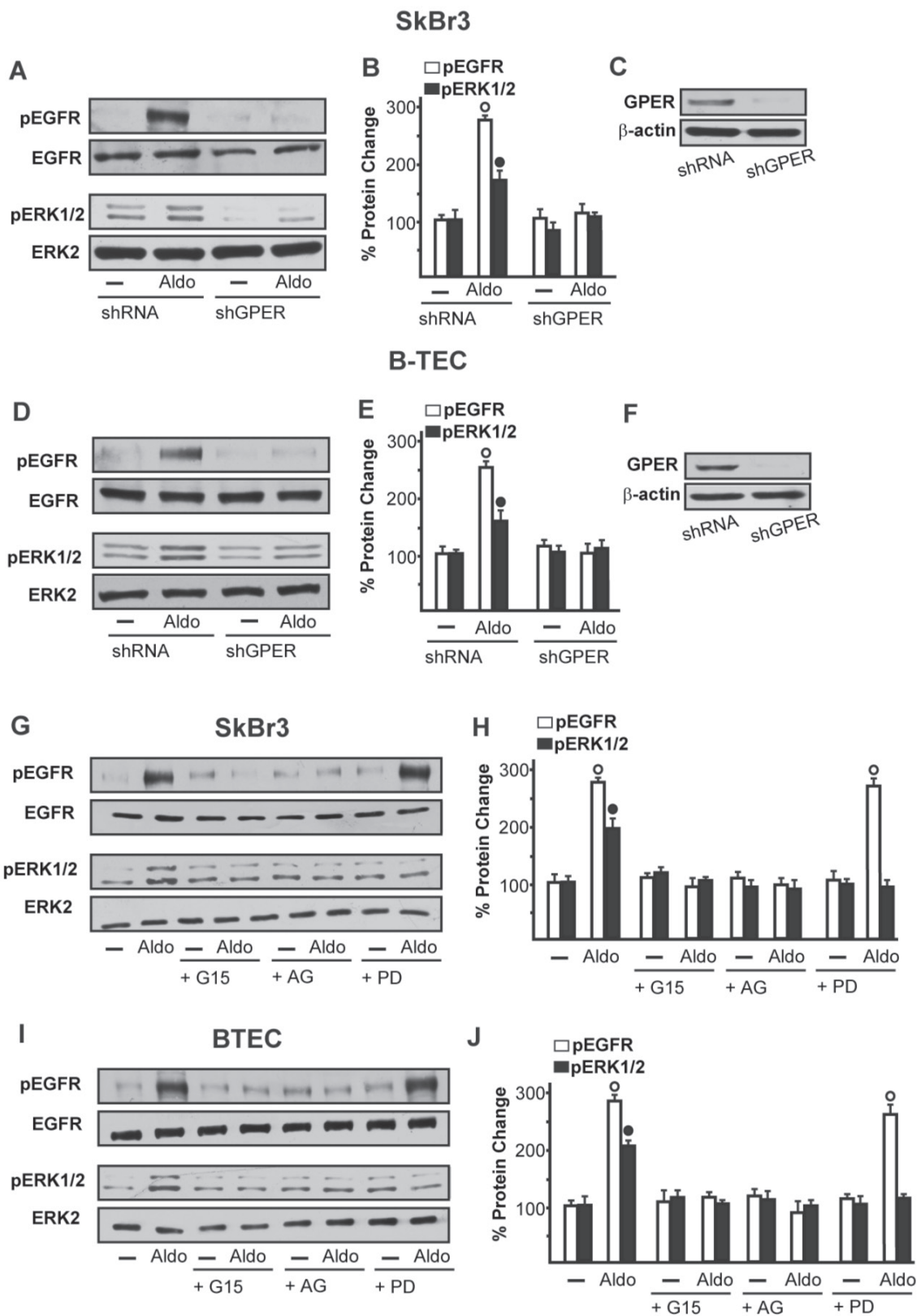


**Figure 3: EGFR and ERK1/2 phosphorylation in SkBr3 cells.** A., B. and B-TEC D., E. transfected for 24 h with shRNA or shGPER and then treated with 10 pM Aldo for 15 min. C., F. Efficacy of GPER silencing. EGFR and ERK1/2 activation in SkBr3 cells G., H. and B-TEC I., J. treated for 15 min with 10 pM Aldo alone and in combination with 10 μM EGFR inhibitor AG1478 (AG), 10 μM MEK inhibitor PD98059 (PD) and 100 nM GPER antagonist G15. The blots were normalized to EGFR or ERK2 and each data point represents the mean ± SD of three independent experiments. (○) and (●) indicate  $p < 0.05$  for cells receiving vehicle (-) versus Aldo treatment.

Aldosterone/MR signalling stimulates the activity and expression of NHE-1, which has been involved in tumor cell migration, invasion and metastasis particularly in breast cancer [6-7, 45]. In this regard, we assessed that aldosterone prompts NHE-1 activity in both SkBr3 cells and B-TEC as evaluated by a fluorescent indicator of cytoplasmic pH changes (Figure 4A). In addition, aldosterone up-regulated NHE-1 at both the mRNA and protein levels as determined by real time PCR (Figure 4B) and immunofluorescence studies performed in SkBr3 cells and B-TEC (Figure 4C-4F). Next, the stimulatory effects induced by aldosterone on NHE-1 protein expression were abolished silencing MR (Figure 5) as well as GPER (Figure 6). Collectively, these findings suggest that NHE-1 regulation by aldosterone requires MR along with GPER.

### **Aldosterone induces biological responses through both MR and GPER**

Functionally, we studied the role of MR and GPER in the proliferative effects of aldosterone in breast tumor cells as well as in the migration of tumor endothelial cells. Indeed, aldosterone triggered growth effects in SkBr3 cells, as assessed by cell counting (Figure 7A) and evidenced by time-lapse video microscopy (Videos 1-2). Cell proliferation stimulated by 10pM aldosterone was no longer evident silencing MR (Figure 7B-7C) or knocking-down GPER expression (Figure 7D-7E) and using the NHE-1 inhibitor cariporide (Figure 7F). Similar results were obtained using aldosterone concentrations up to 10 nM (data not shown). Furthermore, aldosterone promoted the migration of B-TEC as evidenced by time-lapse video microscopy (Videos 3-4) and scratch assay (Figure 8). The observed aldosterone-induced motility was abrogated silencing MR (Figure 8A, 8B, 8F) or GPER (Figure 8C-8D, 8G) and in the presence of cariporide (Figure 8E). Overall, these results indicate that the functional interaction between MR and GPER is involved in the aforementioned stimulatory action of aldosterone in both SkBr3 cells and B-TEC.

## **DISCUSSION**

In the present study we provide novel evidence regarding the molecular mechanisms by which GPER may contribute to the biological responses induced by aldosterone in breast cancer cells and breast tumor-derived endothelial cells. In particular, we have demonstrated that aldosterone activates the EGFR/ERK transduction signalling through the classic MR and the involvement of GPER, as evidenced by gene silencing experiments and pharmacological inhibitors. In addition, we have shown that both MR and GPER mediate the aldosterone-induced up-regulation of Na<sup>+</sup>/H<sup>+</sup> exchanger-1 (NHE-1), a well-known MR target involved in cancer progression

[7, 45]. We have also evidenced that aldosterone does not bind to GPER in accordance with previous studies [44], however it triggers the direct interaction between MR and GPER as well as GPER and EGFR. Interestingly, we have determined that both MR and GPER are required for the proliferation and migration of breast cancer cells and B-TEC mediated by NHE-1 upon aldosterone exposure.

Aldosterone elicits important biological effects in several physio-pathological conditions, spanning from electrolyte and fluid homeostasis to the regulation of fibrotic, inflammatory, proliferative and angiogenic responses in cardiovascular, metabolic diseases and cancer [12-13, 46-49]. As it concerns the breast tissue, it has been demonstrated that aldosterone potentiates prolactin stimulation of casein synthesis in pregnant rabbit mammary gland and contributes to mammary gland development and differentiation [50].

The actions exerted by aldosterone mainly occur through the binding to MR, a ligand-inducible transcription factor that belongs to the nuclear receptor superfamily [1]. The enzyme 11 $\beta$ -hydroxysteroid dehydrogenase type II (11 $\beta$ HSD2), which catalyzes the conversion of 11 $\beta$ -hydroxycorticosteroids like cortisol and corticosterone to the respective 11-keto metabolites namely cortisone and 11-dehydrocorticosterone, does allow the aldosterone binding to MR [51]. 11 $\beta$ HSD2 is mainly expressed in mineralcorticoid target tissues like kidney, colon, salivary glands and placenta [51]. In addition, immunohistochemical studies have detected in normal and malignant breast tissues high levels of 11 $\beta$ -HSD2 that co-localize with MR [52]. Previous studies have also evaluated the 11 $\beta$ -HSD2 activity in breast cancer cells, suggesting that this enzyme may play a regulatory role of aldosterone action in breast malignancy [53]. According to the classical model of MR signalling, the interaction between aldosterone and un-liganded receptor promotes the dissociation of the heat shock proteins from MR, which translocates into the nucleus [1]. Then, the aldosterone/MR complex binds to specific response elements located within the regulatory region of target genes, hence resulting in gene expression changes [1]. In addition, aldosterone induces rapid effects through alternate mechanisms including the activation of the EGFR/ERK transduction pathway, as demonstrated in different animal and cell models [3-4]. The existence of aldosterone receptors structurally unrelated to the classic MR paved also the way for analyzing the role of further mediators of the multifaceted action elicited by aldosterone [49].

GPER has been largely demonstrated to mediate estrogenic signalling in a wide number of physio-pathological conditions, including cancer [54-64]. GPER has been also involved in functional responses to aldosterone in various experimental contexts [37-40]. For instance, the ability of aldosterone in activating ERK1/2 in vascular smooth muscle cells and sensitizing

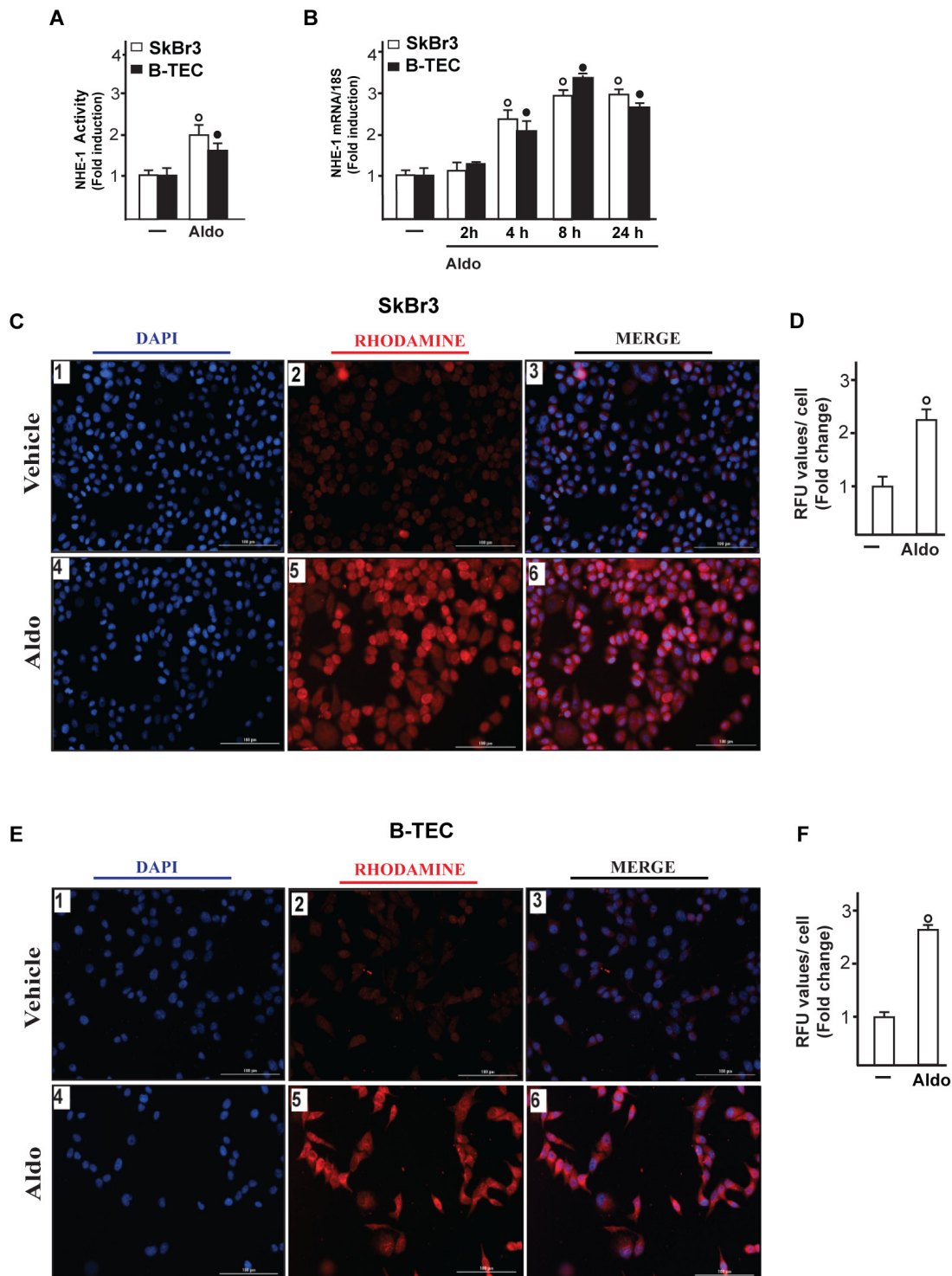


**Figure 4: Na<sup>+</sup>/H<sup>+</sup> Exchanger 1 (NHE-1) activity in SkBr3 cells and B-TEC treated with 10 pM Aldo, as evaluated by fluorescence intensity measurement.** A. Each data point represents the mean  $\pm$  SD of three independent experiments. mRNA expression of NHE-1 in SkBr3 cells and B-TEC treated with 10 pM Aldo, as evaluated by real-time PCR B. Values are normalized to the 18S expression and shown as fold changes of the mRNA expression induced by Aldo respect to cells treated with vehicle (-). NHE-1 expression as evaluated by immunofluorescence in SkBr3 cells C. and B-TEC E. treated with ethanol as vehicle or 10 pM Aldo for 8 hours. NHE-1 accumulation is shown by the red signal, nuclei were stained by DAPI (blue signal). Images shown are representative of three independent experiments. D., F. Fluorescence intensities for the red channel were quantified in 10 random fields for each condition and results are expressed as fold change of relative fluorescence units (RFU) over the vehicle-treated cells. (○) and (●) indicate  $p < 0.05$  for cells receiving vehicle (-) versus Aldo treatment.

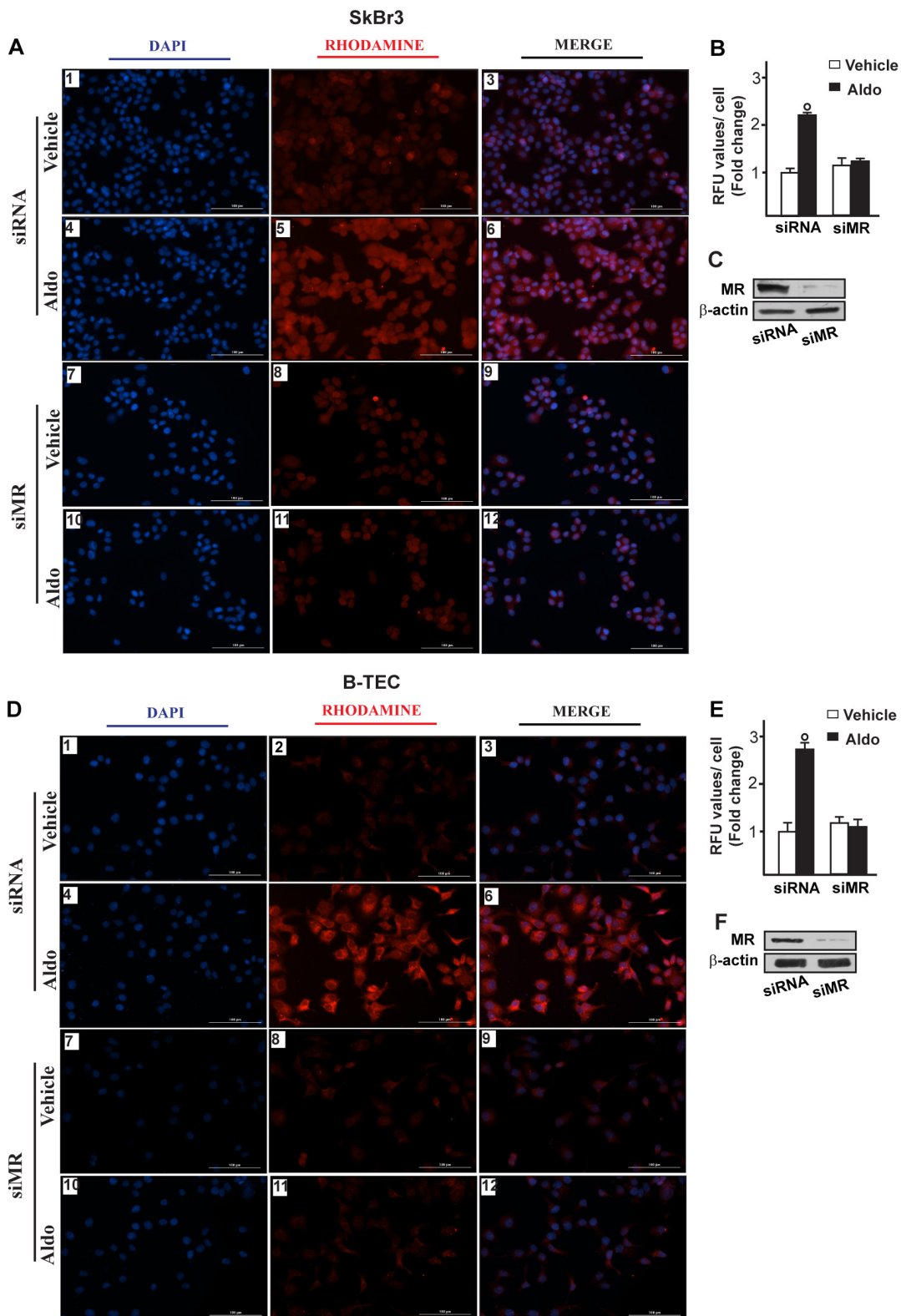


**Figure 5: Na<sup>+</sup>/H<sup>+</sup> Exchanger 1 (NHE-1) expression as evaluated by immunofluorescence in SkBr3 cells. A. and B-TEC D. transfected for 24 hours with siRNA (panels 1-6) or siMR (panels 7-12) and then treated with ethanol as vehicle or 10 pM Aldosterone (Aldo) for 8 hours. NHE-1 accumulation is shown by the red signal, nuclei were stained by DAPI (blue signal). Images shown are representative of three independent experiments. B., E. Fluorescence intensities for the red channel were quantified in 10 random fields for each condition and results are expressed as fold change of relative fluorescence units (RFU) over the vehicle-treated cells. C., F. Efficacy of MR silencing. (○) indicates  $p < 0.05$  for cells receiving vehicle *versus* Aldo treatment.**

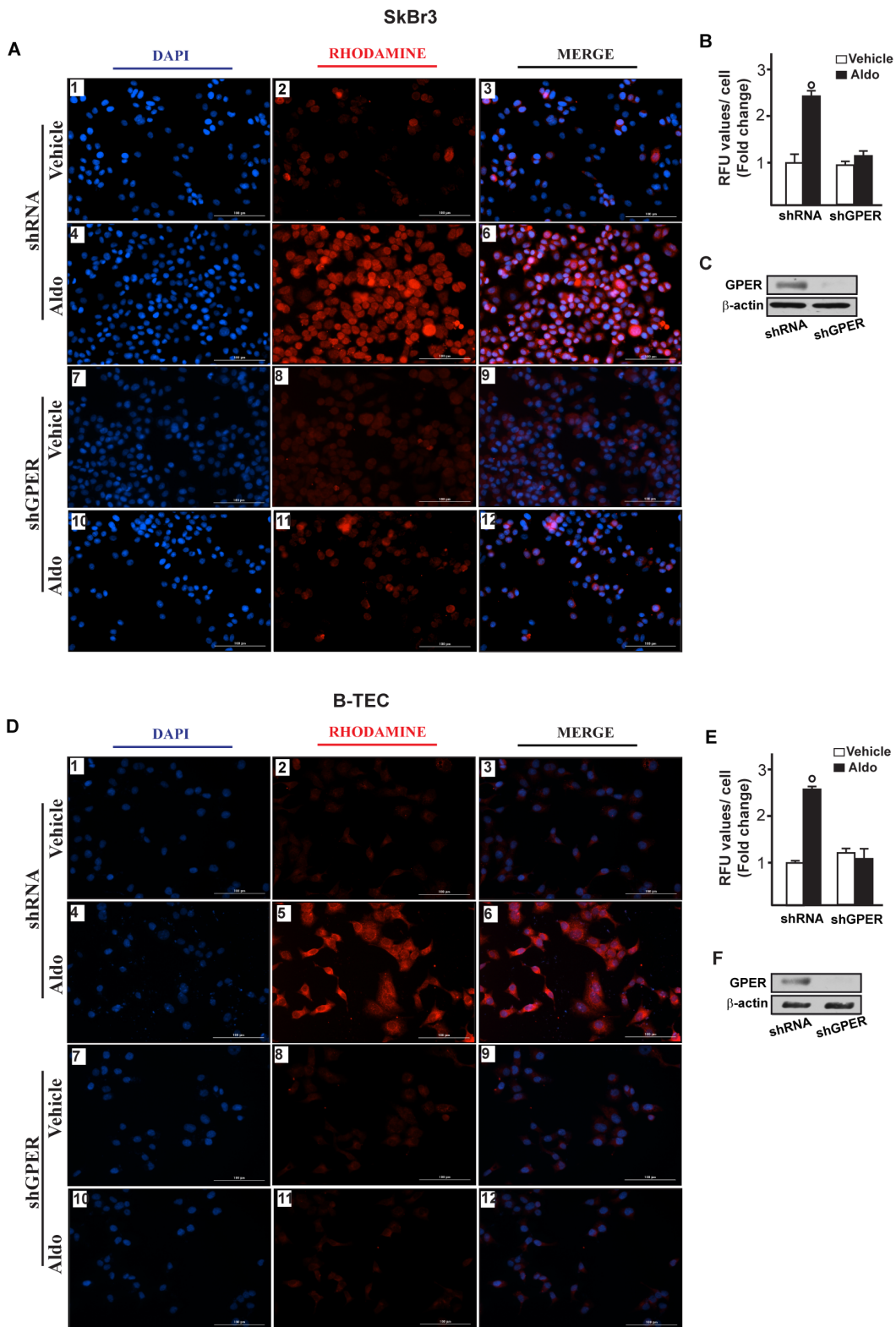


**Figure 6: Na<sup>+</sup>/H<sup>+</sup> Exchanger 1 (NHE-1) expression as evaluated by immunofluorescence in SkBr3 cells. A. and B-TEC D. transfected for 24 hours with shRNA (panels 1-6) or shGPER (panels 7-12) and then treated with ethanol as vehicle or 10 pM aldosterone (Aldo) for 8 hours. NHE-1 accumulation is shown by the red signal, nuclei were stained by DAPI (blue signal). Images shown are representative of three independent experiments. B., E. Fluorescence intensities for the red channel were quantified in 10 random fields for each condition and results are expressed as fold change of relative fluorescence units (RFU) over the vehicle-treated cells. C., F. Efficacy of GPER silencing. (o) indicates  $p < 0.05$  for cells receiving vehicle (-) versus Aldo treatment.**

the connecting tubule glomerular feedback in afferent arterioles was prevented using both MR and GPER blockers [38-40]. Other studies evidenced that the increase of cardiac vagal tone observed upon aldosterone treatment is abolished in the presence of the GPER antagonist G36 but not using the MR antagonists spironolactone and eplerenone [39]. In rat aortic endothelial cells devoid of MR, the biological effects triggered by aldosterone were mimicked by the GPER agonist G-1 and prevented using pharmacological inhibitors of GPER as well as knocking down its expression [38]. The aforementioned

observations suggest that GPER is involved in the effects exerted by aldosterone either through MR or acting as an alternate aldosterone receptor. However, it should be pointed out that diverse controversies argue against the last conclusion, as pharmacologic criteria for GPER to be considered as an aldosterone-responsive receptor are not still adequately fulfilled [41-43]. Indeed, binding studies performed in HEK cells overexpressing GPER (HEK-GPER-1) showed that aldosterone and the MR antagonists, spironolactone and eplerenone, do not compete for specific [<sup>3</sup>H]E2 binding to membrane of HEK-GPER-1 cells [44].

### SkBr3

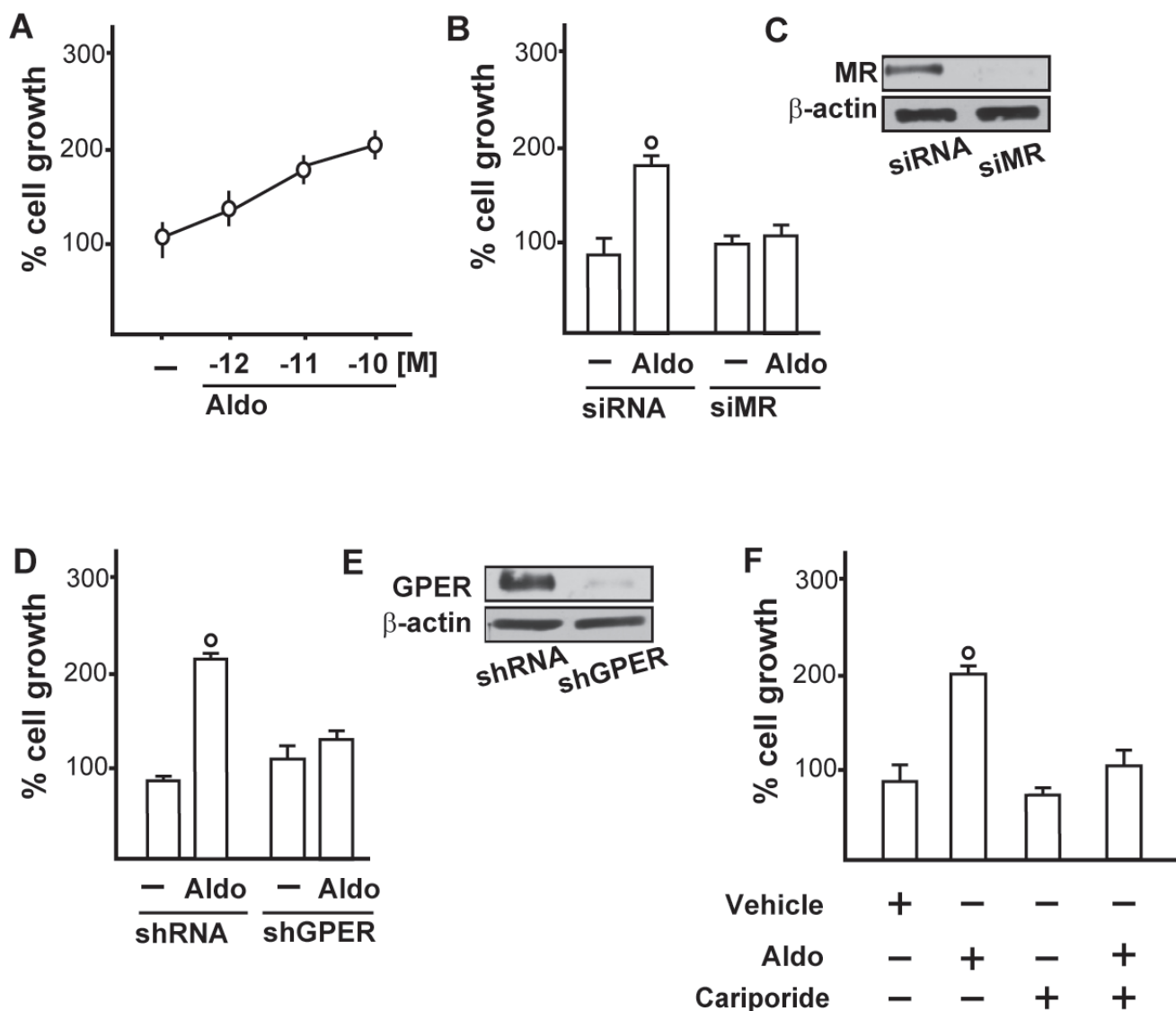


**Figure 7:** A. SkBr3 cell proliferation upon treatment for 5 days with increasing concentrations of Aldosterone (Aldo). Proliferation of SkBr3 cells transfected with siMR B., C. and shGPER D., E. and treated for 5 days with 10 pM Aldo. SkBr3 cell proliferation stimulated by 10 pM Aldo in the presence of 50 μM Na<sup>+</sup>/H<sup>+</sup> Exchanger 1 (NHE-1) inhibitor named cariporide F. Values shown are mean ± SD of three independent experiments performed in triplicate. (○) indicates *p* < 0.05 for cells receiving vehicle (-) versus Aldo treatment.

In accordance with these findings, in the present study aldosterone failed to bind to GPER in competition assays based on experimental approaches used in previous investigations in order to characterize the binding properties of GPER ligands [28, 31-32, 34-36]. Worthy, we found that aldosterone stimulates the interaction of GPER with MR and EGFR, thus suggesting a further mechanism through which ligand-activated MR triggers EGFR signalling [49, 65-67]. Nicely supporting the functional cross-talk between MR and GPER, we ascertained that both receptors are required for the aldosterone-induced expression of NHE-1 which is considered as a molecular

sensor of MR activation [45]. In this respect, our data are reminding of previous findings showing that EGFR and GPER cooperate toward the regulation of NHE-1 function upon aldosterone treatment [40, 66]. Importantly, we found that the stimulatory effects elicited by aldosterone on the proliferation and migration of breast cancer cells and breast tumor-derived endothelial cells are mediated by NHE-1 and involve both GPER and MR. Hence, the current results further extend the well-known action played by NHE-1 toward negative biological features, in particular in breast cancer [7, 68]. In this regard, it is worth mentioning that in tumor metabolic microenvironment

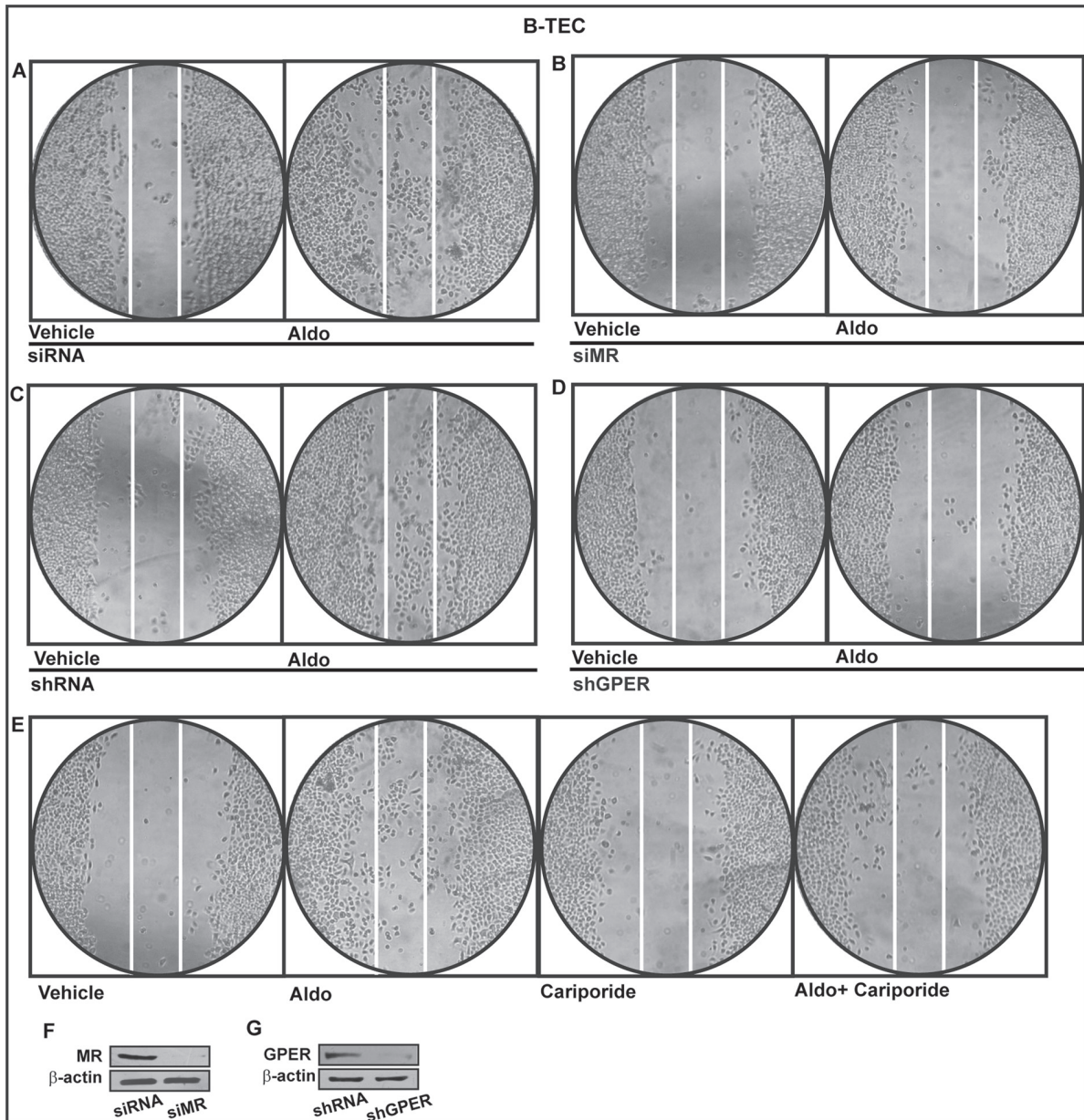


**Figure 8: Cell migration in B-TEC transfected for 24 h with siRNA. A., siMR B., shRNA C. or shGPER D. and then treated for 48 hours with ethanol as vehicle or 10 pM Aldosterone (Aldo). E. Cell migration stimulated by 10 pM Aldo in B-TEC in the presence of 50  $\mu$ M Na<sup>+</sup>/H<sup>+</sup> Exchanger 1 (NHE-1) inhibitor cariporide. F., G. Efficacy of MR and GPER silencing. Data are representative of three independent experiments performed in triplicate.**

characterized by hypoxic-acidic milieu [69], the dysregulation of pH homeostasis mediated by NHE-1 may actually contribute to key steps in tumor progression like increased cell proliferation, loss of cell-cell contact and detachment from the extracellular matrix [68]. In breast cancer cells and breast cancer associated fibroblasts exposed to hypoxia, we have previously assessed that GPER cooperates with hypoxia inducible factor-1 (HIF-1) toward the regulation of vascular endothelial growth factor (VEGF) and tumor angiogenesis [70-73]. Hence, the present findings suggest further mechanisms through which GPER may play a role in the complex adaptive responses to hypoxic-acidic tumor microenvironment. Additionally, our results indicate that GPER contributes to the effects mediated by aldosterone/MR signalling, as evidenced by other ligand-activated steroid receptors [74-75].

Collectively, our findings provide novel insights into the controversial mechanisms through which GPER contributes to aldosterone-mediated signalling. On the basis of our data showing that the functional interaction between MR and GPER triggers certain stimulatory effects exerted by aldosterone, GPER may be considered as a further target within the intricate transduction network activated by aldosterone in particular in breast cancer.

## MATERIALS AND METHODS

### Reagents

Aldosterone (Aldo), 17 $\beta$ -estradiol (E2) and Cariporide were purchased from Sigma Aldrich (Milan, Italy). G15 ((3aS,4R,9bR)-4-(6-bromo-1,3-benzodioxol-5-yl)-3a,4,5,9b-3H-cyclopenta[c]quinolone) was obtained from Tocris Bioscience (distributed by Space, Milan, Italy). Tyrphostin AG1478 (AG) was purchased from DBA (Milan, Italy). PD98059 (PD) was obtained from Calbiochem (DBA, Milan, Italy). All compounds were dissolved in dimethyl sulfoxide (DMSO) except Aldosterone and E2 which were solubilized in ethanol.

### Cell cultures

SkBr3 breast cancer cells were maintained in RPMI-1640 without phenol red, supplemented with 10% fetal bovine serum (FBS) and 100  $\mu$ g/ml penicillin/streptomycin (Life Technologies, Milan, Italy). Breast tumor-derived endothelial cells (B-TEC) were obtained from human breast carcinomas and characterized as previously described [76]. B-TEC showed constant expression of endothelial markers and increased angiogenic properties, migration and drug resistance in respect to normal microendothelial cells [76-78]. Briefly, specimens were finely minced with scissors and

then digested by incubation for 1 h at 37°C in DMEM containing collagenase IV (Sigma Aldrich, Milan, Italy). After washings in medium plus 10% FCS (Life Technologies, Milan, Italy), the cell suspension was forced through a graded series of meshes to separate the cell components from stroma and aggregates. Endothelial cells were isolated from cells suspension using anti-CD105 Ab coupled to magnetic beads, by magnetic cell-sorting using the MACS system (Miltenyi Biotech, Auburn, CA). B-TEC were seeded on collagen-coated flasks (Sigma-Aldrich Srl, Milan, Italy) and cultured in Endothelial Growth Medium (EGM) (Lonza, Milan, Italy), supplemented with 5% FBS (Lonza, Milan, Italy). MCF-7 breast cancer cells were maintained in DMEM F12 supplemented with 10% FBS and 100  $\mu$ g/mL penicillin/streptomycin (Life Technologies, Milan, Italy). All cell lines were grown in a 37° C HeraCell incubator (ThermoScientific-Heraeus, Milan, Italy) with 5% CO<sub>2</sub>. Cells were switched to medium without serum the day before experiments.

### Saturation curve and scatchard plot analysis

SkBr3 cells were grown in 10-cm cell culture dishes and incubated with increasing concentrations of [2, 4, 6, 7-3H] E2 (89 Ci/mmol; GE Healthcare) or [1, 2, 6, 7-3H] Aldosterone (85 Ci/mmol; Perkinelmer). Cells were then washed with ice-cold phosphate-buffered saline (PBS); after 100% ethanol extraction of cells, radioactivity was measured by liquid scintillation counting. The plot of the bound radioactivity (cpm) *versus* the concentration of the radiotracer (nM) was fitted to the saturation binding curve using Prism GraphPad program (GraphPad Software, San Diego, CA), which was used to calculate the binding dissociation constant (Kd) and binding capacity (Bmax).

### Ligand binding assay

SkBr3 cells were grown in 10-cm cell culture dishes and incubated with 4 nM [2, 4, 6, 7-3H] E2 (89 Ci/mmol; GE Healthcare) or 100 pM [1, 2, 6, 7-3H] Aldosterone (85 Ci/mmol; Perkinelmer) in the presence or absence of increasing concentrations of nonlabeled E2 or aldosterone for 2 hours at 37°C. Cells were then washed with ice-cold PBS; after 100% ethanol extraction of cells, radioactivity was measured by liquid scintillation counting. The displacement of [<sup>3</sup>H]E2 or [<sup>3</sup>H]Aldo binding by the competitors was expressed as a percentage of the maximum specific binding of E2 or Aldo.

### Na<sup>+</sup>/H<sup>+</sup> Exchanger 1 (NHE-1) activity assay

SkBr3 cells and B-TEC were grown in 10-cm cell culture dishes and then shifted for 24h to medium

lacking serum. Then,  $4 \times 10^7$  cells/ml were suspended in HEPES buffer solution 1M (Sigma Aldrich, Milan, Italy) and incubated with a membrane-permeable fluorescent indicator for the measurement of cytoplasmic pH namely SPIRO(ISOBENZOFURAN-1(3H),9<sup>2</sup>-(9H) XANTHENE)-2',7'-DIPROPANOIC ACID (BCECF-AM) (0,3 $\mu$ M) (Santa Cruz Biotechnology, Milan, Italy) for 30 min at 37°C. Then, cells were washed with HEPES buffer saline and a cell suspension of  $3 \times 10^6$  cells/ml was prepared. Fluorescence ratio from the dye was measured using an FLX-800 micro plate fluorimeter (Bio-Tek Instruments, Inc., Winooski, VT, USA).

## Gene expression studies

Total RNA was extracted from cell cultures using the TRIzol commercial kit (Life Technologies, Milan, Italy) according to the manufacturer's protocol. RNA was quantified spectrophotometrically and quality was checked by electrophoresis through agarose gels stained with ethidium bromide. Only samples that were not degraded and showed clear 18 S and 28 S bands under UV light were used for RT-PCR. Total cDNA was synthesized from the RNA by reverse transcription using the murine leukemia virus reverse transcriptase (Life Technologies, Milan, Italy), following the protocol provided by the manufacturer. The expression of selected genes was quantified by real-time PCR using Step One<sup>(TM)</sup> sequence detection system (Applied Biosystems Inc, Milan, Italy), following the manufacturer's instructions. Gene-specific primers were designed using Primer Express version 2.0 software (Applied Biosystems, Inc., Milan, Italy) and are as follows: GPER Fwd: 5'-ACACACCTGGGTGGACACAA-3' and Rev: 5'-GGAGCCAGAAGCCACATCTG-3'; MR Fwd: 5'-GCTTTGATGGTAACTGTGAAGG-3' and Rev: 5'-TGTGTTGCCCTTCCACTGCT-3'; ER $\alpha$  Fwd: 5'-AGAGGGCATGGTGGAGATCTT-3' and Rev: 5'-CAAACCTCTCCCTGCAGATT-3'; NHE-1 Fwd: 5'-AAGGACCAGTTCATCATCGC-3' and Rev: 5'-TTCTTACAGCCAACAGGTC-3'; 18S Fwd: 5'-GGCGTCCCCAACTTCTTA-3 and Rev: 5'-GGGCATCACAGACCTGTTATT-3'. Assays were performed in triplicate and the RNA expression values were normalized using 18S expression and then calculated as fold induction.

## Gene silencing experiments

For the silencing of GPER expression, cells were plated onto 10-cm dishes and transfected using X-treme GENE 9 DNA Transfection Reagent (Roche Diagnostics, Milan, Italy) for 24 hours with two shRNA and two different shGPER. The silencing of GPER expression was obtained by using constructs which we have

previously described and used [79]. For knocking down MR expression, cells were seeded in six-well multidishes and transiently transfected the consecutive day at 50% confluence. For transfection, X-treme GENE 9 DNA Transfection Reagent (Roche Diagnostics, Milan, Italy) was mixed with two small interfering RNAs (siRNA) specific for silencing MR or two siRNA controls (Origene, distributed by Tema Ricerca, Milan, Italy) for 24 hours, prior to treatments.

## Western blot analysis

SkBr3 cells and B-TEC were processed according to a previously described protocol [80-81] to obtain protein lysate that was electrophoresed through a reducing SDS/10% (w/v) polyacrylamide gel, electroblotted onto a nitrocellulose membrane and probed with primary antibodies against MR (PA1594) (Boster Immunoleader, distributed by Tema Ricerca, Milan, Italy), phosphorylated ERK 1/2 (E-4), ERK2 (C-14), EGFR (1005), pEGFR<sup>Tyr</sup><sup>1173</sup> (sc-12351-R), GPER (N15), ER $\alpha$  (F10) and  $\beta$ -actin (C2), all purchased from DBA (Milan, Italy). Proteins were detected by horseradish peroxidase-linked secondary antibodies (DBA, Milan, Italy) and revealed using the ECL System (GE Healthcare). Precision Plus Protein<sup>TM</sup> Dual Color Standard (Bio-Rad Laboratories, Milan, Italy) was used to estimate molecular weights and then antigen specificity.

## Coimmunoprecipitation

After stimulation with 10 pM Aldo, SkBr3 breast cancer cells were washed with PBS and lysed using 500  $\mu$ l RIPA buffer with a mixture of protease inhibitors containing 1.7 mg/ml aprotinin, 1mg/ml leupeptin, 200 mmol/liter phenylmethylsulfonyl fluoride, 200 mmol/liter sodium orthovanadate, and 100 mmol/liter sodium fluoride. Samples were then centrifuged at 13,000 rpm for 10 min, and protein concentrations were determined using Bradford reagent. Protein (250  $\mu$ g) was then incubated for 2 hours with 900  $\mu$ l of immunoprecipitation buffer with inhibitors, 2  $\mu$ g of GPER, MR or EGFR antibody and 20  $\mu$ l of Protein A/G agarose immunoprecipitation reagent (DBA, Milan, Italy). Samples were then centrifuged at 13,000 rpm for 5 min at 4° C to pellet beads. Pellets were washed four times with 500  $\mu$ l of PBS and centrifuged at 13,000 rpm for 5 min at 4° C. Supernatants were collected, resuspended in 20  $\mu$ l RIPA buffer with protease inhibitors, 2X SDS sample buffer (40 mM Tris-HCl; 4% glycerol; 2% SDS) and  $\beta$ -mercaptoethanol and heated to 95° C for 5 min. Samples were then run on 10% SDS-PAGE, transferred to nitrocellulose, and probed with rabbit anti-GPER, rabbit anti-MR or rabbit anti-EGFR antibody. Western blot analysis and ECL detection were performed as described above.

## Immunofluorescence and colocalization studies

50 % confluent cultured SkBr3 cells and B-TEC grown on coverslips were serum deprived and then treated for 8 hours with 10 pM Aldo, as indicated. Where required, cells previously transfected for 24 hours with shGPER or siMR and respective control (as described above) and then treated for 8 hours with 10 pM Aldo. Then cells were fixed in 4% paraformaldehyde, permeabilized with 0.2% Triton X-100, washed three times with PBS and incubated overnight with a goat primary antibody against NHE-1 (C20) (DBA, Milan, Italy). After incubation, the slides were extensively washed with PBS and incubated with 4',6-diamidino-2-phenylindole dihydrochloride (DAPI), (1:1000), (Sigma-Aldrich, Milan, Italy) and donkey anti-goat IgG-Rhodamine (1:100; purchased from DBA, Milan, Italy). The slides were imaged on the Cytation 3 Cell Imaging Multimode reader (BioTek, Winooski, VT) and analysed using the software Gen5 (BioTek, Winooski, VT).

For colocalization studies SkBr3 cells seeded on chamber slides were serum deprived for 24 hours and then treated for 15 min with 10 pM Aldo. Next, cells were fixed, permeabilized and incubated overnight with anti-rabbit GPER (N15) and anti-mouse MR (H10E4C9F) antibodies (DBA, Milan, Italy) alone and in combination. Slides were then incubated with secondary antibodies (donkey anti-rabbit IgG-Rhodamine, DBA, Milan, Italy) and donkey anti-mouse IgG-Fitch (Alexa Fluor, Life Technologies, Milan, Italy), stained by DAPI and then imaged on the Cytation 3 Cell Imaging Multimode reader (BioTek, Winooski, VT).

## Proliferation assay

For quantitative proliferation assay, SkBr3 cells ( $1 \times 10^5$ ) were seeded in 24-well plates in regular growth medium. Cells were washed once they had attached and then incubated in medium containing 2.5% charcoal-stripped FBS, transfected for 24 hours, and then treated, as indicated, with transfection and treatments renewed every 2 days. Cells were counted on day 5 using the Countess Automated Cell Counter, as recommended by the manufacturer's protocol (Life Technologies, Milan, Italy).

## Migration assay

Twelve-well plates were coated with 500  $\mu$ L fibronectin for 2 hours at 37°C (Sigma Aldrich, Milan, Italy). B-TEC were allowed to grow in regular growth medium until they reached a 70% to 80% confluence. Next, cells were incubated in medium containing 2.5% charcoal-stripped FBS and transfected for 24 hours, as

indicated. To create a scratch of the cell monolayer, a p200 pipette tip was used. Cells were then washed twice with PBS and treated. The migration assay was evaluated after 48 hours of treatment.

## Time-lapse microscopy

SkBr3 cells and B-TEC ( $1 \times 10^5$ ) were seeded in 24-well plates in regular growth medium until they reached a 70% to 80% confluence. The culture wells were then incubated in medium containing 2.5% charcoal-stripped FBS, treated and transferred into a time-lapse microscopy platform, equipped with a heated stage chamber (Cytation™3 Cell Imaging Multi-Mode Reader, Biotek, Winooski, VT). Cells were maintained at routine incubation settings (37 °C, 5% CO<sub>2</sub>) using temperature and gas controllers. To evaluate cell proliferation and motility, the images were recorded using Cytation 3 Cell Imaging Multimode Reader and the software Gen5 (BioTek, Winooski, VT) in 10 min intervals for 24 hours (cell proliferation) and 10 hours (cell motility). Then, the images were processed as a movie using the software Adobe Creative Cloud Premier Pro CC. Frames collected every 10 minutes are displayed at a rate of 10 frames s<sup>-1</sup>.

## Statistical analysis

Statistical analysis was performed using ANOVA followed by Newman-Keuls' testing to determine differences in means.  $p < 0.05$  was considered as statistically significant.

## ACKNOWLEDGMENTS

We thank A. Brossa and N. Fico for the technical support.

## COMPETING INTERESTS

The authors declare that they have no competing interests.

## GRANT SUPPORT

This work was supported by Associazione Italiana per la Ricerca sul Cancro (AIRC grant 16719/2015), Programma Operativo Nazionale "Ricerca e Competitività 2007-2013" (PON 01\_01078), Ministero della Salute (grant n. 67/GR-2010-2319511). EMDF was supported by "International Cancer Research Fellowships AIRC-iCARE.

## REFERENCES

1. Arriza JL, Weinberger C, Cerelli G, Glaser TM, Handelin BL, Housman DE, Evans RM. Cloning of human mineralocorticoid receptor complementary DNA: structural and functional kinship with the glucocorticoid receptor. *Science*. 1987; 237: 268-275.
2. Meinel S, Gekle M, Grossmann C. Mineralocorticoid receptor signaling: crosstalk with membrane receptors and other modulators. *Steroids*. 2014; 91: 3-10.
3. Williams JS. Evolving research in nongenomic actions of aldosterone. *Curr Opin Endocrinol Diabetes Obes*. 2013; 20: 198-203.
4. Krug AW, Grossmann C, Schuster C, Freudinger R, Mildenerger S, Govindan MV, Gekle M. Aldosterone stimulates epidermal growth factor receptor expression. *J Biol Chem*. 2003; 278: 43060-43066.
5. Paul M, Poyan Mehr A, Kreutz R. Physiology of local renin-angiotensin systems. *Physiol Rev*. 2006; 86: 747-803.
6. De Giusti VC, Orłowski A, Ciancio MC, Espejo MS, Gonano LA, Caldiz CI, Vila Petroff MG, Villa-Abrille MC, Aiello EA. Aldosterone stimulates the cardiac sodium/bicarbonate cotransporter via activation of the g protein-coupled receptor gpr30. *J Mol Cell Cardiol*. 2015; [Epub ahead of print] PMID: 26497404.
7. Amith SR, Fliegel L. Regulation of the Na<sup>+</sup>/H<sup>+</sup> Exchanger (NHE-1) in Breast Cancer Metastasis. *Cancer Res*. 2013; 73: 1259-1264.
8. Luther JM, Brown NJ. The renin-angiotensin-aldosterone system and glucose homeostasis. *Trends Pharmacol Sci*. 2011; 32: 734-739.
9. Briet M, Schiffrin EL. Vascular actions of aldosterone. *J Vasc Res*. 2013; 50: 89-99.
10. Calvier L, Miana M, Reboul P, Cachofeiro V, Martinez-Martinez E, de Boer RA, Poirier F, Lacolley P, Zannad F, Rossignol P, López-Andrés N. Galectin-3 mediates aldosterone-induced vascular fibrosis. *Arterioscler Thromb Vasc Biol*. 2013; 33: 67-75.
11. Bienvenu LA1, Morgan J, Rickard AJ, Tesch GH, Cranston GA, Fletcher EK, Delbridge LM, Young MJ. Macrophage mineralocorticoid receptor signaling plays a key role in aldosterone-independent cardiac fibrosis. *Endocrinology*. 2012; 153: 3416-3425.
12. King S, Bray S, Galbraith S, Christie L, Fleming S. Evidence for aldosterone-dependent growth of renal cell carcinoma. *Int J Exp Pathol*. 2014; 95: 244-250.
13. Kaji K, Yoshiji H, Kitade M, Ikenaka Y, Noguchi R, Shirai Y, Yoshii J, Yanase K, Namisaki T, Yamazaki M, Tsujimoto T, Kawaratani H, Fukui H. Selective aldosterone blocker, eplerenone, attenuates hepatocellular carcinoma growth and angiogenesis in mice. *Hepatol Res*. 2010; 40: 540-549.
14. Maggiolini M, Picard D. The unfolding stories of GPR30, a new membrane-bound estrogen receptor. *J Endocrinol*. 2010; 204: 105-114.
15. Prossnitz ER, Barton M. The G-protein-coupled estrogen receptor GPER in health and disease. *Nat Rev Endocrinol*. 2011; 7: 715-726.
16. Barton M. Position paper: The membrane estrogen receptor GPER—Clues and questions. *Steroids*. 2012; 77: 935-942.
17. Filardo EJ, Thomas P. Minireview: G protein-coupled estrogen receptor-1, GPER-1: its mechanism of action and role in female reproductive cancer, renal and vascular physiology. *Endocrinology*. 2012; 153: 2953-2962.
18. Meyer MR, Prossnitz ER, Barton M. The G protein-coupled estrogen receptor GPER/GPR30 as a regulator of cardiovascular function. *Vascul Pharmacol*. 2011; 55: 17-25.
19. Lindsey SH, Chappell MC. Evidence that the G protein-coupled membrane receptor GPR30 contributes to the cardiovascular actions of estrogen. *Gend Med*. 2011; 8: 343-354.
20. Prossnitz ER, Maggiolini M. Mechanisms of estrogen signaling and gene expression via GPR30. *Molecular and Cellular Endocrinology*. 2009; 308: 32-38.
21. Filardo EJ, Quinn JA, Bland KI, Frackelton AR Jr. Estrogen-induced activation of Erk-1 and Erk-2 requires the G protein-coupled receptor homolog, GPR30, and occurs via trans-activation of the epidermal growth factor receptor through release of HB-EGF. *Mol Endocrinol*. 2000; 14: 1649-1660.
22. Revankar CM, Cimino DF, Sklar LA, Arterburn JB, Prossnitz ER. A transmembrane intracellular estrogen receptor mediates rapid cell signaling. *Science*. 2005; 307: 1625-1630.
23. Pandey DP, Lappano R, Albanito L, Madeo A, Maggiolini M, Picard D. Estrogenic GPR30 signalling induces proliferation and migration of breast cancer cells through CTGF. *EMBO J*. 2009; 28: 523-532.
24. Santolla MF, Lappano R, De Marco P, Pupo M, Vivacqua A, Sisci D, Abonante S, Iacopetta D, Cappello AR, Dolce V, Maggiolini M. G protein-coupled estrogen receptor mediates the up-regulation of fatty acid synthase induced by 17 $\beta$ -estradiol in cancer cells and cancer-associated fibroblasts. *J Biol Chem*. 2012; 287: 43234-43245.
25. Vivacqua A, De Marco P, Santolla MF, Cirillo F, Pellegrino M, Panno ML, Abonante S, Maggiolini M. Estrogenic gper signalling regulates mir144 expression in cancer cells and cancer-associated fibroblasts (cafs). *Oncotarget*. 2015; 6: 16573-16587. Doi: 10.18632/oncotarget.4117.
26. Lappano R, Pisano A, Maggiolini M. GPER Function in Breast Cancer: An Overview. *Front Endocrinol (Lausanne)*. 2014; 5:66.
27. Santolla MF, Avino S, Pellegrino M, De Francesco EM, De Marco P, Lappano R, Vivacqua A, Cirillo F, Rigiracciolo DC, Scarpelli A, Abonante S, Maggiolini M. SIRT1 is involved in oncogenic signaling mediated by GPER in breast cancer. *Cell Death and Disease*. 2015; 6:e1834.

28. Santolla MF, De Francesco EM, Lappano R, Rosano C, Abonante S, Maggiolini M. Niacin activates the G protein estrogen receptor (GPER)-mediated signalling. *Cell Signal*. 2014; 26: 1466-1475.
29. Lappano R, Rosano C, De Marco P, De Francesco EM, Pezzi V, Maggiolini M. Estriol acts as a GPR30 antagonist in estrogen receptor-negative breast cancer cells. *Mol Cell Endocrinol*. 2010; 320: 162-170.
30. Pupo M, Pisano A, Lappano R, Santolla MF, De Francesco EM, Abonante S, Rosano C, Maggiolini M. Bisphenol A induces gene expression changes and proliferative effects through GPER in breast cancer cells and cancer-associated fibroblasts. *Environ Health Perspect*. 2012; 120: 1177-1182.
31. Lappano R, Santolla MF, Pupo M, Sinicropi MS, Caruso A, Rosano C, Maggiolini M. MIBE acts as antagonist ligand of both estrogen receptor  $\alpha$  and GPER in breast cancer cells. *Breast Cancer Res*. 2012; 14:R12.
32. Maggiolini M, Santolla MF, Avino S, Aiello F, Rosano C, Garofalo A, Grande F. Identification of two benzopyrroloxazines acting as selective GPER antagonists in breast cancer cells and cancer-associated fibroblasts. *Future Med Chem*. 2015; 7: 437-448.
33. Sinicropi MS, Lappano R, Caruso A, Santolla MF, Pisano A, Rosano C, Capasso A, Panno A, Lancelot JC, Rault S, Saturnino C, Maggiolini M. (6-bromo-1,4-dimethyl-9H-carbazol-3-yl-methylene)-hydrazine (carbhydraz) acts as a GPER agonist in breast cancer cells. *Curr Top Med Chem*. 2015; 15: 1035-1042.
34. Lappano R, Rosano C, Pisano A, Santolla MF, De Francesco EM, De Marco P, Dolce V, Ponassi M, Felli L, Cafeo G, Kohnke FH, Abonante S, Maggiolini M. A calixpyrrole derivative acts as a GPER antagonist: mechanisms and models. *Dis Model Mech*. 2015; 8: 1237-1246.
35. Albanito L, Lappano R, Madeo A, Chimento A, Prossnitz ER, Cappello AR, Dolce V, Abonante S, Pezzi V, Maggiolini M. Effects of Atrazine on Estrogen Receptor  $\alpha$ - and G Protein-Coupled Receptor 30-Mediated Signalling and Proliferation in Cancer Cells and Cancer-Associated Fibroblasts. *Environ Health Perspect*. 2015; 123: 493-499.
36. Lappano R, Rosano C, Santolla MF, Pupo M, De Francesco EM, De Marco P, Ponassi M, Spallarossa A, Ranise A, Maggiolini M. Two novel GPER agonists induce gene expression changes and growth effects in cancer cells. *Curr Cancer Drug Targets*. 2012; 12: 531-542.
37. Funder JW. GPR30, mineralocorticoid receptors, and the rapid vascular effects of aldosterone. *Hypertension*. 2011; 57: 370-372.
38. Gros R, Ding Q, Liu B, Chorazyczewski J, Feldman RD. Aldosterone mediates its rapid effects in vascular endothelial cells through GPER activation. *Am J Physiol Cell Physiol*. 2013; 304: C532-540.
39. Brailoiu GC, Benamar K, Arterburn JB, Gao E, Rabinowitz JE, Koch WJ, Brailoiu E. Aldosterone increases cardiac vagal tone via G protein-coupled oestrogen receptor activation. *J Physiol*. 2013; 591: 4223-4235.
40. Ren Y, D'Ambrosio MA, Garvin JL, Leung P, Kutskill K, Wang H, Peterson EL, Carretero OA. Aldosterone sensitizes connecting tubule glomerular feedback via the aldosterone receptor GPR30. *Am J Physiol Renal Physiol*. 2014; 307: F427-434.
41. Wendler A, Wehling M. Is GPR30 the membrane aldosterone receptor postulated 20 years ago? *Hypertension*. 2011; 57:e16.
42. Barton M, Meyer MR. Nicolaus Copernicus and the rapid vascular responses to aldosterone. *Trends Endocrinol Metab*. 2015; 26: 396-398.
43. Feldman RD, Limbird LE. Copernicus Revisited: Overturning Ptolemy's View of the GPER Universe. *Trends Endocrinol Metab*. 2015; 26: 592-594.
44. Cheng SB, Dong J, Pang Y, LaRocca J, Hixon M, Thomas P, Filardo EJ. Anatomical location and redistribution of G protein-coupled estrogen receptor-1 during the estrus cycle in mouse kidney and specific binding to estrogens but not aldosterone. *Mol Cell Endocrinol*. 2014; 382: 950-959.
45. Karmazyn M, Liu Q, Gan XT, Brix BJ, Fliegel L. Aldosterone increases NHE-1 expression and induces NHE-1-dependent hypertrophy in neonatal rat ventricular myocytes. *Hypertension*. 2003; 42: 1171-1176.
46. Bruder-Nascimento T, da Silva MA, Tostes RC. The involvement of aldosterone on vascular insulin resistance: implications in obesity and type 2 diabetes. *Diabetol Metab Syndr*. 2014; 6:90.
47. Brown NJ. Contribution of aldosterone to cardiovascular and renal inflammation and fibrosis. *Nat Rev Nephrol*. 2013; 9: 459-469.
48. Queisser N, Oteiza PI, Link S, Hey V, Stopper H, Schupp N. Aldosterone activates transcription factor Nrf2 in kidney cells both *in vitro* and *in vivo*. *Antioxid Redox Signal*. 2014; 21: 2126-2142.
49. Grossmann C, Husse B, Mildenerger S, Schreier B, Schuman K, Gekle M. Colocalization of mineralocorticoid and EGF receptor at the plasma membrane. *Biochim. Biophys. Acta*. 2010; 1803: 584-590.
50. Jahn GA, Moguilewsky M, Houdebine LM, Djiane J. Binding and action of glucocorticoids and mineralocorticoids in rabbit mammary gland. Exclusive participation of glucocorticoid type II receptors for stimulation of casein synthesis. *Mol Cell Endocrinol*. 1987; 52: 205-212.
51. Rabbitt EH, Gittoes NJ, Stewart PM, Hewison M. 11 $\beta$ -hydroxysteroid dehydrogenases, cell proliferation and malignancy. *J Steroid Biochem Mol Biol*. 2003; 85: 415-421.
52. Sasano H, Frost AR, Saitoh R, Matsunaga G, Nagura H, Krozowski ZS, Silverberg SG. Localization of mineralocorticoid receptor and 11  $\beta$ -hydroxysteroid dehydrogenase type II in human breast and its disorders.

- Anticancer Res. 1997; 17: 2001-2007.
53. Kim CH, Cho YS. Selection and optimization of MCF-7 cell line for screening selective inhibitors of 11 $\beta$ -hydroxysteroid dehydrogenase 2. *Cell Biochem Funct.* 2010; 28: 440-447.
  54. De Francesco EM, Angelone T, Pasqua T, Pupo M, Cerra MC, Maggiolini M. GPER mediates cardiotropic effects in spontaneously hypertensive rat hearts. *PLoS One.* 2013; 8: e69322.
  55. Filice E, Angelone T, De Francesco EM, Pellegrino D, Maggiolini M, Cerra MC. Crucial role of phospholamban phosphorylation and S-nitrosylation in the negative lusitropism induced by 17 $\beta$ -estradiol in the male rat heart. *Cell Physiol Biochem.* 2011; 28: 41-52.
  56. Lappano R, Maggiolini M. G protein-coupled receptors: novel targets for drug discovery in cancer. *Nat Rev Drug Discov.* 2011; 10: 47-60.
  57. Lappano R, Maggiolini M. GPCRs and cancer. *Acta Pharmacol Sin.* 2012; 33: 351-362.
  58. Vivacqua A, Romeo E, De Marco P, De Francesco EM, Abonante S, Maggiolini M. GPER mediates the Egr-1 expression induced by 17 $\beta$ -estradiol and 4-hydroxitamoxifen in breast and endometrial cancer cells. *Breast Cancer Res Treat.* 2012; 133: 1025-1035.
  59. Lappano R, De Marco P, De Francesco EM, Chimento A, Pezzi V, Maggiolini M. Cross-talk between GPER and growth factor signalling. *J Steroid Biochem Mol Biol.* 2013; 137: 50-56.
  60. De Marco P, Cirillo F, Vivacqua A, Malaguarnera R, Belfiore A, Maggiolini M. Novel Aspects Concerning the Functional Cross-Talk between the Insulin/IGF-I System and Estrogen Signalling in Cancer Cells. *Front Endocrinol (Lausanne).* 2015; 6:30.
  61. Bartella V, De Marco P, Malaguarnera R, Belfiore A, Maggiolini M. New advances on the functional cross-talk between insulin-like growth factor-I and estrogen signalling in cancer. *Cell Signal.* 2012; 24: 1515-1521.
  62. Madeo A, Maggiolini M. Nuclear alternate estrogen receptor GPR30 mediates 17 $\beta$ -estradiol-induced gene expression and migration in breast cancer-associated fibroblasts. *Cancer Res.* 2010; 70: 6036-6046.
  63. Pupo M, Pisano A, Abonante S, Maggiolini M, Musti AM. GPER activates Notch signalling in breast cancer cells and cancer-associated fibroblasts (CAFs). *Int J Biochem Cell Biol.* 2014; 46: 56-67.
  64. Pupo M, Vivacqua A, Perrotta I, Pisano A, Aquila S, Abonante S, Gasperi-Campani A, Pezzi V, Maggiolini M. The nuclear localization signal is required for nuclear GPER translocation and function in breast Cancer-Associated Fibroblasts (CAFs). *Mol Cell Endocrinol.* 2013; 376: 23-32.
  65. McEneaney V, Harvey BJ, Thomas W. Aldosterone rapidly activates protein kinase D via a mineralocorticoid receptor/EGFR trans-activation pathway in the M1 kidney CCD cell line. *J Steroid Biochem Mol Biol.* 2007; 107: 180-190.
  66. De Giusti VC, Nolly MB, Yeves AM, Caldiz CI, Villa-Abrille MC, Chiappe de Cingolani GE, Ennis IL, Cingolani HE, Aiello EA. Aldosterone stimulates the cardiac Na(+)/H(+) exchanger via transactivation of the epidermal growth factor receptor. *Hypertension.* 2011; 58: 912-919.
  67. Morgado-Pascual JL, Rayego-Mateos S, Valdivielso JM, Ortiz A, Egido J, Ruiz-Ortega M. Paricalcitol Inhibits Aldosterone-Induced Proinflammatory Factors by Modulating Epidermal Growth Factor Receptor Pathway in Cultured Tubular Epithelial Cells. *Biomed Res Int.* 2015; 2015:783538.
  68. Fang JS, Gillies RD, Gatenby RA. Adaptation to hypoxia and acidosis in carcinogenesis and tumor progression. *Semin Cancer Biol.* 2008; 18: 330-337.
  69. Martinez-Outschoorn U, Sotgia F, Lisanti MP. Tumor microenvironment and metabolic synergy in breast cancers: critical importance of mitochondrial fuels and function. *Semin Oncol.* 2014; 41: 195-216.
  70. De Francesco EM, Lappano R, Santolla MF, Marsico S, Caruso A, Maggiolini M. HIF-1 $\alpha$ /GPER signalling mediates the expression of VEGF induced by hypoxia in breast cancer associated fibroblasts (CAFs). *Breast Cancer Res.* 2013; 15:R64.
  71. De Francesco EM, Pellegrino M, Santolla MF, Lappano R, Ricchio E, Abonante S, Maggiolini M. GPER mediates activation of HIF1 $\alpha$ /VEGF signalling by estrogens. *Cancer Res.* 2014; 74: 4053-4064.
  72. Recchia AG, De Francesco EM, Vivacqua A, Sisci D, Panno ML, Andò S, Maggiolini M. The G protein-coupled receptor 30 is up-regulated by hypoxia-inducible factor-1 $\alpha$  (HIF-1 $\alpha$ ) in breast cancer cells and cardiomyocytes. *J Biol Chem.* 2011; 286: 10773-10782.
  73. Rigracciolo DC, Scarpelli A, Lappano R, Pisano A, Santolla MF, De Marco P, Cirillo F, Cappello AR, Dolce V, Belfiore A, Maggiolini M, De Francesco EM. Copper activates HIF-1 $\alpha$ /GPER/VEGF signalling in cancer cells. *Oncotarget.* 2015; 6:34158-77. doi: 10.18632/oncotarget.5779.
  74. Barton M, Prossnitz ER. Emerging roles of GPER in diabetes and atherosclerosis. *Trends Endocrinol Metab.* 2015; 26: 185-192.
  75. Feldman RD, Gros R. scular effects of aldosterone: sorting out the receptors and the ligands. *Clin Exp Pharmacol Physiol.* 2013; 40: 916-921.
  76. Brossa A, Grange C, Mancuso L, Annaratone L, Satolli MA, Mazzone M, Camussi G, Bussolati B. Sunitinib but not VEGF blockade inhibits cancer stem cell endothelial differentiation. *Oncotarget.* 2015; 6: 11295-11309. doi: 10.18632/oncotarget.3123.
  77. Grange C, Bussolati B, Bruno S, Fonsato V, Sapino A, Camussi G. Isolation and characterization of human breast tumor-derived endothelial cells. *Oncol Rep.* 2006; 15: 381-386.
  78. Fiorio Pla A, Ong HL, Cheng KT, Brossa A, Bussolati B,

Lockwich T, Paria B, Munaron L, Ambudkar IS. TRPV4 mediates tumor-derived endothelial cell migration via arachidonic acid-activated actin remodeling. *Oncogene*. 2012; 31: 200-212.

79. Albanito L, Sisci D, Aquila S, Brunelli E, Vivacqua A, Madeo A, Lappano R, Pandey DP, Picard D, Mauro L, Andò S, Maggiolini M. Epidermal growth factor induces G protein-coupled receptor 30 expression in estrogen receptor-negative breast cancer. *Endocrinology*. 2008; 149: 3799-3808.
80. De Marco P, Bartella V, Vivacqua A, Lappano R, Santolla MF, Morcavallo A, Pezzi V, Belfiore A, Maggiolini M. Insulin-like growth factor-I regulates GPER expression and function in cancer cells. *Oncogene*. 2013; 32: 678-688.
81. De Marco P, Romeo E, Vivacqua A, Malaguarnera R, Abonante S, Romeo F, Pezzi V, Belfiore A, Maggiolini M. GPER1 is regulated by insulin in cancer cells and cancer-associated fibroblasts. *Endocr Relat Cancer*. 2014; 21: 739-753.

# GPER, IGF-IR, and EGFR Transduction Signaling Are Involved in Stimulatory Effects of Zinc in Breast Cancer Cells and Cancer-Associated Fibroblasts

Assunta Pisano,<sup>1</sup> Maria Francesca Santolla,<sup>1</sup> Ernestina Marianna De Francesco,<sup>1</sup> Paola De Marco,<sup>1</sup> Damiano Cosimo Rigracciolo,<sup>1</sup> Maria Grazia Perri,<sup>1</sup> Adele Vivacqua,<sup>1</sup> Sergio Abonante,<sup>2</sup> Anna Rita Cappello,<sup>1</sup> Vincenza Dolce,<sup>1</sup> Antonino Belfiore,<sup>3</sup> Marcello Maggiolini,<sup>1\*</sup> and Rosamaria Lappano<sup>1</sup>

<sup>1</sup>Department of Pharmacy, Health and Nutritional Sciences, University of Calabria, Rende, Italy

<sup>2</sup>Breast Cancer Unit, Regional Hospital, Cosanza, Italy

<sup>3</sup>Division of Endocrinology, Department of Health, University Magna Graecia of Catanzaro, Catanzaro, Italy

Zinc (Zn) is an essential trace mineral that contributes to the regulation of several cellular functions; however, it may be also implicated in the progression of breast cancer through different mechanisms. It has been largely reported that the classical estrogen receptor (ER), as well as the G protein estrogen receptor (GPER, previously known as GPR30) can exert a main role in the development of breast tumors. In the present study, we demonstrate that zinc chloride (ZnCl<sub>2</sub>) involves GPER in the activation of insulin-like growth factor receptor I (IGF-IR)/epidermal growth factor receptor (EGFR)-mediated signaling, which in turn triggers downstream pathways like ERK and AKT in breast cancer cells, and main components of the tumor microenvironment namely cancer-associated fibroblasts (CAFs). Further corroborating these findings, ZnCl<sub>2</sub> stimulates a functional crosstalk of GPER with IGF-IR and EGFR toward the transcription of diverse GPER target genes. Then, we show that GPER contributes to the stimulatory effects induced by ZnCl<sub>2</sub> on cell-cycle progression, proliferation, and migration of breast cancer cells as well as migration of CAFs. Together, our data provide novel insights into the molecular mechanisms through which zinc may exert stimulatory effects in breast cancer cells and CAFs toward tumor progression. © 2016 Wiley Periodicals, Inc.

Key words: zinc; breast cancer cells; cancer-associated fibroblasts; EGFR; GPER; IGF-IR

## INTRODUCTION

Zinc (Zn) is the second most abundant heavy metal in human tissues and contributes to the regulation of crucial cellular functions [1]. As an essential mineral, Zn is required for protein, nucleic acid, carbohydrate, and lipid metabolism and is involved in gene transcription, growth, development, and differentiation [1]. Zn is normally found in air, water, and soil; however, Zn concentrations may be boosted by several industrial activities including mining, coal, and waste combustion and steel processing [2]. For instance, soils located in areas where Zn is mined, refined, or used as fertilizer, are heavily contaminated with the metal [2]. The Recommended Daily Allowance of Zn in adults is 8–11 mg/day, with a tolerable upper intake level of 40 mg/day [3–5]. The adverse effects associated with a high Zn intake include acute gastrointestinal effects and headache, impaired immune function, changes in lipoprotein and cholesterol levels, reduced copper levels, and zinc–iron interactions as well as various other disorders [6–8]. In addition, Zn has been involved in the development of several types of tumors including breast cancer [9,10]. In this regard, previous studies have reported an association

between dysregulated Zn homeostasis and breast cancer progression together with higher Zn levels in breast tumor specimens as compared to normal mammary tissues [11,12]. Compelling evidence has also linked an aberrant expression of Zn transporter proteins with the proliferation and migration of

Abbreviations: CAFs, cancer associated fibroblasts; CTGF, connective tissue growth factor; EGFR, epidermal growth factor receptor; EGR-1, early related gene; ERK, extracellular signal-regulated kinase; GPER, G protein estrogen receptor; IGF-IR, insulin-like growth factor I; PI3K, phosphatidylinositol 3-kinase; ROS, reactive oxygen species; ZnCl<sub>2</sub>, zinc chloride.

Assunta Pisano and Maria Francesca Santolla contributed equally to the work.

Grant sponsor: Associazione Italiana per la Ricerca sul Cancro; Grant number: 16719/2015 14066/13; Grant sponsor: Programma Operativo Nazionale “Ricerca e Competitività 2007–2013”; Grant number: PON 01\_01078; Grant sponsor: Ministero della Salute; Grant number: 67/GR-2010-2319511; Grant sponsor: International Cancer Research Fellowship iCARE; Grant sponsor: European Union (Marie Curie Actions)

\*Correspondence to: Department of Pharmacy, Health and Nutritional Sciences, University of Calabria, Rende, Italy.

Received 29 January 2016; Revised 8 June 2016; Accepted 22 June 2016

DOI 10.1002/mc.22518

Published online 4 July 2016 in Wiley Online Library (wileyonlinelibrary.com).

breast cancer cells [13–15]. A recent study has also suggested that specific dysregulations of Zn transporters may characterize grade, invasiveness, metastatic potential, and response to therapy in breast cancer [16]. Of note, zinc regulated transporters (ZIP) that control Zn influx into the cytosol, were found to be up-regulated by estrogens [17], and increased ZIP levels in breast tumors resulted to be associated with a poor prognosis [15]. Noteworthy, Zn may activate tyrosine kinase receptors as EGFR, IGF-IR, and the insulin receptor, which then trigger the mitogen-activated protein kinase (MAPK) and phosphatidylinositol 3-kinase (PI3-K)/AKT signaling [18–20]. These transduction pathways have been largely implicated in cancer growth and invasion together with other important signal molecules like the G protein-coupled receptors (GPCRs) [21]. Notably, both EGF and IGF-I mediated signaling were shown to functionally interact with the G protein estrogen receptor (GPER, previously known as GPR30) transduction pathway in breast cancer cells [22,23]. In this regard, it has been reported that GPER activation induces important responses like proliferation and migration in several types of cancer cells, and stromal cells that contribute to the malignant progression like cancer-associated fibroblasts (CAFs) [24].

In the present study, we therefore, aimed to evaluate whether Zn might trigger the transduction signaling mediated by GPER through a crosstalk with IGF-IR, and EGFR in breast cancer cells and CAFs. Our results provide novel mechanistic insights regarding a multifaceted network through which Zn may lead to stimulatory effects in breast tumor cells and CAFs derived from breast cancer patients.

## METHODS

### Reagents

We purchased zinc chloride ( $ZnCl_2$ ), zinc sulfate ( $ZnSO_4$ ), wortmannin (WM), N,N,N',N'-tetrakis (2-pyridylmethyl)ethane-1,2-diamine (TPEN), N-acetyl-L-cysteine (NAC), and 2',7'-dichlorofluorescein diacetate (DCFDA) from Sigma–Aldrich (Milan, Italy); tyrphostin AG1478 from Biomol Research Laboratories (Milan, Italy); PD98059 (PD), and 3-bromo-5-t-butyl-4-hydroxybenzylidenemalonitrile (AG1024) from Calbiochem (Milan, Italy); (3aS,4R,9bR)-4-(6-Bromo-1,3-benzodioxol-5-yl)-3a,4,5,9b-3H-cyclopenta[c]quinolone (G15) from Tocris Bioscience (Bristol, UK); human Connective Tissue Growth Factor (CTGF) Recombinant Protein from MBL International (Eppendorf, Milan, Italy). All compounds were solubilized in DMSO except  $ZnCl_2$ ,  $ZnSO_4$ , NAC, and human CTGF recombinant protein, which were dissolved in water. Treatments with the inhibitors AG1478, AG1024, G15, NAC, PD, TPEN, and WM were performed concomitantly with  $ZnCl_2$  exposure, as indicated.

### Cell Cultures

SkBr3 breast cancer cells were obtained by ATCC, used less than 6 months after resuscitation and maintained in RPMI 1640 without phenol red supplemented with 10% FBS, and 100 mg/ml penicillin/streptomycin (Life Technologies, Milan, Italy). CAFs were extracted as previously described in Ref. [25]. Briefly, breast cancer specimens were collected from primary tumors of patients who had undergone surgery. Signed informed consent was obtained from all the patients and from the institutional review board(s) of the Regional Hospital of Cosenza. Tissues from tumors were placed in digestion solution (400 IU collagenase, 100 IU hyaluronidase, and 10% serum, containing antibiotics and antimycotic) and incubated overnight at 37°C. Cells were separated by differential centrifugation at 90g for 2 min. Supernatant containing fibroblasts was centrifuged at 485g for 8 min, pellet obtained was suspended in fibroblasts growth medium (Medium 199 and Ham's F12 mixed 1:1, supplemented with 10% FBS, and antibiotics), and cultured at 37°C in 5%  $CO_2$ . The characterization of primary cells cultures of breast fibroblasts was assessed as described previously in Ref. [26]. Cells were switched to medium without serum the day before immunoblots and reverse transcription-PCR experiments.

### Plasmids and Luciferase Assays

The luciferase reporter plasmid for c-fos encoding a 2.2-kb 5' upstream fragment of human c-fos was a gift from Dr. K. Nose (Hatanodai, Shinagawa-ku, Tokyo). EGR1-luc plasmid, containing the –600 to +12 5'-flanking sequence from the human EGR1 gene, was kindly provided by Dr. Safe (Texas A&M University). The *Renilla* luciferase expression vector pRL-TK (Promega, Milan, Italy) was used as internal transfection control. Cells ( $1 \times 10^5$ ) were plated into 24-well plates with 500  $\mu$ l of regular growth medium/well the day before transfection. Cell medium was replaced on the day of transfection with serum-free medium and transfection was performed using X-tremeGENE 9 DNA Transfection Reagent (Sigma–Aldrich), and a mixture containing 0.5  $\mu$ g of each reporter plasmid and 5 ng of pRL-TK. After 6 h, treatments were added and cells were incubated for 18 h. Luciferase activity was measured using the Dual Luciferase Kit (Promega, Milan, Italy) according to the manufacturer's recommendations. Firefly luciferase activity was normalized to the internal transfection control provided by the *Renilla* luciferase activity. Normalized relative light unit values obtained from cells treated with vehicle were set as onefold induction upon which the activity induced by treatments was calculated.

### Gene Silencing Experiments

SkBr3 cells and CAFs were plated in 10-cm dishes and transiently transfected by X-treme GENE 9 DNA

Transfection Reagent for 24 h before treatments with a control vector, a specific shRNA sequence for each target gene. The short hairpin (sh)RNA constructs to knock down the expression of GPER and CTGF, and the unrelated shRNA control constructs have been described previously in Ref. [27]. Short hairpin (sh) RNA constructs against human GPER were bought from Open Biosystems (www.Biocat.de) with catalog no. RHS4533-M001505. The targeting strands generated from the shRNA vectors sh1, 2, 3, 4, and unrelated control are complementary to the following sequences, respectively: CGAGTTAAAGAGGA-GAAGGAA, CTCCCTCATGAGGTGTTCAA, CGCTCCCTGCAAGCAGTCTTT, GCAGTACGT-GATCGGCCTGTT, and CGACATGAAACCGTC-CATGTT. Considering that sh3 showed the highest efficacy, after the first use it has been referred to as shGPER. The shRNA construct for CTGF was obtained from the same supplier (Open Biosystems; www.Biocat.de). It has clone ID TRCN0000061950 and is based on the same lentiviral expression vector pLKO.1 as the other shRNA constructs. The targeting strand generated from the CTGF shRNA construct is TAGTACAGCGATTCAAAGATG.

#### Gene Expression Studies

Total RNA was extracted and cDNA was synthesized by reverse transcription as previously described in Ref. [28]. The expression of selected genes was quantified by real-time PCR using Step One (TM) sequence detection system (Applied Biosystems Inc, Milan, Italy). Gene-specific primers were designed using Primer Express version 2.0 software (Applied Biosystems Inc). For *c-fos*, CTGF, *Cyr61*, *EGR1*, *MT1X*, *MT2A*, *cyclin D1*, *cyclin A*, GPER, and the ribosomal protein 18S, which was used as a control gene to obtain normalized values, the primers were: 5'-CGAGCCCTTTGATGACTTCCT-3' (*c-fos* forward), 5'-GGAGCGGGCTGTCTCAGA-3' (*c-fos* reverse); 5'-ACCTGTGGGATGGGCATCT-3' (CTGF forward), 5'-CAGGCGGCTCTGCTTCTCTA-3' (CTGF reverse); 5'-GAGTGGTCTGTGACGAGGAT-3' (*Cyr61* forward) and 5'-GGTTGTATAGGATGCGAGGCT-3' (*Cyr61* reverse); 5'-GCCTGCGACATCTGTGGAA-3' (*EGR1* forward), 5'-CGCAAGTGGATCTTGGTATGC-3' (*EGR1* reverse); 5'-TGTCCCGCTGCGTGTTT-3' (*MT1X* forward) and 5'-TTCGAGGCAAGGAGAAGCA-3' (*MT1X* reverse); 5'-CCCCTCCAGATGTAAAGA-3' (*MT2A* forward) and 5'-GGTCACGGTCAGGGTTGTACATA-3' (*MT2A* reverse); 5'-GTCTGTGCATTTCTGGTTGCA-3' (*cyclin D1* forward) and 5'-GCTGGAACATGCCGGTTA-3' (*cyclin D1* reverse); 5'-GCATGT-CACCGTTCCTCCTTG -3' (*cyclin A* forward) and 5'-GGGCATTTACGCTCTATTTT -3' (*cyclin A* reverse); 5'-CCTGGACGAGCAGTATTACGATATC-3' (GPER forward) and 5'-TGCTGTACATGTTGATCTG-3' (GPER reverse) and 5'-GGCGTCCCCCACTTCTTA-3' (18S forward) and 5'-GGGCATCACAGACCTGT-TATT -3' (18S reverse), respectively. Assays were

performed in triplicate and the results were normalized for 18S expression, and then calculated as fold induction of RNA expression.

#### Western Blot Analysis

Cells were grown in 10 cm dishes, exposed to ligands, and then lysed as previously described in Ref. [29]. Equal amounts of whole protein extract were resolved on a 10% SDS-polyacrylamide gel and transferred to a nitrocellulose membrane (Amersham Biosciences, GE Healthcare, Milan, Italy), which were probed with primary antibodies against antiphosphotyrosine antibody (4G10) (Merck Millipore, Milan, Italy), pEGFR Tyr 1173 (sc-12351), EGFR (1005), phosphorylated ERK1/2 (E-4), ERK2 (C-14), p-AKT1/2/3 (Ser 473)-R, AKT1/2/3 (H-136), IGF-1R (7G11), GPER (N-15), *c-fos* (H-125), *EGR1* (C-19), CTGF (L-20), *cyclin D1* (M-20), *cyclin A* (H-432), and  $\beta$ -actin (C2) (Santa Cruz Biotechnology, DBA, Milan, Italy) and then revealed using the ECL system from GE Healthcare (Milan, Italy).

#### Immunoprecipitation Assays

Cells were lysed using 200  $\mu$ l RIPA buffer with a mixture of protease inhibitors containing 1.7 mg/ml aprotinin, 1 mg/ml leupeptin, 200 mmol/L phenylmethylsulfonyl fluoride, 200 mmol/L sodium orthovanadate, and 100 mmol/L sodium fluoride. A total of 100  $\mu$ g proteins were incubated for 2 h with 2  $\mu$ g of the appropriate antibody (GPER, N-15; IGF-1R, 7G11) and 20  $\mu$ l of protein A/G agarose immunoprecipitation reagent (Santa Cruz Biotechnology). Samples were centrifuged at 13 000 rpm for 5 min at 4°C to pellet beads. After four washes in PBS, samples were resuspended in RIPA buffer with protease inhibitors and SDS sample buffer. Western Blot analysis was performed as described above.

#### ROS Production

The non-fluorescent 2',7'-dichlorofluorescein diacetate (DCFDA) probe, which becomes highly fluorescent on reaction with ROS, was used to evaluate intracellular ROS production. Briefly, cells ( $2 \times 10^5$ ) were incubated with 10  $\mu$ M DCFDA (Sigma-Aldrich) at 37°C for 30 min, washed with PBS, and then exposed to treatments, as indicated. Cells were washed with PBS and the fluorescent intensity of DCF was measured (excitation at 485 nm and emission at 530 nm).

#### Cell Cycle Analysis

Cells synchronized for 24 h in serum-free medium were transfected, treated, and subjected to fluorescence-activated cell sorting (FACS) analysis. Adherent and floating cells were centrifuged, and resuspended in PBS containing 20  $\mu$ g/ml propidium iodide plus 40  $\mu$ g/ml ribonuclease (Sigma-Aldrich) for 1 h. Cells were then subjected to FACS analysis (FACS Jazz, BD, Milan, Italy) and results were expressed in terms of percentage.

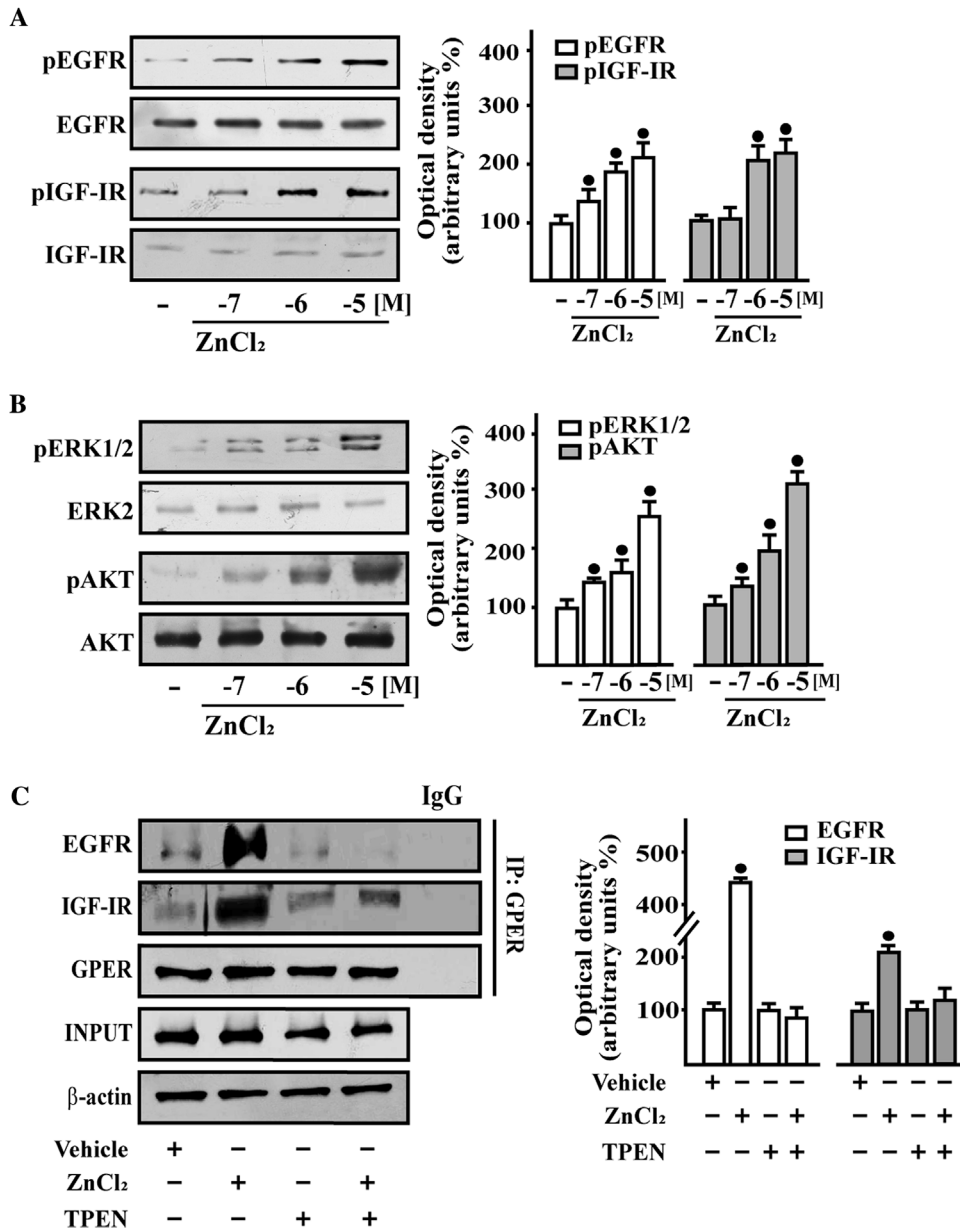


Figure 1. ZnCl<sub>2</sub> triggers rapid responses and stimulates the co-immunoprecipitation of EGFR and IGF-IR with GPER in breast cancer cells. (A and B) Phosphorylation of EGFR (A), IGF-IR (A), ERK1/2 (B) and AKT (B) in SkBr3 cells treated for 15 min with vehicle (–) and increasing concentrations of ZnCl<sub>2</sub>, as indicated. Side panels show densitometric analysis of the blots normalized to EGFR, IGFIR, ERK2, and AKT that served as loading controls, respectively for pEGFR, pIGF-IR, pERK1/2, and pAKT. (C) Co-immunoprecipitation assays performed in SkBr3 cells

treated with 10 μM ZnCl<sub>2</sub> for 15 min using the antibody against GPER followed by immunoblotting for EGFR or IGF-IR, as indicated. In control samples, nonspecific IgG was used instead of the primary antibody. IP, Immunoprecipitation. Input represents the blots probed with the antibody against GPER. Side panels show densitometric analysis of the blots normalized to β-actin. Data shown are the mean ± SD of three independent experiments. (●) indicates *P* < 0.05 for cells treated with vehicle (–) versus treatments.

Proliferation Assay

Cells were seeded in 24-well plates in regular growth medium. After cells attached, they were incubated in medium containing 2.5% charcoal-stripped FBS, transfected for 24 h, and treated as indicated, with transfection and treatments renewed every 2 d. Cells were counted using an automated cell counter (Life Technologies) following the manufacturer’s recommendations.

Migration Assays

Migration assays were performed using Boyden chambers (Costar Transwell, 8 mm polycarbonate membrane, Sigma–Aldrich). Cells were transfected in in regular growth medium. After 24 h, cells were trypsinized and seeded in the upper chambers. Treatments were added to the medium without serum in the bottom wells where applicable, cells on the bottom side

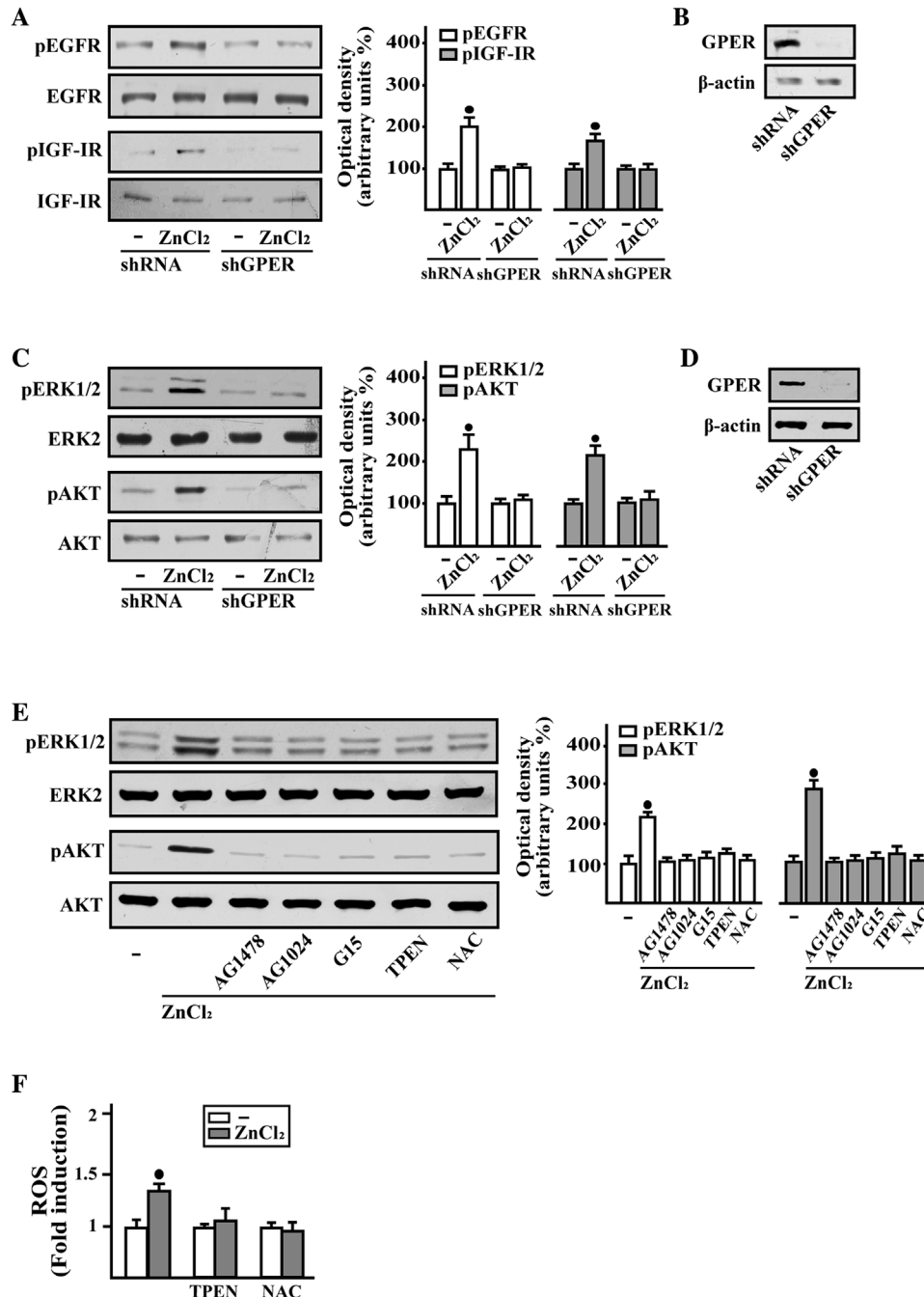


Figure 2. GPER is involved in the rapid action of ZnCl<sub>2</sub> in breast cancer cells. (A–D) Phosphorylation of EGFR (A), IGF-IR (A), ERK1/2 (C) and AKT (C) in SkBr3 cells after silencing GPER expression. Cells were transfected with control shRNA or shGPER, and treated for 15 min with vehicle (–) and 10  $\mu$ M ZnCl<sub>2</sub>. (B and D) Efficacy of GPER silencing. (E) ERK1/2 and AKT activation in SkBr3 cells treated for 15 min with vehicle (–) or 10  $\mu$ M ZnCl<sub>2</sub> alone or in combination with 10  $\mu$ M EGFR inhibitor AG1478, 10  $\mu$ M IGF-IR inhibitor tyrphostin AG1024, 100 nM GPER antagonist G15, 20  $\mu$ M zinc chelator TPEN, and 300  $\mu$ M free radical scavenger NAC. Side panels show densitometric analysis of the blots

normalized to EGFR, IGFIR, ERK2, and AKT that served as loading controls, respectively for pEGFR, pIGF-IR, pERK1/2, and pAKT. (F) ROS production determined as DCF fluorescence in SkBr3 cells treated for 1 h with vehicle (–) or 10  $\mu$ M ZnCl<sub>2</sub> alone and in combination with 20  $\mu$ M zinc chelator TPEN, and 300  $\mu$ M free radical scavenger NAC. DCF fluorescence obtained in cells treated with vehicle (–) was set as onefold induction upon which ROS levels induced by treatments was calculated. Data shown are the mean  $\pm$  SD of three independent experiments. (●) indicates  $P < 0.05$  for cells treated with vehicle (–) versus treatments.

of the membrane were fixed and counted 6 h after seeding. Wound-healing assays were also performed in order to further assess cell migration. Cells were seeded into 12-well plates in regular growth medium. When at

70–80% confluence, cells were transfected in medium without serum. After 24 h, medium was replaced with 2.5% charcoal-stripped FBS and cells were treated. We then used a p200 pipette tip to scratch the cell

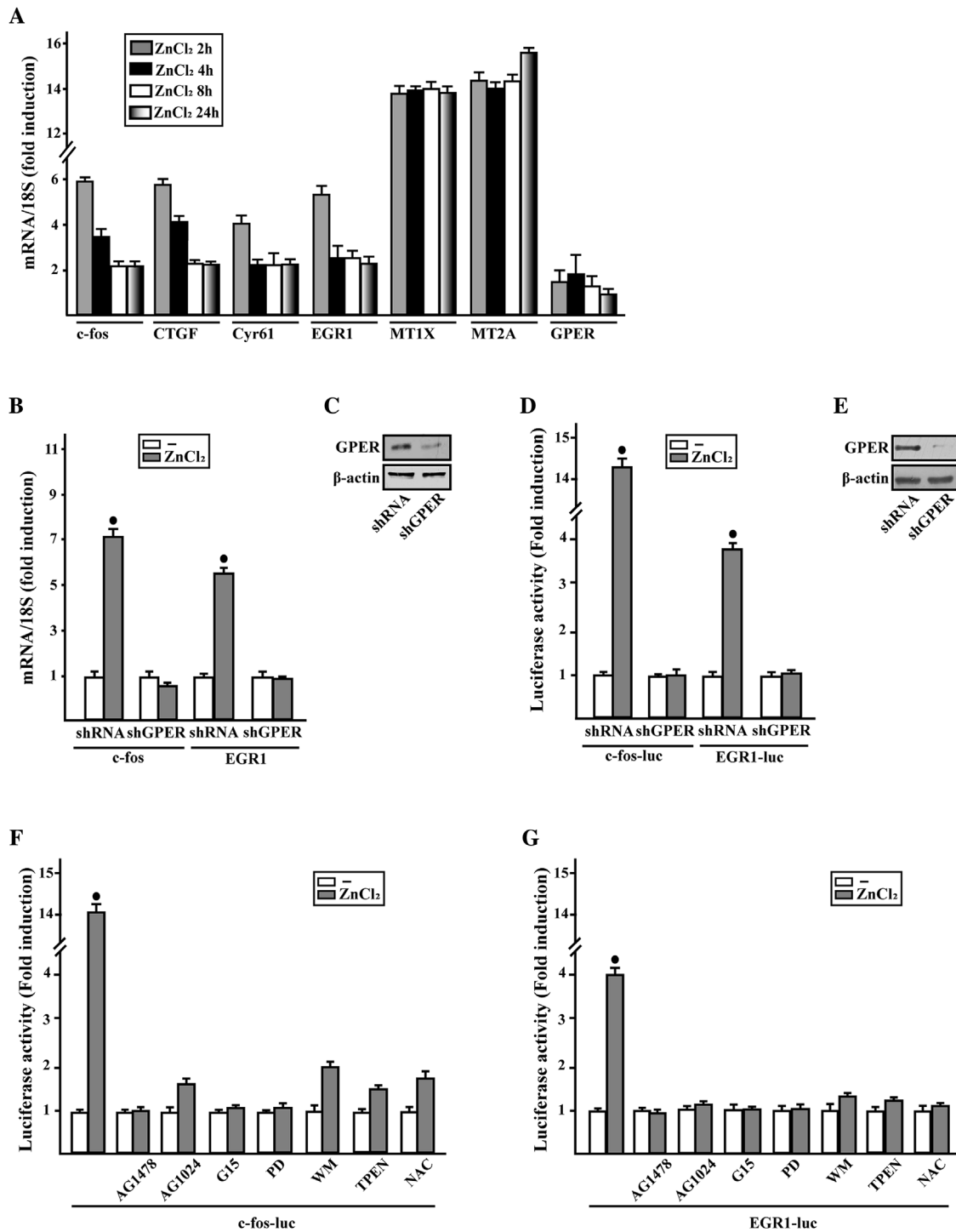


Figure 3. ZnCl<sub>2</sub> regulates the expression of GPER target genes in breast cancer cells. (A) The mRNA expression of c-fos, CTGF, Cyr61, EGR1, MT1X, MT2A and GPER was evaluated by real-time PCR in SkBr3 cells treated with vehicle (–) and 10 μM ZnCl<sub>2</sub>, as indicated. (B) Evaluation of c-fos and EGR1 mRNA expression in SkBr3 cells transfected with shRNA or shGPER, and treated for 2 h with vehicle (–) and 10 μM ZnCl<sub>2</sub>. (C) Efficacy of GPER silencing. Results obtained from experiments performed in triplicate were normalized for 18S expression and shown as fold change of RNA expression compared to cells treated with vehicle. (D) Evaluation of c-fos and EGR1 luciferase reporter genes in SkBr3 cells transfected with shRNA or shGPER, and treated for 18 h

with vehicle (–) and 10 μM ZnCl<sub>2</sub>. (E) Efficacy of GPER silencing. (F and G) Evaluation of c-fos and EGR1 luciferase reporter genes in SkBr3 cells treated for 18 h with vehicle (–) or 10 μM ZnCl<sub>2</sub> alone or in combination with 10 μM EGFR inhibitor AG1478, 10 μM IGF-IR inhibitor tyrphostin AG1024, 100 nM GPER antagonist G15, 10 μM MEK inhibitor PD98089 (PD), 1 μM PI3K inhibitor wortmannin (WM), 20 μM Zn chelator TPEN, and 300 μM free radical scavenger NAC. Luciferase activity was normalized to the internal transfection control; values are presented as fold change (mean ± SD) of vehicle control and represent three independent experiments, each performed in triplicate. (●) indicates *P* < 0.05 for cells receiving vehicle (–) versus treatments.

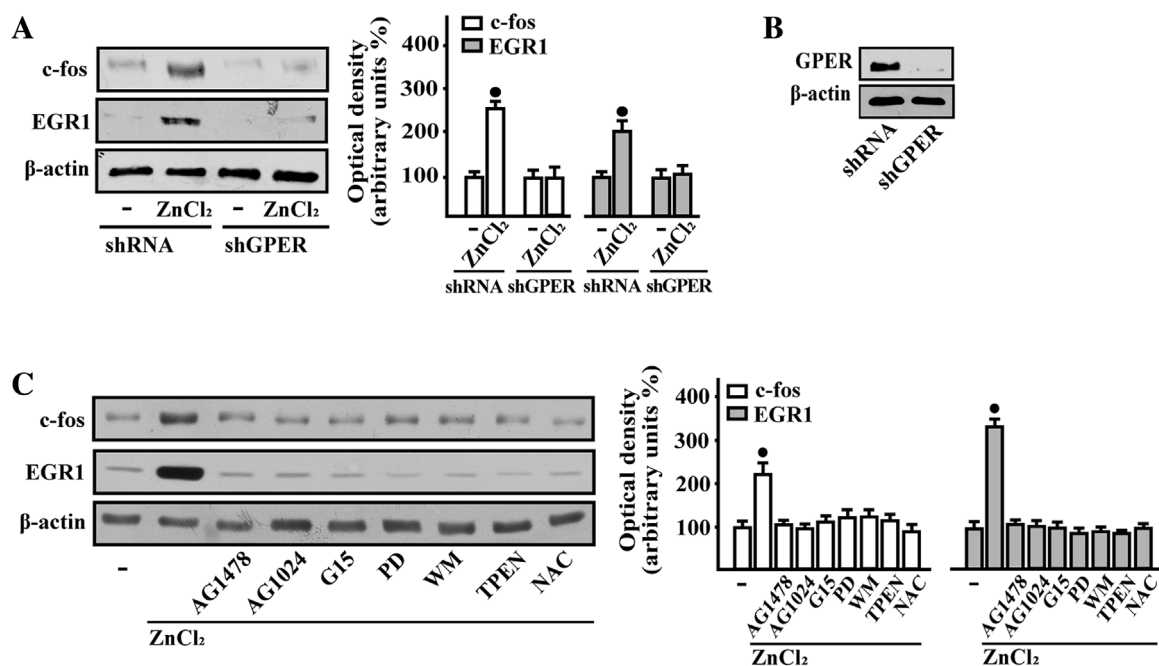


Figure 4. GPER is involved in c-fos and EGR1 protein increase induced by ZnCl<sub>2</sub> in breast cancer cells. (A and B) Protein levels of c-fos and EGR1 in SkBr3 cells transfected with shRNA or shGPER, and treated with vehicle (–) or 10 μM ZnCl<sub>2</sub> for 4 h. (B) Efficacy of GPER silencing. (C) Immunoblots showing c-fos and EGR1 protein expression in SkBr3 cells treated for 4 h with vehicle (–), and 10 μM ZnCl<sub>2</sub> alone or in combination with 10 μM EGFR inhibitor AG1478, 10 μM IGF-IR

inhibitor tyrphostin AG1024, 100 nM GPER antagonist G15, 10 μM MEK inhibitor PD98089 (PD), 1 μM PI3K inhibitor wortmannin (WM), 20 μM Zn chelator TPEN, and 300 μM free radical scavenger NAC. Side panels show densitometric analysis of the blots normalized to β-actin. Values represent the mean ± SD of three independent experiments. (●) indicates *P* < 0.05 for cells treated with vehicle (–) versus treatments.

monolayer. Cells were allowed to migrate for 24 h, the gap area was then photographed and migration distances were measured.

#### Statistical Analysis

Statistical analysis was done using ANOVA followed by Newman–Keuls' testing to determine differences in means. *P* < 0.05 was considered as statistically significant.

## RESULTS

### GPER Is Involved in the Activation of EGFR and IGF-IR by Zn in Breast Cancer Cells

As a dysregulated Zn homeostasis may contribute to breast carcinogenesis through different mechanisms [12], including the activation of growth factors transduction pathways [18–20], we began our study by ascertaining that Zn chloride (ZnCl<sub>2</sub>) triggers the rapid phosphorylation of EGFR and IGF-IR (Figure 1A), as well as the activation of downstream kinases such as ERK and AKT (Figure 1B) in a dose-dependent manner. Similar results were obtained using Zn sulfate (ZnSO<sub>4</sub>) (data not shown). On the basis of these findings, and considering that Zn serum concentration is approximately 15 μM [30], in subsequent assays 10 μM ZnCl<sub>2</sub> were used. As our previous studies have shown that, in cancer cells, both EGFR

and IGF-IR transduction signaling are involved in GPER regulation [29,31–34], we evaluated whether the activation of EGFR and IGF-IR by ZnCl<sub>2</sub> may involve GPER. By co-immunoprecipitation studies performed in SkBr3 cells, we ascertained that ZnCl<sub>2</sub> increases a direct interaction of GPER with EGFR and IGF-IR, while the Zn chelator TPEN prevented this response (Figure 1C). On the basis of these findings, we asked whether the ZnCl<sub>2</sub>-dependent phosphorylation of EGFR and IGF-IR as well as ERK and AKT may involve GPER. Of note, the silencing of GPER expression by a specific shRNA abrogated the activation of both EGFR and IGF-IR, and their downstream signaling molecules ERK and AKT induced by ZnCl<sub>2</sub> treatment (Figure 2A–D). Next, we investigated the mechanisms through which ZnCl<sub>2</sub> may induce the activation of ERK and AKT in breast cancer cells. As shown in Figure 2E, the treatment with the EGFR inhibitor AG1478, the IGF-IR inhibitor AG1024, and the GPER antagonist G15 prevented the phosphorylation of both kinases upon exposure to ZnCl<sub>2</sub>. Likewise, the activation of ERK and AKT triggered by ZnCl<sub>2</sub> was no longer evident in the presence of the Zn chelator TPEN, and the scavenger of reactive oxygen species (ROS) NAC (Figure 2E). Taken together, these data suggest that EGFR, IGF-IR, and GPER are involved in ERK and AKT activation induced by ZnCl<sub>2</sub>. Moreover, the inhibitory effects elicited by

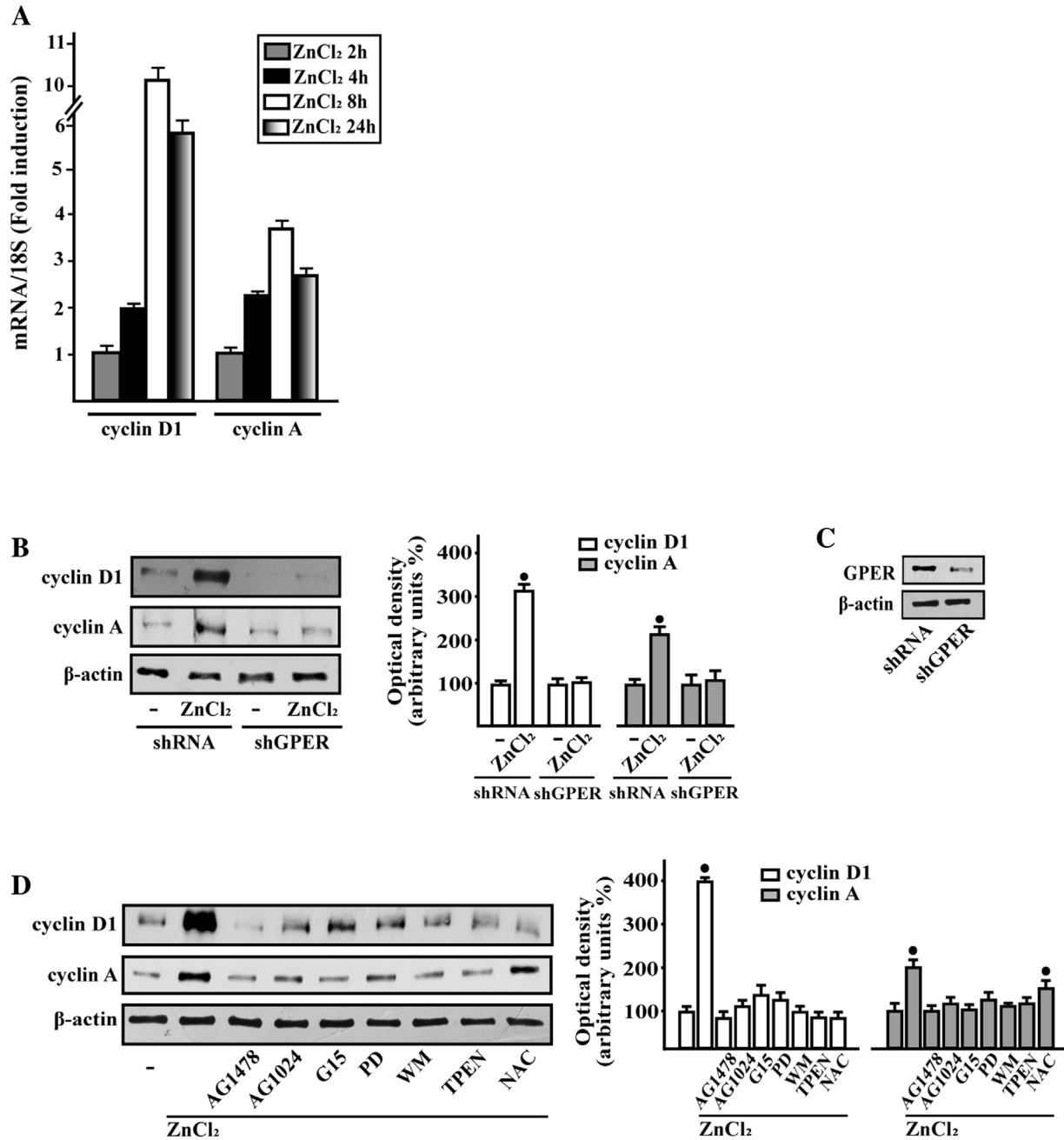


Figure 5. GPER is involved in the up-regulation of cyclins by ZnCl<sub>2</sub> in breast cancer cells. (A) The mRNA expression of cyclin D1 and cyclin A was evaluated by real-time PCR in SkBr3 cells treated with vehicle (–) or 10 μM ZnCl<sub>2</sub>, as indicated. Results obtained from experiments performed in triplicate were normalized for 18S expression and shown as fold change of RNA expression compared to cells treated with vehicle. (B) Cyclin D1 and cyclin A protein levels in SkBr3 cells transfected with shRNA or shGPER, and treated with vehicle (–) and 10 μM ZnCl<sub>2</sub> for 12 h. (C) Efficacy of GPER silencing. (D) Cyclin D1 and

cyclin A immunoblots in SkBr3 cells treated for 12 h with vehicle (–), and 10 μM ZnCl<sub>2</sub> alone or in combination with 10 μM EGFR inhibitor AG1478, 10 μM IGF-IR inhibitor tyrphostin AG1024, 100 nM GPER antagonist G15, 10 μM MEK inhibitor PD98089 (PD), 1 μM PI3K inhibitor wortmannin (WM), 20 μM zinc chelator TPEN, and 300 μM free radical scavenger NAC. Side panels show densitometric analysis of the blots normalized to β-actin. Values represent the mean ± SD of three independent experiments. (●) indicates *P* < 0.05 for cells treated with vehicle (–) versus treatments.

TPEN and NAC indicate that the aforementioned responses triggered by ZnCl<sub>2</sub> are strictly dependent on the metal and occur through the ROS generation. On the basis of these data and previous results showing that Zn is able to increase ROS levels [19,20], we first

confirmed this finding in our experimental model, and thereafter, established that TPEN and NAC inhibit ROS generation triggered by ZnCl<sub>2</sub> (Figure 2F). Hence, the production of ROS observed in SkBr3 cells is involved in the rapid activation of

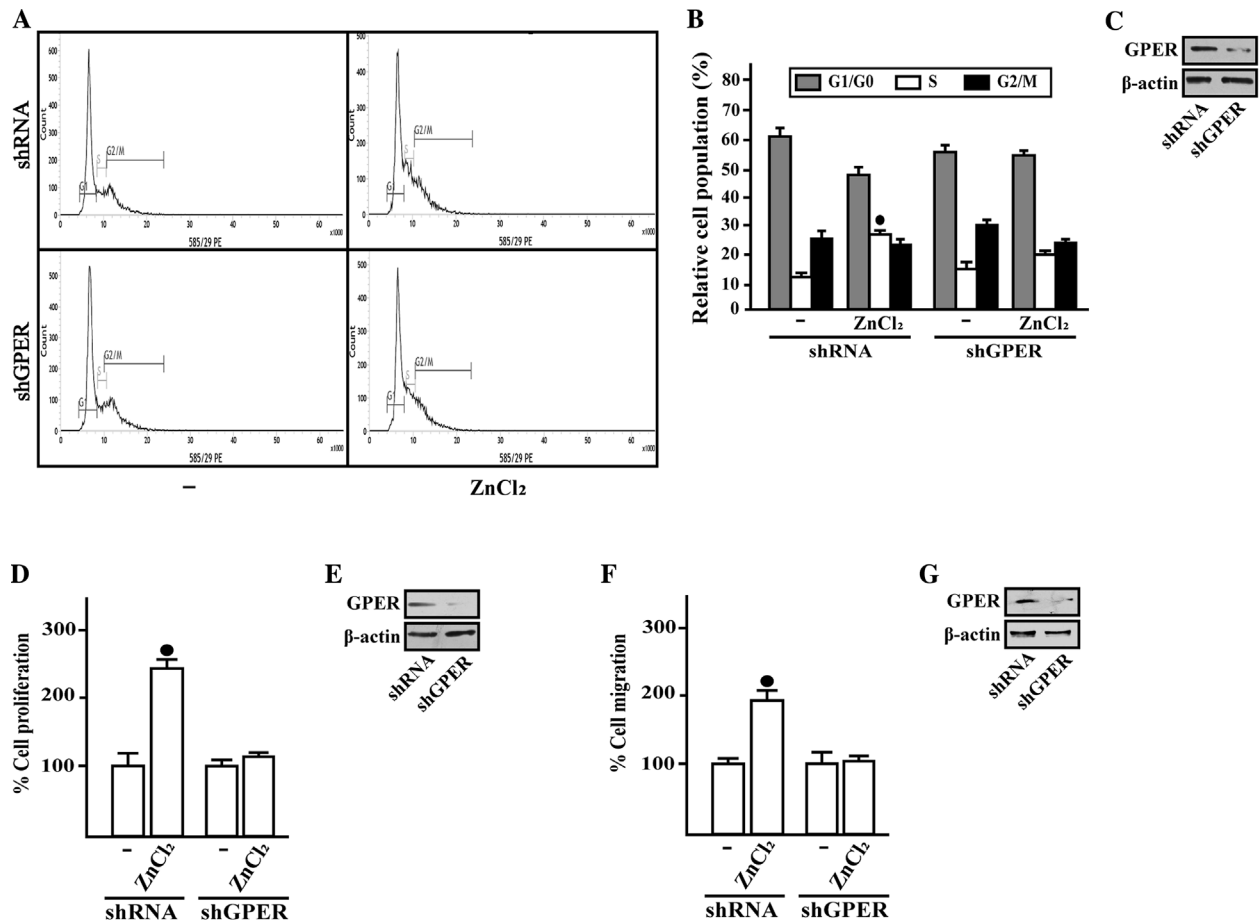


Figure 6. GPER contributes to ZnCl<sub>2</sub> induced cell-cycle progression and proliferation of breast cancer cells. (A) Cell-cycle analysis performed in SkBr3 cells transfected with shRNA or shGPER, and treated with vehicle (–) and 10 μM ZnCl<sub>2</sub> for 18 h. (B) The histograms show the percentages of cells in G1/G0, S, and G2/M phases of the cell cycle, as determined by flow cytometry analysis. (D) The proliferation of SkBr3 cells upon treatment with 10 μM ZnCl<sub>2</sub> is prevented knocking down GPER expression. Cells were transfected with shRNA or shGPER and treated every 2 d with vehicle

(–) or ZnCl<sub>2</sub> as indicated, and then counted on day 6. Proliferation of cells treated with vehicle was set as 100% upon which cell growth induced by treatments was calculated. (F) The migration of SkBr3 cells upon 6 h treatment with 10 μM ZnCl<sub>2</sub> is abrogated knocking down GPER expression, as evaluated by Boyden Chamber assay. (C, E, and G) Efficacy of GPER silencing. Each data point is the mean ± SD of three independent experiments performed in triplicate. (●) indicates  $P < 0.05$  for cells treated with vehicle (–) versus treatments.

GPER/EGFR/IGF-IR transduction signaling upon ZnCl<sub>2</sub> exposure. Collectively, these observations indicate that ZnCl<sub>2</sub> activates a complex transduction signaling that may involve GPER together with EGFR and IGF-IR, and downstream effectors like ERK and AKT, hence, leading to important biological outcomes (see below).

#### GPER Contributes to Gene Expression Changes Induced by Zn in Breast Cancer Cells

Considering that GPER triggers a specific gene signature [27], we then assessed that ZnCl<sub>2</sub> up-regulates in SkBr3 cells the mRNA expression of certain GPER target genes like *c-fos*, *CTGF*, *Cyr61*, *EGR1*, *MT1X*, and *MT2A*, without changing GPER levels in our experimental conditions (Figure 3A). Of note, GPER silencing prevented the mRNA induction of two main GPER target genes as *c-fos* and *EGR1*

(Figure 3B and C) [27]. Accordingly, the transactivation of *c-fos* and *EGR1* promoter constructs observed upon ZnCl<sub>2</sub> exposure was no longer evident knocking down GPER expression (Figure 3D and E). Moreover, the EGFR inhibitor AG1478, the IGF-IR inhibitor AG1024, the GPER antagonist G15, the MEK inhibitor PD, the PI3K inhibitor WM, the zinc chelator TPEN, and the ROS scavenger NAC abolished the luciferase activity of *c-fos* and *EGR1* reporter plasmids induced by ZnCl<sub>2</sub> (Figure 3F and G). Next, we sought to determine whether ZnCl<sub>2</sub> could regulate *c-fos* and *EGR1* at protein level as well as the transduction pathways involved in this response. According to the results obtained in real-time PCR and luciferase experiments, *c-fos* and *EGR-1* protein expression triggered by ZnCl<sub>2</sub> was prevented by GPER silencing (Figure 4A and B) as well as in the presence of the EGFR inhibitor AG1478, the IGF-IR inhibitor AG1024, the GPER antagonist

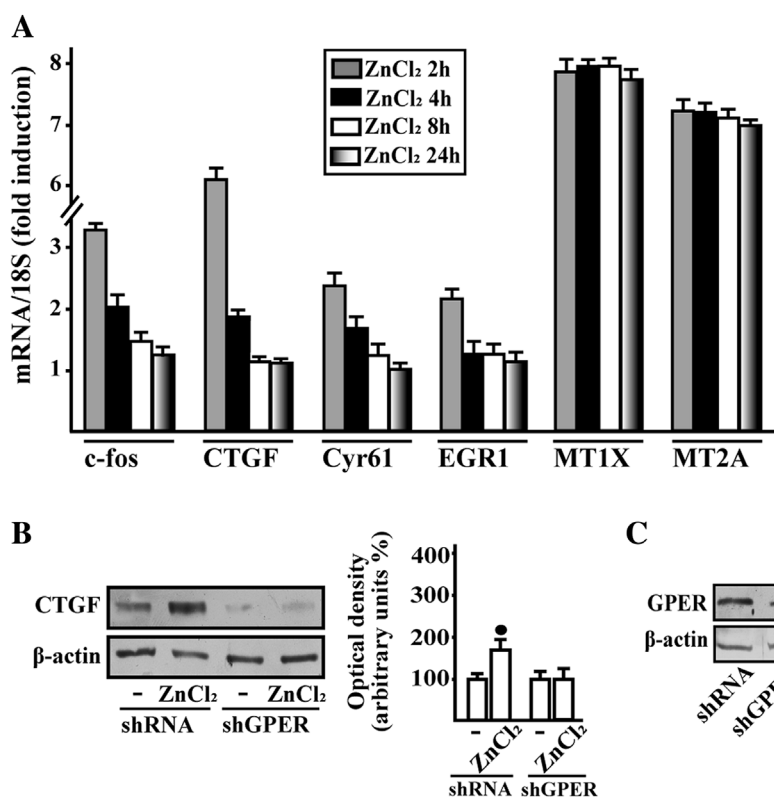


Figure 7. GPER is involved in gene expression changes induced by ZnCl<sub>2</sub> in CAFs. (A) The mRNA expression of c-fos, CTGF, Cyr61, EGR1, MT1X, and MT2A was evaluated by real-time PCR in CAFs treated with vehicle (–) and 10 μM ZnCl<sub>2</sub>, as indicated. Results obtained from experiments performed in triplicate were normalized for 18S expression and shown as fold change of RNA expression compared to cells treated with vehicle. (B)

Immunoblots showing CTGF protein expression in CAFs transfected with shRNA or shGPER, and treated for 4 h with vehicle (–) and 10 μM ZnCl<sub>2</sub>. Side panel shows densitometric analysis of the blot normalized to β-actin. (C) Efficacy of GPER silencing. Values represent the mean ± SD of three independent experiments. (●) indicates  $P < 0.05$  for cells treated with vehicle (–) versus treatments.

G15, the MEK inhibitor PD, the PI3K inhibitor WM, the zinc chelator TPEN, and the ROS scavenger NAC (Figure 4C). Altogether, these data indicate novel transduction mechanisms and gene responses triggered by Zn in breast cancer cells.

#### GPER Is Involved in the Biological Responses to Zn in Breast Cancer Cells

As cyclin D1 and cyclin A have been implicated in the development of several tumors including breast cancer [35], we next evaluated the potential of ZnCl<sub>2</sub> to induce these cell cycle regulators. We found that ZnCl<sub>2</sub> stimulates the expression of both cyclins (Figure 5A and B); however, this response was abrogated silencing GPER (Figure 5B and C) as well as in the presence of AG1478, AG1024, G15, PD, WM, TPEN (Figure 5D). As it concerns NAC, its inhibitory action was mainly exerted on cyclin D1 protein increase by ZnCl<sub>2</sub> whereas, the up-regulation of cyclin A upon NAC treatment was blunted but still evident (Figure 5D). Indeed, although the chelator TPEN does not act in a selective manner, its ability to prevent the aforementioned responses to Zn may further confirm our findings on the biological properties of this metal. On the basis of

the results obtained, it could be therefore, argued that GPER is involved in Zn-dependent gene expression that occurs through both EGFR and IGF-IR transduction pathways. As cyclins are mainly involved in cell cycle progression, we assessed that ZnCl<sub>2</sub> increases the percentage of SkBr3 cells in the S phase of the cell cycle (Figure 6A–C). Moreover, we determined that this response to ZnCl<sub>2</sub> is abrogated by GPER silencing (Figure 6A–C). In accordance with these findings, the proliferative effects observed in SkBr3 cells treated with ZnCl<sub>2</sub> were no longer evident knocking down the expression of GPER (Figure 6D and E). In addition, SkBr3 cell migration induced by ZnCl<sub>2</sub> was prevented silencing GPER (Figure 6F and G). Taken together, these data further extend the current knowledge regarding the stimulatory effects exerted by Zn in breast cancer cells.

#### GPER Contributes to Zn Action in CAFs

In order to further ascertain whether GPER may contribute to the action of Zn, we used CAFs that play an active role toward the growth, expansion, and dissemination of breast cancer cells [36,37]. Remarkably, ZnCl<sub>2</sub> increased the mRNA levels of diverse GPER target genes like c-fos, CTGF, Cyr61, EGR1, MT1X, and MT2A in

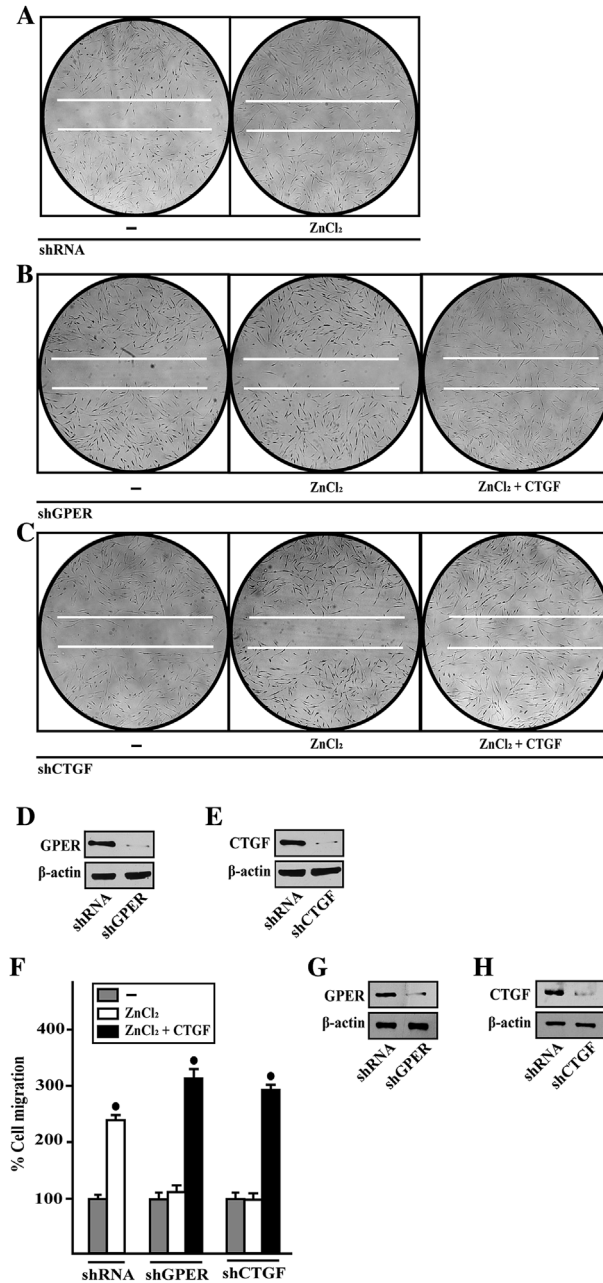


Figure 8. GPER and its target gene CTGF contribute to the migration of CAFs induced by ZnCl<sub>2</sub>. (A–C) The migration of CAFs upon treatment with 10 μM ZnCl<sub>2</sub> for 24 h is prevented knocking down GPER and CTGF expression, as assessed by wound-healing assay. Cell migration is rescued in CAFs transfected with shGPER (B) or shCTGF (C) exposed to 10 μM ZnCl<sub>2</sub> for 24 h and treated with 100 ng/ml CTGF. Images shown are representative of three independent experiments. (F) The migration of CAFs induced by

a 6 h treatment with 10 μM ZnCl<sub>2</sub> is prevented knocking down GPER and CTGF expression, as evaluated by Boyden Chamber assay. Cell migration is rescued in CAFs transfected with shGPER and shCTGF, exposed to 10 μM ZnCl<sub>2</sub> for 6 h and treated with 100 ng/ml CTGF. Efficacy of GPER (D and G) and CTGF (E and H) silencing. Values represent the mean ± SD of three independent experiments. (●) indicates *P* < 0.05 for cells treated with vehicle (–) versus treatments.

CAFs obtained from breast cancer specimens (Figure 7A). Gene expression profile displayed responses to ZnCl<sub>2</sub> similar to those observed in SkBr3 cells (Figure 3A), as the induction of *c-fos*, CTGF, *Cyr61*, and *EGR1* was rapid (2–4 h) but declined thereafter, whereas, the expression of *MT1X* and *MT2A* was still evident up to

24 h. Then, we observed that the up-regulation of CTGF protein levels upon ZnCl<sub>2</sub> treatment is prevented knocking down GPER expression in CAFs (Figure 7B and C). As CTGF exerts an acknowledged role in migratory properties of different cell types [27,38], we evaluated whether GPER signaling

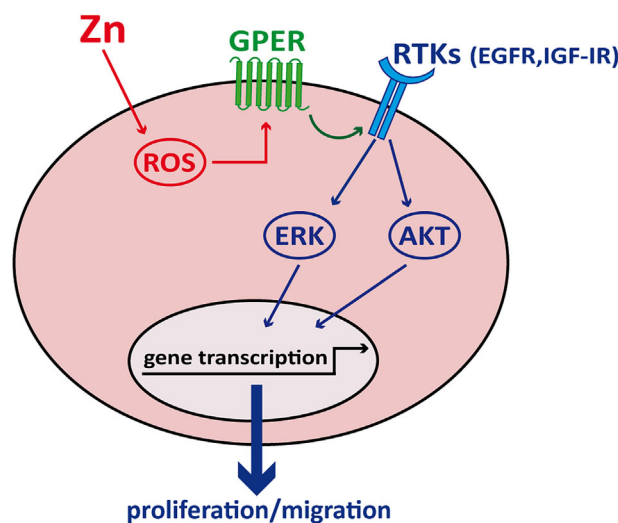


Figure 9. Schematic representation of the functional cooperation of GPER with IGF-IR and EGFR upon zinc exposure.

through CTGF may trigger the migration of CAFs. Scratch experiments and Boyden chamber assays revealed that  $\text{ZnCl}_2$ -stimulated migration of CAFs is abolished silencing GPER or CTGF expression, whereas, adding CTGF the migratory response was rescued (Figure 8). Collectively, the aforementioned results indicate that Zn-activated GPER signaling mediates a similar gene expression profile as well as important biological responses in both breast cancer cells and CAFs. On the basis of these findings, it could be argued that Zn may trigger through GPER a functional interplay between cancer cells and CAFs toward breast tumor progression.

#### DISCUSSION

Several human activities as well as natural events can lead to heavy metals pollution and therefore, increased incidence of various tumors [39–41]. In the present study, we have demonstrated that one important pollutant such as Zn may trigger a functional interplay of GPER with EGFR and IGF-IR, which leads to the activation of main transduction pathways, gene expression changes, and important biological responses like proliferation and migration in breast cancer cells and CAFs (Figure 9).

Breast cancers have been reported to show an increased Zn uptake and tissue concentration as compared to the normal breast tissue [10,42], while patients with advanced breast tumors show decreased serum Zn levels; hence, the determination of serum Zn levels has been proposed as a prognostic marker in breast cancer patients [9,43,44]. Of note, tamoxifen-resistant breast cancer cells that display an aggressive and invasive phenotype, show increased levels of Zn and its transporter ZIP7, which are involved in the activation of EGFR and IGF-IR transduction signaling toward cell proliferation, and invasion [15]. In

accordance with these findings, the growth factors-mediated effects of Zn promoted the activation of kinases, gene expression changes, and growth responses [19,20].

Numerous studies have shown that GPER contributes to the progression of certain tumors including breast cancer [45–50]. In addition, clinical studies have indicated that GPER may be a predictor of aggressive cancer behavior as its expression has been associated with negative clinical outcomes in several cancer histotypes [51–55]. The activation of GPER has been shown to trigger EGFR transactivation, subsequent transduction events such as the activation of MAPK and PI3K cascades, gene expression changes, and relevant biological responses such as proliferation, migration, and angiogenesis in diverse cancer cell types and CAFs [56,57]. In this context, it should be mentioned that the metal cadmium may induce cAMP increase, ERK1/2 activation, and proliferation of breast cancer cells in a GPER-dependent manner [58]. Recently, we also demonstrated that copper activates the HIF-1 $\alpha$ /GPER/VEGF signaling in cancer cells leading to angiogenesis and tumor progression [57]. Further extending these findings, in the present study we have demonstrated that in breast cancer cells exposed to Zn the activation of GPER leads to rapid signaling events such as the phosphorylation of EGFR and IGF-IR, and their downstream effectors ERK and AKT, the up-regulation of c-fos and EGR1, two main GPER target genes largely involved in growth responses. It is worth noting that Zn induced also GPER targets namely metallothioneins MT1X and MT2A, whose overexpression correlates with chemoresistance and poor prognosis in breast tumors [59,60]. Moreover, in line with the known capability of GPER to trigger the transcription of genes associated with cell growth [27], we assessed the potential of Zn to regulate the

expression of two members of the cyclin family as cyclin D1 and A. According to their regulatory role of cell-cycle progression, proliferation, and notably migration [61], we detected also that Zn through GPER significantly increases the percentage of SkBr3 cells in the S phase of the cell cycle as well as stimulates cell proliferation and migration.

Several studies have suggested the active role exerted by the cancer microenvironment on the growth and spread of neoplastic cells [62]. For instance, CAFs contribute to breast cancer aggressiveness through the production of secreted factors that promote migration, invasion, and angiogenesis [62]. Further extending these findings, we have ascertained that Zn promotes the migration of CAFs through GPER and the induction of its target gene CTGF, which has been widely involved in cancer cells dissemination and metastasis [27,38]. Moreover, we have assessed that Zn may influence analogous transcriptional and functional responses in both breast cancer cells, and main components of the reactive stroma like CAFs toward more aggressive tumor features.

Altogether, the present data provide novel insights into the molecular mechanisms through which Zn may elicit stimulatory effects in breast cancer cells and tumor microenvironment components such as CAFs. In particular, our findings indicate that GPER may be included together with EGFR and IGF-IR among the transduction mediators of relevant biological responses to Zn in breast cancer cells, and the surrounding stroma.

#### ACKNOWLEDGMENTS

This work was supported by Associazione Italiana per la Ricerca sul Cancro (MM grant n. 16719/2015 and AB grant n. 14066/13), Programma Operativo Nazionale "Ricerca e Competitività 2007–2013" (PON01\_01078) and Ministero della Salute (grant n. 67/GR-2010-2319511). EMDF was supported by International Cancer Research Fellowship iCARE and European Union (Marie Curie Actions).

#### REFERENCES

1. Vallee BL, Falchuk KH. The biochemical basis of zinc physiology. *Physiol Rev* 1993;73:79–118.
2. Wuana RA, Okieimen FE. Heavy metals in contaminated soils: A review of sources, chemistry, risks, and best available strategies for remediation. *ISRN Ecology* 2011;11:1–20.
3. Institute of Medicine (US) Panel on Micronutrients, Institute of Medicine (US) Food and Nutrition Board DRI, dietary reference intakes for vitamin A, vitamin K, arsenic, boron, chromium, copper, iodine, iron, manganese, molybdenum, nickel, silicon, vanadium, and zinc. Washington, DC: National Academies Press; 2001.
4. Otten JJ, Hellwig JP, Meyers LD. DRI, dietary reference intakes: The essential guide to nutrient requirements. Washington, DC: National Academies Press; 2006.
5. Solomons NW, Ruz M. Trace element requirements in humans: An update. *The journal of trace elements in experimental medicine*. Oxford, UK: Wiley-Liss, Inc.; 1998. 11: pp. 177–195.
6. Haase H, Rink L. The immune system and the impact of zinc during aging. *Immun Ageing* 2009;6:9.
7. Prasad AS. Impact of the discovery of human zinc deficiency on health. *J Am Coll Nutr* 2009;28:257–265.
8. Sensi SL, Paoletti P, Bush AI, Sekler I. Zinc in the physiology and pathology of the CNS. *Nat Rev Neurosci* 2009;10:780–791.
9. Chakravarty PK, Ghosh A, Chowdhury JR. Zinc in human malignancies. *Neoplasma* 1986;33:85–90.
10. Margalioth EJ, Schenker JG, Chevion M. Copper and zinc levels in normal and malignant tissues. *Cancer* 1983;52:868–872.
11. Cui Y, Vogt S, Olson N, Glass AG, Rohan TE. Levels of zinc, selenium, calcium, and iron in benign breast tissue and risk of subsequent breast cancer. *Cancer Epidemiol Biomarkers Prev* 2007;16:1682–1685.
12. Kelleher SL, Seo YA, Lopez V. Mammary gland zinc metabolism: Regulation and dysregulation. *Genes Nutr* 2009;4:83–94.
13. Kagara N, Tanaka N, Noguchi S, Hirano T. Zinc and its transporter ZIP10 are involved in invasive behavior of breast cancer cells. *Cancer Sci* 2007;98:692–697.
14. Taylor KM. A distinct role in breast cancer for two LIV-1 family zinc transporters. *Biochem Soc Trans* 2008;36:1247–1251.
15. Taylor KM, Vichova P, Jordan N, Hiscox S, Hendley R, Nicholson RL. ZIP7-mediated intracellular zinc transport contributes to aberrant growth factor signaling in anti-hormone-resistant breast cancer cells. *Endocrinology* 2008;149:4912–4920.
16. Chandler P, Kochupurakkal BS, Alam S, Richardson AL, Soybel D, Kelleher SL. Subtype-specific accumulation of intracellular zinc pools is associated with the malignant phenotype in breast cancer. *Mol Cancer* 2016;15:2.
17. Dressman MA, Walz TM, Lavedan C, et al. Genes that cocluster with estrogen receptor alpha in microarray analysis of breast biopsies. *Pharmacogenomics J* 2001;1:135–141.
18. Fukada T, Yamasaki S, Nishida K, Murakami M, Hirano T. Zinc homeostasis and signaling in health and diseases: Zinc signaling. *J Biol Inorg Chem* 2011;16:1123–1134.
19. Haase H, Maret W. Intracellular zinc fluctuations modulate protein tyrosine phosphatase activity in insulin/insulinlike growth factor-1 signaling. *Exp Cell Res* 2003;291:289–298.
20. Samet JM, Dewar BJ, Wu W, Graves LM. Mechanisms of Zn<sup>2+</sup>-induced signal initiation through the epidermal growth factor receptor. *Toxicol Appl Pharmacol* 2003;191:86–93.
21. Lappano R, Maggiolini M. G protein-coupled receptors: Novel targets for drug discovery in cancer. *Nat Rev Drug Discov* 2011;10:47–60.
22. Lappano R, De Marco P, De Francesco EM, et al. Cross-talk between GPER and growth factor signaling. *J Steroid Biochem Mol Biol* 2013;137:50–56.
23. Lappano R, Pisano A, Maggiolini M. GPER function in breast cancer: An overview. *Front Endocrinol (Lausanne)* 2014;5:66.
24. Jacenik D, Cygankiewicz AI, Krajewska WM. The G protein-coupled estrogen receptor as a modulator of neoplastic transformation. *Mol Cell Endocrinol* 2016;429:10–18.
25. Madeo A, Maggiolini M. Nuclear alternate estrogen receptor GPR30 mediates 17beta-estradiol-induced gene expression and migration in breast cancer-associated fibroblasts. *Cancer Res* 2010;70:6036–6046.
26. Pupo M, Pisano A, Lappano R, et al. Bisphenol A induces gene expression changes and proliferative effects through GPER in breast cancer cells and cancer-associated fibroblasts. *Environ Health Perspect* 2012;120:1177–1182.
27. Pandey DP, Lappano R, Albanito L, Madeo A, Maggiolini M, Picard D. Estrogenic GPR30 signaling induces proliferation and migration of breast cancer cells through CTGF. *EMBO J* 2009;28:523–532.
28. Lappano R, Rosano C, Santolla MF, et al. Two novel GPER agonists induce gene expression changes and growth effects in cancer cells. *Curr Cancer Drug Targets* 2012;12:531–542.

29. Lappano R, Santolla MF, Pupo M, et al. MIBE acts as antagonist ligand of both estrogen receptor  $\alpha$  and GPER in breast cancer cells. *Breast Cancer Res* 2012;14:R12.
30. Vardatsikos G, Pandey NR, Srivastava AK. Insulino-mimetic and anti-diabetic effects of zinc. *J Inorg Biochem* 2013;120:8–17.
31. Albanito L, Sisci D, Aquila S, et al. Epidermal growth factor induces G protein-coupled receptor 30 expression in estrogen receptor-negative breast cancer cells. *Endocrinology* 2008;149:3799–3808.
32. Bartella V, De Marco P, Malaguarnera R, Belfiore A, Maggiolini M. New advances on the functional cross-talk between insulin-like growth factor-I and estrogen signaling in cancer. *Cell Signal* 2012;24:1515–1521.
33. De Marco P, Bartella V, Vivacqua A, et al. Insulin-like growth factor-I regulates GPER expression and function in cancer cells. *Oncogene* 2013;32:678–688.
34. Vivacqua A, Lappano R, De Marco P, et al. G protein-coupled receptor 30 expression is up-regulated by EGF and TGF  $\alpha$  in estrogen receptor  $\alpha$ -positive cancer cells. *Mol Endocrinol* 2009;23:1815–1826.
35. Casimiro MC, Crosariol M, Loro E, Li Z, Pestell RG. Cyclins and cell cycle control in cancer and disease. *Genes Cancer* 2012;3:649–657.
36. Gao MQ, Kim BG, Kang S, et al. Stromal fibroblasts from the interface zone of human breast carcinomas induce an epithelial-mesenchymal transition-like state in breast cancer cells in vitro. *J Cell Sci* 2010;123:3507–3514.
37. Bhowmick NA, Neilson EG, Moses HL. Stromal fibroblasts in cancer initiation and progression. *Nature* 2004;432:332–337.
38. Aguiar DP, de Farias GC, de Sousa EB, et al. New strategy to control cell migration and metastasis regulated by CCN2/CTGF. *Cancer Cell Int* 2014;14:61.
39. Liu R, Wang M, Chen W, Peng C. Spatial pattern of heavy metals accumulation risk in urban soils of Beijing and its influencing factors. *Environ Pollut* 2015;210:174–181.
40. Pellegri G, De Vathaire F, Scollo C, et al. Papillary thyroid cancer incidence in the volcanic area of Sicily. *J Natl Cancer Inst* 2009;101:1575–1583.
41. Russo M, Malandrino P, Addario WP, et al. Several site-specific cancers are increased in the volcanic area in Sicily. *Anticancer Res* 2015;35:3995–4001.
42. Tupper R, Watts RW, Wormal A. The incorporation of  $^{65}\text{Zn}$  in mammary tumours and some other tissues of mice after injection of the isotope. *Biochem J* 1955;59:264–268.
43. Gupta SK, Shukla VK, Vaidya MP, Roy SK, Gupta S. Serum trace elements and Cu/Zn ratio in breast cancer patients. *J Surg Oncol* 1991;46:178–181.
44. Yucl I, Arpacı F, Ozet A, et al. Serum copper and zinc levels and copper/zinc ratio in patients with breast cancer. *Biol Trace Elem Res* 1994;40:31–38.
45. Albanito L, Lappano R, Madeo A, et al. Effects of atrazine on estrogen receptor  $\alpha$ - and G protein-coupled receptor 30-mediated signaling and proliferation in cancer cells and cancer-associated fibroblasts. *Environ Health Perspect* 2015;123:493–499.
46. Maggiolini M, Picard D. The unfolding stories of GPR30, a new membrane-bound estrogen receptor. *J Endocrinol* 2010;204:105–114.
47. Marjon NA, Hu C, Hathaway HJ, Prossnitz ER. G protein-coupled estrogen receptor regulates mammary tumorigenesis and metastasis. *Mol Cancer Res* 2014;12:1644–1654.
48. Santolla MF, Avino S, Pellegrino M, et al. SIRT1 is involved in oncogenic signaling mediated by GPER in breast cancer. *Cell Death Dis* 2015;6:e1834.
49. Bartella V, De Francesco EM, Perri MG, et al. The G protein-coupled estrogen receptor (GPER) is regulated by endothelin-1 mediated signaling in cancer cells. *Cell Signal* 2016;28:61–71.
50. Rigracciolo DC, Scarpelli A, Lappano R, et al. GPER is involved in the stimulatory effects of aldosterone in breast cancer cells and breast tumor-derived endothelial cells. *Oncotarget* 2015;7:94–111.
51. Filardo EJ, Graeber CT, Quinn JA, et al. Distribution of GPR30, a seven membrane-spanning estrogen receptor, in primary breast cancer, and its association with clinicopathologic determinants of tumor progression. *Clin Cancer Res* 2006;12:6359–6366.
52. Smith HO, Arias-Pulido H, Kuo DY, et al. GPR30 predicts poor survival for ovarian cancer. *Gynecol Oncol* 2009;114:465–471.
53. Smith HO, Leslie KK, Singh M, et al. GPR30: A novel indicator of poor survival for endometrial carcinoma. *Am J Obstet Gynecol* 2007;196:386.
54. Sjöström M, Hartman L, Grabau D, et al. Lack of G protein-coupled estrogen receptor (GPER) in the plasma membrane is associated with excellent long-term prognosis in breast cancer. *Breast Cancer Res Treat* 2014;145:61–71.
55. Prossnitz ER, Arterburn JB. G protein-coupled estrogen receptor and its pharmacologic modulators. *Pharmacol Rev* 2015;67:505–540.
56. Prossnitz ER, Maggiolini M. Mechanisms of estrogen signaling and gene expression via GPR30. *Mol Cell Endocrinol* 2009;308:32–38.
57. Rigracciolo DC, Scarpelli A, Lappano R, et al. Copper activates HIF-1 $\alpha$ /GPER/VEGF signalling in cancer cells. *Oncotarget* 2015;6:34158–34177.
58. Yu X, Filardo EJ, Shaikh ZA. The membrane estrogen receptor GPR30 mediates cadmium-induced proliferation of breast cancer cells. *Toxicol Appl Pharmacol* 2010;245:83–90.
59. Bay BH, Jin R, Huang J, Tan PH. Metallothionein as a prognostic biomarker in breast cancer. *Exp Biol Med* 2006;231:1516–1521.
60. Surowiak P, Matkowski R, Materna V, et al. Elevated metallothionein (MT) expression in invasive ductal breast cancers predicts tamoxifen resistance. *Histol Histopathol* 2005;20:1037–1044.
61. Pestell RG. New roles of cyclin D1. *Am J Pathol* 2013;183:3–9.
62. Kalluri R, Zeisberg M. Fibroblasts in cancer. *Nat Rev Cancer* 2006;6:392–301.

## Stimulatory actions of IGF-I are mediated by IGF-IR cross-talk with GPER and DDR1 in mesothelioma and lung cancer cells

Silvia Avino<sup>1,\*</sup>, Paola De Marco<sup>1,\*</sup>, Francesca Cirillo<sup>1</sup>, Maria Francesca Santolla<sup>1</sup>, Ernestina Marianna De Francesco<sup>1</sup>, Maria Grazia Perri<sup>1</sup>, Damiano Rigracciolo<sup>1</sup>, Vincenza Dolce<sup>1</sup>, Antonino Belfiore<sup>2</sup>, Marcello Maggiolini<sup>1</sup>, Rosamaria Lappano<sup>1,\*\*</sup> and Adele Vivacqua<sup>1,\*\*</sup>

<sup>1</sup> Department of Pharmacy, Health and Nutritional Sciences, University of Calabria, Rende, Italy

<sup>2</sup> Endocrinology, Department of Health Sciences, University Magna Graecia of Catanzaro, Catanzaro, Italy

\* These authors have contributed equally to this work

\*\* Joint senior Authors

**Correspondence to:** Marcello Maggiolini, **email:** marcellomaggiolini@yahoo.it

**Keywords:** DDR1, GPER, IGF-I, IGF-IR, mesothelioma, lung cancer, Pathology Section

**Received:** April 06, 2016

**Accepted:** June 17, 2016

**Published:** June 30, 2016

### ABSTRACT

**Insulin-like growth factor-I (IGF-I)/IGF-I receptor (IGF-IR) system has been largely involved in the pathogenesis and development of various tumors. We have previously demonstrated that IGF-IR cooperates with the G-protein estrogen receptor (GPER) and the collagen receptor discoidin domain 1 (DDR1) that are implicated in cancer progression. Here, we provide novel evidence regarding the molecular mechanisms through which IGF-I/IGF-IR signaling triggers a functional cross-talk with GPER and DDR1 in both mesothelioma and lung cancer cells. In particular, we show that IGF-I activates the transduction network mediated by IGF-IR leading to the up-regulation of GPER and its main target genes CTGF and EGR1 as well as the induction of DDR1 target genes like MATN-2, FBN-1, NOTCH 1 and HES-1. Of note, certain DDR1-mediated effects upon IGF-I stimulation required both IGF-IR and GPER as determined knocking-down the expression of these receptors. The aforementioned findings were nicely recapitulated in important biological outcomes like IGF-I promoted chemotaxis and migration of both mesothelioma and lung cancer cells. Overall, our data suggest that IGF-I/IGF-IR system triggers stimulatory actions through both GPER and DDR1 in aggressive tumors as mesothelioma and lung tumors. Hence, this novel signaling pathway may represent a further target in setting innovative anticancer strategies.**

### INTRODUCTION

Lung cancer is the most frequent cause of cancer incidence and mortality worldwide at least in part due to the increasing number of risk factors in diverse developing countries [1-2]. To date, smoking has been considered the main etiologic factor for lung cancer [3-4], however, several environmental contaminants like asbestos, arsenic, cadmium, nickel and silica, play an important role toward the development of this neoplasia [5]. Among the aforementioned environmental pollutants, asbestos has been particularly acknowledged as prompting

factor in malignant mesothelioma (MM), which is an aggressive cancer that arises from mesothelial cells lining lung, pleura or peritoneum [6-7]. Chronic inflammatory processes caused by the deposition of asbestos fibers and the subsequent release of cytokines and growth factors by macrophages and mesothelial cells have been shown to play an active role toward the development of both pleural MM and lung cancer [7-8].

In this vein, the IGF system, the complex system involving the insulin-like growth factors (IGFs) and related receptors as well as IGF-binding proteins, has been established as an important regulator of tumor initiation

and progression in several malignancies, including pleural MM and lung cancer [9-13]. In particular, the IGF-I receptor (IGF-IR), which is often overexpressed in diverse cancer cell types, affects tumor development, progression and resistance to therapies [11, 14-16]. Moreover, a dysregulated IGF system has been shown to be implicated in various chronic diseases, such as pulmonary fibrosis [17-18].

An increasing body of data has demonstrated that the biological responses mediated by IGF-I involve functional interactions of IGF-IR with diverse signal molecules belonging to other members of the receptor tyrosine kinase (RTK) family [19-20]. In this context, we recently discovered a novel functional cross-talk between IGF-IR and the collagen receptor discoidin domain receptor 1 (DDR1), a molecule also overexpressed in diverse malignancies, including lung carcinomas, and implicated in cancer progression [21]. Interestingly, this cross-talk occurs also independently of the collagen binding actions of DDR1 and, in human breast cancer cells, amplifies the stimulatory biological effects of IGF-I toward proliferation, migration and colony formation. Moreover, through a signaling pathway involving Akt/miR-199a-5p, IGF-I is able to upregulate DDR1 [12, 22].

In addition to RTKs, IGF-IR interacts with other important signaling molecules like G protein-coupled receptors (GPCRs) [19, 23]. These functional interactions have also important implications in the development and progression of diverse types of tumors [23-24]. In particular, we found that IGF-IR activation engages the G protein estrogen receptor (GPER/GPR30)-mediated signaling toward the stimulation of proliferation and migration of different cancer cell types [25-26]. Interestingly, high expression levels of GPER were detected in lung cancer cells and involved in growth stimulatory effects [24, 27-28]. To date, other signaling molecules have been implicated in the development of MM including the estrogen receptor (ER) $\beta$  that may act as a tumor suppressor [29-30]. Therefore, the multifaceted mechanisms and the transduction network of factors involved in the progression of the aforementioned malignancies remain to be fully understood.

In this study, we found that mesothelioma and lung cancer cells show a new complex functional cross-talk involving IGF-IR, GPER and DDR1, which affects gene expression and biological effects in response to IGF-I. Our data, therefore, further extend the molecular mechanisms by which IGF-I may affect tumor progression in mesothelioma and lung cancer, hence providing novel targets in the aforementioned aggressive malignancies.

## RESULTS

### IGF-I stimulates GPER expression through IGF-IR/ERK/p-38 transduction signaling

On the basis of previous studies showing that IGF-I triggers stimulatory effects in malignant mesothelioma as well as in lung cancer cells [31-32], we began our study evaluating the transduction signaling activated by IGF-I in IST-MES1 mesothelioma and A549 lung cancer cells, which were used as model system. First, we determined that in both cell types IGF-I induces the phosphorylation of IGF-IR (Figure 1A) and both ERK (Figure 1B) and p-38 (Figure 1C). As expected, these responses were no longer observed after IGF-IR silencing (Figure 1A-1E). The activation of ERK triggered by IGF-I was abolished in the presence of the IGF-IR inhibitor AG and the MEK inhibitor PD, but it still persisted using the p-38 inhibitor SB (Figure 1F). The phosphorylation of p-38 was prevented by AG and SB, but not in the presence of PD (Figure 1G). In addition, we assessed that the phosphorylation of IGF-IR induced by IGF-I is inhibited exclusively by AG, but not in the presence of PD and SB (data not shown), then suggesting that the activation of both ERK and p-38 relies directly on IGF-IR phosphorylation upon IGF-I exposure. On the basis of our previous data showing that IGF-I signaling cooperates with several GPCR family members, including GPER, toward cancer progression [19, 25], we evaluated whether IGF-I regulates GPER expression in IST-MES1 and A549 cells. In this regard, time-course experiments demonstrated that IGF-I up-regulates GPER at both mRNA (Figure 2A) and protein levels (Figure 2B). Moreover, we ascertained that these responses to IGF-I occurred through IGF-IR, as the induction of GPER mRNA (data not shown) and protein levels (Figure 2C-2E) was abolished by knocking-down IGF-IR expression. Recapitulating the aforementioned findings, the transactivation of the GPER promoter by IGF-I was prevented by IGF-IR silencing (Figure 2F), and the IGF-I induced GPER protein up-regulation was abrogated in the presence of AG, PD and SB (Figure 2G). Taken together, these results indicate that the IGF-I/IGF-IR transduction pathway stimulates GPER expression through ERK and p-38 signaling. In order to further investigate this functional cross-talk between IGF-IR and GPER, we performed co-immunoprecipitation studies determining that IGF-I triggers also a direct interaction between these receptors in both IST-MES1 and A549 cells upon either 1 h (data not shown) or 8 h treatment with IGF-I (Figure 2H-2I), thus suggesting that the interaction between IGF-IR and GPER may occur without a newly protein expression of GPER.

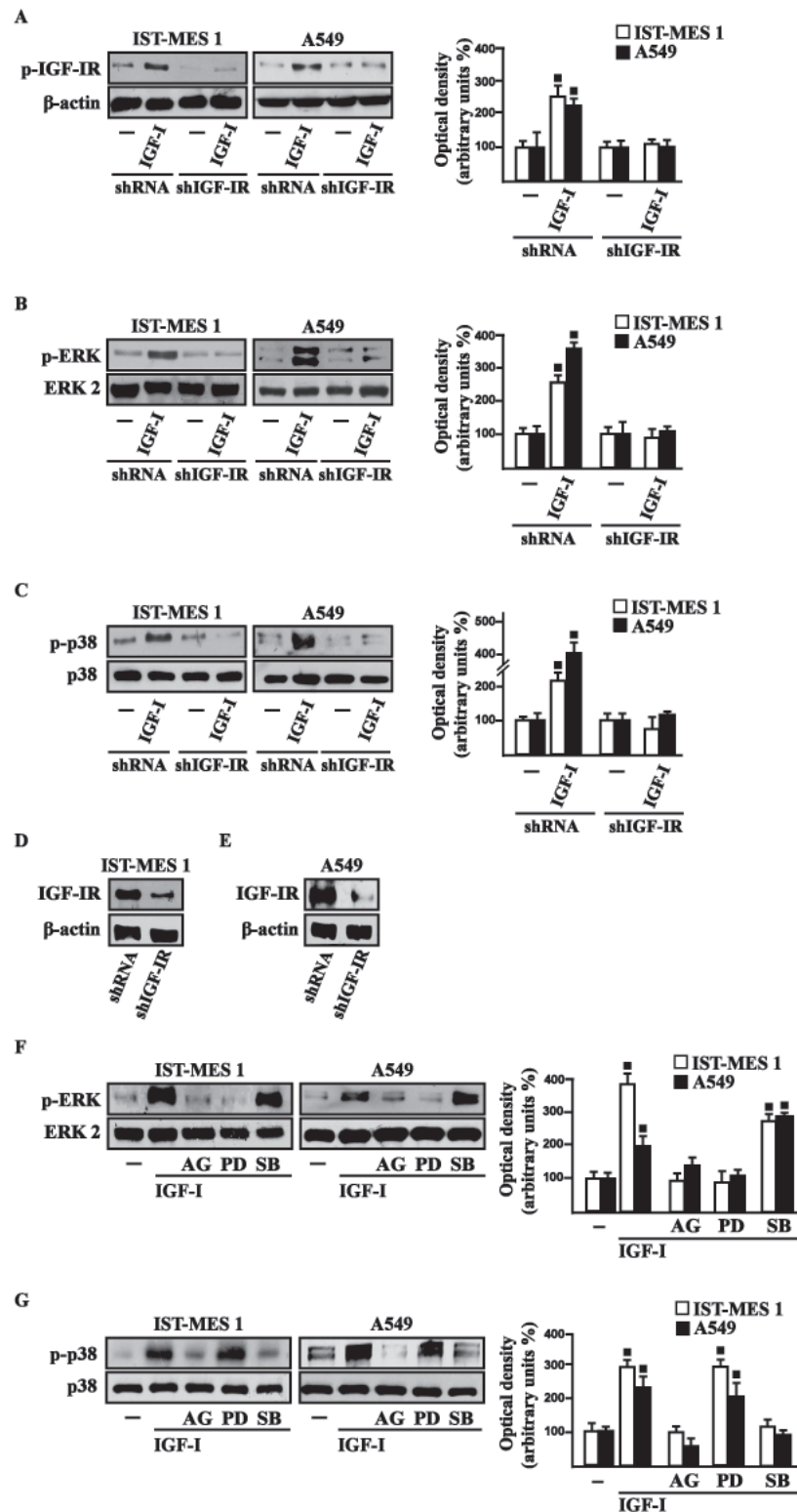


**Figure 1: Rapid activation of transduction signaling by IGF-I in IST-MES 1 and A549 cells.** IGF-IR **A.**, ERK **B.** and p-38 **C.** phosphorylation in cells transfected for 24 h with shRNA or shIGF-IR treated with vehicle (-) or 100 ng/ml IGF-I for 15 min. **D.-E.** Efficacy of IGF-IR silencing. ERK **F.** and p-38 **G.** activation in cells treated for 15 min with vehicle (-) or 100 ng/ml IGF-I alone and in combination with either 1  $\mu$ M IGF-IR inhibitor tyrphostin AG1024 (AG), or 1  $\mu$ M MEK inhibitor PD98059 (PD) or 1  $\mu$ M p38 inhibitor SB202190 (SB). Side panels show densitometric analysis of the blots normalized to  $\beta$ -actin, ERK2 and p38 that served as loading controls respectively for pIGF-IR, pERK and p-p38. Data shown are the mean  $\pm$  SD of three independent experiments. (■)  $p < 0.05$  for cells receiving vehicle (-) versus treatments.

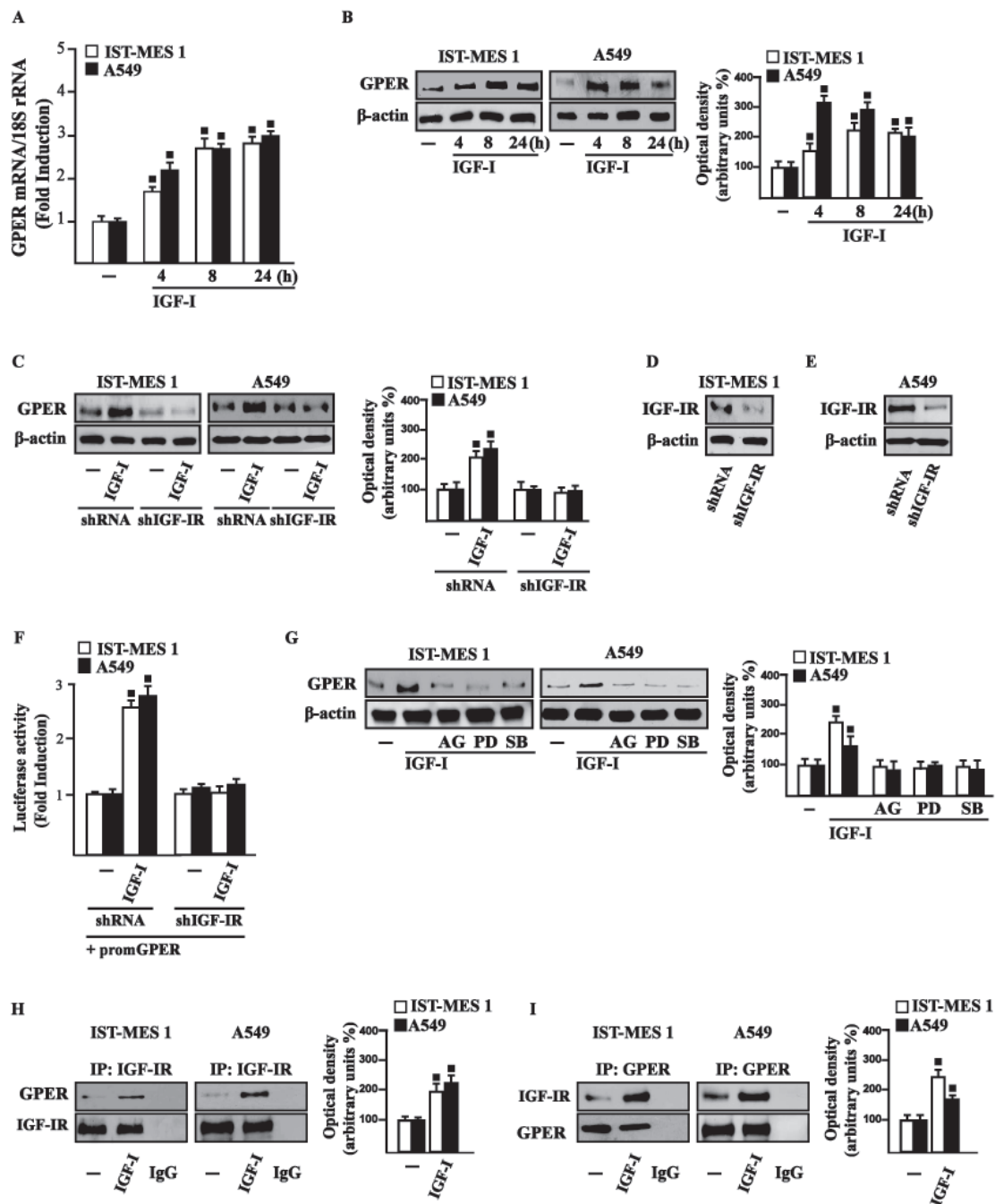


**Figure 2: IGF-I up-regulates GPER expression in IST-MES 1 and A549 cells.** **A.** mRNA expression of GPER in cells treated with either vehicle (-) or 100 ng/ml IGF-I, as evaluated by real-time PCR. Results obtained from experiments performed in triplicate were normalized for 18S expression and shown as fold change of RNA expression compared to cells treated with vehicle. **B.** GPER protein levels were evaluated by immunoblotting in cells treated with either vehicle (-) or 100 ng/ml IGF-I, as indicated. **C.** GPER protein expression in cells transfected for 24 h with either shRNA or shIGF-IR and then treated for 8 h with vehicle (-) or 100 ng/ml IGF-I. **D.-E.** Efficacy of IGF-IR silencing. **F.** Cells were transfected for 24 h with shRNA or shIGF-IR together with the GPER promoter construct. Then, cells were treated for 18 h with vehicle (-) or 100 ng/ml IGF-I. The luciferase activities were normalized to the internal transfection control, and values of cells receiving vehicle (-) were set as one fold induction upon which the activity induced by treatments was calculated. **G.** GPER protein levels in cells treated for 8 h with vehicle (-) or 100 ng/ml IGF-I alone or in combination with 1  $\mu$ M IGF-IR inhibitor tyrphostin AG1024 (AG), 1  $\mu$ M MEK inhibitor PD98059 (PD) and 1  $\mu$ M p38 inhibitor SB202190 (SB). Side panels show densitometric analysis of the blots normalized to  $\beta$ -actin. **H.-I.** Co-immunoprecipitation studies performed in cells treated for 8 h with vehicle (-) or 100 ng/ml IGF-I, as indicated. In control samples, non-specific IgG was used instead of the primary antibody. **H.** Side panel show densitometric analysis of the blot normalized to IGF-IR. **I.** Side panel show densitometric analysis of the blot normalized to GPER. Data shown are the mean  $\pm$  SD of three independent experiments. (■)  $p < 0.05$  for cells receiving vehicle (-) versus treatments.

## IGF-I triggers the expression of GPER target genes

In our previous study [33] we established that GPER mediates a specific gene signature, therefore, we evaluated

whether, in IST-MES1 and A549 cells, IGF-I is able to affect the expression of certain GPER target genes like CTGF and EGR1, which have been involved in fibrotic responses in mesothelioma and lung cancer cells [34-36]. Indeed, in time-course experiments we found that

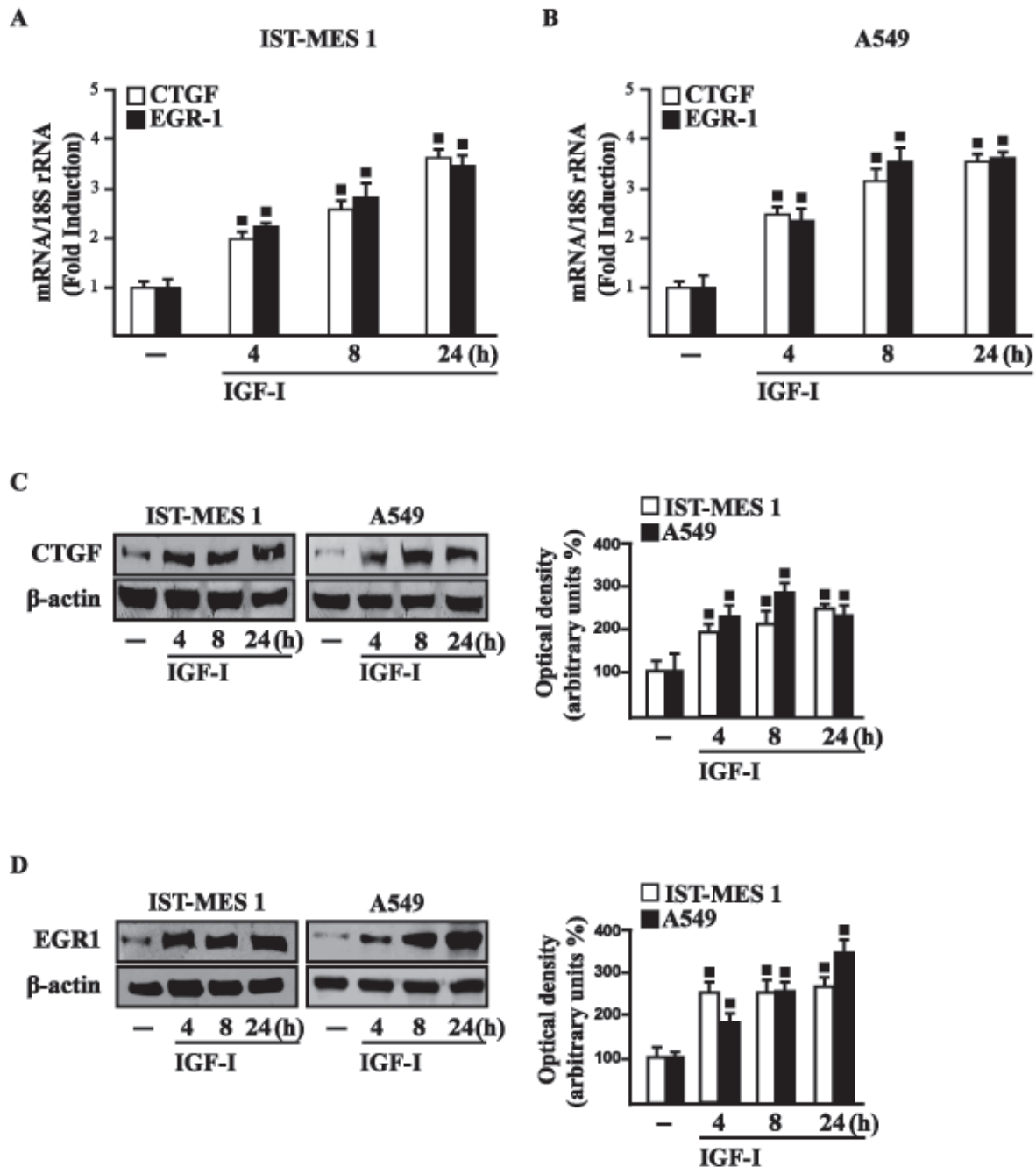


**Figure 3: IGF-I up-regulates CTGF and EGR1 expression in IST-MES 1 and A549 cells.** (A-B) mRNA expression of CTGF and EGR1 in cells treated with either vehicle (-) or 100 ng/ml IGF-I, as evaluated by real-time PCR. Results obtained from experiments performed in triplicate were normalized for 18S expression and shown as fold change of RNA expression compared to cells treated with vehicle. CTGF C. and EGR1 D. protein levels were evaluated by immunoblotting in cells treated with vehicle (-) or 100 ng/ml IGF-I, as indicated. Side panels show densitometric analysis of the blots normalized to  $\beta$ -actin and each data point represents the mean  $\pm$  SD of three independent experiments. (■)  $p < 0.05$  for cells receiving vehicle (-) versus treatments.

IGF-I increases the mRNA (Figure 3A-3B) and protein levels (Figure 3C-3D) of both CTGF and EGR1. Next, we determined that this action of IGF-I involves not only the IGF-IR but also GPER, as the silencing of each of these receptors prevented gene changes (Figure 4A-4H). In accordance with these observations, the IGF-I transactivation of CTGF (Figure 4I) and EGR1 (Figure 4J) promoters required both IGF-IR and GPER, as demonstrated by knocking down the expression of these receptors. As *c-fos* plays a main role in the up-regulation of GPER target genes [33, 37], we next determined that the promoter transactivation of both CTGF and EGR1 is abrogated by co-transfecting a dominant-negative form of *c-fos* (DN/*c-fos*) in IST-MES1 and A549 cells (Figure 4K). Collectively, these findings provide novel mechanisms through which IGF-I/IGF-IR transduction signaling regulates GPER target genes like CTGF and EGR1 in mesothelioma and lung cancer cells.

### **IGF-IR and GPER are both involved in IGF-I regulation of DDR1 target genes**

Considering that in diverse model systems IGF-I stimulates the synthesis of collagen [38-40], we next established that IGF-I regulates in both IST-MES1 and A549 cells the mRNA expression of COL1A1 (Figure 5A) that encodes the major component of type I collagen [41]. We previously reported that IGF-IR functionally interacts with DDR1, which is activated by various collagen types including type I collagen. Therefore, we first ascertained that, in both IST-MES1 and A549 cells, several DDR1 target genes such as matrilin-2 (MATN-2), fibrillin-1 (FBN-1), NOTCH 1 and HES-1, are induced by the DDR1 agonist COL1 (Figure 5B-5C) and abrogated by the DDR1 inhibitor (DDR1 IN) (Figure 5D-5E). Then, we assessed that these DDR1 target genes are also stimulated by IGF-I (Figure 6A-6B) and that this response was inhibited by DDR1 IN (Figure 6C-6D) as well as by silencing IGF-IR (Figure 6E-6F) or GPER (Figure 6G-6H). In accordance with these findings, we determined that the NOTCH 1 protein induction by COL1 and IGF-I is prevented in the presence of the DDR1 IN in IST-MES1 and A549 cells (Figure 7). Accordingly, IGF-I was not able to trigger NOTCH 1 protein expression when IGF-IR (Figure 8A-8C) or GPER (Figure 8D-8F) were silenced. Altogether, these results indicate that, in both mesothelioma and lung cancer cells, IGF-I may up-regulate DDR1 target genes, and this action involves not only IGF-IR but also a cross-talk with GPER.

### **DDR1, IGF-IR and GPER contribute to the chemotaxis and migration of mesothelioma and lung cancer cells**

Previous studies have reported that IGF-I stimulates chemotactic and chemokinetic motility in mesothelioma cells [32]. Moreover, DDR1 also plays an important role in promoting cell-cell interactions and cell migration in various cell contexts [42-45]. Further extending these data, in IST-MES1 cells, we found that both IGF-I and COL1 induce chemotactic motility, which requires DDR1, as these responses were abolished by DDR1 IN (Videos 1-6). Moreover, we ascertained that the chemotactic motility induced by IGF-I requires also IGF-IR and GPER as the aforementioned effect was prevented silencing the expression of these receptors (Videos 7-12). Similar findings occurred in A549 cells (data not shown). Likewise, we determined that IST-MES1 and A549 cell migration induced by both IGF-I and COL1 is abolished using DDR1 IN (Figure 9A), whereas the silencing of IGF-IR or GPER abolished cell migration triggered by IGF-I, as determined by Boyden chamber assay (Figure 9B). Collectively, our data indicate novel cross-talk and biological functions exerted by IGF-I toward tumor progression.

### **DISCUSSION**

In the present study we provide novel evidence regarding the molecular mechanisms by which IGF-I triggers biological responses in mesothelioma and lung cancer cells. In particular, we show a complex functional cooperation involving IGF-IR, GPER and DDR1 through which IGF-I up-regulates first the expression of COL1A1 and certain DDR1 target genes, thereafter stimulating cancer cell motility and chemotactic response (Figure 10).

Lung cancer is a highly heterogeneous tumor that can arise in different sites of the bronchial tree [1-2]. The incidence of lung cancer depends on toxic effects of inhaled substances such as tobacco, asbestos, arsenic, cadmium, nickel and silica [46]. The environmental pollutant asbestos is also considered the main cause of the insurgence of malignant mesothelioma (MM), which is a rare and aggressive tumor that springs from mesothelial cells lining lung, pleura or peritoneum [5-7, 47-48]. The deposition of asbestos fibers has been also related to chronic inflammatory processes as well as to pulmonary fibrosis, which in turn may create a favorable environment for the development of lung and pleura malignancies [6, 49]. As it concerns the multifaceted mechanisms and factors involved in pulmonary fibrosis and neoplasia, an increased expression and activation of DDR1 have been reported [50-53]. To date, DDR1 has been shown to play an important role in cancer progression by regulating the interactions of tumor cells with the surrounding

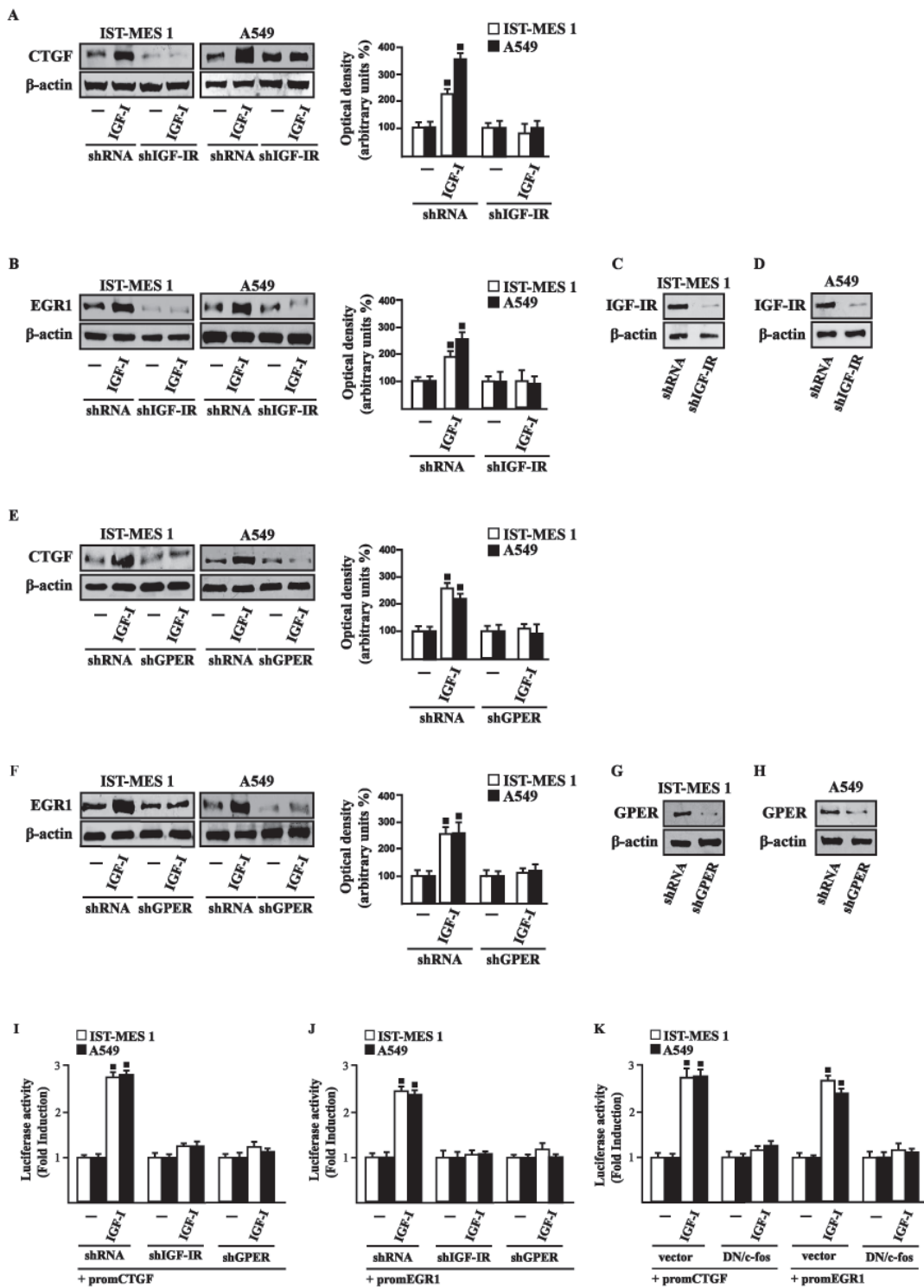


**Figure 4: IGF-IR and GPER mediate CTGF and EGR1 stimulation by IGF-I in IST-MES 1 and A549 cells. A-F.** CTGF and EGR1 protein levels in cells transfected for 24 h with shRNA, shIGF-IR or shGPER and then treated for 8 h with either vehicle (-) or 100 ng/ml IGF-I. Efficacy of IGF-IR C.-D. and GPER G.-H. silencing. Side panels show densitometric analysis of the blots normalized to  $\beta$ -actin. **I.-J.** Cells were transfected for 24 h with shRNA, shIGF-IR or shGPER together with the CTGF or EGR1 promoter construct. Then, cells were treated for 18 h with vehicle (-) or 100 ng/ml IGF-I. **K.** Cells were transfected for 24 h with a dominant negative form of c-fos (DN/c-fos) together with the CTGF or EGR1 promoter construct. Then, cells were treated for 18 h with vehicle (-) or 100 ng/ml IGF-I. The luciferase activities were normalized to the internal transfection control, and values of cells receiving vehicle (-) were set as one fold induction upon which the activity induced by treatments was calculated. Data shown are the mean  $\pm$  SD of three independent experiments. (■)  $p < 0.05$  for cells receiving vehicle (-) versus treatments.

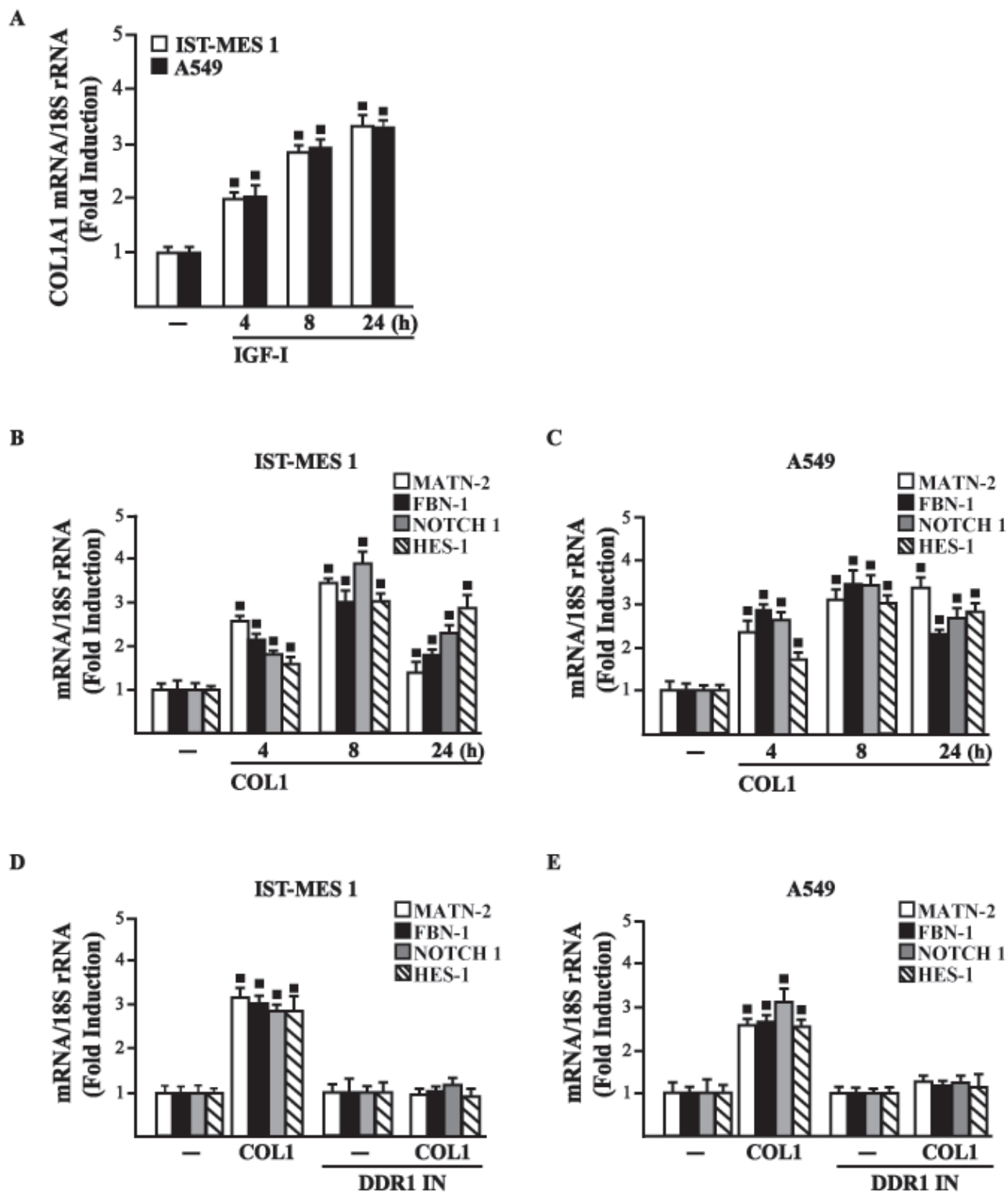


**Figure 5:** A. mRNA expression of COL1A1 in IST-MES 1 and A549 cells treated with vehicle (-) or 100 ng/ml IGF-I, as evaluated by real-time PCR. mRNA expression of MATN-2, FBN-1, NOTCH 1 and HES-1 in IST-MES 1 B., D. and A549 C., E. cells treated with vehicle (-) or 10  $\mu$ g/ml COL1 alone or in combination with 1  $\mu$ M DDR1 inhibitor (DDR1 IN), as indicated. Results obtained from experiments performed in triplicate were normalized for 18S expression and shown as fold change of RNA expression compared to cells treated with vehicle. (■)  $p < 0.05$  for cells receiving vehicle (-) versus treatments.

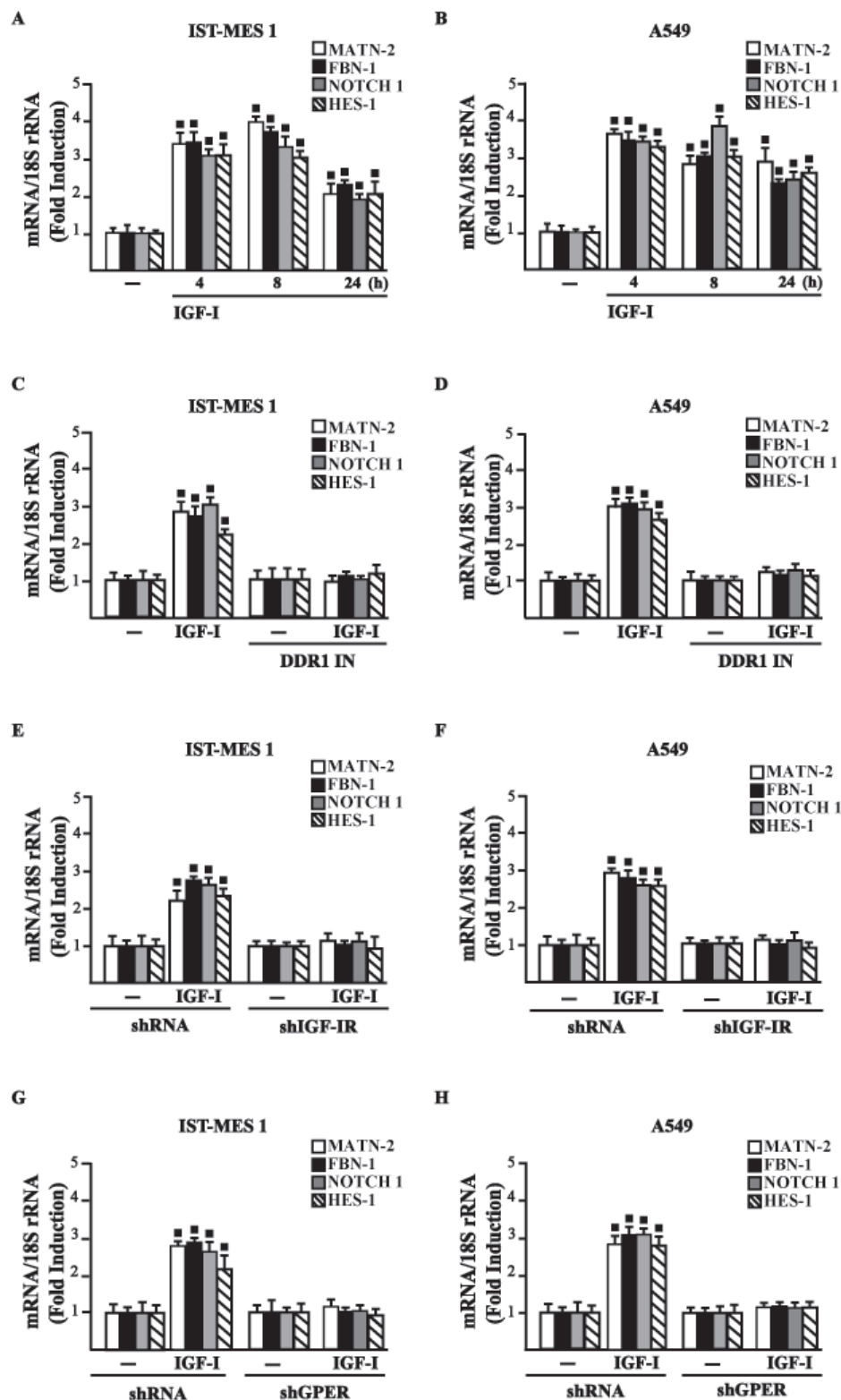


**Figure 6: IGF-IR and GPER mediate the IGF-I induced up-regulation of COL1A1/DDR1 target genes in IST-MES 1 and A549 cells.** A.-D. mRNA expression of MATN-2, FBN-1, NOTCH 1 and HES-1 in cells treated with vehicle (-) or 100 ng/ml IGF-I alone or in combination with 1  $\mu$ M DDR1 inhibitor (DDR1 IN), as indicated. E.-H. mRNA expression of MATN-2, FBN-1, NOTCH 1 and HES-1 in cells transfected for 24 h with shRNA, shIGF-IR or shGPER and then treated for 8 h with vehicle (-) or 100 ng/ml IGF-I. Results obtained from experiments performed in triplicate were normalized for 18S expression and shown as fold change of RNA expression compared to cells treated with vehicle. (■)  $p < 0.05$  for cells receiving vehicle (-) versus treatments.

collagen matrix, therefore leading to pro-migratory and pro-invasive responses [21]. Furthermore, collagen activated DDR1 triggers diverse pro-survival pathways toward anti-apoptotic, proliferative and aggressive features in cancer cells [21]. In this regard, it should be noted that several types of collagen are able to bind to and activate DDR1, which then regulates cell and tissue homeostasis acting as a collagen sensor [21, 54]. Of note, an abnormal expression and deposition of collagen has been associated with cancer development [55-56]. As it concerns the synthesis and extracellular accumulation of diverse types of collagen, cytokines and growth factors like IGF-I, the epidermal growth factor (EGF) and the transforming growth factor- $\beta$ 1 have been reported to promote these effects [38-40, 57]. Notably, we previously showed that, in breast cancer cells, IGF-I may upregulate DDR1 expression through a signaling pathway involving the DDR1 regulatory miR-199a-5p [12]. Moreover, the activation of one of the main IGF-I transduction signaling, the IGF-IR/PI3K/Akt cascade, inhibits miR-199a-5p expression, thus relieving its inhibition upon DDR1 gene and allowing DDR1 upregulation. In turn, DDR1 increases IGF-IR expression through post-transcriptional mechanisms and amplifies IGF-I downstream signaling and biological effects, such as proliferation, migration and colony formation [12]. Indeed, we previously showed that DDR1 directly interacts with IGF-IR, and that this interaction is enhanced by IGF-I stimulation, which promotes rapid DDR1 tyrosine-phosphorylation and co-internalization of the DDR1 - IGF-IR complex [22]. This interaction was shown to occur in a panel of human breast cancer cells as well as in mouse fibroblasts (R- cells) co-transfected with the human IGF-IR and DDR1, indicating that it is not cell-specific. Notably, the formation of this DDR1 - IGF-IR complex did not require the presence of collagen, the canonical DDR1 ligand. In addition, the critical role of IGF-IR in DDR1 activation and biological actions is supported by the finding that collagen-dependent DDR1 phosphorylation was impaired in the absence of IGF-IR [22].

Extending these previous studies, we now show that IGF-I through the cognate receptor IGF-IR is able to induce COL1A1 expression [54]. Moreover, a panel of DDR1 target genes could be also induced by IGF-I through the previously described functional cross-talk involving IGF-IR and DDR1. Taken together, these findings show that DDR1, besides enhancing the activation of typical IGF-IR downstream cascades, the PI3K/Akt and the ERK1/2 cascades, following cell exposure to IGF-I, modifies significantly these IGF-I effects by allowing the induction of typical DDR1 target genes. These effects confirm the relevance of DDR1 in the amplification and diversification of IGF-I signaling pathways in cancer. We have previously demonstrated that IGF-IR may also functionally interact with the non-canonical estrogen receptor GPER. Indeed, through the

IGF-IR/PKC $\delta$ /ERK/c-fos/AP1 transduction pathway, IGF-I up-regulates GPER, which plays an important role in sustaining proliferation and migration in response to IGF-I in breast and endometrial human cancer cells [25]. In close accordance with these findings, we now show that the functional cooperation between IGF-IR and DDR1 also requires GPER, and that both DDR1 and GPER are critical to the chemotactic motility stimulated by IGF-I in mesothelioma and lung cancer cells. Notably, we now show that GPER and IGF-IR co-immunoprecipitate in lung and mesothelioma cells (Figure 2), indicating that GPER and IGF-IR also interact. Taken together all these data strongly suggest the possible formation of a ternary functional complex involving IGF-IR - DDR1 - GPER. However, further studies are needed to fully elucidate this aspect. These data may be of a particular interest as GPER expression has been associated with negative clinical features and poor survival rates in diverse types of malignancies [58-61]. In the last years, extensive studies were therefore performed in order to better characterize the role of GPER in cancer development, including the mechanisms and factors involved in its expression. For instance, we determined that EGF and IGF-I, insulin and further tumorigenic factors like hypoxia and endothelin-1 up-regulate GPER expression in diverse cancer cell contexts [25, 62-68].

Our present findings provide significant new insights on the well-established role played by the IGF axis in cancer [9-11, 14-16, 20, 23, 69-71] that involves also the interaction of IGF-IR with other RTKs and GPCRs in diverse tumor histotypes [19, 23, 72-73]. In particular, our findings might be relevant in devising new therapeutical strategies in cancers with a dysregulated IGF system. In the last decade, much effort has been made in targeting the IGF-IR in these malignancies [74]. In particular, both small-molecule IGF-IR tyrosine kinase inhibitors, and humanized monoclonal antibodies with blocking activity to the IGF-IR, have been investigated in Phase III trials of advanced non-small cell lung cancers [13]. Unfortunately, in spite of very promising preclinical studies, clinical trials have clearly indicated that only a small minority of malignancies do respond to target therapies when IGF-IR is the sole target [75], because the frequent occurrence of resistance mechanisms arising by the complex signaling network involving the IGF-IR [76].

Overall, on the basis of our data the multifaceted signaling network between IGF-IR, GPER and DDR1 could be taken into account in setting innovative combined strategies targeting these pathways in mesothelioma and lung cancers.

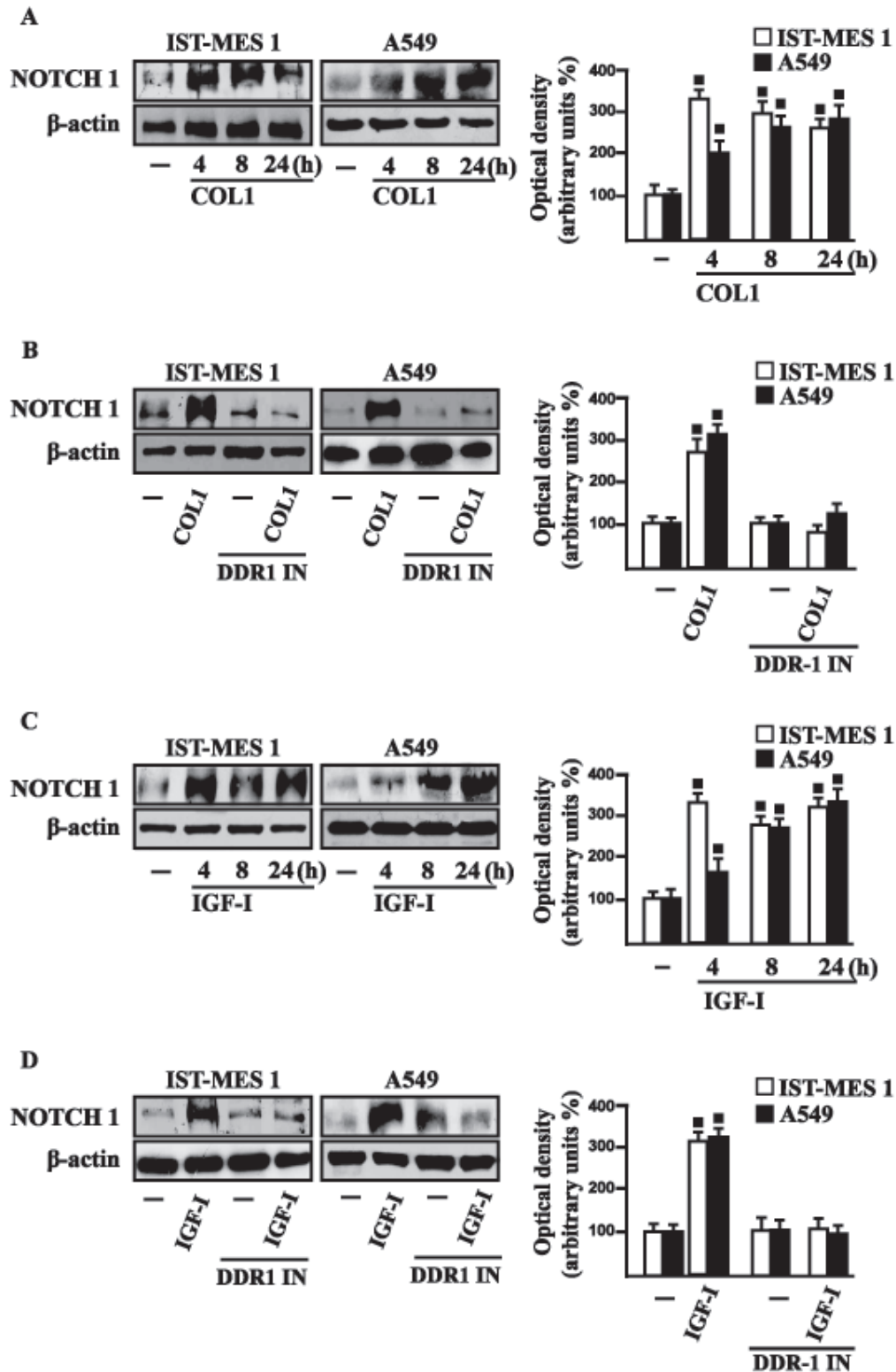


**Figure 7: COL1 and IGF-I stimulate NOTCH 1 expression through DDR1 in IST-MES 1 and A549 cells.** A. NOTCH 1 protein levels in cells treated with vehicle (-) or 10 µg/ml COL1, as indicated. B. NOTCH 1 protein levels in cells treated for 8 h with vehicle (-) or 10 µg/ml COL1 alone and in combination with 1 µM DDR1 inhibitor (DDR1 IN). C. NOTCH 1 protein levels in cells treated with vehicle (-) or 100 ng/ml IGF-I, as indicated. D. NOTCH 1 protein levels in cells treated for 8 h with vehicle (-) or 100 ng/ml IGF-I alone and in combination with 1 µM DDR1 inhibitor (DDR1 IN). Side panels show densitometric analysis of the blots normalized to β-actin and each data point represents the mean ± SD of three independent experiments. (■)  $p < 0.05$  for cells receiving vehicle (-) versus treatments.

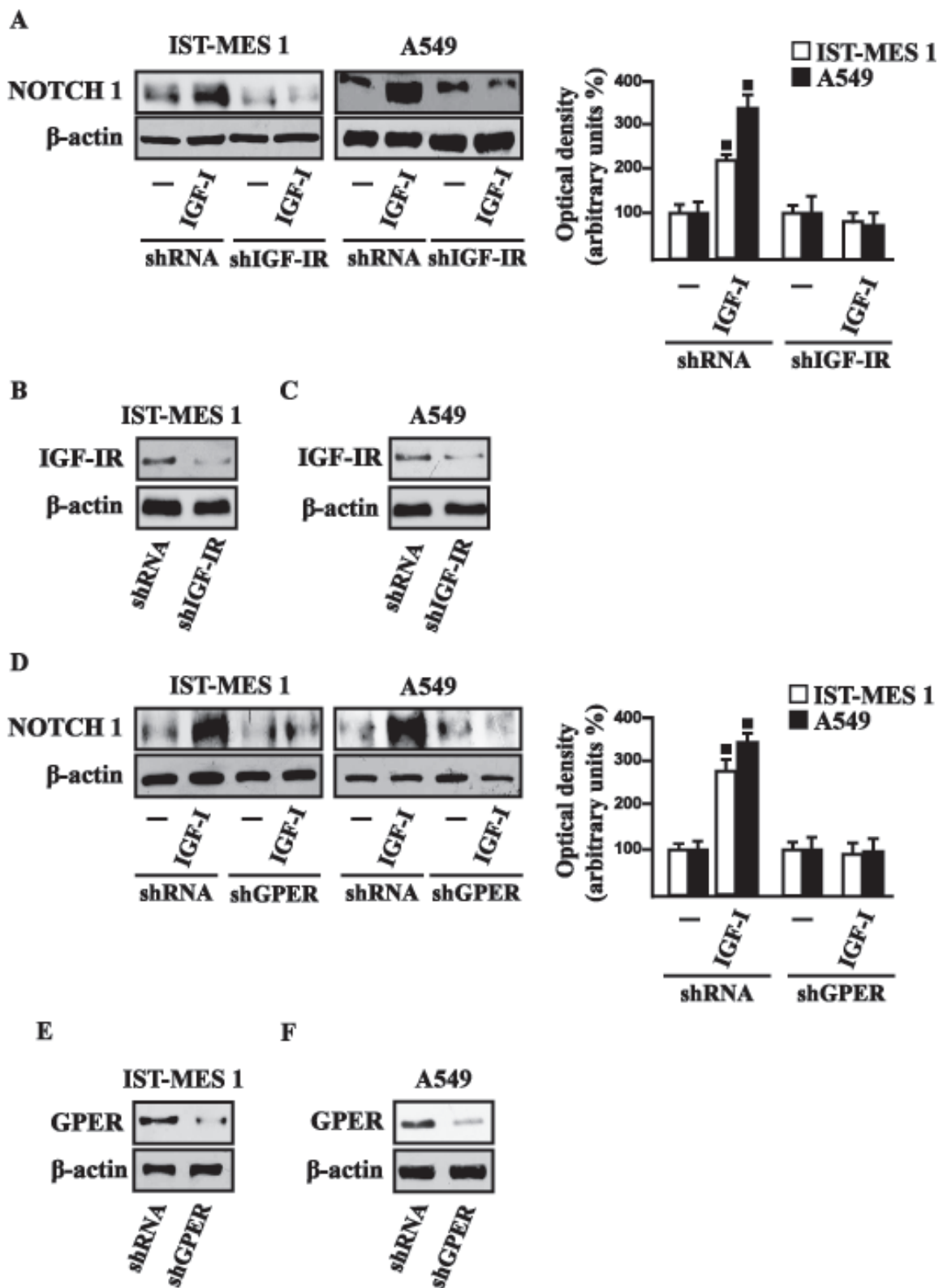


**Figure 8: IGF-IR and GPER mediate the IGF-I induced up-regulation of NOTCH 1 in IST-MES 1 and A549 cells.** NOTCH 1 protein levels in cells transfected for 24 h with shIGF-IR **A**. or shGPER **D**. and then treated for 8 h with vehicle (-) or 100 ng/ml IGF-I. Efficacy of IGF-IR **B**.-**C**. and GPER **E**.-**F**. silencing. Side panels show densitometric analysis of the blots normalized to  $\beta$ -actin. (■)  $p < 0.05$  for cells receiving vehicle (-) versus treatments.

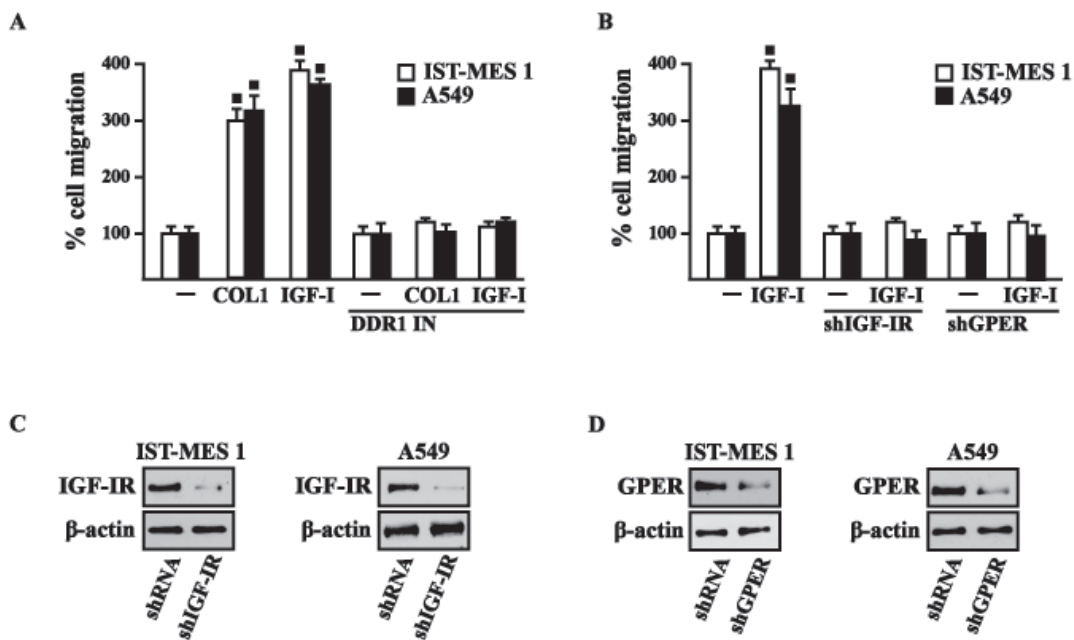


**Figure 9: COL1 and IGF-I stimulate IST-MES 1 and A549 cell migration through DDR1, IGF-IR and GPER.** A. The migration of IST-MES 1 and A549 cells upon 8 h treatment with vehicle (-), 10  $\mu\text{g/ml}$  COL1 or 100 ng/ml IGF-I alone and in combination with 1  $\mu\text{M}$  DDR1 inhibitor (DDR1 IN), as evaluated by Boyden Chamber assay. B. The migration of IST-MES 1 and A549 cells induced by 8 h treatment with 100 ng/ml IGF-I was prevented knocking down IGF-IR and GPER expression, as evaluated by Boyden Chamber assay. Efficacy of IGF-IR C.-D. and GPER E.-F. silencing. Values represent the mean  $\pm$  SD of three independent experiments. (•) indicates  $p < 0.05$  for cells treated with vehicle (-) versus treatments.

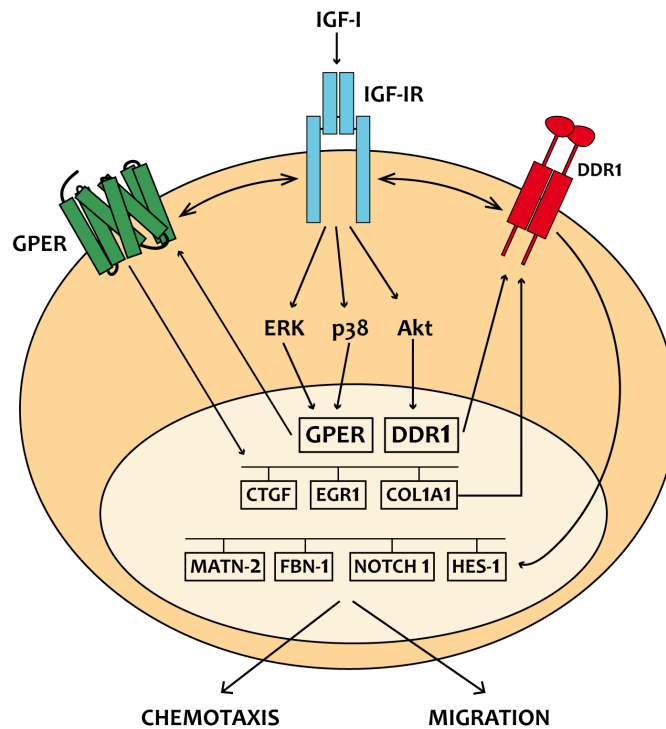


**Figure 10: Schematic representation of the signaling network between IGF-IR, GPER and DDR1 activated by IGF-I.** IGF-I stimulates the expression of GPER and its target genes, then IGF-IR and GPER trigger the IGF-I regulation of DDR1 target genes. The functional cross-talk of IGF-IR, GPER and DDR1 contributes to the chemotaxis and migration observed in cancer cells.

## MATERIALS AND METHODS

### Reagents

IGF-I, SB202190 (SB) and collagen I from rat tail were obtained from Sigma-Aldrich Inc. (Milan, Italy). PD98059 (PD) and 3-bromo-5-t-butyl-4-hydroxybenzylidenemalonitrile (AG1024) were purchased from Calbiochem (DBA, Milan, Italy). All compounds were solubilized in dimethylsulfoxide, except PD and IGF-I, which were dissolved in ethanol and in water, respectively. DDR1IN1 dihydrochloride (DDR-1 in) was purchased from Tocris Bioscience (Space, Milan, Italy).

### Cell cultures

IST-MES1 malignant mesothelioma cells were kindly provided by Dr. Orengo (Istituto Nazionale per la Ricerca sul Cancro, Genova, Italy). Cells were previously characterized [77] and were grown in Nutrient Mixture F-10 Ham (Ham's F-10) medium supplemented with 10% fetal bovine serum (FBS) and 100 µg/ml penicillin/streptomycin. A549 lung cancer cells were obtained by ATCC, used < 6 months after resuscitation and maintained in DMEM/F12 (Dulbecco's modified Eagle's medium) supplemented with phenol red 10% FBS and 100 µg/ml penicillin/streptomycin. All cell lines were cultured at 37°C in 5% CO<sub>2</sub> and switched to medium without serum the day before immunoblots and reverse transcription-PCR experiments.

### Plasmids and luciferase assays

The GPER luciferase expression vector (promGPER) was previously described [65]. The CTGF luciferase reporter plasmid (promCTGF) (-1999/+ 36)-luc was a gift from Dr. Chaqour. EGR1-luc plasmid, containing the -600 to +12 5'-flanking sequence from the human EGR1 gene, was kindly provided by Dr. Safe (Texas A&M University). The plasmid DN/cfos, which encodes a c-fos mutant that heterodimerizes with c-fos dimerization partners but does not allow DNA binding [78], was a kind gift from Dr C Vinson (NIH, Bethesda, MD, USA). The Renilla luciferase expression vector pRL-TK (Promega, Milan, Italy) was used as internal transfection control. Cells (1×10<sup>5</sup>) were plated into 24-well dishes with 500 µl/well culture medium containing 10% FBS. Transfection were performed using X-treme GENE 9 DNA transfection reagent as recommended by the manufacturer (Roche Diagnostics, Milan, Italy), with a mixture containing 0.5 µg of reporter plasmid and 10 ng of pRL-TK. After 24 h, treatments were added and cells were incubated for 18 h. Luciferase activity was measured using

the Dual Luciferase Kit (Promega, Milan, Italy) according to the manufacturer's recommendations. Firefly luciferase activity was normalized to the internal transfection control provided by the Renilla luciferase activity. Normalized relative light unit values obtained from cells treated with vehicle were set as 1-fold induction upon which the activity induced by treatments was calculated.

### Gene silencing experiments

Cells were plated onto 10-cm dishes and transfected by X-treme GENE 9 DNA Transfection Reagent for 24 h before treatments with a control vector, a specific shRNA sequence for each target gene. The shIGF-IR and the respective control plasmids (shRNA) were purchased from SA Bioscience Corp. (Frederick, MD, USA) and used according to the manufacturer's recommendations. The short hairpin (sh)RNA constructs to knock down the expression of GPER and the unrelated shRNA control construct have been described previously [64].

### Gene expression studies

Total RNA was extracted and cDNA was synthesized by reverse transcription as previously described [79-80]. The expression of selected genes was quantified by real-time PCR using Step One sequence detection system (Applied Biosystems, Milan, Italy). Gene-specific primers were designed using Primer Express version 2.0 software (Applied Biosystems Inc. Milan, Italy) and are as follows: GPER Fwd 5'-ACACACCTGGGTGGACACAA-3' and Rev 5'-GGAGCCAGAAGCCACATCTG-3'; HES-1 Fwd 5'-TCAACACGACACCCGATAAA-3' and Rev 5'-CCGCGAGCTATCTTTCTTCA-3'; NOTCH 1 Fwd 5'-AATGGCGGGAAGTGTGAAGC-3' and Rev 5'-GCATAGTCTGCCACGCCTCT-3'; MTN-2 Fwd 5'-CTCCGAGTGGGCCAGTAAAG-3' and Rev 5'-CTGGCTCAGATTCTGTTGGCT-3'; FBN-1 Fwd 5'-GCCGCATATCTCCTGACCTC-3' and Rev 5'-GTCGATACACGCGGAGATGT-3'; 18S Fwd 5'-GGCGTCCCCCAACTTCTTA-3' and Rev 5'-GGGCATCACAGACCTGTTATT-3'. Assays were performed in triplicate and the results were normalized for 18S expression and then calculated as fold induction of RNA expression.

### Western blot analysis

Cells were processed according to a previously described protocol [81] to obtain protein lysate that was electrophoresed through a reducing SDS/10% (w/v) polyacrylamide gel, electroblotted onto a nitrocellulose membrane and probed with primary antibodies against antiphosphotyrosine antibody (4G10) (Merck Millipore,

Milan, Italy), IGF-IR (7G11), GPER (N-15), CTGF (L-20), phosphorylated ERK1/2 (E-4), ERK2 (C-14), NOTCH 1 (C-20), EGR1 (588), phosphorylated p-38 (D-8), p-38 (A-12),  $\beta$ -actin (C2), (Santa Cruz Biotechnology, DBA, Milan, Italy). Proteins were detected by horseradish peroxidase-linked secondary antibodies (DBA, Milan, Italy) and revealed using the ECL System (GE Healthcare).

### Co-immunoprecipitation

Cells were lysed using 200  $\mu$ l RIPA buffer with a mixture of protease inhibitors containing 1.7mg/ml aprotinin, 1mg/ml leupeptin, 200mmol/L phenylmethylsulfonyl fluoride, 200mmol/L sodium orthovanadate, and 100mmol/L sodium fluoride. A total of 100  $\mu$ g proteins were incubated for 2 h with 2  $\mu$ g of the appropriate antibody (GPER, N-15; IGF-1R, 7G11) and 20  $\mu$ l of protein A/G agarose immunoprecipitation reagent (Santa Cruz Biotechnology, DBA, Milan, Italy). Samples were centrifuged at 13,000 rpm for 5 min at 4°C to pellet beads. After four washes in PBS, samples were resuspended in RIPA buffer with protease inhibitors and SDS sample buffer. Western Blot analysis was performed as described above.

### Migration assay

Migration assays were performed using Boyden chambers (Costar Transwell, 8 mm polycarbonate membrane, Sigma Aldrich, Milan, Italy). Cells were transfected in regular growth medium. After 8 h, cells were trypsinized and seeded in the upper chambers. Treatments were added to the medium without serum in the bottom wells where applicable, cells on the bottom side of the membrane were fixed and counted 8 hours after seeding.

### Time-lapse microscopy

Cells ( $1 \times 10^5$ ) were seeded in 6-well plates and maintained in regular growth medium for 24 h. For knockdown experiments, cells were transfected for 24 h with shRNA constructs directed against IGF-IR or GPER and with an unrelated shRNA construct. Thereafter, cells were treated and transferred into a time-lapse microscopy platform, equipped with a heated stage chamber (Cytation™3 Cell Imaging Multi-Mode Reader, Biotek, Winooski, VT). Cells were maintained at routine incubation settings (37 °C, 5% CO<sub>2</sub>) using temperature and gas controllers. To evaluate chemotaxis the images were recorded using Cytation 3 Cell Imaging Multimode Reader and the software Gen5 (BioTek, Winooski, VT) in 10 min intervals for 8 hours. Then, the images were processed as a movie using the software Adobe Creative Cloud Premier Pro CC. Frames collected every 10 minutes

are displayed at a rate of 10 frames s<sup>-1</sup>.

### Statistical analysis

Statistical analysis was performed using ANOVA followed by Newman-Keuls' testing to determine differences in means.  $P < 0.05$  was considered as statistically significant.

### GRANT SUPPORT

This work was supported by Associazione Italiana per la Ricerca sul Cancro (MM: IG 16719/2015; AB: IG 14066/2013), Ministero della Salute (grant n. 67/GR-2010-2319511); SA was supported by Fellowships INAIL-Regione Calabria; EMDF was supported by an iCARE fellowship from the Associazione Italiana per la Ricerca sul Cancro (AIRC) cofunded by Marie Curie Actions.

### CONFLICTS OF INTEREST

The authors declare no conflict of interest.

### REFERENCES

1. Travis WD, Brambilla E, Noguchi M, Nicholson AG, Geisinger K, Yatabe Y, Powell CA, Beer D, Riely G, Garg K, Austin JH, Rusch VW, Hirsch FR et al. International Association for the Study of Lung Cancer/American Thoracic Society/European Respiratory Society: international multidisciplinary classification of lung adenocarcinoma: executive summary. *Proc Am Thorac Soc.* 2011; 8: 381-5.
2. Guo L, Zhang T, Xiong Y, Yang Y. Roles of NOTCH1 as a Therapeutic Target and a Biomarker for Lung Cancer: Controversies and Perspectives. *Dis Markers.* 2015; 2015: 520590.
3. Abdel-Rahman O. Targeting the MEK signaling pathway in non-small cell lung cancer (NSCLC) patients with RAS aberrations. *Ther Adv Respir Dis.* 2016.
4. Silvestri GA, Gonzalez AV, Jantz MA, Margolis ML, Gould MK, Tanoue LT, Harris LJ, Detterbeck FC. Methods for staging non-small cell lung cancer: Diagnosis and management of lung cancer, 3rd ed: American College of Chest Physicians evidence-based clinical practice guidelines. *Chest.* 2013; 143: e211S-50S.
5. Rajer M, Zwitter M, Rajer B. Pollution in the working place and social status: co-factors in lung cancer carcinogenesis. *Lung Cancer.* 2014; 85: 346-50.
6. Carbone M, Ly BH, Dodson RF, Pagano I, Morris PT, Dogan UA, Gazdar AF, Pass HI, Yang H. Malignant mesothelioma: facts, myths, and hypotheses. *J Cell Physiol.* 2012; 227: 44-58.

7. Rascoe PA, Jupiter D, Cao X, Littlejohn JE, Smythe WR. Molecular pathogenesis of malignant mesothelioma. *Expert Rev Mol Med*. 2012; 14: e12.
8. Valavanidis A, Vlachogianni T, Fiotakis K, Loridas S. Pulmonary oxidative stress, inflammation and cancer: respirable particulate matter, fibrous dusts and ozone as major causes of lung carcinogenesis through reactive oxygen species mechanisms. *Int J Environ Res Public Health*. 2013; 10: 3886-907.
9. Belfiore A, Frasca F, Pandini G, Sciacca L, Vigneri R. Insulin receptor isoforms and insulin receptor/insulin-like growth factor receptor hybrids in physiology and disease. *Endocr Rev*. 2009; 30: 586-623.
10. Belfiore A, Malaguarnera R. Insulin receptor and cancer. *Endocr Relat Cancer*. 2011; 18: R125-47.
11. Kai K, D'Costa S, Sills RC, Kim Y. Inhibition of the insulin-like growth factor 1 receptor pathway enhances the antitumor effect of cisplatin in human malignant mesothelioma cell lines. *Cancer Lett*. 2009; 278: 49-55.
12. Matà R, Palladino C, Nicolosi ML, Lo Presti AR, Malaguarnera R, Ragusa M, Sciortino D, Morrione A, Maggiolini M, Vella V, Belfiore A. IGF-I induces upregulation of DDR1 collagen receptor in breast cancer cells by suppressing MIR-199a-5p through the PI3K/AKT pathway. *Oncotarget*. 2016; 7: 7683-700. doi: 10.18632/oncotarget.6524.
13. Scagliotti GV and Novello S. The role of the insulin-like growth factor signaling pathway in non-small cell lung cancer and other solid tumors. *Cancer Treat Rev*. 2012; 38: 292-302.
14. Carboni JM, Lee AV, Hadsell DL, Rowley BR, Lee FY, Bol DK, Camuso AE, Gottardis M, Greer AF, Ho CP, Hurlburt W, Li A, Saulnier M, et al. Tumor development by transgenic expression of a constitutively active insulin-like growth factor I receptor. *Cancer Res*. 2005; 65: 3781-7.
15. Franks SE, Briah R, Jones RA, Moorehead RA. Unique roles of Akt1 and Akt2 in IGF-IR mediated lung tumorigenesis. *Oncotarget*. 2016; 7: 3297-316. doi: 10.18632/oncotarget.6489.
16. Hoang CD, Zhang X, Scott PD, Guillaume TJ, Maddaus MA, Yee D, Kratzke RA. Selective activation of insulin receptor substrate-1 and -2 in pleural mesothelioma cells: association with distinct malignant phenotypes. *Cancer Res*. 2004; 64: 7479-85.
17. Lee H, Kim SR, Oh Y, Cho SH, Schleimer RP, Lee YC. Targeting insulin-like growth factor-I and insulin-like growth factor-binding protein-3 signaling pathways. A novel therapeutic approach for asthma. *Am J Respir Cell Mol Biol*. 2014; 50: 667-77.
18. Hung CF, Rohani MG, Lee SS, Chen P, Schnapp LM. Role of IGF-1 pathway in lung fibroblast activation. *Respir Res*. 2013; 14: 102.
19. Lappano R and Maggiolini M. G protein-coupled receptors: novel targets for drug discovery in cancer. *Nat Rev Drug Discov*. 2011; 10: 47-60.
20. Liu C, Zhang Z, Tang H, Jiang Z, You L, Liao Y1. Crosstalk between IGF-1R and other tumor promoting pathways. *Curr Pharm Des*. 2014; 20: 2912-21.
21. Valiathan RR, Marco M, Leitinger B, Kleer CG, Fridman R. Discoidin domain receptor tyrosine kinases: new players in cancer progression. *Cancer Metastasis Rev*. 2012; 31: 295-321.
22. Malaguarnera R, Nicolosi ML, Sacco A, Morcavallo A, Vella V, Voci C, Spatuzza M, Xu SQ, Iozzo RV, Vigneri R, Morrione A, Belfiore A. Novel cross talk between IGF-IR and DDR1 regulates IGF-IR trafficking, signaling and biological responses. *Oncotarget*. 2015; 6: 16084-105. doi: 10.18632/oncotarget.3177.
23. Rozengurt E, Sinnott-Smith J, Kisfalvi K. Crosstalk between insulin/insulin-like growth factor-1 receptors and G protein-coupled receptor signaling systems: a novel target for the antidiabetic drug metformin in pancreatic cancer. *Clin Cancer Res*. 2010; 16: 2505-11.
24. Liu C, Liao Y, Fan S, Tang H, Jiang Z, Zhou B, Xiong J, Zhou S, Zou M, Wang J. G protein-coupled estrogen receptor (GPER) mediates NSCLC progression induced by 17 $\beta$ -estradiol (E2) and selective agonist G1. *Med Oncol*. 2015; 32: 104.
25. De Marco P, Bartella V, Vivacqua A, Lappano R, Santolla MF, Morcavallo A, Pezzi V, Belfiore A, Maggiolini M. Insulin-like growth factor-I regulates GPER expression and function in cancer cells. *Oncogene*. 2013; 32: 678-88.
26. De Marco P, Cirillo F, Vivacqua A, Malaguarnera R, Belfiore A, Maggiolini M. Novel Aspects Concerning the Functional Cross-Talk between the Insulin/IGF-I System and Estrogen Signaling in Cancer Cells. *Front Endocrinol (Lausanne)*. 2015; 6: 30.
27. Jala VR, Radde BN, Haribabu B, Klinge CM. Enhanced expression of G-protein coupled estrogen receptor (GPER/GPR30) in lung cancer. *BMC Cancer*. 2012; 12: 624.
28. Siegfried JM, Hershberger PA, Stabile LP. Estrogen receptor signaling in lung cancer. *Semin Oncol*. 2009; 36: 524-31.
29. Pinton G, Brunelli E, Murer B, Puntoni R, Puntoni M, Fennell DA, Gaudino G, Mutti L, Moro L. Estrogen receptor-beta affects the prognosis of human malignant mesothelioma. *Cancer Res*. 2009; 69: 4598-604.
30. Pillai K, Pourgholami MH, Chua TC, Morris DL. Oestrogen receptors are prognostic factors in malignant peritoneal mesothelioma. *J Cancer Res Clin Oncol*. 2013; 139: 987-94.
31. Kim, JS, Kim, ES, Liu, D, Lee, JJ, Solis, L, Behrens, C, Lippman, SM, Hong, WK, Wistuba, II, Lee, HY. Prognostic implications of tumoral expression of insulin like growth factors 1 and 2 in patients with non-small-cell lung cancer. *Clinical Lung Cancer*. 2014; 15: 213-221.
32. Liu Z and Klominek J. Chemotaxis and chemokinesis of

- malignant mesothelioma cells to multiple growth factors. *Anticancer Res.* 2004; 24: 1625-30.
33. Pandey DP, Lappano R, Albanito L, Madeo A, Maggiolini M, Picard D. Estrogenic GPR30 signalling induces proliferation and migration of breast cancer cells through CTGF. *EMBO J.* 2009; 28: 523-32.
  34. Fujii M, Nakanishi H, Toyoda T, Tanaka I, Kondo Y, Osada H, Sekido Y. Convergent signaling in the regulation of connective tissue growth factor in malignant mesothelioma: TGF $\beta$  signaling and defects in the Hippo signaling cascade. *Cell Cycle.* 2012; 11: 3373-9.
  35. Wang L, Chen Z, Wang Y, Chang D, Su L, Guo Y, Liu C. TR1 promotes cell proliferation and inhibits apoptosis through cyclin A and CTGF regulation in non-small cell lung cancer. *Tumour Biol.* 2014; 35: 463-8.
  36. Shan LN, Song YG, Su D, Liu YL, Shi XB, Lu SJ. Early Growth Response Protein-1 Involves in Transforming Growth factor- $\beta$ 1 Induced Epithelial-Mesenchymal Transition and Inhibits Migration of Non-Small-Cell Lung Cancer Cells. *Asian Pac J Cancer Prev.* 2015; 16: 4137-42.
  37. Maggiolini M, Picard D. The unfolding stories of GPR30, a new membrane-bound estrogen receptor. *J Endocrinol.* 2010; 204: 105-14.
  38. Blackstock CD, Higashi Y, Sukhanov S, Shai SY, Stefanovic B, Tabony AM, Yoshida T, Delafontaine P. Insulin-like growth factor-1 increases synthesis of collagen type I *via* induction of the mRNA-binding protein LARP6 expression and binding to the 5' stem-loop of COL1a1 and COL1a2 mRNA. *J Biol Chem* 2014; 289: 7264-74.
  39. Sukhanov S, Higashi Y, Shai SY, Blackstock C, Galvez S, Vaughn C, Titterington J, Delafontaine P. Differential requirement for nitric oxide in IGF-1-induced anti-apoptotic, anti-oxidant and anti-atherosclerotic effects. *FEBS Lett.* 2011; 585: 3065-72.
  40. Sukhanov S, Higashi Y, Shai SY, Vaughn C, Mohler J, Li Y, Song YH, Titterington J, Delafontaine P. IGF-1 reduces inflammatory responses, suppresses oxidative stress, and decreases atherosclerosis progression in ApoE-deficient mice. *Arterioscler Thromb Vasc Biol.* 2007 Dec; 27: 2684-90.
  41. Inamori Y, Ota M, Inoko H, Okada E, Nishizaki R, Shiota T, Mok J, Oka A, Ohno S, Mizuki N. The COL1A1 gene and high myopia susceptibility in Japanese. *Hum Genet.* 2007; 122: 151-7.
  42. Wang CZ, Yeh YC, Tang MJ. DDR1/E-cadherin complex regulates the activation of DDR1 and cell spreading. *Am J Physiol Cell Physiol.* 2009; 297: C419-29.
  43. Yeh YC, Wu CC, Wang YK, Tang MJ. DDR1 triggers epithelial cell differentiation by promoting cell adhesion through stabilization of E-cadherin. *Mol Biol Cell.* 2011; 22: 940-53.
  44. Eswaramoorthy R, Wang CK, Chen WC, Tang MJ, Ho ML, Hwang CC, Wang HM, Wang CZ. DDR1 regulates the stabilization of cell surface E-cadherin and E-cadherin-mediated cell aggregation. *J Cell Physiol.* 2010; 224: 387-97.
  45. Hidalgo-Carcedo C, Hooper S, Chaudhry SI, Williamson P, Harrington K, Leitinger B, Sahai E. Collective cell migration requires suppression of actomyosin at cell-cell contacts mediated by DDR1 and the cell polarity regulators Par3 and Par6. *Nat Cell Biol.* 2011; 13:49-58.
  46. Ahuja J, Kanne JP, Meyer CA. Occupational lung disease. *Semin Roentgenol.* 2015; 50: 40-51.
  47. Lenters V, Vermeulen R, Dogger S, Stayner L, Portengen L, Burdorf A, Heederik D. A meta-analysis of asbestos and lung cancer: is better quality exposure assessment associated with steeper slopes of the exposure-response relationships? *Environ Health Perspect.* 2011; 119: 1547-55.
  48. Straif K, Benbrahim-Tallaa L, Baan R, Grosse Y, Secretan B, El Ghissassi F, Bouvard V, Guha N, Freeman C, Galichet L, Cogliano V; WHO International Agency for Research on Cancer Monograph Working Group. A review of human carcinogens—Part C: metals, arsenic, dusts, and fibres. *Lancet Oncol.* 2009; 10:453-4.
  49. Mossman BT, Lippmann M, Hesterberg TW, Kelsey KT, Barchowsky A, Bonner JC. Pulmonary endpoints (lung carcinomas and asbestosis) following inhalation exposure to asbestos. *J Toxicol Environ Health B Crit Rev.* 2011; 14: 76-121.
  50. Avivi-Green C, Singal M, Vogel WF. Discoidin domain receptor 1-deficient mice are resistant to bleomycin-induced lung fibrosis. *Am J Respir Crit Care Med.* 2006; 174: 420-7.
  51. Lemeer S, Bluwstein A, Wu Z, Leberfinger J, Müller K, Kramer K, Kuster B. Phosphotyrosine mediated protein interactions of the discoidin domain receptor 1. *J Proteomics.* 2012; 75: 3465-77.
  52. Matsuyama W, Watanabe M, Shirahama Y, Oonakahara K, Higashimoto I, Yoshimura T, et al. Activation of discoidin domain receptor 1 on CD14-positive bronchoalveolar lavage fluid cells induces chemokine production in idiopathic pulmonary fibrosis. *J Immunol* 2005; 174: 6490-8.
  53. Heinzelmann-Schwarz VA, Gardiner-Garden M, Henshall SM, Scurry J, Scolyer RA, Davies MJ, Heinzelmann M, Kalish LH, Bali A, Kench JG, et al. Overexpression of the cell adhesion molecules DDR1, Claudin 3, and Ep-CAM in metaplastic ovarian epithelium and ovarian cancer. *Clin Cancer Res* 2004; 10: 4427-4436.
  54. Vogel WF, Abdulhussein R, Ford CE. Sensing extracellular matrix: an update on discoidin domain receptor function. *Cell Signal.* 2006; 18: 1108-16.
  55. Tavazoie SF, Alarcón C, Oskarsson T, Padua D, Wang Q, Bos PD, Gerald WL, Massagué J. Endogenous human microRNAs that suppress breast cancer metastasis. *Nature.* 2008; 451: 147-52.

56. Ramaswamy S, Ross KN, Lander ES, Golub TR. A molecular signature of metastasis in primary solid tumors. *Nat Genet.* 2003; 33: 49-54.
57. Grande JP, Melder DC, Zinsmeister AR. Modulation of collagen gene expression by cytokines: stimulatory effect of transforming growth factor-beta1, with divergent effects of epidermal growth factor and tumor necrosis factor-alpha on collagen type I and collagen type IV. *J Lab Clin Med.* 1997; 130: 476-86.
58. Filardo EJ, Graeber CT, Quinn JA, Resnick MB, Giri D, DeLellis RA, Steinhoff MM, Sabo E. Distribution of GPR30, a seven membrane-spanning estrogen receptor, in primary breast cancer and its association with clinicopathologic determinants of tumor progression. *Clin Cancer Res.* 2006; 12: 6359-66.
59. Smith HO, Arias-Pulido H, Kuo DY, Howard T, Qualls CR, Lee SJ, Verschraegen CF, Hathaway HJ, Joste NE, Prossnitz ER. GPR30 predicts poor survival for ovarian cancer. *Gynecol Oncol.* 2009; 114: 465-71.
60. Smith HO, Leslie KK, Singh M, Qualls CR, Revankar CM, Joste NE, Prossnitz ER. GPR30: a novel indicator of poor survival for endometrial carcinoma. *Am J Obstet Gynecol.* 2007; 196: 386.e1-11.
61. Marjon NA, Hu C, Hathaway HJ, Prossnitz ER. G protein-coupled estrogen receptor regulates mammary tumorigenesis and metastasis. *Mol Cancer Res.* 2014; 12: 1644-54.
62. De Marco P, Romeo E, Vivacqua A, Malaguarnera R, Abonante S, Romeo F, Pezzi V, Belfiore A, Maggiolini M. GPER1 is regulated by insulin in cancer cells and cancer-associated fibroblasts. *Endocr Relat Cancer.* 2014; 21:739-53.
63. Vivacqua A, Lappano R, De Marco P, Sisci D, Aquila S, De Amicis F, Fuqua SA, Andò S, Maggiolini M. G protein-coupled receptor 30 expression is up-regulated by EGF and TGF alpha in estrogen receptor alpha-positive cancer cells. *Mol Endocrinol.* 2009; 23: 1815-26.
64. Albanito L, Sisci D, Aquila S, Brunelli E, Vivacqua A, Madeo A, Lappano R, Pandey DP, Picard D, Mauro L, Andò S, Maggiolini M. Epidermal growth factor induces G protein-coupled receptor 30 expression in estrogen receptor-negative breast cancer cells. *Endocrinology.* 2008; 149: 3799-808.
65. Recchia AG, De Francesco EM, Vivacqua A, Sisci D, Panno ML, Andò S, Maggiolini M. The G protein-coupled receptor 30 is up-regulated by hypoxia-inducible factor-1alpha (HIF-1alpha) in breast cancer cells and cardiomyocytes. *J Biol Chem.* 2011; 286: 10773-82.
66. De Francesco EM, Lappano R, Santolla MF, Marsico S, Caruso A, Maggiolini M. HIF-1 $\alpha$ /GPER signaling mediates the expression of VEGF induced by hypoxia in breast cancer associated fibroblasts (CAFs). *Breast Cancer Res.* 2013; 15: R64.
67. De Francesco EM, Pellegrino M, Santolla MF, Lappano R, Ricchio E, Abonante S, Maggiolini M. GPER mediates activation of HIF1 $\alpha$ /VEGF signaling by estrogens. *Cancer Res.* 2014; 74: 4053-64.
68. Bartella V, De Francesco EM, Perri MG, Curcio R, Dolce V, Maggiolini M, Vivacqua A. The G protein estrogen receptor (GPER) is regulated by endothelin-1 mediated signaling in cancer cells. *Cell Signal.* 2016; 28: 61-71.
69. Baserga R, Peruzzi F, Reiss K. The IGF-1 receptor in cancer biology. *Int J Cancer.* 2003; 107: 873-7.
70. Yakar S, Leroith D, Brodt P. The role of the growth hormone/insulin-like growth factor axis in tumor growth and progression: Lessons from animal models. *Cytokine Growth Factor Rev.* 2005; 16: 407-420.
71. Novosyadlyy R, Lann DE, Vijayakumar A, Rowzee A, Lazzarino DA, Fierz Y, et al. Insulin-mediated acceleration of breast cancer development and progression in a nonobese model of type 2 diabetes. *Cancer Res.* 2010; 70: 741-751.
72. Kisfalvi K, Eibl G, Sinnott-Smith J, Rozengurt E. Metformin disrupts crosstalk between G protein-coupled receptor and insulin receptor signaling systems and inhibits pancreatic cancer growth. *Cancer Res.* 2009; 69: 6539-45.
73. Akekawatchai C, Holland JD, Kochetkova M, Wallace JC, McColl SR. Transactivation of CXCR4 by the insulin-like growth factor-1 receptor (IGF-1R) in human MDA-MB-231 breast cancer epithelial cells. *J Biol Chem.* 2005; 280: 39701-8.
74. Gombos A, Metzger-Filho O, Dal Lago L, Awada-Hussein A. Clinical development of insulin-like growth factor receptor—1 (IGF-1R) inhibitors: at the crossroad? *Invest New Drugs.* 2012; 30: 2433-42.
75. Fidler MJ, Shersher DD, Borgia JA, Bonomi P. Targeting the insulin-like growth factor receptor pathway in lung cancer: problems and pitfalls. *Ther Adv Med Oncol.* 2012; 4: 51-60.
76. Scotlandi K and Belfiore A. Targeting the Insulin-Like Growth Factor (IGF) System Is Not as Simple as Just Targeting the Type 1 IGF Receptor. *Am Soc Clin Oncol Educ Book.* 2012: 599-604.
77. Orengo AM, Spoletini L, Procopio A, Favoni RE, De Cupis A, Ardizzoni A, Castagneto B, Ribotta M, Betta PG, Ferrini S, Mutti L. Establishment of four new mesothelioma cell lines: characterization by ultrastructural and immunophenotypic analysis. *Eur Respir J.* 1999; 13: 527-34.
78. Gerdes MJ, Myakishev M, Frost NA, Rishi V, Moitra J, Acharya A, Levy MR, Park SW, Glick A, Yuspa SH, Vinson C. Activator protein-1 activity regulates epithelial tumor cell identity. *Cancer Res* 2006; 66: 7578-7588.
79. Rigiacciolo DC, Scarpelli A, Lappano R, Pisano A, Santolla MF, De Marco P, Cirillo F, Cappello AR, Dolce V, Belfiore A, Maggiolini M, De Francesco EM. Copper activates HIF-1 $\alpha$ /GPER/VEGF signalling in cancer

- cells. *Oncotarget*. 2015; 6: 34158-77. doi: 10.18632/oncotarget.5779.
80. Rgiracciolo DC, Scarpelli A, Lappano R, Pisano A, Santolla MF, Avino S, De Marco P, Bussolati B, Maggiolini M, De Francesco EM. GPER is involved in the stimulatory effects of aldosterone in breast cancer cells and breast tumor-derived endothelial cells. *Oncotarget*. 2016; 7: 94-111. doi: 10.18632/oncotarget.6475.
81. De Marco P, Lappano R, De Francesco EM, Cirillo F, Pupo M, Avino S, Vivacqua A, Abonante S, Picard D, Maggiolini M. GPER signalling in both cancer-associated fibroblasts and breast cancer cells mediates a feedforward IL1 $\beta$ /IL1R1 response. *Scientific Reports* 2016, in press.

## Review Article

Theme: Heterotrimeric G Protein-based Drug Development: Beyond Simple Receptor Ligands  
Guest Editor: Shelley Hooks

# Recent Advances on the Role of G Protein-Coupled Receptors in Hypoxia-Mediated Signaling

Rosamaria Lappano,<sup>1</sup> Damiano Rigiracciolo,<sup>1</sup> Paola De Marco,<sup>1</sup> Silvia Avino,<sup>1</sup> Anna Rita Cappello,<sup>1</sup> Camillo Rosano,<sup>2</sup> Marcello Maggiolini,<sup>1,3</sup> and Ernestina Marianna De Francesco<sup>1</sup>

Received 1 October 2015; accepted 28 January 2016; published online 10 February 2016

**Abstract.** G protein-coupled receptors (GPCRs) are cell surface proteins mainly involved in signal transmission; however, they play a role also in several pathophysiological conditions. Chemically heterogeneous molecules like peptides, hormones, lipids, and neurotransmitters activate second messengers and induce several biological responses by binding to these seven transmembrane receptors, which are coupled to heterotrimeric G proteins. Recently, additional molecular mechanisms have been involved in GPCR-mediated signaling, leading to an intricate network of transduction pathways. In this regard, it should be mentioned that diverse GPCR family members contribute to the adaptive cell responses to low oxygen tension, which is a distinguishing feature of several illnesses like neoplastic and cardiovascular diseases. For instance, the G protein estrogen receptor, namely G protein estrogen receptor (GPER)/GPR30, has been shown to contribute to relevant biological effects induced by hypoxia via the hypoxia-inducible factor (HIF)-1 $\alpha$  in diverse cell contexts, including cancer. Likewise, GPER has been found to modulate the biological outcome of hypoxic/ischemic stress in both cardiovascular and central nervous systems. Here, we describe the role exerted by GPCR-mediated signaling in low oxygen conditions, discussing, in particular, the involvement of GPER by a hypoxic microenvironment.

**KEYWORDS:** angiogenesis; GPCRs; GPER; hypoxia; signal transduction.

## INTRODUCTION

G protein-coupled receptors (GPCRs) are seven transmembrane-spanning receptors that regulate many cellular functions upon ligand activation (1). The biological responses mediated by GPCRs involve the recruitment of proteins prompting the receptor internalization and desensitization, like arrestins and GPCR kinases (GRKs) as well as membrane-bound partners, namely heterotrimeric G proteins (1,2). In the inactive state, G proteins consist of a G $\beta\gamma$  monomer which maintains a high affinity for a guanine diphosphate (GDP)-bound G $\alpha$  subunit (1,2). On the basis of the sequence identity, four subtypes of G $\alpha$  subunit (G $\alpha_s$ , G $\alpha_i$ , G $\alpha_q$ , and G $\alpha_{12}$ ) have been extensively characterized (1,2). Ligand binding promotes conformational modifications that result in the exchange of GDP for GTP on the G $\alpha$  subunit, leading to a decreased affinity of G $\alpha$  for the G $\beta\gamma$  subunit. The dissociation of the heterotrimer allows that both GTP-

bound G $\alpha$  and free G $\beta\gamma$  activate numerous transduction pathways like mitogen-activated protein kinase (MAPK), phosphatidylinositol 3-kinase (PI3-K), small GTP-binding proteins (Ras and Rho GTPases), and other mediators that contribute to various physiopathological responses (1,2). For instance, an aberrant expression of GPCRs and/or their activation have been associated to several types of tumors (3,4). Consequently, the pharmacological manipulation of certain GPCR-mediated signaling may represent a promising anti-cancer strategy (3,4). As demonstrated for many GPCRs (3,4), the G protein estrogen receptor (GPER, also known as GPR30) may trigger oncogenic signaling (5,6). GPER binds to estrogens, phyto- and xenoestrogens, and also estrogen receptor (ER) antagonists that may act as GPER agonists (7–12). GPER mediates the activation of a network of transduction pathways; however, the actual role elicited by GPER in tumorigenesis is still controversial. Previous studies have shown that GPER may induce cell cycle arrest and inhibition of cancer cell growth (13–16). Nevertheless, other *in vitro* and *in vivo* studies have revealed that GPER triggers cancer cell migration and proliferation (5,17). In addition, GPER expression was associated to inflammatory breast tumor (18), was found reduced during breast cancer tumorigenesis (19), and was related to a poor relapse-free survival in breast cancer patients treated with tamoxifen (20). The lack of GPER in the plasma membrane was linked to a

<sup>1</sup> Department of Pharmacy, Health and Nutritional Sciences, University of Calabria, Via Bucci, 87036, Rende, CS, Italy.

<sup>2</sup> UOS Proteomics IRCCS AOU San Martino-IST National Institute for Cancer Research, Largo R. Benzi 10, 16132, Genoa, Italy.

<sup>3</sup> To whom correspondence should be addressed. (e-mail: marcellomaggiolini@yahoo.it; marcello.maggiolini@unical.it)

favorable prognosis in breast cancer (21), whereas its expression was associated with aggressive features of breast, endometrial, and ovarian tumors (22–24). In this context, we have demonstrated that GPER is upregulated by EGF, insulin-like growth factor (IGF)-I, insulin, and a main factor contributing to tumor aggressiveness like hypoxia (25–31). A low oxygen tension characterizes the growth of solid tumors, where it promotes adaptive responses like anaerobic glycolysis, reduction of macromolecule synthesis, and angiogenesis (32). In addition, hypoxia is critical for the pathogenesis of heart disease and stroke, the major causes of human mortality (33). The effects of hypoxia are mainly mediated by hypoxia-inducible factor (HIF) family members, which orchestrate the complex responses to low oxygen tension (34). In particular, HIF-1 $\alpha$  regulates the expression of several pro-angiogenic factors involved in tumor angiogenesis progression (34,35). Many signaling cascades are engaged by hypoxia toward HIF-1 $\alpha$  activation such as receptor tyrosine kinases (RTKs) and GPCRs (30,31,36). Here, we discuss the involvement of certain GPCRs, including GPER, in hypoxia-mediated signaling toward cancer development and cardiovascular diseases.

### GPCR INVOLVEMENT IN HYPOXIA-MEDIATED SIGNALING

A low oxygen tension characterizes relevant pathophysiological conditions like cancer and cardiovascular diseases (32–34). Multiple mechanisms for oxygen sensing have been developed and conserved in both prokaryotic and eukaryotic organisms (32–34). In particular, HIF-1 acts as a master regulator of the adaptive cell response to limited oxygen availability mainly by activating the transcription of genes that regulate physiological processes as glycolysis, survival, and angiogenesis (34–37). HIF-1 is a heterodimer of two helix-loop-helix-PAS proteins, namely HIF-1 $\alpha$  and HIF-1 $\beta$  or ARNT (38). Upon hypoxia, HIF-1 $\alpha$  and HIF-1 $\beta$  dimerize and bind to the hypoxia-responsive elements (HREs) located within the promoter region of target genes (38). Several factors contribute to HIF-1 $\alpha$ -mediated action in hypoxic conditions, including diverse GPCRs (30,39). For instance, GPR41 was shown to be a hypoxia-induced receptor that drives p53-dependent apoptosis in rat cardiomyocytes subjected to ischemia and reoxygenation injury (40) whereas GPR22 was involved in cardioprotection as its ablation increased the susceptibility to functional decompensation following hemodynamic stress (41). The adrenergic signaling axis, consisting of catecholamines and their adrenergic receptors, has been included among GPCRs that play a primary role in oxygen-related diseases like hypertension, cardiac hypertrophy, and heart failure (42). Moreover, the adrenoreceptors have been shown to functionally interact with opioid receptors (43), which elicit protective actions in response to pre- and post-conditioning stimuli upon cardiac and cerebral damages (44,45). It is worth noting that certain ligand-activated GPCRs induce HIF-1 expression and function (46–48), thus mimicking hypoxic conditions. For instance, the recruitment of transcription factors to the promoter sequence of HIF-1 as well as the stabilization of HIF-1 protein levels may occur upon activation of GPCRs by

endothelin-1 (ET-1),  $\beta$ -adrenoceptor agonists, and lysophosphatidic acid (46–48).

### GPCR INVOLVEMENT IN TUMOR ANGIOGENESIS UPON HYPOXIA

Tumor microenvironment is often characterized by hypoxia, which is a distinguishing feature of an aggressive cancer phenotype and disease recurrence (32). The metabolic changes occurring in rapidly growing cells, the increasing diffusion distances between the blood vessels and certain tumor areas, and the compressive action elicited by the expanding mass on local blood vessels may cumulatively account for low intra-tumor oxygenation (32). The effects of hypoxia on the malignant progression are mediated by complex mechanisms that allow tumor cells to survive and/or escape their oxygen-deficient environment (32,34). Moreover, the adaptive responses to hypoxic stress in the tumor microenvironment trigger the formation of new blood vessels stimulated by pro-angiogenic factors (35,37). Along with the activation of endothelial cells (ECs) and the subsequent degradation of the basement membrane, the angiogenic response leads to the migration and proliferation of ECs, which then form tubes generating new blood vessels (49). Moreover, tumor angiogenesis prompts cancer cells to grow, evade the host surveillance, form the pre-metastatic niche, and invade distant sites (49); hence, the molecular players driving this complex process are intensively investigated toward effective anti-tumor strategies (49). To date, the major growth factors involved in the formation of blood vessels are members of the vascular endothelial growth factor (VEGF) family (50). It includes placental growth factor (PlGF), VEGF-A, VEGF-B, VEGF-C, VEGF-D, and VEGF-E, which bind to the tyrosine kinase receptors, namely VEGF receptor (VEGFR)-1, VEGFR-2, and VEGFR-3 (50). VEGF-A mainly mediates new blood vessel formation within the tumor mass as its binding to VEGFR-2 promotes EC proliferation, migration, and vascular permeability (50). Hormones, cytokines, and growth factors have been shown to boost VEGF-dependent tumor angiogenesis; however, hypoxia represents the primary stimulus for VEGF production and release in the tumor microenvironment (50). Diverse members of the GPCR family are involved in the angiogenic action induced by thrombin, prostaglandins, lysophosphatidic acid, chemokines, and sphingosine 1-phosphate in different pathophysiological conditions, suggesting that certain GPCRs contribute to the development of blood vessels (51–54). In addition, the heterotrimeric G proteins G $\alpha_q$  and G $\alpha_{11}$  may contribute to angiogenic responses by interacting with VEGFR-2 (55) and the G protein-coupled receptor kinase 2 (GRK2) has recently emerged as an integrative node toward the development of cancer-associated vascularization (56). In the tumor microenvironment, chemokines and their receptors elicit relevant paracrine actions, as suggested by the ability of CCL2, CCL5, and CXCL8/IL-8 to recruit within the tumor mass leukocytes and macrophages, which release VEGF and other angiogenic factors (57). Furthermore, cytokines may stimulate the production of prostaglandin E2 (PGE2), which increases the secretion of VEGF, CXCL8, and CXCL5 by tumor and stromal cells (57). Overall, these data suggest that GPCR-mediated signaling may modulate the angiogenic

process together with the VEGF/VEGFR axis. Further corroborating these observations, the anti-tumor activity exhibited by several GPCR antagonists has been correlated with their anti-angiogenic properties and anti-proliferative effects (58). Among the GPCRs contributing to the formation of new blood vessels in hypoxic conditions, the chemokine receptor CXCR4 that binds to the stromal cell-derived factor-1 (SDF-1)/CXCL12 has been shown to stimulate tumor outgrowth and metastasis as well as angiogenesis upon hypoxia (59). The angiogenic factor named adrenomedullin (ADM) signals through the calcitonin receptor-like receptor (CRLR), which is a GPCR expressed in several tumors like the high-vascular clear renal cell carcinoma (RCC) (60,61). A functional consensus HRE was identified within the promoter region of the human CRLR gene, thus corroborating the role of CRLR in the formation of new blood vessels upon hypoxic conditions (60,61). Among the vasoactive pro-angiogenic molecules, ET-1 and the cognate receptors (ETRs) are aberrantly activated in diverse malignancies and regulated by low oxygen tension through HIF-1 $\alpha$  (62). In this regard, HIF-1 $\alpha$ /VEGF signaling has been considered as a downstream transduction pathway activated by the ET-1 axis (62). For instance, in human chondrosarcoma cells, ET-1 promoted the expression of VEGF, angiogenesis, and cell migration by activating integrin-linked kinase (ILK), Akt, and HIF-1 $\alpha$ -mediated signaling cascades (63). In ovarian carcinoma, in both normoxic and hypoxic conditions, ET-1 induced the transcription and accumulation of HIF-1 $\alpha$  and the upregulation of VEGF, suggesting that ET-1 action may be linked to hypoxia and HIF-1 $\alpha$ -dependent angiogenesis (64). In our recent study (65), we also found that ET-1 may trigger GPER expression and function leading to angiogenic responses. Recently, the adrenergic system has been shown to boost tumor angiogenesis and aggressive features through the upregulation of diverse angiogenic factors like VEGF, IL-6, IL-8, matrix metalloproteinase (MMP)-2, and MMP-9 (66,67). The involvement of HIF-1 $\alpha$  in the aforementioned biological responses to catecholamine-mediated stress was also evidenced in other studies showing that the  $\beta$ 2-adrenergic receptor (AR)/HIF-1 $\alpha$  axis regulates angiogenesis and stress-induced pancreatic tumor growth in mouse models (68). In hypoxic melanoma cells,  $\beta$ 3-ARs have been found to be upregulated and involved in the increase of VEGF, as evidenced by using two  $\beta$ 3-AR blockers (69). Additionally, in ovarian cancer cells, the  $\alpha$ 1-AR blocker doxazosin prevented VEGF-mediated cell migration, proliferation, and capillary-like structure tube formation (70). These effects were dependent on the activation of VEGFR-2 and downstream signaling including HIF-1 $\alpha$  (70). Altogether, these observations may suggest that the adrenergic system plays a role in tumor angiogenesis and progression, in particular through HIF-1 $\alpha$ -mediated responses and VEGF expression in hypoxic conditions. Virally encoded GPCRs may also contribute to cancer angiogenesis and progression as evidenced by the human herpesvirus-8 (HHV-8 or Kaposi's sarcoma-associated herpesvirus (KSHV))-encoded G protein-coupled receptor (vGPCR) (71). In this regard, it has been demonstrated that KSHV stimulates the expression of the angiogenic factor angiopoietin-like 4 (71) as well as the production of

VEGF through HIF-1 $\alpha$  (72). Accordingly, the expression of vGPCR in human umbilical vein endothelial cells (HUVECs) triggered cell immortalization together with a constitutive expression and activation of VEGFR-2, thus proposing a role for vGPCRs in the acquisition of the KS-angiogenic phenotype in the model system used (73).

## GPER IS INVOLVED IN HYPOXIA-MEDIATED SIGNALING

GPER has been recently characterized toward its ability to mediate estrogen action in reproductive, immune, skeletal, cardiovascular, and central nervous systems (5). In addition, our and other studies have largely demonstrated the involvement of GPER in the stimulatory effects elicited by estrogens in cancer cells and tumor microenvironment (6,9–11). Significantly, several studies performed in different cell and animal models have ascertained the role exerted by GPER in certain pathological conditions characterized by oxygen deficiency (30,31,74–78). In this regard, it has been demonstrated that GPER activation may decrease myocardial damage and increase functional recovery after ischemia-reperfusion (I/R) injury, which often induces dangerous complications like arrhythmia in patients with myocardial infarction (74–78). Likewise, in rat hearts of both sexes exposed to I/R injury, the activation of GPER reduced myocardial inflammation and infarct size as well as improved immunosuppression and myocardial mechanical performance (79–81). Interestingly, the expression levels of both GPER and HIF-1 $\alpha$  were found to be increased in spontaneously hypertensive rat hearts compared to normotensive controls, suggesting that HIF-1 $\alpha$ /GPER signaling may represent a transduction mediator in certain conditions characterized by elevated blood pressure (74), which is tightly linked to hypoxia (82). Of note, the selective GPER agonist G-1 markedly lowered blood pressure in normotensive and hypertensive rats (83,84), thus supporting the hypothesis that GPER may be a valuable pharmacological target for the prevention/treatment of certain cardiovascular diseases. Further supporting the role elicited by GPER in hypoxic conditions, previous studies have reported that its activation may attenuate the detrimental effects induced by oxygen deficiency in some areas of the central nervous system like the hypothalamic-pituitary axis, hippocampal formation, brainstem autonomic nuclei, and spinal cord (85,86). For instance, GPER activation promoted neuronal survival after global ischemia through the activation of pro-survival and anti-apoptotic signaling cascades (86). An improvement in cerebral microvascular function upon hypoxia/reoxygenation injury was also observed upon GPER activation in male and female rats (87), although sex-dependent protective effects mediated by GPER have been also shown to influence the outcome of ischemic stroke (88). In this regard, it has been demonstrated that GPER expression increases after stroke in the brain of male but not female mice, thus suggesting that a gender-specific regulation of GPER may occur and influence the recovery from cerebral I/R (88). The regulation of GPER expression following hypoxia has been evaluated in breast cancer cells as well as in cancer-associated fibroblasts (CAFs) obtained from breast malignancies (30,31). In these cells, hypoxia-stimulated HIF-1 $\alpha$  was found recruited to the HRE sequences located

within the promoter region of the human GPER gene (30,31). Accordingly, HIF-1 $\alpha$  was required for both the transactivation of a GPER promoter reporter gene as well as for the upregulation of GPER expression upon hypoxia (30,31). These observations were further corroborated by the involvement of HIF-1 $\alpha$ /GPER signaling in VEGF expression toward tumor angiogenesis and progression (31,89). In addition, HIF-1 $\alpha$ /GPER/VEGF transduction pathway was triggered in cancer cells upon exposure to copper, which showed the ability to mimic the hypoxia-mediated signaling (90). Interestingly, the copper-chelating agent TEPA exerted an inhibitory action on the activation of the aforementioned pathway (90), in accordance with previous studies demonstrating that copper-chelating agents can exert anti-tumor effects (91). Altogether, these results indicate that diverse stimuli including hypoxia may trigger relevant biological responses through GPER, which was recently shown to be also involved in the stimulatory effects exerted by aldosterone in breast cancer cells and breast tumor-derived endothelial cells (92) as well as in pregnancy-induced vasodilation of rat uterine arteries (93).

### GPCRS AND HYPOXIA: IMPLICATIONS FOR DRUG DISCOVERY

The multifaceted mechanisms of oxygen sensing mainly orchestrated by HIF-1 represent an essential response to cope with hypoxic stress, which often occurs in cancer, heart disease, and stroke (32,33). As many members of the GPCR family elicit a role in the intricate cell adaptation to oxygen deficiency, a cross talk between HIF-1 and GPCR-mediated pathways may be involved in the biological responses to hypoxia in the aforementioned pathological conditions. In recent years, the discovery and development of several different strategies to block HIF-1 action directly or indirectly has been suggested as a promising tool to overcome the resistance to conventional chemotherapeutic agents in hypoxic microenvironment (34,94). In this vein, HIF-1 inhibitors may be regarded as golden candidates in combination treatment targeting the molecular mediators activated by hypoxia. For instance, a further approach toward new therapeutic strategies may combine the pharmacological manipulation of both HIF-1- and GPCR-mediated signaling. In addition to the therapeutic purposes, GPCRs along with HIF-1 may be regarded as further hallmarks of hypoxia signature in different pathophysiological conditions. As it concerns GPER, on the basis of its involvement in biological responses to low oxygen tension, new GPER-targeted therapies might pioneer for innovative drug discovery strategies aimed to improve the efficacy of HIF blockers and conventional angiogenic inhibitors.

### CONCLUSIONS

A significant progress has been made in the past few years toward the characterization of the molecular mechanisms involved in GPCR action. In particular, many members of the GPCR family have been shown to contribute to the adaptive cell responses to low oxygen tension, which is a distinguishing feature of tumor development and certain cardiovascular diseases. In this regard, GPER may be

included among the HIF-1 $\alpha$  target genes that drive cancer cell survival and malignant progression. In addition, HIF-1 $\alpha$ /GPER signaling may play a relevant role toward VEGF stimulation, angiogenesis, and cancer development. Furthermore, the role elicited by GPER in heart failure, stroke, and hypertension has been largely elucidated, paving the way for novel therapeutic approaches in these relevant illnesses that are characterized by hypoxia and ischemia.

### ACKNOWLEDGMENTS

This work was supported by the Associazione Italiana per la Ricerca sul Cancro (AIRC, grant 16719/2015) and Ministero della Salute (grant 67/GR-2010-2319511). EMDF was supported by the International Cancer Research Fellowships AIRC-iCARE.

### REFERENCES

- Rosenbaum DM, Rasmussen SG, Kobilka BK. The structure and function of G-protein-coupled receptors. *Nature*. 2009;459:356–63.
- Pierce KL, Premont RT, Lefkowitz RJ. Seven-transmembrane receptors. *Nat Rev Mol Cell Biol*. 2002;3:639–50.
- Dorsam RT, Gutkind JS. G-protein-coupled receptors and cancer. *Nat Rev Cancer*. 2007;7:79–94.
- Lappano R, Maggiolini M. G protein-coupled receptors: novel targets for drug discovery in cancer. *Nat Rev Drug Discov*. 2011;10:47–60.
- Maggiolini M, Picard D. The unfolding stories of GPR30, a new membrane-bound estrogen receptor. *J Endocrinol*. 2010;204:105–14.
- Lappano R, Pisano A, Maggiolini M. GPER function in breast cancer: an overview. *Front Endocrinol (Lausanne)*. 2014;5:66.
- Albanito L, Lappano R, Madeo A, Chimento A, Prossnitz ER, Cappello AR, *et al.* Effects of atrazine on estrogen receptor  $\alpha$ - and G protein-coupled receptor 30-mediated signaling and proliferation in cancer cells and cancer-associated fibroblasts. *Environ Health Perspect*. 2015;5:493–9.
- Maggiolini M, Vivacqua A, Fasanella G, Recchia AG, Sisci D, Pezzi V, *et al.* The G protein-coupled receptor GPR30 mediates c-fos up-regulation by 17 $\beta$ -estradiol and phytoestrogens in breast cancer cells. *J Biol Chem*. 2004;279:27008–16.
- Pandey DP, Lappano R, Albanito L, Madeo A, Maggiolini M, Picard D. Estrogenic GPR30 signalling induces proliferation and migration of breast cancer cells through CTGF. *EMBO J*. 2009;28:523–32.
- Pupo M, Pisano A, Lappano R, Santolla MF, De Francesco EM, Abonante S, *et al.* Bisphenol A induces gene expression changes and proliferative effects through GPER in breast cancer cells and cancer-associated fibroblasts. *Environ Health Perspect*. 2012;120:1177–82.
- Madeo A, Maggiolini M. Nuclear alternate estrogen receptor GPR30 mediates 17 $\beta$ -estradiol-induced gene expression and migration in breast cancer-associated fibroblasts. *Cancer Res*. 2010;70:6036–46.
- Lappano R, Rosano C, De Marco P, De Francesco EM, Pezzi V, Maggiolini M. Estriol acts as a GPR30 antagonist in estrogen receptor-negative breast cancer cells. *Mol Cell Endocrinol*. 2010;320:162–70.
- Ariazi EA, Brailoiu E, Yerrum S, Shupp HA, Slifker MJ, Cunliffe HE, *et al.* The G protein-coupled receptor GPR30 inhibits proliferation of estrogen receptor-positive breast cancer cells. *Cancer Res*. 2010;70:1184–94.
- Wei W, Chen ZJ, Zhang KS, Yang XL, Wu YM, Chen XH, *et al.* The activation of G protein-coupled receptor 30 (GPR30) inhibits proliferation of estrogen receptor-negative breast cancer cells in vitro and in vivo. *Cell Death Dis*. 2014;5, e1428.

15. Weißenborn C, Ignatov T, Ochel HJ, Costa SD, Zenclussen AC, Ignatova Z, *et al.* GPER functions as a tumor suppressor in triple-negative breast cancer cells. *J Cancer Res Clin Oncol.* 2014;140:713–23.
16. Weißenborn C, Ignatov T, Poehlmann A, Wege AK, Costa SD, Zenclussen AC, *et al.* GPER functions as a tumor suppressor in MCF-7 and SK-BR-3 breast cancer cells. *J Cancer Res Clin Oncol.* 2014;140:663–71.
17. Marjon NA, Hu C, Hathaway HJ, Prossnitz ER. G protein-coupled estrogen receptor regulates mammary tumorigenesis and metastasis. *Mol Cancer Res.* 2014;12:1644–54.
18. Arias-Pulido H, Royce M, Gong Y, Joste N, Lomo L, Lee SJ, *et al.* GPR30 and estrogen receptor expression: new insights into hormone dependence of inflammatory breast cancer. *Breast Cancer Res Treat.* 2010;123:51–8.
19. Ignatov T, Weißenborn C, Poehlmann A, Lemke A, Semczuk A, Roessner A, *et al.* GPER-1 expression decreases during breast cancer tumorigenesis. *Cancer Invest.* 2013;31:309–15.
20. Ignatov A, Ignatov T, Weissenborn C, Eggemann H, Bischoff J, Semczuk A, *et al.* G-protein-coupled estrogen receptor GPR30 and tamoxifen resistance in breast cancer. *Breast Cancer Res Treat.* 2011;128:457–66.
21. Sjöström M, Hartman L, Grabau D, Fornander T, Malmström P, Nordenskjöld B, *et al.* Lack of G protein-coupled estrogen receptor (GPER) in the plasma membrane is associated with excellent long-term prognosis in breast cancer. *Breast Cancer Res Treat.* 2014;145:61–71.
22. Smith HO, Leslie KK, Singh M, Qualls CR, Revankar CM, Joste NE, *et al.* GPR30: a novel indicator of poor survival for endometrial carcinoma. *Am J Obstet Gynecol.* 2007;196:386.e1–11.
23. Smith HO, Arias-Pulido H, Kuo DY, Howard T, Qualls CR, Lee SJ, *et al.* GPR30 predicts poor survival for ovarian cancer. *Gynecol Oncol.* 2009;114:465–71.
24. Filardo EJ, Graeber CT, Quinn JA, Resnick MB, Giri D, DeLellis RA, *et al.* Distribution of GPR30, a seven membrane-spanning estrogen receptor, in primary breast cancer and its association with clinicopathologic determinants of tumor progression. *Clin Cancer Res.* 2006;12:6359–66.
25. Albanito L, Sisci D, Aquila S, Brunelli E, Vivacqua A, Madeo A, *et al.* Epidermal growth factor induces G protein-coupled receptor 30 expression in estrogen receptor-negative breast cancer cells. *Endocrinology.* 2008;149:3799–808.
26. Vivacqua A, Lappano R, De Marco P, Sisci D, Aquila S, De Amicis F, *et al.* G protein-coupled receptor 30 expression is up-regulated by EGF and TGF alpha in estrogen receptor alpha-positive cancer cells. *Mol Endocrinol.* 2009;23:1815–26.
27. Bartella V, De Marco P, Malaguarnera R, Belfiore A, Maggiolini M. New advances on the functional cross-talk between insulin-like growth factor-I and estrogen signalling in cancer. *Cell Signal.* 2012;24:1515–21.
28. De Marco P, Bartella V, Vivacqua A, Lappano R, Santolla MF, Morcavallo A, *et al.* Insulin-like growth factor-I regulates GPER expression and function in cancer cells. *Oncogene.* 2013;32:678–88.
29. De Marco P, Romeo E, Vivacqua A, Malaguarnera R, Abonante S, Romeo F, *et al.* GPER1 is regulated by insulin in cancer cells and cancer-associated fibroblasts. *Endocr Relat Cancer.* 2014;21:739–53.
30. Recchia AG, De Francesco EM, Vivacqua A, Sisci D, Panno ML, Andò S, *et al.* The G protein-coupled receptor 30 is up-regulated by hypoxia-inducible factor-1alpha (HIF-1alpha) in breast cancer cells and cardiomyocytes. *J Biol Chem.* 2011;286:10773–82.
31. De Francesco EM, Lappano R, Santolla MF, Marsico S, Caruso A, Maggiolini M. HIF-1 $\alpha$ /GPER signaling mediates the expression of VEGF induced by hypoxia in breast cancer associated fibroblasts (CAFs). *Breast Cancer Res.* 2013;15:R64.
32. Harris AL. Hypoxia—a key regulator factor in tumor growth. *Nat Rev Cancer.* 2002;2:38–47.
33. Bishop T, Ratcliffe PJ. HIF hydroxylase pathways in cardiovascular physiology and medicine. *Circ Res.* 2015;117:65–79.
34. Semenza GL. Hypoxia-inducible factors: mediators of cancer progression and targets for cancer therapy. *Trends Pharmacol Sci.* 2012;33:207–14.
35. Manalo DJ, Rowan A, Lavoie T, Natarajan L, Kelly BD, Ye SQ, *et al.* Transcriptional regulation of vascular endothelial cell responses to hypoxia by HIF-1. *Blood.* 2005;105:659–69.
36. Glück AA, Aebersold DM, Zimmer Y, Medová M. Interplay between receptor tyrosine kinases and hypoxia signaling in cancer. *Int J Biochem Cell Biol.* 2015;62:101–14.
37. Wang GL, Semenza GL. General involvement of hypoxia-inducible factor 1 in transcriptional response to hypoxia. *Proc Natl Acad Sci U S A.* 1993;90:4304–8.
38. Semenza GL, Agani F, Booth G, Forsythe J, Iyer N, Jiang H, *et al.* Structural and functional analysis of hypoxia-inducible factor 1. *Kidney Int.* 1997;51:553–5.
39. Guo M, Cai C, Zhao G, Qiu X, Zhao H, Ma Q, *et al.* Hypoxia promotes migration and induces CXCR4 expression via HIF-1 $\alpha$  activation in human osteosarcoma. *PLoS One.* 2014;9:e90518.
40. Kimura M, Mizukami Y, Miura T, Fujimoto K, Kobayashi S, Matsuzaki M. Orphan G protein-coupled receptor, GPR41, induces apoptosis via a p53/Bax pathway during ischemic hypoxia and reoxygenation. *J Biol Chem.* 2001;276:26453–60.
41. Adams JW, Wang J, Davis JR, Liaw C, Gaidarov I, Gatlin J, *et al.* Myocardial expression, signaling, and function of GPR22: a protective role for an orphan G protein-coupled receptor. *Am J Physiol Heart Circ Physiol.* 2008;295:H509–21.
42. Corbi G, Conti V, Russomanno G, Longobardi G, Furgi G, Filippelli A, *et al.* Adrenergic signaling and oxidative stress: a role for sirtuins? *Front Physiol.* 2013;4:324.
43. Jordan BA, Gomes I, Rios C, Filipovska J, Devi LA. Functional interactions between mu opioid and alpha 2A-adrenergic receptors. *Mol Pharmacol.* 2003;64:1317–24.
44. Headrick JP, See Hoe LE, Du Toit EF, Peart JN. Opioid receptors and cardioprotection-opioidergic conditioning' of the heart. *Br J Pharmacol.* 2015;172:2026–50.
45. Gao CJ, Niu L, Ren PC, Wang W, Zhu C, Li YQ, *et al.* Hypoxic preconditioning attenuates global cerebral ischemic injury following asphyxial cardiac arrest through regulation of delta opioid receptor system. *Neuroscience.* 2012;202:352–62.
46. Caprara V, Scappa S, Garrafa E, Di Castro V, Rosanò L, Bagnato A, *et al.* Endothelin-1 regulates hypoxia-inducible factor-1 $\alpha$  and -2 $\alpha$  stability through prolyl hydroxylase domain 2 inhibition in human lymphatic endothelial cells. *Life Sci.* 2014;118:185–90.
47. Hu HT, Ma QY, Zhang D, Shen SG, Han L, Ma YD, *et al.* HIF-1alpha links beta-adrenoceptor agonists and pancreatic cancer cells under normoxic condition. *Acta Pharmacol Sin.* 2010;31:102–10.
48. Lee SJ, No YR, Dang DT, Dang LH, Yang VW, Shim H, *et al.* Regulation of hypoxia-inducible factor 1 $\alpha$  (HIF-1 $\alpha$ ) by lysophosphatidic acid is dependent on interplay between p53 and Krüppel-like factor 5. *J Biol Chem.* 2013;288:25244–53.
49. Baeriswyl V, Christofori G. The angiogenic switch in carcinogenesis. *Semin Cancer Biol.* 2009;19:329–37.
50. Ferrara N, Gerber HP, LeCouter J. The biology of VEGF and its receptors. *Nat Med.* 2003;9:66–76.
51. Richard DE, Vouret-Craviari V, Pouyssegur J. Angiogenesis and G-protein-coupled receptors: signals that bridge the gap. *Oncogene.* 2001;20:1556–62.
52. Sumida H, Noguchi K, Kihara Y, Abe M, Yanagida K, Hamano F, *et al.* LPA4 regulates blood and lymphatic vessel formation during mouse embryogenesis. *Blood.* 2010;116:5060–70.
53. Moore BB, Keane MP, Addison CL, Arenberg DA, Strieter RM. CXC chemokine modulation of angiogenesis: the importance of balance between angiogenic and angiostatic members of the family. *J Invest Med.* 1998;46:113–20.
54. Liu Y, Wada R, Yamashita T, Mi Y, Deng CX, Hobson JP, *et al.* Edg-1, the G protein-coupled receptor for sphingosine-1-phosphate, is essential for vascular maturation. *J Clin Invest.* 2000;106:951–61.
55. Zeng H, Zhao D, Yang S, Datta K, Mukhopadhyay D. Heterotrimeric G $\alpha$ q/G $\alpha$ 11 proteins function upstream of vascular endothelial growth factor (VEGF) receptor-2 (KDR) phosphorylation in vascular permeability factor/VEGF signaling. *J Biol Chem.* 2003;278:20738–45.
56. Rivas V, Carmona R, Muñoz-Chápuli R, Mendiola M, Nogués L, Reglero C, *et al.* Developmental and tumoral vascularization is

- regulated by G protein-coupled receptor kinase 2. *P J Clin Invest.* 2013;123:4714–30.
57. Sarvaiya PJ, Guo D, Ulasov I, Gabikian P, Lesniak MS. Chemokines in tumor progression and metastasis. *Oncotarget.* 2013;4:2171–85.
  58. Guha S, Eibl G, Kisfalvi K, Fan RS, Burdick M, Reber H, *et al.* Broad-spectrum G protein-coupled receptor antagonist, [D-Arg1, D-Trp5,7,9, Leu11]SP: a dual inhibitor of growth and angiogenesis in pancreatic cancer. *Cancer Res.* 2005;65:2738–45.
  59. Jin F, Brockmeier U, Otterbach F, Metz E. New insight into the SDF-1/CXCR4 axis in a breast carcinoma model: hypoxia-induced endothelial SDF-1 and tumor cell CXCR4 are required for tumor cell intravasation. *Mol Cancer Res.* 2012;10:1021–31.
  60. Nikitenko LL, Leek R, Henderson S, Pillay N, Turley H, Generali D, *et al.* The G-protein-coupled receptor CRLR is upregulated in an autocrine loop with adrenomedullin in clear cell renal cell carcinoma and associated with poor prognosis. *Clin Cancer Res.* 2013;19:5740–8.
  61. Nikitenko LL, Smith DM, Bicknell R, Rees MC. Transcriptional regulation of the CRLR gene in human microvascular endothelial cells by hypoxia. *FASEB J.* 2003;17:1499–501.
  62. Yamashita K, Discher DJ, Hu J, Bishopric NH, Webster KA. Molecular regulation of the endothelin-1 gene by hypoxia. Contributions of hypoxia-inducible factor-1, activator protein-1, GATA-2, AND p300/CBP. *J Biol Chem.* 2001;276:12645–53.
  63. Wu MH, Huang CY, Lin JA, Wang SW, Peng CY, Cheng HC, *et al.* Endothelin-1 promotes vascular endothelial growth factor-dependent angiogenesis in human chondrosarcoma cells. *Oncogene.* 2014;33:1725–35.
  64. Spinella F, Rosanò L, Di Castro V, Natali PG, Bagnato A. Endothelin-1 induces vascular endothelial growth factor by increasing hypoxia-inducible factor-1 $\alpha$  in ovarian carcinoma cells. *J Biol Chem.* 2002;277:27850–5.
  65. Bartella V, De Francesco EM, Perri MG, Curcio R, Dolce V, Maggiolini M, *et al.* The G protein estrogen receptor (GPER) is regulated by endothelin-1 mediated signaling in cancer cells. *Cell Signal.* 2016;2:61–71.
  66. Moretti S, Massi D, Farini V, Baroni G, Parri M, Innocenti S, *et al.*  $\beta$ -Adrenoceptors are upregulated in human melanoma and their activation releases pro-tumorigenic cytokines and metalloproteases in melanoma cell lines. *Lab Invest.* 2013;279.
  67. Yang EV, Kim SJ, Donovan EL, Chen M, Gross AC, Webster Marketon JI, *et al.* Norepinephrine upregulates VEGF, IL-8, and IL-6 expression in human melanoma tumor cell lines: implications for stress-related enhancement of tumor progression. *Brain Behav Immun.* 2009;23:267–75.
  68. Shan T, Ma J, Ma Q, Guo K, Guo J, Li X, *et al.*  $\beta$ 2-AR-HIF-1 $\alpha$ : a novel regulatory axis for stress-induced pancreatic tumor growth and angiogenesis. *Curr Mol Med.* 2013;13:1023–34.
  69. Dal Monte M, Casini G, Filippi L, Nicchia GP, Svetlo M, Bagnoli P. Functional involvement of  $\beta$ 3-adrenergic receptors in melanoma growth and vascularization. *J Mol Med (Berl).* 2013;91:1407–19.
  70. Park MS, Kim BR, Dong SM, Lee SH, Kim DY, Rho SB. The antihypertension drug doxazosin inhibits tumor growth and angiogenesis by decreasing VEGFR-2/Akt/mTOR signaling and VEGF and HIF-1 $\alpha$  expression. *Oncotarget.* 2014;5:4935–44.
  71. Ma T, Jham BC, Hu J, Friedman ER, Basile JR, Molinolo A, *et al.* Viral G protein-coupled receptor up-regulates angiopoietin-like 4 promoting angiogenesis and vascular permeability in Kaposi's sarcoma. *Proc Natl Acad Sci U S A.* 2010;107:14363–8.
  72. Sodhi A, Montaner S, Patel V, Zohar M, Bais C, Mesri EA, *et al.* The Kaposi's sarcoma-associated herpes virus G protein-coupled receptor up-regulates vascular endothelial growth factor expression and secretion through mitogen-activated protein kinase and p38 pathways acting on hypoxia-inducible factor 1 $\alpha$ . *Cancer Res.* 2000;60:4873–80.
  73. Bais C, Van Geelen A, Eroles P, Mutlu A, Chiozzini C, Dias S, *et al.* Kaposi's sarcoma associated herpesvirus G protein-coupled receptor immortalizes human endothelial cells by activation of the VEGF receptor-2/ KDR. *Cancer Cell.* 2003;3:131–43.
  74. De Francesco EM, Angelone T, Pasqua T, Pupo M, Cerra MC, Maggiolini M. GPER mediates cardioprotective effects in spontaneously hypertensive rat hearts. *PLoS One.* 2013;8, e69322.
  75. Patel VH, Chen J, Ramanjaneya M, Karteris E, Zachariades E, Thomas P, *et al.* G-protein coupled estrogen receptor 1 expression in rat and human heart: protective role during ischaemic stress. *Int J Mol Med.* 2010;26:193–9.
  76. Meyer MR, Prossnitz ER, Barton M. The G protein-coupled estrogen receptor GPER/GPR30 as a regulator of cardiovascular function. *Vascul Pharmacol.* 2011;55:17–25.
  77. Deschamps AM, Murphy E, Sun J. Estrogen receptor activation and cardioprotection in ischemia reperfusion injury. *Trends Cardiovasc Med.* 2011;20:73–8.
  78. Deschamps AM, Murphy E. Activation of a novel estrogen receptor, GPER, is cardioprotective in male and female rats. *Am J Physiol Heart Circ Physiol.* 2009;297:H1806–13.
  79. Weil BR, Manukyan MC, Herrmann JL, Wang Y, Abarbanell AM, Poynter JA, *et al.* Signaling via GPR30 protects the myocardium from ischemia/reperfusion injury. *Surgery.* 2010;148:436–43.
  80. Zhang B, Subramanian S, Dziennis S, Jia J, Uchida M, Akiyoshi K, *et al.* Estradiol and G1 reduce infarct size and improve immunosuppression after experimental stroke. *J Immunol.* 2010;184:4087–94.
  81. Li WL, Xiang W, Ping Y. Activation of novel estrogen receptor GPER results in inhibition of cardiocyte apoptosis and cardioprotection. *Mol Med Rep.* 2015;12:2425–30.
  82. Czibik G. Complex role of the HIF system in cardiovascular biology. *J Mol Med (Berl).* 2010;88:1101–1.
  83. Lindsey SH, Cohen JA, Brosnihan KB, Gallagher PE, Chappell MC. Chronic treatment with the G protein-coupled receptor 30 agonist G-1 decreases blood pressure in ovariectomized mRen2.Lewis rats. *Endocrinology.* 2009;150:3753–8.
  84. Meyer MR, Prossnitz ER, Barton M. GPER/GPR30 and regulation of vascular tone and blood pressure. *Immunol, Endocr Metab Agents Med Chem.* 2011;11:255–61.
  85. Brailoiu E, Dun SL, Brailoiu GC, Mizuo K, Sklar LA, Oprea TI, *et al.* Distribution and characterization of estrogen receptor G protein-coupled receptor 30 in the rat central nervous system. *J Endocrinol.* 2007;193:311–21.
  86. Chen J, Hu R, Ge H, Duanmu W, Li Y, Xue X, *et al.* G-protein-coupled receptor 30-mediated antiapoptotic effect of estrogen on spinal motor neurons following injury and its underlying mechanisms. *Mol Med Rep.* 2015;12:1733–40.
  87. Murata T, Dietrich HH, Xiang C, Dacey Jr RG. G protein-coupled estrogen receptor agonist improves cerebral microvascular function after hypoxia/reoxygenation injury in male and female rats. *Stroke.* 2013;44:779–85.
  88. Broughton BR, Brait VH, Guida E, Lee S, Arumugam TV, Gardiner-Mann CV, *et al.* Stroke increases G protein-coupled estrogen receptor expression in the brain of male but not female mice. *Neurosignals.* 2013;21:229–39.
  89. De Francesco EM, Pellegrino M, Santolla MF, Lappano R, Ricchio E, Abonante S, *et al.* GPER mediates activation of HIF1 $\alpha$ /VEGF signaling by estrogens. *Cancer Res.* 2014;74:4053–64.
  90. Rigracciolo DC, Scarpelli A, Lappano R, Pisano A, Santolla MF, De Marco P, *et al.* Copper activates HIF-1 $\alpha$ /GPER/VEGF signalling in cancer cells. *Oncotarget.* 2015;33:34158–77.
  91. Brewer GJ. Anticopper therapy against cancer and diseases of inflammation and fibrosis. *Drug Discov Today.* 2005;10:1103–19.
  92. Rigracciolo DC, Scarpelli A, Lappano R, Pisano A, Santolla MF, Avino S, *et al.* GPER is involved in the stimulatory effects of aldosterone in breast cancer cells and breast tumor-derived endothelial cells. *Oncotarget.* 2015 Dec 5. doi: 10.18632/oncotarget.6475.
  93. Tropea T, De Francesco EM, Rigracciolo D, Maggiolini M, Wareing M, Osol G, *et al.* Pregnancy augments G protein estrogen receptor (GPER) induced vasodilation in rat uterine arteries via the nitric oxide—cGMP signaling pathway. *PLoS One.* 2015;10(11), e0141997.
  94. Xia Y, Choi HK, Lee K. Recent advances in hypoxia-inducible factor (HIF)-1 inhibitors. *Eur J Med Chem.* 2012;49:24–40.

## Estrogen Receptors and Chronic Venous Disease

R. Serra <sup>a,b,\*</sup>, L. Gallelli <sup>c,f</sup>, P. Perri <sup>b</sup>, E.M. De Francesco <sup>d</sup>, D.C. Rigracciolo <sup>d</sup>, P. Mastroroberto <sup>e</sup>, M. Maggiolini <sup>d,f</sup>, S. de Franciscis <sup>a,b,f</sup>

<sup>a</sup> Interuniversity Center of Phlebology (CIFL), International Research and Educational Program in Clinical and Experimental Biotechnology, University Magna Graecia of Catanzaro, Viale Europa, Catanzaro 88100, Italy

<sup>b</sup> Department of Medical and Surgical Sciences, University of Catanzaro, Catanzaro 88100, Italy

<sup>c</sup> Department of Health Sciences, University of Catanzaro, Catanzaro 88100, Italy

<sup>d</sup> Department of Pharmacy, Health and Nutritional Sciences, University of Calabria, Rende (CS) 87036, Italy

<sup>e</sup> Department of Experimental and Clinical Medicine, University of Catanzaro, Catanzaro 88100, Italy

### WHAT THIS PAPER ADDS

The present study may help physicians to better understand the underlying pathophysiology of chronic venous disease by focusing on the role of estrogen receptors, in order to improve the knowledge and treatment of its clinical manifestations.

**Objective/Background:** Chronic venous disease (CVD) is a common and relevant problem affecting Western people. The role of estrogens and their receptors in the venous wall seems to support the major prevalence of CVD in women. The effects of the estrogens are mediated by three estrogen receptors (ERs): ER $\alpha$ , ER $\beta$ , and G protein-coupled ER (GPER). The expression of ERs in the vessel walls of varicose veins is evaluated.

**Methods:** In this prospective study, patients of both sexes, with CVD and varicose veins undergoing open venous surgery procedures, were enrolled in order to obtain vein samples. To obtain control samples of healthy veins, patients of both sexes without CVD undergoing coronary artery bypass grafting with autologous saphenous vein were recruited (control group). Samples were processed in order to evaluate gene expression.

**Results:** Forty patients with CVD (10 men [25%], 30 women [75%], mean age 54.3 years [median 52 years, range 33–74 years]) were enrolled. Five patients without CVD (three men, two women [aged 61–73 years]) were enrolled as the control group. A significant increase of tissue expression of ER $\alpha$ , ER $\beta$  and GPER in patients with CVD was recorded ( $p < .01$ ), which was also related to the severity of venous disease.

**Conclusion:** ERs seem to play a role in CVD; in this study, the expression of ERs correlated with the severity of the disease, and their expression was correlated with the clinical stage.

© 2016 European Society for Vascular Surgery. Published by Elsevier Ltd. All rights reserved.

Article history: Received 7 December 2015, Accepted 20 April 2016, Available online 21 May 2016

**Keywords:** Chronic venous disease, ER $\alpha$ , ER $\beta$ , Estrogen receptors, GPER, Varicose veins

### INTRODUCTION

Chronic venous disease (CVD) is a very common problem affecting the Western adult population with a prevalence of up to 57% and 77% in men and women respectively. It may also be associated with other clinical manifestations.<sup>1–4</sup> The spectrum of CVD ranges from varicose veins to leg edema and serious skin changes such as hyper-pigmentation, eczema, lipodermatosclerosis, and venous ulceration.<sup>5</sup> To date, several factors have been implicated in the pathophysiology of CVD,

such as alteration of extracellular matrix (ECM) or matrix metalloproteinases (MMPs), or endothelial dysfunction,<sup>6–9</sup> even if none of these can properly explain its genesis. Recently, a higher prevalence of CVD in patients with breast cancer compared with the general population has been shown, especially in patients that were positive for estrogen receptor (ER) expression.<sup>10</sup> Mashiah et al. documented increased concentrations of ERs in varicose veins.<sup>11</sup> Endogenous estrogens, which are important regulators of vascular homeostasis, mainly act through ER $\alpha$  and ER $\beta$ , which are ligand-gated transcription factors.<sup>12</sup> Recently, it has been shown that the G protein-coupled ER (GPER) mediates estrogen signaling in several types of cells, including those of the cardiovascular system.<sup>13–15</sup> However, the molecular mechanisms related to the development of CVD remain to be elucidated. Therefore, in this study, the expression of the different types of ER in vessel walls of varicose veins, through the entire clinical spectrum of CVD, was evaluated.

<sup>f</sup> R.S., L.G., M.M. and S.d.F. contributed equally to this study.

\* Corresponding author. Interuniversity Center of Phlebology (CIFL), International Research and Educational Program in Clinical and Experimental Biotechnology, University Magna Graecia of Catanzaro, Viale Europa, Catanzaro 88100, Italy.

E-mail address: [rserra@unicz.it](mailto:rserra@unicz.it) (R. Serra).

1078-5884/© 2016 European Society for Vascular Surgery. Published by Elsevier Ltd. All rights reserved.

<http://dx.doi.org/10.1016/j.ejvs.2016.04.020>

## MATERIALS AND METHODS

### Study design

A single center open label study was performed between 1 January and 3 August 2015. The study involved surgeons of the Department of Medical and Surgical Sciences, University “Magna Graecia”, Catanzaro, Italy. The study was approved by two independent ethics committees: (a) the investigational review board (IRB) of the Interuniversity Center of Phlebology (CIFL) International Research and Educational Program in Clinical and Experimental Biotechnology (CIFL IRB, independent ethics committee approval number: ER.ALL.2013.31.A); and (b) the ethics committee of the University Hospital “Mater Domini”, University Magna Graecia, Catanzaro, Italy (approval number: Prot. N. 30/CE) in accordance with the Declaration of Helsinki and the Guideline for Good Clinical Practice. Before starting the study, all participants provided written informed consent. The protocol was properly registered in a public trials registry ([www.clinicaltrials.gov](http://www.clinicaltrials.gov); trial identifier NCT02558426).

### Study population

**Inclusion criteria.** Patients of both sexes with CVD who were > 18 years of age, with C2–C6 varicose veins, according to CEAP classification,<sup>5</sup> and who were eligible to receive open venous surgery procedures in order to obtain vein samples after stab avulsion of varicosities were included.

Patients with concomitant peripheral artery disease (PAD), previous venous thromboembolism (VTE), pregnant or breast feeding women, and women receiving estrogen therapy were excluded.

A further group of patients with coronary artery disease (CAD), and without clinical or laboratory evidence of CVD, PAD, or VTE, undergoing coronary artery bypass grafting (CABG) with autologous saphenous veins, were recruited to collect healthy samples of vein segments (control group).

### Experimental protocol

**Venous sample collection, tissue homogenate preparation, and gene expression studies.** Samples obtained from patients undergoing surgical removal of varicose veins were collected and immediately preserved at  $-80^{\circ}\text{C}$ . Briefly, venous tissues were excised, homogenized with a motor driven homogenizer, and total RNA was isolated using Trizol reagent (Invitrogen, Milan, Italy), according to the manufacturer’s instructions. RNA was quantified spectrophotometrically and quality was checked by electrophoresis via agarose gels stained with ethidium bromide. Only samples that were not degraded and showed clear 18 S and 28 S bands under ultraviolet light were used for reverse transcription polymerase chain reaction (PCR). Total cDNA was synthesized from the RNA by reverse transcription using the murine leukemia virus reverse transcriptase (Life Technologies, Milan, Italy) following the protocol provided by the manufacturer. The expression of ER $\alpha$ , ER $\beta$ , and GPER was quantified by real time PCR using the Step One sequence detection system (Applied

**Table 1.** Reproducibility of the assay.

Intra-assay CV (%)			
	ER $\alpha$	ER $\beta$	GPER
C2	1.32	0.75	1.29
C3	2.01	0.36	1.42
C4	1.98	1.73	0.33
C5	0.77	2.29	0.58
C6	1.54	2.18	1.14
Controls	0.63	1.13	2.33
Inter-assay CV (%)			
	ER $\alpha$	ER $\beta$	GPER
C2	2.23	1.20	1.01
C3	2.18	2.44	0.75
C4	1.32	2.12	0.82
C5	1.45	0.89	1.13
C6	0.55	1.99	2.43
Controls	1.72	2.03	2.12

Note. CV = coefficient of variation; ER = estrogen receptor; GPER = G protein-coupled ER.

Biosystems, Milan, Italy), following the manufacturer’s instructions. Specific primers for  $\beta$ -actin, which was used as internal control, ER $\alpha$ , ER $\beta$ , and GPER were designed using Primer Express version 2.0 software (Applied Biosystems). The sequences were as follows:  $\beta$ -actin forward 5'-AAGCCACCC-CACTTCTCTCTAA-3', reverse 5'-CACCTCCCCTGTGTGGACTT-3'; ER $\alpha$  forward 5'-AGAGGGCATGGTGGAGATCTT-3', reverse 5'-CAAACCTCTCTCCCTGCAGATT-3'; ER $\beta$  forward 5'-GACCA-CAAGCCAAATGTGTT-3', reverse 5'-ACTGGCGATGGACCAC-TAAA-3'; GPER forward 5'-CCTGGACGAGCAGTATTACGATATC-3', reverse 5'-TGCTGTACATGTTGATCTG-3'.

To quantify the expression of ER $\alpha$ , ER $\beta$ , and GPER in venous tissues, standard curves were generated using serially diluted solutions of cDNA from a mixture of all samples. cDNA (5  $\mu\text{L}$ ) of each sample was mixed to obtain the solution of the standard stock (tube 1, first dilution point), which was used to prepare the other four dilution points. Each dilution point (in triplicate) was added into well plates containing the Master Mix solution and, according to the protocol of the real time software, the concentration of each solution (ng/mL) was recorded. The absolute quantification of unknown values was obtained by interpolating the PCR signals into the standard curve provided by the serially diluted solutions. The content of ER $\alpha$ , ER $\beta$ , and GPER transcript was normalized to the  $\beta$ -actin content. To evaluate the sensitivity of the assay, serial dilutions of ER $\alpha$ , ER $\beta$ , and GPER plasmid DNA ranging from 4 to 640 (4, 40, 80, 160, 320 and 640) pg/mL were tested in 20 replicates. Following 40 amplification cycles, the lowest product of amplification, which was consistently differentiated from the negative controls ( $\text{H}_2\text{O}$ ), was set as the lowest limit and used to evaluate the sensitivity of the assay. The lowest concentration for ER $\alpha$  was 2.5 pg/mL. The lowest concentration for ER $\beta$  was 3.2 pg/mL. The lowest concentration of GPER cDNA was 6.5 pg/mL. The specificity of the assay was determined using MCF-7 human breast cancer cells and LnCAP human prostate cancer cells as positive controls. In particular, MCF-7 served as a positive control for both ER $\alpha$  and GPER, while LnCAP served as a positive control for ER $\beta$ .

Absence of amplification for ER $\alpha$ , ER $\beta$ , and GPER was detected in HEK293 cells. In order to determine the reproducibility of the assay, the intra- and inter-assay coefficients of variation of ER $\alpha$ , ER $\beta$ , and GPER cDNA (Ct values) were calculated, as reported in Table 1.

### Statistical analysis

PCR amplification was carried out in triplicate for each sample and the results are expressed as mean  $\pm$  SD. A student *t* test was performed in order to analyze the difference between each group with their control. The ANOVA test was used to evaluate the difference between the groups. Differences identified by ANOVA were pinpointed by an unpaired Student *t* test. The ANCOVA test was used to evaluate the correlation between the age of the patients and the tissue expression of ERs and GPER.

Multiple linear regression analyses were performed to evaluate the associations between body mass index (BMI), smoking, diabetes, lipid disorders, and cardiovascular diseases with the tissue expression of ERs and GPER.

The threshold of statistical significance was set at  $p < .05$ . SPSS (IBM, Armonk, NY, USA) was used for the statistical analyses.

As this was a pilot study, it was not possible to do power calculations.

## RESULTS

Forty patients with CVD were enrolled (group 1; 10 men [25%], 30 women [75%], mean age 54.3 years [median age 52.0 years; range 33.0–74.0 years]); 20 patients (50%) with C2, 10 patients (25%) with C3, six patients (15%) with C4, two patients (5%) with C5, and two patients (5%) with C6 varicose veins. Full patient demographics are given in Table 2.

Five patients (three men, two women, aged 61–73 years) with CAD undergoing CABG with autologous saphenous vein were recruited and represented the control group (group 2).

A significant increase ( $p < .01$ ) in tissue expression of ER $\alpha$ , ER $\beta$ , and GPER, which was related to the severity of venous disease (Table 3), was recorded. Tissue expression of

ER $\alpha$ , ER $\beta$ , and GPER in patients without CVD was significantly lower than in patients with CVD ( $p < .01$ ).

### Correlation

Using the ANCOVA test, no significant correlation between age and expression of ER $\alpha$ , ER $\beta$ , and GPER was documented ( $p = .080$ ,  $p = .805$ , and  $p = .066$ , respectively;  $R^2 = .284$ ;  $R^2$  correct = .125).

Using multiple regression analysis, no correlation between BMI, smoking, lipid disorders, cardiovascular disease and ERs or GPER expression in patients with a C2 CVD was recorded (Table 4). In contrast, a significant correlation was documented between smoking and ER $\beta$  expression in patients with C3 CVD, and between BMI and cardiovascular diseases and the expression of GPER receptors in patients with C3 and C4 CVD, respectively (Table 4). Owing to the small numbers with C5 and C6 CVD, statistical analysis was not possible for these patients.

Student *t* test analysis did not show any correlation between mild and moderate stages of venous disease (C2–C4) and the expression of ER $\alpha$ , ER $\beta$ , and GPER, while a significant correlation at the most severe stages of venous disease (C5 and C6) was recorded (Table 5).

## DISCUSSION

In the present study, information on ER and GPER content in varicose veins of patients with CVD has been provided. Thereafter, the expression of the different types of ER with clinical stage was correlated.

In this study, an association between patient age and expression of ER $\alpha$ , ER $\beta$ , and GPER has been documented, suggesting that age plays a role in ER expression.

Moreover, a linear correlation between the expression of the ERs and the severity of CVD was also found, with a maximum ER expression reached in the ulceration stage (CEAP classification C6).

Asbeutah et al., in studying the changes in the leg veins during the menstrual cycle in university students, showed a significant increase in vein diameter and valve closure time (VCT) of five venous segments, including the common femoral vein, femoral vein, popliteal vein, and great and

**Table 2.** Demographic data and risk factors of enrolled patients with varicose veins (CEAP C2–C6).

	Group 1 ( <i>n</i> = 40)						Group 2 (controls) ( <i>n</i> = 5)
	Total	C2	C3	C4	C5	C6	
Men	10 (25)	2 (10)	3 (30)	3 (50)	1 (50)	1 (50)	3 (60)
Women	30 (75)	18 (90)	7 (70)	3 (50)	1 (50)	1 (50)	2 (40)
Mean age (y)	54.3	53.0	53.1	54.5	62.0	57.5	67.4
Median age (y)	52.0	54.3	50.0	54.5	62.0	57.5	68.0
Age range (y)	33–74	33–73	43–66	39–70	51–73	41–74	61–73
Mean BMI	26.95	25.97	27.74	27.35	31.08	23.38	26.60
Smoke	10 (25)	2 (10)	5 (50)	1 (17)	1 (50)	1 (50)	3 (60)
Diabetes	5 (13)	1 (5)	1 (1)	1 (17)	1 (50)	1 (50)	2 (40)
Lipid disorders	5 (13)	1 (5)	1 (1)	1 (17)	1 (50)	1 (50)	4 (80)
Cardiovascular disease	10 (25)	4 (20)	3 (30)	1 (17)	1 (50)	1 (50)	5 (100)
Total	40 (100)	20 (50)	10 (25)	6 (15)	2 (5)	2 (5)	5 (100)

Note. Data are *n* (%) unless otherwise indicated. BMI = body mass index.

**Table 3.** Expression of estrogen receptor (ER) $\alpha$ , ER $\beta$ , and G protein-coupled ER (GPER) in venous tissues of enrolled patients with or without (controls) varicose veins (CEAP C2–C6).

	C2	C3	C4	C5	C6	Controls
ER $\alpha$	26.95 $\pm$ 13.24	29.50 $\pm$ 20.84	47.33 $\pm$ 1.03	72.52 $\pm$ 3.98	102.50 $\pm$ 4.94	20.00 $\pm$ 12.84
ER $\beta$	47.00 $\pm$ 23.08	146.30 $\pm$ 82.32	185.83 $\pm$ 56.07	275.50 $\pm$ 18.67	1310.00 $\pm$ 14.14	31.00 $\pm$ 17.39
GPER	17.00 $\pm$ 14.38	28.00 $\pm$ 11.4	57.33 $\pm$ 11.09	93.40 $\pm$ 1.13	1960.79 $\pm$ 197.28	15.40 $\pm$ 10.50

Note. Data are mean  $\pm$  SD.

small saphenous veins.<sup>16</sup> In a subsequent study, the same authors demonstrated that first pregnancy is associated with changes in diameter and VCT in the lower limbs veins.<sup>17</sup> These changes also seemed to cause the development of varicose veins in some patients as pregnancy progressed.

In a study performed in women with breast cancer, a strong correlation between breast cancer and CVD, influenced by hormonal receptor expression in tumor tissue, was shown.<sup>10</sup> ER-positive status was associated with a severe manifestation of CVD.

An experimental *in vitro* study performed on the inferior vena cava of both male and female Sprague-Dawley rats, suggested that ERs were involved in sex related differences of venous contraction and relaxation and therefore in the genesis of varicose veins.<sup>18</sup>

A previous study documented that estrogens, including their physiologically most important form, 17 $\beta$ -estradiol, affect vascular function through ER $\alpha$ , ER $\beta$ , and GPER.<sup>19</sup>

GPER is widely distributed in peripheral tissues and plays a pivotal role in vasculature and is expressed in human mammary artery and saphenous vein cells.<sup>19,20</sup> GPER may also function in conjunction with ERs to assemble a complex for rapid and synergic estrogen signaling.<sup>19</sup> In endothelial cells and vascular smooth muscle cells, estrogens activating ERs and GPER may also cause relaxation of endothelium denuded vessels.<sup>21,22</sup>

**Table 5.** Student *t* test correlation between venous disease class and tissue expression of estrogen receptors (ERs) and G protein-coupled ER (GPER) in enrolled patients with chronic venous disease.

CEAP vascular disease classification	ER $\alpha$	ER $\beta$	GPER
C2	.591	.457	-.085
C3	.425	-.699	.096
C4	-.516	-.296	.222
C5	1.000*	1.000*	-1.000*
C6	1.000*	1.000*	-1.000*

Note. Data are expressed with respect to control patients.

\**p* < .01.

Robertson et al. evaluated 120 patients with varicose veins, and documented that smoking, obesity, and restricted ankle movement increase the risk of severe disease and ulceration.<sup>23</sup>

In the present study, it has been shown that the expression of both ERs and GPER is not related to other factors such as age, BMI, lipid disorders, diabetes, smoking, or cardiovascular disease in patients with a low grade of disease, suggesting that estrogens may elicit a primary action in the modulation of venous disease. In contrast, in C3 and C4 patients, these risk factors are related to the expression of the receptors.

**Table 4.** Multiple regression analysis evaluated the correlation between demographic values and estrogen receptors (ERs) and G protein-coupled ER (GPER) tissue expression in enrolled patients with chronic venous disease.

	Demographic data	C2		C3		C4	
		Student <i>t</i>	<i>p</i>	Student <i>t</i>	<i>p</i>	Student <i>t</i>	<i>p</i>
ER $\alpha$	Age	.664	.517	-.374	.728	-1.007	.388
	BMI	.634	.536	.028	.979	-.306	.779
	Smoking	.142	.889	.496	.646	1.732	.333
	Diabetes	.850	.407	1.020	.365	-.577	.667
	Lipid disorders	.653	.524	-.678	.535	-.577	.667
	Cardiovascular disease	-.660	.520	3.380	.010	-1.732	.333
ER $\beta$	Age	-1.910	.075	.489	.651	.361	.742
	BMI	.436	.669	-2.277	.085	-1.159	.330
	Smoking	-1.440	.170	4.021	.016*	-4.041	.154
	Diabetes	-.389	.702	-2.222	.090	-2.021	.293
	Lipid disorders	-.037	.971	-.358	.738	-.289	.821
	Cardiovascular disease	-1.637	.119	1.065	.318	-1.299	.418
GPER	Age	-1.002	.332	-.735	.503	.357	.745
	BMI	1.232	.237	-3.114	.036*	.220	.840
	Smoking	-.766	.455	2.042	.111	-19.053	.033*
	Diabetes	.842	.411	.574	.597	1.732	.333
	Lipid disorders	.638	.533	-.151	.887	1.732	.333
	Cardiovascular disease	.174	.864	.171	.868	21.362	.030

Note. BMI = body mass index.

\**p* < .05.

In particular, the present data suggest that smoking is related to the expression of ER $\beta$  in patients with C3 CVD, while BMI and cardiovascular disease are related to the expression of GPER receptor in patients with C3 and C4 CVD patients, respectively, suggesting that inflammation is able to modulate the expression of either ER $\beta$  and GPER  $\beta$  receptors but not that of ER $\alpha$  receptor.

Taken together, these data suggest a disease related increase of ERs and GPER expression, and these receptors may play a mechanistic role in the development of the venous disease, suggesting a causative association between ER expression and grade of disease.

The development of CVD may be related to several mechanisms, such as vascular remodeling, ECM alterations, and endothelial dysfunction, that could be related to MMP activation.<sup>1,2,5,8–10</sup> Furthermore, the vascular effects of estrogens may reflect, at least in part, their concentration dependent effects on MMPs. For instance, low doses of estrogens could inhibit MMPs and attenuate collagen deposition, whereas at high doses they may activate MMPs and promote vascular lesions.<sup>22</sup>

MMP expression was not evaluated in the current study; thus, a correlation between ER expression and MMP activation could not be shown, which represents a limitation of the study. Another limitation is related to the small number of patients enrolled. Therefore, further studies are required to clarify the transduction mechanisms and mediators involved in the pathophysiology of CVD.

In conclusion, ERs seem to play a role in CVD; in this study, their expression was correlated with disease severity. Moreover, expression of the different types of ER was correlated with each clinical class.

#### CONFLICT OF INTEREST

None.

#### FUNDING

None.

#### REFERENCES

- Serra R, Grande R, Butrico L, Fugetto F, de Franciscis S. Epidemiology, diagnosis and treatment of chronic venous disease: a systematic review. *Chirurgia* 2016;**29**(2):34–45.
- Serra R, Buffone G, de Franciscis A, Mastrangelo D, Molinari V, Montemurro R, et al. A genetic study of chronic venous insufficiency. *Ann Vasc Surg* 2012;**26**:636–42.
- Robertson L, Evans C, Fowkes FG. Epidemiology of chronic venous disease. *Phlebology* 2008;**23**:103–11.
- Beebe-Dimmer JL, Pfeifer JR, Engle JS, Schottenfeld D. The epidemiology of chronic venous insufficiency and varicose veins. *Ann Epidemiol* 2005;**15**:175–84.
- Eklöf B, Rutherford RB, Bergan JJ, Carpentier PH, Gloviczki P, Kistner RL, et al. Revision of the CEAP classification for chronic venous disorders: consensus statement. *J Vasc Surg* 2004;**40**:1248–52.
- Serra R, Buffone G, Costanzo G, Montemurro R, Scarcello E, Stillitano DM, et al. Altered metalloproteinase-9 expression as the least common denominator between varicocele, inguinal hernia and chronic venous disorders. *Ann Vasc Surg* 2014;**28**:705–9.
- de Franciscis S, Serra R. Matrix Metalloproteinases and endothelial dysfunction: the search for new prognostic markers and for new therapeutic targets for vascular wall imbalance. *Thromb Res* 2015;**136**:5–6.
- Kucukguven A, Khalil RA. Matrix metalloproteinases as potential targets in the venous dilation associated with varicose veins. *Curr Drug Targets* 2013;**14**:287–324.
- Lim CS, Davies AH. Pathogenesis of primary varicose veins. *Br J Surg* 2009;**96**:1231–4.
- Serra R, Buffone G, Miglietta AM, Abonante S, Giordano V, Renne M, et al. Breast cancer and venous disease: a retrospective cohort study. *Ann Vasc Surg* 2013;**27**:762–6.
- Mashiah A, Berman V, Thole HH, Rose SS, Pasik S, Schwarz H, et al. Estrogen and progesterone receptors in normal and varicose saphenous veins. *Cardiovasc Surg* 1999;**7**:327–31.
- Moriarty K, Kim KH, Bender JR. Mini review: estrogen receptor-mediated rapid signaling. *Endocrinology* 2006;**147**:5557–63.
- Barton M, Prossnitz ER. Emerging roles of GPER in diabetes and atherosclerosis. *Trends Endocrinol Metab* 2015;**26**:185–92.
- De Francesco EM, Angelone T, Pasqua T, Pupo M, Cerra MC, Maggiolini M. GPER mediates cardiotropic effects in spontaneously hypertensive rat hearts. *PLoS One* 2013;**8**:e69322.
- Filice E, Recchia AG, Pellegrino D, Angelone T, Maggiolini M, Cerra MC. A new membrane G protein-coupled receptor (GPR30) is involved in the cardiac effects of 17 $\beta$ -estradiol in the male rat. *J Physiol Pharmacol* 2009;**60**:3–10.
- Asbeutah A, Al enezi M, Al-Sharifi N, Almajran A, Cameron J, McGrath B, et al. Changes of the diameter and valve closure time in leg veins across the menstrual cycle. *J Ultrasound Med* 2014;**4**:4–9.
- Asbeutah A, Al-Azemi M, Al-Sarhan S, Almajran A, Asfar SK. Changes in the diameter and valve closure time of leg veins in primigravida women during pregnancy. *J Vasc Surg* 2015;**3**:147–53.
- Raffetto JD, Qiao X, Beauregard KG, Khalil RA. Estrogen receptor-mediated enhancement of venous relaxation in female rat: implications in sex-related differences in varicose veins. *J Vasc Surg* 2010;**51**:972–81.
- Haas E, Meyer MR, Schurr U, Bhattacharya I, Minotti R, Nguyen HH, et al. Differential effects of 17 $\beta$ -estradiol on function and expression of estrogen receptor alpha, estrogen receptor beta, and GPER in arteries and veins of patients with atherosclerosis. *Hypertension* 2007;**49**:1358–63.
- Miller VM, Duckles SP. Vascular actions of estrogens: functional implications. *Pharmacol Rev* 2008;**60**:210–41.
- Orshal JM, Khalil RA. Gender, sex hormones, and vascular tone. *Am J Physiol Regul Integr Comp Physiol* 2004;**286**:R233–49.
- Khalil RA. Estrogen, vascular estrogen receptor and hormone therapy in postmenopausal vascular disease. *Biochem Pharmacol* 2013;**86**:1627–42.
- Robertson L, Lee AJ, Gallagher K, Carmichael SJ, Evans CJ, McKinstry BH, et al. Risk factors for chronic ulceration in patients with varicose veins: a case control study. *J Vasc Surg* 2009;**49**:1490–8.

## Copper activates HIF-1 $\alpha$ /GPER/VEGF signalling in cancer cells

Damiano Cosimo Rigracciolo<sup>1</sup>, Andrea Scarpelli<sup>1</sup>, Rosamaria Lappano<sup>1</sup>, Assunta Pisano<sup>1</sup>, Maria Francesca Santolla<sup>1</sup>, Paola De Marco<sup>1</sup>, Francesca Cirillo<sup>1</sup>, Anna Rita Cappello<sup>1</sup>, Vincenza Dolce<sup>1</sup>, Antonino Belfiore<sup>2</sup>, Marcello Maggiolini<sup>1</sup> and Ernestina Marianna De Francesco<sup>1</sup>

<sup>1</sup> Department of Pharmacy, Health and Nutritional Sciences, University of Calabria, Rende, Italy

<sup>2</sup> Endocrinology, Department of Health, University Magna Graecia of Catanzaro, Catanzaro, Italy

**Correspondence to:** Marcello Maggiolini, **email:** marcellomaggiolini@yahoo.it

**Keywords:** copper, cancer, angiogenesis, GPER, HIF-1 $\alpha$ , VEGF, Pathology Section

**Received:** June 15, 2015

**Accepted:** August 31, 2015

**Published:** September 22, 2015

This is an open-access article distributed under the terms of the Creative Commons Attribution License, which permits unrestricted use, distribution, and reproduction in any medium, provided the original author and source are credited.

### ABSTRACT

**Copper promotes tumor angiogenesis, nevertheless the mechanisms involved remain to be fully understood. We have recently demonstrated that the G-protein estrogen receptor (GPER) cooperates with hypoxia inducible factor-1 $\alpha$  (HIF-1 $\alpha$ ) toward the regulation of the pro-angiogenic factor VEGF. Here, we show that copper sulfate (CuSO<sub>4</sub>) induces the expression of HIF-1 $\alpha$  as well as GPER and VEGF in breast and hepatic cancer cells through the activation of the EGFR/ERK/c-fos transduction pathway. Worthy, the copper chelating agent TEPA and the ROS scavenger NAC prevented the aforementioned stimulatory effects. We also ascertained that HIF-1 $\alpha$  and GPER are required for the transcriptional activation of VEGF induced by CuSO<sub>4</sub>. In addition, in human endothelial cells, the conditioned medium from breast cancer cells treated with CuSO<sub>4</sub> promoted cell migration and tube formation through HIF-1 $\alpha$  and GPER.**

**The present results provide novel insights into the molecular mechanisms involved by copper in triggering angiogenesis and tumor progression. Our data broaden the therapeutic potential of copper chelating agents against tumor angiogenesis and progression.**

### INTRODUCTION

Copper, which is an essential trace element naturally occurring in soil, water and air, acts as a catalytic and/or structural cofactor in a wide array of important biological processes like embryogenesis, growth, homeostasis and angiogenesis [1, 2]. An elevated exposure to copper may be mainly consequent to environmental pollution from the manufacture of wire, sheet metal, pipe and other metal products [2]. In addition, mining, waste dumps, combustion of fossil fuels, wood production and phosphate fertilizers release copper in the environment, thus contributing to the actual exposure in humans [2-4]. To date, mismanaged or high copper levels have been involved in the generation of oxidative stress [5] which plays an important role in cancer development [6]. In this regard, it should be mentioned that physiological concentrations of copper range approximately from

18 to 31  $\mu$ M [7], while serum copper levels have been found in cancer patients from 50  $\mu$ M to 205  $\mu$ M or even at mM concentrations [8-10]. Of note, elevated copper concentrations were correlated with cancer stage and/or progression in diverse types of tumors, thus suggesting that copper may be a useful prognostic factor and a marker of responsiveness to therapy [reviewed in 8]. On the basis of these findings, a number of studies investigated the stimulatory action of copper on VEGF production and tumor angiogenesis [11-13] and the repressive effects exerted by copper-chelating on HIF-1 $\alpha$  mediated expression of VEGF [14, 15].

Numerous G-protein coupled receptors (GPCRs) contribute to the angiogenic switch through mechanisms that include their functional interaction with HIF-1 $\alpha$  toward VEGF expression [16]. In this regard, our recent study has shown that the G protein estrogen receptor (GPER) cooperates with HIF-1 $\alpha$  in order to modulate

VEGF in hypoxic breast tumor microenvironment [17]. In addition, we have demonstrated that estrogenic GPER signalling activates HIF-1 $\alpha$ /VEGF transduction pathway leading to angiogenesis and tumor growth [18].

Here, we provide novel evidence on the mechanisms by which copper triggers the EGFR/ERK/c-fos signalling cascade along with GPER and HIF-1 $\alpha$  toward VEGF expression and function in cancer cells. We also show that GPER may be considered as an additional target of copper chelating agents, hence broadening the therapeutic potential of these chemicals against tumor angiogenesis and progression.

## RESULTS

### CuSO<sub>4</sub> induces the expression of the pro-angiogenic factor VEGF

Considering that copper and its chelating agents have been involved in tumor angiogenesis [5], we asked whether copper sulfate (CuSO<sub>4</sub>) may induce the expression of the pro-angiogenic factor VEGF and its transcriptional regulator HIF-1 $\alpha$  in SkBr3 breast cancer cells and HepG2 hepatocellular carcinoma cells. Of note, CuSO<sub>4</sub> induced the mRNA expression of both HIF-1 $\alpha$  (Figure 1A) and VEGF (Figure 1B) in a dose dependent manner, starting from 25  $\mu$ M and reaching the strongest stimulation upon concentrations ranging from 100 to 200  $\mu$ M. Taking into account these results and considering that in previous studies relevant biological responses to copper exposure were observed up to 500  $\mu$ M [19-21], in the subsequent assays of the current study 200  $\mu$ M CuSO<sub>4</sub> were used. First, we determined that CuSO<sub>4</sub> up-regulates in a time-dependent manner the mRNA expression of HIF-1 $\alpha$  (Figure 1C) and VEGF (Figure 1D) in SkBr3 and HepG2 cells. Thereafter, we ascertained that the well-acknowledged copper chelating agent TEPA [14, 22] as well as the extensively used ROS scavenger NAC [reviewed in 23] prevent the mRNA induction of HIF-1 $\alpha$  (Figure 1E) and VEGF (Figure 1F) and the transactivation of a VEGF promoter construct (Figure 1G) upon treatment with CuSO<sub>4</sub>. As copper has been previously involved in HIF-1 $\alpha$  responses to low oxygen conditions [14, 15], we then assessed the effect of TEPA on the action of the hypoxia-mimetic agent CoCl<sub>2</sub>. As expected, CoCl<sub>2</sub> induced the mRNA expression of HIF-1 $\alpha$  (Figure 2A) and VEGF (Figure 2B) as well as the transactivation of a VEGF promoter construct (Figure 2C) in SkBr3 and HepG2 cells. Interestingly, these effects were abolished in the presence of TEPA and rescued adding CuSO<sub>4</sub> to SkBr3 and HepG2 cells (Figure 2). Results similar to those observed using CoCl<sub>2</sub> were obtained culturing SkBr3 and HepG2 cells in a low oxygen tension (2% O<sub>2</sub>) (Supplementary Figure 1A-1C).

Collectively, these findings suggest that CuSO<sub>4</sub> may be involved in the activation of HIF-1 $\alpha$ /VEGF transduction signalling in cancer cells. On the basis of our recent findings suggesting that a functional cross-talk between HIF-1 $\alpha$  and GPER may occur toward the VEGF expression in hypoxic conditions [24, 17-18], we next determined that the up-regulation of GPER mRNA expression induced by CuSO<sub>4</sub> in SkBr3 and HepG2 cells (Figure 3A, 3B) is abolished in the presence of both TEPA and NAC (Figure 3C). Moreover, the transactivation of a GPER promoter construct triggered by CuSO<sub>4</sub> was prevented using TEPA and NAC (Figure 3D). Notably, the GPER mRNA induction and the GPER promoter transactivation induced by CoCl<sub>2</sub> were prevented in the presence of TEPA and rescued adding CuSO<sub>4</sub> (Figure 3E, 3F). Results comparable to those observed upon CoCl<sub>2</sub> treatment were obtained culturing cells in a low oxygen tension (2% O<sub>2</sub>) (Supplementary Figure 1D-1E). Cumulatively, these data recall previous studies showing that the inhibitory effects of TEPA on hypoxia-induced responses are rescued by CuSO<sub>4</sub> in a dose-dependent manner [14].

Altogether, these data indicate that GPER may be included among the transduction mediators triggered by copper, in particular in stressful conditions characterized by a low oxygen tension in cancer cells.

### Molecular mechanisms involved in the stimulatory actions elicited by CuSO<sub>4</sub>

As c-fos expression is a molecular sensor of both GPER and HIF-1 $\alpha$  signalling [18, 25-26], we also demonstrated that c-fos mRNA increase upon CuSO<sub>4</sub> stimulation (Figure 3G, 3H) is abrogated in the presence of TEPA and NAC (Figure 3I). Nicely fitting with these results, the transactivation of a c-fos luciferase construct and AP1-luc promoter sequence induced by CuSO<sub>4</sub> was repressed in the presence of TEPA and NAC (Figure 3J). Recapitulating the aforementioned findings, the protein induction of c-fos, HIF-1 $\alpha$  and GPER observed upon CuSO<sub>4</sub> treatment was abrogated in the presence of TEPA and NAC in SkBr3 and HepG2 cells (Figure 4A-4D). Given that the activation of EGFR/ERK signalling triggers transduction mechanisms leading to gene expression changes as mentioned above [17-18, 25, 27-28], we ascertained that the EGFR and ERK1/2 phosphorylation induced by CuSO<sub>4</sub> in both SkBr3 and HepG2 cells (Figure 5A, 5B) is blocked in the presence of the EGFR tyrosine kinase inhibitor AG1478 (AG) and the MEK inhibitor PD98059 (PD) (Figure 5C, 5D) as well as using TEPA and NAC (Figure 5E, 5F). Further corroborating these data, the up-regulation of c-fos, HIF-1 $\alpha$ , GPER and VEGF mRNA expression (Figure 6A-6D) as well as the transactivation of fos-luc, AP1-luc, GPER-luc and VEGF-luc reporter constructs (Figure 6E, 6F) induced by CuSO<sub>4</sub>

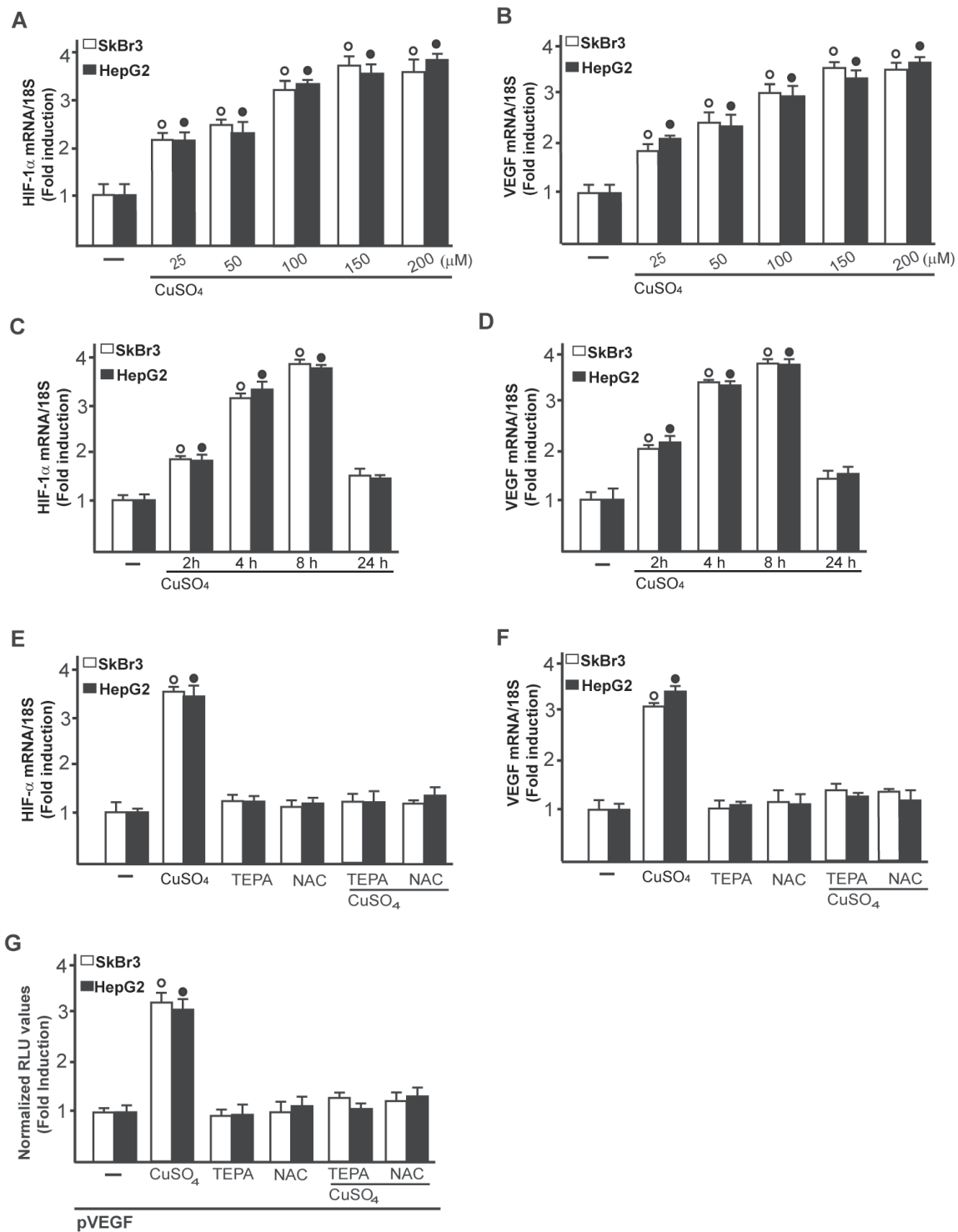


**Figure 1: CuSO<sub>4</sub> induces the mRNA expression of HIF-1 $\alpha$  and VEGF.** mRNA expression of HIF-1 $\alpha$  **A.** and VEGF **B.** in SkBr3 and HepG2 cells treated with increasing concentrations of CuSO<sub>4</sub> for 8 hours, as evaluated by real-time PCR. CuSO<sub>4</sub> (200  $\mu$ M) induces the mRNA expression of HIF-1 $\alpha$  **C.** and VEGF **D.** in a time-dependent manner. In SkBr3 and HepG2 cells treated with 200  $\mu$ M CuSO<sub>4</sub> for 8 hours, the mRNA induction of HIF-1 $\alpha$  **E.** and VEGF **F.** is abrogated in the presence of the copper chelating agent TEPA (50  $\mu$ M) and the ROS scavenger NAC (300  $\mu$ M). Values are normalized to the 18S expression and shown as fold changes of the mRNA expression induced by CuSO<sub>4</sub> compared to cells treated with vehicle (-). **G.** The transactivation of a VEGF promoter plasmid (pVEGF) observed in SkBr3 and HepG2 cells treated with 200  $\mu$ M CuSO<sub>4</sub> for 12 hours is prevented by TEPA (50  $\mu$ M) and NAC (300  $\mu$ M). The luciferase activities were normalized to the internal transfection control and values of cells receiving vehicle (-) were set as 1-fold induction upon which the activities induced by CuSO<sub>4</sub> treatment were calculated. Each data point represents the mean  $\pm$  SD of three independent experiments performed in triplicate. (o), (●)  $p < 0.05$  for cells receiving vehicle (-) versus CuSO<sub>4</sub> treatment.

were abolished in the presence of AG and PD. Analogous findings were obtained evaluating the regulation of c-fos, HIF-1 $\alpha$  and GPER protein expression in SkBr3 and HepG2 cells (Figure 6G, 6H).

Immunofluorescence experiments performed in SkBr3 cells showed that TEPA, NAC, AG and PD prevent also the increase of VEGF protein expression upon CuSO<sub>4</sub> treatment (Figure 7). In addition, the HIF-1 $\alpha$  protein increase triggered by CuSO<sub>4</sub> was no longer evident transfecting SkBr3 and HepG2 cells with a plasmid encoding a dominant/negative c-fos mutant (DN/c-fos) (Figure 8A, 8B). In accordance with the aforementioned results, the up-regulation of GPER (Figure 8A, 8B) and VEGF (Figure 8C, 8D) protein levels

upon CuSO<sub>4</sub> treatment was prevented by DN/c-fos, as evaluated by immunoblotting and immunofluorescence assays, respectively. As demonstrated in our previous investigations, in hypoxic tumor microenvironment HIF-1 $\alpha$  mediates the expression of GPER that contributes to the regulation and function of VEGF [17, 24]. Likewise, we found that the GPER protein up-regulation induced by CuSO<sub>4</sub> as well as the transactivation of the GPER promoter were abolished knocking down HIF-1 $\alpha$  expression (Figure 9A-9F). In addition, the silencing of HIF-1 $\alpha$  prevented the CuSO<sub>4</sub>-induced activation of the VEGF promoter construct (Figure 9G, 9H) as well as the up-regulation of VEGF protein expression (Figure 9I-9K). Of note, GPER was required for VEGF protein induction

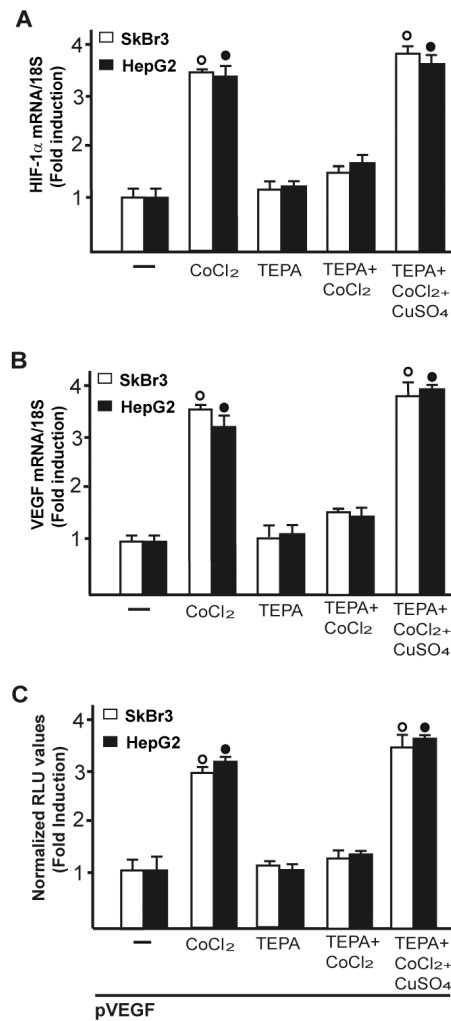


**Figure 2: CuSO<sub>4</sub> rescues the inhibitory effects of TEPA on CoCl<sub>2</sub>-induced transcription of HIF-1 $\alpha$  and VEGF.** In SkBr3 and HepG2 cells, the up-regulation of HIF-1 $\alpha$  **A.** and VEGF **B.** mRNA expression induced upon CoCl<sub>2</sub> treatment (100  $\mu$ M for 8 hours) is no longer evident in the presence of TEPA (50  $\mu$ M) but rescued using CoCl<sub>2</sub> (100  $\mu$ M for 8 hours) in combination with 200  $\mu$ M CuSO<sub>4</sub>, as determined by real-time PCR. Values are normalized to the 18S expression and shown as fold changes of mRNA expression induced by treatments respect to cells treated with vehicle (-). **C.** The transactivation of a VEGF promoter plasmid (pVEGF) observed in SkBr3 and HepG2 cells treated with 100  $\mu$ M CoCl<sub>2</sub> for 12 hours is prevented by TEPA (50  $\mu$ M) and rescued using CoCl<sub>2</sub> (100  $\mu$ M for 12 hours) in combination with 200  $\mu$ M CuSO<sub>4</sub>. The luciferase activities were normalized to the internal transfection control and values of cells receiving vehicle (-) were set as 1-fold induction upon which the activities induced by CoCl<sub>2</sub> treatment were calculated. Each data point represents the mean  $\pm$  SD of three independent experiments performed in triplicate. (○), (●)  $p < 0.05$  for cells receiving vehicle (-) *versus* treatments.

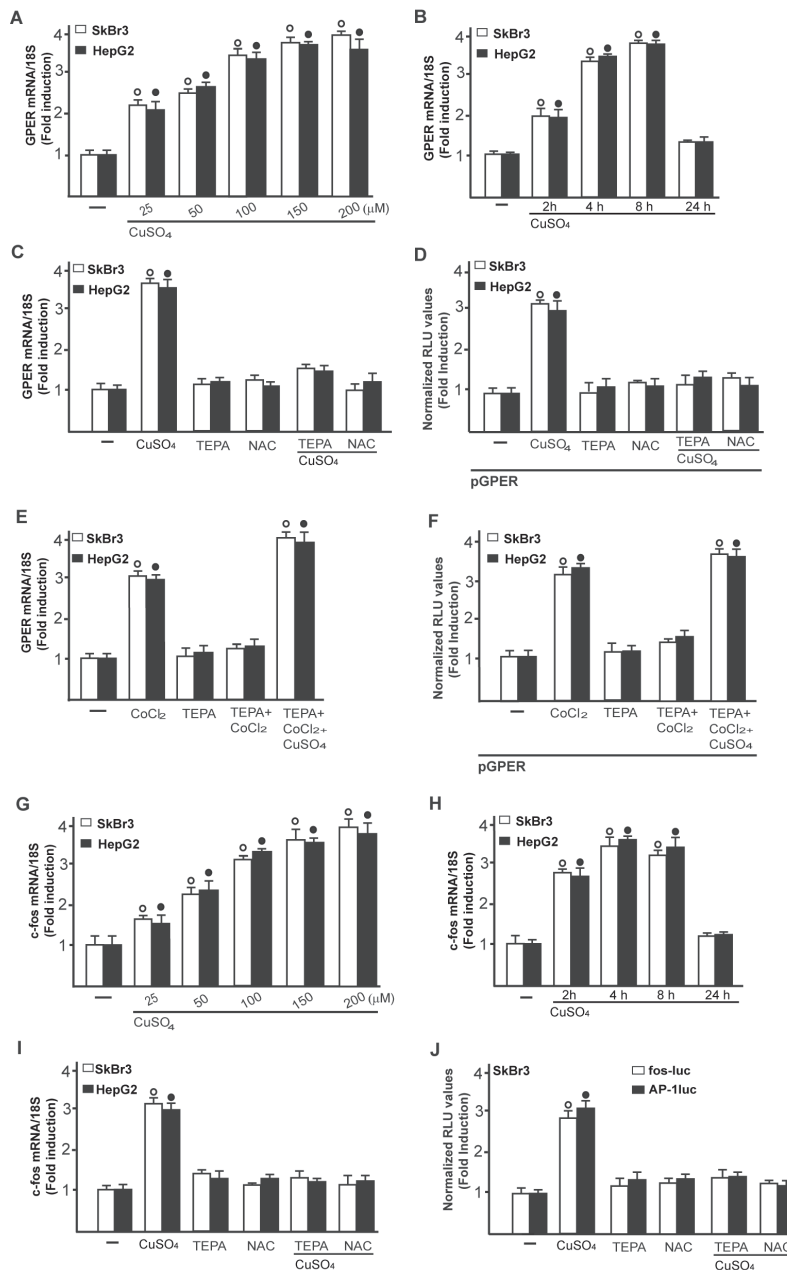


**Figure 3: CuSO<sub>4</sub> induces the mRNA expression of GPER.** mRNA expression of GPER in SkBr3 and HepG2 cells treated with increasing concentrations of CuSO<sub>4</sub> for 8 hours, as evaluated by real-time PCR **A**. CuSO<sub>4</sub> (200 μM) induces the mRNA expression of GPER in a time-dependent manner **B**. The increase in GPER mRNA observed treating SkBr3 and HepG2 cells for 8 hours with 200 μM CuSO<sub>4</sub> is abrogated in the presence of TEPA (50 μM) and NAC (300 μM) **C**. The transactivation of a GPER promoter plasmid (pGPER) observed in SkBr3 and HepG2 cells treated with 200 μM CuSO<sub>4</sub> for 12 hours is prevented by TEPA (50 μM) and NAC (300 μM) **D**. The mRNA induction of GPER observed in SkBr3 and HepG2 cells treated with 100 μM CoCl<sub>2</sub> for 8 hours is abrogated in the presence of TEPA (50 μM) and rescued using CoCl<sub>2</sub> (100 μM for 8 hours) in combination with 200 μM CuSO<sub>4</sub>, as determined by real-time PCR **E**. The transactivation of a GPER promoter plasmid (pGPER) observed in SkBr3 and HepG2 cells treated with 100 μM CoCl<sub>2</sub> for 12 hours is prevented by TEPA (50 μM) and rescued using CoCl<sub>2</sub> (100 μM for 12 hours) in combination with 200 μM CuSO<sub>4</sub> **F**. Dose-response increase of c-fos mRNA expression in SkBr3 and HepG2 cells treated with CuSO<sub>4</sub> for 8 hours, as evaluated by real-time PCR **G**. CuSO<sub>4</sub> (200 μM) induces the mRNA expression of c-fos in a time-dependent manner **H**. The mRNA increase of c-fos observed treating SkBr3 and HepG2 cells for 8 hours with 200 μM CuSO<sub>4</sub> is abrogated in the presence of TEPA (50 μM) and NAC (300 μM) **I**. The transactivation of c-fos (fos-luc) and AP-1 (AP-1luc) reporter plasmids observed in SkBr3 cells treated with 200 μM CuSO<sub>4</sub> for 12 hours is prevented by TEPA (50 μM) and NAC (300 μM) **J**. In transfection assays, the luciferase activities were normalized to the internal transfection control and values of cells receiving vehicle (-) were set as 1-fold induction upon which the activities induced by treatments were calculated. In RNA experiments, values are normalized to the 18S expression and shown as fold changes of mRNA expression induced by treatments compared to cells treated with vehicle (-). Each data point represents the mean ± SD of three independent experiments performed in triplicate. (○), (●) *p* < 0.05 for cells receiving vehicle (-) versus treatments.

and the transactivation of a VEGF promoter construct by  $\text{CuSO}_4$ , as demonstrated by silencing experiments (Figure 10A-10E). Overall, these data highlight the transduction mechanisms involved by copper toward the stimulation of VEGF in cancer cells.

### HIF-1 $\alpha$ and GPER are required for VEGF-induced endothelial tube formation, cell migration and proliferation induced by $\text{CuSO}_4$

Having established that HIF-1 $\alpha$  and GPER cooperate in triggering the up-regulation of VEGF by

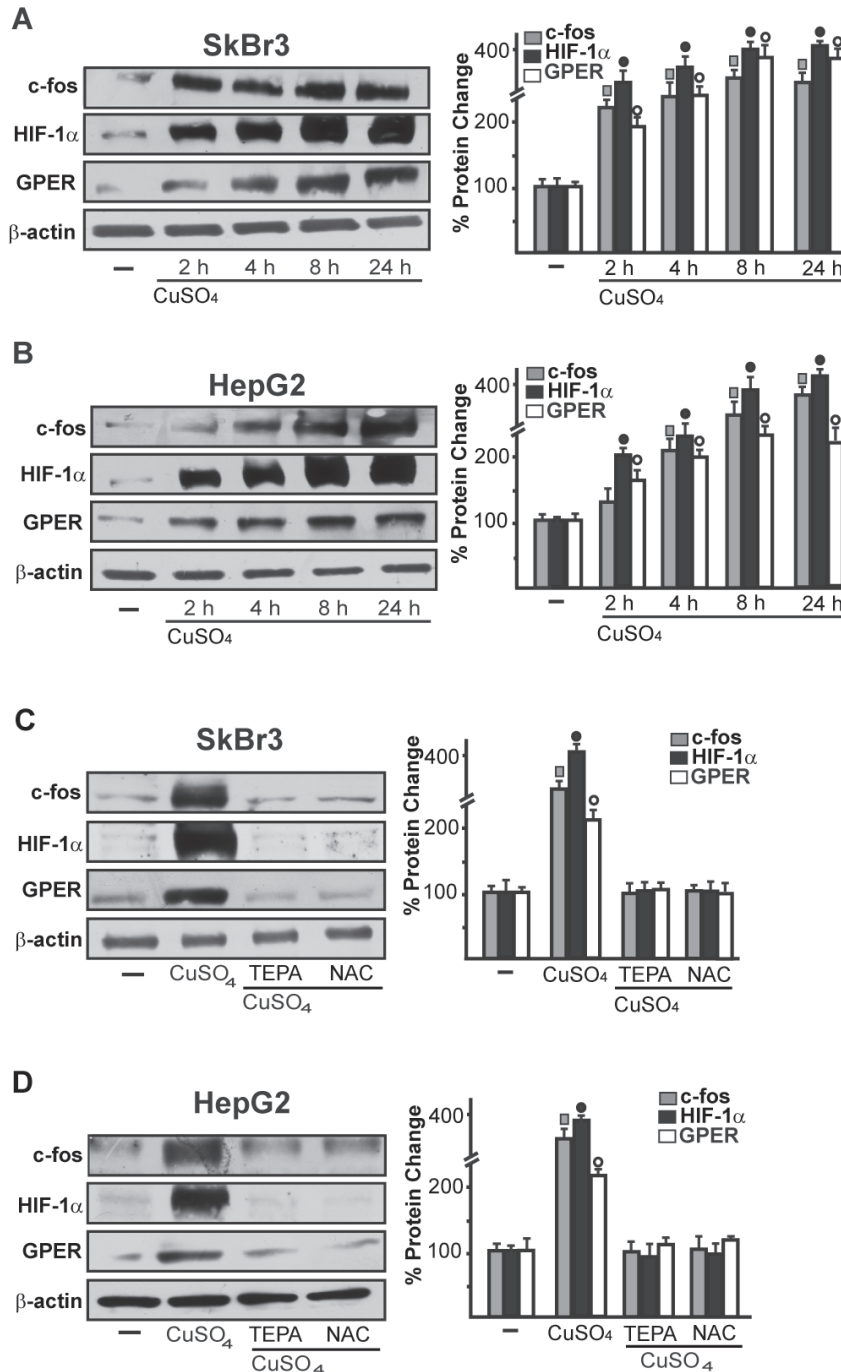


**Figure 4:  $\text{CuSO}_4$  induces the protein expression of c-fos, HIF-1 $\alpha$  and GPER.** Up-regulation of c-fos, HIF-1 $\alpha$  and GPER protein expression in SkBr3 and HepG2 cells treated with 200  $\mu\text{M}$   $\text{CuSO}_4$  for 8 hours **A**, **B**. The induction of c-fos, HIF-1 $\alpha$  and GPER protein expression observed upon treatment with 200  $\mu\text{M}$   $\text{CuSO}_4$  for 8 hours is abolished in the presence of TEPA (50  $\mu\text{M}$ ) and NAC (300  $\mu\text{M}$ ) **C**, **D**. Results shown are representative of three independent experiments. Side panels show densitometric analysis of the blots normalized to  $\beta$ -actin. (■), (●), (○),  $p < 0.05$  for cells receiving vehicle (-) versus  $\text{CuSO}_4$  treatment.

CuSO<sub>4</sub>, we assessed in HUVECs the involvement of HIF-1 $\alpha$  and GPER in the formation of tubule-like structures that represent a useful experimental model of angiogenic process [29]. Interestingly, a ramified network of tubules was generated in HUVECs cultured in conditioned medium from CuSO<sub>4</sub>-treated SkBr3 cells (Figure 11A). However this effect was prevented by knocking down the expression of HIF-1 $\alpha$  or GPER (Figure 11B-11H). The addition of VEGF to the medium collected from CuSO<sub>4</sub>-treated and GPER-silenced SkBr3 cells rescued the generation of tubule structures in HUVECs (Figure 11C). Figure 11 (panels D-F) recapitulates these results, suggesting that VEGF may be considered as a target of copper-activated HIF-1 $\alpha$ /GPER signalling toward new blood vessels formation. As in previous studies VEGF boosted endothelial cells migration [30-31] we then evaluated whether HIF-1 $\alpha$  and GPER are involved in the migration of HUVECs. Conditioned medium from SkBr3 cells exposed to CuSO<sub>4</sub> induced the migration of HUVECs (Figure 12A), however this response was abrogated silencing HIF-1 $\alpha$  and GPER expression (Figure 12B-12E). Indeed, the addition of VEGF rescued cell migration

culturing HUVECs in medium collected from SkBr3 cells which were GPER-silenced and treated with CuSO<sub>4</sub> (Figure 12C). Next, we determined that HIF-1 $\alpha$  and GPER are required for SkBr3 cell proliferation induced by CuSO<sub>4</sub>, as this response was prevented knocking-down their expression (Supplementary Figure S2A-C). Likewise, the growth effects elicited by CuSO<sub>4</sub> was abolished in the presence of TEPA (Supplementary Figure S2D). Altogether, these findings suggest that copper may trigger relevant biological actions through HIF-1 $\alpha$ /GPER/VEGF transduction signalling in both cancer and endothelial cells toward angiogenesis and tumor progression.

## DISCUSSION

The present study provides novel evidence regarding the molecular mechanisms by which copper may trigger the expression and function of VEGF toward angiogenesis and tumor progression. In particular, we have shown that copper activates the EGFR/ERK/c-fos transduction pathway leading to the expression of HIF-1 $\alpha$ , GPER and VEGF in breast and hepatic cancer cells. In this regard,

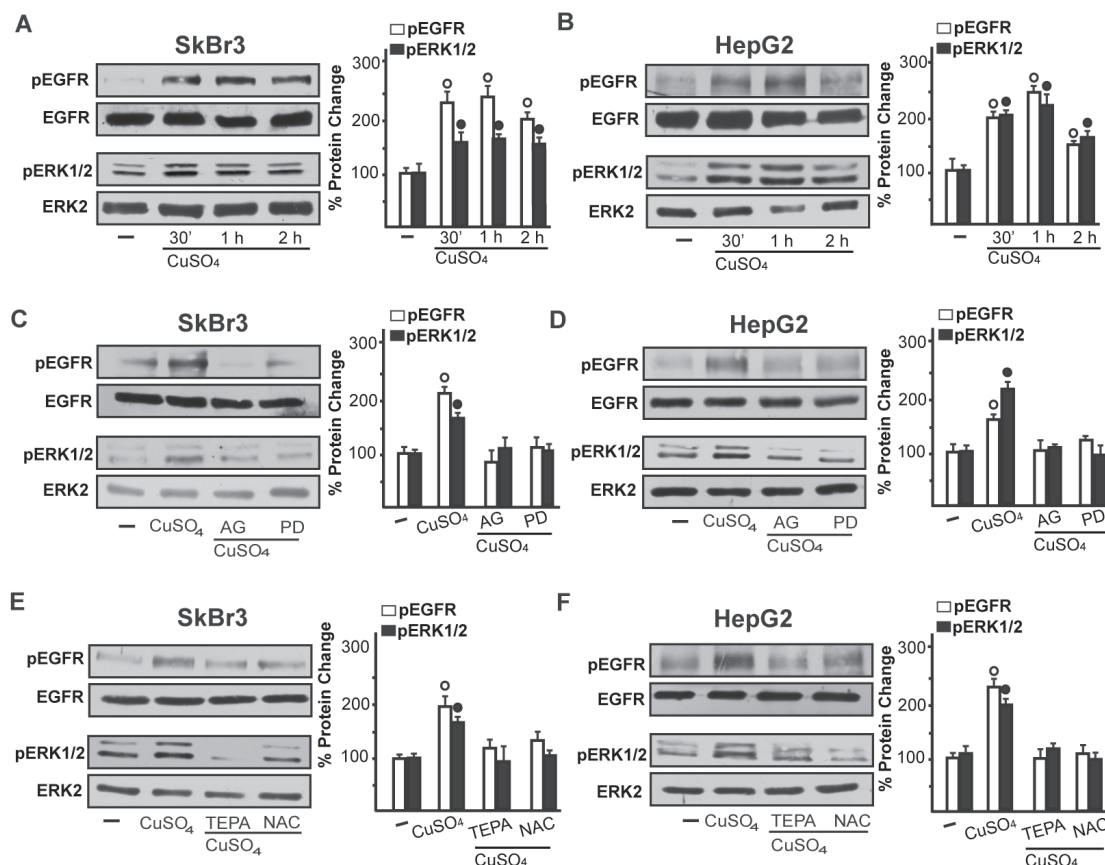


**Figure 5: CuSO<sub>4</sub> induces EGFR and ERK activation.** The exposure to 200  $\mu$ M CuSO<sub>4</sub> induces EGFR (Tyr 1173) and ERK1/2 phosphorylation in SkBr3 and HepG2 cells **A.**, **B.** The activation of EGFR and ERK1/2 observed in SkBr3 and HepG2 cells treated with 200  $\mu$ M CuSO<sub>4</sub> for 30 min is abrogated in the presence of the EGFR inhibitor AG1478 (AG, 10  $\mu$ M) and the MEK inhibitor PD98059 (PD, 10  $\mu$ M) **C.**, **D.** as well as TEPA (50  $\mu$ M) and NAC (300  $\mu$ M) **E.**, **F.** Side panels show densitometric analysis of the blots normalized to EGFR or ERK2. Each data point represents the mean  $\pm$  SD of three independent experiments. ( $\circ$ ), ( $\bullet$ )  $p < 0.05$  for cells receiving vehicle (-) versus CuSO<sub>4</sub> treatment.

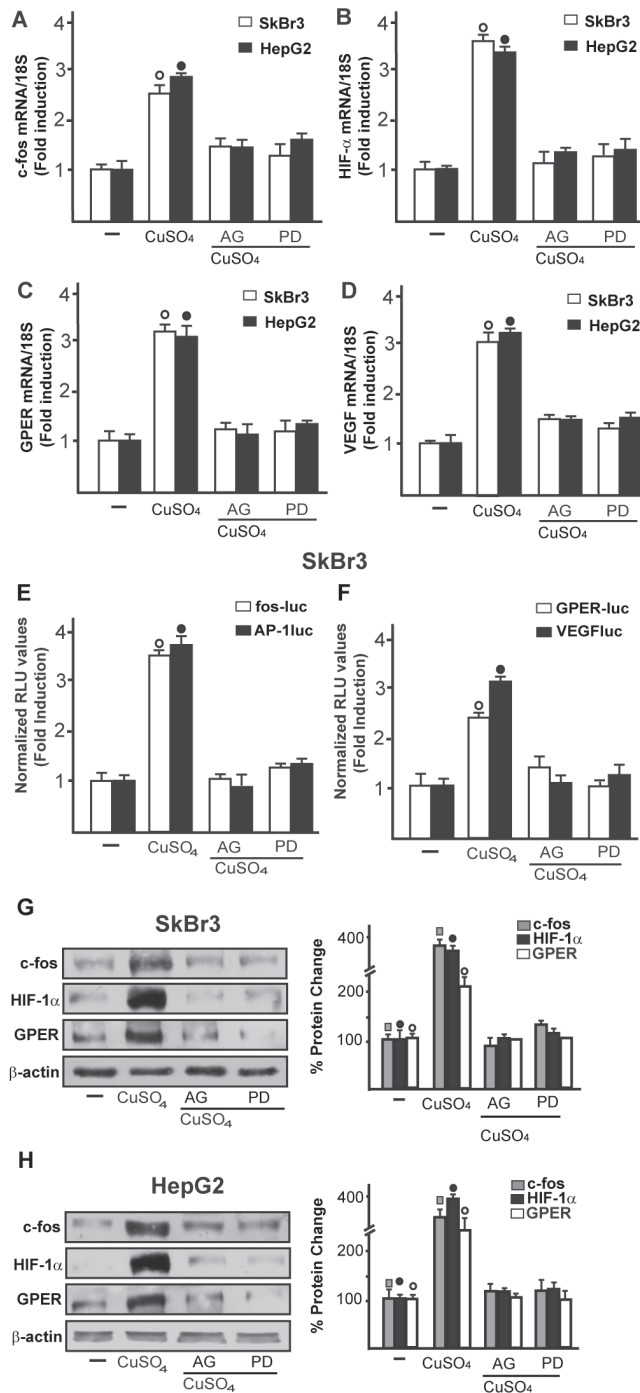


**Figure 6: The EGFR/ERK transduction pathway is involved in the stimulatory responses induced by CuSO<sub>4</sub>.** The mRNA increase of c-fos **A**, HIF-1α **B**, GPER **C**, and VEGF **D**, observed in SkBr3 and HepG2 cells upon treatment with 200 μM CuSO<sub>4</sub> for 8 hours is prevented by AG (10 μM) and PD (10 μM), as evaluated by real-time PCR. Values are normalized to the 18S expression and shown as fold changes of mRNA expression induced by CuSO<sub>4</sub> compared to cells treated with vehicle (-). The transactivation of c-fos, AP-1, GPER and VEGF reporter plasmids induced in SkBr3 cells upon treatment with 200 μM CuSO<sub>4</sub> for 12 hours is abolished using AG (10 μM) and PD (10 μM) **E**, **F**. The luciferase activities were normalized to the internal transfection control and values of cells receiving vehicle (-) were set as 1-fold induction upon which the activities induced by CuSO<sub>4</sub> treatment were calculated. Each data point represents the mean ± SD of three independent experiments performed in triplicate. The up-regulation of c-fos, HIF-1α and GPER protein expression observed in SkBr3 **G**, and HepG2 **H**, cells treated with 200 μM CuSO<sub>4</sub> for 8 hours is abolished in the presence of AG (10 μM) and PD (10 μM) **G**, **H**. Results shown are representative of three independent experiments. Side panels show densitometric analysis of the blots normalized to β-actin. (■), (●) (○), *p* < 0.05 for cells receiving vehicle (-) versus CuSO<sub>4</sub> treatment.

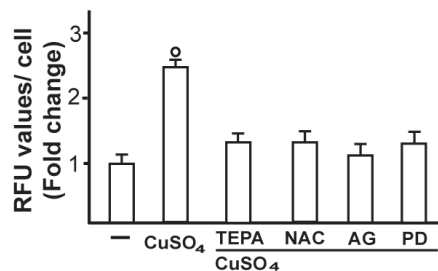
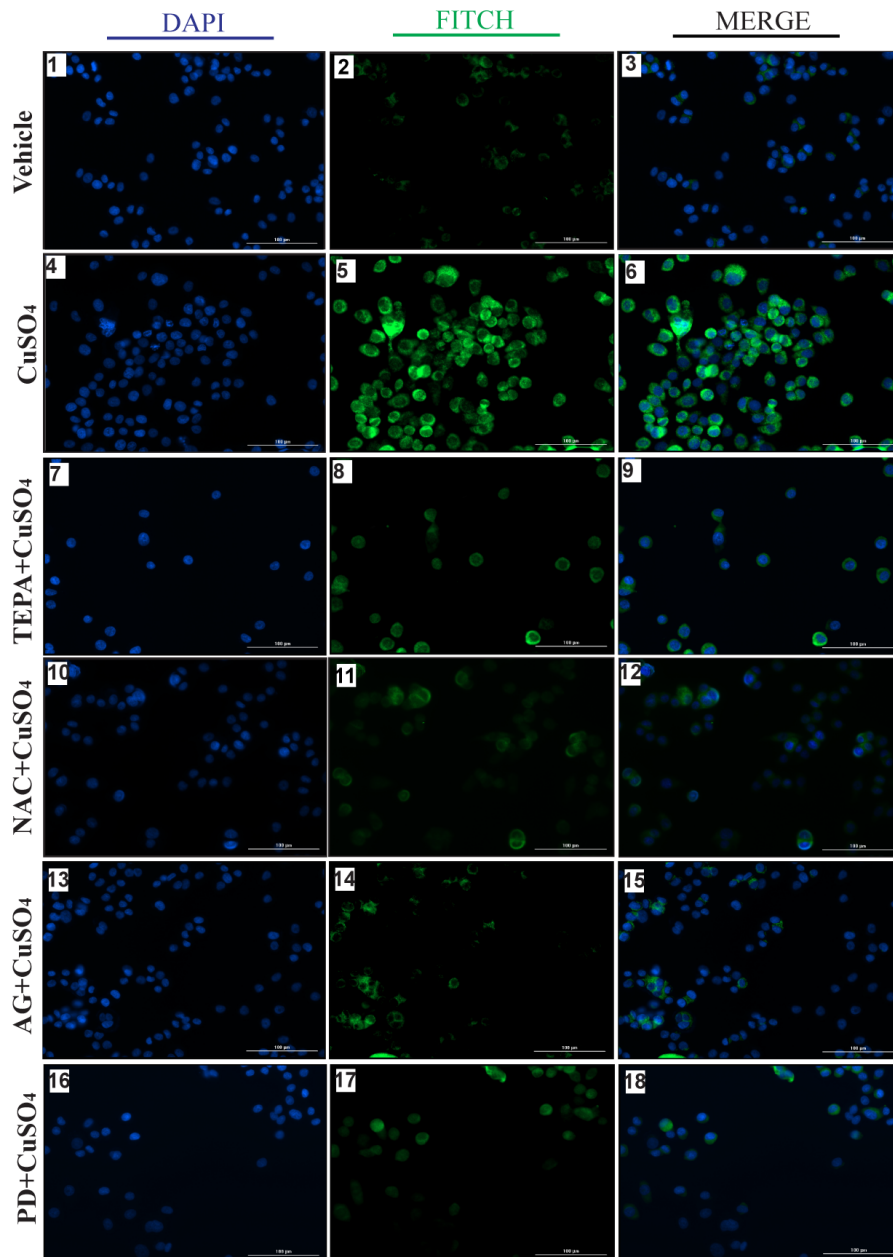


**Figure 7: CuSO<sub>4</sub> induces VEGF protein expression as evaluated by immunofluorescence assay.** SkBr3 cells were treated for 12 hours with vehicle (panels 1-3), 200 μM CuSO<sub>4</sub> alone (panels 4-6) or in combination with TEPA (50 μM) (panels 7-9), NAC (300 μM) (panels 10-12), AG (10 μM) (panels 13-15) and PD (10 μM) (panels 16-18). VEGF accumulation is shown by the green signal, nuclei were stained by DAPI (blue signal). The slides were imaged on the Cytation 3 Cell Imaging Multimode Reader (BioTek, Winooski, VT). Images shown are representative of three independent experiments. Fluorescence intensities for the green channel were quantified in 10 random fields for each condition and results are expressed as fold change of relative fluorescence units (RFU) over the vehicle-treated cells (as indicated in the lower panel). Values are mean ± SD of three independent experiments. (○)  $p < 0.05$  for cells receiving vehicle (-) versus CuSO<sub>4</sub> treatment.

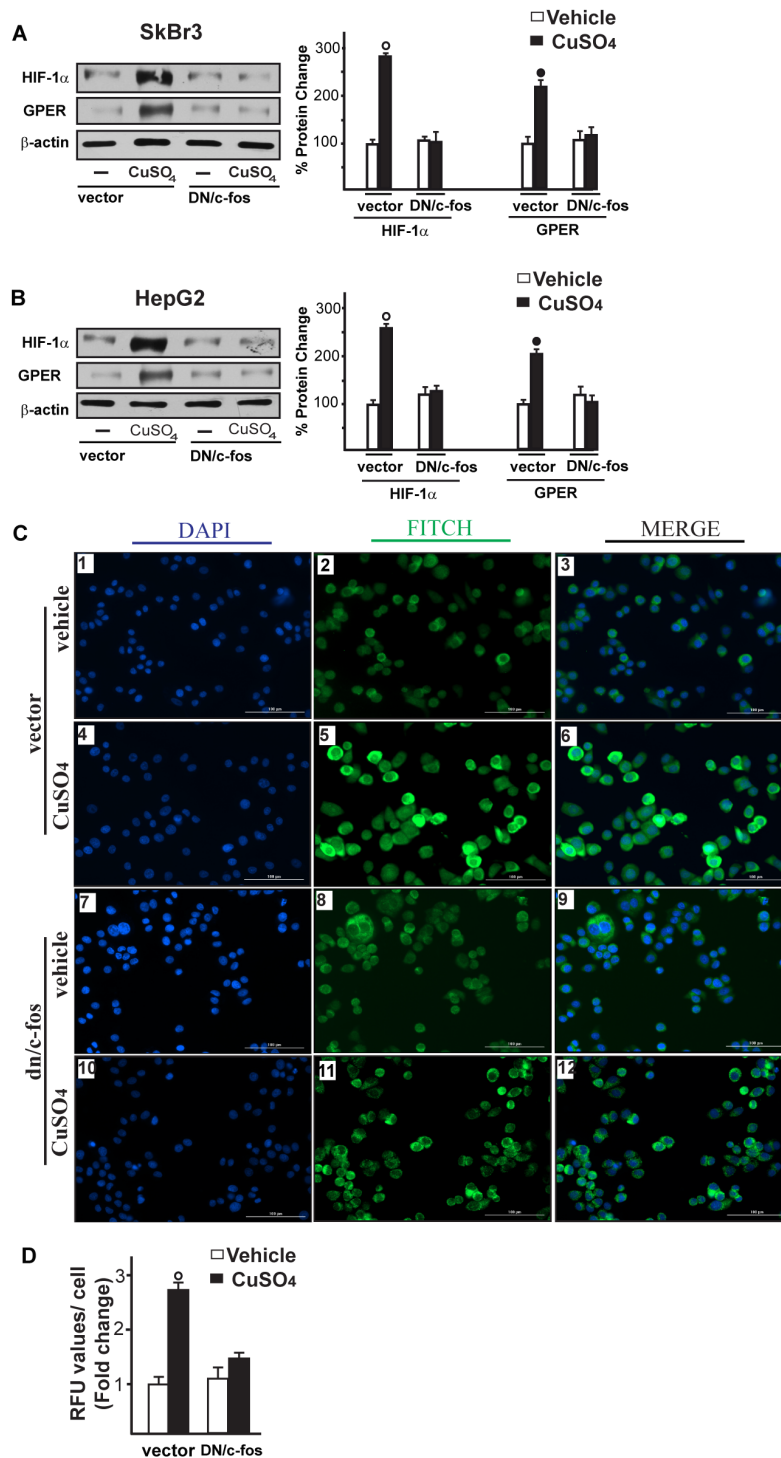


**Figure 8: c-fos is involved in the up-regulation of HIF-1 $\alpha$ , GPER and VEGF induced by CuSO<sub>4</sub>.** Evaluation of HIF-1 $\alpha$  and GPER protein expression in SkBr3 and HepG2 cells transfected for 24 hours with a vector or a plasmid encoding for a dominant negative form of c-fos (DN/c-fos) and then treated with 200  $\mu$ M CuSO<sub>4</sub> for 8 hours (A., B.). Side panels show densitometric analysis of the blots normalized to  $\beta$ -actin. Each data point represents the mean  $\pm$  SD of three independent experiments. Evaluation of VEGF protein expression by immunofluorescence assay in SkBr3 cells transfected for 24 hours with a vector (panels 1-6) or a plasmid encoding for a dominant negative form of c-fos (DN/c-fos) (panels 7-12) and then treated with vehicle or 200  $\mu$ M CuSO<sub>4</sub> for 12 hours, as indicated. VEGF accumulation is shown by the green signal, nuclei were stained by DAPI (blue signal). The slides were imaged on the Cytation 3 Cell Imaging Multimode Reader (BioTek, Winooski, VT). Images shown are representative of three independent experiments C. Fluorescence intensities for the green channel were quantified in 10 random fields for each condition and results are expressed as fold change of relative fluorescence units (RFU) over the vehicle-treated cells D. Values are mean  $\pm$  SD of three independent experiments. (○), (●)  $p < 0.05$  for cells receiving vehicle (-) *versus* CuSO<sub>4</sub> treatment.

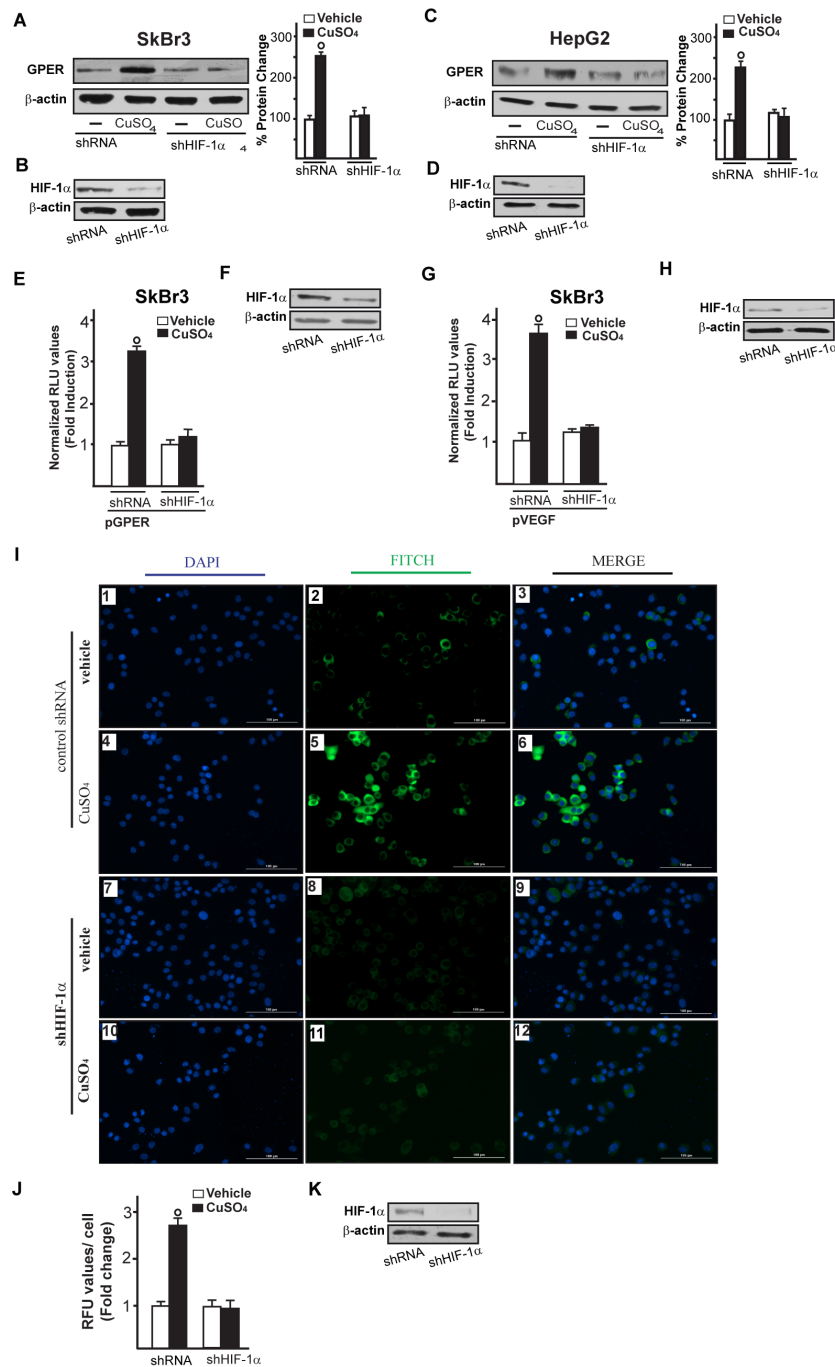


**Figure 9: HIF-1 $\alpha$  is involved in the up-regulation of GPER and VEGF induced by CuSO<sub>4</sub>.** Evaluation of GPER protein expression in SkBr3 and HepG2 cells transfected with shRNA or shHIF-1 $\alpha$  for 24 hours and then treated with 200  $\mu$ M CuSO<sub>4</sub> for 8 hours **A**, **C**. Side panels show densitometric analysis of the blots normalized to  $\beta$ -actin. Efficacy of HIF-1 $\alpha$  silencing in SkBr3 and HepG2. Each data point represents the mean  $\pm$  SD of three independent experiments **B**, **D**. **E**-**H**. The transactivation of the GPER (pGPER) **E** and VEGF (pVEGF) **G**, promoter plasmids observed in SkBr3 cells treated with 200  $\mu$ M CuSO<sub>4</sub> for 12 hours is abrogated silencing the expression of HIF-1 $\alpha$ . (**F**, **H**) Efficacy of HIF-1 $\alpha$  silencing. The luciferase activities were normalized to the internal transfection control and values of cells receiving vehicle were set as 1-fold induction, upon which the activities induced by treatments were calculated. Each data point represents the mean  $\pm$  SD of three independent experiments performed in triplicate. **I**. Evaluation of VEGF protein expression by immunofluorescence assay in SkBr3 cells transfected for 24 hours with shRNA (panels 1-6) or shHIF-1 $\alpha$  (panels 7-12) and treated with 200  $\mu$ M CuSO<sub>4</sub> for 12 hours, as indicated. VEGF accumulation is shown by the green signal, nuclei were stained by DAPI (blue signal). The slides were imaged on the Cytation 3 Cell Imaging Multimode Reader (BioTek, Winooski, VT). Images shown are representative of three independent experiments. **J**. Fluorescence intensities for the green channel were quantified in 10 random fields for each condition and results are expressed as fold change of relative fluorescence units (RFU) over the vehicle-treated cells. Values are mean  $\pm$  SD of three independent experiments. **K**. Efficacy of HIF-1 $\alpha$  silencing. ( $\circ$ )  $p < 0.05$  for cells receiving vehicle *versus* CuSO<sub>4</sub> treatment.

we demonstrated that a functional cooperation between HIF-1 $\alpha$  and GPER contributes to VEGF regulation in cancer cells exposed to copper. Recalling previous studies on the capability of copper chelating agents to elicit anti-

tumor effects [5, 32], we have also evidenced that these chemicals exert an inhibitory action on HIF-1 $\alpha$ /GPER/VEGF transduction pathway. Next, we have found that HIF-1 $\alpha$  and GPER are required for endothelial tube

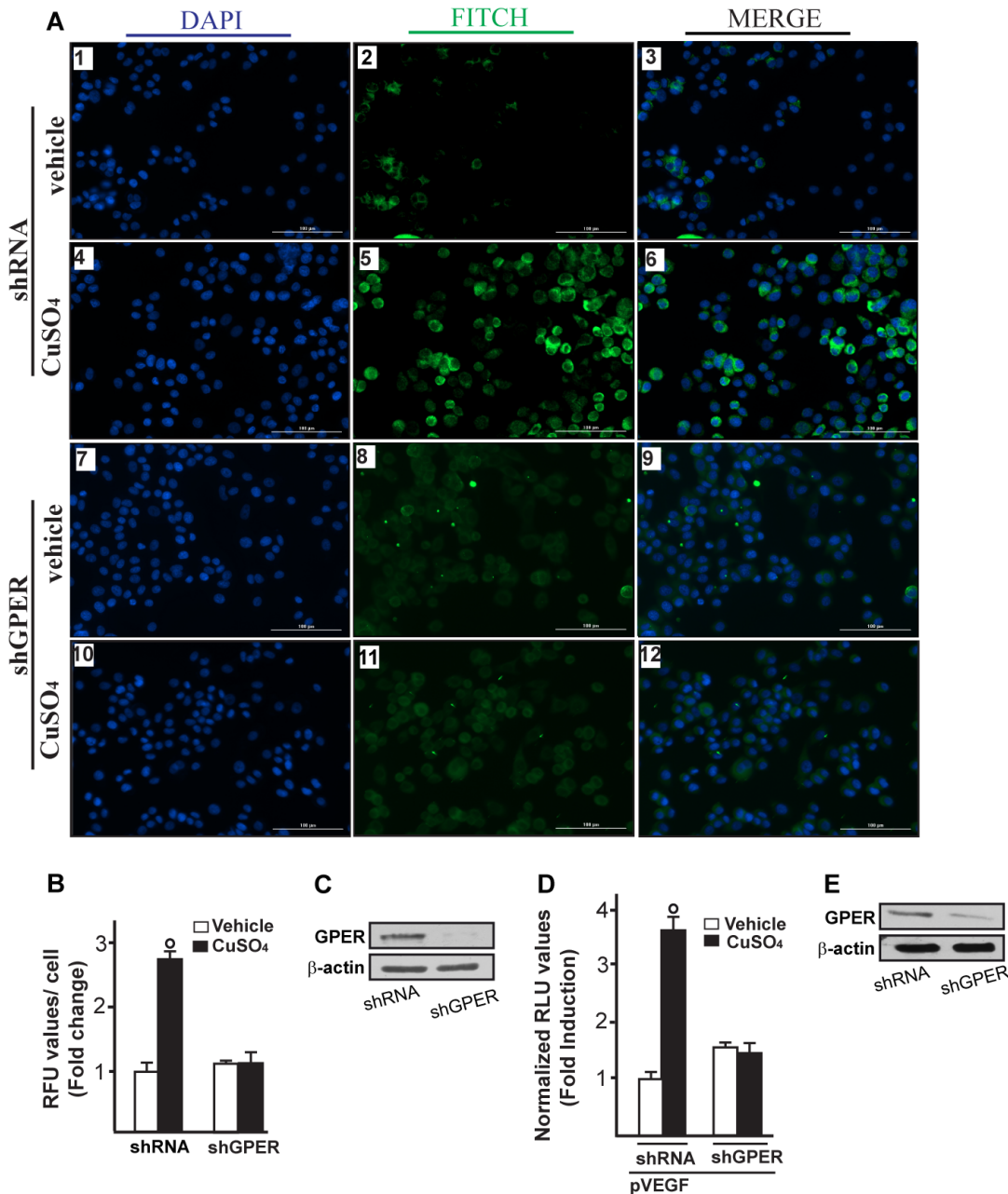


**Figure 10: GPER is involved in VEGF protein increase induced by CuSO<sub>4</sub>.** Evaluation of VEGF protein expression by immunofluorescence assay in SkBr3 cells transfected for 24 hours with shRNA (panels 1-6) or shGPER (panels 7-12) and treated with 200  $\mu$ M CuSO<sub>4</sub> for 12 hours, as indicated. VEGF accumulation is evidenced by the green signal, nuclei were stained by DAPI (blue signal). The slides were imaged on the Cytation 3 Cell Imaging Multimode Reader (BioTek, Winooski, VT). Images shown are representative of three independent experiments **A**. Fluorescence intensities for the green channel were quantified in 10 random fields for each condition and results are expressed as fold change of relative fluorescence units (RFU) over the vehicle-treated cells **B**. Values are mean  $\pm$  SD of three independent experiments. Efficacy of GPER silencing **C**. The transactivation of the VEGF (pVEGF) promoter plasmid observed in SkBr3 cells treated with 200  $\mu$ M CuSO<sub>4</sub> for 12 hours is abrogated silencing the expression of GPER **D**. The luciferase activities were normalized to the internal transfection control and values of cells receiving vehicle were set as 1-fold induction, upon which the activities induced by treatments were calculated. Efficacy of GPER silencing **E**. Each data point represents the mean  $\pm$  SD of three independent experiments performed in triplicate. (o)  $p < 0.05$  for cells receiving vehicle (-) versus CuSO<sub>4</sub> treatment.

formation and cell migration stimulated by VEGF as well as for copper-induced proliferation of breast cancer cells.

The role of copper in tumor initiation and progression has been extensively investigated both *in*

*vitro* and *in vivo* [8, 33]. In this context, high copper levels ranging from 50 to 200  $\mu$ M have been correlated with incidence and recurrence in cancer patients [8, 9]. In accordance with these findings, we have ascertained

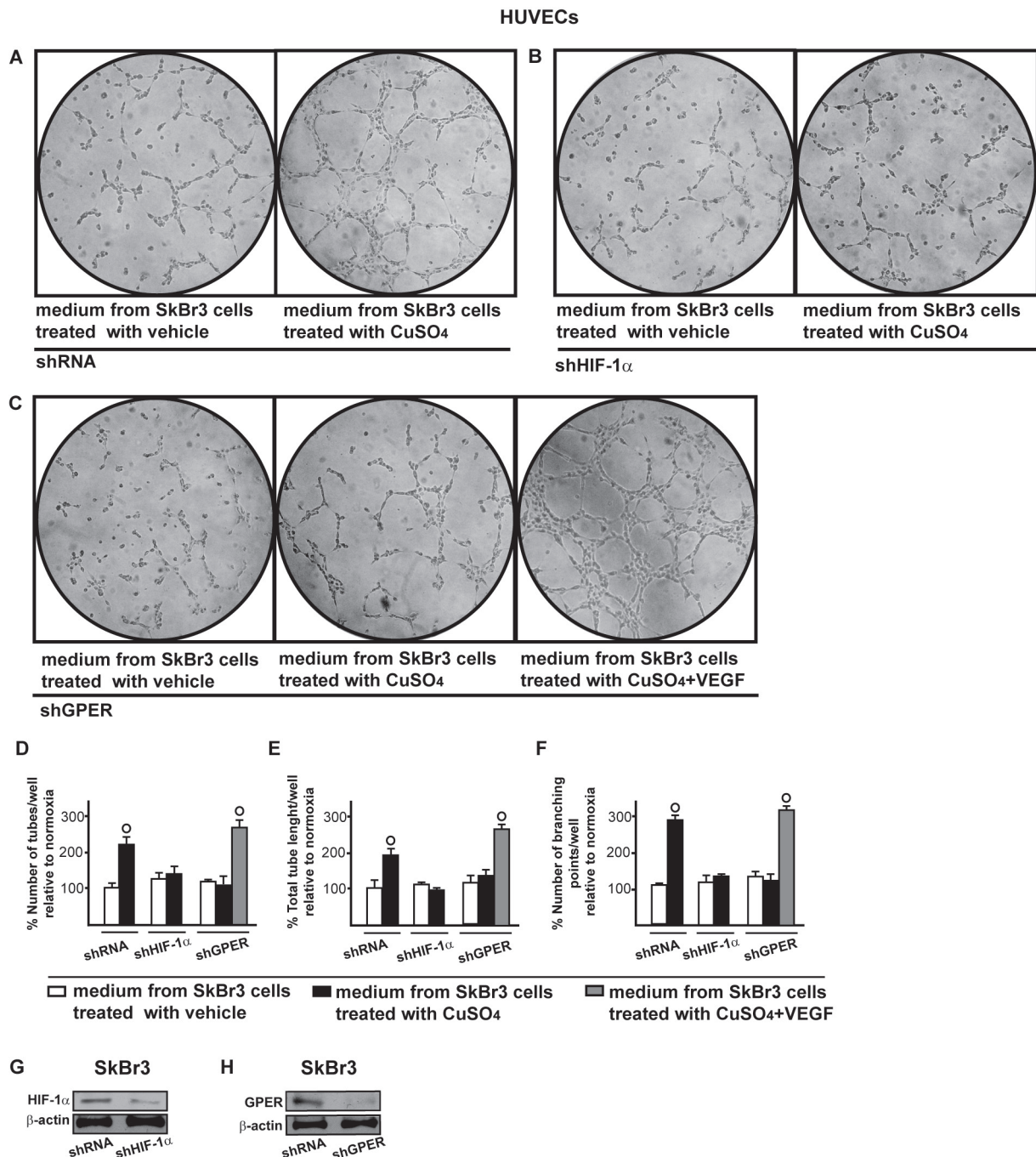


**Figure 11: HIF-1 $\alpha$  and GPER contribute to the endothelial tube formation triggered by CuSO<sub>4</sub>.** Tube formation in HUVECs cultured for 2 hours in medium collected from SkBr3 cells which were transfected for 24 hours with shRNA **A**, shHIF-1 $\alpha$  **B**, or shGPER **C**, and then treated for 18 hours with vehicle or 200  $\mu$ M CuSO<sub>4</sub>, as indicated. **C**. In HUVECs cultured in conditioned medium from SkBr3 cells that were transfected with shGPER and treated with 200  $\mu$ M CuSO<sub>4</sub>, tube formation is rescued adding 10 ng/mL VEGF for 2 hours. Data are representative of three independent experiments performed in triplicate. Quantification of the number of tubes **D**., total tube length **E**., and number of branching points **F**., observed in HUVECs, as indicated. Data are representative of three independent experiments performed in triplicate. (○)  $p < 0.05$  for cells receiving medium from SkBr3 cells treated with vehicle *versus* cells receiving medium from SkBr3 cells treated with CuSO<sub>4</sub>. Efficacy of HIF-1 $\alpha$  **G**, and GPER **H**, silencing in SkBr3 cells.

that copper exerts stimulatory effects on gene expression starting from a concentration of 25  $\mu\text{M}$ , even though the maximal responses were observed using a concentration of 200  $\mu\text{M}$ . Hence, the last amount was used in all assays to better evaluate the potential of copper to activate the aforementioned biological activity. Previous studies have disclosed that certain effects elicited by copper in cancer cells rely on the generation of reactive oxygen species (ROS), which act as second messenger in triggering stimulatory signals [8]. In this regard, it has been shown the transduction mechanisms involved, that include the activation of the EGFR/ERK pathway and the expression of genes mediating growth responses like c-fos [reviewed in 5]. On the basis of these observations, it could be argued that copper may mimic some biological features which characterize the hypoxic tumor environment.

HIF-1 acts as a survival factor upon low oxygen conditions regulating the expression of genes involved

in cell metabolism, migration, invasion and angiogenesis [34-35]. In this vein, it is worth mentioning that copper was shown to increase HIF-1 $\alpha$  stabilization and accumulation [19]. Further extending these findings, our current results indicate that copper is also able to induce HIF-1 $\alpha$  expression, thus providing a new mechanism through which this chemical may be involved in cancer progression. Previous studies have determined that GPER contributes together with HIF-1 $\alpha$  to the adaptive responses to hypoxic tumor microenvironment [17, 24]. Nicely fitting with these observations, the present data reveal that copper induces the expression of GPER through HIF-1 $\alpha$ , leading to the regulation of VEGF in breast cancer cells and cancer associated fibroblasts (CAFs) [17]. The stimulatory role of copper in cancer development has been also proved by copper chelating agents as a reduction in tumor volume, vascular permeability, tumor's microvascular supply and micrometastasis generation has been reported

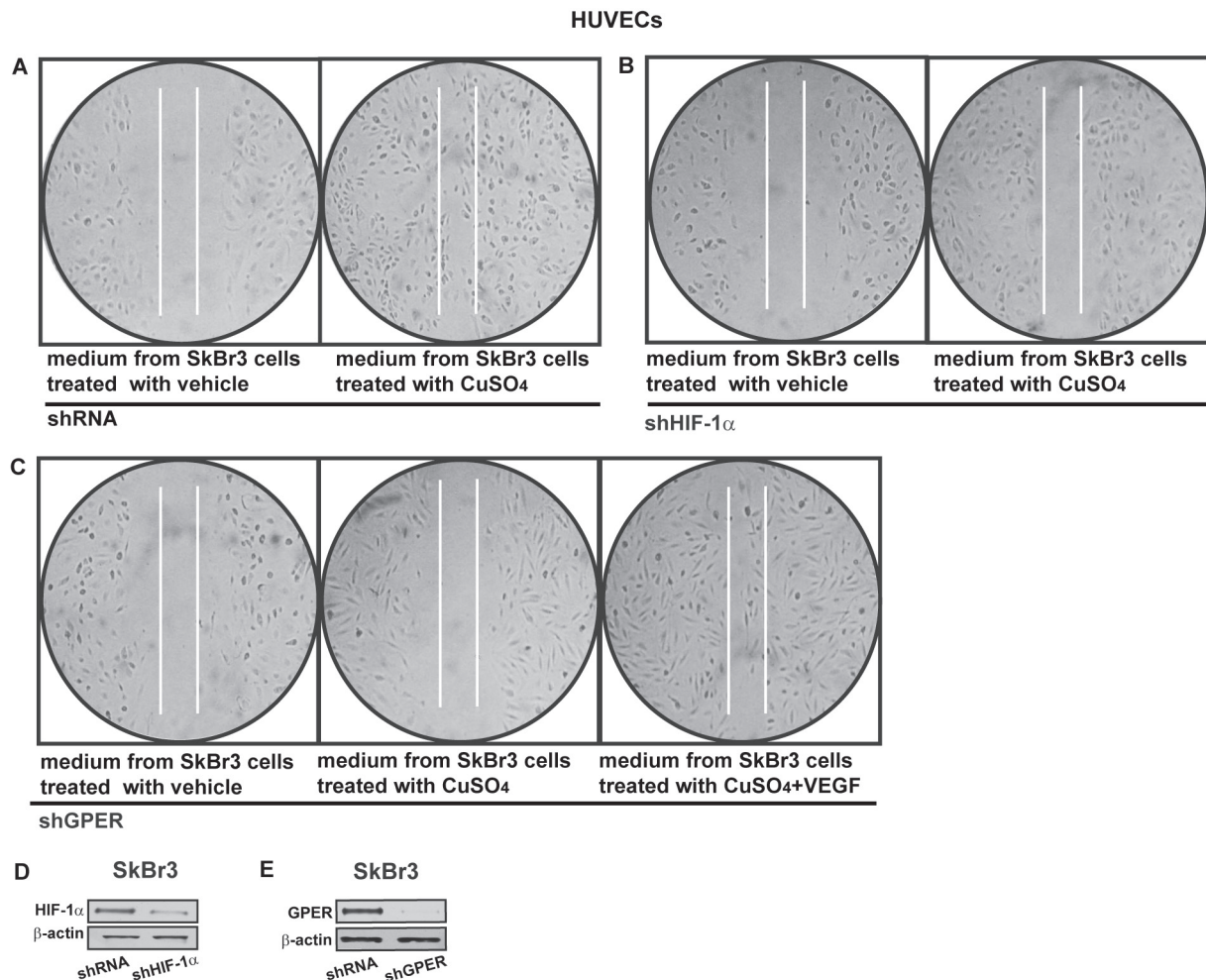


**Figure 12: HIF-1 $\alpha$  and GPER contribute to the endothelial cell migration induced by  $\text{CuSO}_4$ .** Cell migration in HUVECs cultured for 24 hours in medium collected from SkBr3 cells which were transfected for 24 hours with control shRNA **A.**, shHIF-1 $\alpha$  **B.** or shGPER **C.** and then treated for 18 hours with vehicle or 200  $\mu\text{M}$   $\text{CuSO}_4$ , as indicated. **C.** In HUVECs cultured in medium from SkBr3 cells which were transfected with shGPER and treated with 200  $\mu\text{M}$   $\text{CuSO}_4$ , cell migration is rescued adding 10 ng/mL VEGF for 36 hours. Data are representative of three independent experiments performed in triplicate. Efficacy of HIF-1 $\alpha$  **D.** and GPER **E.** silencing in SkBr3 cells.

lowering copper levels in diverse experimental models [5]. Extending the current knowledge on the action of anti-copper drugs like TEPA, our data indicate that these chemicals may also target HIF-1 $\alpha$ /GPER signalling among the multifaceted responses triggered in cancer cells.

To date, the expression of GPER has been associated with negative clinical features and poor survival rates in a variety of tumors [36-38]. Consequently, huge efforts are currently underway to better understand the mechanisms involved in the regulation of GPER [28, 39-58] which belongs to the GPCRs family widely involved in cancer progression [59, 60]. Of note, several studies have demonstrated that estrogenic GPER signalling mediates relevant biological effects like proliferation and migration in cancer cells and CAFs [61-63] that are largely acknowledged to contribute to tumor cell metabolism and disease progression [64-66]. In this regard, additional investigations are needed to determine whether copper could be also able to activate GPER signalling in a direct manner, as previously demonstrated using other metals [67].

Here, we have provided novel evidence regarding the action elicited by copper toward tumor angiogenesis and progression. On the basis of the present findings GPER may be included together with HIF-1 $\alpha$  and VEGF among the molecular targets of copper chelating agents in combination therapies. Nevertheless, further studies are needed to better define the role of copper on the functional interaction between GPER, HIF-1 $\alpha$  and VEGF in malignant cells and tumor microenvironment.

## MATERIALS AND METHODS

### Materials

Copper sulfate (CuSO<sub>4</sub>), cobalt chloride (CoCl<sub>2</sub>), tetraethylenepentamine (TEPA) and ROS scavenger N-acetyl-L-cysteine (NAC) were purchased from Sigma-Aldrich Srl (Milan, Italy). Tyrphostin AG1478 (AG) was purchased from Biomol Research Laboratories, Inc (Milan, Italy). PD98059 (PD) was obtained from Calbiochem (Milan, Italy). Human VEGF was purchased from Peprotech (Rocky Hill, New Jersey, USA). All compounds were dissolved in DMSO, except VEGF, CuSO<sub>4</sub> and NAC which were solubilized in water.

### Cell cultures

We used SkBr3 breast cancer cells and HepG2 hepatocarcinoma cells that represent a valuable tool for the evaluation of the transduction pathways activated by copper in cancer cells. As both cell lines express GPER, which has been involved with the angiogenic process within the tumor microenvironment [17-18], this model

system is suitable to ascertain the contribution of GPER to copper action toward tumor angiogenesis.

The SkBr3 breast cancer cells were maintained in RPMI-1640 (Life Technologies, Milan, Italy) without phenol red, supplemented with 10% fetal bovine serum (FBS) and 100  $\mu$ g/ml penicillin/streptomycin. The hepatocarcinoma cells HepG2 were cultured in DMEM (Dulbecco's modified Eagle's medium) (Life Technologies, Milan, Italy) with phenol red, supplemented with 10% FBS and 100  $\mu$ g/ml penicillin/streptomycin. Human umbilical vein endothelial cells (HUVECs) were seeded on collagen-coated flasks (Sigma-Aldrich Srl, Milan, Italy) and cultured in Endothelial Growth Medium (EGM) (Lonza, Milan, Italy), supplemented with 5% FBS (Lonza, Milan, Italy). All cell lines were grown in a 37 $^{\circ}$  C HeraCell incubator (ThermoScientific-Heraeus, Milan, Italy) with 5% CO<sub>2</sub>. For hypoxic stimulation, cells were treated with CoCl<sub>2</sub> (100  $\mu$ M) or cultured in the presence of a low oxygen tension (2% O<sub>2</sub>) in a multi-gas HeraCell incubator (ThermoScientific-Heraeus, Milan, Italy). Cells were switched to medium without serum the day before experiments.

### Gene reporter assays

The 2.6 kb VEGF promoter-luciferase construct containing full-length VEGF promoter sequence (22,361 to +298 bp relative to the transcription start site) used in luciferase assays was a kind gift from dr. P. Soumitro (Harvard Medical School, Boston, Massachusetts). The GPER promoter-luciferase construct (pGPER 2.9 kb) was obtained as previously described [24].

The luciferase reporter plasmid for AP-1 responsive collagen promoter was a kind gift from H. Van Dam (Department of Molecular Cell Biology, Leiden University, Leiden, Netherlands). The luciferase reporter plasmid for c-fos, encoding a -2.2 kb 5' upstream fragment of human c-fos, kindly provided by K. Nose (Department of Microbiology, Showa University School of Pharmaceutical Sciences, Hatanodai, Shinagawa-ku, Tokyo, Japan). SkBr3 and HepG2 cells (1 x 10<sup>5</sup>) were plated into 24-well dishes with 500 $\mu$ L/well culture medium containing 10% FBS. Transfections were performed using X-treme GENE 9 DNA transfection reagent as recommended by the manufacturer (Roche Diagnostics, Milan, Italy), with a mixture containing 0.5 $\mu$ g of reporter plasmid and 10 ng of pRL-TK. After 24 h, cells were treated with CuSO<sub>4</sub>, alone and in combination with TEPA, NAC, AG1478 and PD98059, as indicated. For co-transfection experiments, cells were previously transfected with control shRNA, shHIF-1 $\alpha$  or shGPER using X-treme GENE 9 DNA transfection reagent (Roche Diagnostics, Milan, Italy). A mixture containing 0.5  $\mu$ g of reporter plasmid and 10 ng of pRL-TK was then transfected by using X-treme GENE 9 DNA Transfection. After 8 hours, cells were treated for 18 hours with CuSO<sub>4</sub>

in serum free medium. Luciferase activity was measured with the Dual Luciferase Kit (Promega, Milan, Italy) normalized to the internal transfection control provided by Renilla luciferase activity. The normalized relative light unit values obtained from cells treated with vehicle were set as 1-fold induction, upon which the activity induced by treatments was calculated.

### Gene expression studies

Total RNA was extracted from cell cultures using the TRIzol commercial kit (Life Technologies, Milan, Italy) according to the manufacturer's protocol. RNA was quantified spectrophotometrically and quality was checked by electrophoresis through agarose gels stained with ethidium bromide. Only samples that were not degraded and showed clear 18 and 28 S bands under UV light were used for RT-PCR. Total cDNA was synthesized from the RNA by reverse transcription as previously described [17]. The expression of selected genes was quantified by real-time PCR using Step One<sup>(TM)</sup> sequence detection system (Applied Biosystems Inc, Milan, Italy), following the manufacturer's instructions. Gene-specific primers were designed using Primer Express version 2.0 software (Applied Biosystems, Inc., Milan, Italy) and are as follows: : HIF-1 $\alpha$  Fwd: 5'-TGCATCTCCATCTTCTACCCAAGT-3' and Rev: 5'-CCGACTGTGAGTGCCACTGT-3'; VEGF Fwd: 5'- TGCAGATTATGCGGATCAAACC-3' and Rev: 5'- TGCATTACATTTGTTGTGCTGTAG-3'; GPER Fwd: 5'-CCTGGACGAGCAGTATTACGATATC-3' and Rev 5'-TGCTGTACATGTTGATCTG-3'; c-FOS Fwd: 5'-GAGCCCTTTGATGACTTCCT-3' and Rev: 5'-GAGCGGGCTGTCTCAGA-3'; 18S Fwd: 5'- GGCGTCCCCCAACTTCTTA -3' and Rev: 5'-GGGCATCACAGACCTGTTATT -3'. Assays were performed in triplicate and the results were normalized for 18S expression and then calculated as fold induction of RNA expression.

### Western blot analysis

SkBr3 and HepG2 cells were processed according to the previously described protocol [17] to obtain protein lysate that was electrophoresed through a reducing SDS/10% (w/v) polyacrylamide gel, electroblotted onto a nitrocellulose membrane and probed with primary antibodies against HIF-1 $\alpha$  (R&D Systems, Inc. Celbio, Milan, Italy), GPER (N-15), c-fos (H-125), phosphorylated ERK 1/2 (E-4), ERK2 (C-14), EGFR (1005), pEGFR Tyr 1173 (sc-12351-R) and  $\beta$ -actin (C2), all purchased from Santa Cruz Biotechnology, (DBA, Milan, Italy). Proteins were detected by horseradish peroxidase-linked secondary antibodies (Santa Cruz Biotechnology, DBA) and revealed using the ECL System (GE Healthcare).

### Gene silencing experiments

Cells were plated onto 10-cm dishes and prior to treatments cells were transfected for 24 hours using X-treme GENE 9 DNA Transfection Reagent (Roche Diagnostics, Milan, Italy) with a control shRNA, shHIF-1 $\alpha$ , shGPER, a control vector and the plasmid DN/c-fos, encoding a c-fos mutant that heterodimerizes with c-fos dimerization partners but not allowing DNA binding (kindly obtained from Dr. C. Vinson, NIH, Bethesda, MD, USA). The HIF-1 $\alpha$  shRNA and the respective control plasmid were purchased from SABioscience Corporation (Frederick, MD, USA). The silencing of GPER expression was obtained by the construct which we have previously described and used [68].

### Immunofluorescence assay

Fifty percent confluent cultured SkBr3 cells grown on coverslips were serum deprived and then treated for 12 hours with CuSO<sub>4</sub> alone and in combination with TEPA, NAC, AG1478 and PD98059, as indicated. Where required, cells previously transfected for 24 h with shHIF-1 $\alpha$  or shGPER and respective negative control plasmids (as described above) and then treated for 18 hours with CuSO<sub>4</sub>. Then cells were fixed in 4% paraformaldehyde, permeabilized with 0.2% Triton X-100, washed three times with PBS and incubated overnight with a mouse primary antibody against VEGF (C-1) (Santa Cruz Biotechnology, DBA, Milan, Italy). After incubation, the slides were extensively washed with PBS and incubated with 4',6-diamidino-2-phenylindole dihydrochloride (DAPI), (1:1000), (Sigma-Aldrich, Milan, Italy) and donkey anti-mouse IgG-FITC (1:300; purchased from Alexa Fluor, Life Technologies, Milan, Italy). The slides were imaged on the Cytation 3 Cell Imaging Multimode reader (BioTek, Winooski, VT) and analysed using the software Gen5 (BioTek, Winooski, VT).

### Conditioned medium

SkBr3 cells were cultured in regular growth medium, then cells were washed twice with PBS and transfected for 24 hours in serum-free RPMI-1640 with shHIF-1 $\alpha$ , shGPER or control shRNA using X-treme GENE 9 DNA Transfection Reagent (Roche Diagnostics, Milan, Italy). Cells were treated for 18 hours with CuSO<sub>4</sub>, culture medium was then replaced for additional 18 hours with medium without serum. Thereafter, the supernatants were collected, centrifuged at 3,500 rpm for 5 minutes to remove cell debris and used as conditioned medium in HUVECs.

## Tube formation assay

The day before the experiment, confluent HUVECs were starved overnight at 37 °C in serum free medium (EBM, Lonza, Milan, Italy). Growth factor-reduced Matrigel® (Cultrex, Trevigen Inc, USA) was thawed overnight at 4 °C on ice, plated on the bottom of prechilled 96well-plates and left at 37°C for 1 h for gelification. Starved HUVECs were collected by enzymatic detachment (0.25% trypsin-EDTA solution, Life Technologies, Milan, Italy), counted and resuspended in conditioned medium from CAFs. Then, 10,000 cells/well were seeded on Matrigel and incubated at 37 °C. Tube formation was observed starting from 2 h after cell seeding and quantified by using the software NIH ImageJ (National Institutes of Health (NIH), Rockville Pike, Bethesda, Maryland, USA)

## Migration assay

Twelve-well plates were coated with 500 µL fibronectin for 2 hours at 37°C (Sigma Aldrich, Milan, Italy). HUVECs were allowed to grow in regular growth medium until they reached a 70% to 80% confluence. Next, to create a scratch of the cell monolayer, a p200 pipette tip was used. Cells were washed twice with PBS and then incubated in medium collected from SkBr3 cells as previously described. The migration assay was evaluated after 24 hours of treatment.

## MTT growth assay

For quantitative proliferation assay, cells ( $1 \times 10^5$ ) were seeded in 24-well plates in regular growth medium. Cells were washed once they had attached and then incubated in medium containing 2.5% charcoal-stripped FBS with the indicated treatments; medium was renewed every day (with treatments) before dimethylthiazoldiphenyltetrazoliumbromide (MTT, Sigma-Aldrich, Milan, Italy) assay which was performed according to the manufacturer's protocol. A concentration of 250ng/L of the control shRNA, shHIF-1 $\alpha$  or shGPER plasmids was transfected using X-treme GENE 9 DNA Transfection Reagent the day before treatments. The absorbance was measured using a FLX-800 microplate fluorimeter (Bio-Tek Instruments, Inc., Winooski, VT, USA) at a test wavelength of 570 nm. Each experiment was performed at in triplicate.

## Statistical analysis

Statistical analysis was performed using ANOVA followed by Newman-Keuls' testing to determine differences in means.  $p < 0.05$  was considered statistically

significant.

## ACKNOWLEDGMENTS AND FUNDING

This work was supported by Associazione Italiana per la Ricerca sul Cancro (AIRC), PROGRAMMA OPERATIVO NAZIONALE "RICERCA E COMPETITIVITA' 2007-2013" (PON01\_01078) and Ministero della Salute (grant n. 67/GR-2010-2319511).

## CONFLICTS OF INTERESTS

The authors declare no conflict of interest.

## REFERENCES

1. Kim BE, Nevitt T, Thiele DJ. Mechanisms for copper acquisition, distribution and regulation. *Nat Chem Biol.* 2008; 3: 176-185.
2. Georgopoulos PG, Roy A, Yonone-Lioy MJ, Opiekun RE, Lioy PJ. Environmental copper: its dynamics and human exposure issues. *J Toxicol Environ Health B Crit Rev.* 2001; 4: 341-394.
3. Agency for Toxic Substances and Disease Registry. Toxicological Profile for Copper. Atlanta, GA: US Public Health Service, 1990, p. 43.
4. Rocha GH, Lini RS, Barbosa F Jr, Batista BL, de Oliveira Souza VC, Nerilo SB, Bando E, Mossini SA, Nishiyama P. Exposure to heavy metals due to pesticide use by vineyard farmers. *Int Arch Occup Environ Health.* 2015; 88:875-80.
5. Antoniadis V, Sioga A, Dietrich EM, Meditskou S, Ekonomou L, Antoniadis K. Is copper chelation an effective anti-angiogenic strategy for cancer treatment? *Med Hypotheses.* 2013; 6: 1159-1163.
6. Sabharwal SS, Schumacker PT. Mitochondrial ROS in cancer: initiators, amplifiers or an Achilles' heel? *Nat Rev Cancer.* 2014; 11: 709-721.
7. Olusi S, Al-Awadhi A, Abiaka C, Abraham M, George S. Serum copper levels and not zinc are positively associated with serum leptin concentrations in the healthy adult population. *Biol Trace Elem Res.* 2003; 91: 137-144.
8. Gupte A, Mumper RJ. Elevated copper and oxidative stress in cancer cells as a target for cancer treatment. *Cancer Treat Rev.* 2009; 1: 32-46.
9. Lewis RA, Hultquist DE, Baker BL, Falls HF, Gershowitz H, Penner JA. Hypercupremia associated with a monoclonal immunoglobulin. *J Lab Clin Med.* 1976; 88: 375-388.
10. Baharvand M, Manifar S, Akkafan R, Mortazavi H, Sabour S. Serum levels of ferritin, copper, and zinc in patients with oral cancer. *Biomed J.* 2014; 37(5):331-6.
11. Lowndes SA, Harris AL. The role of copper in tumour angiogenesis. *J Mammary Gland Biol Neoplasia.* 2005; 10: 299-310.
12. Finney L, Vogt S, Fukai T, Glesne D. Copper and

- angiogenesis: unravelling a relationship key to cancer progression. *Clin Exp Pharmacol Physiol*. 2009; 36: 88-94.
13. Sen CK, Khanna S, Venojarvi M, Trikha P, Ellison EC, Hunt TK, Roy S. Copper-induced vascular endothelial growth factor expression and wound healing. *Am J Physiol Heart Circ Physiol*. 2002; 282: H1821-1827.
  14. Feng W, Ye F, Xue W, Zhou Z, Kang YJ. Copper regulation of hypoxia-inducible factor-1 activity. *Mol Pharmacol*. 2009; 1: 174-182.
  15. Qiu L, Ding X, Zhang Z, Kang YJ. Copper is required for cobalt-induced transcriptional activity of hypoxia-inducible factor-1. *J Pharmacol Exp Ther*. 2012; 342: 561-567.
  16. Richard DE, Vouret-Craviari V, Pouyssegur J. Angiogenesis and G-protein-coupled receptors: signals that bridge the gap. *Oncogene*. 2001; 20: 1556-1562.
  17. De Francesco EM, Lappano R, Santolla MF, Marsico S, Caruso A, Maggiolini M. HIF-1 $\alpha$ /GPER signalling mediates the expression of VEGF induced by hypoxia in breast cancer associated fibroblasts (CAFs). *Breast Cancer Res*. 2013; 15: R64.
  18. De Francesco EM, Pellegrino M, Santolla MF, Lappano R, Ricchio E, Abonante S, Maggiolini M. GPER mediates activation of HIF1 $\alpha$ /VEGF signalling by estrogens. *Cancer Res*. 2014; 74: 4053-4064.
  19. Martin F, Linden T, Katschinski DM, Oehme F, Flamme I, Mukhopadhyay CK, Eckhardt K, Tröger J, Barth S, Camenisch G, Wenger RH. Copper-dependent activation of hypoxia-inducible factor (HIF)-1: implications for ceruloplasmin regulation. *Blood*. 2005; 105: 4613-4619.
  20. Hu GF. Copper stimulates proliferation of human endothelial cells under culture. *J Cell Biochem*. 1998; 69: 326-335.
  21. Song MO, Li J, Freedman JH. Physiological and toxicological transcriptome changes in HepG2 cells exposed to copper. *Physiol Genomics*. 2009; 38: 386-401.
  22. Dong D, Xu X, Wen Y and Kang YJ. Changes in copper concentrations affect the protein levels but not the mRNA levels of copper chaperones in human umbilical vein endothelial cells. *Metallomics*. 2014; 6: 554-559.
  23. Sun, SY. N-acetylcysteine, reactive oxygen species and beyond. *Cancer Biol. Ther*. 2010; 9: 109-110.
  24. Recchia AG, De Francesco EM, Vivacqua A, Sisci D, Panno ML, Andò S, Maggiolini M. The G protein-coupled receptor 30 is up-regulated by hypoxia-inducible factor-1 $\alpha$  (HIF-1 $\alpha$ ) in breast cancer cells and cardiomyocytes. *J Biol Chem*. 2011; 286: 10773-10782.
  25. Maggiolini M, Vivacqua A, Fasanella G, Recchia AG, Sisci D, Pezzi V, Montanaro D, Musti AM, Picard D, Andò S. The G Protein-coupled Receptor GPR30 Mediates c-fos up-regulation by 17 $\beta$ -Estradiol and Phytoestrogens in Breast Cancer Cells. *J Biol Chem*. 2004; 279: 27008-27016.
  26. Maggiolini M, Picard D. The unfolding stories of GPR30, a new membrane-bound estrogen receptor. *J Endocrinol*. 2010; 204: 105-114.
  27. Pandey DP, Lappano R, Albanito L, Madeo A, Maggiolini M, Picard D. Estrogenic GPR30 signalling induces proliferation and migration of breast cancer cells through CTGF. *EMBO J*. 2009; 28: 523-532.
  28. Lappano R, De Marco P, De Francesco EM, Chimento A, Pezzi V, Maggiolini M. Cross-talk between GPER and growth factor signalling. *J Steroid Biochem Mol Biol*. 2013; 137: 50-56.
  29. Staton CA, Reed MW, Brown NJ. A critical analysis of current *in vitro* and *in vivo* angiogenesis assays. *Int J Exp Pathol*. 2009; 90: 195-221.
  30. Byzova TV, Goldman CK, Pampori N, Thomas KA, Bett A, Shattil SJ, Plow EF. A mechanism for modulation of cellular responses to VEGF: activation of the integrins. *Mol Cell*. 2000; 6: 851-860.
  31. Morales-Ruiz M, Fulton D, Sowa G, Languino LR, Fujio Y, Walsh K, Sessa WC. Vascular endothelial growth factor-stimulated actin reorganization and migration of endothelial cells is regulated via the serine/threonine kinase Akt. *Circ Res*. 2000; 86: 892-896.
  32. Brewer GJ. Anticopper therapy against cancer and diseases of inflammation and fibrosis. *Drug Discov Today*. 2005; 10: 1103-1119.
  33. Ishida S, Andreux P, Poitry-Yamate C, Auwerx J, Hanahan D. Bioavailable copper modulates oxidative phosphorylation and growth of tumors. *Proc Natl Acad Sci U S A*. 2013; 110: 19507-19512.
  34. Wang GL, Semenza GL. General involvement of hypoxia-inducible factor 1 in transcriptional response to hypoxia. *Proc Natl Acad Sci USA*. 1993; 90: 4304-4308.
  35. Semenza GL. Hypoxia-inducible factors: mediators of cancer progression and targets for cancer therapy. *Trends Pharmacol Sci*. 2012; 33: 207-214.
  36. Filardo EJ, Graeber CT, Quinn JA, Resnick MB, Giri D, DeLellis RA, Steinhoff MM, Sabo E. Distribution of GPR30, a seven membrane spanning estrogen receptor, in primary breast cancer and its association with clinicopathologic determinants of tumor progression. *Clin Cancer Res*. 2006; 12: 6359-6366.
  37. Smith HO, Leslie KK, Singh M, Qualls CR, Revankar CM, Joste NE, Prossnitz ER. GPR30: a novel indicator of poor survival for endometrial carcinoma. *Am J Obstet Gynecol*. 2007; 196: 386.e1-9; discussion 386.e9-11.
  38. Smith HO, Arias-Pulido H, Kuo DY, Howard T, Qualls CR, Lee SJ, Verschaegen CF, Hathaway HJ, Joste NE, Prossnitz ER. GPR30 predicts poor survival for ovarian cancer. *Gynecol Oncol*. 2009; 114: 465-471.
  39. Vivacqua A, De Marco P, Santolla MF, Cirillo F, Pellegrino M, Panno ML, Abonante S, Maggiolini M. Estrogenic gper signalling regulates mir144 expression in cancer cells and cancer-associated fibroblasts (cafs). *Oncotarget*. 2015; 6:16573-87. doi: 10.18632/oncotarget.4117.
  40. De Marco P, Cirillo F, Vivacqua A, Malaguarnera R, Belfiore A, Maggiolini M. Novel Aspects Concerning the

- Functional Cross-Talk between the Insulin/IGF-I System and Estrogen Signalling in Cancer Cells. *Front Endocrinol (Lausanne)*. 2015; 6: 30. doi: 10.3389/fendo.2015.00030.
41. Lappano R, Pisano A, Maggiolini M. GPER Function in Breast Cancer: An Overview. *Front Endocrinol (Lausanne)*. 2014; 5: 66. doi: 10.3389/fendo.2014.00066.
  42. Santolla MF, De Francesco EM, Lappano R, Rosano C, Abonante S, Maggiolini M. Niacin activates the G protein estrogen receptor (GPER)-mediated signalling. *Cell Signal*. 2014; 7: 1466-1475.
  43. Santolla MF, Lappano R, De Marco P, Pupo M, Vivacqua A, Sisci D, Abonante S, Iacopetta D, Cappello AR, Dolce V, Maggiolini M. G protein-coupled estrogen receptor mediates the up-regulation of fatty acid synthase induced by 17 $\beta$ -estradiol in cancer cells and cancer-associated fibroblasts. *J Biol Chem*. 2012; 287: 43234-43245.
  44. De Francesco EM, Angelone T, Pasqua T, Pupo M, Cerra MC, Maggiolini M. GPER mediates cardiotropic effects in spontaneously hypertensive rat hearts. *PLoS One*. 2013; 8: e69322.
  45. Pupo M, Pisano A, Lappano R, Santolla MF, De Francesco EM, Abonante S, Rosano C, Maggiolini M. Bisphenol A induces gene expression changes and proliferative effects through GPER in breast cancer cells and cancer-associated fibroblasts. *Environ Health Perspect*. 2012; 120: 1177-1182.
  46. Filice E, Angelone T, De Francesco EM, Pellegrino D, Maggiolini M, Cerra MC. Crucial role of phospholamban phosphorylation and S-nitrosylation in the negative lusitropism induced by 17 $\beta$ -estradiol in the male rat heart. *Cell Physiol Biochem*. 2011; 28: 41-52.
  47. Lappano R, Rosano C, De Marco P, De Francesco EM, Pezzi V, Maggiolini M. Estriol acts as a GPR30 antagonist in estrogen receptor-negative breast cancer cells. *Mol Cell Endocrinol*. 2010; 320: 162-170.
  48. Lappano R, Santolla MF, Pupo M, Sinicropi MS, Caruso A, Rosano C, Maggiolini M. MIBE acts as antagonist ligand of both estrogen receptor  $\alpha$  and GPER in breast cancer cells. *Breast Cancer Res*. 2012; 14: R12.
  49. Maggiolini M, Santolla MF, Avino S, Aiello F, Rosano C, Garofalo A, Grande F. Identification of two benzopyrroloxazines acting as selective GPER antagonists in breast cancer cells and cancer-associated fibroblasts. *Future Med Chem*. 2015; 7: 437-448.
  50. Sinicropi MS, Lappano R, Caruso A, Santolla MF, Pisano A, Rosano C, Capasso A, Panno A, Lancelot JC, Rault S, Saturnino C, Maggiolini M. (6-bromo-1,4-dimethyl-9H-carbazol-3-yl-methylene)-hydrazine (carbhydraz) acts as a GPER agonist in breast cancer cells. *Curr Top Med Chem*. 2015; 15: 1035-42.
  51. Bartella V, De Marco P, Malaguarnera R, Belfiore A, Maggiolini M. New advances on the functional cross-talk between insulin-like growth factor-I and estrogen signalling in cancer. *Cell Signal*. 2012; 24 : 1515-1521.
  52. De Marco P, Bartella V, Vivacqua A, Lappano R, Santolla MF, Morcavallo A, Pezzi V, Belfiore A, Maggiolini M. Insulin-like growth factor-I regulates GPER expression and function in cancer cells. *Oncogene*. 2013; 32 :678-688.
  53. De Marco P, Romeo E, Vivacqua A, Malaguarnera R, Abonante S, Romeo F, Pezzi V, Belfiore A, Maggiolini M. GPER1 is regulated by insulin in cancer cells and cancer-associated fibroblasts. *Endocr Relat Cancer*. 2014; 21: 739-753.
  54. Santolla MF, Avino S, Pellegrino M, De Francesco EM, De Marco P, Lappano R, Vivacqua A, Cirillo F, Rigracciolo DC, Scarpelli A, Abonante S and Maggiolini M. SIRT1 is involved in oncogenic signaling mediated by GPER in breast cancer. *Cell Death and Disease*. 2015 Cdx.doi.org/10.1038/cddis.2015.201.
  55. Lappano R, Rosano C, Pisano A, Santolla MF, De Francesco EM, De Marco P, Dolce V, Ponassi M, Felli L, Cafeo G, Kohnke FH, Abonante S, Maggiolini M. A calixpyrrole derivative acts as a GPER antagonist: mechanisms and models. *Dis Model Mech*. 2015; pii: dmm.021071.
  56. Albanito L, Lappano R, Madeo A, Chimento A, Prossnitz ER, Cappello AR, Dolce V, Abonante S, Pezzi V, Maggiolini M. Effects of Atrazine on Estrogen Receptor  $\alpha$ - and G Protein-Coupled Receptor 30-Mediated Signalling and Proliferation in Cancer Cells and Cancer-Associated Fibroblasts. *Environ Health Perspect*. 2015; 123: 493-499.
  57. Vivacqua A, Romeo E, De Marco P, De Francesco EM, Abonante S, Maggiolini M. GPER mediates the Egr-1 expression induced by 17 $\beta$ -estradiol and 4-hydroxitamoxifen in breast and endometrial cancer cells. *Breast Cancer Res Treat*. 2012; 133: 1025-1035.
  58. Lappano R, Rosano C, Santolla MF, Pupo M, De Francesco EM, De Marco P, Ponassi M, Spallarossa A, Ranise A, Maggiolini M. Two novel GPER agonists induce gene expression changes and growth effects in cancer cells. *Curr Cancer Drug Targets*. 2012; 12: 531-542.
  59. Lappano R, Maggiolini M. G protein-coupled receptors: novel targets for drug discovery in cancer. *Nat Rev Drug Discov*. 2011; 10: 47-60.
  60. Lappano R, Maggiolini M. GPCRs and cancer. *Acta Pharmacol Sin*. 2012; 33: 351-362.
  61. Madeo A, Maggiolini M. Nuclear alternate estrogen receptor GPR30 mediates 17 $\beta$ -estradiol-induced gene expression and migration in breast cancer-associated fibroblasts. *Cancer Res*. 2010; 70: 6036-6046. doi: 10.1158/0008-5472.CAN-10-0408.
  62. Pupo M, Pisano A, Abonante S, Maggiolini M, Musti AM. GPER activates Notch signalling in breast cancer cells and cancer-associated fibroblasts (CAFs). *Int J Biochem Cell Biol*. 2014; 46: 56-67.
  63. Pupo M, Vivacqua A, Perrotta I, Pisano A, Aquila S, Abonante S, Gasperi-Campani A, Pezzi V, Maggiolini M. The nuclear localization signal is required for nuclear GPER translocation and function in breast Cancer-Associated Fibroblasts (CAFs). *Mol Cell Endocrinol*. 2013; 376: 23-32.

64. Martinez-Outschoorn UE, Lisanti MP, Sotgia F. Semin Cancer Biol. Catabolic cancer-associated fibroblasts transfer energy and biomass to anabolic cancer cells, fueling tumor growth. 2014; 25: 47-60.
65. Martinez-Outschoorn U, Sotgia F, Lisanti MP. Tumor microenvironment and metabolic synergy in breast cancers: critical importance of mitochondrial fuels and function. Semin Oncol. 2014; 41: 195-216.
66. Sotgia F, Martinez-Outschoorn UE, Lisanti MP. Cancer metabolism: new validated targets for drug discovery. Oncotarget. 2013; 4: 1309-1316.
67. Yu X, Filardo EJ, Shaikh ZA. The membrane estrogen receptor GPR30 mediates cadmium-induced proliferation of breast cancer cells. Toxicol Appl Pharmacol. 2010; 245: 83-90.
68. Albanito L, Sisci D, Aquila S, Brunelli E, Vivacqua A, Madeo A, Lappano R, Pandey DP, Picard D, Mauro L, Andò S, Maggiolini M. Epidermal growth factor induces G protein-coupled receptor 30 expression in estrogen receptor-negative breast cancer. Endocrinology. 2008; 149: 3799-3808.

RESEARCH ARTICLE

# Pregnancy Augments G Protein Estrogen Receptor (GPER) Induced Vasodilation in Rat Uterine Arteries via the Nitric Oxide - cGMP Signaling Pathway

Teresa Tropea<sup>1</sup>, Ernestina Marianna De Francesco<sup>2</sup>, Damiano Rigracciolo<sup>2</sup>, Marcello Maggiolini<sup>2</sup>, Mark Wareing<sup>3</sup>, George Osol<sup>4</sup>, Maurizio Mandalà<sup>1\*</sup>

**1** Department of Biology, Ecology and Earth Sciences, University of Calabria, Rende, Italy, **2** Department of Pharmacy, Health and Nutritional Sciences, University of Calabria, Rende, Italy, **3** Maternal and Fetal Health Research Centre, The University of Manchester, Manchester, United Kingdom, **4** Department of Obstetrics, Gynecology and Reproductive Sciences, University of Vermont, Burlington, Vermont, United States of America

\* [m.mandala@unical.it](mailto:m.mandala@unical.it)



**OPEN ACCESS**

**Citation:** Tropea T, De Francesco EM, Rigracciolo D, Maggiolini M, Wareing M, Osol G, et al. (2015) Pregnancy Augments G Protein Estrogen Receptor (GPER) Induced Vasodilation in Rat Uterine Arteries via the Nitric Oxide - cGMP Signaling Pathway. PLoS ONE 10(11): e0141997. doi:10.1371/journal.pone.0141997

**Editor:** Christopher Torrens, University of Southampton, UNITED KINGDOM

**Received:** March 16, 2015

**Accepted:** October 15, 2015

**Published:** November 4, 2015

**Copyright:** This is an open access article, free of all copyright, and may be freely reproduced, distributed, transmitted, modified, built upon, or otherwise used by anyone for any lawful purpose. The work is made available under the [Creative Commons CC0](https://creativecommons.org/licenses/by/4.0/) public domain dedication.

**Data Availability Statement:** All relevant data are within the paper.

**Funding:** This work was supported by the University of Calabria with a contribution named "ex 60%" to MM. The funder had a role in study design and in analysis and interpretation of data.

**Competing Interests:** The authors have declared that no competing interests exist.

## Abstract

### Background

The regulation of vascular tone in the uterine circulation is a key determinant of appropriate uteroplacental blood perfusion and successful pregnancy outcome. Estrogens, which increase in the maternal circulation throughout pregnancy, can exert acute vasodilatory actions. Recently a third estrogen receptor named GPER (G protein-coupled estrogen receptor) was identified and, although several studies have shown vasodilatory effects in several vascular beds, nothing is known about its role in the uterine vasculature.

### Aim

The aim of this study was to determine the function of GPER in uterine arteries mainly during pregnancy. Uterine arteries were isolated from nonpregnant and pregnant rats.

### Methods

Vessels were contracted with phenylephrine and then incubated with incremental doses ( $10^{-12}$ – $10^{-5}$  M) of the selective GPER agonist G1.

### Results

G1 induced a dose-dependent vasodilation which was: 1) significantly increased in pregnancy, 2) endothelium-dependent, 3) primarily mediated by NO/cGMP pathway and 4) unaffected by BK<sub>Ca</sub> channel inhibition.

## Conclusion

This is the first study to show the potential importance of GPER signaling in reducing uterine vascular tone during pregnancy. GPER may therefore play a previously unrecognized role in the regulation of uteroplacental blood flow and normal fetus growth.

## Introduction

During pregnancy, uteroplacental blood flow increases significantly to allow the normal growth of the fetus. Reduced blood flow to the uteroplacental unit is observed in gestational diseases such as fetal growth restriction and preeclampsia, with serious consequences for pregnancy outcome. Estrogens may modulate uteroplacental vascular function since its plasma concentrations increase significantly during pregnancy, and an effect on vascular tone has been documented in many experimental and clinical contexts [1]. Estrogens act on the vasculature via three different receptors: the two classical nuclear estrogen receptors, ER $\alpha$  and ER $\beta$ , function traditionally as ligand-activated nuclear transcription factors [2], while a third membrane estrogen receptor termed G-protein coupled estrogen receptor (GPER, formerly GPR30) was recently identified as an orphan 7-transmembrane G protein-coupled receptor [3–7]. In the last decade, several studies have shown that GPER [8,9] mediates the action of estrogens and estrogen-like compounds in diverse pathophysiological conditions [10–15]. In addition, using the specific GPER agonists and antagonists namely G1 [16] and G15 [17], respectively, several studies have shown that GPER plays a role in the nervous, immune, reproductive and vascular systems [18]. The potential vascular relevance of GPER function was first observed in human vascular endothelial cells, in which flow (shear stress) induced its expression [7]. GPER is also expressed in both endothelial and smooth muscle cells throughout the cardiovascular system [19–21]. Although several vessel types have been assessed [22–24], GPER has not been investigated in the uterine vasculature, which supplies blood flow to the uterus and placenta and plays a crucial role in providing sufficient blood for normal placental exchange [25].

In this study we ascertained that GPER is expressed in the uterine circulation, its activation triggers a vasoactive effect primarily through the NO-cGMP signaling system in uterine arteries and that its effects may be altered during pregnancy.

## Material and Methods

### Animals

All experiments were conducted in accordance with the European Guidelines for the care and use of laboratory animals (Directive 2010/63/EU) and were approved by the local ethical committee of the University of Calabria. Surgery was performed under anesthesia to minimize pain and suffering. Female Sprague-Dawley rats were purchased from Harlan Laboratories (Italy). All animals were housed under controlled conditions on a 12-hour light/dark cycle and provided commercial chow and tap water *ad libitum*. Experiments were performed on age-matched pregnant and non-pregnant animals at 12–15 weeks of age. Pregnant animals were obtained by placing a female in proestrus with a fertile male overnight; detection of spermatozoa using a vaginal smear on the following morning was used to confirm day 1 of pregnancy. Animals were euthanized with inhalation of Diethyl ether followed by decapitation, the uterus was removed and uterine arteries were dissected free from connective and adipose tissue for subsequent experimentation.

## Pressure myography

Radial uterine arteries were obtained from non pregnant (NP) and pregnant animals (P) at 14 days of gestational age, i.e. approximately one week before term. Arterial segments (1–2 mm long) were transferred to the chamber of a small-vessel arteriograph. One end of the vessel was tied onto a glass cannula and flushed of any luminal contents by increasing the pressure before securing the distal end onto a second cannula using a servo-null pressure system (Living Systems Instrumentation). All vessels were continuously superfused with HEPES-physiological saline solution (HEPES-PSS) at 37°C, pressurized to 50 mmHg, and equilibrated for 45 min before beginning experimentation. Lumen diameter was measured by trans-illuminating each vessel segment and using a video dimension analyzer (Living Systems Instrumentation) in conjunction with data-acquisition software (Ionoptix) to continuously record lumen diameter.

Following equilibration, all vessels were pre-constricted with phenylephrine (0.1–1 μM) to produce a 40–50% reduction in baseline diameter [26]. Once constriction was achieved and stable for about 10 minutes, the specific agonist of GPER, 1-(4-(6-Bromobenzol(1,3)diodo-5-yl)3a,4,5,9b-tetrahydro-3Hcyclopenta(c)-quinolin-8yl)ethanone (G-1), dissolved in DMSO to prepare a stock solution of 1 mg/ml was added at a concentration of  $10^{-12} \div 10^{-6}$  M. In some arteries the endothelium was removed (denuded artery) mechanically by hair and air perfusion, and the effectiveness of denudation confirmed by the lack of dilation to acetylcholine ( $10^{-5}$  M). Additional pharmacological experiments were carried out using the following inhibitors: 1) (3aS\*,4R\*,9bR\*)-4-(6-Bromo-1,3-benzodioxol-5-yl)-3a,4,5,9b-3H-cyclopenta[c]quinoline (G-15,  $10^{-5}$  M) a specific antagonist of GPER; 2) N-nitro-L-arginine (L-NNA,  $10^{-4}$  M) + Nω-nitro-L-arginine methyl ester (L-NAME,  $10^{-4}$  M) for NOS and 3) ODQ ( $10^{-5}$  M) for guanylate cyclase and 4) Paxilline ( $10^{-5}$  M) for BK<sub>Ca</sub> channels. Vessels were pre-incubated with inhibitors for 20 minutes before pre-constriction with phenylephrine and addition of G1.

## Western blotting

Frozen uterine arteries from non pregnant and pregnant rats were powdered with a mortar and homogenized in 50 mM Hepes solution, pH 7.4, containing 1% (v/v) Triton X-100, 4 mM EDTA, 1 mM sodium fluoride, 0.1 mM sodium orthovanadate, 2 mM PMSF, 10 mg/ml leupeptin and 10 mg/ml aprotinin. In order to increase the amount of tissue for accurate measurements, uterine arteries from two rats were pooled. Homogenates were centrifuged at 13,000 rpm for 10 min and protein concentrations in the supernatant were determined according to the Bradford assay. Tissue lysates (40 μg of protein) were electrophoresed through a reducing SDS/10% (w/v) polyacrylamide gel and electroblotted onto a nitrocellulose membrane. After the transfer, the membranes were stained with Red Poinceau to confirm equal loading and transfer. Membranes were blocked and incubated with primary polyclonal IgG antibody GPER (N-15), β-tubulin (H-235-2) and appropriate secondary HRP-conjugated antibodies, all purchased from Santa Cruz Biotechnology (DBA, Milan, Italy). The levels of proteins were detected with horseradish peroxidase-linked secondary antibodies, and revealed using the Enhanced Chemiluminescence system (GE Healthcare, Milan, Italy).

## Drugs and Solutions

The HEPES-PSS contained the following (in mmol/L): sodium chloride 141.8, potassium chloride 4.7, magnesium sulfate 1.7, calcium chloride 2.8, potassium phosphate 1.2, HEPES 10.0, EDTA 0.5, and dextrose 5.0. All drugs tested were administered from stock solutions prepared daily, except for G1 and G15 where the stock solutions were frozen in small aliquots. G1 and G-15 were purchased from TOCRIS, distributed by R&D Systems (Milano, Italy), all the other

chemicals were purchased from Sigma-Aldrich, Fisher Scientific, Cayman Chemical Co. unless otherwise specified.

## Statistical analysis

Vasodilation to G1 was expressed as percent of maximally-relaxed diameter which was determined at the end of each experiment by the addition of a relaxing HEPES-PSS solution containing diltiazem (10  $\mu$ M) + papaverine (100  $\mu$ M). Data are expressed as means  $\pm$  SEM, where n is the number of arterial segments studied. The n values refer to both number of vessels and number of animals. A normal distribution for all datasets was confirmed by Kolmogorov-Smirnov test, and differences in responses between groups were determined with two-way ANOVA for repeated measures analysis. Differences were considered significant at  $P \leq 0.05$ .

## Results

Phenylephrine is a potent vasoconstrictor of radial uterine arteries from NP and P rats as showing in the traces A and C respectively in [Fig 1](#). Phenylephrine hold stable the constriction of the vessels for enough time necessary to observe clearly the action of the G1 showed in traces B and D respectively for NP and P. Several experiments were done and the data were summarized in [Fig 1E](#) that suggested G1, tested in the range ( $10^{-12}$ – $10^{-6}$ M), induced vasodilation in a concentration-dependent manner in precontracted radial uterine arteries from both NP and P rats. The vasodilation was significantly greater in vessels from P vs NP rats with a maximal efficacy of  $97,8 \pm 2,5\%$  in P vs  $66,5 \pm 3,7\%$  in NP;  $p < 0.001$  ([Fig 1](#)). Also GPER protein expression was significant higher in uterine artery from P rat vs NP with a  $p < 0.05$  ([Fig 2](#)). The vasodilatory effect of G1 was almost entirely abolished in presence of the specific GPER antagonist, G15, as evidenced by an approximately 80% of reduction from  $90,7 \pm 2,6\%$  (G1) to  $18,2 \pm 2,4\%$  (G1 + G15),  $p < 0.001$  ([Fig 3](#)). To understand the mechanism underlying the G1-induced vasodilation in radial uterine artery, several pharmacological experiments were carried out and the results shown that G1 vasodilation ( $90,7 \pm 2,6\%$ ) was abolished by the inhibition of nitric oxide production ( $2,5 \pm 2,5\%$ ;  $p < 0.001$ ) and also in denuded artery ( $6,6 \pm 2,2\%$ ;  $p < 0.001$ ), [Fig 4](#). Further, a significant reduction was observed by the inhibition of cGMP ( $23,1 \pm 2,1\%$ ;  $p < 0.001$ ), while the inhibitor of BK channels (paxilline) did not affect the G1-induced vasodilation ([Fig 5](#)).

## Discussion

There were four principal findings in this study: 1) GPER activation with G1 induced significant vasodilation of rat uterine radial arteries; 2) G1 vasodilation was significantly augmented in pregnancy, 3) as was the expression of its protein in the arterial wall; 4) GPER vasodilation, which was effectively antagonized by the G15 inhibitor, was also endothelium-dependent and mediated by the NO-cGMP pathway without BK<sub>Ca</sub> channel involvement.

During pregnancy, the maternal uterine circulation both vasodilates and undergoes a process of three-dimensional expansive remodeling [27]. Together, these processes result in a many-fold increase in uteroplacental blood flow that is requisite for normal fetal growth and myometrial function during parturition. Estrogen, whose concentrations increase progressively in the maternal circulation throughout pregnancy, has been reported to play a role in both processes of vasodilation [1,28] and remodeling [29]. In addition to ER $\alpha$  and ER $\beta$ , the classic nuclear estrogen receptors, a membrane G protein-coupled estrogen receptor termed GPER has recently been identified. There is increasing evidence that GPER is expressed in the cardiovascular system and may mediate some vascular estrogenic effects [30], although there have not been any studies to date on the uterine vasculature. The aim of this study was to evaluate

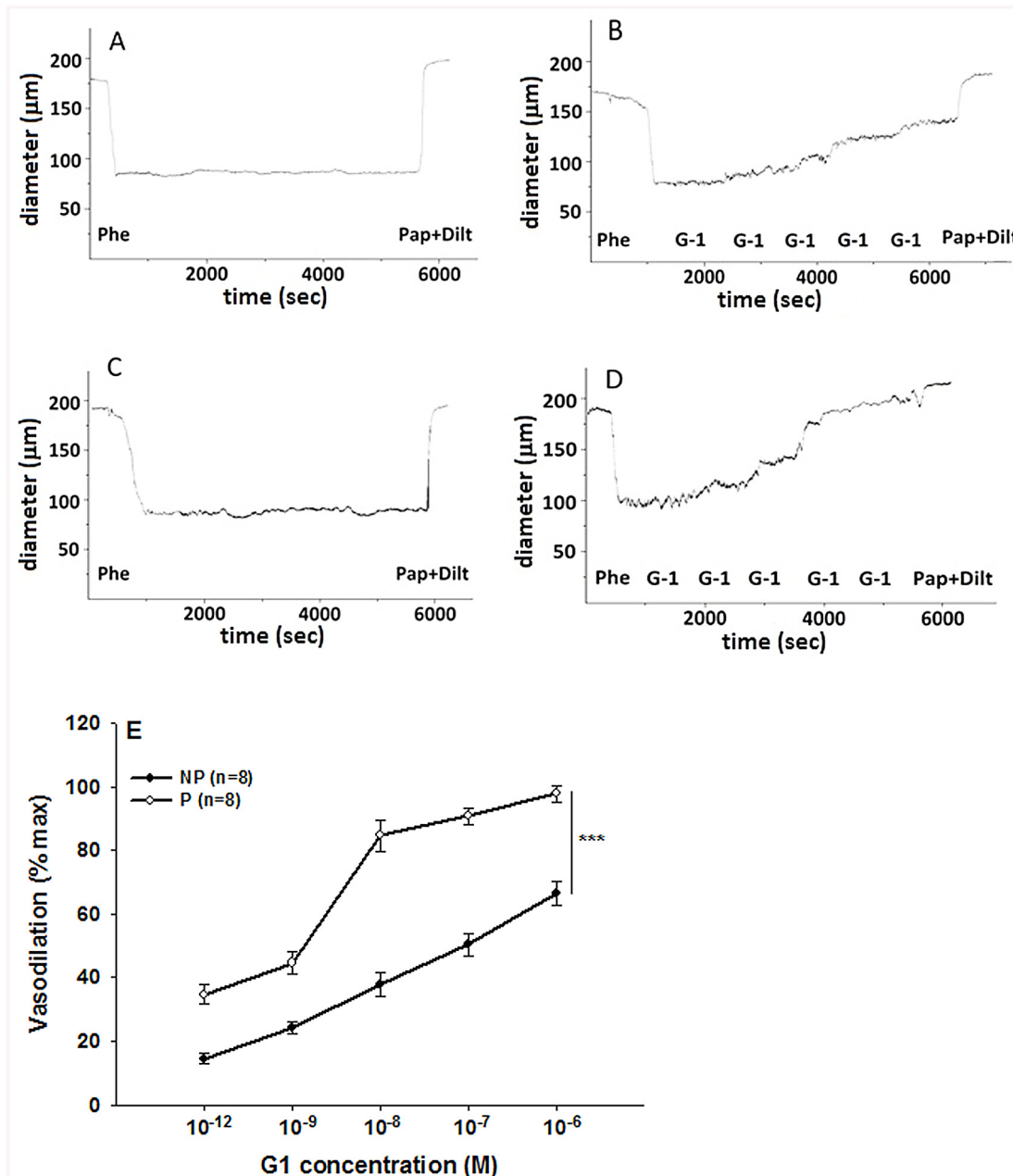


**Fig 1. Concentration-response curves to G1 vasodilation in pressurized uterine radial arteries from non-pregnant (NP) vs. pregnant (P) rats.** Uterine arteries were constricted with phenylephrine and then treated with the GPER agonist G1 at different concentration. An example of experimental records are shown in trace A and B for NP rat and in traces C and D for P rat. The Vasodilation of G1 was summarized in E and is expressed as a percentage of maximal relaxation (max) obtained in presence of papaverine and diltiazem. Data are reported as mean  $\pm$  SEM; n indicates number of experiments. \*\*\*p < 0.001.

doi:10.1371/journal.pone.0141997.g001

the effects of GPER activation on uterine artery vascular tone, and to probe the underlying mechanisms by using the high affinity GPER-selective agonist (G1) and antagonist (G15). Neither compound shows any detectable activity towards the classical estrogen receptors [16,17]. Our study shows a potent vasodilator effect of G1-induced GPER activation in uterine resistance (radial) arteries. A similar vasorelaxant effect has been observed in several different types of arteries (cerebral, aorta, mesenteric, coronary, internal mammary), and in different species:

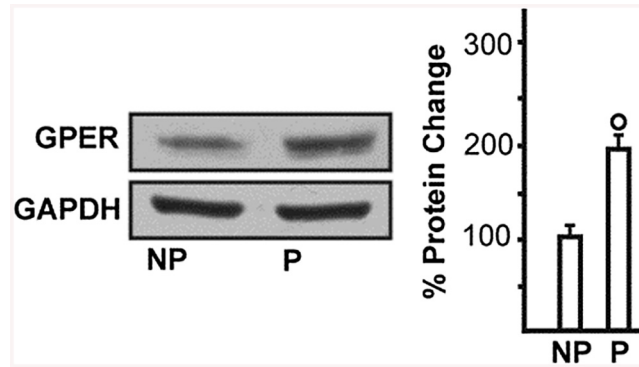


**Fig 2. GPER expression in uterine radial arteries from nonpregnant and pregnant rats. Western blot showing.** GPER protein expression in uterine arteries homogenates from non-pregnant (NP) and pregnant (P) rats. Side panel shows densitometric analysis of the blot normalized to  $\beta$ -tubulin. Percentage changes were evaluated as mean  $\pm$  SEM of 3 experiments for each group. \* $p < 0.05$  for the expression in P vs NP.

doi:10.1371/journal.pone.0141997.g002

rat, swine, human [22–24,31]. In human uterine arteries, there is one report of suggesting a lack of vasodilatory effect [32] but this may have to do with the use of U46619, a thromboxane receptor agonist, to contract the vessels since stimulus-specific effects have been reported previously; for example GPER agonists attenuated contractions to endothelin-1 but not serotonin [33]. Notably, we used Phe as the agonist in view of the rich adrenergic innervation of the uterine vasculature, and the fact that uterine vessels are more sensitive to catecholeamines than any other regional vascular bed [34]. We also found that GPER protein expression was increased significantly in uterine arteries from pregnant vs. non pregnant rats, an observation that may explain the greater magnitude of vasodilation.

G1-induced uterine artery vasodilation was endothelium dependent, and that this effect was mediated by NO since pharmacological inhibition of nitric oxide synthase virtually abolished the G1 vasodilation. Species differences may exist in this regard, however, since vessels from eNOS knockout mice were somewhat less reactive to G1 than wild type controls (data not

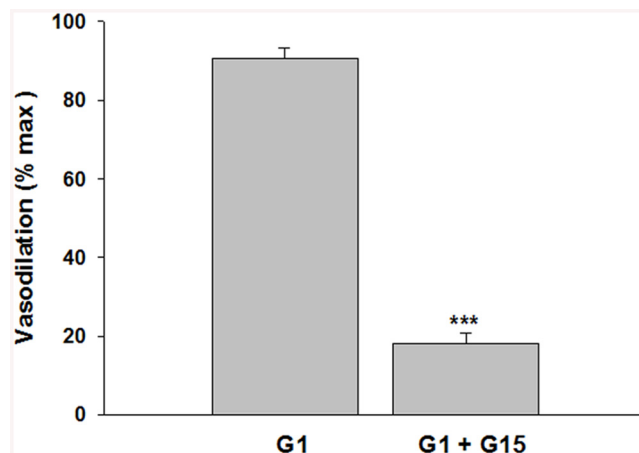


**Fig 3. Effect of the specific GPER antagonist, G15, on G1 vasodilation in uterine radial arteries from pregnant rats.** Inhibition of G1 ( $10^{-7}$ M;  $n = 8$ ) induced vasodilation of uterine arteries from pregnant rats by the GPER-specific antagonist G15 ( $10^{-5}$ M, G1  $\pm$  G15,  $n = 5$ ). Vasodilation is expressed as a percentage of maximal relaxation (% max) measured in a relaxing solution containing papaverine and diltiazem. Data are reported as mean  $\pm$  SEM. \*\*\* $p < 0.001$ .

doi:10.1371/journal.pone.0141997.g003

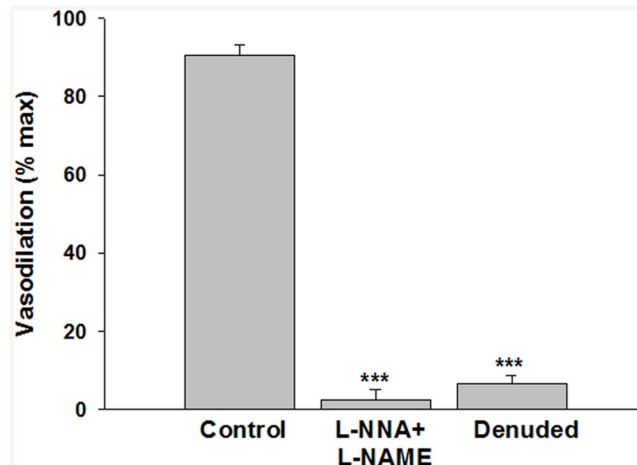


**Fig 4. Effects of NOS inhibition and endothelial denudation on G1 vasodilation in uterine radial arteries from pregnant rats.** G1 ( $10^{-7}$  M) was tested on intact radial uterine arteries in absence (Control,  $n = 8$ ) vs. the presence of the nitric oxide synthase inhibition using a combination of L-NNA+L-NAME ( $n = 5$ ). G1 was also tested on radial uterine arteries without endothelium (Denuded,  $n = 5$ ). Vasodilation is expressed as a percentage of maximal relaxation (max) in papaverine and diltiazem. Data are reported as mean  $\pm$  SEM. \*\*\* $p < 0.001$ .

doi:10.1371/journal.pone.0141997.g004

shown), but a significant degree of relaxation nevertheless remained. This may reflect the existence of compensatory mechanism secondary to the loss of eNOS, e.g. upregulation of prostanooids or another endothelial vasodilator. We also found that, while NO acted via the canonical cGMP pathway (based on the effectiveness of ODQ in blocking dilation), this effect did not involve  $BK_{Ca}$  channel activation. Activation of the NO-cGMP pathway following GPER stimulation was reported in several different types of arteries, e.g. mesenteric [24], cerebral [23], coronary [33] and carotid [20]. In denuded porcine coronary arteries, G1 did activate  $BK_{Ca}$  channels with consequent vasodilation that was not affected by the inhibition of nitric oxide

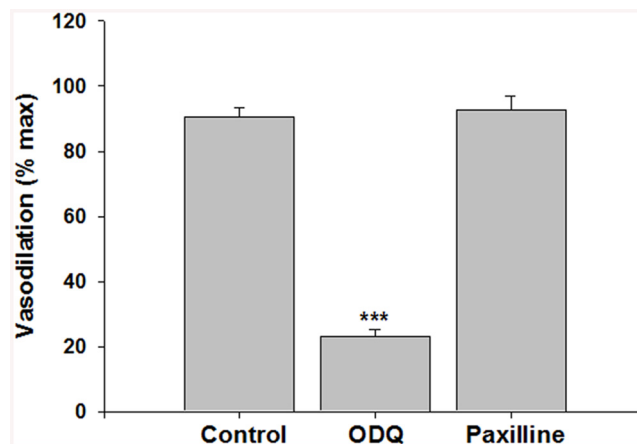


**Fig 5. Effects of guanylate cyclase and  $BK_{Ca}$  channel inhibition on G1 vasodilation of rat uterine radial arteries.** G1 ( $10^{-7}$  M) was tested on radial uterine arteries in absence (Control,  $n = 8$ ) vs. presence of guanylate cyclase (ODQ,  $10^{-9}$  M,  $n = 5$ ) or  $BK_{Ca}$  channel (paxilline  $10^{-5}$  M,  $n = 5$ ) inhibition. Vasodilation is expressed as a percentage of maximal response (max) obtained in papaverine and diltiazem. Data are reported as mean  $\pm$  SEM. \*\*\* $p < 0.001$ .

doi:10.1371/journal.pone.0141997.g005

synthase [35]. Thus, there may be both regional and species variations in post-receptor GPER coupling in endothelial and vascular smooth muscle cells.

In conclusion, this study is the first to show a GPER vasodilation in the uterine vasculature that is augmented in pregnancy, most likely secondary to upregulation of receptor expression, and involves endothelial NO release. Additional studies are warranted to determine whether GPER activation may offer a novel therapeutic mechanism for regulating uterine vascular tone and hemodynamics in gestational diseases associated with a reduction in uteroplacental blood flow such as preeclampsia and intrauterine growth restriction (IUGR).

## Author Contributions

Conceived and designed the experiments: M. Mandalà. Performed the experiments: TT ED DR. Analyzed the data: M. Mandalà M. Maggiolini. Contributed reagents/materials/analysis tools: M. Mandalà M. Maggiolini. Wrote the paper: TT M. Mandalà. Critical revision for important intellectual content: GO MW.

## References

1. Pastore MB, Jobe SO, Ramadoss J, Magness RR. Estrogen receptor- $\alpha$  and estrogen receptor- $\beta$  in the uterine vascular endothelium during pregnancy: functional implications for regulating uterine blood flow. *Semin Reprod Med.* 2012; 30:46–61. doi: [10.1055/s-0031-1299597](https://doi.org/10.1055/s-0031-1299597) PMID: [22271294](https://pubmed.ncbi.nlm.nih.gov/22271294/)
2. Carroll JS, Brown M. Estrogen receptor target gene: an evolving concept. *Mol Endocrinol.* 2006; 20:1707–14. PMID: [16396959](https://pubmed.ncbi.nlm.nih.gov/16396959/)
3. Carmeci C, Thompson DA, Ring HZ, Francke U, Weigel RJ. Identification of a gene (GPR30) with homology to the G-protein-coupled receptor superfamily associated with estrogen receptor expression in breast cancer. *Genomics* 1997; 45:607–17. PMID: [9367686](https://pubmed.ncbi.nlm.nih.gov/9367686/)
4. Kvingedal AM, Smeland EB. A novel putative G-protein-coupled receptor expressed in lung, heart and lymphoid tissue. *FEBS Lett.* 1997; 407:59–62. PMID: [9141481](https://pubmed.ncbi.nlm.nih.gov/9141481/)
5. O'Dowd BF, Nguyen T, Marchese A, Cheng R, Lynch KR, Heng HH, et al. Discovery of three novel G-protein coupled receptor genes. *Genomics* 1998; 47:310–3. PMID: [9479505](https://pubmed.ncbi.nlm.nih.gov/9479505/)
6. Owman C, Blay P, Nilsson C, Lolait SJ. Cloning of human cDNA encoding a novel heptahelix receptor expressed in Burkitt's lymphoma and widely distributed in brain and peripheral tissues. *Biochem Biophys Res Commun.* 1996; 228:285–92. PMID: [8920907](https://pubmed.ncbi.nlm.nih.gov/8920907/)
7. Takada Y, Kato C, Kondo S, Korenaga R, Ando J. Cloning of cDNAs encoding G protein-coupled receptor expressed in human endothelial cells exposed to fluid shear stress. *Biochem Biophys Res Commun.* 1997; 240:737–41. PMID: [9398636](https://pubmed.ncbi.nlm.nih.gov/9398636/)
8. Thomas P, Pang Y, Filardo EJ, Dong J. Identity of an estrogen membrane receptor coupled to a G-protein in human breast cancer cells. *Endocrinology* 2005; 146:624–32. PMID: [15539556](https://pubmed.ncbi.nlm.nih.gov/15539556/)
9. Revankar CM, Cimino DF, Sklar LA, Arterburn JB, Prossnitz ER. A transmembrane intracellular estrogen receptor mediates rapid cell signaling. *Science* 2005; 307:1625–30. PMID: [15705806](https://pubmed.ncbi.nlm.nih.gov/15705806/)
10. Maggiolini M, Picard D. The unfolding stories of GPR30, a new membrane-bound estrogen receptor. *J Endocrinol.* 2010; 204:105–114. doi: [10.1677/JOE-09-0242](https://doi.org/10.1677/JOE-09-0242) PMID: [19767412](https://pubmed.ncbi.nlm.nih.gov/19767412/)
11. De Francesco EM, Lappano R, Santolla MF, Marsico S, Caruso A, Maggiolini M. HIF-1 $\alpha$ /GPER signaling mediates the expression of VEGF induced by hypoxia in breast cancer associated fibroblasts (CAFs). *Breast Cancer Res.* 2013; 15:R64. PMID: [23947803](https://pubmed.ncbi.nlm.nih.gov/23947803/)
12. De Francesco EM, Pellegrino M, Santolla MF, Lappano R, Ricchio E, Abonante S, et al. GPER mediates activation of HIF1 $\alpha$ /VEGF signaling by estrogens. *Cancer Res.* 2014; 74:4053–64. doi: [10.1158/0008-5472.CAN-13-3590](https://doi.org/10.1158/0008-5472.CAN-13-3590) PMID: [24894716](https://pubmed.ncbi.nlm.nih.gov/24894716/)
13. Lappano R, Rosano C, De Marco P, De Francesco EM, Pezzi V, et al. Estriol acts as a GPR30 antagonist in estrogen receptor-negative breast cancer cells. *Mol Cell Endocrinol.* 2010; 320:162–170. doi: [10.1016/j.mce.2010.02.006](https://doi.org/10.1016/j.mce.2010.02.006) PMID: [20138962](https://pubmed.ncbi.nlm.nih.gov/20138962/)
14. Pupo M, Pisano A, Lappano R, Santolla MF, De Francesco EM, et al. Bisphenol A Induces Gene Expression Changes and Proliferative Effects through GPER in Breast Cancer Cells and Cancer-Associated Fibroblasts. *Environ Health Perspec.* 2012; 120:1177–1182.
15. Albanito L, Lappano R, Madeo A, Chimento A, Prossnitz ER, Cappello AR, et al. Effects of Atrazine on Estrogen Receptor  $\alpha$ - and G Protein-Coupled Receptor 30-Mediated Signaling and Proliferation in Cancer Cells and Cancer-Associated Fibroblasts. *Environ Health Perspec.* 2015 (in press).

16. Bologa CG, Revankar CM, Young SM., Edwards BS., Arterburn JB., Kiselyov AS, et al. Virtual and bio-molecular screening converge on a selective agonist for GPR30. *Nat Chem Biol.* 2006; 2:207–12. PMID: [16520733](#)
17. Dennis MK, Burai R, Ramesh C, Petrie WK, Alcon SN, Nayak TK, et al. In vivo effects of a GPR30 antagonist. *Nat Chem Biol.* 2009; 5(6):421–7. doi: [10.1038/nchembio.168](#) PMID: [19430488](#)
18. Meyer MR, Prossnitz ER, Barton M. The G protein-coupled estrogen receptor GPER/GPR30 as a regulator of cardiovascular function. *Vascul Pharmacol.* 2011; 55:17–25. doi: [10.1016/j.vph.2011.06.003](#) PMID: [21742056](#)
19. Isensee J, Meoli L, Zazzu V, Nabzdyk C, Witt H, Soewarto D, et al. Expression pattern of G protein-coupled receptor 30 in LacZ reporter mice. *Endocrinology* 2009; 150:1722–30. doi: [10.1210/en.2008-1488](#) PMID: [19095739](#)
20. Broughton BRS, Miller AA, Sobey CG. Endothelium-dependent relaxation by G protein-coupled receptor 30 agonists in rat carotid arteries. *Am J Physiol Heart Circ Physiol.* 2010; 298: H1055–H1061. doi: [10.1152/ajpheart.00878.2009](#) PMID: [20061543](#)
21. Lindsey SH, Carver KA, Prossnitz ER, Chappell MC. Vasodilation in response to the GPR30 agonist G-1 is not different from estradiol in the mRen2.Lewis female rat. *J Cardiovasc Pharmacol.* 2011; May; 57(5):598–603. PMID: [21326105](#)
22. Haas E, Bhattacharya I, Brailoiu E. Regulatory Role of G Protein-Coupled Estrogen Receptor for Vascular Function and Obesity. *Circ Res.* 2009; 104(3):288–291. doi: [10.1161/CIRCRESAHA.108.190892](#) PMID: [19179659](#)
23. Patkar S, Farr TD, Cooper E, Dowell FJ, Carswell HV. Differential vasoactive effects of oestrogen, oestrogen receptor agonists and selective oestrogen receptor modulators in rat middle cerebral artery. *Neurosci Res.* 2011; Sep; 71(1):78–84. doi: [10.1016/j.neures.2011.05.006](#) PMID: [21624404](#)
24. Lindsey SH, Liu L, Chappell MC. Vasodilation by GPER in mesenteric arteries involves both endothelial nitric oxide and smooth muscle cAMP signaling. *Steroids.* 2014; 81:99–102. doi: [10.1016/j.steroids.2013.10.017](#) PMID: [24246735](#)
25. Mandala M, Osol G. Physiological remodeling of the maternal uterine circulation during Pregnancy. *Basic Clin Pharmacol Toxicol.* 2012; Jan; 110(1):12–8. doi: [10.1111/j.1742-7843.2011.00793.x](#) PMID: [21902814](#)
26. Colton I, Mandalà M, Morton J, Davidge ST, Osol G. Influence of constriction, wall tension, smooth muscle activation and cellular deformation on rat resistance artery vasodilator reactivity. *Cell Physiol Biochem.* 2012; 29(5–6):883–92. doi: [10.1159/000178465](#) PMID: [22613988](#)
27. Osol G, Mandala M. Maternal uterine vascular remodeling during pregnancy. *Physiology* 2009; 24:58–71. doi: [10.1152/physiol.00033.2008](#) PMID: [19196652](#)
28. Byers MJ, Zangl A, Phernetton TM, Lopez G, Chen DB, Magness RR. Endothelial vasodilator production by ovine uterine and systemic arteries: ovarian steroid and pregnancy control of ERalpha and ERbeta levels. *J Physiol.* 2005; May 15; 565(Pt 1):85–99. PMID: [15774511](#)
29. Van der Heijden OW, Essers YP, Spaanderman ME, De Mey JG, van Eys GJ, Peeters LL. Uterine artery remodeling in pseudopregnancy is comparable to that in early pregnancy. *Biol Reprod.* 2005; 73(6):1289–93. PMID: [16120827](#)
30. Haas E, Meyer MR, Schurr U, Bhattacharya I, Minotti R, Nguyen HH, et al. Differential effects of 17β-Estradiol on function and expression of estrogen receptor α, estrogen receptor β, and GPR30 in arteries and veins of patients with atherosclerosis. *Hypertension.* 2007; 49:1358–1363. PMID: [17452498](#)
31. Arefin S, Simoncini T, Wieland R, Hammarqvist F, Spina S, Goglia L, et al. Vasodilatory effects of the selective GPER agonist G-1 is maximal in arteries of postmenopausal women. *Maturitas.* 2014; 78:123–30. doi: [10.1016/j.maturitas.2014.04.002](#) PMID: [24796498](#)
32. Corcoran JJ, Nicholson C, Sweeney M, Charnock JC, Robson SC, Westwood M, et al. Human uterine and placental arteries exhibit tissue-specific acute responses to 17β-estradiol and estrogen-receptors specific agonists. *Mol Hum Reprod.* 2014; 20(5):433–41. doi: [10.1093/molehr/gat095](#) PMID: [24356876](#)
33. Meyer MR, Baretella O, Prossnitz ER, Barton M. Dilation of epicardial coronary arteries by the G protein-coupled estrogen receptor agonists G-1 and ICI 182,780. *Pharmacology* 2010; 86:58–64. doi: [10.1159/000315497](#) PMID: [20639684](#)
34. Magness RR, Rosenfeld CR. Systemic and uterine responses to alpha-adrenergic stimulation in pregnant and nonpregnant ewes. *Am J Obstet Gynecol.* 1986; 155(4):897–904. PMID: [3766646](#)
35. Yu X, Ma H, Barman SA, Liu AT, Sellers M, Stallone JN, et al. Activation of G protein-coupled estrogen receptor induces endothelium independent relaxation of coronary artery smooth muscle. *Am J Physiol Endocrinol Metab.* 2011; 301:E882–E888. doi: [10.1152/ajpendo.00037.2011](#) PMID: [21791623](#)

# SIRT1 is involved in oncogenic signaling mediated by GPER in breast cancer

MF Santolla<sup>1</sup>, S Avino<sup>1</sup>, M Pellegrino<sup>1</sup>, EM De Francesco<sup>1</sup>, P De Marco<sup>1</sup>, R Lappano<sup>1</sup>, A Vivacqua<sup>1</sup>, F Cirillo<sup>1</sup>, DC Rigracciolo<sup>1</sup>, A Scarpelli<sup>1</sup>, S Abonante<sup>2</sup> and M Maggiolini<sup>\*1</sup>

A number of tumors exhibit an altered expression of sirtuins, including NAD<sup>+</sup>-dependent histone deacetylase silent information regulator 1 (SIRT1) that may act as a tumor suppressor or tumor promoter mainly depending on the tumor types. For instance, in breast cancer cells SIRT1 was shown to exert an essential role toward the oncogenic signaling mediated by the estrogen receptor- $\alpha$  (ER $\alpha$ ). In accordance with these findings, the suppression of SIRT1 led to the inhibition of the transduction pathway triggered by ER $\alpha$ . As the regulation of SIRT1 has not been investigated in cancer cells lacking ER, in the present study we ascertained the expression and function of SIRT1 by estrogens in ER-negative breast cancer cells and cancer-associated fibroblasts obtained from breast cancer patients. Our results show that 17 $\beta$ -estradiol (E2) and the selective ligand of GPER, namely G-1, induce the expression of SIRT1 through GPER and the subsequent activation of the EGFR/ERK/c-fos/AP-1 transduction pathway. Moreover, we demonstrate that SIRT1 is involved in the pro-survival effects elicited by E2 through GPER, like the prevention of cell cycle arrest and cell death induced by the DNA damaging agent etoposide. Interestingly, the aforementioned actions of estrogens were abolished silencing GPER or SIRT1, as well as using the SIRT1 inhibitor Sirtinol. In addition, we provide evidence regarding the involvement of SIRT1 in tumor growth stimulated by GPER ligands in breast cancer cells and xenograft models. Altogether, our data suggest that SIRT1 may be included in the transduction network activated by estrogens through GPER toward the breast cancer progression.

*Cell Death and Disease* (2015) 6, e1834; doi:10.1038/cddis.2015.201; published online 30 July 2015

Estrogens are involved in multiple patho-physiological processes, including the development of diverse types of tumors.<sup>1,2</sup> For instance, in breast cancer cells 17 $\beta$ -estradiol (E2) triggers stimulatory effects binding to the estrogen receptor- $\alpha$  (ER $\alpha$ ) and ER $\beta$  that regulate the expression of genes which contribute to cell proliferation, migration and survival.<sup>3,4</sup> In the last few years, increasing evidence have demonstrated that the G-protein ER (GPER, formerly known as GPR30), can mediate the action of estrogens and certain antiestrogens in both normal and malignant cells.<sup>5–9</sup> The ligand binding to GPER induces the release of the membrane-tethered heparin-bound epidermal growth factor, which binds to and activate the epidermal growth factor receptor (EGFR).<sup>10,11</sup> Then, the transactivation of EGFR stimulates a transduction network which includes calcium mobilization, MAPK and PI3-K activation in cancer cells and cancer-associated fibroblasts (CAFs), suggesting that GPER may trigger a functional interaction between tumor cells and important components of the tumor micro-environment.<sup>10,11–13</sup> As ascertained by microarray analysis,<sup>10</sup> GPER regulates a peculiar gene signature involved in the stimulation of estrogen-sensitive malignancies.<sup>7,10,14,15</sup> In accordance with these findings, GPER has been associated with negative clinical features and poor survival rates in patients with breast, endometrial and ovarian carcinomas.<sup>5</sup>

Recent studies have linked an altered expression of sirtuins family members with several diseases, including different types of tumors.<sup>16</sup> In particular, the NAD<sup>+</sup>-dependent histone deacetylase silent information regulator 1 (SIRT1) deacetylates several histone and non-histone proteins, leading to the inactivation of tumor-suppressor genes and further target proteins.<sup>16</sup> SIRT1 influences many hallmarks of longevity, gene silencing, cell cycle progression, differentiation and apoptosis and was found upregulated in a variety of malignancies.<sup>17,18</sup> The role of SIRT1 in cancer has been extensively evaluated, however, its potential to act as tumor promoter or suppressor remains controversial.<sup>19–21</sup> For instance, SIRT1-mediated deacetylation repressed the functions of several tumor suppressors like p53, p73 and HIC1, suggesting that SIRT1 may be involved in tumor progression.<sup>22,23</sup> In contrast, SIRT1 exerted anti-proliferative effects through the inhibition of NF- $\kappa$ B,<sup>24,25</sup> a transcription factor having a central role in the regulation of the immune response and carcinogenesis.<sup>26</sup> As it concerns breast cancer, tumor samples displayed elevated levels of SIRT1 with respect to non-transformed counterparts and the expression of SIRT1 was upregulated by estrogens through ER $\alpha$ .<sup>17,18</sup> In addition, it was demonstrated that ER $\alpha$  physically interacts and functionally cooperates with SIRT1 toward the stimulation of breast tumor cells.<sup>18</sup> In accordance with these findings, the inhibition of SIRT1 led to the inhibition of ER-mediated signaling, thus

<sup>1</sup>Department of Pharmacy, Health and Nutritional Sciences, University of Calabria, Rende, Italy and <sup>2</sup>Breast Cancer Unit, Regional Hospital, Cosenza, Italy

\*Corresponding author: M Maggiolini, Department of Pharmacy, Health and Nutritional Sciences, University of Calabria, Rende 87036, Italy. Tel: +39 09 8449 3076; Fax: +39 09 8449 3458; E-mail: marcellomaggiolini@yahoo.it

**Abbreviations:** GPER, G-protein estrogen receptor; CAFs, cancer-activated fibroblasts; SIRT1, silent information regulator 1; EGFR, epidermal growth factor receptor; ERK, extracellular signal-regulated kinase; AP-1, activator protein 1; HDACs, histone deacetylases

Received 13.4.15; revised 17.6.15; accepted 24.6.15; Edited by A Oberst

indicating that SIRT1 may act as a co-activator of ER $\alpha$ .<sup>27</sup> In the present study, using the GPER-positive and ER-negative SkBr3 breast cancer cells and CAFs obtained from breast cancer patients, we demonstrate that estrogens upregulate SIRT1 expression through the GPER/EGFR/ERK/c-fos/AP-1 transduction pathway. Moreover, we disclose that GPER and SIRT1 have an important role in the pro-survival effects prompted by E2 and the selective GPER ligand G-1 in cancer cells and CAFs treated with etoposide. Noteworthy, SIRT1 contributes to tumor growth elicited by ligand-activated GPER as assessed both *in vitro* as well as in breast tumor xenografts. Collectively, our data provide novel insights into the multifaceted action triggered by estrogenic GPER signaling, which engages also SIRT1, toward breast cancer progression.

## Results

**E2 and G-1 induce SIRT1 expression in ER-negative SkBr3 cells and CAFs.** Previous studies have reported that SIRT1 expression is upregulated by estrogens through ER $\alpha$  in breast cancer cells.<sup>10,18</sup> Hence, we aimed to evaluate whether estrogens may regulate SIRT1 levels also in ER-negative cancer cells. To this end, we used as a model system the SkBr3 breast cancer cells and CAFs, that are both ER-negative and GPER-positive (Supplementary Figure 1). In time course experiments, E2 and G-1 upregulated SIRT1

expression at both mRNA and protein levels, as determined by real-time PCR (Figures 1a and b) and confirmed by a semi-quantitative PCR evaluation (data not shown).<sup>28</sup> In line with these results, immunoblotting studies revealed that SIRT1 protein levels are also induced by E2 and G-1 in SkBr3 cells (Figures 1c and d) and CAFs (Figures 1e and f).

**SIRT1 expression is regulated by estrogens through GPER along with the EGFR/ERK/c-fos/AP-1 transduction pathway.** These findings prompted us to evaluate the molecular mechanisms involved in the upregulation of SIRT1 elicited by estrogens in our experimental models. Silencing GPER through a specific short-hairpin GPER construct (shGPER) in SkBr3 cells and CAFs, E2 and G-1 lost the ability to increase SIRT1 expression (Figures 2a and d), suggesting that GPER mediates this effect in both cell types. Next, we found that the upregulation of SIRT1 upon E2 and G-1 treatments is abrogated in the presence of the EGFR inhibitor AG1478 (AG) or the MEK inhibitor PD98059 (PD), whereas the PKA and PI3-K inhibitors, namely H89 and LY294002 (LY), respectively, had no effect (Figures 2e and h). In accordance with these data, E2 and G-1 induced a rapid activation of both EGFR and ERK in SkBr3 cells and CAFs (Figures 2i and j). As the GPER/EGFR/ERK transduction signaling triggers c-fos expression,<sup>6,13,15</sup> we determined the occurrence of this response to E2 and G-1 in both SkBr3 cells

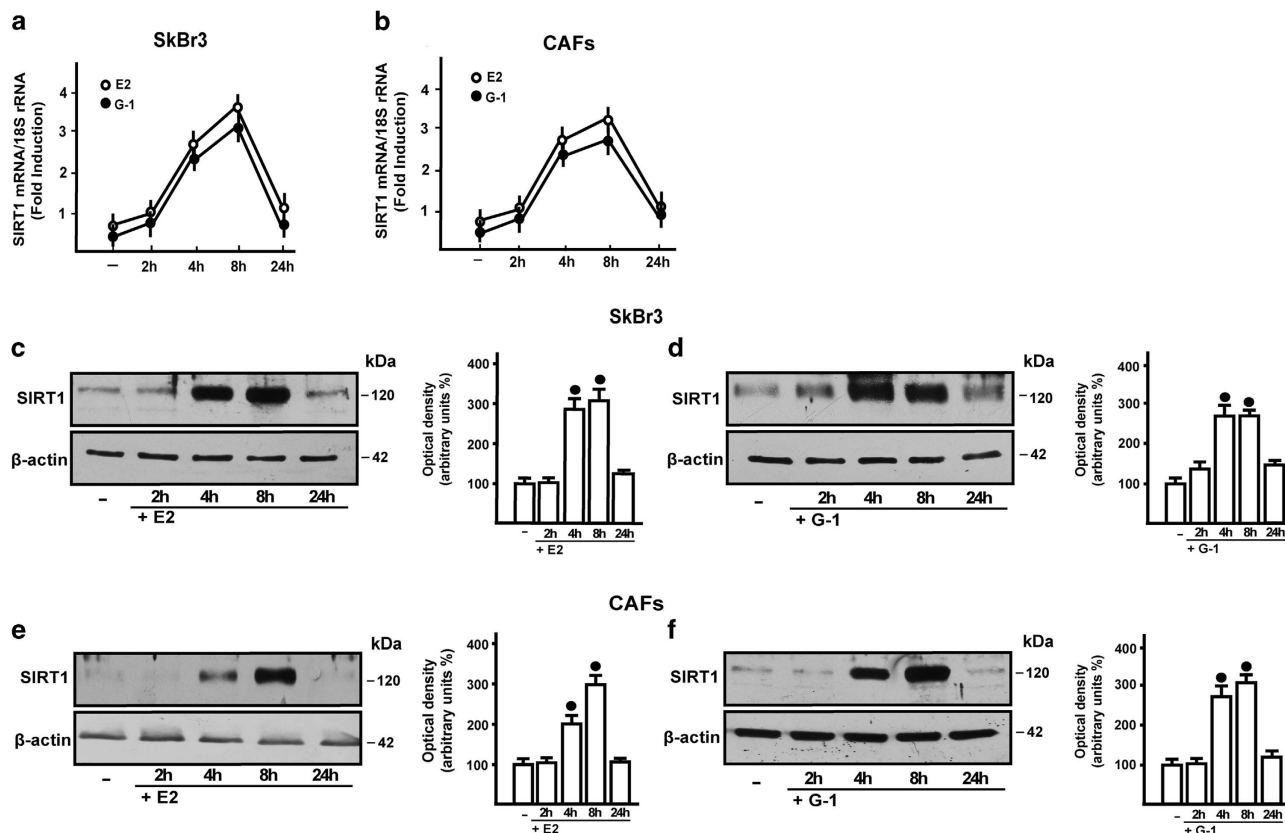


**Figure 1** E2 and G-1 induce SIRT1 expression. In SkBr3 cells and CAFs, 100 nM E2 and 1  $\mu$ M G-1 upregulate the mRNA (a and b) and protein levels (c–f) of SIRT1, as evaluated respectively by real-time PCR and immunoblotting. In RNA experiments, gene expression was normalized to 18 S expression and results are shown as fold changes of mRNA expression compared with the cells treated with vehicle (–). Side panels show densitometric analyses of the blots normalized to  $\beta$ -actin. Each data point represents the mean  $\pm$  S.D. of three independent experiments. \* indicates  $P < 0.05$  for cells receiving vehicle (–) versus treatments

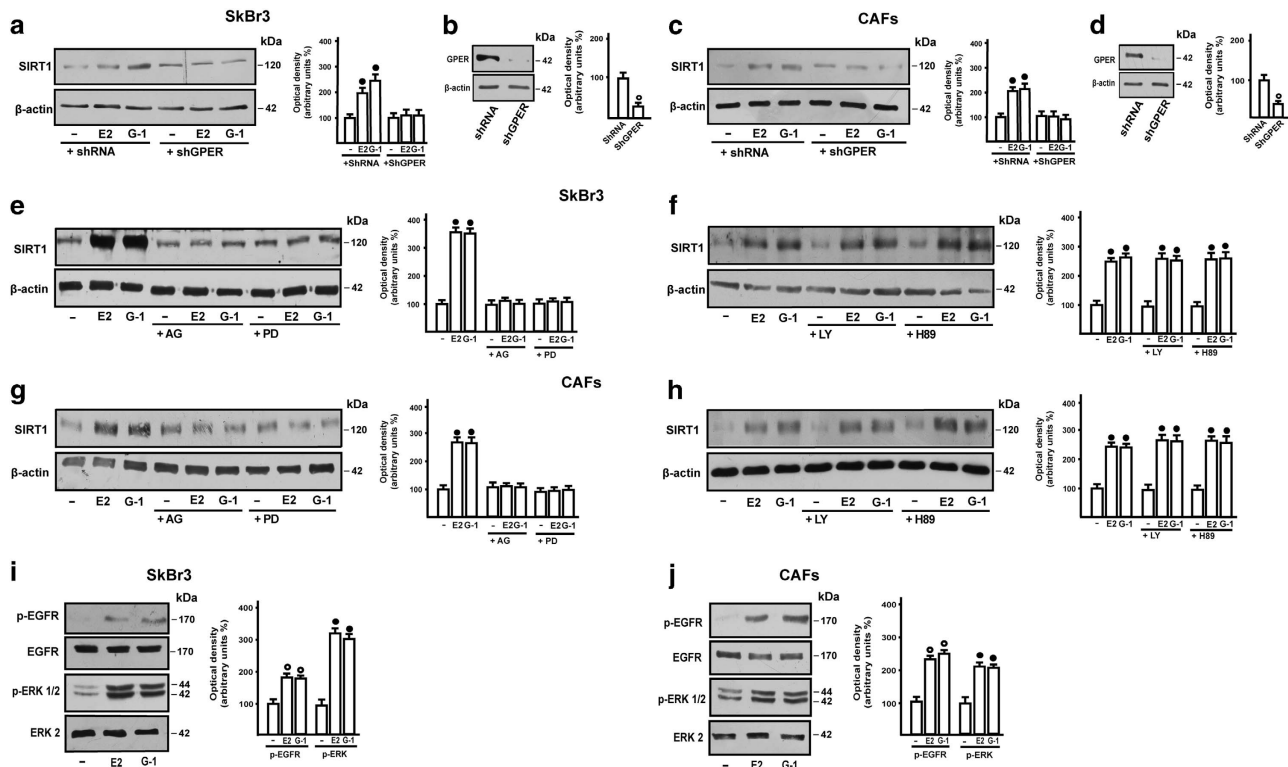


**Figure 2** The upregulation of SIRT1 protein levels by E2 and G-1 is mediated by the GPER/EGFR/ERK transduction pathway. SIRT1 protein expression induced by 100 nM E2 and 1  $\mu$ M G-1 is abolished in SkBr3 cells (a) and CAFs (c) by silencing GPER with a shGPER construct (b and d). SIRT1 protein expression in SkBr3 cells (e and f) and CAFs (g and h) treated for 8 h with vehicle (–), 100 nM E2 and 1  $\mu$ M G-1 alone and in combination with 10  $\mu$ M EGFR inhibitor AG1478 (AG), 10  $\mu$ M MEK inhibitor PD98089 (PD), 10  $\mu$ M PKA inhibitor H89, 10  $\mu$ M PI3-K inhibitor LY294002 (LY), as indicated. ERK1/2 activation and EGFR<sup>Tyr1173</sup> phosphorylation in SkBr3 cells (i) and CAFs (j) treated with vehicle (–), 100 nM E2 and 1  $\mu$ M G-1 for 15 min. Side panels show densitometric analyses of the blots normalized to  $\beta$ -actin for SIRT1 expression, ERK2 for p-ERK1/2, EGFR for p-EGFR. Each data point represents the mean  $\pm$  S.D. of three independent experiments. \*<sup>o</sup> indicate  $P < 0.05$  for cells receiving vehicle (–) versus treatments

and CAFs (Figures 3a and b), then establishing that both ligands prompt the recruitment of c-fos to the AP-1 site located within the promoter sequence of SIRT1 (Figures 3c and d). Further supporting these results, the transactivation of the SIRT1 promoter construct by E2 and G-1 was abolished co-transfecting a dominant negative form of c-fos (DN/c-fos; Figures 3e and f). Taken together, the aforementioned findings suggest that GPER along with the EGFR/ERK/c-fos/AP-1 transduction pathway mediate SIRT1 expression induced by E2 and G-1.

**SIRT1 is involved in the pro-survival effects elicited by estrogens through GPER.** Previous studies have reported that E2 through ER $\alpha$  protects breast cancer cells from oxidative stress and DNA injury.<sup>29</sup> DNA damage triggers p53 protein acetylation which leads to cell cycle arrest.<sup>30</sup> This process is mediated by many mechanisms and factors, including the increased expression of the cell cycle inhibitor p21, which facilitates cell accumulation in G0/G-1 phase in order to allow the repair of the damaged DNA.<sup>31</sup> As p21 expression is controlled by p53 which is regulated by SIRT1, for instance through deacetylation at Lys382 residue,<sup>23</sup> we investigated the role of SIRT1 in the pro-survival effects elicited by E2 and G-1 via GPER. In this regard, we performed western blot analysis to examine the p53 acetylation at residue Lys382 and the expression levels of p21 in SkBr3 cells and CAFs upon treatment with the DNA

damaging agent etoposide (ETO), which was also used in combination with E2 and G-1. As shown in Figures 4a–d, the treatment with E2 and G-1 prevented the activation of p53 and the increase of p21 protein levels triggered by ETO. Of note, this effect was abrogated in both cell types silencing GPER expression by a shGPER construct (Figures 4a and d and Supplementary Figure 2) or treating cells with the SIRT1 inhibitor namely Sirtinol (Figures 4e and h). Next, we performed cell cycle analysis determining that E2 prevents cell cycle arrest induced by ETO in SkBr3 cells and CAFs, however, this effect was no longer evident silencing GPER or in the presence of Sirtinol (Figures 5a and d). Then, we analyzed by TUNEL assay the involvement of GPER and SIRT1 in the pro-survival effects elicited by E2 in ETO-induced apoptosis. The DNA fragmentation induced by ETO was prevented treating with E2 both SkBr3 cells (Figure 6) and CAFs (Supplementary Figure 3), however the effect of E2 was abrogated silencing GPER, using the SIRT1 inhibitor Sirtinol or silencing SIRT1 expression with shSIRT1 (Supplementary Figure 4). Collectively, these findings suggest that GPER and SIRT1 contribute to the protective effects of estrogens upon exposure to the DNA damaging agent ETO.

**GPER and SIRT1 promote tumor growth both *in vitro* and *in vivo*.** In order to evaluate the potential of GPER along with SIRT1 to stimulate growth effects, we first assessed that in

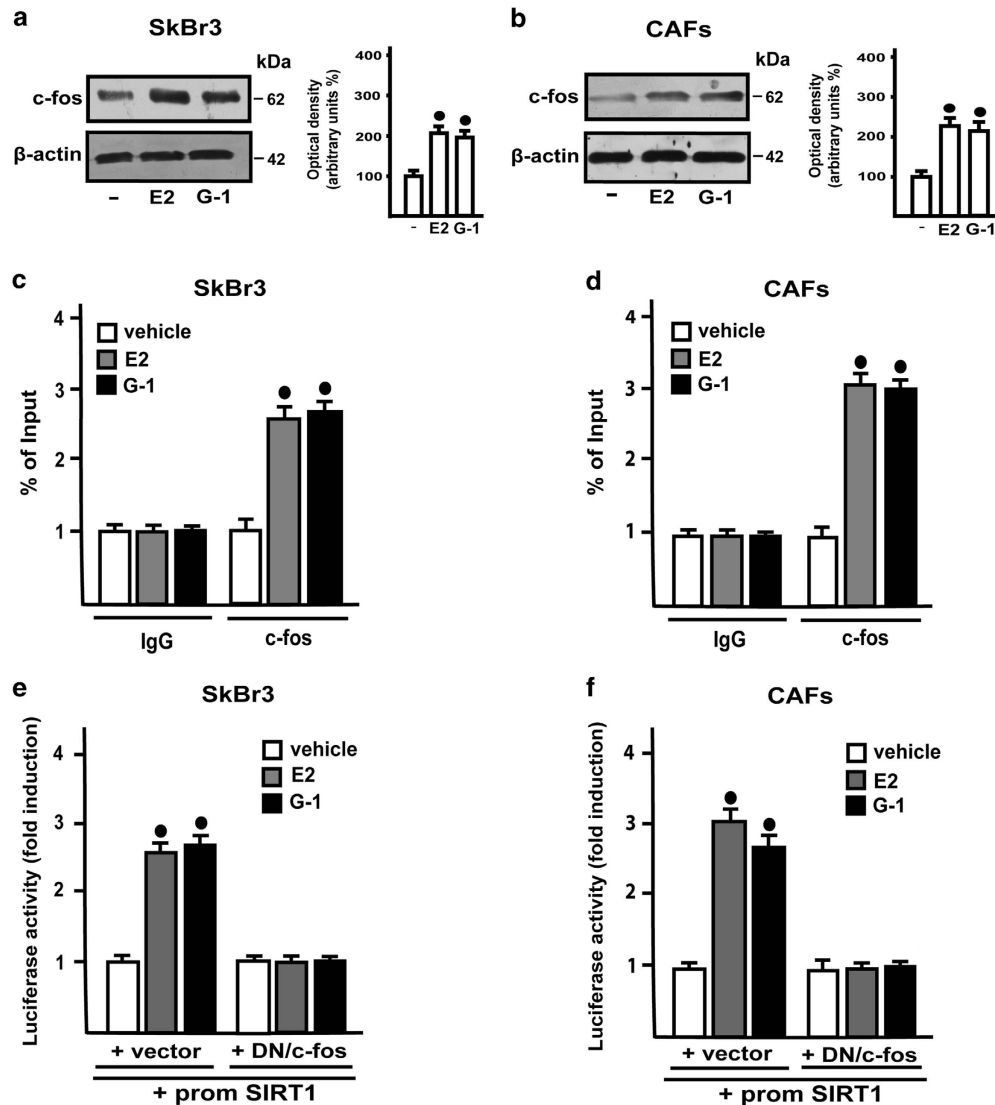


**Figure 3** E2 and G-1 induce the expression of c-fos which is recruited to the AP-1 site located within the SIRT1 promoter sequence. In SkBr3 cells (a) and CAFs (b), the treatment with 100 nM E2 and 1  $\mu$ M G-1 for 2 h upregulate c-fos, which is recruited to the AP-1 site located within the SIRT1 promoter sequence (c and d), as ascertained by ChIP assay. The transactivation of the SIRT1 promoter construct induced by an 18 h treatment with 100 nM E2 and 1  $\mu$ M G-1 is prevented transfecting cells with a construct encoding for a dominant negative form of c-fos (DN/c-fos) (e and f). In immunoblotting, side panels show densitometric analyses of the blots normalized to  $\beta$ -actin. Each data point represents the mean  $\pm$  S.D. of three independent experiments. \* indicates  $P < 0.05$  for cells receiving vehicle (-) versus treatments. Each transfection experiment was performed in triplicate, the luciferase activities from three independent experiments were normalized to the internal transfection control and values for cells receiving vehicle were set as 1 fold induction upon which the activities induced by treatments were calculated

SkBr3 cells the induction of Cyclin D1 by E2 and G-1 is abolished silencing GPER expression, as well as in the presence of the DN/c-fos construct or Sirtinol (Figures 7a and e). In agreement with these results, the proliferation of SkBr3 cells upon exposure to E2 and G-1 was no longer evident of knocking down GPER expression (Figure 7f), in the presence of the DN/c-fos construct (Figure 7g) or Sirtinol (Figure 7h), as well as silencing SIRT1 expression (Figure 7i). Afterward, we evaluated the influence of SIRT1 on tumor growth *in vivo* in 45-day-old female nude mice bearing into the intrascapular region the SkBr3 cells. Tumor xenografts were treated with vehicle, G-1 at 0.5 mg/kg/day alone and in combination with Sirtinol at 10 mg/kg/day.<sup>32–34</sup> These administrations were well tolerated as no change in body weight or in food and water

consumption was observed together with no evidence of reduced motor function. No significant difference in the mean weights or histologic features of the major organs (liver, lung, spleen and kidney) was also detected after killing among vehicle and ligand-treated mice, thus indicating a lack of toxic effects. After 40 days of treatment, histologic examination of SkBr3 xenografts revealed that tumors explanted were primarily composed of human epithelial cells (Supplementary Figure 5). Moreover, we assessed that tumor growth induced by G-1 is prevented by Sirtinol (Figures 8a and b). Of note, increased Cyclin D1, Ki-67 and SIRT1 protein levels were found in tumor homogenates obtained from G-1 stimulated mice with respect to mice treated with vehicle, however, these stimulatory effects were prevented in the group of animals

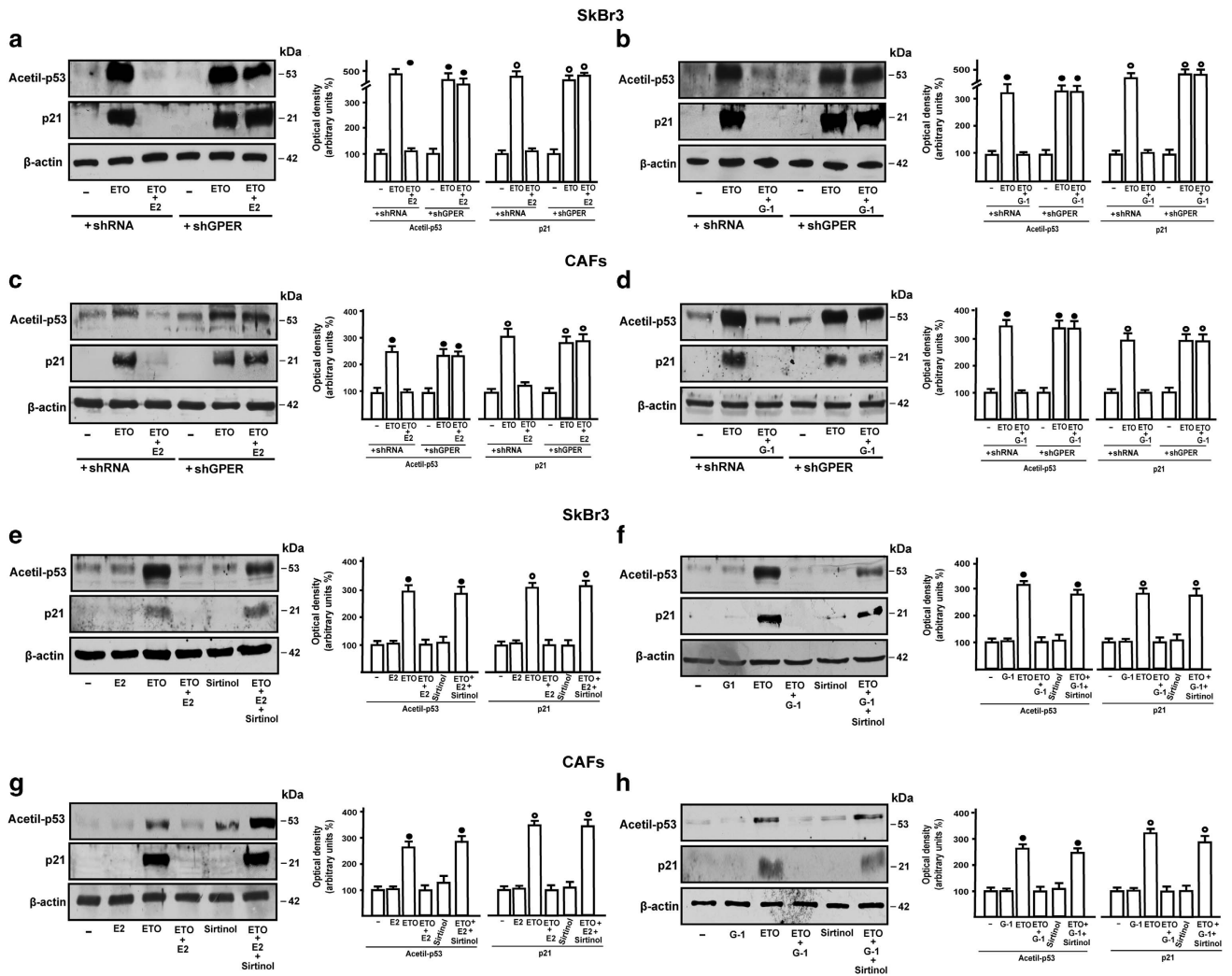


**Figure 4** p53 acetylation and p21 upregulation induced by etoposide (ETO) are prevented by E2 and G-1 through GPER and SIRT1. SkBr3 cells (**a** and **b**) and CAFs (**c** and **d**) were transfected with shRNA or shGPER and then treated for 6 h with vehicle (–), 20 μM ETO alone and in combination with 100 nM E2 and 1 μM G-1. Immunoblots showing p53 acetylation at residue Lys382 and p21 protein expression in SkBr3 cells (**e** and **f**) and CAFs (**g** and **h**) treated for 6 h with vehicle (–), 20 μM ETO alone and in combination with 100 nM E2, 1 μM G-1 and 25 μM Sirtinol. Side panels show densitometric analysis of the blots normalized to β-actin. Each data point represents the mean ± S.D. of three independent experiments. \* ° indicate  $P < 0.05$  for cells receiving vehicle (–) versus treatments

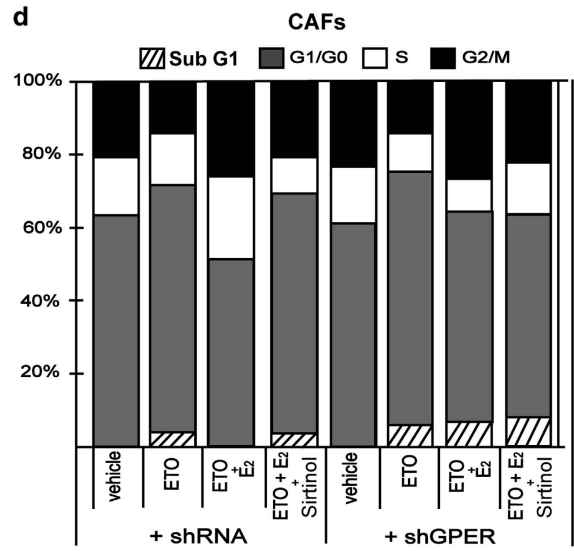
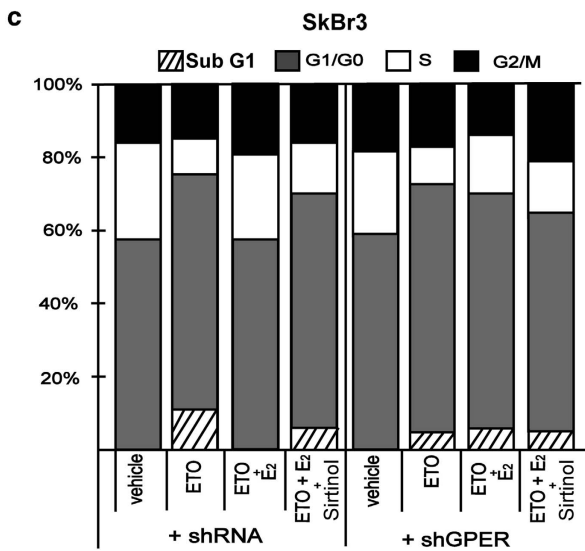
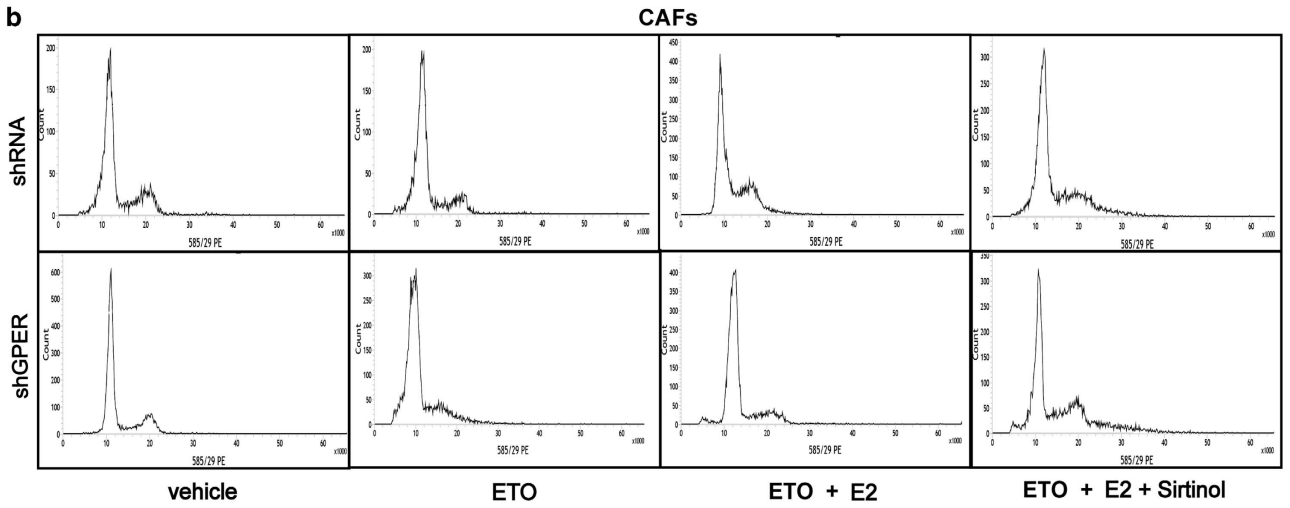
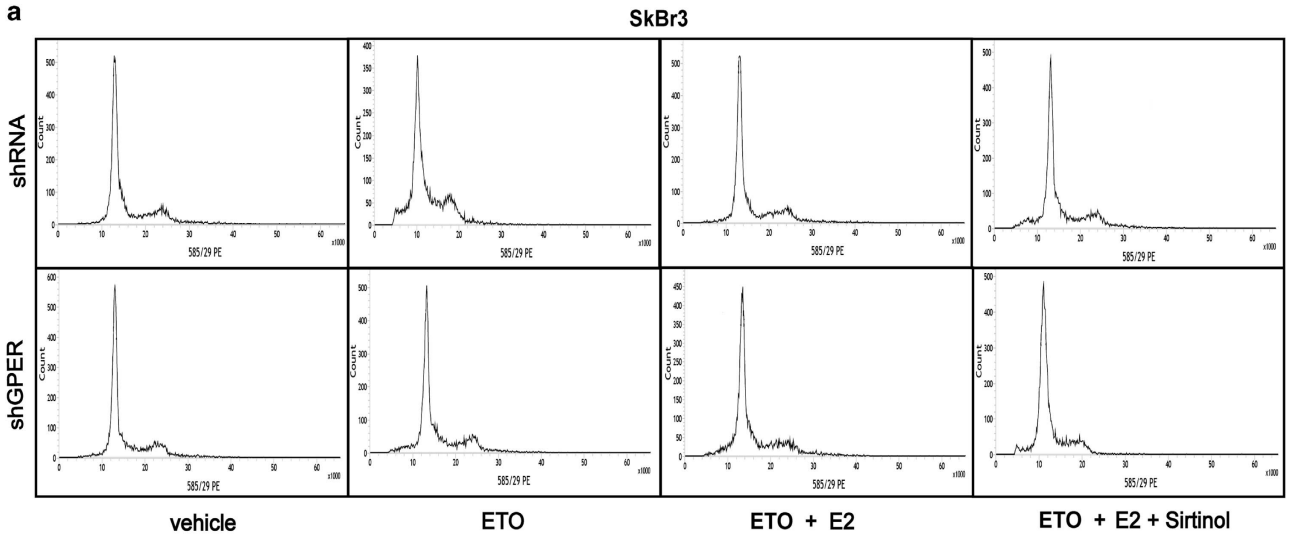
receiving G-1 in combination with Sirtinol (Figure 8c). Taken together, these results indicate that SIRT1 is also involved in tumor growth prompted by G-1 *in vivo*.

## Discussion

In the present study, we provide novel insights into the regulation and function of SIRT1 by estrogens in ER-negative breast cancer cells and CAFs. In particular, we demonstrate that E2 and the selective GPER agonist G-1 induce SIRT1 expression through the rapid activation of the EGFR/ERK1/2 signaling and the stimulation of c-fos expression which is recruited to the AP-1 site located within the SIRT1 promoter sequence. Noteworthy, GPER mediates the upregulation of SIRT1 by E2 and G-1, as ascertained by silencing experiments. Using the DNA damaging agent ETO, we also disclose that GPER along with SIRT1 are involved in the pro-survival effects elicited by these ligands, as demonstrated knocking

down GPER expression and using the SIRT1 inhibitor Sirtinol. Biologically, we show that GPER and SIRT1 contribute to the growth effects triggered by E2 and G-1 *in vitro*, as well as in breast tumor xenografts. In accordance with these findings, Sirtinol abrogated the increase of both Cyclin D1 and the proliferative index Ki-67 upon G-1 treatment, as assessed in tumor homogenates. Collectively, our data reveal that SIRT1 may be engaged by GPER signaling toward tumor progression and pro-survival effects elicited by estrogens in cancer cells and main components of the tumor microenvironment like CAFs.

Sirtuins have drawn increasing attention due to their action in various patho-physiological processes as lifespan extension, aging, neurodegeneration, obesity, heart disease, inflammation and cancer.<sup>16</sup> In mammals, the sirtuins family includes seven members (SIRT1-7) that show distinct structure, distribution and functions.<sup>35</sup> SIRT1 is the mammalian homolog of the yeast silent information regulator 2 (sir2)



and the most extensively studied sirtuins member.<sup>16</sup> SIRT1 deacetylates several histone and non-histone proteins involved in the regulation of numerous cellular and metabolic processes including gene silencing, cell cycle progression, differentiation, apoptosis and aging.<sup>17,36,37</sup> For instance, SIRT1 inactivates the tumor suppressor p53 deacetylating the Lys382 residue.<sup>38,39</sup> Inactive p53 then leads to a defective apoptotic response to DNA damage, suggesting that SIRT1 may contribute to cancer initiation and progression.<sup>40</sup> Other SIRT1 downstream targets include NF- $\kappa$ B, PPAR- $\gamma$ , p63, p73, FOXO, Ku70 and the androgen receptor.<sup>22,39,41–43</sup> To date, the function of SIRT1 remains controversial as previous data suggest that SIRT1 can act as a tumor promoter or a tumor suppressor likely depending on cell type, its distribution and biological targets.<sup>19–21</sup> SIRT1-deficient mice developed tumors in many tissues<sup>44</sup> and the overexpression of SIRT1 prevented intestinal tumorigenesis in transgenic mice,<sup>45</sup> nevertheless SIRT1 activity was suggested to have a role in breast and prostate cancer cell growth.<sup>46,47</sup> In addition, SIRT1 was involved in oncogenic signaling in mammary epithelial cancer cells<sup>48</sup> and SIRT1 knockout mice exhibited p53 hyperacetylation and increased apoptosis upon radiation exposure.<sup>49</sup> SIRT1 was also shown to suppress senescence and apoptosis indicating that its inhibition may be beneficial in diverse types of cancer.<sup>50,51</sup> Consequently, a number of SIRT1 inhibitors have been identified in order to interfere with cell proliferation in various types of tumors.<sup>19,52–55</sup>

Estrogens exert diverse patho-physiological functions, including the development and maintenance of female reproductive system and the progression of breast cancer.<sup>56</sup> The action of estrogens is mainly mediated by the classical ER, however, these steroids act also through GPER in both normal and malignant cell contexts, like breast cancer cells and CAFs that are main factors of the tumor microenvironment.<sup>5,8,10,11,56,57</sup> In particular, the stromal contribution to the development of a wide variety of tumors has been extensively assessed using both *in vitro* and *in vivo* model systems.<sup>58–60</sup> For instance, it has been shown that malignant cells may recruit into the tumor mass diverse components of the microenvironment like CAFs, inflammatory and vascular cells that actively cooperate toward cancer progression.<sup>58</sup> Increasing evidence has suggested that CAFs contribute to cancer aggressiveness through the production of secreted factors, which target numerous stromal components and cancer cell types.<sup>59,61</sup> In breast carcinoma ~80% of stromal fibroblasts exhibit the activated features of CAFs that stimulate the proliferation of cancer cells also at the metastatic sites.<sup>62</sup> CAFs may also promote the local production of estrogens, which largely contribute to the development of breast carcinomas through an intricate cross-talk with many transduction pathways activated by growth factors.<sup>63</sup> In addition, the ER antagonist tamoxifen was shown to upregulate the aromatase expression through GPER in both breast cancer cells and CAFs, suggesting that GPER may be

involved in the tamoxifen resistance in breast cancer.<sup>64</sup> In this context, our current results provide evidence regarding a novel mechanism by which estrogens through GPER engages SIRT1 toward the stimulation of breast cancer cells, CAFs and breast tumor xenografts. Previous studies have demonstrated that ER $\alpha$  is involved in cell survival and oncogenic transformation triggered by E2 via activation of anti-oxidative enzymes, MAPK, PI3-K and p53 inhibition.<sup>18,29</sup> In addition, it has been shown that ER $\alpha$  and SIRT1 actively cooperate in mediating the protection elicited by E2 against DNA damaging agents.<sup>18</sup> Further extending these mechanisms of estrogen action, the current results indicate that E2 through GPER protect ER-negative breast cancer cells and CAFs from the DNA damage occurring upon ETO treatment. For instance, we have found that GPER and SIRT1 are involved in the prevention of cell cycle arrest and apoptosis prompted by ETO. Hence, GPER targets SIRT1 as ER $\alpha$  toward cell survival and tumor growth, suggesting that appropriate combination therapies could offer more effective interventions according to the ER expression pattern in breast cancer.

#### Materials and Methods

**Materials.** Tyrphostin AG1478 (AG) was purchased from Biomol Research Laboratories (Milan, Italy). PD98059 (PD) and Sirtinol were obtained from Calbiochem (Milan, Italy). 1-[4-(6-Bromobenzol1,3-diodo-5-yl)-3a,4,5,9b-tetrahydro-3H-cyclopenta[c-]quinolin-8yl] ethanone (G-1) was purchased from Tocris Bioscience (Bristol, UK). E2, H89, LY294002 (LY) and ETO were purchased from Sigma-Aldrich Srl (Milan, Italy). All compounds were solubilized in dimethyl sulfoxide (DMSO), except E2 and PD which were dissolved in ethanol.

**Cell culture.** SkBr3 and MCF-7 breast cancer cells and LNCaP prostate cancer cells were obtained by ATCC (Manassas, VA, USA) and used <6 months after resuscitation. SkBr3 and LNCaP were maintained in RPMI-1640 without phenol red, MCF-7 was maintained in DMEM medium, with a supplement of 10% fetal bovine serum (FBS; Sigma-Aldrich Srl) and 100  $\mu$ g/ml of penicillin/streptomycin (Life Technologies, Milan, Italy). CAFs obtained from breast cancer patients, were characterized and maintained as we previously described.<sup>57,65</sup> Signed informed consent from all the patients was obtained and all samples were collected, identified and used in accordance with approval by the Institutional Ethical Committee Board (Regional Hospital, Cosenza, Italy). All cell lines were grown in a 37 °C incubator with 5% CO<sub>2</sub>. Cells were switched to medium without serum 24 h before experiments.

**Gene silencing experiments and plasmids.** Cells were plated onto 10-cm dishes and transfected by X-treme GENE 9 DNA transfection reagent (Roche Molecular Biochemicals, Milan, Italy) for 24 h before treatments with a control vector, a specific shRNA sequence for each target gene, the DN/c-fos construct which encodes for c-fos mutant that heterodimerizes with c-fos dimerization partners but not allowing DNA binding (kindly obtained from Dr C Vinson, NIH, Bethesda, MD, USA). The silencing of GPER expression was obtained by a construct (shGPER) previously described,<sup>66</sup> whereas the silencing of SIRT1 expression was obtained by a construct (shSIRT1) kindly provided by Dr H Cha, (Sogang University, Seoul, Korea).

**Gene expression studies.** Total RNA was extracted and cDNA was synthesized by reverse transcription as previously described.<sup>13</sup> The expression of selected genes was quantified by real-time PCR using Step One sequence detection system (Applied Biosystems, Milan, Italy). Gene-specific primers were

**Figure 5** The cell cycle arrest induced by etoposide (ETO) is blunted by E2 via GPER and SIRT1. Cell-cycle analysis performed in SkBr3 cells (a) and CAFs (b) transfected with shRNA or shGPER for 24 h and then treated for 12 h with 20  $\mu$ M ETO alone and in combination with 100 nM E2 and 25  $\mu$ M Sirtinol. (c and d) histograms show the percentages of cells in subG1, G0/G-1, S and G2/M phases of the cell cycle, as determined by flow cytometry analysis. Values represent the mean  $\pm$  S.D. of three independent experiments

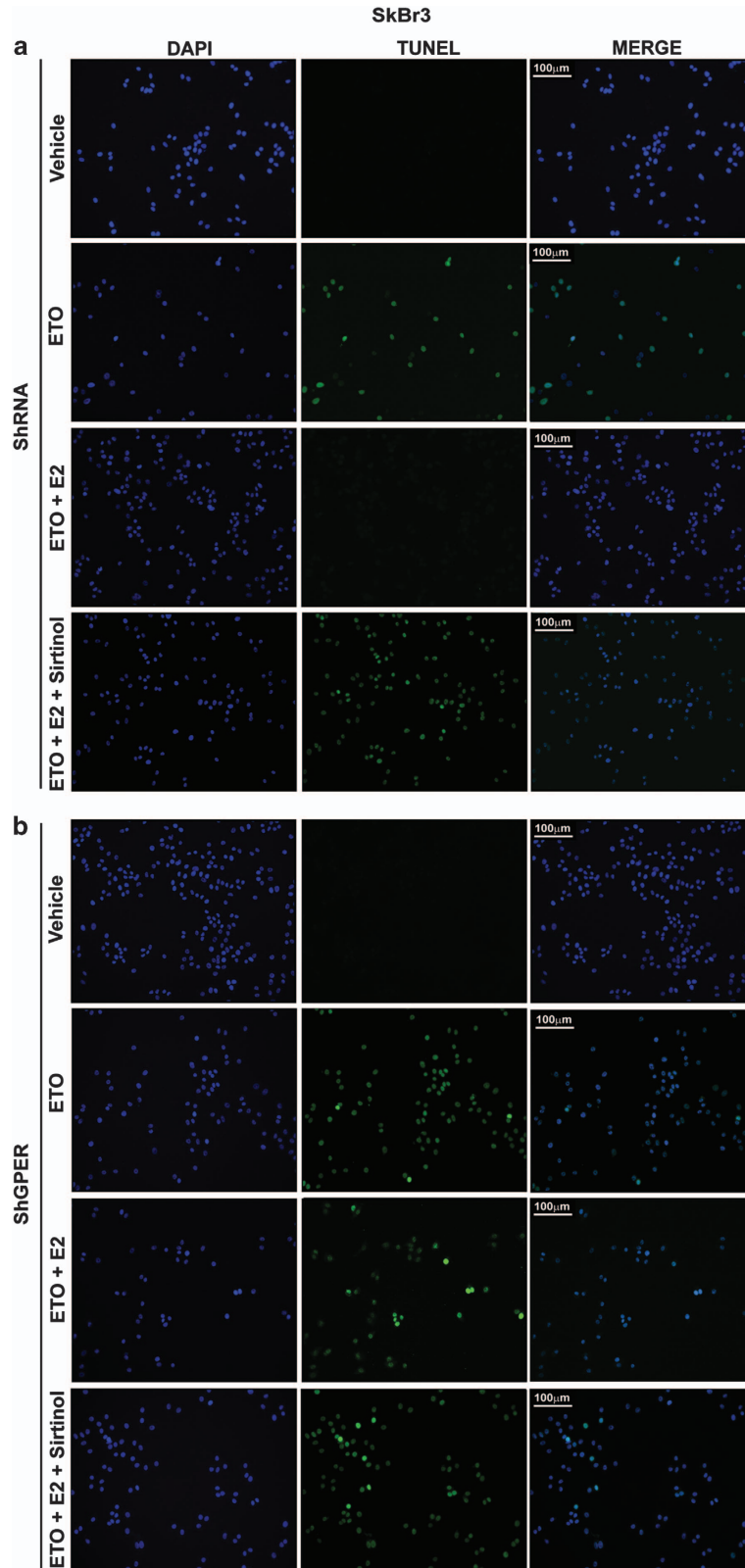


**Figure 6** Apoptosis induced by etoposide (ETO) is prevented by E2 via GPER and SIRT1. In SkBr3 cells transfected with shRNA (a) or shGPER (b), apoptotic changes were detected using TUNEL (green) and DAPI (blue) staining after 24 h of treatment with 20  $\mu$ M ETO alone and in combination with 100 nM E2 and 25  $\mu$ M Sirtinol. Each experiment shown is representative of 20 random fields. Data are representative of three independent experiments

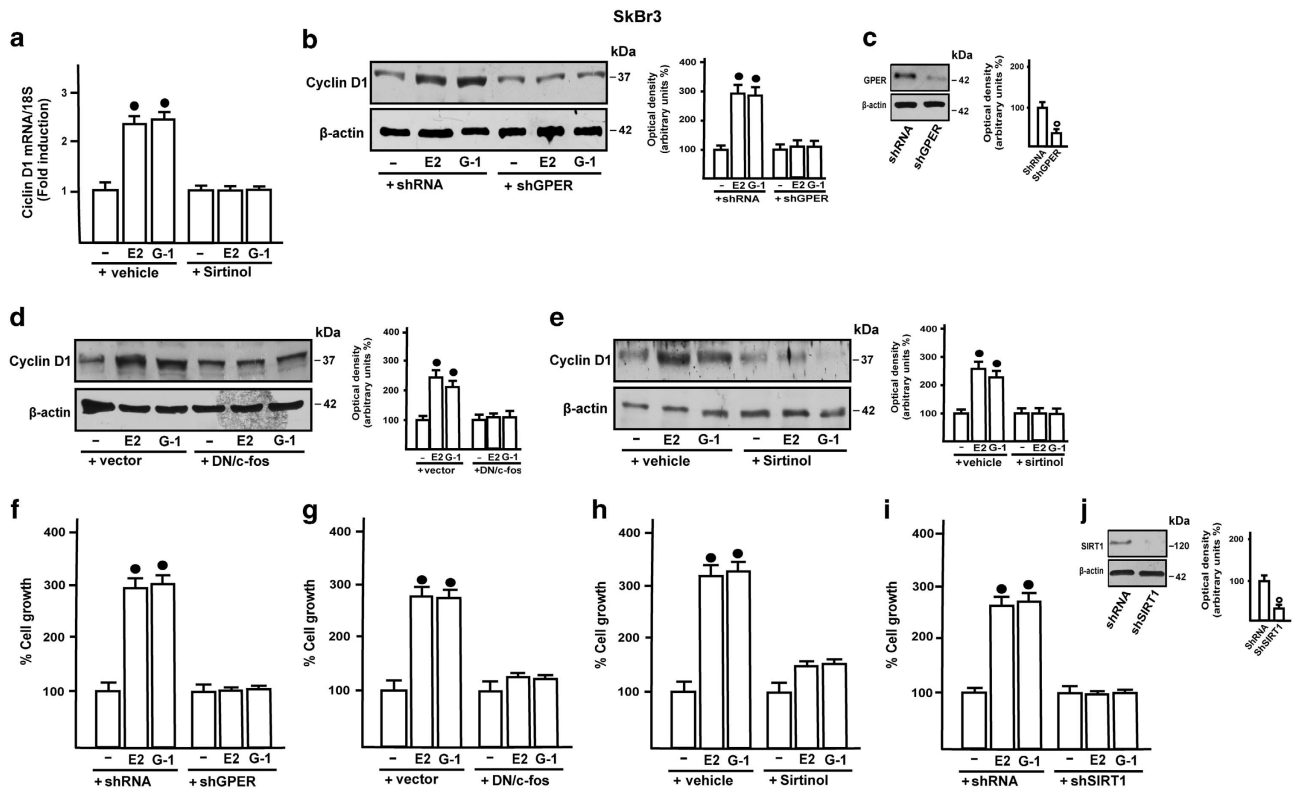


**Figure 7** SIRT1 mediates the proliferative effects induced by E2 and G-1 in SkBr3 cells. (a) Evaluation of Cyclin D1 mRNA expression upon exposure to 100 nM E2 and 1  $\mu$ M G-1 alone and in combination with 25  $\mu$ M Sirtinol. The upregulation of Cyclin D1 protein levels by 100 nM E2 and 1  $\mu$ M G-1 was abolished transfecting cells with shGPER (b and c), with the DN/c-fos construct (d) or treating cells also with 25  $\mu$ M Sirtinol (e). Cell proliferation induced by 100 nM E2 and 100 nM G-1 was abrogated transfecting cells with shGPER (f), with the DN/c-fos construct (g), treating cells with 25  $\mu$ M Sirtinol (h) or transfecting cells with shSIRT1 (i). In RNA experiments, gene expression was normalized to 18 S expression and results are shown as fold changes of mRNA expression induced by treatments with respect to cells treated with vehicle (-). In immunoblots experiments side panels show densitometric analyses of the blots normalized to  $\beta$ -actin. Each data point represents the mean  $\pm$  S.D. of three independent experiments. \*,  $\circ$  indicate  $P < 0.05$  for cells receiving vehicle (-) versus treatments

designed using Primer Express version 2.0 software (Applied Biosystems). For SIRT1, Cyclin D1 and the ribosomal protein 18 S, which was used as a control gene to obtain normalized values, the primers were: 5'-CTCTAGTGACTCC AAGG-3' (SIRT1 forward), 5'-AAGATCTGGGAAGTCTACAGCA-3' (SIRT1 reverse), 5'-GTCTGTGCATTCTGTTGCA-3' (Cyclin D1 forward), 5'-GCTGGAAC ATGCCGGTGA-3' (Cyclin D1 reverse), 5'-GGCGTCCCCAACTTCTTA-3' (18 S forward) and 5'-GGGCATCACAGACTGTATT-3' (18 S reverse). Assays were performed in triplicate and the results were normalized to 18 S expression and then calculated as fold induction of RNA expression.

**Western blot analysis.** SkBr3 cells, CAFs and tumor homogenates obtained from nude mice were processed according to the previously described protocol.<sup>67-69</sup> Protein lysates were electrophoresed through a reducing SDS/10% (w/v) polyacrylamide gel, electroblotted onto a nitrocellulose membrane probed with primary antibodies against SIRT1 (D739) and acetyl-p53 (Lys382) purchased from Cell Signaling Technology, Euroclone (Milan, Italy), c-fos (H-125), phosphorylated ERK1/2 (E-4), ERK2 (C-14), EGFR (1005), p-EGFR<sup>Tyr1173</sup> (sc-12351), p21 (H164), GPER (N-15), Cyclin D1 (M-20), Ki-67 (H-300) and  $\beta$ -actin (C2) purchased from Santa Cruz Biotechnology (DBA, Milan, Italy). The levels of proteins and phosphoproteins were detected, after incubation with the horseradish peroxidase-linked secondary antibodies (Santa Cruz Biotechnology), by the ECL System (GE Healthcare, Milan, Italy).

**Chromatin immunoprecipitation (ChIP) assay.** Cells grown in 10-cm plates were shifted for 24 h to medium lacking serum and then treated with vehicle, 100 nM E2 and 1  $\mu$ M G-1. Chip assay was performed as previously described.<sup>70</sup> In brief, the immune-cleared chromatin was immunoprecipitated with anti-c-fos (H-125) or nonspecific IgG (Santa Cruz Biotechnology). A 4- $\mu$ l volume of each immunoprecipitated DNA sample was used as template to amplify, by real-time

PCR, a region containing an AP-1 site located in the SIRT1 promoter region. The primers used to amplify this fragment were: 5'-GCTCACGCTAGAAGGAAGG-3' (forward) and 5'-GGAAGACCTTTGACGTGGAG-3' (reverse). The data were normalized with respect to unprocessed lysates (input DNA). Inputs DNA quantification was performed by using 4  $\mu$ l of the template DNA. The relative antibody-bound fractions were normalized to a calibrator that was chosen to be the basal, untreated sample. Final results were expressed as percent differences with respect to the relative input.

**Gene reporter assays.** The 2.2 kb SIRT1 promoter-luciferase construct containing full-length SIRT1 promoter sequence used in luciferase assays was a kind gift from Dr M Thangaraju, (Georgia Health Sciences University, Augusta, GA, USA). SkBr3 cells and CAFs ( $1 \times 10^5$ ) were plated into 24-well dishes with 500  $\mu$ l/well culture medium containing 10% FBS and transfected for 24 h with control vector and DN/c-fos construct. A mixture containing 0.5  $\mu$ g of reporter plasmid and 10 ng of pRL-TK was then transfected by using X-treme GENE 9 DNA transfection reagent, as recommended by the manufacturer (Roche Diagnostics). After 8 h, cells were treated for 18 h with E2 and G-1 in serum-free medium. Luciferase activity was measured with Dual Luciferase Kit (Promega, Milan, Italy) and normalized to the internal transfection control provided by Renilla luciferase. The normalized relative light unit values obtained from cells treated with vehicle were set as onefold induction, upon which the activity induced by treatments was calculated.

**FACS analysis.** Around  $1 \times 10^5$  cells per well were seeded into 12-well plates and maintained in medium for 24 h. For knockdown experiments, cells were transfected for 48 h with shRNA constructs directed against GPER and with an unrelated shRNA construct (3  $\mu$ g DNA/well transfected with X-treme GENE 9 DNA transfection reagent in medium without serum). Cells were then treated with 20  $\mu$ M ETO alone and in combination with 100 nM E2, as well as in presence of 25  $\mu$ M

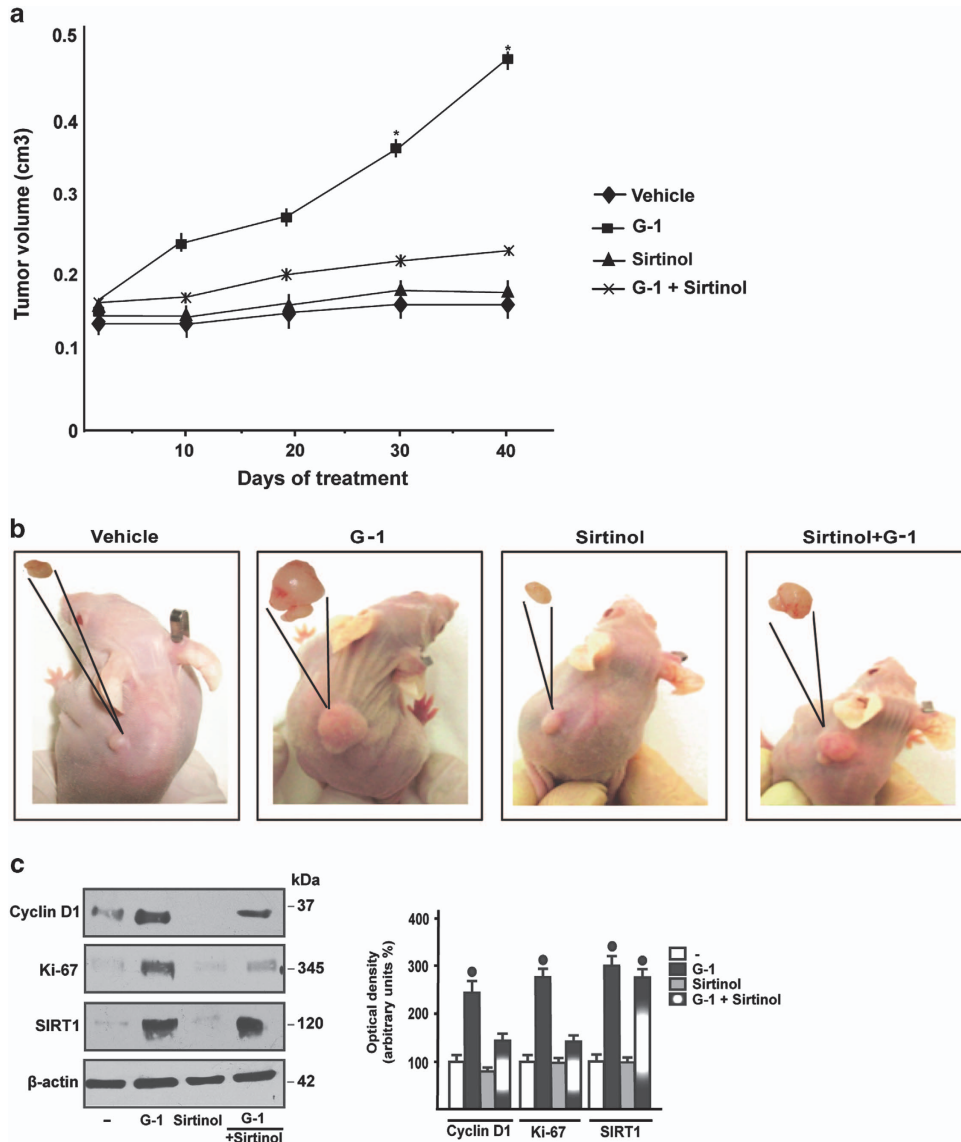


**Figure 8** SIRT1 is involved in the growth of SkBr3 xenografts. (a) Tumor volume from SkBr3 xenografts implanted in female athymic nude mice treated for 40 days with vehicle, G-1 (0.50 mg/kg/die), Sirtinol (10 mg/kg/die) or a combination of these agents, as indicated. \* indicates  $P < 0.05$  for animals treated with G-1 versus animals treated with vehicle. (b) Representative images of mice and relative explanted tumors at day 40, scale bar, 0.3 cm. (c) Cyclin D1, Ki-67 and SIRT1 protein levels in tumor homogenates from SkBr3 xenografts treated as reported above. Side panels show densitometric analysis of the blots normalized to  $\beta$ -actin. \* indicates  $P < 0.05$  for G-1-treated animals versus vehicle-treated animals

Sirtinol. After 8 h, cells were pelleted, washed once with phosphate buffered saline (PBS) and resuspended in 0.5 ml of a 50  $\mu$ g/ml propidium iodide in 1 x PBS (PI) solution containing 20 U/ml RNAse-A and 0.1% triton and incubated for 1 h (Sigma-Aldrich). Cells were analyzed for DNA content by FACS (BD, FACS JAZZ). Cell phases were estimated as a percentage of a total of 10 000 events.

**Tunel assay.** SkBr3 cells and CAFs were seeded into coverslips and maintained in medium for 24 h. Next, cells were serum-deprived, transfected and treated as indicated. Therefore, cells were fixed in 4% buffered paraformaldehyde for 15 min. Slides were rinsed twice in PBS, pH 7.4. For the detection of DNA fragmentation at the cellular level, cells were stained using DeadEnd Fluorometric Tunel System (Promega) following the manufacturer's instructions. Nuclei of cells were stained with 4',6-Diamidino-2-phenylindole dihydrochloride (DAPI; 1 : 1000; Sigma-Aldrich). The Leica AF6000 Advanced Fluorescence Imaging System supported by quantification and image processing software Leica Application Suite

Advanced Fluorescence (Leica Microsystems CMS, GmbH Mannheim, Germany) was used for the microscopy evaluation.

**Proliferation assay.** For quantitative proliferation assay, SkBr3 cells ( $1 \times 10^5$ ) were seeded in 24-well plates in regular growth medium. Cells were washed once they had attached and then incubated in medium containing 2.5% charcoal-stripped FBS with the indicated treatments; medium was renewed every 2 days (with treatments) and cells were counted using the Countess Automated Cell Counter, as recommended by the manufacturer's protocol (Life Technologies).

**In vivo studies.** Female 45-day-old athymic nude mice (nu/nu Swiss; Harlan Laboratories, Milan, Italy) were maintained in a sterile environment. At day 0, exponentially growing SkBr3 cells ( $8.0 \times 10^6$  per mouse) were inoculated into the intrascapular region in 0.1 ml of Matrigel (Cultrex, Trevigen, Gaithersburg, MD, USA). When the tumors reached average  $\sim 0.15$  cm<sup>3</sup> (i.e., in about 1 week after implantation), mice were randomized and divided into four groups, according to

treatments administered by intramuscular injection for 40 days. The first group of mice ( $n=7$ ) was treated daily with vehicle (0.9% NaCl with 0.1% albumin and 0.1% Tween-20), (Sigma-Aldrich), the second group of mice ( $n=7$ ) was treated daily with G-1 (0.5 mg/kg/die), the third group of mice ( $n=7$ ) was treated daily with Sirtinol (10 mg/kg/die) and the fourth group of mice ( $n=7$ ) was treated daily with G-1 in combination with Sirtinol (at the concentrations described above). G-1 and Sirtinol were dissolved in DMSO at 1 mg/ml. SkBr3 xenograft tumor growth was monitored twice a week by caliper measurements, along two orthogonal axes: length (L) and width (W). Tumor volumes (in cubic centimeters) were estimated by the following formula:  $TV=L \times (W^2)/2$ . At 40 days of treatment, the animals were killed following the standard protocols and tumors were dissected from the neighboring connective tissue. Specimens of tumors were frozen in nitrogen and stored at  $-80^\circ\text{C}$ ; the remaining tumor tissues of each sample were fixed in 4% paraformaldehyde and embedded in paraffin for the histologic analyses. Animal care, death and experiments were done in accordance with the US National Institutes of Health Guide for the Care and Use of Laboratory Animals (NIH Publication No 85-23, revised 1996) and in accordance with the Italian law (DL 116, 27 January 1992).

**Histologic analysis.** Morphologic analyses were carried out on formalin-fixed, paraffin-embedded sections of tumor xenografts were cut at  $5\ \mu\text{m}$  and allowed to air dry. Deparaffinized, rehydrated sections were stained with hematoxylin and eosin (Bio-Optica, Milan, Italy) or immunolabeled with human cytoheratin 18 (Santa Cruz Biotechnology) to verify that the tumors explanted will be primarily composed of human epithelial cells. Sections were then dehydrated, cleared with xylene, and mounted with resinous mounting medium.

**Statistical analysis.** Statistical analysis was performed using ANOVA followed by Newman-Keuls' testing to determine differences in means. Statistical comparisons for *in vivo* studies were made using the Wilcoxon-Mann-Whitney test.  $P < 0.05$  was considered statistically significant.

### Conflict of Interest

The authors declare no conflict of interest.

**Acknowledgements.** This work was supported by Associazione Italiana per la Ricerca sul Cancro (AIRC), PON01\_01078 and Ministero della Salute grant no. 67/GR-2010-2319511.

- Hall JM, Couse JF, Korach KS. The multifaceted mechanisms of estradiol and estrogen receptor signalling. *J Biol Chem* 2001; **276**: 36869–36872.
- Pearce ST, Jordan VC. The biological role of estrogen receptors alpha and beta in cancer. *Crit Rev Oncol Hematol* 2004; **50**: 3–22.
- Sanchez R, Nguyen D, Rocha W, White JH, Mader S. Diversity in the mechanisms of gene regulation by estrogen receptors. *Bioessays* 2002; **24**: 244–254.
- Métivier R, Penot G, Hübnér MR, Reid G, Brand H, Koš M et al. Estrogen receptor-alpha directs ordered, cyclical, and combinatorial recruitment of cofactors on a natural target promoter. *Cell* 2003; **115**: 751–763.
- Maggiolini M, Picard D. The unfolding stories of GPR30, a new membrane-bound estrogen receptor. *J Endocrinol* 2010; **204**: 105–114.
- Lappano R, Maggiolini M. G protein-coupled receptors: novel targets for drug discovery in cancer. *Nat Rev Drug Discov* 2011; **10**: 47–60.
- Maggiolini M, Vivacqua A, Fasanella G, Recchia AG, Sisci D, Pezzi V et al. The G protein-coupled receptor GPR30 mediates c-fos up-regulation by 17beta-estradiol and phytoestrogens in breast cancer cells. *J Biol Chem* 2004; **279**: 27008–27016.
- Albanito L, Madeo A, Lappano R, Vivacqua A, Rago V, Carpino A et al. G protein-coupled receptor 30 (GPR30) mediates gene expression changes and growth response to 17beta-estradiol and selective GPR30 ligand G-1 in ovarian cancer cells. *Cancer Res* 2007; **67**: 1859–1866.
- Prossnitz ER, Maggiolini M. Mechanisms of estrogen signalling and gene expression via GPR30. *Mol Cell Endocrinol* 2009; **308**: 32–38.
- Pandey DP, Lappano R, Albanito L, Madeo A, Maggiolini M, Picard D. Estrogenic GPR30 signalling induces proliferation and migration of breast cancer cells through CTGF. *EMBO J* 2009; **28**: 523–532.
- Madeo A, Maggiolini M. Nuclear alternate estrogen receptor GPR30 mediates 17beta-estradiol - Induced gene expression and migration in breast cancer-associated fibroblasts. *Cancer Res* 2010; **70**: 6036–6046.
- Pupo M, Vivacqua A, Perrotta I, Pisano A, Aquila S, Abonante S et al. The nuclear localization signal is required for nuclear GPER translocation and function in breast cancer-associated fibroblasts (CAFs). *Mol Cell Endocrinol* 2013; **376**: 23–32.
- Santolla MF, Lappano R, De Marco P, Pupo M, Vivacqua A, Sisci D et al. G protein-coupled estrogen receptor mediates the up-regulation of fatty acid synthase induced by 17beta-estradiol in cancer cells and cancer-associated fibroblasts. *J Biol Chem* 2012; **287**: 43234–43245.
- Lappano R, Rosano C, De Marco P, De Francesco EM, Pezzi V, Maggiolini M. Estriol acts as a GPR30 antagonist in estrogen receptor-negative breast cancer cells. *Mol Cell Endocrinol* 2010; **320**: 162–170.
- Lappano R, Santolla MF, Pupo M, Sinicropi MS, Caruso A, Rosano C et al. MIBE acts as antagonist ligand of both estrogen receptor  $\alpha$  and GPER in breast cancer cells. *Breast Cancer Res* 2012; **14**: R12.
- Moore RL, Dai Y, Faller D V. Sirtuin 1 (SIRT1) and steroid hormone receptor activity in cancer. *J Endocrinol* 2012; **213**: 37–48.
- Liu T, Liu PY, Marshall GM. The critical role of the class III histone deacetylase SIRT1 in cancer. *Cancer Res* 2009; **69**: 1702–1705.
- Elangovan S, Ramachandran S, Venkatesan N, Ananth S, Gnana-Prakasam JP, Martin PM et al. SIRT1 is essential for oncogenic signalling by estrogen/ estrogen receptor  $\alpha$  in breast cancer. *Cancer Res* 2011; **71**: 6654–6664.
- Lain S, Hollick JJ, Campbell J, Staples OD, Higgins M, Aoubala M et al. Discovery, *in vivo* activity, and mechanism of action of a small-molecule p53 activator. *Cancer Cell* 2008; **13**: 454–463.
- Di Sante G, Pestell TG, Casimiro MC, Bisetto S, Powell MJ, Lisanti MP et al. Loss of Sirt1 promotes prostatic intraepithelial neoplasia, reduces mitophagy, and delays Park2 translocation to mitochondria. *Am J Pathol* 2015; **185**: 266–279.
- Deng CX. SIRT1, is it a tumor promoter or tumor suppressor?. *Int J Biol Sci* 2009; **5**: 147–152.
- Jin MD, Zhi YW, Dao CS, Ru XL, Sheng QW. SIRT1 interacts with p73 and suppresses p73-dependent transcriptional activity. *J Cell Physiol* 2007; **210**: 161–166.
- Wen YC, Wang DH, RayWhay CY, Luo J, Gu W, Baylin SB. Tumor suppressor HIC1 directly regulates SIRT1 to modulate p53-dependent DNA-damage responses. *Cell* 2005; **123**: 437–448.
- Kong S, Kim SJ, Sandal B, Lee SM, Gao B, Zhang DD et al. The type III histone deacetylase Sirt1 protein suppresses p300-mediated histone H3 lysine 56 acetylation at Bclaf1 promoter to inhibit T cell activation. *J Biol Chem* 2011; **286**: 16967–16975.
- Yeung F, Hoberg JE, Ramsey CS, Keller MD, Jones DR, Frye RA et al. Modulation of NF-kappaB-dependent transcription and cell survival by the SIRT1 deacetylase. *EMBO J* 2004; **23**: 2369–2380.
- Kiernan R, Brès V, Ng RWM, Coudart MP, El Messaoudi S, Sartet C et al. Post-activation turn-off of NF-kB-dependent transcription is regulated by acetylation of p65. *J Biol Chem* 2003; **278**: 2758–2766.
- Yao Y, Brodie AMH, Davidson NE, Kensler TW, Zhou Q. Inhibition of estrogen signalling activates the NRF2 pathway in breast cancer. *Breast Cancer Res Treat* 2010; **124**: 585–591.
- Maggiolini M, Donzé O, Picard D. A non-radioactive method for inexpensive quantitative RT-PCR. *Biol Chem* 1999; **380**: 695–697.
- Viña J, Borrás C, Gambini J, Sastre J, Pallardó F V. Why females live longer than males? Importance of the upregulation of longevity-associated genes by oestrogenic compounds. *FEBS Lett* 2005; **579**: 2541–2545.
- Dai Y, Faller DV. Transcription regulation by class III histone deacetylases (HDACs)-sirtuins. *Transl Oncogenomics* 2008; **3**: 53–65.
- Brugarolas J, Chandrasekaran C, Gordon JI, Beach D, Jacks T, Hannon GJ. Radiation-induced cell cycle arrest compromised by p21 deficiency. *Nature* 1995; **377**: 552–557.
- Huffman DM, Grizzle WE, Bamman MM, Kim JS, Eltoum IA, Elgavish A et al. SIRT1 is significantly elevated in mouse and human prostate cancer. *Cancer Res* 2007; **67**: 6612–6618.
- Brooks CL, Gu W. How does SIRT1 affect metabolism, senescence and cancer? *Nat Rev Cancer* 2009; **9**: 123–128.
- Gong D-J, Zhang J-M, Yu M, Zhuang B, Guo Q-Q. Inhibition of SIRT1 combined with gemcitabine therapy for pancreatic carcinoma. *Clin Interv Aging* 2013; **8**: 889–897.
- Inoue T, Hiratsuka M, Osaki M, Oshimura M. The molecular biology of mammalian SIRT proteins: SIRT2 in cell cycle regulation. *Cell Cycle* 2007; **6**: 1011–1018.
- Houtkooper RH, Pirinen E, Auwerx J. Sirtuins as regulators of metabolism and healthspan. *Nat Rev Mol Cell Biol* 2012; **13**: 225–238.
- Zschoernig B, Mahlknecht U. SIRTUIN 1: regulating the regulator. *Biochem Biophys Res Commun* 2008; **376**: 251–255.
- Rufini A, Tucci P, Celardo I, Melino G. Senescence and aging: the critical roles of p53. *Oncogene* 2013; **32**: 5129–5143.
- Lane DP, Cheek CF, Lain S. p53-based cancer therapy. *Cold Spring Harb Perspect Biol* 2010; **2**: a001222.
- Vaziri H, Dessain SK, Eaton EN, Imai SI, Frye RA, Pandita TK et al. hSIR2/SIRT1 functions as an NAD-dependent p53 deacetylase. *Cell* 2001; **107**: 149–159.
- Saunders LR, Verdin E. Sirtuins: critical regulators at the crossroads between cancer and aging. *Oncogene* 2007; **26**: 5489–5504.
- Motta MC, Divecha N, Lemieux M, Kamel C, Chen D, Gu W et al. Mammalian SIRT1 represses forkhead transcription factors. *Cell* 2004; **116**: 551–563.
- Cohen HY, Lavu S, Bitterman KJ, Hekking B, Imahiyerobo TA, Miller C et al. Acetylation of the C terminus of Ku70 by CBP and PCAF controls Bax-mediated apoptosis. *Mol Cell* 2004; **13**: 627–638.

44. Wang RH, Sengupta K, Li C, Kim HS, Cao L, Xiao C *et al*. Impaired DNA damage response, genome instability, and tumorigenesis in SIRT1 mutant mice. *Cancer Cell* 2008; **14**: 312–323.
45. Firestein R, Blander G, Michan S, Oberdoerffer P, Ogino S, Campbell J *et al*. The SIRT1 deacetylase suppresses intestinal tumorigenesis and colon cancer growth. *PLoS One* 2008; **3**: e2020.
46. Ota H, Tokunaga E, Chang K, Hikasa M, Iijima K, Eto M *et al*. Sirt1 inhibitor, Sirtinol, induces senescence-like growth arrest with attenuated Ras-MAPK signalling in human cancer cells. *Oncogene* 2006; **25**: 176–185.
47. Jung-Hynes B, Nihal M, Zhong W, Ahmad N. Role of sirtuin histone deacetylase SIRT1 in prostate cancer: a target for prostate cancer management via its inhibition? *J Biol Chem* 2009; **284**: 3823–3832.
48. Ford J, Jiang M, Milner J. Cancer-specific functions of SIRT1 enable human epithelial cancer cell growth and survival. *Cancer Res* 2005; **65**: 10457–10463.
49. Fang Y, Nicholl MB. Sirtuin 1 in malignant transformation: friend or foe? *Cancer Lett* 2011; **306**: 10–14.
50. Yao Y, Li H, Gu Y, Davidson NE, Zhou Q. Inhibition of SIRT1 deacetylase suppresses estrogen receptor signalling. *Carcinogenesis* 2010; **31**: 382–387.
51. Zhao W, Kruse J-P, Tang Y, Jung SY, Qin J, Gu W. Negative regulation of the deacetylase SIRT1 by DBC1. *Nature* 2008; **451**: 587–590.
52. Solomon JM, Pasupuleti R, Xu L, McDonagh T, Curtis R, DiStefano PS *et al*. Inhibition of SIRT1 catalytic activity increases p53 acetylation but does not alter cell survival following DNA damage. *Mol Cell Biol* 2006; **26**: 28–38.
53. Heltweg B, Gattbonton T, Schuler AD, Posakony J, Li H, Goehle S *et al*. Antitumor activity of a small-molecule inhibitor of human silent information regulator 2 enzymes. *Cancer Res* 2006; **66**: 4368–4377.
54. Lara E, Mai A, Calvanese V, Altucci L, Lopez-Nieva P, Martinez-Chantar ML *et al*. Salermide, a Sirtuin inhibitor with a strong cancer-specific proapoptotic effect. *Oncogene* 2009; **28**: 781–791.
55. Peck B, Chen C-Y, Ho K-K, Di Fruscia P, Myatt SS, Coombes RC *et al*. SIRT inhibitors induce cell death and p53 acetylation through targeting both SIRT1 and SIRT2. *Mol Cancer Ther* 2010; **9**: 844–855.
56. Deroo BJ, Korach KS. Estrogen receptors and human disease. *J Clin Invest* 2006; **116**: 561–570.
57. Pupo M, Pisano A, Lappano R, Santolla MF, de Francesco EM, Abonante S *et al*. Bisphenol A induces gene expression changes and proliferative effects through GPER in breast cancer cells and cancer-associated fibroblasts. *Environ Health Perspect* 2012; **120**: 1177–1182.
58. Kalluri R, Zeisberg M. Fibroblasts in cancer. *Nat Rev Cancer* 2006; **6**: 392–401.
59. Calon A, Lonardo E, Berenguer-Illego A, Espinet E, Hernando-momblona X, Iglesias M *et al*. Stromal gene expression defines poor-prognosis subtypes in colorectal cancer. *Nat Genet* 2015; **47**: 320–329.
60. Isella C, Terrasi A, Bellomo SE, Petti C, Galatola G, Muratore A *et al*. Stromal contribution to the colorectal cancer transcriptome. *Nat Genet* 2015; **47**: 312–319.
61. Bhowmick NA, Neilson EG, Moses HL. Stromal fibroblasts in cancer initiation and progression. *Nature* 2004; **432**: 332–337.
62. Orimo A, Gupta PB, Sgroi DC, Arenzana-Seisdedos F, Delaunay T, Naeem R *et al*. Stromal fibroblasts present in invasive human breast carcinomas promote tumor growth and angiogenesis through elevated SDF-1/CXCL12 secretion. *Cell* 2005; **121**: 335–348.
63. Yamaguchi Y, Hayashi S. Estrogen-related cancer microenvironment of breast carcinoma. *Endocr J* 2009; **56**: 1–7.
64. Catalano S, Giordano C, Panza S, Chemi F, Bonfiglio D, Lanzino M *et al*. Tamoxifen through GPER upregulates aromatase expression: a novel mechanism sustaining tamoxifen-resistant breast cancer cell growth. *Breast Cancer Res Treat* 2014; **146**: 273–285.
65. Santolla MF, De Francesco EM, Lappano R, Rosano C, Abonante S, Maggolini M. Niacin activates the G protein estrogen receptor (GPER)-mediated signalling. *Cell Signal* 2014; **26**: 1466–1475.
66. Albanito L, Sisci D, Aquila S, Brunelli E, Vivacqua A, Madeo A *et al*. Epidermal growth factor induces G protein-coupled receptor 30 expression in estrogen receptor-negative breast cancer cells. *Endocrinology* 2008; **149**: 3799–3808.
67. De Francesco EM, Pellegrino M, Santolla MF, Lappano R, Ricchio E, Abonante S *et al*. GPER mediates activation of HIF1/VEGF signalling by estrogens. *Cancer Res* 2014; **74**: 4053–4064.
68. Maggolini M, Santolla MF, Avino S, Aiello F, Rosano C, Garofalo A *et al*. Identification of two benzopyrrolinoxazines acting as selective GPER antagonists in breast cancer cells and cancer-associated fibroblasts. *Future Med Chem* 2015; **7**: 437–448.
69. Vivacqua A, De Marco P, Santolla MF, Cirillo F, Pellegrino M, Panno ML *et al*. Estrogenic gper signaling regulates mir144 expression in cancer cells and cancer-associated fibroblasts (cafs). *Oncotarget*; e-pub ahead of print 12 May 2015.
70. De Marco P, Bartella V, Vivacqua A, Lappano R, Santolla MF, Morcavallo A *et al*. Insulin-like growth factor-I regulates GPER expression and function in cancer cells. *Oncogene* 2013; **32**: 678–688.



**Cell Death and Disease** is an open-access journal published by Nature Publishing Group. This work is licensed under a Creative Commons Attribution 4.0 International License. The images or other third party material in this article are included in the article's Creative Commons license, unless indicated otherwise in the credit line; if the material is not included under the Creative Commons license, users will need to obtain permission from the license holder to reproduce the material. To view a copy of this license, visit <http://creativecommons.org/licenses/by/4.0/>

Supplementary Information accompanies this paper on Cell Death and Disease website (<http://www.nature.com/cddis>)



UNIVERSITÀ DELLA CALABRIA  
DIPARTIMENTO DI FARMACIA E  
SCIENZE DELLA SALUTE E DELLA  
NUTRIZIONE

*Prof. Marcello Maggiolini*

Tel. 0984/493076 – 3382993190

[marcellomaggiolini@yahoo.it](mailto:marcellomaggiolini@yahoo.it)

[marcello.maggiolini@unical.it](mailto:marcello.maggiolini@unical.it)

## **Giudizio del Supervisore sull'attività del dottorando Damiano Cosimo Rigracciolo**

### **Dottorato di Ricerca in Medicina Traslazionale (XXX Ciclo)**

**Coordinatore Prof. Sebastiano Andò**

Il Dottor Damiano Cosimo Rigracciolo ha iniziato il corso di dottorato di ricerca in "Medicina Traslazionale" - XXX ciclo - il 02-11-2014.

Nel corso del Dottorato, il progetto di ricerca del Dr. Rigracciolo ha riguardato inizialmente i meccanismi molecolari coinvolti dal rame nella stimolazione dell'angiogenesi in cellule tumorali. Gli esperimenti condotti e i risultati ottenuti hanno dimostrato che il rame (CuSO<sub>4</sub>), attraverso la generazione di radicali liberi ed il coinvolgimento del pathway trasduzionale EGFR/ERK/MAPK, è in grado di indurre l'up-regolazione dei livelli di mRNA e proteici del fattore trascrizionale indotto dall'ipossia HIF-1 $\alpha$ , del fattore di crescita dell'endotelio vascolare VEGF e del recettore di membrana responsivo agli estrogeni GPER, sia in cellule tumorali mammarie SkBr3 che epatiche HepG2. In tale contesto, utilizzando specifici silenziatori è stato inoltre osservato il coinvolgimento di HIF-1 $\alpha$  e GPER nell'up-regolazione di VEGF indotta dal rame. E' stato infine valutato il ruolo del cross-talk funzionale tra HIF-1 $\alpha$ , VEGF e GPER nelle risposte biologiche mediate dal rame, utilizzando come modello sperimentale cellule HUVECs (Human Umbilical Vein Endothelial Cells), nelle quali il metallo ha indotto la formazione di un intricato network di strutture tubulari simil-vascolari e la migrazione cellulare.

Le attività di ricerca del Dr. Rigracciolo hanno inoltre riguardato la caratterizzazione dei pathway trasduzionali coinvolti negli effetti mediati dall'aldosterone in cellule tumorali mammarie. Attraverso saggi di co-immunoprecipitazione ed immunofluorescenza è stata dimostrata l'esistenza di un'interazione diretta tra il recettore dell'aldosterone MR e GPER, il quale è stato coinvolto nella regolazione dello scambiatore Na<sup>+</sup>/H<sup>+</sup> denominato NHE-1 la cui attività è regolata dal complesso aldosterone/MR. Gli studi condotti hanno infine specificato il ruolo di MR e GPER in alcuni effetti biologici mediati dall'aldosterone, utilizzando come modello sperimentale cellule endoteliali



UNIVERSITÀ DELLA CALABRIA  
DIPARTIMENTO DI FARMACIA E  
SCIENZE DELLA SALUTE E DELLA  
NUTRIZIONE

*Prof. Marcello Maggiolini*  
Tel. 0984/493076 – 3382993190  
[marcellomaggiolini@yahoo.it](mailto:marcellomaggiolini@yahoo.it)  
[marcello.maggiolini@unical.it](mailto:marcello.maggiolini@unical.it)

derivate da tumore mammario denominate B-TEC. In tale contesto cellulare, il silenziamento dell'espressione di GPER e di MR ha infatti inibito la capacità dell'aldosterone di indurre la proliferazione e la migrazione cellulare.

Il Dr. Rigracciolo ha svolto uno stage di un anno (Gennaio 2016-Dicembre 2016) a San Diego presso il Laboratorio diretto dal Prof. J. Silvio Gutkind – John & Rebecca Moores Cancer Center, dell'Università della California (USA).

Durante tale stage, il progetto di ricerca del Dr. Rigracciolo ha riguardato il ruolo esercitato da una proteina citoplasmatica ad attività tirosin-chinasica associata ai recettori per le integrine, denominata FAK (focal adhesion kinase), nella progressione del Melanoma Uveale. A riguardo, si precisa che tale tumore è caratterizzato dalla presenza di mutazioni somatiche attivanti a carico degli oncogeni GNAQ e GNA11, che codificano per due diverse subunità  $\alpha$  delle proteine G. Attraverso analisi bioinformatica lo studio ha inizialmente determinato che il gene codificante per FAK (PTK2) è over-espresso nel 56% dei casi di Melanoma Uveale. Sulla base di tale osservazione, sono stati successivamente valutati i meccanismi mediati da GNAQ nell'attivazione di FAK, utilizzando come modelli sperimentali cellule di Melanoma Uveale OMM1.3 (GNAQ/11 mutate) e cellule denominate HEK293 DREADD/Gq che sono state ingegnerizzate per l'espressione di un recettore di membrana accoppiato a proteine-G (Gaq) attivato da ligandi sintetici. I saggi biologici effettuati hanno dimostrato l'attività antitumorale di specifici inibitori di FAK, come osservato negli esperimenti realizzati in cellule di Melanoma Uveale derivanti sia da lesioni primarie che da metastasi epatiche. Infine, attraverso l'innovativo approccio genetico CRISPR/Cas9, il silenziamento dell'espressione di FAK ha ridotto significativamente la crescita del melanoma uveale anche in saggi condotti in vivo.

L'attività sperimentale descritta è stata pianificata e realizzata autonomamente dal Dr. Rigracciolo, che ha inoltre curato la disamina critica dei risultati ottenuti ai fini delle seguenti pubblicazioni su riviste internazionali peer-reviewed:



*Prof. Marcello Maggiolini*

Tel. 0984/493076 – 3382993190

[marcellomaggiolini@yahoo.it](mailto:marcellomaggiolini@yahoo.it)

[marcello.maggiolini@unical.it](mailto:marcello.maggiolini@unical.it)

1. **Rigiracciolo DC**, Xiadong F, Maggiolini M, Gutkind JS. Targeting systems vulnerabilities in uveal melanoma by CRISPR/Cas9 focal adhesion kinase (FAK) genome editing and therapeutic inhibition. *Cancer Research*, Submitted.
2. GPER is involved in the regulation of the estrogen-metabolizing CYP1B1 enzyme in breast cancer. Cirillo F, Pellegrino M, Malivindi R, Rago V, Avino S, Muto L, Dolce V, Vivacqua A, **Rigiracciolo DC**, De Marco P, Sebastiani A, Abonante S, Nakajima M, Lappano R, Maggiolini M. *Oncotarget*. 2017 Nov 20;8(63):106608-106624. doi: 10.18632/oncotarget.22541.
3. Lappano R, Sebastiani A, Cirillo F, **Rigiracciolo DC**, Galli GR, Curcio R, Malaguarnera R, Belfiore A, Cappello AR, Maggiolini M. The lauric acid-activated signaling prompts apoptosis in cancer cells. *Cell Death Discov*, 2017. 3:17063
4. Cirillo F, Pellegrino M, Malivindi R, Rago V, Avino S, Muto L, Dolce V, Vivacqua A, **Rigiracciolo DC**, De Marco P, Sebastiani A, Abonante S, Nakajima M, Lappano R, Maggiolini M. GPER is involved in the regulation of the estrogen-metabolizing CYP1B1 enzyme in breast cancer. *Oncotarget*, in press, 2017.
5. De Francesco EM, Rocca C, Scavello F, Amelio D, Pasqua T, **Rigiracciolo DC**, Scarpelli A, Avino S, Cirillo F, Amodio N, Cerra MC, Maggiolini M, Angelone T. Protective Role of GPER Agonist G-1 on Cardiotoxicity Induced by Doxorubicin. *J Cell Physiol*, 2017. 232:1640-1649.
6. **Rigiracciolo DC**, Scarpelli A, Lappano R, Pisano A, Santolla MF, Avino S, De Marco P, Bussolati B, Maggiolini M, De Francesco EM. GPER is involved in the stimulatory effects of aldosterone in breast cancer cells and breast tumor-derived endothelial cells. *Oncotarget*, 2016. 7:94-111.
7. Serra R, Gallelli L, Perri P, De Francesco EM, **Rigiracciolo DC**, Mastroberto P, Maggiolini M, de Francis S. Estrogens Receptors and Chronic Venous Disease. *J Vasc Surg*, 2016. 64:538.
8. **Rigiracciolo DC**, Scarpelli A, Lappano R, Pisano A, Santolla MF, De Marco P, Cirillo F, Cappello AR, Dolce V, Belfiore A, Maggiolini M, De Francesco EM. Copper activates HIF-1 $\alpha$ /GPER/VEGF signalling in cancer cells. *Oncotarget*, 2015. 6:34158-34177.
9. Pisano A, Santolla MF, De Francesco EM, De Marco P, **Rigiracciolo DC**, Perri MG, Vivacqua A, Abonante S, Cappello AR, Dolce V, Belfiore A, Maggiolini M, Lappano R. GPER, IGF-1R, and EGFR transduction signaling are involved in stimulatory effects of zinc in breast cancer cells and cancer-associated fibroblasts. *Mol Carcinog*, 2017. 56:580-593.



UNIVERSITÀ DELLA CALABRIA  
DIPARTIMENTO DI FARMACIA E  
SCIENZE DELLA SALUTE E DELLA  
NUTRIZIONE

*Prof. Marcello Maggiolini*

Tel. 0984/493076 – 3382993190

[marcellomaggiolini@yahoo.it](mailto:marcellomaggiolini@yahoo.it)

[marcello.maggiolini@unical.it](mailto:marcello.maggiolini@unical.it)

10. Avino S, De Marco P, Cirillo F, Santolla MF, De Francesco EM, Perri MG, **Rigiracciolo DC**, Dolce V, Belfiore A, Maggiolini M, Lappano R, Vivacqua A. Stimulatory actions of IGF-1 are mediated by IGF-1R cross-talk with GPER and DDR1 in mesothelioma and lung cancer cells. *Oncotarget*, 2016. 7:52710-52728.

11. Lappano R, **Rigiracciolo DC**, De Marco P, Avino S, Cappello AR, Rosano C, Maggiolini M, De Francesco EM. Recent Advances on the Role of G Protein-Coupled Receptors in Hypoxia-Mediated Signaling. *AAPS J*, 2016. 18:305-310.

12. Tropea T, De Francesco EM, **Rigiracciolo DC**, Maggiolini M, Wareing M, Osol G, Mandalà M. Pregnancy Augments G Protein Estrogen Receptor (GPER) Induced Vasodilation in Rat Uterine Arteries via the Nitric Oxide-cGMP Signaling Pathway. *PloS One*, 2015. 10:e0141997.

13. Santolla MF, Avino S, Pellegrino M, De Francesco EM, De Marco P, Lappano R, Vivacqua A, Cirillo F, **Rigiracciolo DC**, Scarpelli A, Abonante S, Maggiolini M. SIRT1 is involved in oncogenic signaling mediated by GPER in breast cancer. *Cell Death Dis*, 2015. 6:e1834.

Il giudizio complessivo sull'attività di ricerca svolta dal Dottor Damiano Cosimo Rigiracciolo è, pertanto, ampiamente positivo.

Rende 30/01/2018

Il supervisore

Prof. Marcello Maggiolini